Intrinsic properties of Hellenic "Marls"

George Tsifoutidis

INTRINSIC PROPERTIES OF HELLENIC "MARLS"

Ph.D THESIS

presented by

George Tsifoutidis B.Sc, M.Sc, F.G.S.

February 1993

Durham
United Kingdom

INTRINSIC PROPERTIES OF HELLENIC "MARLS"

a thesis submitted to the Faculty of Science in fulfilment of the requirements for the degree of Doctor of Philosophy at the School of Engineering and Computer Science, University of Durham, U.K.

by

George Tsifoutidis, B.Sc, M.Sc, F.G.S

February 1993.

Dedicated to my parents, my brother and the land
I spent most of my life, beautiful Macedonia,
beautiful Hellas.

DECLARATION

I hereby declare that the work reported in this thesis has not been previously submitted for any degree. All material in this thesis is original except where indicated by reference to other work.

George Tsifoutidis B.Sc, M.Sc, F.G.S.

TABLE OF CONTENTS

Abstract i
Acknowledgements ii
List of Abbreviations iv
List of Symbols v

chapter 1 INTRODUCTION

1.1 The background of the thesis 1
1.2 Aims of this thesis 2
1.3 Glossary 2
1.3 Format of the thesis 3

chapter 2 THE GEOLOGICAL EVOLUTION OF HELLAS

2.1 General Geological Background 7
2.2 Evolution of the Mediterranean: Recent and Present 8
2.3 The Hellenides Mountain Ranges 11
2.3.1 Geographical Position 11
2.3.2 Evolution of the Aegean Region 12
2.3.2.1 General 12
2.3.2.2 Seismicity and Regional Dynamics 12
2.4 On the Geotectonical Zoning of the Hellenides 15
2.5 Hellenic Post Alpine Formations 16
2.5.1 General 16
2.5.2 The Molassic Sediments 17
2.5.3 Neogene and Quaternary Deposits 18

chapter 3 FIELDWORK

3.1 General Information 22
3.2 Sampling Techniques 23
3.3 Korinthos Sampling Area 25
3.3.1 General Structure and Seismisity 25
3.3.2 Korinthos Sampling Area Boundaries 26
3.3.3 The Lithology of Korinthos Sampling Area 26
3.3.4 Sampling Sites. 27
3.3.4.1 General 27
3.3.4.2 Solomos Junction. 27
3.3.4.3 Arvanitis. 29
3.3.4.4 Penteskoufi 30
3.3.4.5 Tsakiri - Rentaiika 31
3.3.4.6 Roumania 32
3.4 Preveza - Igoumenitsa Road Axis Sampling Area. 32
3.4.1 Geographical Boundaries 32
3.4.2 Structural Evolution of the Area 33
3.4.3 Lithology of Sampling Area. 34
3.4.4 Geomorphology of Sampling Area. 35

3.4.5 Sampling Sites 36
3.4.5.1 General 36
3.4.5.2 Kanali (Mytikas) 36
3.4.5.3 Loutsa 37
3.4.5.4 Agios Nikolaos 37
3.4.5.5 Gourounaki 38
3.4.5.6 Lakka Lefkas 38
3.4.5.7 Tsoumba Laxi 39
3.4.5.8 Krevatina 39
3.4.5.9 Kastro Despos 41
3.4.5.10 Lakka Lampes 41
3.4.5.11 Apidoules 42
3.4.5.12 Xynomelia 43
3.4.5.13 Koukos 43
3.5 Amalias - Goumeron Sampling Area. 43
3.5.1 Geographical Boundaries. 43
3.5.2 Geomorphology of the Area. 44
3.5.3 General Structure. 44
3.5.4 Lithology of the Sampling Area. 45
3.5.5 Sampling Sites 46
3.5.5.1 General 46
3.5.5.2 Hill 183 (near Pineios Reservoir) 47
3.5.5.3 Nesia 47
3.5.5.4 Tzami 48
3.5.5.5 Merovigli 48
3.5.5.6 Palaiostani 48
3.5.5.7 Skoufia 48
3.5.5.8 Oenoi 49
3.5.5.9 Koutsohera 49
3.5.5.10 Rodia 49

chapter 4 PHYSICAL CHARACTERISTICS AND MINERALOGY

4.1 On the Classification of "Marls" 50
4.1.1 General 50
4.1.2 Definitions on Marls 50
4.1.2.1 General 50
4.1.2.2 Mineralogical Considerations 51
4.1.2.3 Engineering Geological Considerations 52
4.1.3 Hellenic Marls and Marly Fine Grained Sediments 55
4.2 Engineering Classification Tests in the Laboratory 56
4.2.1 General 56
4.2.2 Methods of Testing 57
4.2.2.1 Atterberg Limits 57
4.2.2.2 Specific Gravity 57
4.2.2.3 Grain Size Distribution 57
4.2.2.4 Free Swell Test 58
4.2.3 Presentation of Results 58
4.2.4 Analysis of the Test Results 69

4.2.4.1 Atterberg Limits 69
4.2.4.2 Activity 69
4.2.4.3 Grain Size Analysis 71
4.2.4.5 The Effect of Drying on Plasticity 72
4.2.4.6 Free Swelling 73
4.3 Mineralogical Analysis 74
4.3.1 General 74
4.3.2 Theoretical Considerations 74
4.3.2.1 General on X-ray Fluoresence 74
4.3.2.2 General on X-ray Diffraction 74
4.3.2.3 Sample Pretreatment 76
4.3.2.4 Mineral Identification 76
4.3.3 Preparation of Samples 77
4.3.4 Equipment and Testing Parameters 78
4.3.5 Mineral Identification 78
4.3.6 Quantification of Diffractograph Result 80
4.3.7 Presentation of Results 80
4.3.8 Analysis of Results 81
4.3.8.1 Mineral Species and Suites 81
4.4 Discussion 88
4.4.1 General 88
4.4.2 Plasticity and Grain Size. 88
4.4.3 Specific Gravity 88
4.4.4 The Effect of Drying on Plasticity 89
4.4.5 Free Swelling 89
4.4.6 Mineralogical contents 89
4.4.7 Aggregation Ratio 91
4.4.8 Minerals and Grain Size 95

chapter 5 RESIDUAL STRENGTH

5.1 Literature Review 99
5.1.1 Introduction 99
5.1.2 Major Contributions to the residual strength concept. 99
5.1.2.1 4th Rankine Lecture (Skempton, 1964) 99
5.1.2.2 Lupini's contribution 100
5.1.2.3 Skempton's (1985) contribution 101
5.1.3. Slope stability and residual strength 101
5.1.4 Apparatuses for measuring residual shear strength 104
5.1.4.1 Apparatus Types 104
5.1.4.2 Comparative Studies and Testing Methods 105
5.1.5. Grain Size and Residual Strength 107
5.1.6. Plasticity Indices and Residual Strength 108
5.1.7. Mineralogy and Pore Water Chemistry Effects. 111
5.1.8. The effects of vertical effective (normal) stress 114
5.1.9. The role of shear effects on residual strength 115
5.1.10 Granular Void ratio 117
5.2 The residual strength testing programme. 119
5.2.1. General 119

5.2.2. Apparatuses used. 119
5.2.2.1 Bromhead ring shear apparatus. 119
5.2.2.2 Armfield ring shear apparatus. 119
5.3. Methods of testing. 128
5.3.1 Testing with the Bromhead apparatus. 128
5.3.1.1 Preparation of Specimens. 128
5.3.1.2. Shearing Procedure 128
5.3.2 Testing with the Armfield apparatus 129
5.3.2.1 Preparation of Specimen 129
5.3.2.2 Shearing Procedure 130
5.3.2.3 Comparison against Bromhead ring shear measurements 132
5.3.2.4 Comparisons against reversible shear box measurements 133
5.3.3 Experimental Errors 133
5.3.4 Calibration 135
5.3.5 Data Recording 136
5.4 Calculating the Shear Strength Parameters 136
5.5. Test Results 137
5.6 Analysis of Test results. 146
5.6.1 Residual stress ratio and shear stress envelopes 146
5.6.2. Granular Void ratio 148
5.7 Discussion 152
5.7.1 Comparisons with results from other Hellenic formations 152
5.7.2 Testing Procedures and the curved envelope 153
5.7.2.1. General 153
5.7.2.2.Physico-Chemical swelling and curved envelope implications 153
5.7.2.3 Mechanical swelling and curved envelope implications 154
5.7.2.4 Concuding remarks 154
5.7.3 Granular Void Ratio 155

chapter 6 COMPRESSIBILITY OF RECONSTITUTED "MARLS"

6.1 Literature Review 157
6.1.1 From Sedimentation to Consolidation 157
6.1.2 Compressibility and Permeability 158
6.1.3 Virgin Compression of Clays 159
6.1.4 Double Layer Theory and the Compressibility of Clays 160
6.1.5 Compressibility of Reconstituted Clays and Intrinsic Parameters 162
6.1.6 The Effect of Initial Moisture Content and Load Increment Duration 165
6.1.7 The Effect of Ageing 165
6.2 Testing programme 166
6.2.1. General 166
6.2.2. Equipment 167
6.2.3. Method of testing 167

6.2.3.1 Specimen Preparation 167
6.2.3.2 Testing Procedure 169
6.2.4. Calculation of compression parameters e, Cc, and Iv 170
6.2.5. Presentation of results 172
6.2.6 Analysis of test results 179
6.2.6.1 The e-logσ_v' curves convergence 179
6.2.6.2 The I_v - logσ_v' curves 179
6.2.6.3 Constants of intrinsic compressibility 182
6.3 Discussion 183
6.3.1 Effects of plasticity on e-logσ_v'curves 183
6.3.2 The effect of mixing ratio w_i/w_L on the e-logσ_v' curves 185
6.3.3 Intrinsic compression lines 185

chapter 7 DISCUSSION

7.1 The effects of grain size on the residual strength 191
7.1.1 General 191
7.1.2 The Effect of Grain Size on the Residual Strength of Hellenic "Marls" 191
7.1.3 The effects of grain size as modelled by a computer program 197
7.1.3.1 The program 197
7.1.3.2 The model 199
7.1.3.3. Concluding remarks 200
7.2 The effects of mineralogy on the residual strength 200
7.2.1 General 200
7.2.2 Clay minerals associations 201
7.2.3 Non clay mineral associations 204
7.2.4 Mineralogical suites and ϕ_r' 206
7.3 The effect of aggregation on the residual stress-linear displacement relationship 209
7.4 The effect of plasticity on the residual strength 209
7.5 Mineralogical associations with the intrinsic compression index 212
7.5.1 General 212
7.5.2 Mineralogical suites and intrinsic compression 213
7.6 A comparison between reconstituted and intact e-logsv' curves 222

chapter 8 SUMMARY AND CONCLUSIONS

8.1 General 231
8.2 On the classification and physical characteristics of "marls" 231
8.3 On the aggregation ratio of "marls" 234
8.4 On the residual strength of "marls" 234
8.5 On the intrinsic compressibility of Hellenic "marls" 239
8.6 Proposals for further research 242

REFERENCES-BIBLIOGRAPHY 248

APPENDIX A -
APPENDIX B -
APPENDIX C -
APPENDIX D -

ABSTRACT

Post-alpine deposits cover substantial areas of Hellas. The fine grained facies of these deposits, comprise a wide range of over consolidated materials of varying grading and mineralogy. On average, however, these deposits cover different depositional environments and may be classed as silty clays and clayey silts of low to intermediate plasticity containing calcite in their mineralogical suite. Such deposits have been collectively known to practising engineers as *marls*. A concerted effort to collect field and laboratory data and interpret the behaviour of these materials was recently launched in view of the involvement of the aforesaid mentioned deposits in a series of geotechnical problems. This thesis aspires to contribute to this knowledge and provide a framework on which the field performance of such materials may be interpreted.

To that end, disturbed and high quality undisturbed samples from the geologically dissimilar areas of Korinthos, Preveza-Igoumenitsa road axis and Amalias-Goumeron were obtained and tested in order to ascertain their physical characteristics and mineralogical composition. Further, engineering properties which are independent of stress history, i.e. *intrinsic*, of the materials sampled, were determined. These were the residual strength as determined by ring shearing and the compressibility of reconstituted samples.

The performance of the samples was assessed in terms of grain size distribution and mineralogy. The results show that any attempt to explain or predict *intrinsic* properties of Hellenic fine grained calcareous sediments without taking simultaneous account of gradation and mineralogy is incomplete and therefore inaccurate.

ACKNOWLEDGEMENTS

This thesis would have not existed if it wasn't for the unquestioned and unconditional love and continuous support from my parents and brother. They have been the only source of motivation and encouragement through thick and thin, the shield against miserable thoughts, the safe harbour in stormy weather, the lifeline when my dreams scuppered, the only reason left to me to finish what I had started whenever I realised that I might have been better off pursuing other interests in life. To them I will be eternally grateful.

My life would have been no different than a blank piece of paper if it was not for the people that I have the luck to have befriended during my stay in the U.K. and certainly first of all David and Christine Heppell and their parents whose long lasting friendship and support means a lot to me. Apart from their friendship I would also like to thank my house mate Dr. Steve Lavelle for providing an excellent company and for all the late night most interesting conversations, my colleagues Jonathan Welch for his altruism and Vasiliki Malandraki for moaning at my laziness, Susanne Hitchinson for showing me how spoiled I used to be, Dr. Yiannis Georgantopoulos for the trips to Scotland, Dr. Efharis Scarvelis for the most entertaining shopping trips, Dr. Yannos Michopoulos for being ...ωραιος, Nikolas Antoniu for the received artistic enlightment and last but certainly not least uncle Nikos and auntie Soultana for their love and all the sweets they sent from Thessaloniki.

To all those who stood by me during my presidency in the Graduate Society 1988-1989 I extend my warmest thanks. For being such a sport I'd like to thank all the good people in St' Cuthbert's Society, especially the guys of S.C.S.B.C. 2nd VIII 1991-2 and 1992-3 as well as Nick "Nikolai" Weston, Jed "Biggie" Gargan, Rob "the Fat Boy" Meek and Jon "Digger" Carr Brown. Thanks are also due to Cirion "Casey" Jones for being completely bonkers, all the good people of the "Reggata Tea Rooms", Ala Hola, Panayiotis and Dida, Kostas, crazy Zoe, Aris, Eleni for a big lesson in life, Julia, "little" Peter, Theakstons XB and the good people of the Highlands for their Uisge Beatha.

On the academic front I extend my gratitude to my supervisor Dr. David Toll for his interest and help even before he took over the supervision, his continuous support, immense patience, openness and willingness to discuss, his constructive criticism

and useful suggestions thought the three years of our co-operation which helped me to maintain the focus on the subject of this research and shape up this thesis. Thanks are due to Dr. David Hirst who meticulously supervised my mineralogical work and Mr. R. Hardy for the technical and analytical support offered during the mineralogical testing. Thanks are also due to Dr. A.R. Selby for his constructive comments on aspects of the thesis. Messrs B. McEleavey and S. Richardson for all their technical assistance and much needed witty humour are gratefully acknowledged.

To Prof. G. Koukis who kept on advising me since my days as a geology undergraduate I extend my gratitude. The contribution of the Division of Geotechnical Engineering of the Central Public Works Laboratory, Ministry for the Environment, Physical Planning and Public Works, the Engineering Geology Division of the Institute of Geology and Mineral Exploration and the Geological Mapping Division of the Public Petroleum Corporation to the successful accomplishment of my fieldwork by providing all the necessary field and/or laboratory assistance is gratefully acknowledged. I would in particular like to thank Dr. G.Tsiambaos and Dr. D. Rozos for their continuous support, suggestions and critical guidance during the fieldwork, as well as Messrs D. Tsaligopoulos, A. and S. Megremis for their excellent laboratory support.

If, however, I have managed to fail to mention people, who have contributed in any way towards the completion of the "beast" and my well being, in this section this was done out of no intention and certainly by accident

Durham 3 February 1993

LIST OF ABBREVIATIONS

A.D.	Anno Domini
A.S.T.M.	Americal Society of Testing and Materials
B.C.	Before Christ
B.S.	British Standards
B.S.I.	British Standards Institution
C.P.W.L.	Central Public Works Laboratory (Κ.Ε.Δ.Ε.)
E	East
G.D.P.U.	Geology Department of Patras University (Τ.Γ.Π.Π.)
G.S.H.A.F.	Geography Service of the Hellenic Armed Forces (Γ.Υ.Σ.)
I.C.L.	Intrinsic Compression Line
I.G.M.E.	Institute of Geological and Mineral Exploration (Ι.Γ.Μ.Ε.)
I.G.S.R.	Institute of Geology and Subsurface Research, former name of I.G.M.E
L.V.D.T.	Low Voltage Data Transducer
M.E.P.P.P.W.	Ministry for the Environment, Physical Planning and Public Works (Υ.ΠΕ.ΧΩ.ΔΕ)
min.	Minute
Mys	Million years
N	North
NNW, SSE, NE,...	North-northwest, South-southeast, Northeast,...
O.C.R.	Overconsolidation ratio
P.C.	Personal Computer
P.P.C.	Public Petroleum Corporation (Δ.Ε.Π.)
S	South
S.E.C.S.	School of Engineering and Computer Science
S.S.E.	Errors Sum of Square
S.S.R.	Regression Sum of Squares
S.S.T.	Total Sum of Squares
U.C.S.	Unconfined Compressive Stress
U.S.S.	Unconfined Shear Stress
W	West
X.R.D.	X - Ray Diffraction
X.R.F.	X - Ray Fluorescence

LIST OF SYMBOLS

a	Distance between the proving ring reaction and the axis of the shearing head of the ring shear apparatus
A	1 Ampere (mA=10^{-3}A)
A	Surface area
A_r	Aggregation ratio
Å	1 Ångström (=10^{-10} m)
Atm	1 Atmosphere (=100 kPa)
B	Base exchange capacity (equivalents / gram)
c	Cohesion intercept for a total stress failure envelope (Coulomb)
c'	Cohesion intercept for an effective stress failure envelope (Coulomb)
c_r	Residual cohesion intercept
c_v	Coefficient of consolidation (=$k/\gamma_w m_v$)
c.f	Clay size fraction
C_c	Compression index
C^*_c	Intrinsic compression index
C_s	Swelling index
γ_w	Bulk unit weight of water
d	Distance between planes of atoms
$D_1, D_2,...$	Proving rings' divisions
de	Void ratio change at any stage of an oedometer test
dH	Loss in specimen's height at any stage of an oedometer test
Δe	Total change in void ratio
e	Void ratio
e_o	Initial void ratio
e_f	Final void ratio
e_L	Void ratio at liquid limit
e^*_{100}	Intrinsic void ratio at σ_n'=100kPa
e^*_{1000}	Intrinsic void ratio at σ_n'=1000kPa
e_g	Granular void ratio
$F_1, F_2,...$	Calibration constants for the proving rings
g	1 gram (1 kg=10^3g, 1 Mg=10^6g)
G_s	Specific gravity
H_o	Initial height of an oedometer specimen
H_f	Final height of an oedometer specimen
θ	Angle of incidence of an x-ray on a crystal

I_B	Brittleness index
I_p	Plasticity index
I_p/w_p	Plastic ratio
I_v	Void index
k	Permeability
l	1 litre ($=10^{-3}$ m^3)
λ	Wavelength of x-rays
m	1 metre (cm=10^{-2}m, mm=10^{-3}m, μm=10^{-6}m, nm=10^{-9}m, km=10^3m)
M	Magnitude of an earthquake in the Richter scale
m_d	Dry mass of a specimen
m_i	Initial mass of a specimen
m_v	Compressibility
m_w	Mass of water
N	1 Newton
N_s	Frequency of seismic shocks inside an area
p	Effective vertical stress during an oedometer test
p'_m	Mean effective vertical stress during a ring shear test
p'_{mL}	Mean effective vertical stress during a ring shear test at liquid limit
p'_{mP}	Mean effective vertical stress during a ring shear test at plastic limit
Pa	1 Pascal (=1 N/m^2), kPa=10^3Pa, MPa=10^6Pa
P.I	Plasticity index
r	Radius at a point of a ring shear specimen from the apparatus rotation axis
r^2	Coefficient of determination
r_{vc}	Volume ratio
R	(in chapter 2) 1 Richter
R	Total interparticle repulsion
R_i	Inner radius of the rings shear apparatus
R_o	Outer radius of the rings shear apparatus
R_ϕ	Relative residual strength
ρ	Bulk density
ρ_d	Dry density
S	Specific surface area of a crystal (m^2/g)
S_{ey}	Standard error estimate for the independent parameter y
σ	Total stress
σ_1	Vertical principal stress (z axis)
σ_2	Horizontal principal stress (x axis)
σ_3	Horizontal principal stress (y axis)

σ'_n	Effective stress normal to the shearing plane
σ'_{ni}, σ'_{nj},...	Effective normal stress at shearing stage i, j,...
σ'_v	Effective vertical stress
T	Torque
τ	Shear stress
τ/σ'_n	Stress ratio
τ_i, τ_j,...	Shear stress at shearing stages i, j,...
τ_{res}	Residual shear stress
τ_p	Peak shear stress
u_a	Pore air pressure
u_w	Pore water pressure
φ	Udden-Wentworth grain size class
ϕ	Angle of internal friction
ϕ'	Effective angle of internal friction
ϕ'_r	Residual effective angle of internal friction
ϕ'_{ri}, ϕ'_{rj},...	Residual effective angle of internal friction at shearing stage i, j,...
ν	Specific volume (V/V_s)
V	Total volume of a sample
V_s	Volume of solids (=1+e)
w_i	Initial moisture content
w_i/w_L	Mixing ratio for a slurry
w_f	Final moisture content
w_L	Liquid limit
w_o	Moisture content at the start of slurry consolidation test
w_P	Plastic limit

CHAPTER 1
INTRODUCTION

1.1 The background of the thesis

Hellas is situated in a geologically continuously evolving domain of the Eurasian tectonic plate. The present subduction of the African plate along the Hellenic arc generates intense deformation resulting in seismic activity along major tensional fault zones and an accumulated vertical displacement along normal faults of approximately 1500m since Pliocene (5mys).

Thick successions of fine and coarse grained sediments deposited into active basins since the early Neogene (Miocene, 22mys) have daylighted and been subjected to seismic & gravitational deformation, to weathering and erosion and lately to the human activities. These sediments are called *post-alpine* and vary significantly in petrological and geotechnical terms.

The fine grained sediments (mudstones, marls, calcareous clays and silts, etc) cover extensive areas of Hellas frequently intercalated with sands, silty sands, sandstones and conglomerates of varying grain size and levels of cementation. Many slope stability and foundation engineering problems are related to the incomplete understanding of the engineering geological performance of these sediments.

The recent understanding of the behaviour of Hellenic argillaceous-calcareous fine grained sediments, collectively referred to in this thesis as "marls", was mainly based on the international experience with over-consolidated clayey soils and some patchy coverage of special cases of marls and calcareous mudstones, such as the Korinthos Canal marls and the deposits forming the Piraeus Marl. However useful the international experience may be with over-consolidated clayey soils, it cannot answer adequately problems arising from the mineralogy and different evolutionary processes endemic to these Hellenic formations. A working engineering geological and geotechnical framework of knowledge specific to these "marls" is clearly needed.

Only recently a more concerted effort has started shedding light on the general behaviour of these fine grained facies instead of focusing on very special case

studies such as the Korinth Canal marls, which although interesting as they may be, are very localised and bare no relevance to the vast majority of the Hellenic "marls".

1.2 Aims of this thesis

The present thesis aspires to contribute to the already accumulating knowledge on the Hellenic "marls" by:

i) provide field information about the sampled sediments and classify those sediments based on their physical and mineralogical characters;

ii) report and discuss *intrinsic* (see below) geotechnical properties of Hellenic "marls" as measured in the laboratory; and finally,

iii) examine the existence of esoteric relationships between the reported geotechnical properties and the constituent particles and mineralogy of the samples and discuss the implications of such relationships on the behaviour of Hellenic "marls" as this is portrayed by the measured *intrinsic* properties.

To ensure the maximum independence from special geological conditions, the fieldwork was extended to include sampling sites in three geologically dissimilar Quaternary basins. Particular effort was paid to cover the diverse range of fine grained calcareous materials present in each site.

1.3 Glossary

Owing to their cross-disciplinary nature, engineering geology and geotechnical engineering frequently use terms and methods of analysis borrowed from other fields of science and engineering. Inevitably, certain terms have been used in different contexts which has lead to misunderstandings. In order to avoid that, a number of such terms used in this thesis are defined below.

The term *marl* has generally been applied to a range of materials which share one common characteristic, namely the presence of calcite. Occasionally, other fine grained materials other than plastic brown clays have been described as marls. Although discussion on the definition of the term marl is presented later in the thesis, the author uses the term in quotes ("marls") to indicate those sediments that have

been sampled and rightly or wrongly have already been named as marls by previous researchers.

The geotechnical properties presented in this thesis are stress history independent and depend only on the reaction of the constituent particles and minerals of the tested samples to externally imposed testing conditions. Such properties are termed *intrinsic* and help to produce boundary conditions with reference to which properties of the intact materials can be categorised and their behaviour interpreted. To that end, the residual shear strength and the compression of destructured/reconstituted Hellenic "marls" have been seen as intrinsic properties.

In describing the mineralogical contents of the samples, the terms *species* or *mineral type* and *mineral group* or *mineralogical group* are used to indicate a specific mineral, e.g. calcite, and a family or group of them, e.g. carbonates, respectively. However, the term *mica* has often been used by geotechnical engineers as a mineral type outside the clay minerals. The author takes the mineralogical and geological definition of mica as the correct one, namely a mineralogical group of crystalline as well as hydrated aluminium phyllosilicate (i.e. clay) minerals, such as muscovite, hydrous muscovite, biotite and illite. The term mica or mica group is also used as the collective term for the above clay minerals since the x-ray diffraction identification of them is based on the reflection patterns of the more crystalline members of the group and cannot distinguish easily between, say, muscovite and illite.

Linear Regression (or least squares best fit) may be used to fit a curve (or multidimensional function) to a data set if the equation can be linearised by transforming the variables; e.g. in the equation $g(x)=a_0x^2$, the function x^2 may be transformed by the function ω such that $g(x)=a_0x^2=a_0\omega$. The data is transformed (i.e. squared) prior to the use of the well known linear regression technique. The function g(x) may then be considered linear with respect to the unknown parameter a_0.

1.4 Format of the thesis

The contents of this thesis are divided into eight (8) chapters and additional information may also be found in four (4) appendices. The chapters that follow this introduction are described below.

Chapter 2 describes the geological evolution of Hellas as part of the alpine orogene, attempts to discuss the current state of stress distribution as this has been revealed by the study of earthquakes and refers to the geological zoning and the distinction between alpine and post-alpine formation in order to provide a brief and comprehensive general geological overview.

Chapter 3 is devoted to the fieldwork which was conducted. In its first part, the background and the criteria for the choice of sampling sites and type of sampling are given. In the second part, the geology, geomorphology and position of the individual sampling areas with descriptions of their sampling sites and the obtained samples is provided.

Chapter 4 is divided up in four sections. The first section discusses the classification of "marls" in terms of their mineralogy and engineering properties and reviews some important studies on Hellenic "marls". In the second section the engineering tests used to ascertain the physical characteristics of the studied sediments and the test results are presented. In the analysis sub-section the test results are interpreted and discussed in order to provide an engineering classification. The third section deals with the mineralogical analysis which involves XRD and XRF spectrometry. A brief discussion on mineral identification and sample preparation, as well as a description of equipment and testing methods are provided. The results are presented and analysed in order to give a petrological classification of the sampled sediments. The fourth section compares the findings of this chapter with similar studies on Hellenic fine grained sediments and discusses phenomena arising from the interaction of the presented results, such as the aggregation ratio

Chapter 5 is dedicated to the residual strength of the sampled sediments. The first section reviews the literature on the concept of residual strength, testing methods and equipment and discusses proposed correlations between residual strength parameters and other soil properties and mineralogy. The second section describes the testing equipment, the third section describes the testing procedures used and the fourth section shows how the calculation of results is done. The fifth section presents the test results in tables and graphs. In the sixth section the analysis of the results concentrates on the shape of the failure envelopes, identification of trends per sampling area and shows results in terms of the granular void ratio concept. The seventh section discusses the results of this chapter with results presented on other

Hellenic fine grained sediments, proposes a mechanism for the observed curvatures of the failure envelopes and finally discusses the granular void ratio results.

Chapter 6 deals with the compressibility of reconstituted "marls". The first section reviews the literature on the mechanisms that control the behaviour of slurries under one-dimensional compression and discusses the concept of the compressibility of reconstituted clays and intrinsic parameters. The second section presents the testing procedure and equipment used, the calculation of the compression parameters and the test results. In the same section, the analysis of the results discusses the shape of the compression curves and presents the constants of intrinsic compressibility. The void index normalised curves are discussed and expressions which describe them are presented. The third section discusses the effects of plasticity on the void index normalised curves and compares the latter ones to the intrinsic compression line presented by Burland (1990).

Chapter 7 discusses the effects of grain size distribution (section 1) and mineralogy (section 2) on the residual shear strength and assesses the contribution of their contents as modelling parameters. The effect of particle aggregation on the residual stress-displacement (section 3) and the effect of plasticity on the residual strength (section 4) are also discussed. Section 5 discusses the mineralogical associations with the intrinsic compression index and assesses the contribution of the identified mineralogical suites in modelling the intrinsic compression index of the tested soils. Finally, section 6 compares the reconstituted compression lines with compression curves from intact samples and discusses the outcome of the comparison.

Chapter 8 concludes the findings of this thesis.

Appendix A presents the results of the ring shearing tests per tested sample in the form of a τ/σ_n' vs. σ_n' , a τ vs. σ_n' and a τ vs. linear displacement graphs.

Appendix B presents the results of ring shearing trial tests from the Armfield apparatus in comparison to test results from a Bromhead apparatus and a standard shear box.

Appendix C presents the void ratios and void indices versus their corresponding load increments from compression tests on reconstituted Hellenic "marls" and results from incremental loading tests on some intact samples of Hellenic "marls".

Appendix D contains 1:50,000 maps representing the surface geology of the sampling areas showing the approximate position of the various sampling sites. A more detailed 1:5,000 geological sketch of the Solomos site of Korinthos with the sampling positions indicated is included.

CHAPTER 2
THE GEOLOGICAL EVOLUTION OF HELLAS

2.1 General geological background

The main orogenetic episode, responsible for the present form of the Mediterranean region, is part of a wider movement which spanned throughout the Triassic to the Quarternary periods covering a geographical area from the Maghreb-Atlas to the Himalayan mountain ranges. This episode, known as the closing of the Tethys ocean, was caused by the progressive convergence of the Eurasian and the remnants of the Gondwana supercontinents and it is termed the Alpine Orogene. It is the alpine orogentic movements that have shaped Neo-Europe comprising Italy, the Alps, the Dinarides and the Hellenides. Although, as a term, Neo-Europe was established according to old geotectonic concepts, mainly by Stille(1924), it still remains valid in practice. Palaeo-Europe, with Western Scandinavia and Britain, formed during the Cambrian-Lower Devonian Caledonian orogene and Meso-Europe, with Iberia, France and Central Europe, formed during the Middle Devonian-Permian Hercynian-Variskan orogene, completing Stille's picture (fig 2.1).

Not only different strata but also whole geographical areas can be identified relative to the development of the alpine geosyncline in palaeogeographical and/or depositional terms. These may, then, be classified as *pro-*, *syn-*, *post-alpine*. The former comprise sedimentary and igneous strata, metamorphosed or not, of the bedrock massifs on which, during Triassic time, the ingression of the Tethys took place. The *syn-*, or simply, *alpine* are those domains that have been directly affected by the main folding episodes, the geological sequences of which were deposited inside or intruded the alpine geosyncline. The upper age limit to those stratigraphic columns may vary regionally as it is determined by geotectonic rather than stratigraphic factors. Finally, all sediments deposited and igneous bodies formed after the new mountain ranges emerged and which have not been affected by alpine folding are collectively characterised as *post-alpine*.

The strata that emerged after the alpine orogenetic movements, constructed a complex system of mountain ranges (fig. 2.2). In Europe, two major structural belts of the system are distinguished. The Alpides, firstly, comprise the Swiss Alps, the Pennine range, the Carpathian and the Balkan ranges and continues into Northern

Anatolia (Turkey) forming the Pontos Chain. The Dinarides, secondly, comprise the Apennines, the southern Alps, the Dinaric Alps and continue into Asia with the Taurus and Zagros mountains across to the Himalayas. In between these belts, surrounded, is the Rodopi massif consisting mainly of old crystalline rocks. According to Kober (1931) the Rodopi massif was an old craton that had no involvement in the alpine orogene. Kroneberg et. al. (1970), however, reinforced Dimitrev's (1955, 1959) indication that Rodopi has been an intermediate belt affected by alpine movements.

Fig. 2.1 Stille's tectonic model of Europe (from Stille, 1924).

2.2 Evolution of the Mediterranean: Recent and Present

Seismicity and present day deformations are an instantaneous picture, at geological scale, of the tectonic evolution of a region (Philip, 1988). Therefore, tectonic history gives us the logical explanation to understand present day tectonic deformations which may be associated, or not, with seismicity.

The Mediterranean region corresponds to a quite complex plate boundary between Eurasia and Africa. This domain is a wide mobile zone made up of different blocks trapped between two large relatively indeformable continental plates (Jacobshagen et

al, 1978). From 190 to 80 million years (Mys) the relative motion between Africa and Eurasia corresponds to a sinistral movement, (Tapponnier, 1977). This movement induced the opening of numerous oceanic or thinned continental crust basins in the Mediterranean area. At about 70 million years ago the relative displacement vector of the Eurasian and African plates changed, becoming roughly N-S to NNW-SSE remaining relatively unchanged until present time, fig.2.3a and fig 2.3b (Dercourt et al, 1986).

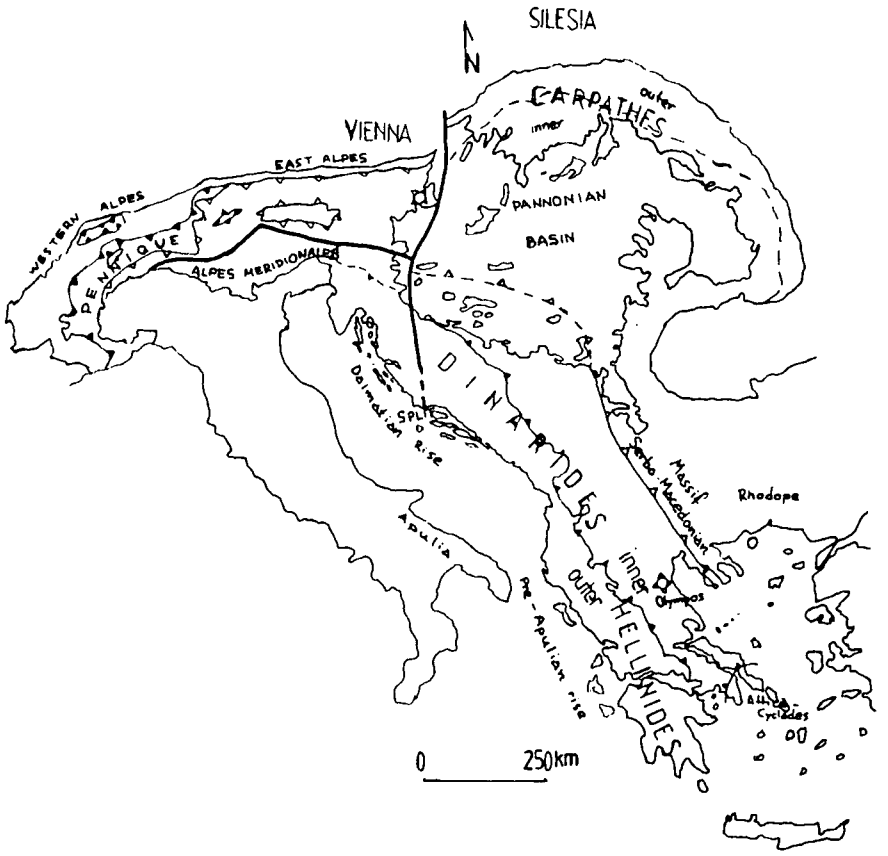

Fig. 2.2 Geotectonic plan of the alpine system by Chorowicz (1977).

One by one, from north to south, all the basins created during Mesozoic time were absorbed by subduction, collision or other mechanisms, depending on the different areas and epochs considered (fig. 2.4). The north-south convergence resulting from this last relative displacement has also led to the opening of new oceanic basins (Algero-Provencal, Alboran basin; Tyrrhenian Sea; Panonian basin etc). But each individual geodynamic stage was of short duration regardless of the block sizes that were affected (Philip, 1988) (fig. 2.5).

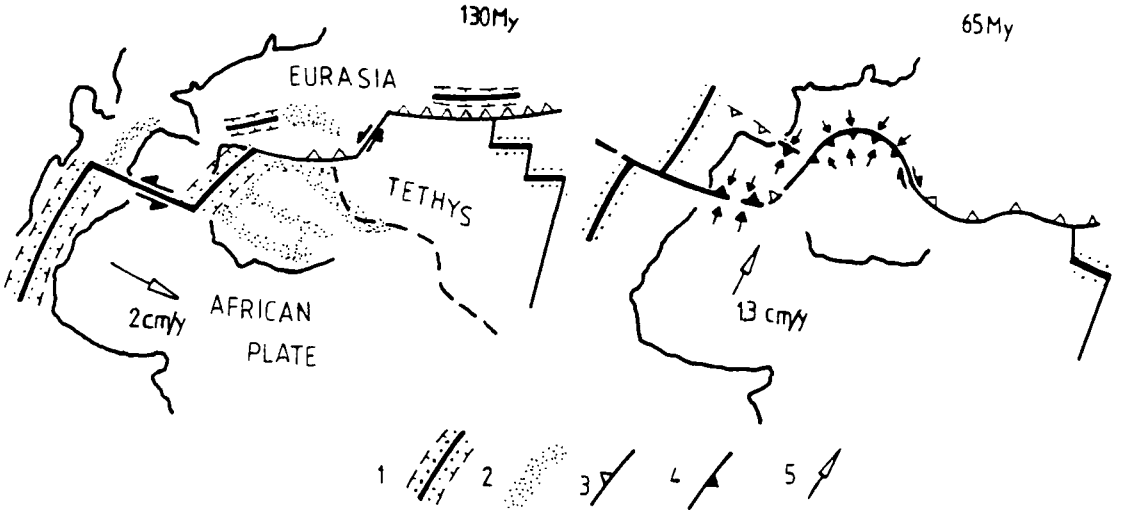

Fig. 2.3(a) Simplified plate scheme during the two main stages of Atlantic ocean opening (modified from Dercourt et al., 1986). 1: oceanic accretion, 2: thin continental crust, 3: oceanic subduction, 4: continental collision, 5: relative motion of Africa with respect to Eurasia

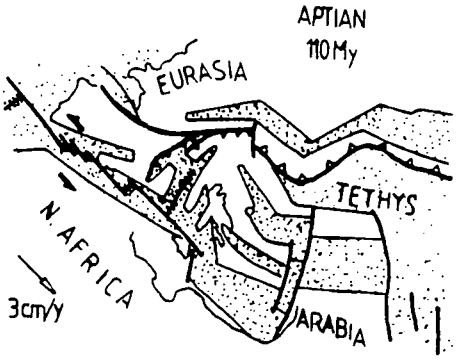

Fig. 2.3(b) Mediterranean region during Aptian time. Dotted pattern indicates oceanic and continental basins. Notation is as in fig. 2.3(a); (modified from Dercourt et al., 1986)

Various geodynamic contexts can be present during the same period. For example at the end of the Miocene (6 Mys) we can observe:

1. The Apennines and the Calabrian arc have been under subduction since Tortonian times (9 Mys);
2. Subduction in the Aegean arc has just begun;
3. Collision started in the Maghreb chain and the Betic Cordillera;
4. Collision existed in the Alps since Cretaceous times and is still active (130mys).

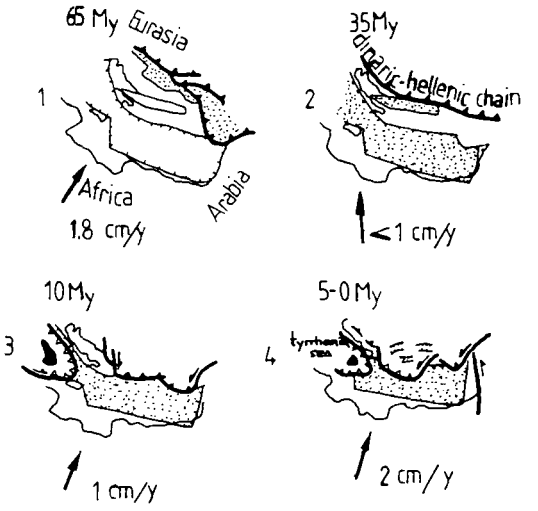

Fig.2.4 Southward progressive closure of the Mesozoic basins in the eastern Mediterranean region, from upper Cretaceous (1) to present time (4); (Philip, 1988).

2.3 The Hellenides mountain ranges

2.3.1 Geographical position

The Dinaric Alps continue through Yugoslavia into Albania and then into Greece (Hellas) to form the Hellenides mountain ranges. The predominant direction that these mountains (e.g. Pindos, Agrapha, Taygetos) bear is NNW-SSE, bending E-W in Crete, and through the Dodecanesa continue into Turkey where they meet with the Taurus mountain range changing direction to NE-SW.

Further, to the north east, the inner Hellenic mountain ranges of Voras, Vermion, Pieria, Olympos, Ossa and Pelion form a continuous chain of NNW-SSE direction which bends E-W into the Aegean Sea through to Northern Anatolia, Turkey. A similar curved configuration is followed by the north-east Mediterranean trench along the Ionian Sea and to the south of Crete.

Together with its corresponding shallow sea and volcanic belts, the entire system is known as the Hellenic Arc, a subduction zone between the African and the Eurasian tectonic plates.

2.3.2 Evolution of the Aegean Region

2.3.2.1 General

The Aegean Region includes the Hellenic arc and the Aegean Sea. Almost every year at least one earthquake with magnitude M>6.5 occurs in this relatively small but at present highly active region (fig.1.6; from Papazachos, 1988).

Tectonics related to oceanic subduction have been studied mostly from local earthquake mechanisms (McKenzie, 1972). Different conditions can exist above subduction and might be related to the characteristics of the subduction such as its velocity and dip (Nacamura & Vyeda, 1980; Megand & Philip, 1976). In the Aegean region, compressive tectonics are continuous in the external domain of the arc and are related to the existence of an accretionary prism, (fig. 2.5). In the back-arc regions, normal faulting characterises the preponderance of tensile stress regimes. The extension directions may be quite variable and microtectonic analysis of deformation reveals that horizontal stresses σ_2 and σ_3 are generally of similar magnitude, i.e. radial extension (Doutsos, 1980; Doutsos & Ferentinos, 1984).

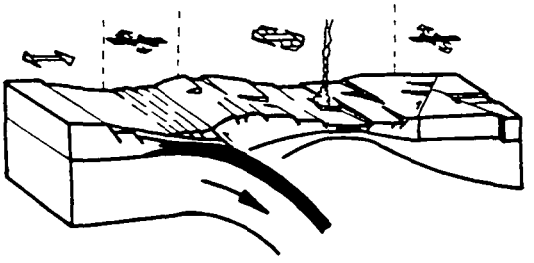

Fig. 2.5 Oceanic subduction: distribution of the deformation types according to Aegean example (Papazachos, 1988).

2.3.2.2 Seismicity and regional dynamics

One of the main contributions of Seismology to the new global tectonics is the determination of boundaries of lithospheric plates by determining the seismic zones which define these boundaries. Good knowledge of the spatial distribution of the seismic activity requires homogeneous and complete data in respect to the magnitude

of the socks and of acceptable accuracy in respect to their location as expressed by focal depth and epicentre.

Figure 2.6 shows epicentre maps of shallow (h≤60km) earthquakes which occurred in the Aegean Region (Papazachos, 1973; Komninakis & Papazachos, 1978). It is seen that there is not one or two lithospheric plates but several aseismic blocks surrounded by active zones, the most noticeable of which lies in the Aegean region. Figure 2.6 shows the epicentre map of the Aegean region for all known shallow shocks with magnitude M>6.0. The differing notation reflects the different source of reference and magnitude. So, open circles represent epicentres of shocks during historical times from 600BC to 1900AD, described to us by means of reporting secondary phenomena to the shock. Black circles denote epicentres of shocks recorded by instrumented stations from 1901 to 1986 A.D. The varying diameters of these circles correspond to levels of magnitude. It is evident from fig. 2.6, that the external seismic zones form a continuous large belt along the convex aspect of the Hellenic arc. All the other zones constitute the internal seismic zones which have a general E-W direction more pronounced in the eastern parts of the region.

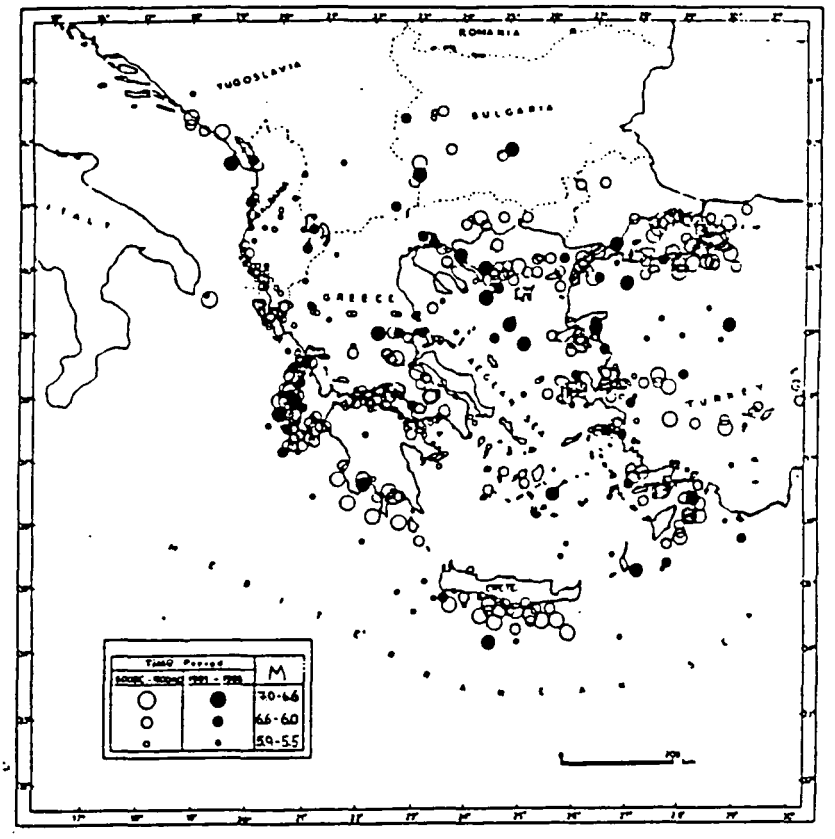

Fig. 2.6 Epicentres of historical and present time earthquakes in the Aegean area.

Therefore, the available data indicate that the directions of recent and present seismic fracture zones show little correlation with the alpine induced geotectonic zoning. Hatzidimitriou et al (1985), however, observed a systematic decrease of the parameter b in the frequency-magnitude Gütenberg-Richter (1954) relationship,

$$logNs = a\text{-}b*M$$

for shallow earthquakes in Hellas, from the outer towards the inner geotectonic zones, where the *Ns* is the frequency of shocks in a given volume area, M is the magnitude, *a* is the intercept depending on the amount of seismicity and *b* depends on mechanical properties of the given volume area. The whole region was divided into three zones A, B and C where the Gütenberg-Richter parameter b, averages 1.03, 0.84 and 0.6 respectively. In region A, for instance, the material must have a higher degree of heterogeneity than in regions B and C. This is in agreement with the fact that region A has experienced stronger tectonisation in recent geological times. It is, therefore, clear that the seismicity deduced zones A,B and C correspond in an almost identical way to the outer Hellenides, the inner Hellenides and the Hellenic hinterland respectively. Similar correlations have been suggested by Westaway (1992) for Britain and SSW Turkey.

Komninakis & Papazachos (1980) and Panagiotopoulos et al (1984) studied the intermediate local depth earthquakes that occurred between 1964-1984 A.D. with reference to their spatial distribution. The most extensive deep seismic activity is associated with the southern and south western part of the Hellenic arc. A systematic increase in focal depths from the outer towards the inner parts of the arc was identified, thus defining the Benioff zone for the Aegean region. The Benioff zone dips slightly more steeply (37º) at the eastern and western sections than at the central section (32º) of the arc.

Fault plane solutions for almost all major earthquakes (M>6) have been examined and presented by Papazachos & Kiratzi (1984-1986b). The interpretation of the plane solutions is summarised in fig. 2.7, where the region's main features of active tectonics are reproduced after Papazachos & Kiratzi, 1986a.

The fault plane solutions presented above, show that thrust faulting is dominant along the convex aspect of the arc, except for the North Western part where strike-slip faulting with a thrust component is observed. The latter has been considered to

be a dextral transform fault, in agreement with known relative motions between the Aegean arc and the Appoulian platform to the west of the Ionian Sea (Scordilis et al, 1985). Normal faulting is mainly observed in the inner part of the Aegean region. Consequent geomorphologic features such as the Patras and Corinthos gulfs, the Plataees basin, the Amvrakikos gulf, the Trichonis basin, run approximately E-W. That seems in agreement with the Pliocene till present tensional field that follows an almost N-S trend. However, close to the boundary with the outer thrust zone, The tensional field seems to become parallel to the compressional field, inducing a NNW-SSE oriented geomorphological environment clearly seen in areas such as the Amalias-Olympia basin and the Preveza coastal sub-basins on the west coast of Ipeiros (NW Hellas).

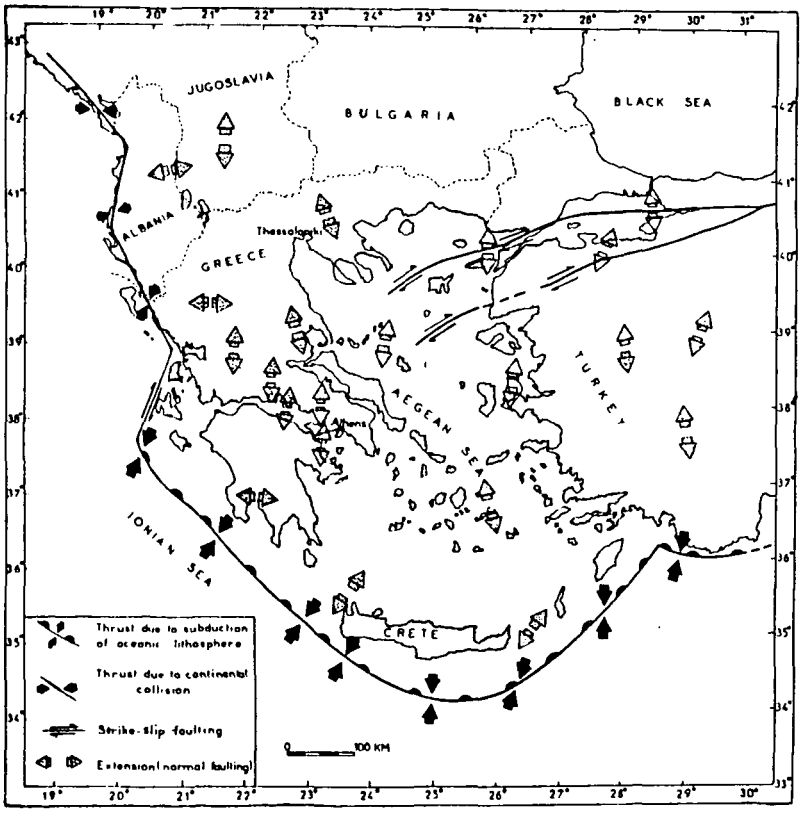

Fig. 2.7 The main features of active tectonics in the Aegean and the surrounding area (Papazachos et al, 1986a).

2.4 On the Geotectonical Zoning of the Hellenides

The situation of the Hellenides is a direct consequence of the geotectonic evolution of the Hellenic Arc. This evolution advanced from approximately East to West, affecting different palaeogeographical entities at each time, resulting in areas of distinctive character both in a stratigraphic and geotectonic sense. The various

proposals on the division of the Hellenic domain into zones were based, up until the middle 1970s, on a hypothetical alpine palaeogeographical model, developed by Aubouin (1965). In that model, the concept of a binary system of troughs and ridges was introduced. The alternating nature of that binary system was attributed to Hercynian folds of the Permo-Carboniferous. During the depositional phase of the geosyncline's development isostatic movements led to temporary surfacing of parts of the sea floor. The local manner of such exposures was held responsible for phenomena occurring perpendicular to the main orogenetic axis, such as gravity controlled normal faulting, erosional surfaces, unconformities etc, as well as providing the necessary conditions for the formation of lateritic mineral ore deposits.

With the development of plate (or global) tectonics and the subsequent proposition of new models of the geodynamic evolution of the alpine system, the question of zones was seen from a different angle. Today, the distinction between zones is based on their individual role played inside a system of dynamic evolution. That role is partially translated into a palaeogeographic position. Hence, each geotectonic zone consists of a specific stratigraphic succession with its own characteristic lithological types and tectonic behaviour.

The zoning of the Hellenides is the result of work by many researchers since the end of the last century. As Moundrakis (1985) notes, most recent geologists accept the term zone in the new context of global tectonics for Hellas. The term zone will be used in its conventional form as *an area or region more or less set off or characterised as distinct from surrounding parts,* (A.G.I., 1976).

It is generally accepted that nine (9) isopique alpine zones compose the geological structure of Hellas. They are roughly grouped as inner and outer geotectonic zones being on the east or west margins respectively of the Hellenic arc. The zones from east to west as shown in fig. 2.8 are shown in table 2.1.

2.5 Hellenic Post Alpine formations

2.5.1 General

After the paroxysmic phase of the alpine orogene, a series of formations were deposited in newly formed basins. These deposits have been affected principally by fault tectonics: horsts and grabens between normal and dextral faults. Two major

categories of post alpine deposits are associated with the Hellenic arc: 1) the molassic sediments of Eocene-Middle Miocene and ii) the Neogene and Quaternary deposits. The distinction between the two categories is related not only to age but also to genetic relations with the pre-existing adjacent alpine zones.

2.5.2 The molassic sediments

The molassic sediments were deposited in sizeable basins under continental, freshwater and occasionally saline environments. The basins, which were formed during the paroxysmic phase of the orogenetic movements, were filled soon after the main "folding front" migrated further to the west. (fig.2.9). The sediments associated with these basins formed long and thick sequences of varying lithological types; the latter is closely linked to the adjacent source-alpine zones and it is controlled by concurring tectonic events.

A classic example is the molassic sequence of the Mesohellenic basin deposited between Oligocene and Miocence, between the Pindos and Pelagonian geotectonic zones. It stretches 130km SE-NW from West Macedonia to Thessalia with an average width of 40km. The deposits may vary significantly in terms of energy and geochemistry (Soliman & Zygoyannis, 1980).

Table 2.1

Hellenic geotectonic zones (from E to W)

Hellenic Hinterland	Rodopi massif (**Rh**) Serbo-Macedonian massif (or zone) (**Sm**) Peri-Rodopi zone (**CR**)
Inner Hellenides	Paeonia zone (**Pe**)# These three are better Paikon zone (**Pa**)# known collectively as Almopia zone (**Al**)# the Axios Zone Pelagonian zone (**Pl**) Attica-Cyclades zone (**AC**) Sub-Pelagonian zone (**Ps**)
Outer Hellenides	Parnasos-Giona zone (**Pk**) Olonos-Pindos zone (**P**) Gavrovon-Tripolis zone(**G**) Ionian zone(**I**) Paxoi or Pre-Apulian zone(**Px**)

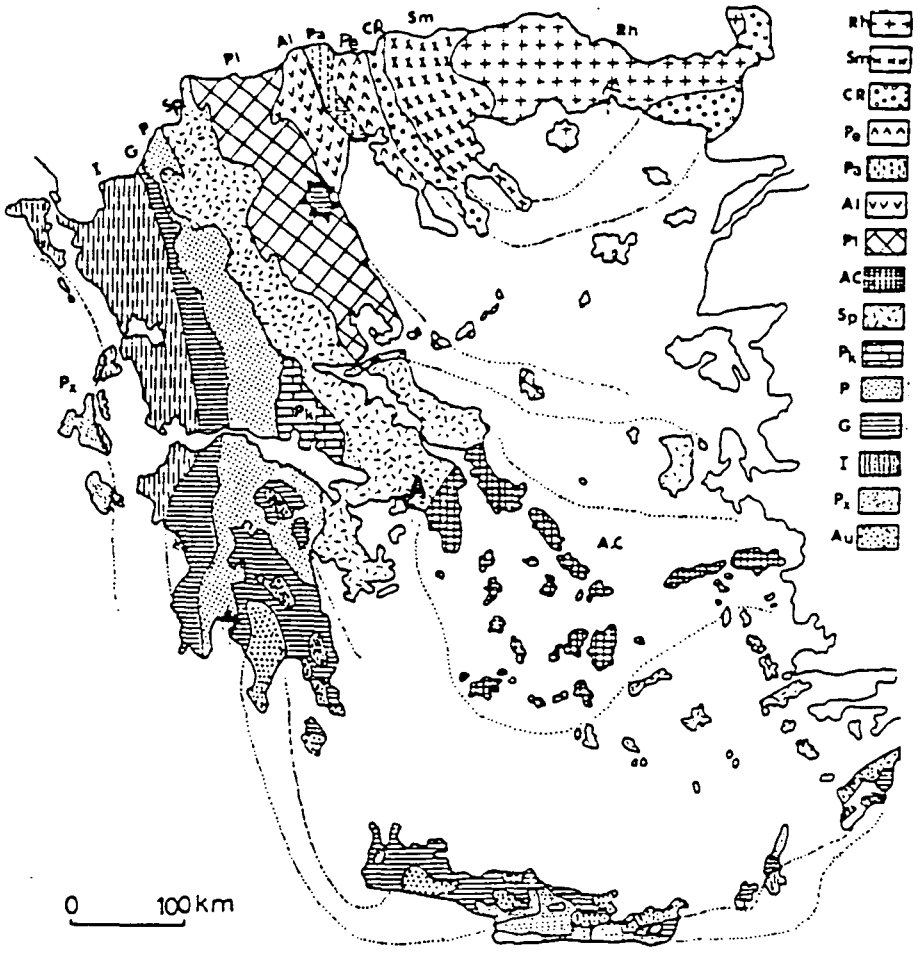

Fig 2.8. Geotectonic map of Hellas; key to legend in Table 2.1.

2.5.3 Neogene and Quaternary deposits

Neogene deposition has taken place and Quaternary deposition still takes place in trenches or other non-tectonism related basins which were developed further behind the folding-front, and certainly behind active molassic basins. Both Neogene and Quaternary deposits have not been affected by any alpine-type deformation. The direction and size of such basins is variable.

A significant episode which characterises most of the Neogene sequences is the Messinian salinity crisis, caused by the cutting off of the Mediterranean from both the Atlantic and Indian oceans. This event resulted in increased salinity and a significant deposition of evaporites in many marine basins during the Upper

Miocene (west coast of Ipeiros, N.W. Hellas), reaching thicknesses of up to 300m. Diapyric movements of those evaporites inflicted further faulting and deformation to overlying beds. Such movements are known to still progress.

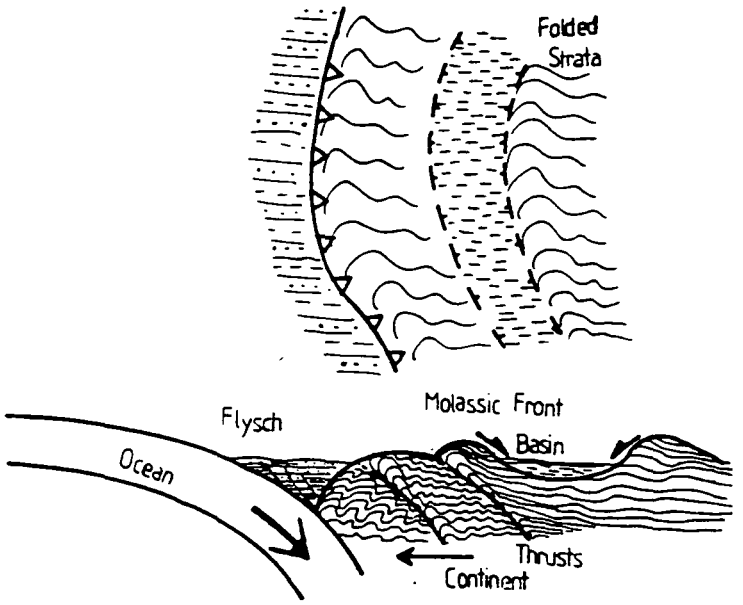

Fig.2.9. Simplified depiction of molassic tectonics in an advancing orogenetic front (adopted from Moundrakis, 1985)

Many of these basins follow the general NNW-SSE axis imposed by the alpine orogenetic movements; such as the Strymon and Axios valleys. The Florina and Ptolemais basin, the Pyrgos-Amalias-Kylini basin (N.W. Peloponnesos), the N.E Peloponnesos basin stretching between Argos, Corinthos and Xylocastron, the Preveza-Souli etc (fig.1.10). However, there are basins extending NE-SW and even E-W; such as the Corinthos and Patra gulfs, the vale of Spercheios, the Thessalia plain etc. The departure of those basins from the typical NNW-SSE alpine direction is due to complicated neotectonic local regimes.

The depositional environments, to which these basins were or still are subjected, are variable and indeed changing. It is not uncommon to encounter marine and fluvial facies next to each other, often without transitional beds or a hiatus or unconformity, as might be expected. In the majority of cases, the associated deposits tend to change laterally and vertically over relatively short distances. Significant deposits of lignite and other organic materials were deposited around the margins of such basins, e.g. Ptolemais, Aliverion, Megalopolis etc.

Fig.2.10. The main Neogene-Quaternary basins in Hellas

A common characteristic of these successions is the presence of base conglomerates. The majority of the fine grained facies is frequently intercalated with coarser members. The degree of lithification varies with stratigraphic age and burial depth. The fine sediments are in their majority thin to medium bedded and many would have been classified as silty to silty sandy clays and clayey silts of variable colours, mainly green, blue, white-yellow and shades of these colours. Quite often the deposition of fine grained sediments was accompanied by the precipitation of carbonates and thus such sedimentary successions were named marls.

Marls have been subjected to tensional normal faulting of appreciable displacement. It was estimated that approximately 1500 m of uplift is a reasonable average which may however vary significantly from one basin to another. Seismic loading frequently activates slopes the hangingwall of which is formed by such sediments along normal faults. The overburden relief together with the tensional tectonics are the dominant feature leading to further degradation of these sediments which is frequently expressed as randomly oriented tension cracks. Further loosening of these sediments may occur due to seasonal variations in their degree of saturation with the opening up of desiccation cracks as the material between the cracks contracts and stiffens up. However, weathering profiles are quite often incomplete due to the continuous denudation of the loosened materials downslope.

CHAPTER 3
FIELDWORK

3.1 General Information

Fieldwork preparation began at Durham University in early November 1988 with the preparation of letters of intent to the Institute of Geology and Mineral Exploration (I.G.M.E), the Geology Dept at Patras University (G.D.P.U) and the Central Public Works Laboratory (C.P.W.L), Athens, asking for any assistance they could provide. The Geology Dept (Patras) provided letters of authorisation essential for the acquisition of topographic maps from the Geography Service of the Hellenic Armed Forces (G.S.H.A.F). The author arranged to meet Ass. Prof. G.Koukis of G.D.P.U at his arrival in Athens at the end of January 1989 and further meetings were arranged with Dr. G.Tsiambaos (C.P.W.L) and Dr. D.Rozos (I.G.M.E) in early February.

During these meetings the feasibility of various fieldwork plans and laboratory back up were examined. The original proposal was to concentrate on sequential sampling with depth for the examination of weathering induced effects on the shear strength of Hellenic marls with special reference to calcium carbonate depletion. The original proposal could not be supported because of a lack in available core samples and because intense drought rendered hand sampling of intact samples quite problematic (table 3.1). The aquisition of large volume disturbed samples and intact ones wherever possible remained the only solution. As a result, the entire research proposal had to be reappraised to suit the local conditions. It seemed reasonable at that time that a switch to testing reconstituted samples was the only solution to keep the reseach programme alive.

Further, a number of sites were reviewed as possible candidates. The critiria for choosing the sites were:

i) independent geological evolution from each other;
ii) the diversity of fine grained facies;
iii) the presence or the probability of geotechical problems;
iv) reasonable amount of geological background information;
v) reasonable access roads

Table 3.1

National Meteorogical Service *

rainfall values in mm

Area	December mean value	December 1989	January mean value	January 1989
Athens	61.2	18.3	49.0	3.0
Thessaloniki	54.5	49.0	38.2	2.0
Alexandropoli	85.2	72.7	69.5	0.0
Corfu	188.9	180.2	154.4	1.2
Rhodos	165.6	108.0	162.1	70.4
Naxos	71.2	60.1	72.9	1.0
Irakleion	81.5	43.0	97.4	32.0

*from Mesimvrini Daily , 20th February 1989.

The sites that fit the above criteria were the wider area to the west and south west of Korinthos and part of the coastal section between Preveza and Igoumenitsa. A third site was considered as control site. After consultation with Dr. E.Kamberis (Public Petroleum Corporation, Athens) the third site was decided to be the wider area to the west of Amalias. The sites are shown in fig. 3.1.

3.2 Sampling Techniques

Owing to the arid conditions that dominated the entire period of the fieldwork and the nature of most sampled natural slopes the excavation of trial pits was necessary. The depth of every pit varied with the amount of soil that had to be removed before reasonably unweathered material was exposed. The minimum depth was approximately 0.3 m in freshly cut slopes and reached a maximum of 2.5 m in a more weathered slope. The description and categorisation of geological bodies with regard to weathering was based on published work by Chandler (1969, 1970, 1972, 1974). All trial pits were dug by hand and samples were taken from the bottom or from various depths depending on the existence of distinguishable weathering levels.

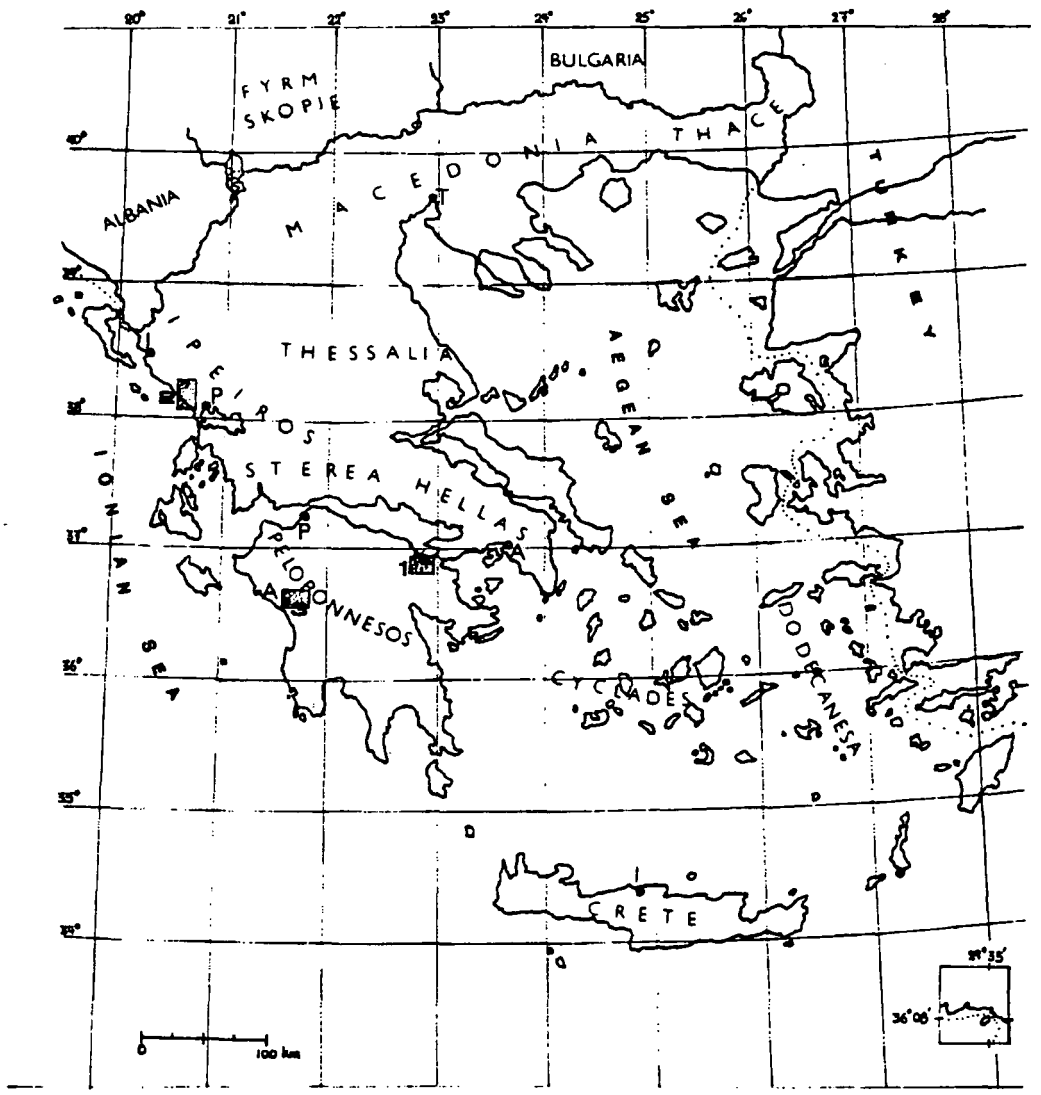

Fig. 3.1 The position of the sampling sites in Hellas
1: Korinthos, 2: Preveza - Igoumenitsa, 3: Amalias - Goumeron

The undisturbed samples were obtained by means of forming a cavity around and behind the sampled mass and carefully removing it from its bed by undercutting. Dimensions varied but on average they were 0.3x0.3x0.3 m. The undisturbed samples were then immediately wrapped in aluminium foil and covered in wax to prevent losses of moisture. The orientation (i.e upper and lower surfaces) of the samples were noted on the samples' surfaces with a marker pen. Further wrapping and waxing was applied once away from the actual site. The disturbed samples were placed in thick plastic bags and were carefully sealed with tape to minimise moisture losses. Prior to any sampling the area was surveyed using the available topographic and geological maps. Where the map's resolution was not high enough extra

geological mapping was conducted in order to confirm the stratigraphy of the sampled horizon.

3.3 Korinthos Sampling Area

3.3.1 General Structure and Seismicity

The Korinthos basin is one sub-basin of the gulf of Korinthos basin system which trends ESE-WNW. The area is seismically active, undergoing normal faulting due to a N-S extension (Jackson et al, 1982 a,b). Rifting was initiated in the late Miocene or early Pliocene, superimposing approximately E-W striking normal faults on the Hillsides mountain belt (Doutsos et al, 1987).

Various studies lead to the conclusion that since the Pliocene a total overburden relief of 3.5 km in thickness can be estimated (Brooks & Ferentinos, 1984; Heezen et al, 1966). Relative vertical motion of 1mm per year was estimated (Tselentis & Makropoulos, 1986) based on slip movements along seismogenic faults. Keraudren & Sorel (1987), based on uplifted marine terraces, point at a displacement rate of 1.5 mm/year for the last 500,000 years and Collier (1990) suggests that the area is undergoing an uplift phase, since marine deposits are found more than 100 m above the maximum Quaternary sea level. However, Vita-Finzi & King (1985) had considered these morphological features as fault controlled continental surfaces.

The fault induced geometry, syn-depositional deformation and intrabasin growth faulting define periods of increased intensity of tectonism (Leeder & Gawthorpe, 1987). The recent (Pleistocene to Holocene) evolution of the area is directly related to strong and frequent earthquakes. Seismic risk for shallow shocks, expressed as the return period for a surface of one square degree is shown below (Galanopoulos, 1968).

Table 3.2

Magnitude (R)	Return Period (years)
over 7	135-170
over 6.5	55-70
over 6	23-28
over 5.5	9-12

3.3.2 Korinthos Sampling Area Boundaries

The area of sampling is confined by the Korinthos-Patras national road to the north; the Arvanitis, Prophetis Helias and Tsoumba hills to the south; the Platani stream and Solomos village to the east; the Tsakiri, Pournari and Roumania hills to the west.

The area lies between the following coordinates: 22 degrees 54' E, 22 degrees 45' 30" W, 37 degrees 55' N, 37 degrees 50' S, of the national geographic grid and it is covered in the Korinthos sheet of the Geological Map of Greece, published by the Institute of Geology and Mineral Exploration (formerly Institute for Geology and Subsurface Research), 70 Mesogeion Ave, Athens, Hellas, in 1971. Part of this map with a 1:5000 detail of the Solomos junction with the sampling positions marked is in Appendix D.

3.3.3 The Lithology of Korinthos Sampling Area

The area is characterised by the middle to upper Jurassic limestone masses of Akrokorinthos (574m) and Prophetes Helias (701m) that mark a transition zone between the Pindos and Sub-Pelagonian zones (Bornovas et al, 1971) and a complex system of post alpine lacustrine, lagoonal and fluvial deposits. This system is generally dipping WNW and is interrupted by N-S direction valleys, mainly those of the Potamia stream to the east and Rachiani stream to the west.

The post alpine system consists of i) Tyrrhenian marine and near shore deposits, mainly conglomerates, marls, sands etc which form characteristic benches and terraces. They overly unconformably Pliocene deposits. ii) Pliocene deposits, mainly marls, marly clays with intercalations of sandstones, psephitic conglomerates and marly limestones. They are brackish to lacustrine deposits with the latter dominating the upper members of the sequence. Lignite beds were found among the lacustrine strata by the villages of Penteskoufi and Solomos. The beds dip gently 10º-15º WNW with a main NE strike. Underlying, there are basic conglomerates and psephites which dip with larger angles, typically 30 degrees NW, indicating an angular unconformity. They are generally coarse, cohesive beds with plenty of marly cement (Bornovas et al 1971).

3.3.4 Sampling Sites.

3.3.4.1 General

Sampling took place between March and June 1989. Samples were obtained along the new Korinthos - Tripolis road axis and along local roads. During this period the road axis was still under construction in various places providing access to freshly cut slopes.

3.3.4.2 Solomos Junction.

a) Site Location.

The Solomos Junction site was the main sampling site with an overall total of 19 samples from two sub-sites. The first is located 6+0.000 km to 6+0.400 km south as per the new route plan (or 6+0.800 km to 7+0.200 km on the old route plan at the junction to Argos from the Korinthos Patras national road). The second site can be identified as 8+0.200km to 8+0.400 km on the new route plan further towards Tripolis and near the hamlet of Mpekianika. The distinction between the two sub-sites is made by attaching the letters A and T to their serial code to devote the site subcontractors A.T.E.M.K.E A.E and T.E.Γ.K. A.E. respectively.

b) Description of Site.

The first site (subcontractor A.T.E.M.K.E A.E), when first visited on 1st March 1989, comprised a road cutting 6m high and 2:3 steep on the uphill side and a heap of excavated material on the downhill side. The length of the cutting was 300 m. On completion of the works the junction comprised a 400m long, 12m high and 2:3 steep cutting at positions 6+0.000km to 6+0.400km (new route plan) and an adjacent embankment (4m high at maximum) constructed from recompacted excavation material from the cutting leading to the junction duct.

Samples SLM1A to 8A were obtained progressively from the top to the foot of the excavated slope at position 6+0.220km. The sampled material ranged from a light grey yellow to yellow brown hard sandy clayey silt (SLM1A), grey brown hard clayey silt (SLM2A & 3A), whitish yellow stiff silty clay with carbonate concretions (SLM4A), light grey green fissured hard silty clay with carbonate concretions (SLM6A), grey brown green fissured hard clayey silt with lenses of fine to medium sand (SLM7A & 8A). Intact samples SLMA (1 & 2) were obtained from the same light grey green material as SLM6A and grey brown green material as SLM7A, respectively. Intact sample SLMBi was obtained at position 6+0.250km from a lithified cracked yellow brown hard clayey silt. At position 6+300 intact samples

SLMB1 & B2 were obtained from stiff light green grey silt clay and from green firm to stiff silty clay respectively. Samples SLMG4 and SLMD2 were obtained from the foot and the crest of a landslide at position 6+270km from stiff grey blue clay and red brown firm silty clay respectively. All samples were from the surface of freshly cut slopes.

At 200m to the south of the junction duct there are two more slopes with thinly bedded lithified grey brown (SLM1B & 2B) to yellow brown (SLM3B &4B) hard clayey silts with carbonate concretions and magnesium dendrites intercalated with medium to coarse grained sandstone, the uphill side 3:1 15m high and the downhill side 3:1 5m high running 150m long.

The relief is moderately undulated at both sides of the road axis with small depressions marking runoff drainage lines which lead to the cuting. Olive tree growths characterise the flora on both sides. A simple geological map was constructed on a 1:5,000 scale topographic map which shows the main features of the sub-site and records the positions of the obtained samples (Appendix D).

The 2nd site (subcontractor Τ.Ε.Γ.Κ A.E) sampled on 8th May 1989 comprises 2 adjacent cuttings (bearing 7ºNE from Akrokinthos hillrock), separated by a culvert embankment, 3:1 steep and approximately 5m high, from the position 8.000 + 0.200km (new route plan). At distances 0.035km and 0.060km along the cutting, two samples were obtained (SLM1T & 2T) from 0.5m into a light grey brown friable hard clayey silt, each from the middle of the slope. At a further distance of 0.095km and 0.170km three samples (SLM3T to 5T) were obtained from a depth 0.5m at the middle, the top and the foot of the respective part of the cutting.

c) Problems

In both sites stability problems occured in varying degrees. The greatest and more obvious ones occured on the main slope of the Solomos Junction at positions 6.000 + 0.270 km and 6.000 + 0.320km on the new route. It should be noted that the problems occured after 8 hours of heavy rain on an area that had seen no rain for roughly one month.

The sliding at location 6+0.270km (photograph 3.1) had a crest of 20m and height at maximum of 8m. It was a complicated movement partly planar along the crest and the NE flank and rotational on the rest of the surfaces. The planar failure occured on a preprepared surface consisting of 3-4 cm of very plastic blue grey clay over a

red brown - grey brown argillaceous mudstone. The sliding at location 6+0.320km had a crest of 10m, depth of 7m and height of 7m and could be described as rotational failure in poorly cemented recent fluvial channel deposits over stiff well cemented marl.

Photograph 3.1 Complex slide in Solomos junction

3.3.4.3 Arvanitis.

a) Position and Description

At the foot of Arvanitis hill and at the position marked by 250 degrees WSW from Arvanitis, 70 degrees NE from Prophetes Helias and 90 degrees from Ayios Ioannis chapel, five disturbed samples where taken from the base of road cuttings along the Korinthos - Tripolis new road axis. The road cuts the slope in a uphill and downhill face respectively from the downhill face, two brown, with red and green mottles, stiff to hard argillacous marl samples were obtained at a distance of 50m from each other. These are called ARV1 and ARV2. With an intermission of grey to green grey sandstone of varying bedding thickness and grain size and a further 80m from ARV2 an additional two samples of stiff grey brown argillaceous marl with green to grey green mottles were obtained 50m from each other. They are named ARV3 and ARV4. Finally ARV5 was obtained 50m further from ARV4 in the direction of

Korinthos representing a transitional facies between the marly and sandstone members in the area.

b) Problems

On the uphill face of the slope multiple tension cracks were observed, especially close to the crest of the cutting at varying heights between 10m - 20m. The same can be reported for the downhill face of the cutting for heights varying between 2m - 10m. The frequent and rapid change of lithological types along the two faces acts unfavourably, adding to problems induced by a dense system of Neogene fractures with vertical displacement varying from 0.5 to 18m. The coarser facies tend to dominate the upper parts of the slope. The facies that could in broad terms be grouped as fine-grained, are characterised by a rapid lateral and vertical change of lithology and appear in a loosened state due to many small dessication cracks randomly orientated. This geometry encourages slump failures which develop into debris slides further down slope owing to the intense cracking induced by drought conditions (photograph 3.2).

Photograph 3.2 Slope failure at position ARV3

3.3.4.4 Penteskoufi

At a distance of 70m to the north from the church of the Penteskoufi hamlet, an intact sample (PSF1a) was obtained by hand from a depth of 1 m in a small hand-dug trench. The material was a yellowish light grey marl, very stiff and difficult to seperate even along fissure planes. It is overlain by the Tyrrhenian ingression

formations. Though eroded at the surface it would still be classed as Zone IIb according to Chandler (1972).

3.3.4.5 Tsakiri - Rentaiika

Tsakiri lies 1km to the south of the Korinthos - Patras national road and along the Assos - Veliniatika road. Along the same road Rentaiika hamlet is situated approximately 2km further to the south from Tsakiri.

photograph 3.3 Trial pit at position RTK1. Light greyish marl with varying degrees of degradation with depth Note the extent of desiccation cracks.

Underlying the Tyrrhenian ingression formations and at a stratigraphic depth of 20m below the unconformity level, Neogene deposits consist mainly of fine grained light blue grey marls and yellowish light grey silty marls with thin bands of fine sand. Oxidation occurs along discontinuities with erosion intensifying upwards, as was

observed inside a hand dug trial pit at a depth of 1.5m. The material becomes disintegrated in the top 0.35-0.40m with very little matrix or lithorelicts (Chandler, 1969) (photograph 3.3). Relics of fossilised leaves can be observed.

The slopes are natural ones forming part of the right hand side flank of the valley of the Rachiani stream and it is covered with oregano shrubs and olive trees. At its top the Tyrrhenian terraces consist of conglomerate benches which topple along the rim of the terraces due to lack of support from eroded or even denuded Neogene materials which lie underneath. The loosening up of surface cracks in the Neogene materials is exacerbated by the well defined wetting and drying cycles of weather in the area of Korinthos. This leads to cracks being filled with rain water resulting in small scale mud flows during winter months. The relief is moderately undulaling with slope angles not exceeding 35 degrees. Indications of old landslides exist further upstream though the present mode is probably one of progressive slips. Two samples were obtained, one from each site, named TKR1 (light blue grey marly stiff silty clay) and RTK1 (yellowish light grey hard calcareous silty clay) respectively, at a distance of 2.5 km from each other.

3.3.4.6 Roumania

Along the same flank of the Rachiani stream the site of Roumania lies to the NNW of the Spathovounion hamlet at a distance of 1.5km. The slope forms the south facing bank of one of the tributary streams and consists of argillaceous marls intercalated with sandstones and lignite lenses of maximum thickness approximately 60cm. Two samples were obtained. ER1 was sampled at the foot of the slope whilst ER2 was obtained from a bed of intercalated marl within the sandstone group. The latter contained thin laminae of silty material mixed with pebbles up to 1.8cm maximum size and lies 100m higher that ER1 in stratigraphic terms. Both samples were disturbed and exhibited extensive discolouration with depth, a sign of propagating chemical weathering associated with progressive mineral alterations .

3.4 Preveza - Igoumenitsa road axis Sampling Area.

3.4.1 Geographical Boundaries

The sampling area is part of the coastal section of NW Hellas. It is covered in the Kanalakion Sheet of the Geological Map of Greece, published in 1967 by the Institute for Geological and Subsurface Research. The studied section of the road

axis starts at the village of Loutsa to the North (position 16 + 0.000km on the new route plan) and finishes at the junction to Nikopolis (position 42 + 0.500 km on the new route plan).

The area was studied using 1:5000 maps but is presented here in a part of the IGSR Kanalakion Sheet with the positions of the obtained samples marked (Appendix D).

3.4.2 Structural Evolution of the Area

Ionian zone carbonate and evaporitic sedimentation prevailed until the late Iocene and was superseded by a thick clartic sequence of Oligocene to Early Miocene age (flysch). The latter was laid down in a foreland basin, which heralded the advance of the westward migrating Hellerides thrust front. At the end of the Early Miocene, turbidite deposition was disrupted by a phase of contractional deformation, which lifted the area above depositional base level. Middle Miocene to Pliocene sediments would therefore unconformably overlie the foreland basin deposits and have themselves undergone contractional deformation (Clews, 1989). These two phases of deformation may be related to the two periods of clockwise rotation of mid-Miocene and Plio-Quaternary age (Kissel & Laj, 1988).

A number of locally deformed, fault bounded, late Neogene and Quaternary basin have been recognised: a) a thrust dissected Mio-Pliocene basin centered on Lefkas, Paleros, Mitikas and Kalamos (Clews, 1989), b) east-west trending Plio-Quaternary extensional basins, e.g the gulf of Preveza, and c) NNW - SSE trending basins e.g. the blue marls of *Vindobonien* (Miocene), north of Zaloggos.

Doutsos *et al* (1987) demonstrated that a Miocene to Quaternary WSW-ENE shortening controlled the development and eventual break up of the main Miocene basin. Subsequent structural complexity was probably caused by thrust events which were "out of sequence" in the general foreland - propagating model or by neotectonic reactivation (Underhill, 1989), by virtue of the area's vicinity to areas of outer-arc compression (King *et al*, 1983).

In the studied area the basins are divided into a Miocene to Pliocene series to the west and a mid to late Pliocene to the east. Sedimentological distribution suggest that the Miocene to Pliocene sediments of the western region (sampling area) represent deposition in one large basin with early detritus derived from within the Ionian zone. Sedimentary patterns resulted from the depositional filling of an undulating

topography controlled mainly by pre-existing and reactivated thrust faults (Underhill, 1989).

Evidence for reactivation of both the Ionian thrust and imbricates within the Ionian thrust sheet exist offshore in the Zakynthos channel. Geophysical records across the wider area show the presence of diapyrs of mobilized Triassic evaporites rising along steep reactivated West Hellenides thrust faults (Monopolis & Bruneton, 1982; Brooks and Ferentinos, 1984). In effect that would lead to a dismemberment of Plio-Quaternary sequences into a series of sub-basins in the area between the Ionian Islands and the mainland (Brooks and Ferentinos, 1984; Meulenkamp, 1986).

3.4.3 Lithology of Sampling Area.

The area is dominated by post alpine deposits. The only alpine bedrock exposures occured in the proximity of the village of Loutsa. These are lower to mid Lias limestones of the Pantokrator sequence. Intercalated dolomites and dolomite conglomerates are also to be found to the west of Loutsa.

Along the major anticline of Riza (NNW-SSE) an extensive outcrop of upper Miocene series blue marls is interupted by Triassic evaporitic intrusions which daylight along the foot of the coastal scarp. The series of blue marls in its upper members show transitions from marine type deposition to shallow sea and transgressional facies of base conglomerates with calcitic sandstones of medium to coarse grain size. The thickness of this sequence is not know but it is estimated at approximately 800m.

A number of boreholes, sunk to varying depths, cored Neogene and Quaternary deposits with thicknesses from 422m to 2100m in the vicinity of the village of Archangelos (Bison et al, 1967), confirming significant displacements along the northern flanks of the Preveza Gulf basin.

The Plioene is represented by the sequence of the Archangelos formation. The formation consists of mixed successions of marine and terraneous facies mainly marine clays and marly clays and clayey sands, sandstones and conglomerates respectively. The conglomerates appear to dominate the areas around the villages of Riza, Myrsini and Kastrosykia. They are well graded (Kolovos, G; 1989 private communication) and well cemented in places. Most of the conglomerate beds lie intercalated with clayey sands and fine to medium grained sandstones, and also with

clays and marly clay beds. In the latter case the conglomerates appear less well cemented and often loosened by tension cracks.

3.4.4 Geomorphology of sampling area.

The area is a hilly to almost mountainous zone running roughly parallel to the coastline extending 1km inland. The relief rises from sea level to 300-400m elevation within the area, forming in some places, where significant conglomerate exposures are found, steep scarps. This is partly due to the durability of locally occuring conglomerate beds but most importantly it is due to major fault lines running parallel to the coastline. The area evolves continuously with significant seismic activity recorded (Papazachos 1988; Mountrakis, 1985). This is followed by processes of weathering and erosion that eventually form the present morphology. The major faults are almost vertical trending NNW-SSE parallel to the Riza anticline axis. There is a minor NE-SW trend, too, which combines with the major trend to provide a drainage pattern characterised by seasonally flowing streams along the NE-SW axis whilst larger streams follow the major NNW-SSE axis, bending finally towards a E-W direction into the sea. The former, transversal, streams create deep ravines with steep slopes as a result of their tendency to follow the tectonic uplift of the area (Pachakis *et al*, 1988). The degree of steepness may vary according to the ability of the various formations in resisting erosion, for example, in the coarser beds the joints are sparse and open due to tension, whereas in marls and marly mudstones they are dense, closed and smooth (Gasios et al, 1988).

The steep slopes are subjected to a continuous process of degradation and denudation through contraction, shrinkage and swelling caused by the seasonal variation of temperature and rain fall levels. Western Hellas is by comparison very wet with an annual rainfall of 900-1000 mm (Koukis & Ziourkas, 1989). The slopes of marly formations deteriorate by a series of successive slips, following gradual opening up of fissures during the summer months and swelling caused by the absorption of water during autumn and winter. The latter is exacerbated by existing open cracks allowing water inflow and a change in pore pressures (Wilson, 1970). The coarser grained intercalated conglomerates and sandstones may behave as artesian aquifers, thus adding to the problem. Cavounidis & Sotiropoulos (1980) suggest that the existing fissures are already at about their residual strength value. As the fine grained formations become softened and easily denudated, the courser grained facies creep on them ending in block slides controlled by the nature of the coarse-fine facies contact and the relative degrees of dissintegration of the pertinent formations.

3.4.5 Sampling sites.

3.4.5.1 General

For a number of sites there are descriptions by Gatsios *et al* (1988), Pachakis *et al* (1988) and Ministry of Public Works, C.L.P.W., report 8271000 (1985). The latter contains technical details from boreholes sunk along the problem sections of the Igoumenitsa - Preveza road axis. Sampling was made possible by means of hand-dug pits of varying depths and undisturbed sampling was attempted wherever that was deemed possible. For the needs of sampling and accurate location of pits to enable resampling, a series of 1:5.000 maps, covering 500m on either side of the road, was kindly provided for in premises consultation by the C.L.P.W. staff. Mapping and sampling took place between the end of March and June 1989.

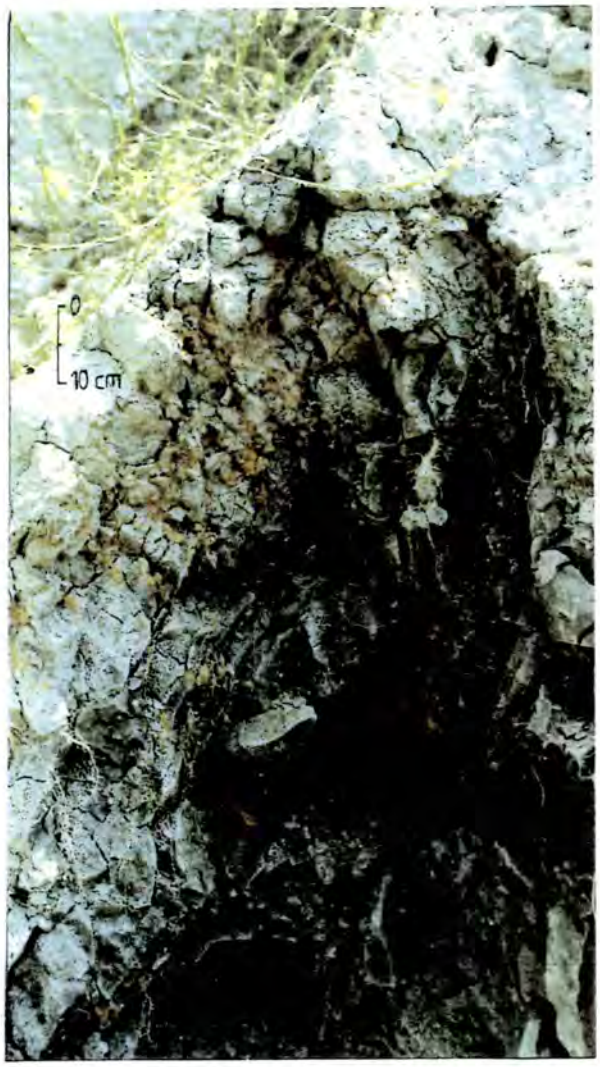

3.4.5.2 Kanali (Mytikas)

At position 39 + 0.650 km the terraced slope supported by a concrete retaining wall had failed following a shallow circular slide with a width of 25m, length of 15m and vertical displacement at the crest of 2m. The formation was mainly green grey in places brown grey slightly sandy, silty in places, firm weathered mudstone. There were disernable fissures of random orientation. Concretions of carbonates were rarely found on fissure surfaces in the green grey facies. No samples were taken. At position 39 + 0.470 km along the same slope, the materials involved beds of alternating blueish, green gray and blue grey silty mudstones and sandstones striking 20 degrees N and dipping 60 degrees E. Four pits were dug.

Photograph 3.4 Haematite concretions (Mytikas).

In general the first 0.50m were taken up by weathered and/or transported materials ranging from medium sand lenses to brown bands of plastic soft clay. From 0.50m to 0.80m the blueish, blue grey and green grey lithorelicts among and amorphous soil matrix became more apparent with depth (Zone III, Chandler, 1969). From 0.80m to the bottom of each pit, grey blue to blue mudrock becomes pervasive with distinctive discolouration and oxidation surfaces. Hematite was frequently encountered in small corrections along fissure lines (photograph 3.4). A sample was obtained from the top pit at a depth of 1.30m (KKS2).

3.4.5.3 Loutsa

Surface sample (LTS) of green grey stiff silty clay was taken from a small cutting at 16+0.300m. The material appeared softened and heavily fissured. Stability problems were confined mainly within the body of the weathered mantle with depths ranging between 1m and 10m and came in the form of shallow slides, especially at the contact of conglomerates and sandstone beds with marly beds. The main feature on the site was an embankment which had failed several times. More information on this site can be found in Gasios et al (1988).

3.4.5.4 Agios Nikolaos

At position 17+0.850 km a trial pit 1.20 m deep was dug in blue marly clay at the top of the downslope face. The sample AGN1 appeared hard with grey green discolouration surfaces. The material was bedded with irregularly orientated fissures which tended to break the material down to blocks of 0.15-0.20m maximum size. The size of these blocks increased with depth (photograph 3.5). At position 18+0.000 km sample AGN2 was obtained from the uphill slope at a depth of 0.80m. The material was a dark brown to green brown hard clayey silt which appeared intercalated in beds of blueish marls and conglomerates. The sampled material was weathered, intensely cracked with a maximum intact block dimension of 5 cm and considerably moistered since it underlies sandy conglomerates. At position 18+0.035 km along the same slope, sample AGN3 was obtained from a 1.20 m deep pit situated 17 m higher from the road surface and at least 20 m deeper, stratigraphically, than AGN 2. The slope is generally stable with the fine grained members appearing weathered at the contact with water bearing sandstones and conglomerates. The thicknesses of the intercalated member reaches a maximum of 5 cm per individual bed.

← Photograph 3.5 Trial pit at AGN1.

3.4.5.5 Gourounaki

At position 1.5km from the Vrachos junction and towards the Vrachos hamlet, a sample of green marly clay was taken from a depth of 1m. The material was rich in flora relicts, coming in large very stiff blocks (approx. dimensions 0.7 x 0.3 x 0.3m). The overlying mantle consists of a thin bed of dark green clay. The sample was called DRV. At position 20+0.000km and 50m to the south of the tunnel, sample GRN, a green silty mudstone which appeared quite weathered coming in brittle cobble size pieces was obtained from a slope which consisted of two small terraces. The coarser facies prevailed with mainly sandstones of medium to fine grain size.

3.4.5.6 Lakka Lefkas

At position 20+0.300km the uphill slope reaches 25m in height. The formations consist of brown red to dark brown red clayey mudstone within yellow and blueish sandstones. Conglomerates daylight at the top of the slope while blue marls daylight at the foot. The sample LLK1 was taken from the brown red mudstone. The material is hard although heavily fissured. Discolouration and decrease in block size appeared closer to the mudstone-sandstone contact surfaces. The sample LLK2 was taken from the blueish marls. The material came out

typically in big blocks of up to 0.30m in width and was silty.

3.4.5.7 Tsoumba Laxi

At position 21+0.800 km the natural slope is fairly even. The material is weathered and softened light brown to grey silty clay. The fissures often contain sand which must have propagated through being washed out from overlying sandstone beds. The sample TLX was taken from the surface of a 30m high cutting slope with varying inclination (3:2 to 2:1 height/base ratio). A shallow slip at the top of the slope overlooks the main slip in the middle of it, with a crest approximately 30m long. The failure has been classed as long term by Kalteziotis et al (1989).

3.4.5.8 Krevatina

From 23+0.080 to 24+0.000 the road cuts through unstable slopes which lead to extensive landsliding. The slopes vary in height from a minimum of 5m at the downhill section to a maximum of 45 m at the uphill section of the site. In the CLPW report (1985) it is noted that the marly formation cracks open due to stress relief independently from existing discontinuity systems. The uphill slope is dominated by a big slide at its centre (photograph 3.6). To the right of the slide yellow to light brown -brown grey sandstones dominate while to the left of the slide blue grey to dark grey clayey mudstones with thin bands (max. thickness 15cm) of sandstone prevail, exhibiting intense loosening and oxidation. From the top of the marly slope and close to the crest of the slide a trial pit reached 1.5 m depth. At the top the material is completely weathered dark grey plastic soft to firm clay with carbonaceous concretions (sample KVT1HPA). With increasing depth the material becomes grey blue and firm coming in pieces up to 7 cm maximum dimension. At the bottom the material becomes firm to stiff and although it retains weathered soil characteristics it contains sizable relics of the parent formation (Zone III, Chandler, 1969) becoming blue marly clay. The sample is called KVT1 HPB.

From the middle of the marly slope sample KVT1 LP was obtained from a depth of 60 cm. The material is stiffer than KVT1 HPB, coming in very stiff blocks (max. 30 x 10 x 12 cm) with weathered surfaces along the opened cracks. The latter tend to close with depth.

Opposite to the landslide on the downhill cutting two samples were obtained. The slope contains fine to medium size sandstones and blue marls interecalated with olive green silty mudstone and greengrey clayey mudstone. The first sample KVT A1, was

taken from the top of the slope at a depth of 0.20m and was olive green silty mudstone, friable with concretions of carbonates. The second sample, KVT A2 was obtained at the foot of the slope from the blue marly formation at a depth of 0.70m.

The main failure which had occurred had a maximum length at the crest of 550m developing different characteristics along its length from block sliding to mudflow, reflecting thus the variability of materials that this slide involved. The displacement along the failure surface was estimated to have reached a maximum of about 30m without taking secondary movements at the foot of the slide into account. This failure has combined with other, by comparison, minor failures of the downhill slopes to completely block the road with several metres thickness of debris material. Kalteziotis et al (1989) concluded that this was a failure that has exhibited both short and long term characteristics.

photograph 3.6 Part of the Krevatina failure at location KVT 1.

At position 24+0.050 km a further two samples of the olive green silty marly mudstone were obtained. The material appeared significantly weathered and ,where close to contact with sandstones, quite discoloured denoting chemical alteration. The slope is dominated by the fine grained facies and bears the marks of block sliding and toppling of unsupported sandstone beds, along its steep, typically 50 degrees, face.

The samples obtained from the top and foot of the slope are called KVT B1 and KVT B2 respectively.

3.4.5.9 Kastro Despos

At position 25+0.200 km the bridge of Despo is founded on very hilly terrain. It connects the two very steep sides of the Despo ravine, cutting through blue marls and base conglomerates with clayey intercalations. The steepness of the natural slopes contributes to unfavourable stability conditions especially at the foot where the flora cover has been stripped off to allow for the bridge foundation. On the south bank the terrain close to the bridge has been flattened allowing only small height (3-4 m) terraced slopes of blue marl on either side of the road axis. At position 25+0.250 km a 1.5 m deep pit was dug into the left hand side slope south of the bridge. From that pit a disturbed sample from the top (KDs) and one intact sample from the floor (KD) were obtained from a loosened jointed but still very stiff blue marl with discontinuities closing with depth. Discolouration and oxidation was quite evident along joint surfaces. Along the same slope and at position 25+0.265 samples KDAg and KDAb were obtained from a similar pit. The acronyms g and b denote grey and blue colour, as the two samples were taken from a contact surface. The grey facies is very argillaceous and weathered exhibiting foliation planes whereas the blue facies appears well stratified though jointed with medium thickness beds (30-45 cm) and stiff to hard intact behaviour. From the opposite slope sample KD B was obtained from the foot of the slope. The 30m high (2:1) slope consists of conglomerate beds and sandstone intercalated with olive green mottled hard clayey marl which would be classed as zone II material according to Chandler (1969).

The slope where KDB was obtained had failed during the spring of 1983 (Kalteziotis et al, 1989). Kalteziotis et al (1989) studied this failure and concluded that the circular rotational movement took place inside the marl bed and its face at its higher points coincides with a vertical fault parallel to the road axis. The authors suggested that the continuous supply of water by the adjacent conglomerates into the marl, loosend by the presence of the fault was greatly to blame since back analysis showed $c'=12kPa$ and $\phi'=28°$ for the marl alone and $c'=140kPa$ and $\phi'=50°$ for the conglomerates.

3.4.5.10 Lakka Lampes

At position 22+0.800km on a small 1:1 slope on the left hand side, a trial pit was opened in blue marl (photograph 3.7). Three samples were obtained LL1, LL2 and LL3 at depths 0.3 m, 1.2 m and 2 m respectively. Sample LL1 is completely

weathered grey light green friable and soft when wetted clay with visible carbonaceous concretions. The discoloured parts of the formation appeared grey brown, light grey green with lithorelicts of frequently small 3cm to 4cm size.

As lithorelicts between the irregularly spaced fissures and soil matrix gain size with depth, the soil mass becomes firm and at approximately 0.50m depth the material became stiff to very stiff with extensive discolouration along the fissures. Sample LL2 comprises 0.1x0.5x0.1m pieces of discoloured along the fissures but fresh in the centre blue very stiff silty clay. The fresh material appeared gradually at depths greater than 1.6 m and was hard blue to blue grey silty clay which could be removed in blocks approximately 0.1 x 0.15 x 0.2 m and above in size. Sample LL3 was excavated at a depth of 2m and could be described as a hard blue grey silty clay

Photograph 3.7 Part of Lakka Lampes trial pit. The yellow tape indicates 1m depth

The intense nature of denudation in the area prevented the full scale development of profiles comparable to those of Lias clay (Chandler, 1972). The slope appeared quite loosened with extension cracks developing inside the top 1.5 m at least.

3.4.5.11 Apidoules

At position 28 + 0.200km and two 27 +0.900km two samples were obtained (ADL1 and ADL2). The area is dominated by conglomerate and sandstone beds. The fine grained facies are mainly represented by silty mudstones and clayey marls.

The slopes are quite steep (approx. 1:1) and terraces had to be constructed for the cuttings. The beds have a general NNW - SSE strike and a 20° E dip. ADL1 is silty slightly sandy brown clay whilst ADL2 is silty red brown to green brown weathered moderately plastic clay.

3.4.5.12 Xynomelia

At position 28+0.800km mixed facies of sandstones and conglomerates alternate with blue silty marls with E-W strike and 30° N dip. On the uphill slope the cutting had failed in a mixed manner. Small, shallow, slips of the fine grained members had forced the sandstones into block slides, loosening up the slope, leading to a circular slip 30 m long and 10 m deep with an apparent displacement at the crest of approximately 5 m. Three samples were obtained from stiff blue silty marl beds at the top (XML HP), the middle (XML MP) and the foot (XML LP) of the slope which is situated to the right of the slide and is formed in two terraces, each of 10 m height and 1:1 steep.

3.4.5.13 Koukos

At position 39+0.380km the main road axis meets a local agricultural track leading into an elongated small depression with a seasonal brook running along its axis. On its south flank the fine grained members of the Archangelos Pliocene formation daylight. The material is very weathered and in places has been replaced by topsoil several tens of centimetres deep due to furrow ploughing. Approximately 100 m from the above junction the KKS1 sample was obtained from a freshly cut face. Stratigraphically it corresponds to the lower members of the Archangelos formation which partly daylight along the Kanali cutting and it consists of a blue grey with light brown mottles firm to stiff silty clay. The beds are jointed with weathering and discolouration advancing along the sides of the joints. Like other cases the joints tend to close up with depth. No signs of recent landslip activity were identified.

3.5 Amalias - Goumeron Sampling Area.

3.5.1 Geographical Boundaries.

The studied area belongs to NW Peloponessos and is confined within the 1:50:000Amalias and Goumeron sheets of the Geological map of Greece. Its grid coordinates are:

21 degrees 25' E, 21 degrees 35'W, 37 degrees 55'N, 37 degrees 45' 30" S.

It lies to the south of Peneios river reservoir, to the east of the town of Amalias, to the west of the villages Rodia, Simopoulon and Velemidion and to the north of the village of Koutsohera and the hamlet of Palaiolanthi. A geological map of the wider area in 1:25,000 scale was kindly offered for consultation by Dr. E.Kamberis (courtesy of the Geological Mapping division of the Public Petroleum Corporation). A 1:50,000 map was prepared based on that map and provides details on the sampling locations (Appendix D)

3.5.2 Geomorphology of the area.

The wider NW Peloponessos can be divided roughly into a west part of even terrain and an undulating east part. The area studied lies along a transition zone of medium to low lying hilly terrain interrupted by many tributary streams of the main rivers of Peneios to the north and Ladon to the east of the area. Generally the relief becomes sharper towards the east, as it gets nearer to the alpine bedrock groups, with deeper V shape valleys. One of the causes responsible for today's relief is uplift movements related to diapyric movements of underlying evaporites (Kamberis, 1987). The geotectonic evolution of the area, on the other hand, led to the break up of the plio-pleistocene relief, determining thus the main directions of flow of surface waters. The two main collectors of surface waters in the area, Peneios and Ladon rivers, have undergone varying stages of development and maturing depending on relative paleogeographical position and geodynamic regime. Results of such variation can be seen in the form of extensive point bars interrupted by buried valleys and in other cases braided river channels. The surface water network has been characterised as one of low energy (Kamberis, 1987).

Red sandy clays cover many parts of the area's surface (1-10m) offering fertile ground for agriculture to the west of the studied area and forested slopes on the hills of the east part of the studied area. The extensive vegetation coverage rendered the use of aerial photography problematic.

3.5.3 General Structure.

NW Peloponnesos is constructed from the alpine groups of the Ionian and Tripolis zones and the formations of the Neogene and Quaternary. The latter formations have been deposited unconformably over the alpine sedimentary groups inside the two main basins of Amalias-Pyrgos and Kyparissia respectively. Possible remains of marine sedimentation between upper Bourdigale-lower Tortogne (Mid. Pliocene) suggested low rates of stratigraphic gaps along the stratigraphical column. An

ingression of sea during upper Pliocene continued through lower Pleistocene forming successive formations from shallow sea to terrain facies (Oenoi, Peristeri, Vounagron & Keramidia) which succeed each other at irregular time intervals (Cita, 1972). The transgression of lower Pleistocene led to the formation of base conglomerates and sands to the east (Chelidoni formation), whilst the lower lying west part of the area experienced coarse grain shallow sea deposition. The transgression of the lower Pleistocene led to the formation of base conglomerates and sands to the east (Chelidoni formation), whilst the lower lying west part of the area experienced coarse grain shallow sea deposition. The Tyrrhenian ingression affected the outmost western parts of the area (Katakolon). The Neogene basins, which accepted most of the post alpine deposition, developed mainly due to alpine faults NNW-SSE, some of which have occassionally reactivated since mid Pliocene. Differential uplift movements caused by Ionian zone evaporites have profited from the activity of fault zones which provided areas of limited resistance. By doing so, the evaporitic diapyric movements have contributed to the vertical and horizontal evolution of the post alpine facies and the thickness of the corresponding deposits. (Hageman,1979).

It should be noted that the evaporitic movements have not ceased as yet, resulting in a continuous transformation, in relatively short geological periods, of the geography and hence the hydrodynamics, ecology and deposition of an area. The transition from, for example, a marine to a terraineous facies could be abrupt, characterised by sandstone beds of 0.1 to 2m thickness, or progressive in which case the transition facies would reach 10-20m thickness. In total the thickness of the post alpine deposits may vary from 800m to 5,000m. Differential uplift meant that 600 to 650 of such deposits have been exposed to the east part of the area (Goumeron), whilst to the west (Amalias) the uplift was relatively small, up to 120m (Makris, 1973).

3.5.4 Lithology of the sampling area.

The formations which cover the studied area are presented in great detail by Kamberis (1987). In addition to stratigraphic succession, they follow a general west-east trend. The west-most formation of Tyrrhenian age consists of ingressional conglomerates and agglomerates with calcarenitic lenses and intercalations of yellowish silts; it is called the *Katakolon formation* and covers the Amalias town and areas around the villages Chavarion and Kardamas. The Pleistocene *formation of Chelidoni* consists of conglomerates, sandstones and red clays which develop laterally to less coarse members including fine grained sands, silty clays and marls, yellow to reddish, and grey white chalk, thinly bedded. The *formation of Keramidia*

is overlain next, through an angular unconformity. It consists of clays and silty clays, blue to grey blue, with lenses of sands, course to medium grained, which exhibit cross bedding. The formation develops to coarser facies close to the village of Kavathas.

The *formation of Vounagros* is the main Neogene body in the area covering almost exclusively the Plio-Pleistocene period. It is subdivided into 5 units/environments. Similar to the two previous formations, Vounagros, too, develops lateral transition zones. Irregular deposition of clays, mudstones and sandstones characterises Vounagros. Conglomerates may be encountered along the periphery of the Vounagos sub-basin. The strata developes from shallow sea to deltaic and lagoon facies at the lower to middle horizons becoming fluvial and/or lacustrine at the upper horisons. The fine grained members are fossilipferous (gasteropoda, ostrea pinae) and tend to host thin beds of chalk and lenses of marly limestones. They vary in colour and structure depending on the type of depositional environment.

The upper Pliocene is dominated by the *formations of Peristeri* and *Prophetis Helias-Oenoe*. The former consists of beds of poorly cemented white conglomerates with silty clay and fine sand intercalations (upper horizon); white grey base conglomerates (gravel size 4-6cm) with calcarenites followed by a succession of yellow sandstones and grey clays thinning out close to the village of Koutsohera; blue-grey blue clays and silty clays mainly with sandstone lenses and poorly cemented conglomerates with brown plastic clay lenses and sands. The *Prophetis Helias-Oenoe* formation consists of plastic clays-silty clays with no bedding, green grey to greyish with gypsum laminae and intercalations of well cemented lenses of fine conglomerates which transform into sandstones (upper); blue and green grey mudstones and clays with fine sand bands (middle) and intercalations of brown-green, mottled clays and mudstones (lower).

3.5.5 Sampling Sites

3.5.5.1 General

Reconaissance and mapping took place during May 1989 while sampling was completed in June 1989. Particular attention was paid to ensure the diversity of formations from which samples were obtained. All samples were obtained by means of hand-dug pits. Attempts to extract undisturbed samples were hampered by the prolonged drought causing materials to develop cracks due to dessication.

3.5.5.2 Hill 183 (Near Pineios reservoir)

At a distance of 1200m from the village Ayios Helias, towards the Pineios reservoir dam, on the south west slope of hill 183 two samples were obtained on either side of a 2.5 metre thick sandstone bed. Sample 183a, from the base of the slope, is a brown-greengrey weathered clay with extensive discolouration surfaces. Sample 183b, from 10m above the sandstone bed, is a grey silty marl, firm with little apparent cohesion and plentyful Lamellibranches. Both horizons belong to the Keraminia formation.

photograph 3.8 South facing bank enscarpment downstream of the Dam at NSA1.

3.5.5.3 Nesia

At a distance of 600m from the downstream face of the Pineios Dam and along the left handside flank of the Pineios river valley there are alternating sandstone and marly clay beds, 5-15m thick, with the latter more prominent (photogaph 3.8). The slope is fractured in many places owing to block sliding caused by wedge failures, exhibiting displacements of up to 5 metres, probably along some very plastic surfaces. Slumping and debris slides were also observed in the vicinity of the Dam. On the 6th of June according to local people at about 11.30am rockfalls were induced by earth tremours. Two samples were obtained. Sample NSA1 was taken from the bottom of the slope. It is light blue greyish hard marly clay. Sample NSA 2 was taken from fragments of the above mentioned rockfall. It is a cohesive stiff, marly

clay, well stratified, with grey blue colour. Both samples belong to horizons of the Keramidia formation.

3.5.5.4 Tzami

At a distance of 50m before the junction to the village of Avgi, towards Oenoi, a sample of stiff brown clay was obtained from a freshly cut clope. The slope was 70 degrees steep with a maximum height of 10m. The sample TZM was extracted from a 2m thick layer of clay sandwiched between yellowish fine grained sandstone at the bottom and blue silty mudstone at the top of the slope at a depth of 40cm. It belongs to the upper horizon of Vounagros formation.

3.5.5.5 Merovigli

Along the same road, at a distance of 1050m before the junction to Avgi, at the foot of Merovigli hill the sample MVG was obtained from the middle of the lower section of a two-terrace slope (4m from the road surface). The top terrace is dominated by a 7m thick sandstone medium-coarse grain size moderately weathered and loosened along fractures. The sample, a firm blue clay, belongs to the upper horizon of Vounagros formation.

3.5.5.6 Palaiostani

On the top of the Palaiostani hill overlooking the hamlet of Asteraiika by the Peristerion - Amalias road the Peristerion formation consists mainly of poorly cemented sandstones with intercalations of mudstones and conglomerates. The sample PLS was obtained at a depth of 1m inside a trial pit. The mudstone is firm, marly showing concretions of carbonaceous material and gypsum, mainly grey with red brown laminae of a soft to firm clay.

3.5.5.7 Skoufia

At a distance 2.5km to the NE of the village Penisterion, sample SKF1 was obtained from the surface of a freshly cut slope. The material, known localy as "γλυνα" (translated as "slippery"), is a firm to stiff blue clay with discolouration marks along discontinuities (the material becomes greyish). Along the same agricultural road and 20m before the junction with Oenoi-Pyrgos road SKF2 was obtained from the weathered mantle of a mildly sloping cutting (5m height, 1:2.5 slope). The sampling depth was 20cm-45 cm and the material obntained was a greyish-blue green silty clay. SKF3 was sampled 1km to the south of the above junction, beside a dislodged drainage culvert. The material is a very stiff grey blue marly clay with intense oxidisation and discolouration surfaces and concretions of carbonaceous material.

The samples SKF2 and SKF3 are from the middle and SKF1 from the bottom horizons of the Prophetes Helias - Oenoi formation.

3.5.5.8 Oenoi

Before the northern entrance to the village Oenoi a waste burial site was under construction. Two samples were obtained from the north and southwest faces of the site. Sample OEN 1 is a brown green to green stiff mudstone. OEN 2 is grey brown weathered and firm clayey material. The slopes of the site were not too high (5-8m) and not steep (approx 1:2.5). The samples belong to the upper horizon of the Proph. Helias - Oenoi formation.

3.5.5.9 Koutsohera

Approximately 500m to the east of Koutsohera village, samples KTR 1 and KTR 2 were obtained from Vounagrou formation beds. Steep sandstone beds (45 degrees NE) overlie green stiff marly clays with carbonate and gypsum concretions along discontinuity surfaces. Where the exposures were fresh (KTR1) the slopes would remain steep (up to 45 degrees) while, where weathered material daylighted (KTR2) extension cracks in the sandstones become more frequent due to lack of support. The weathered material, olive green grey firm clay, can be easily denuded. Plenty of Lamellibrancs were observed. The samples come from upper to middle Vounagros horizons.

3.5.5.10 Rodia

Beside the village of Rodia, at the most easterly point of the studied area the sample RDA was obtained from a steep (80 degrees) slope 4m in height, at a depth of 1m inside the foot of the slope. The material is a silty brown very stiff marly clay. The sampled material belongs to the Keramidia formation.

CHAPTER 4
PHYSICAL CHARACTERISTICS AND MINERALOGY

4.1 On the Classification of "Marls"

4.1.1 General

The problem of how to explain the behaviour of sedimendary formations is closely related to the problem of how to classify them (Blatt, Middleton & Murrey, 1980). In other words the framework within which a particular type of rock or soil is examined influences the resulting model with which we attempt to understand the behaviour and make predictions of the performance of that type of rock or soil.

Marl has been a term with varied meaning depending on the definition based on the percentages of its constituent minerals and also the positioning of the engineering borderlines of behaviour. As far as the former is concerned, the consensus definition is of a calcium carbonate rich (30 to 60 %) clayey fine grained formation (Barth et al, 1939; Krynine & Judd, 1957; Underwood, 1967; Jung, 1969; Fleming et al, 1970; Davi, 1971; Fytrolakis, 1973; and others). In engineering terms, as much as in sedimentological terms, *marls* have always been seen as a special member of the mudrocks family (Gillot, 1968; Attewell & Farmer, 1976; Lindholm, 1987; Selley, 1988; and others) or a calcium carbonate rich overconsolidated clay, depending always on the degree of diagenesis (Millot, 1970; Fytrolakis, 1973; Tsiambaos, 1987; and others).

4.1.2 Definitions on Marls

4.1.2.1 General

Marl, a term first applied to glauconitic sands, was more commonly used to describe carbonate earths accumulated in recent or present day freshwater lakes. Various dictionaries define marls as calcareous clays or intimate mixtures of clays and particles of calcite and/or dolomite with or without fragments of shells, slightly to richly carbonaceous silty clays and silts and fine grained sands. Terzaghi & Peck (1967) distinguished *lake marls* from *marls*, *marls* being light coloured fine grained powdery calcareous deposits precipitated in ponds to stiff or very stiff calcareous clays and *lake marls* being stiff to very stiff calcareous clays of greenish colour. Marls may behave like a soil, a weak rock or a rock depending on the degree of diagenesis and the type of diagenetic evolution (Hawkins et al, 1986; Tsiambaos,

1987; Anagnostopoulos et al, 1991; and others). It is this perplexity that renders marls and marly clays a unique group within the overconsolidated clays - mudrocks families.

4.1.2.2 Mineralogical considerations

With regard to mineralogical composition it is common to define marls as part of a clay-limestone two end-members systems (fig. 4.1.1).

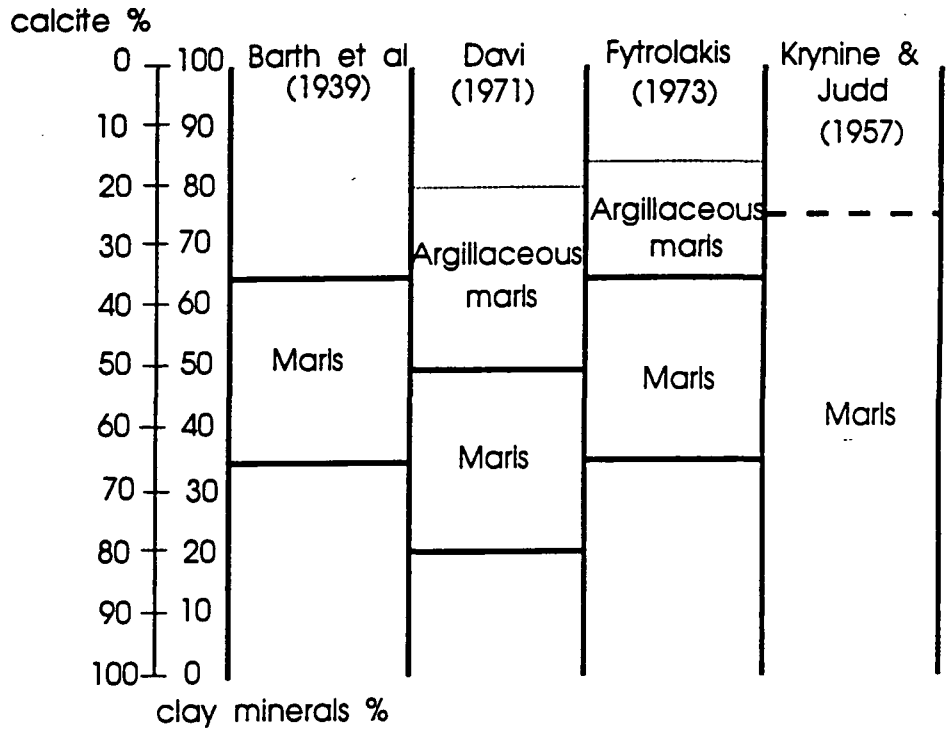

Fig. 4.1.1 Mineralogical classifications of marls based on a calcite - clay minerals configuration

Barth et al (1939) situated marls as lying between 35% and 65% calcium carbonate by weight with a complementary percentage of clay minerals. Jung (1969) placed marls between the same as above $CaCO_3$ percentage levels. Davi (1971) defined marls as a clay - carbonate mineral mixture with clay minerals ranging from 20% to 50%; an argillaceous marl should contain more than 50% clay minerals. Fytrolakis (1973) suggested a range of 35% to 65% $CaCO_3$ for marls and 16% to 35% $CaCO_3$ for argillaceous marls. Attewell & Farmer (1976) adapted a nomeclature system by Krynine & Judd (1957) where marls and marlstones are idendified as clastic materials with clay minerals and calcite as constituent components with calcite being

no less than 25% by weight. Other similar nomeclatures have been proposed by Underwood (1967) and Fleming et al (1970).

Lindholm (1987) and Selley (1988) showed three end-members systems for the classification of mudrocks, where marls were broadly defined in an area in the middle between the clay and carbonate mineral poles with little contribution from the third constituent, the third constituent being sand and organic matter respectively (fig. 4.1.2).

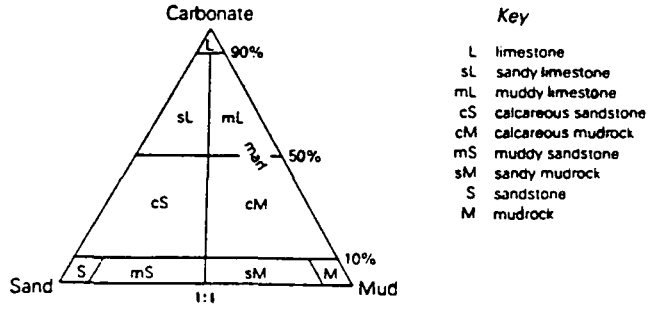

Fig. 4.1.2 Triangular configuration for mudrock-limestone classification system. Carbonate pole includes calcite and aragonite; sand and mud include silicate minerals. For bottom tier of rocks see fig. 4.1.3.

The carbonate component in marls is either of organic origin (shells, sponge fragments etc) or has precipitated as biochemical sediment. The presence of "rock flour" is common in marls and consists mainly of quartz, feldspars and crystalline micaceous clay minerals, their quantities depending on relative durability and travel distance before deposition. Hydrated oxides such as goethite and haematite intermingle with clay minerals promoting the formation of cementation bonds (Perrin, 1971)

4.1.2.3 Engineering Geological considerations

The distinction between marls, clayey or argillaceous marls, marly clays, clays and micrites is predominantly based on mineralogical concerns. In terms of soil mechanics the distinction of marls from other types of formations becomes blurred and subjective. The delimiting values of strength parameters have not yet been agreed as a result of varying interpretations of what is a soil, a weak rock and a rock, clearly exhibited during the 26th Annual Conference of the Engineering Group of

the Geological Society of London with the theme *The Engineering Geology of Weak Rock* (Culshaw, 1993).

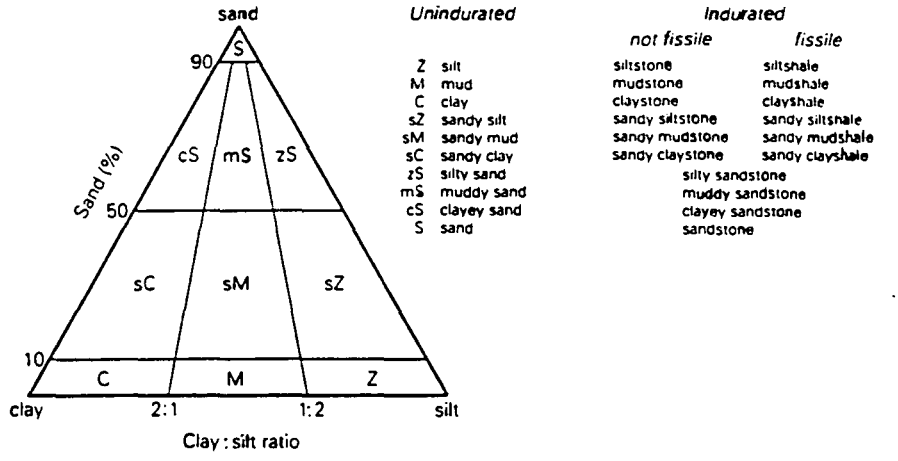

Fig. 4.1.3 Example of usage of triangular plot in classification systems. The terminology for mixtures of sand and mud using Udden-Wentworth size terms (table 4.1.1). Fissile rock names are given without hyphen as done by Potter *et al* (1980).

Many authors view marls as over-consolidated carbonaceous clays with cementation varying according to the degree of diagenesis. Depending on the degree of diagenesis, marls range from stiff marls to soft slightly over-consolidated calcareous clays (Datta et al, 1982; Tsiambaos, 1987; Anagnostopoulos et al, 1991). It is precisely this discrepancy that renders conventional geotechnical investigation and interpretation techniques insufficient (Vaughan et al, 1988). Unlike coarse grained cemented materials, such as sandstones, studies concerning the cementing bonds and their effect on engineering performance have been rare. Only recently has appreciation been given to this subject (Leroueil et al, 1979; McKown & Ladd, 1982; Griffiths et al, 1988; Vaughan, 1988; Vaughan et al,1988; Bressani, 1990; Leroueil & Vaughan, 1990; Anagnostopoulos et al, 1991)

If marls were to be seen within the overconsolidated clays and mudrocks framework, using the conventional initial void ratio - stress history concept, then they could be classed as less compacted and consolidated than limestones and less plastic than pure clays (Tsiambaos, 1987). It would, then, be expected that marls should have no less

than 50% particles ≤ 60μm in diameter (Taylor & Spears, 1981) and have undrained compressive strength values in excess of 100MPa where the diagenetic bonds are strong (Eng. Group, Geol. Soc. London, Working Party, 1977; Cripps & Taylor, 1986). Following Bjerrum (1973), Morgenstern & Eigenbrod (1974) proposed that a fresh rock-type mudstone should have an undrained shear strength greater than 1.8 MPa and U.C.S greater than 3.5 MPa. They noted that strength loss during softening should be less than 40% while a loss of 60% should apply to soil type clays.

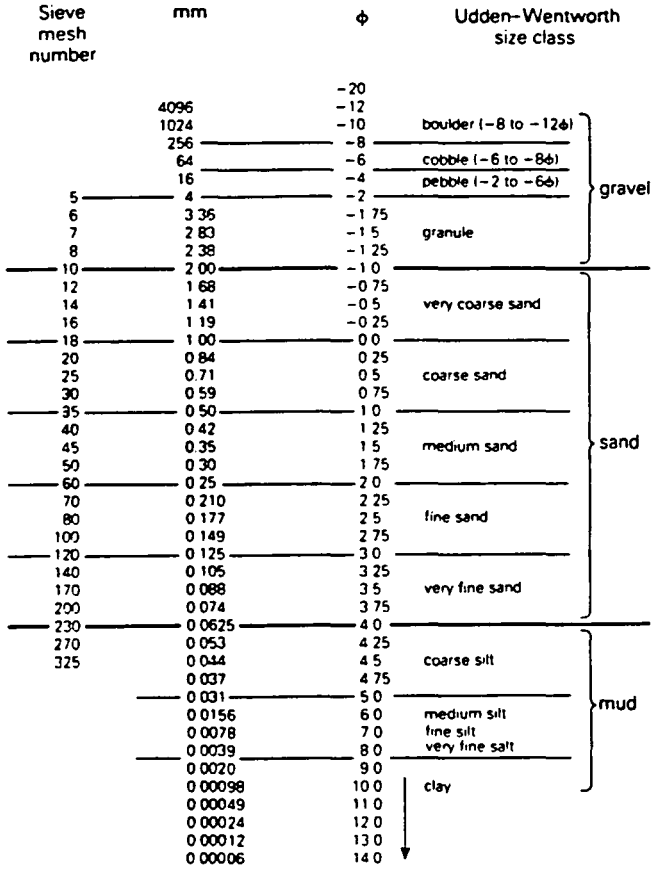

Table 4.1.1 Udden-Wentworth size classes. Nomograms are used to convert mm to ϕ and vice versa; (modified from Folk, 1980).

Cripps & Taylor (1986), based on field evidence, point out that unconfined shear strength (U.S.S) of British Tertiary deposits conform to "weak" rock levels averaging 625kPa with unconfined compressive strength (U.C.S) greater than 1.3 MPa. However the deposits that they have studied displayed a wide variety of behaviour and strength parameters ranging from firm clay (≈ 360kPa U.S.S) to strong rock (≈50MPa U.S.S). The same authors later (Cripps & Taylor, 1987)

agreed that with the exception of some "unusually strong samples" of Gault clay and calcareous Lower Lias clay, the older materials had higher shear strength than the rest of the British Tertiary deposits

4.1.3 Hellenic marls and marly fine grained sediments

Hellenic marls and marly fine grained sediments, often referred to as *Neogene* and/or *Plio-Pleistocene formations* in the literature, they are also referred to as "marls" on the day to day language by many practising colleagues as long as they look reasonably strong and they have not got a brown colour. Only recently there has been a systematic effort to record their properties and classify them accordingly (Fytrolakis, 1973; Koukis, 1977; Technical Chamber of Greece, 1985; Tsiambaos,1987; Kostopoulos, 1988; Rozos, 1991). Values of grain size, plasticity and mineral contents are discussed below.

Koukis (1977) reported on Pyrgos silty clays, clayey silts and stiff marls. He found liquid limits ranging between 20%-57% and plastic limits between 13%-37% with a clay fraction range of 5%-30%, fine silt 15%-40%, medium silt 20%-25%, coarse silt 5%-30%, sand 0%-30%.

Tsiambaos (1987) for the Irakleion Marls identified two sub-groups of the formations. In the first the whitish-yellow and the brown-yellow ones showed a strong presence of calcite with the latter ones showing higher values of quartz. Feldspars and chlorites were present in trace quantities in both whitish-yellow and brown-yellow marls. They contained sand (2-34%), silt (45-62%) and clay fraction (4-38%) with liquid limits from 24-59% and plasticity indices from 35-36 (CL to CH). In the second group, the light-grey and the grey-blue ones, showed more clayey characteristics than the whitish-yellow and the brown-yellow marls with the light-grey ones displaying a remarkable 25% mintomorillonite content. The grey-blue marls showed slightly higher values for calcite and quartz contents and a marked increase in chlorites than the light-grey ones. They showed sand from 4-14%, silt from 65-95% and clay fraction from 4-38% with liquid limit from 33-100% and plasticity index from 10 to 57 (mainly MH).

Kostopoulos (1988) presented results from X-ray diffraction analysis on marls from Korinthos, Ipeiros, Pireeus and Komotini without, however, giving information on the sampling locations. He suggested values for calcite, quartz, feldspars and clay

minerals (totals) and the main clay minerals for the Korinthos specimens. He identified chlorite and montmorillonite as the main clay species (6-7%).

Cavounidis *et al* (1988) studied Hellenic marls under the microscope. They have also given mineral ranges for "a Pliocene marl" from Ipeiros. The suggested ranges for carbonates (20-25%), quartz (20-25%), feldspars(10%) and clay minerals (illite and chlorite at 35-40%)

Rozos (1991) studied silty clay, argillaceous marl and marl samples from N.W. Peloponnesos and reported clay fractions between 21% and 65%, silt 34%-76%, and sand 1%-15% for the "argillaceous marls" of the plio-pleistocene formations and clay 3-33% silt 53-82% and sand 1-44% for some of the deeper "marly" horizons. He showed plasticities ranging between CL to CH for the former while the latter concentrated inside the CL area. The values of specific gravity ranged between 2.65-2.70. Rozos (1991) presented a comprehensive account of X-ray diffraction results. Illite ranged from 2-15%, chlorite from1-7%, kaolinite from 0-5%, quartz from 4-54%, feldspars from 0-11% and inferred calcite from chemical analysis ranged from 5-75%.

U.C.S values may vary significantly. Rozos (1991) reported that the argillaceous marls gave values between 15-154kPa while the marls ranged from 30-247kPa. Kostopoulos (1988) gave a range of values for Korinthos marls (30-8,000kPa), Pireeus marl (40-20,000kPa), Ipeiros marls (50-2,000kPa) and Komotini marls (30-1,000kPa) while Tsiambaos (1987) reported an equally wide range of U.C.S values for the Irakleion marls and calcareous clays from 20 to 1,250kPa.

4.2 Engineering Classification Tests in the Laboratory

4.2.1 General

An extensive test programme was undertaken between April 1989 and May 1991 to ascertain the physical properties of the samples collected. Fifty six samples from Korinthos, Prevesa-Igoumenitsa and Amalias-Goumeron areas were tested for plasticity, specific gravity & grain size distribution. Ten more samples from the mentioned areas were tested for plasticity, specific gravity and coarse grain fraction distribution. For thirty of the above samples a free swell test was performed.

The testing took place partly in Athens at the Central Public Works Laboratory courtesy of the Ministry for the Environment, Physical Planning and Public Works and partly in Durham at the Engineering Geology Laboratory, School of Engineering and Computer Science (S.E.C.S), Durham University. Data on two samples of Irakleion marls, named ts71 and ts26, was kindly provided by Dr. G. Tsiambaos of CPWL.

4.2.2 Methods of Testing

4.2.2.1 Atterberg Limits

Tests were performed on representative sample specimens after air-drying for four days and mechanical crushing in a pestle and mortar for 30 minutes each. The specimens were dry-sieved through a 425μm mesh (BS1377:1975) in Durham and through a 420μm (ASTM D-136) in Athens.

The plastic limit determination was performed according to the BS1377:1975 specification. In Athens, the liquid limit was determined using the Casagrande cup to E106-86/5&6 specifications (M.E.P.P.P.W., 1986). In Durham the fall cone penetrometer method to BS 1377:1975 specification was used.

Much has been published on the advantages and disadvantages of each method (Sherwood & Ryley, 1968; Wood & Wroth, 1978; Littleton & Farmilo, 1977; Wood, 1982; Moon & White, 1985;Christaras, 1991; and others). Since the comparison of the two methods was outside the scope of the present thesis, the author notes the method used next to the corresponding data to allow others to make comparisons should they so desire.

4.2.2.2 Specific Gravity

The BS 1377:1975 pycnometer method was followed for all tested samples.

4.2.2.3 Grain Size Distribution

Samples were allowed to air dry for at least four days and were then mechanically crushed for thirty minutes using a pestle & mortar bowl. The pestle had a rubber crushing edge to minimise the destruction of mineral crystallic forms during breakdown.

In Athens the samples were subjected to dry sieving through a ASTM D-136 standard sieve No40 (420μm). Generally the entire sample went through the above

sieve with the exception of samples SLM 1A and SLM B1. The samples were then tested according to E106-86/7&9 specifications for the determination of the coarse and the fine fractions based on the respective ASTM D-136 and ASTM D-422 specifications. The coarse fraction distribution was determined by means of wet sieving through a succession of sieves from 420μm to 74μm. The fines fraction distribution was determined by means of the hydrometer test. Deflocculation was achieved by means of adding Sodium Hexametaphosphate (at a concentration of 2g/litre water) in a sealed beaker with the sample and shaking the mixture for one hour.

The BS1377:1975 standard specifications were followed in Durham and involved wet sieving through a set of sieves from 200μm to 60μm and using the pipette method for the determination of the fines fraction distribution. Deflocculation was achieved as above.

4.2.2.4 Free Swell Test

The test was first devised by Gibbs and Holtz (1956). The procedure involves 10ml of crushed soil powder passing the 425μm sieve, being placed in a dry 25ml cylinder. The powder should not be compacted or shaken down. 50ml of distilled water were placed in a measuring cylinder. The dry powder was then "drizzled" steadily into the water and was allowed to settle. Once the sample has settled, the volume of settled solids is read off (V). Free swell is then defined as:

$$\text{free swell} = \frac{V - 10}{10} * 100\%$$

4.2.3 Presentation of results

The results are presented in separate tables for every test and sampling area. tables 4.2.1, 4.2.2 and 4.2.3 present the plasticity results for Korinthos, Igoumenitsa-Preveza and Amalias-Goumeron samples respectively. Tables 4.2.4, 4.2.5, 4.2.6 present the grain size distribution percentages for fine sand, coarse, medium and fine silt and clay fractions, accompanied with the respective specific gravity measurements for the various samples. The results from the free swell test are presented in table 4.2.7.

The results from the samples ts71 and ts26 provided by Dr. Tsiambaos are presented separately in table 4.2.8. For every set of data presented, the corresponding testing

method specification is provided. Finally table 4.2.9 presents the results of plasticity tests on eight oven-dried and air-dried samples.

Figures 4.2.1 to 4.2.4 present the grain size distribution curves for the samples from Korinthos, Preveza-Igoumenitsa, Amalias-Goumeron and Irakleion respectively.

The abbreviations w_L, wp and Ip stand for liquid limit, plastic limit and plasticity index respectively.

table 4.2.1 Atterberg Limits Results for Korinthos

sample	wl %	wp %	Ip	test specification
slm 1A	26	17	9	E106-86
slm2 A	32	18	14	E106-86
slm3 A	32	16	16	E106-86
slm 4A	28	16	12	E106-87
slm 5A	28	17	11	E106-88
slm6 A	36	20	16	E106-86
slm 7A	36	17	19	E106-89
slm 8A	24	14	10	E106-90
slm1 T	33	20	14	E106-86
slm2 T	32	22	10	E106-86
slm3 T	31	18	12	E106-86
slm4 T	35	18	17	E106-86
slm5 T	33	19	14	E106-86
slm1 B	28	18	10	E106-86
slm2 B	22	16	6	E106-86
slm B1	34	14	20	E106-86
slm B2	47	19	28	E106-86
slm G4	35	19	23	E106-86
slm D2	42	19	16	E106-86
slm 20	57	19	38	BS 1377:1975
slm 21	46	20	26	E106-86
arv3	40	19	21	BS 1377:1975
arv4	48	23	24	BS 1377:1975
er 1	41	22	19	BS 1377:1975
er 2	45	21	24	BS 1377:1975
psf 1 a	33	19	13	BS 1377:1975
rtk	41	19	22	BS 1377:1975
tkr	45	21	24	BS 1377:1975

table 4.2.2 Atterberg Limits Results for Preveza-Igoumenitsa

sample	wl %	wp %	Ip	test specification
xml HP s	29	17	12	E106-86
xml HP	28	16	12	E106-86
xml MP	49	22	27	E106-86
xml LP	42	19	23	E106-86
ll1	47	24	23	E106-86
ll2	29	13	16	E106-86
ll3	28	13	15	E106-86
lts	51	22	22	BS 1377:1975
apd1	39	15	24	E106-86
apd2	30	14	16	E106-86
kd s	40	18	22	E106-86
kd	43	23	20	E106-86
kd 1 b	56	23	33	BS 1377:1975
kd B1	43	21	22	BS 1377:1975
kvt2	45	19	26	E106-86
kvt A HPs	34	14	20	BS 1377:1975
kvt A HP	32	12	20	E106-86
kvt A LP	45	20	25	E106-86
kvt B1	48	23	25	BS 1377:1975
kvt 1 HP a	55	23	32	BS 1377:1975
kvt 1 HP b	50	22	28	BS 1377:1975
kks1	42	20	22	E106-86
agn1	57	25	32	BS 1377:1975
agn2 s	56	24	32	BS 1377:1975
agn2	53	24	30	BS 1377:1975
agn3	43	19	24	BS 1377:1975
dvr 1	48	22	26	BS 1377:1975

table 4.2.3 Atterberg Limits Results for Amalias - Goumeron

sample	wl %	wp %	Ip	test specification
ktr 1	50	21	29	BS 1377:1975
ktr2	55	23	32	BS 1377:1975
mvg	45	22	23	BS 1377:1975
nsa 1	54	24	30	BS 1377:1975
oen2	47	20	27	BS 1377:1975
pls	43	22	22	BS 1377:1975
rda	53	25	28	BS 1377:1975
skf1	55	24	31	BS 1377:1975
skf2	43	19	24	BS 1377:1975
tlp 183	44	21	23	BS 1377:1975

table 4.2.4 Grain Size and Specific Gravity Results for Korinthos

sample	Gs(*)	clay fraction%	f. silt %	m. silt %	c. silt %	f. sand %	test specification
slm 1A	2.55					37	E106-86
slm2 A	2.55	20	53	16	5	6	E106-86
slm3 A	2.52	26	18	38	11	7	E106-86
slm 4A	2.55					5	E106-86
slm 5A	2.60					5	E106-86
slm6 A	2.54	23	12	33	26	6	E106-86
slm 7A	2.62					3	E106-89
slm 8A	2.55					15	E106-86
slm1 T	2.58	34	35	18	10	3	E106-86
slm2 T	2.58	24	37	23	8	8	E106-86
slm3 T	2.62	28	36	22	12	2	E106-86
slm4 T	2.60	35	31	21	12	1	E106-86
slm5 T	2.52	30	30	25	8	7	E106-86
slm1 B	2.59	18	23	47	7	5	E106-86
slm2 B	2.49	19	12	19	30	20	E106-86
slm B1	2.59	38	12	12	21	17	E106-86
slm B2	2.70	50	28	8	8	6	E106-86
slm G4	2.65	19	18	43	18	3	E106-86
slm D2	2.70	36	32	18	12	2	E106-86
slm 20	2.67	60	21	6	8	5	BS 1377:1975
slm 21	2.65					2	E106-86
arv3	2.68	17	23	24	33	3	BS 1377:1975
arv4	2.64	36	26	35	2	1	BS 1377:1975
er 1	2.60	31	41	18	6	4	BS 1377:1975
er 2	2.68					8	BS 1377:1975
psf 1 a	2.55	18	32	39	11	0	BS 1377:1975
rtk	2.60	35	41	19	3	2	BS 1377:1975
tkr	2.66	38	33	13	7	9	BS 1377:1975

(*) all specific gravity tests according to BS 1377:1975 specifications

table 4.2.5 Grain Size and Specific Gravity Results for Preveza-Igoumenitsa

sample	Gs(*)	clay fraction%	f. silt %	m. silt %	c. silt %	f. sand %	test specification
xml HP s	2.59	23	10	31	32	4	E106-86
xml HP	2.59	25	12	25	32	6	E106-86
xml MP	2.70	50	28	13	8	1	E106-86
xml LP	2.70	41	27	22	9	1	E106-86
ll1	2.70	53	20	18	8	1	E106-86
ll2	2.70	24	9	17	42	8	E106-86
ll3	2.70	25	7	23	38	7	E106-86
lts	2.65	54	23	13	5	5	BS 1377:1975
apd1	2.66	31	14	20	26	9	E106-86
apd2	2.68	21	9	20	31	19	E106-86
kd s	2.67	42	22	23	10	3	E106-86
kd	2.68	41	18	22	18	1	E106-86
kd 1 b	2.66	55	20	21	2	2	BS 1377:1975
kd B1	2.65	44	23	30	2	1	BS 1377:1975
kvt2	2.68	46	21	19	10	4	E106-86
kvt A HPs	2.67	28	12	23	31	6	BS 1377:1975
kvt A HP	2.66	27	11	14	38	10	E106-86
kvt A LP	2.68	29	15	29	25	2	E106-86
kvt B1	2.60	33	20	36	11	0	BS 1377:1975
kvt 1 HP a	2.67	54	28	15	2	1	BS 1377:1975
kvt 1 HP b	2.66	31	41	18	7	3	BS 1377:1975
kks1	2.60	29	14	25	30	1.5	E106-86
agn1	2.67	25	29	43	2	1	BS 1377:1975
agn2 s	2.60	38	16	29	14	3	BS 1377:1975
agn2	2.62	22	21	31	21	5	BS 1377:1975
agn3	2.65	23	17	26	21	13	BS 1377:1975
dvr 1	2.68					8	BS 1377:1975

(*) all specific gravity tests according to BS 1377:1975 specifications

table 4.2.6 Grain Size and Specific Gravity Results for Amalias-Goumeron

sample	Gs(*)	clay fraction%	f. silt %	m. silt %	c. silt %	f. sand %	test specification
ktr 1	2.70					9	BS 1377:1975
ktr2	2.63	49	23	9	11	8	BS 1377:1975
mvg	2.54	32	24	38	4	2	BS 1377:1975
nsa 1	2.70	58	30	10	2	0	BS 1377:1975
oen2	2.52	43	15	21	9	12	BS 1377:1975
pls	2.64	34	13	34	19	0	BS 1377:1975
rda	2.66	23	56	19	1	1	BS 1377:1975
skf1	2.65	51	20	22	6	1	BS 1377:1975
skf2	2.67	34	11	26	24	5	BS 1377:1975
tlp 183	2.61	51	11	21	10	7	BS 1377:1975

(*) all specific gravity tests according to BS 1377:1975 specifications

table 4.2.7 Results of Free Swell Tests

area	sample	free (1) swell %
Prev-Igou	xml HP s	2
Prev-Igou	xml HP	0
Prev-Igou	xml MP	23
Prev-Igou	xml LP	13
Prev-Igou	II1	37
Prev-Igou	II2	13
Prev-Igou	II3	7
Prev-Igou	apd1	20
Prev-Igou	apd2	5
Prev-Igou	kd s	30
Prev-Igou	kd	20
Prev-Igou	kvt2	32
Prev-Igou	kvt A HP	22
Prev-Igou	kvt A LP	22
Prev-Igou	kks1	23
Korithos	slm2 A	1
Korithos	slm3 A	1
Korithos	slm6 A	1
Korithos	slm1 T	1
Korithos	slm2 T	1
Korithos	slm3 T	5
Korithos	slm4 T	3
Korithos	slm5 T	12
Korithos	slm B1	1

(1) Gibbs and Holtz (1956)

table 4.2.8 Test Results for Irakleion Marls

sample	wl %	wp %	Ip	test specification
ts71 (2)	46	20	26	E106-86
ts26 (2)	37	17	20	E106-86

sample	clay fraction%	f. silt %	m. silt %	c. silt %	f. sand %	test specification
ts71 (2)	38	12	10	21	19	E106-86
ts26 (2)	28	18	17	25	12	E106-86

sample	Gs	test specification
ts71 (2)	2.64	BS 1377:1975
ts26 (2)	2.57	BS 1377:1975

(2) Data provided by Dr. G.Tsiambaos (C.P.W.L)

table 4.2.9 Effect of Drying on Plasticity

sample	air dry wl(%)	oven dry wl(%)	air dry wp(%)	oven dry wp(%)	air dry Ip(%)	oven dry Ip(%)	clay fract.(%)
ll1	54	47	24	16	30	31	53
kd	43	41	23	20	20	21	41
kvt Alp	45	40	20	17	25	23	29
kks1	42	32	20	14	22	18	29
slm 6A	36	30	20	18	16	12	23
slm 7A	36	30	17	16	19	14	25
slm 1T	33	30	20	19	13	11	34
slm0+320	40	31	19	16	21	15	22

Fig 4.2.1 Grain Size Distributions for Korinthos

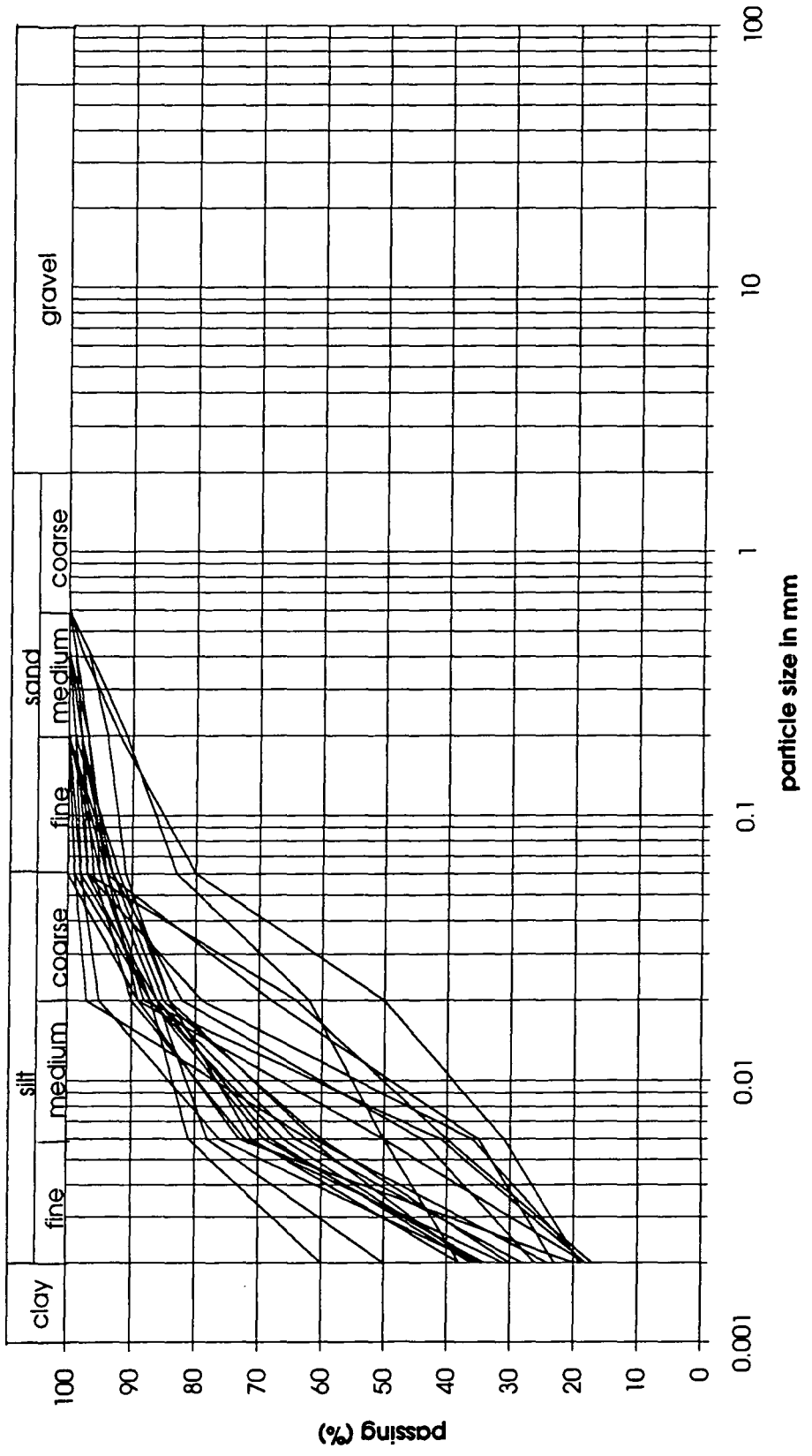

Fig 4.2.2 Grain Size Distributions for Preveza-Igoumenitsa

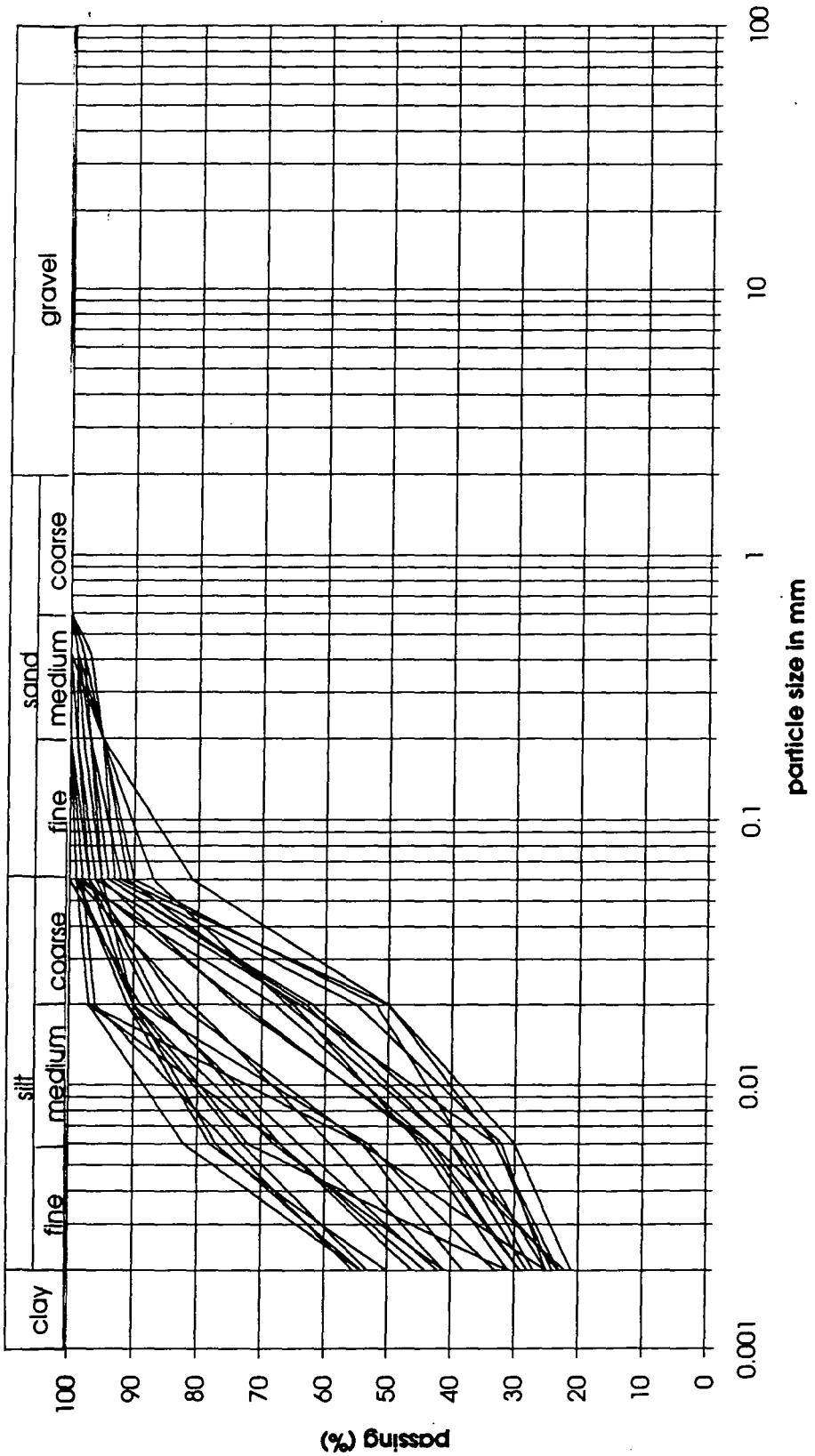

Fig 4.2.3 Grain Size Distributions for Amalias-Goumeron

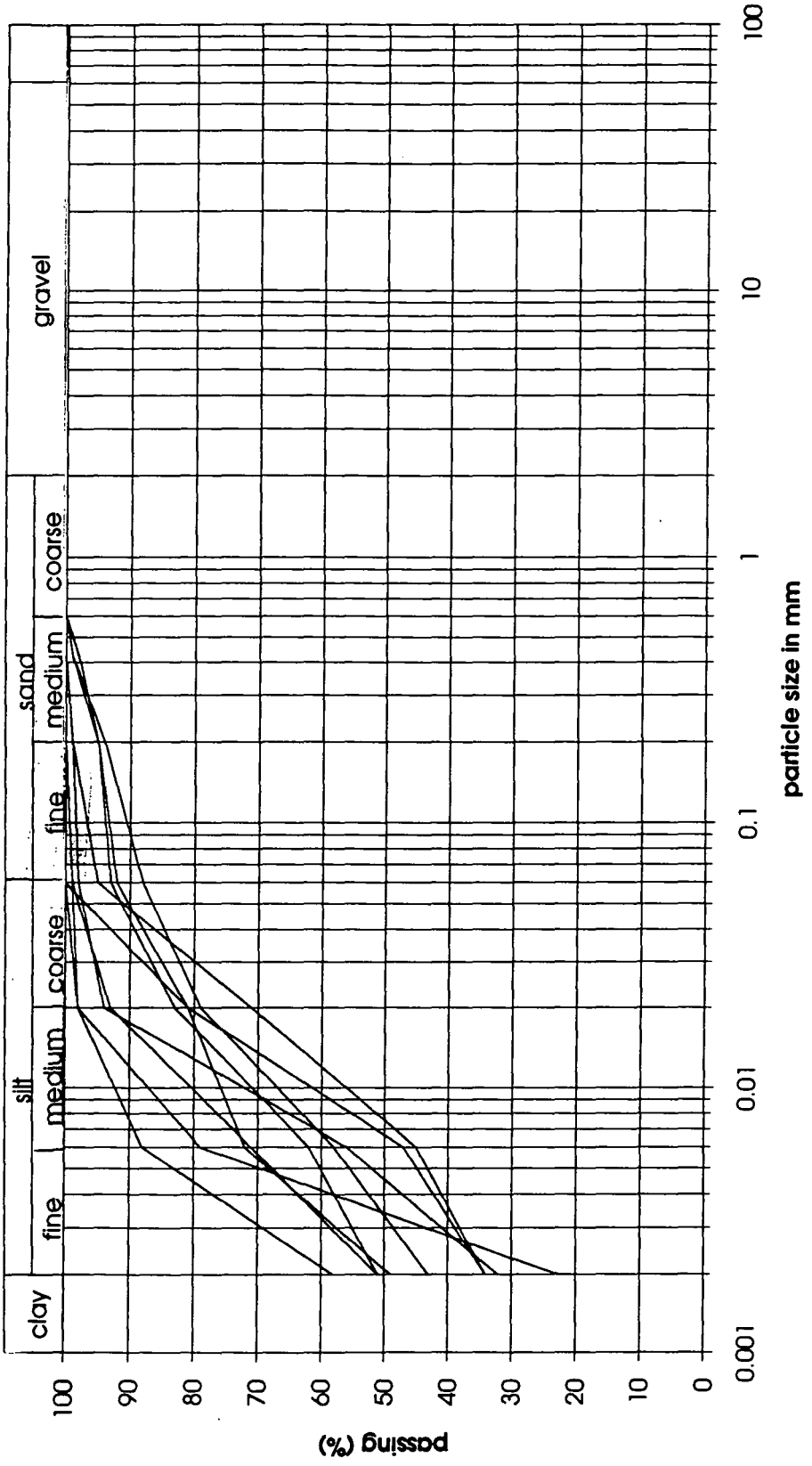

Fig 4.2.4 Grain Size Distributions for Irakleion

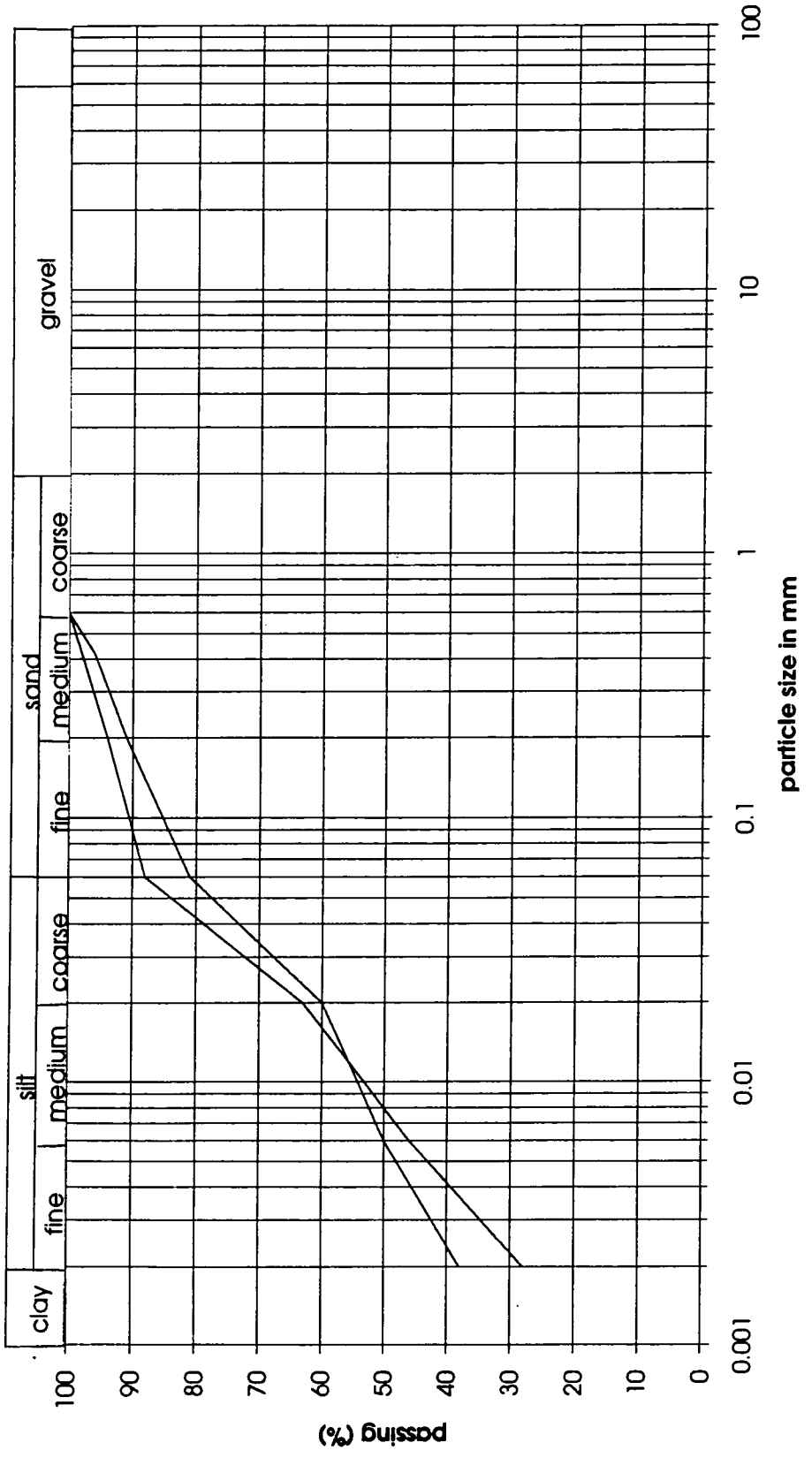

4.2.4 Analysis of the test results

4.2.4.1 Atterberg Limits

Fifty eight test results are plotted onto Cassagrande's (1948) plasticity chart (fig. 4.2.5). It can be seen that the majority of Korinthos samples lie in the low plasticity clay area; the majority of Preveza-Igoumenitsa samples are found inside the intermediate plasticity clay area although an appreciable number can also be found inside the low and high plasticity areas. The Amalias-Goumeron samples are equally divided between the intermediate and high plasticity clay areas of the chart. In summary Korinthos samples are CL-CI, Preveza-Igoumenitsa are CL-CH and Amalias-Goumeron are CI-CH. All samples tested lie above the A-line and the majority lie inside the CL and CI areas.

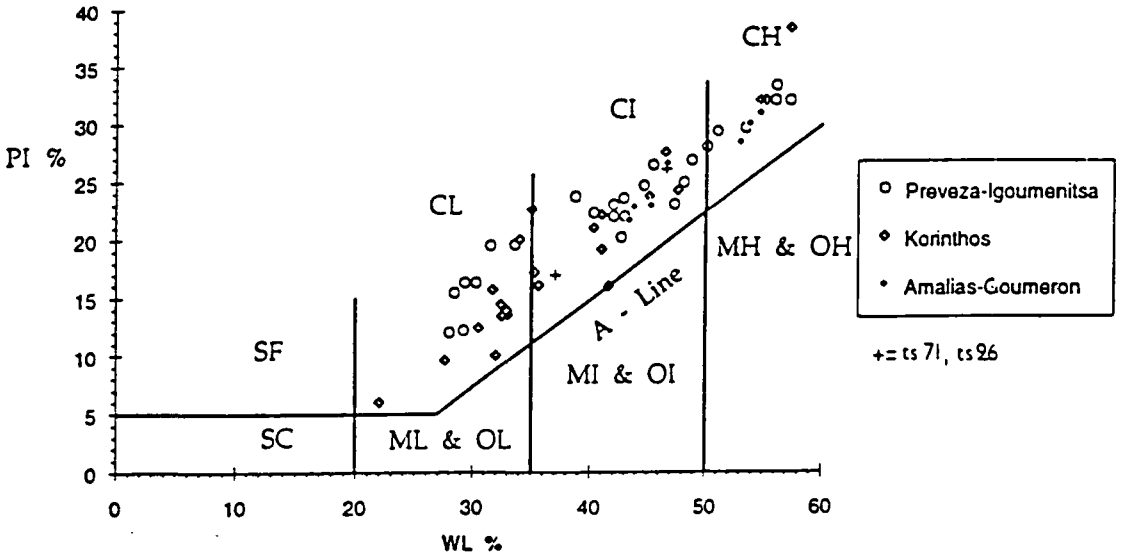

Fig 4.2.5 Unified Soil Classification System plasticity chart

4.2.4.2 Activity

Figure 4.2.6 presents results in the classic Skempton (1953) configuration where the activities of the various samples are shown as a projection of clay fraction values against the corresponding plasticity index values. The activity lines for three key clay minerals, namely kaolinite, illite and montmorillonite, are shown as boundary lines. The majority of the samples are concentrated between the illite and kaolinite lines representing intermediate to low activity values. Some results are inside the illite-montmorillonite zone of intermediate to high activity values.

Figure 4.2.7 presents results in the Williams & Donaldson (1980) configuration which relates activity with potential expansion. This configuration is recommended for use within the mudrock range by Taylor & Smith (1986).

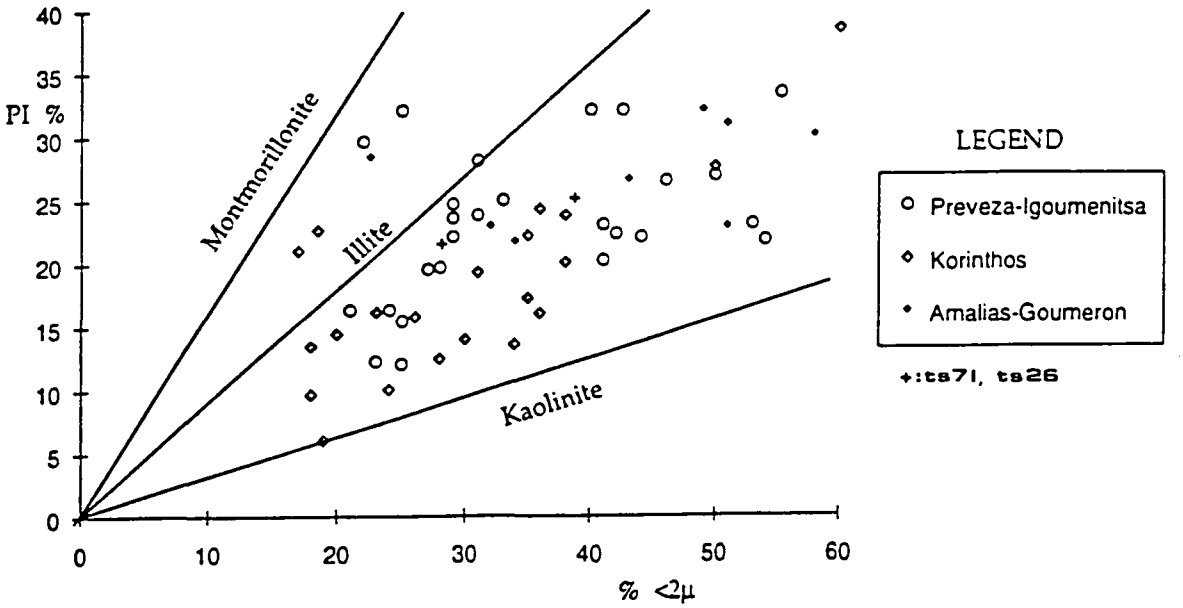

Fig. 4.2.6 Activity Chart (Skempton, 1953). Points ts71 & ts 21 by Tsiambaos (1987).

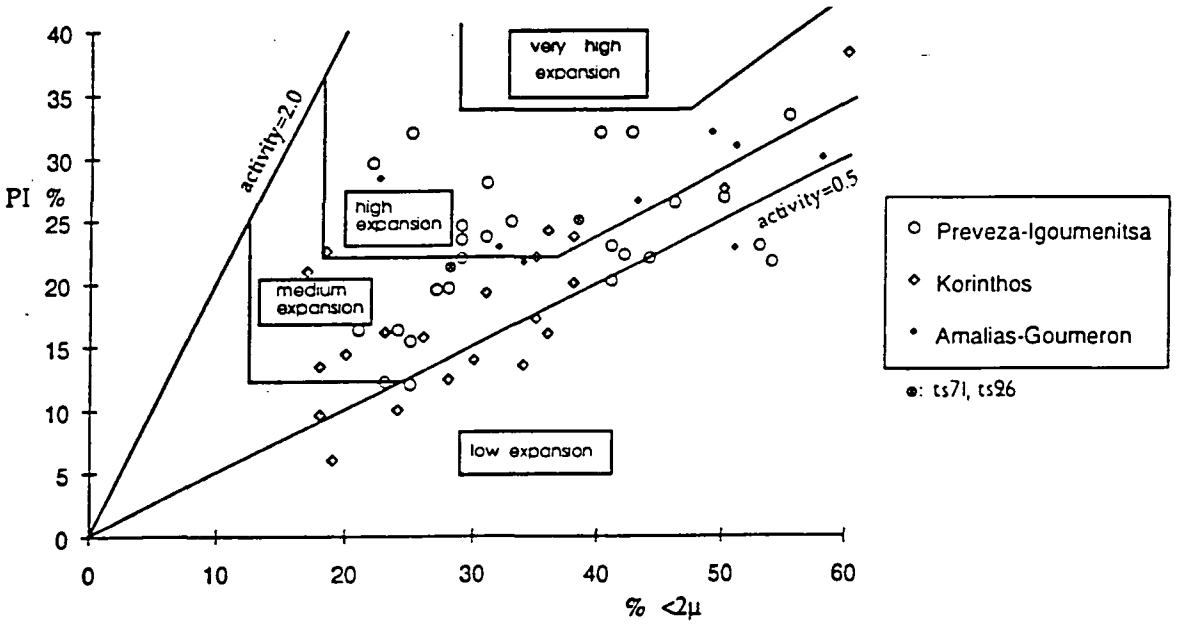

Fig 4.2.7 Activity - Expansion chart (after Williams & Donaldson, 1980).

Taylor & Smith (1986) suggested that better results for the above configuration can be obtained if, instead of the 425μm sieve recommended in BS 1377:1975, samples passing the 75μm sieve were used for the determination of plasticity index. It can be

seen that the Korinthos samples occupy the low to intermediate expansion area which compares comfortably with their position in the plasticity A-line chart (fig 4.2.5). The Preveza-Igoumenitsa samples are almost equally spread between the medium and high expansion areas and the Amalias-Goumeron are mostly inside the high expansion area. In both figures test points ts71 and ts26 refer to data provided by Dr. G. Tsiambaos (C.P.W.L) from Irakleion marls.

4.2.4.3 Grain Size Analysis

A cummulative synoptic picture of the tested samples with regard to grain-size distribution is given in fig. 4.2.8. The plot is adopted from Folk (1980) while the codenames for the categories shown is based on the British Soil Classification system. It can be seen that the majority of the Korinthos soils (K) fall into the clayey silt and silt categories. Two samples are into the silty clay band. These are SLM 20 and SLM B2. The Preveza-Igoumenitsa samples (Pr-Ig) occur across the board from silty clays to silts while the Amalias-Goumeron (Am-Gou) are more clayey lying within the silty clay and clayey silt areas.

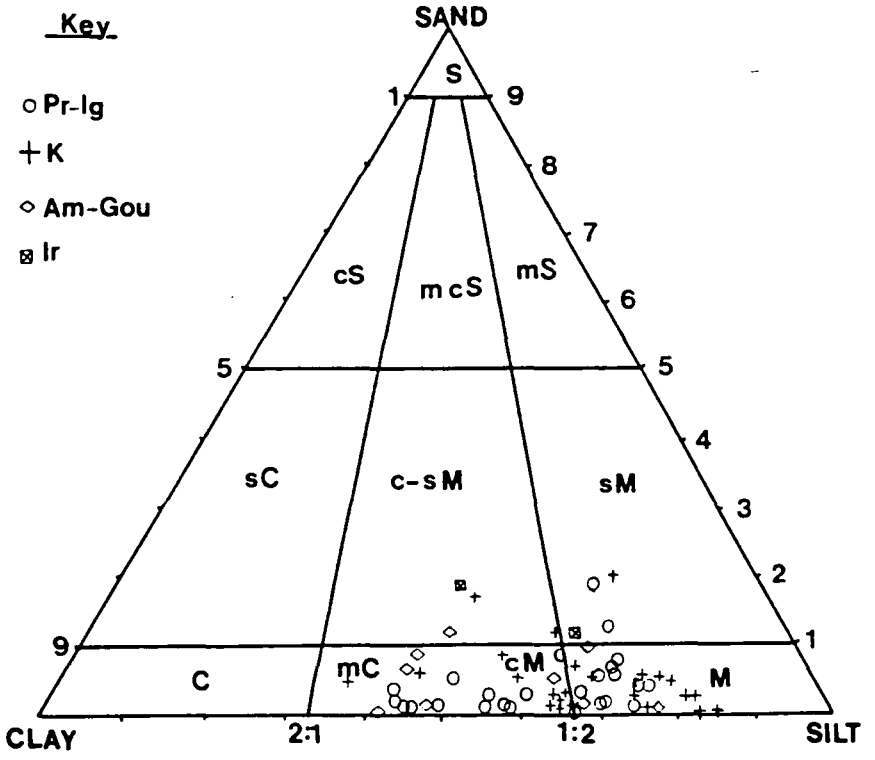

Fig. 4.2.8 Classification triangle based on fig. 4.1.3. S: sand; M: silt; C: clay; c: clayey; m: silty; s: sandy.

From the grain size distribution curves (fig. 4.2.1) it can be shown that Korinthos samples have values for fine silt ranging between 10% to 53% with most of the

values occurring between 23% to 38%. These values are, on average higher than for the other areas. As already mentioned above, Korinthos samples are not particularly clayey, with clay fractions (<2μm) ranging between 17% and 38%. The exceptional samples SLM 20 and SLM B2 gave 60% and 50% respectively.

The samples from Preveza-Igoumenitsa (fig. 4.2.2) gave a clay fraction range of 21%. The fine silt size range between 7% to 29% is split into two groups which become more separated at the medium and coarse silt sizes. The first grouping ranges between 7% to 15% for fine silt, 20% to 43% for medium silt and 18% to 38% for coarse silt corresponding to clayey silts, mainly blue to blue-grey marly clays from lagoon to shallow sea deposits. The second grouping ranges between 17% to 29% for fine silt, 13% to 19% for medium silt and 2% to 14% for coarse silt size corresponding to silty clays and clays of variable colour and mainly terrestial origin (i.e. deltaic, lake or river).

The Amalias-Goumeron samples (fig. 4.2.3) appear mainly as well graded silty clays. The clay fraction values range between 23% to 58%. Only one sample, RDA, appears very silty with a fine silt content at 57%. The same sample has a plasticity index value of 28% which appears high for a sample with a clay fraction at 23% (table 4.2.3). This could suggest that the high fine silt content is a result of aggregation of clay minerals into silt size particles.

The samples ts71 and ts26 from Irakleion (fig. 4.2.4) are typically clayey silts corresponding to whitish-yellow Irakleion marl deposits (Tsiambaos, 1987).

4.2.4.4 The effect of drying on plasticity

The variation of plasticity with drying procedure for 8 samples is shown in table 4.2.9. The table indicates two types of treatment prior to mechanical crushing, air drying for four days or oven drying for 24 hours at 105° C. The plastic limit was then determined according to BS1377:1975 and the liquid limit according to E106:86/5.

In all cases the liquid and plastic limit values are reduced when the samples are subjected to oven drying. The reduction can also be seen as a drop in plasticity index values. Table 4.2.9 shows the plasticity index for air dried samples, the plasticity index for oven dried samples and the clay fraction values for these samples. Two samples, LL1 and KD, with the highest clay fractions 53% and 41% respectively, show in fact a slight increase if little change in the *Ip* values with

increased temperature of pretreatment drying, but samples with lower clay content show a larger drop. It is clear that the liquid limit is more affected than the plastic limit on drying.

4.2.4.5 Free swelling

Twenty four samples from Korinthos and Preveza-Igoumenitsa (table 4.2.7) were tested according to the procedure devised by Gibbs & Holtz (1956). The values from Korinthos samples are markedly lower than those from Preveza-Igoumenitsa averaging 3% and 18% respectively, with extremes at 1%-12% and 0%-37% respectively. Head (1980) suggests that values of free swell below 50% show soils not likely to show expansive properties.

The above findings for Korinthos samples are consistent with the results shown in figure 4.2.7 as the Korinthos samples indicate low to intermediate expansion. In the case of Preveza-Igoumenitsa, samples do not show the same kind of agreement between results from table 4.2.7 and figure 4.2.7 as in Korinthos case, as the majority of results for Preveza-Igoumenitsa fall in the medium to high expansion area. There are however a number of samples in figure 4.2.7 that show a medium to low expansion potential. A weak correlation between plasticity index and free swell for the total of the tested samples can be viewed in figure 4.2.9.

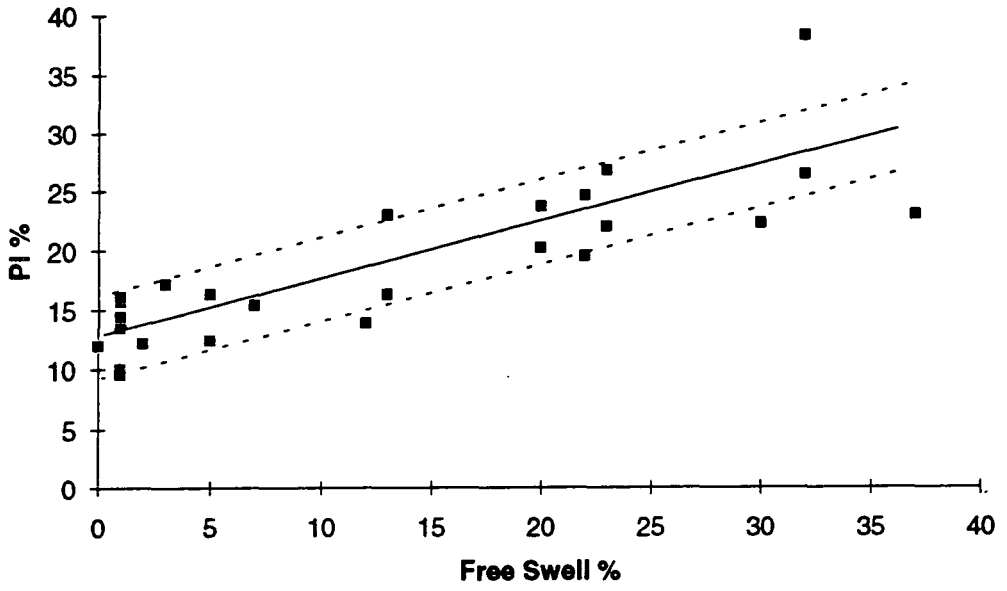

fig. 4.2.9 Correlation between plasticity index Ip and free swell test results

4.3 Mineralogical Analysis

4.3.1 General

The mineralogical identification programme was conducted in the Department of Geological Sciences, Durham University, under the supervision and with the assistance of Dr. D. Hirst and Mr. R. Hardy.

The programme was executed in three phases. During the first phase, a qualitative analysis using X-ray diffraction (XRD), of fifty four (54) samples was conducted along side engineering classification tests (see section 4.2.1) to allow a decision on which of the samples tested required more detailed analysis. During the second phase chemical analysis on thirty (30) selected samples was performed using X-ray fluorescence (XRF). The third phase involved the semi-quantitative analysis of the thirty samples selected for the second phase. The programme was conducted between February1991 and December 1991.

4.3.2 Theoretical considerations

4.3.2.1 General on X-ray fluorescence

The excitation of atoms and the subsequent emission of radiation when bombarded by a short wavelength energy source, such as hard X-rays or γ-rays, is called *fluorescence*. When a compacted powder is bombarded by hard X-rays, the various atoms of the constituent minerals emit radiation at characteristic frequences which can be studied in a spectrometer. The method is called *X-ray fluorescence* and it provides percentages of the constituent in the powder atoms in the form of commonly occuring oxides.

4.3.2.2 General on X-ray diffraction

A monochromatic beam of X-rays passing through a mineral grain is scattered by the atoms that compose the mineral. At specific angles of incidence, the scattered X-rays are in phase producing an intensified secondary beam. This phenomenon is known as *diffraction*. Diffraction can be pictured as a reflection of the X-rays beams by planes of atoms.

Diffraction occurs when the distance traveled by one scattered beam is different, by a length equal to the X-ray wavelength, from the distance traveled by another beam scattered by an adjacent plane of atoms. This diffracted beam is called a *first order reflection.* Diffraction also occurs when the difference in distance traveled by X-rays scattered from two adjacent layers of atoms equals two wavelengths (fig. 4.3.1) The resultant beam is called a *second order reflection.* Higher order reflections occur each time the path difference is a whole numper multiple of the wavelength. The general relationship is expressed by the **Bragg equation:**

$$n\lambda = 2d\sin\theta \qquad (4.3.1)$$

where n is a whole number, λ is the X-ray wavelength, d is the distance between planes of atoms (Å), and θ is the angle of incidence. More on the subject can be read in the 5th Monograph of the Mineralogical Society (Brindley & Brown, eds, 1980).

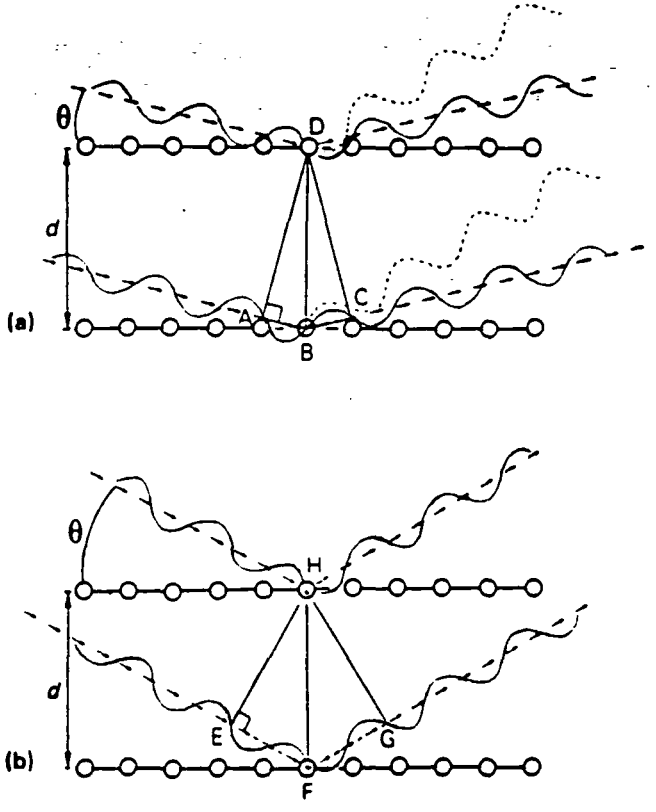

Fig. 4.3.1 Diffraction of X-rays by layers of atoms (from Lindholm, 1987).

When a powdered monomineralic sample is analysed, diffraction occurs for each

angle of incidence that satisfies the Bragg equation. Each angle is related to a set of lattice planes with a characteristic *d* spacing. Because each mineral has a number of distinctive set of lattice parameters, X-ray diffraction produces a unique series of reflections (peaks) on the strip chart, which is known as a diffractogram. This unique character is based on the position of each reflection as measured by 2θ and on the intensity of each reflection. The relative intensity equals the intensity of a particular reflection given as a ratio of the strongest reflection ranging from 0 to 100.

4.3.2.3 Sample Pretreatment

Some authors in geotechnical engineering suggest that carbonate minerals should be acid leached to allow better clay minerals resolution (Tsiambaos, 1987). However, it is believed that such treatment may alter clay minerals sensitive to cation exchange and lattice substitutions, such as Ca-montmorollonites (Grim, 1968).

It is also known that disaggregation methods (chemical or mechanical) affect the quality of the X-ray diffraction analysis because of their destructive effect on the clay mineral crystalinity (Olmstead, 1931; Krumbein, 1933; Takahashi, 1959a,b). Huang(1989) studied varius disaggregation methods and their effect on X-ray diffraction intensity peaks. He found that the change of intensity varied from one mineralogical type to another and from one disaggregation method to another.

Generally, clay microaggregates in the specimen reduce the degree of parallelism between the platy particles in the oriented sample and weaken the basal X-ray reflections. The increasing X-ray intensity of a clay mineral during the early stage of grinding is probably due to the separation of clay aggregates. However, under further processing the disaggregation force begins to break some of the interparticle bonds and produces finer particles through cleaving and fracturing of the clay crystals. These phenomena have been observed by Huang(1989) using electron scanning microscopy.

4.3.2.4 Mineral Identification

Generally, samples of unknown mineralogy are run through a range of 2θ from 2° to 40°. The 2θ of each major reflection is measured and compared with analysis of standards, such as those found in the ASTM Powder Diffraction File. For most of the reflections there is some difference between that measured for the unknown sample and the published standard values. Very weak reflections commonly do not show up, even in monomineralic samples. This problem is worse in samples composed of several different minerals. The signal for weak reflections may not be

strong enough to be picked up on the diffractogram. Alternatively, weak reflections of one mineral may be masked by stronger reflections of another mineral.

Identification of major clay mineral group types, using a sample oriented on the (001) plane is relatively straightforward and satisfactory for most work.

For even the most routine analysis, a sample must be run on the diffractometer three times. On the first run an untreated sample is used. On the second run a glycolated sample is used. The process of glycolation (i.e the exposure of a sample to glycol vapor for 6 hours at 50°C) will force expansive lattices to shift to the left of the diffractogram towards higher 2θ values. On the third run a sample that has been heated to 550°C for an hour is used.

This procedure is followed because minerals with the same or very similar lattice structures react differently to each type of treatment. For example chlorite and kaolinite both have a 7Å reflection. Unlike the chlorite, kaolinite is affected by the heating process and becomes mullite (a meta-kaolinite) with no reflection in that region of *d* spacings. Similarly, chlorite and montmorillonite together with mixed layered minerals give a number of strong reflections between 13Å and 15Å when untreated. When glycolated, montmorillonite and most of the expansive mixed layers move between 16Å and 17Å.

Figure 4.3.2 presents a typical diffractogram with the three runs superimposed to allow comparisons (sample KD Ab).

4.3.3 Preparation of samples

The preparation of samples for both methods of analysis involved pulverisation or at least crushing and seiving through a 425μm mesh. Two small samples were then separated of which one weighed at best 10g and the second at least 1gr at minimum for XRF and for XRD respectively.

1) For XRD, samples were mixed with a well crystaline phylosilicate mineral with a very well defined 001 base reflection (in this case Böhmite or Boehmite) at 10% of the sample's weight to act as an internal standard. To achieve the best possible orientation of the minerals prior to testing, a suspension of the mineral powder and distilled water was placed on a glass slide and was allowed to settle forming a thin film as the distilled water finally evaporates. No acid leaching of carbonates was

applied because of the possible damage the acid solution could inflict on the clay minerals of a sample.

2) For the XRF, samples were thoroughly mixed with *moviol* resin until moist and placed inside a stainless steel mould. The sample was then compressed under 5 Atm (500kPa) to form a thin pellet. The pellet was then placed in an oven at 105°C overnight to allow for the resin to completely evaporate. Prior to the test, the remaining sample was used for the determination of the *loss of ignition*, i.e the percentage of volatile H_2O, CO_2 and C by drying the sample at 1,050°C for 2 hours and measuring the loss in sample weight. The percentage of lost weight with respect to the initial weight determines the *loss of ignition.* It should be noted that the samples are kept dry at all times.

4.3.4 Equipment and testing parameters

For the X-ray diffraction a PHILIPS PW1130 spectrometer with a PHILIPS PW2236 Cobalt K alpha tube were used. The Co radiation wavelength was λ =1.7902Å with Ni filter set at 45kV and 25mA excitation power level. The X-ray fluorescence spectrometer consisted of a PHILIPS PW1400 spectrometer with a Rhodium (Rh) tube and an IBM compatible personal computer for on line interpretation using PHILIPS X41 software as well as software developed in the Department of Geological Sciences, University of Durham by Mr. D.Stevenson.

The accuracy of the spectrometers was assessed to be ±2.5% for the PW1400 and ± 4% for the PW1130. The accuracy was determined by running samples KKS1, PSF1a and SLM21 five times in PW1400 and running sample LL1 three times in PW1130 and calculating the standard deviation for each sample and their average (in the case of the PW1400).

4.3.5 Mineral identification

Identification of minerals from a XRD diffractograph was only possible when a series of characteristic for the species reflections on the diffractograph had been recognised and attributed with confidence to the specific mineralogical species or group.

During the first phase of the mineralogical analysis programme the samples ran only once covering a range of angles of incidence from 2°2θ to 65°2θ to allow a quick assessment of the broad mineralogical composition of every sample (i.e clays,

calcite, quartz etc) with emphasis on the common non clay minerals and less common non clay minerals that have often been referred to as cementing agents (eg pyrite).

For the purposes of this thesis the common hydrated micas, kaolinite, common montmorillonite and chlorite group members were identified. Determination of varieties of chlorite and montmorillonite (smectite) or mixed layer clays is more difficult and outside the scope of the present research. However, details can be obtained in Müller(1967), Carrol(1970) and Brindley & Brown(eds) (1980).

The values attributed to mica group members (such as illite etc) have been calculated on the basis of hydrous muscovite basal (001) reflections as being the closest to those of illite, a hydrated complex mica. Similarly, the values for chlorites were based on basal reflections of Penninite as well as reflections for Ia, IIb Fe-Mg, Ib Al and dioctahedral chlorites as presented in the ASTM Powder Diffraction File. In this case the strongest reflections appeared to be almost at identical 2θ angles. The montmorillonites were interpreted using reflection patterns for both Na and Ca - montmorillonites.

For certain minerals, such as pyrite (FeS_2), that the literature has suspected as having cementing properties, the chemical analysis helped to establish their presence or absence. The total amount of sulphur detected by the XRF analysis was ascribed to the presence of pyrite. However, the chemical analysis (XRF) is not an accurate indicator of clay mineralogy. The formulae for representative clay minerals is show below:

biotite (mica) $K(MgFe)_3(Al,Fe)Si_3O_{10}(HO,F)$
muscovite(mica) $KAl_2(AlSi_3)O_{10}(OH)_2$
penninite(chlorites) $(MgFe^{+2})_5Al(Si,Al)_4O_{10}(OH)_8$
clinochlore(chlorites) $(MgFe^{+2})_5Al(Si,Al)_4O_{10}(OH)_8$
kaolinite (clay) $Al_2Si_2O_5(OH)_4$
montmorillonite(clay) $(Na,Ca)_{0.33}(Al,Mg)_2Si_4O_{10}(OH)_2 * nH_2O$

Depending on the type of feldspars present, the KO_2 may be shared by orthoclase, a K-rich aluminium silicate ($KAlSi_3O_8$), and any of the mica group minerals or Na_2O may be shared by albite, a Na-rich aluminium silicate ($NaAlSi_3O_8$), and Na-

montmorillonites. However it is safer to use Na_2O levels as albite indicators because of the low contribution per unit weight of Na-montmorillonites to the total Na_2O . It is equally safe to assume that in the absence of pyrite, biotite and iron oxides and hydroxides the FeO levels are due to a strong chlorite presence. In any case and because of the interpretation difficulties, the XRF data should only be used as a supplementary tool alongside with the XRD analysis exercised with great care.

4.3.6 Quantification of diffractograph result

The X-ray diffraction analysis of a sample provides a good qualitative picture of the mineralogical contents which can be quantified within some reasonable degree of accuracy when **semi-quantitative analysis** techniques are used. Extensive descriptions of this method of analysis and the various mineral calibration standard charts used can be found in Taylor (1971), Smith (1978) and Hardy & Tucker (1988).

For the purpose of quantification an internal standard was added to the sample powder. The clay mineral Boehmite was added at 10% by weight of the total sample. The background base reflection was then established and marked on the diffractograph and the area under a reflection peak was approximated to a triangle the base of which was formed by the background base reflection. Once the areas under the basal 001 reflection peaks were calculated, the ratio:

$$\frac{A_{\text{mineral}}}{A_{\text{Boehmite}}}$$

was calculated for every mineral main peak. The ratios were then plotted on standard mineral calibration charts and the true value for the corresponding minerals was read off. In some of the calibration charts the degree of crystallinity had to be taken into account. This was achieved by comparing the shape of the experimental peak to standard ones that correspond to various degrees of crystallinity, normally interpreted as the sharper the peak the more crystalline the mineral.

4.3.7 Presentation of results

The results from the XRD analysis can be seen in table 4.3.1. It must be pointed that any values from table 4.3.1 have to be normalised to add up to 100% per sample before they can be of use for any type of analysis involving such data. The normalised values are shown in table 4.3.2. Table 4.3.3 presents the XRF results. No attempt has been made to identify any mixed layered minerals, such as regular

swelling mixed layer chlorites, regular mixed layer chlorite-montmorillonites and mixed illite-montmorilonites. The minerals are presented as groups and where possible as individual species when present in adequate and idendifiable quantities.

4.3.8 Analysis of results

4.3.8.1 Mineral species and suites

As already mentioned, the experimental programme concentrated on the detection of groups of the main mineralogical species normally expected to be present in samples with geological field descriptions such as marl, calcareous clay etc. Quartz and mica were detected using XRD in all samples in all areas. Similarly calcite was detected everywhere in all but one (SKF1) samples. Feldspars, smectites and chlorites were detected in almost all sample with very few exceptions (TS71, TS6, SLM1a). Dolomite and kaolinite were found in small quantities in some samples, but were absent or in trace quantities in most of the samples. The presence of pyrite was inferred in trace quantities for a small number of samples, being completely absent in the rest of the samples.

The X-ray diffraction results are summarised in table 4.3.4 . The values are presented as averages, minimums and maximums of the detected minerals for each area. The results for dolomite have not been included because they are not significant. Also excluded are the results for samples TS71 and TS26 representing Irakleion marls as being statistically not significant. The samples from Korinthos show the highest calcite content and with it the lowest content in every other mineral group detected. The samples from Amalias - Goumeron show the highest value for the mica group. The samples from Preveza - Igoumenitsa are the least calcitic and show slightly higher values than the Amalias - Goumeron for the quartz, chlorite and montmorillonite contents. The samples from Korinthos show the highest maximum, minimum and average calcite content and with it the lowest content in every other mineral group detected.

The majority of the Korinthos samples, shown in fig. 4.3.3 as filled diamonds, lie inside the *"marls"* designated part of the plot, with SLM1T, PSF1a and RTK inside the *"muddy Limestone"* area of the diagram. Sample SLM1a exhibits sandy characteristics and lies within the *"calcareous Sandstone"* area.

It is interesting that samples SLM2a, SLM6a and SLM7a down the same crossection on the uphill cutting slope at S olomos Junction, sampled at 0.30m intrervals, show

Fig. 4.3.2 Typical diffractogram (sample KD Ab) with all three types of runs.

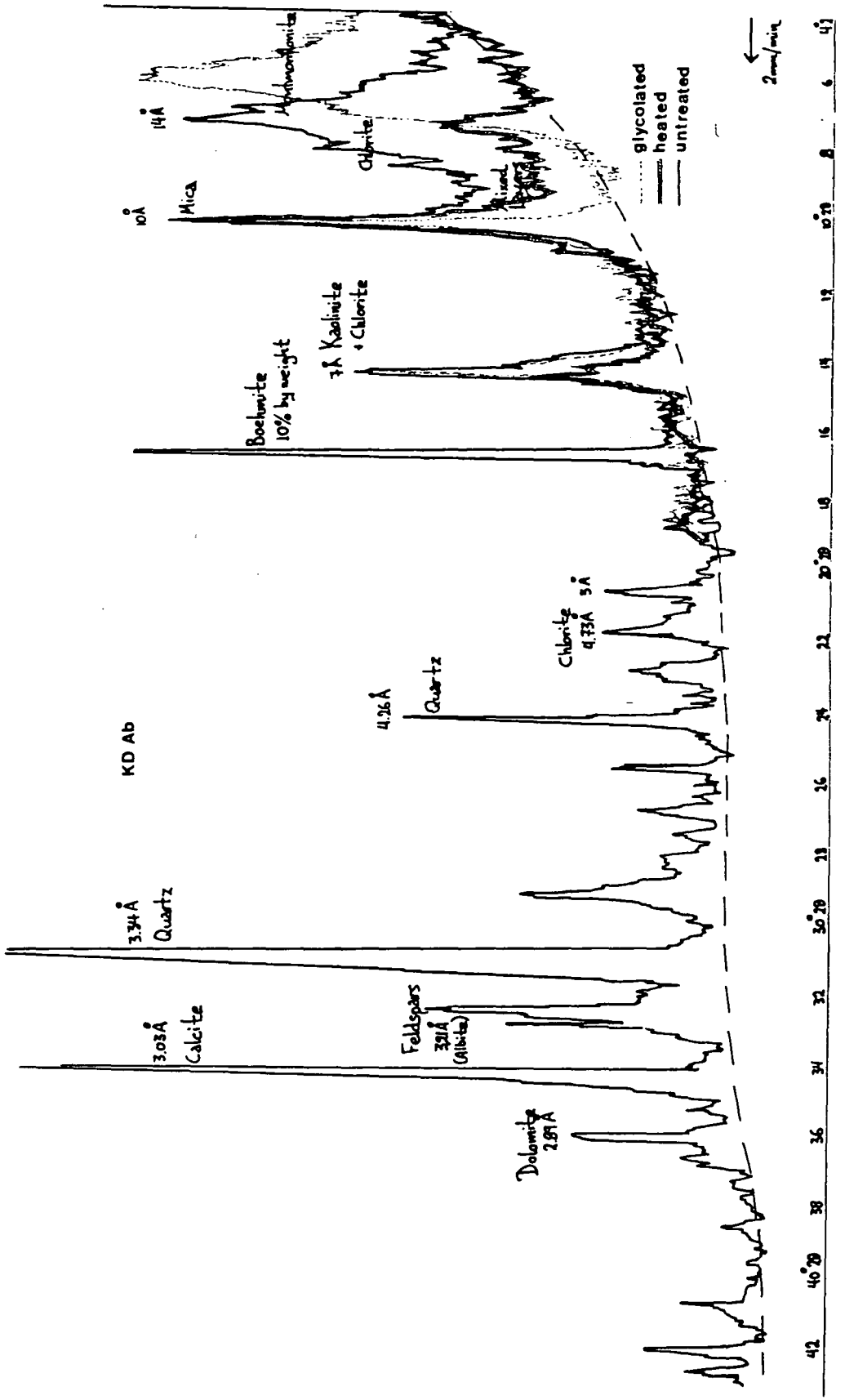

X-Ray Diffraction Analysis Table of Results **CoK alpha wavelength lamda = 1.7902**

sample	feldspars %	quartz %	calcite %	dolomite %	pyrite %	mica group %	kaolinite %	smectites group %	chlorites group %	total %
arv3	4	15	43	0	0	25	2	6	3	98
er1	3	12	37	1	0	22	0	6	14	95
psf1	1	5	72	0	0	12	0	6	2	98
rtk	6	7	58	3	0	12	4	2	5	97
slm1a	15	31	36	3	0	8	0	3	4	100
slm2a	7	20	25	0	0	15	8	10	12	97
slm6a	5	16	38	3	0	18	0	6	12	98
slm7a	7	18	41	3	0	18	0	9	4	100
slm20	6	12	25	7	0	30	2	6	16	104
slmB2	5	16	28	0	0	24	3	9	12	97
slm1t	5	5	76	1	0	5	0	0	5	97
slm4t	2	13	50	0	0	15	2	10	2	94
tkr	2	10	50	0	0	15	5	6	6	94
agn1	5	14	29	0	0	25	4	7	12	96
agn2	6	18	23	0	0	20	6	9	15	97
kd	10	19	20	0	0	30	0	8	14	101
kd1b	5	8	14	5	0	32	0	25	15	104
kks1	10	26	16	2	0	19	3	10	13	99
kvt-a.l.p	10	19	14	0	0	20	5	15	18	101
kvt1h.p.b	4	17	32	0	0	19	6	18	2	98
kvt2	10	20	15	0	0	20	5	14	10	94
ll1	6	13	14	0	0	28	2	16	18	97
lts	8	20	4	0	0	30	5	5	25	97
xlm-m.p	3	20	26	3	0	23	2	11	10	98
ktr2	10	10	46	2	0	20	3	5	3	99
mvg	7	12	13	1	0	35	5	9	18	100
nsa1	4	13	35	0	0	30	0	6	11	99
oen2	10	21	10	0	0	28	6	12	12	99
pls	7	17	19	4	0	28	0	10	12	97
rda	2	10	35	0	0	28	2	10	12	99
skf1	6	25	0	0	0	37	0	16	22	106

table 4.3.1 X-ray diffraction results

table 4.3.2 X-ray diffraction normalised results

XRD normalised results **CoK alpha wavelength lamda = 1.7902**

sample	feldspars %	quartz %	calcite %	dolomite %	non-clays %	mica group %	kaolinite %	smectites group %	chlorites group %	clays %	total %
arv3	4.08	15.31	43.88	0.00	63.27	25.51	2.04	6.12	3.06	36.73	100
er1	3.16	12.63	38.95	1.05	55.79	23.16	0.00	6.32	14.74	44.21	100
psf1	1.02	5.10	73.47	0.00	79.59	12.24	0.00	6.12	2.04	20.41	100
rtk	6.19	7.22	59.79	3.09	76.29	12.37	4.12	2.06	5.15	23.71	100
slm1a	15.00	31.00	36.00	3.00	85.00	8.00	0.00	3.00	4.00	15.00	100
slm2a	7.22	20.62	25.77	0.00	53.61	15.46	8.25	10.31	12.37	46.39	100
slm6a	5.10	16.33	38.78	3.06	63.27	18.37	0.00	6.12	12.24	36.73	100
slm7a	7.00	18.00	41.00	3.00	69.00	18.00	0.00	9.00	4.00	31.00	100
slm20	5.77	11.54	24.04	6.73	48.08	28.85	1.92	5.77	15.38	51.92	100
slmB2	5.15	16.49	28.87	0.00	50.52	24.74	3.09	9.28	12.37	49.48	100
slm1t	5.15	5.15	78.35	1.03	89.69	5.15	0.00	0.00	5.15	10.31	100
slm4t	2.13	13.83	53.19	0.00	69.15	15.96	2.13	10.64	2.13	30.85	100
tkr	2.13	10.64	53.19	0.00	65.96	15.96	5.32	6.38	6.38	34.04	100
agn1	5.21	14.58	30.21	0.00	50.00	26.04	4.17	7.29	12.50	50.00	100
agn2	6.19	18.56	23.71	0.00	48.45	20.62	6.19	9.28	15.46	51.55	100
kd	9.90	18.81	19.80	0.00	48.51	29.70	0.00	7.92	13.86	51.49	100
kd1b	4.81	7.69	13.46	4.81	30.77	30.77	0.00	24.04	14.42	69.23	100
kks1	10.10	26.26	16.16	2.02	54.55	19.19	3.03	10.10	13.13	45.45	100
kvt-a.l.p	9.90	18.81	13.86	0.00	42.57	19.80	4.95	14.85	17.82	57.43	100
kvt1h.p.b	4.08	17.35	32.65	0.00	54.08	19.39	6.12	18.37	2.04	45.92	100
kvt2	10.64	21.28	15.96	0.00	47.87	21.28	5.32	14.89	10.64	52.13	100
ll1	6.19	13.40	14.43	0.00	34.02	28.87	2.06	16.49	18.56	65.98	100
lts	8.25	20.62	4.12	0.00	32.99	30.93	5.15	5.15	25.77	67.01	100
xlm-m.p	3.06	20.41	26.53	3.06	53.06	23.47	2.04	11.22	10.20	46.94	100
ktr2	10.10	10.10	46.46	2.02	68.69	20.20	3.03	5.05	3.03	31.31	100
mvg	7.00	12.00	13.00	1.00	33.00	35.00	5.00	9.00	18.00	67.00	100
nsa1	4.04	13.13	35.35	0.00	52.53	30.30	0.00	6.06	11.11	47.47	100
oen2	10.10	21.21	10.10	0.00	41.41	28.28	6.06	12.12	12.12	58.59	100
pls	7.22	17.53	19.59	4.12	48.45	28.87	0.00	10.31	12.37	51.55	100
rda	2.02	10.10	35.35	0.00	47.47	28.28	2.02	10.10	12.12	52.53	100
skf1	5.66	23.58	0.00	0.00	29.25	34.91	0.00	15.09	20.75	70.75	100
ts71(*)	0.00	26.00	45.00	0.00	71.00	13.00	0.00	14.00	0.00	27.00	100
ts26(*)	0.00	15.00	61.00	0.00	76.00	9.00	0.00	10.00	0.00	19.00	100

(*) from Tsiambaos (1987)

X-Ray Fluorescence Table of Results

sample	SiO2 %	Al2O3 %	Fe2O3 %	MgO %	CaO %	Na2O %	K2O %	TiO2 %	MnO %	P2O5 %	S %	L.O.I %	total %
ER1	36.57	8.98	3.05	2.58	20.98	0.69	1.96	0.42	0.06	0.09	0.11	22.55	98.04
KVTA lp	52.53	12.00	5.00	3.36	8.36	1.14	1.82	0.62	0.10	0.13	0.01	15.11	100.18
MVG	50.89	12.50	5.56	3.21	8.30	1.15	2.53	0.68	0.08	0.11	0.14	16.13	101.36
KVT1hpb	37.25	8.96	3.88	2.61	18.25	0.40	1.90	0.40	0.12	0.12	0.90	26.01	99.91
KTR2	20.12	7.16	2.46	2.46	25.82	0.35	2.07	0.25	0.19	0.09	0.06	38.57	99.35
KVT2	48.35	12.50	5.58	3.82	8.50	0.99	2.01	0.69	0.08	0.09	0.01	18.49	101.11
ARV3	36.25	8.14	3.16	2.11	25.56	0.55	1.89	0.36	0.09	0.09	0.00	21.94	100.14
RTK	16.89	5.21	1.83	1.79	33.65	0.39	1.48	0.20	0.04	0.07	0.19	37.89	99.63
TKR1	20.19	6.17	2.03	2.03	29.21	0.40	1.60	0.25	0.04	0.08	0.01	39.03	101.04
PFS1	15.62	3.46	1.15	1.33	42.61	0.40	1.00	0.14	0.03	0.05	0.02	34.05	100.31
SLM1T	14.00	1.13	1.05	1.03	44.22	0.10	0.52	0.12	0.02	0.05	0.01	36.52	98.77
SLM4T	19.89	6.24	1.66	1.86	28.99	0.35	1.36	0.23	0.04	0.06	0.01	38.98	99.67
SLM20A	39.23	11.61	5.57	3.78	13.11	0.47	2.72	0.56	0.08	0.09	0.00	23.00	100.22
SLM2A	45.62	8.59	3.38	2.88	16.21	1.09	1.37	0.46	0.08	0.10	0.01	20.51	100.30
SLM7A	38.98	8.27	2.90	3.04	18.80	0.79	1.58	0.40	0.09	0.09	0.00	26.92	101.86
SLM6A	34.39	7.90	3.37	4.60	19.01	0.69	1.57	0.39	0.10	0.08	0.00	29.14	101.24
SKF1	58.00	16.22	7.10	3.64	1.02	1.44	2.75	0.95	0.06	0.06	0.05	10.13	101.42
AGN1	39.96	9.10	4.36	3.32	16.14	0.52	2.11	0.43	0.11	0.10	0.02	24.03	100.21
AGN2	42.72	9.53	4.66	3.47	12.86	0.53	1.86	0.49	0.09	0.15	0.01	26.36	102.73
OEN2	61.16	16.06	6.45	3.14	0.74	1.28	2.41	0.87	0.07	0.03	0.01	8.14	100.36
LTS1	52.57	16.50	8.18	3.66	1.89	0.62	2.66	0.99	0.11	0.08	0.01	15.12	102.39
NSA1	39.05	9.29	4.06	3.29	17.19	0.64	2.44	0.42	0.10	0.08	0.14	22.81	99.51
RDA	36.43	10.56	4.47	2.33	17.54	0.42	2.41	0.45	0.09	0.09	0.00	27.75	102.54
XMLMP	38.91	9.19	4.65	4.00	14.44	0.51	2.02	0.46	0.10	0.12	0.03	28.64	103.07
KD1B	46.51	11.13	5.15	4.43	10.81	1.71	2.54	0.57	0.07	0.08	0.13	15.09	98.22
KKS1	51.37	10.97	4.55	3.99	9.84	1.16	1.83	0.59	0.09	0.11	0.06	14.91	99.47
LL1	49.98	12.87	6.27	3.73	7.84	0.65	2.03	0.71	0.11	0.09	0.01	17.81	102.10
PLS	46.89	12.65	4.80	3.14	10.17	0.90	2.32	0.59	0.08	0.10	0.02	20.91	102.57
KD	43.45	10.90	4.60	4.32	11.50	1.71	2.29	0.51	0.06	0.10	0.18	19.06	98.68

table 4.3.3 X-ray fluorescence results

Table 4.3.4

		Korinthos	Preveza Igoumenitsa	Amalias Goumeron
feldspars	max.	15	10	10
	min.	1	3	2
	average	5.2	7	6.7
quartz	max.	31	26	25
	min.	5	8	10
	average	13.8	17.6	15.4
calcite	max.	76	32	46
	min.	25	4	0
	average	44.5	18.8	22.6
mica	max.	30	30	37
	min.	5	19	20
	average	16.8	24.2	29.4
kaolinite	max.	8	6	6
	min.	0	0	0
	average	2	3.5	2.3
montmoril l	max.	10	25	16
	min.	0	5	6
	average	6.1	12.5	9.7
chlorite	max.	16	25	22
	min.	2	2	3
	average	7.5	13.8	12.8

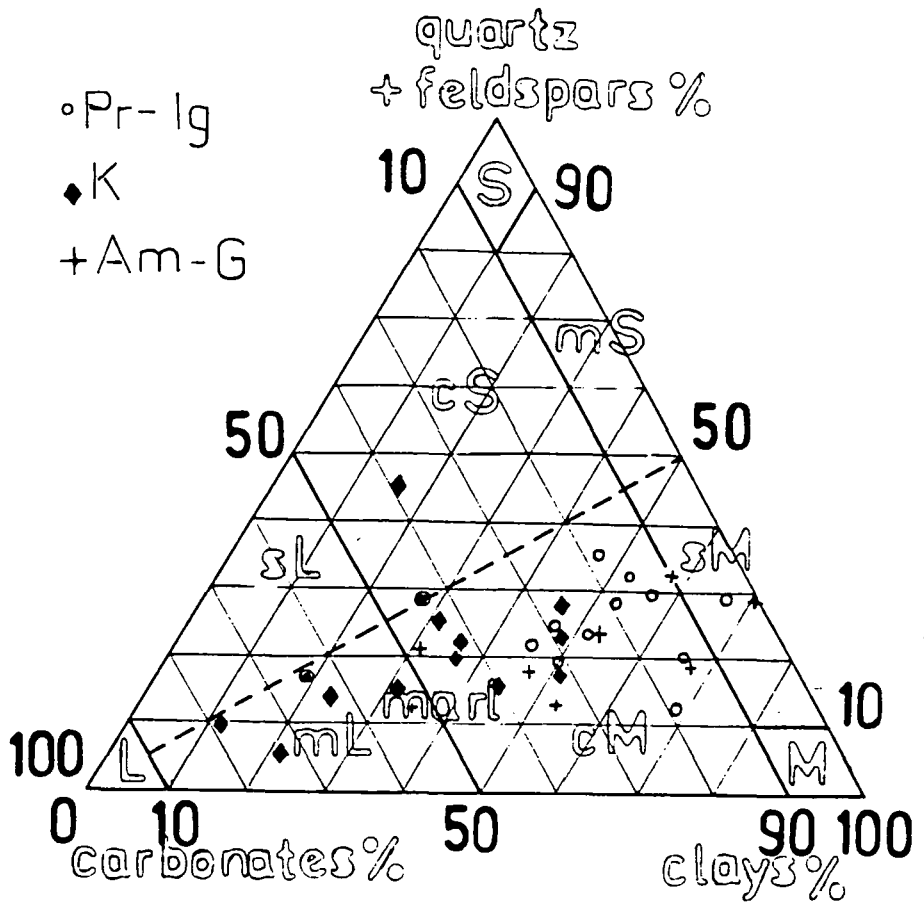

Fig. 4.3.3 Petrological classification of the studied samples. More information on the nomeclature shown can be found in fig. 4.1.2.

different characters between themselves (table 4.3.2). Though the changes may not be dramatic for this particular crossection, it is clear that there are changes in character at short distances both in the vertical and the horizontal sense, typical of the fluvial and lacustrine depositional environments that prevail in the Korinthos area.

The Preveza-Igoumenitsa samples, shown as open circles, display more clayey and slightly sandier characters than those from Korinthos samples and lie inside the *"calcareous Mudstone"* zone. Sample LTS seen here as a *"sandy Mudstone"* has been classified based on grain size as silty clay. By comparison, sample KD Ab, although it contains similar amounts of clay minerals to LTS, it contains 18.3% of carbonates (compared to only 4.1% in LTS) classifying it as *"calcareous Mudstone"*.

The Amalias-Goumeron samples, shown as crosses, exhibit more varied behaviour ranging from *"marl"* (KTR2) to *"sandy Mudstone"* (SKF1) reflecting the wide variety of depositional facies and environments active in the area during the Plio-Pleistocene. The same wide range was also shown for the grain size based classification. The Irakleion samples TS71 and TS26, shown as dotted circles, lie inside the *"marl"* and *"muddy Limestone"* areas respectively.

4.4 Discussion

4.4.1 General

The tested samples have shown a fairly wide range of characters in both terms of mineralogy, plasticity and grain size distribution, although certain local characters may appear as prevalent, e.g. the high percentage of carbonates in Korinthos samples, the silt size fraction groupings of Preveza-Igoumenitsa samples, the more plastic nature of the Amalias-Goumeron samples. These locally occurring characters reflect the geological conditions and evolution of the investigated areas deliberately chosen to ensure the maximum diversity of the sampled materials (see also section 3.1)

4.4.2 Plasticity and Grain Size.

The test results compare comfortably with similar investigations by Koukis (1977;1985), Tsiambaos (1987) and Rozos (1991) on fine grained Neogene formations of Pyrgos, Lefkas, Irakleion and N.W. Peloponessos respectively. Koukis (1977) reported on silty clays, clayey silts and stiff marls from Pyrgos. Rozos (1991) reported clay fractions between 21% and 65%, silt 34%-76%, and sand 1%-15% for the "argillaceous marls" of the plio-pleistocene formations and clay 3-33% silt 53-82% and sand 1-44% for some of the deeper "marly" horizons. He showed plasticities ranging between CL to CH for the former while the latter concentrated inside the CL area.

4.4.3 Specific Gravity

The values of specific gravity may seem lower (range 2.50-2.70) than those quoted by Rozos (1991) (range 2.65-2.70). The majority of the samples presented here, however, lie within the 2.65-2.70 range. This is consistent with tables published by

Goodman (1980) based on specific gravities of common minerals. Low values of Gs may be attributed to increased clay aggregations and\or the presence of poorly crystalline micro porous calcite particles that trap air in their voids (Rozos, 1991).

4.4.4 The Effect of Drying on Plasticity

The effect of temperature variation and most notably of oven drying prior to Atterberg limits determination has been known as source of erroneous results (Voumoos, 1965; Townsend, 1965; Townsend, 1985; Rao et al, 1989; Ctori, 1989). It has been shown that the liquid limit is more affected by oven drying than the plastic limit, but both decrease with increased temperature. This is quite pronounced in the presence of lime while curing time might be of equal importance (Rowlands, Arabi & Delpak, 1987). Possible mechanisms involve increased normality N of the intersticial water resulting in increased concentration of exchangeable ions facilitating stronger particle attraction. The latter leads to stronger capillary stresses and growth of stronger Van den Waals and Coulombic bonds, hence the available interparticle space reduces and so does the specific surface of clay particles resulting in depressed plasticity values (Rao et al, 1989; Muhunthan, 1991). The findings reported in table 4.2.9 are in agreement with Rao et al (1989).

4.4.5 Free Swelling

As already mentioned in section 4.2.6 Head (1980) suggested that values of free swell below 50% show no significant expansive potential. This in conjunction with the found range 0%-37% is in partial disagreement with the Williams & Donaldson (1980) graph shown in figure 4.2.7. The disagreement which shows as a weak correlation in figure 4.2.9 springs from the fact that the test as developed by Gibbs and Holtz (1956) is only indicative of the relative ability of minerals to adsorb water molecules and by no means predictive of exact patterns of expansive behaviour as the minerals are not allowed to compact and come to close proximity prior to the start of the test.

4.4.6 Mineralogical contents

The X-ray diffraction analysis has revealed that the studied formations show diverse characters which do not necessarily justify their commonly held petrological field description as *"marls"*. The localised characters both in terms of wider sampling area and sampling site are in perfect agreement with the nature and depositional history of those formations.

Such diversity has been observed also by Tsiambaos (1987) for the Irakleion Marls who identified two sub-groups of formations. From the first group, the whitish-yellow and the brown-yellow ones showed a strong presence of calcite with the latter ones showing higher values of quartz.. From the second group, the light-grey and the grey-blue ones showed more clayey characteristics than the whitish-yellow and the brown-yellow marls with the light-grey ones displaying a remarkable 25% mintomorillonite content. The grey-blue marls showed slightly higher values for calcite and quartz contents and a marked increase in chlorites than the light-grey ones. In general, there is an agreement in terms of detected mineralogical species but in quantitative terms there was some disagreement on the percentage of feldspars present with those samples studied by the author who found feldspars present in average quantities averaging 5-7%. Finally Tsiambaos (1987) suggested a link between the colour of the formations that he studied and their mineralogical nomeclature. Such link could not be confirmed by the author apart from the apparent observation that the light coloured samples were more likely to have appreciable amounts of calcite.

Kostopoulos (1988) suggested values for calcite, quartz, feldspars and clay minerals (totals) which agree reasonably with the general trends identified by the author with the exception of the main clay minerals for the Korinthos specimens suggested by Kostopoulos (1988). He identified chlorite and montmorillonite as the main clay species (6-7%). The author found that mica minerals were dominant (16.8% on average) while chlorite and montmorillonite were secondary minerals (7.5% and 6.1% respectively). The author believes that the Korinthos samples presented by Kostopoulos came from the Canal area which in itself is a localised special case of deposits.

Cavounidis *et al* (1988) have also given mineral ranges for "a Pliocene marl" from Ipeiros implying the area examined by the author. They suggested ranges for carbonates (20-25%), quartz (20-25%), feldspars(10%) and clay minerals (illite and chlorite at 35-40%) which lie within the lower band of the presented in this thesis range for the Preveza-Igoumenitsa samples. However it is important to note that the authors mentioned have not reported any montmorillonite being present. The author believes that the absence of montmorillonite from the mineralogical suit mentioned by Cavounidis *et al* (1988) may be due to incorporation of the chlorite since montmorillonite was detected in every Pliocene sample from the Preveza-Igoumenitsa area at an average 12.5% content.

From an area with separate Plio-Pleistocene evolution from those presented in this thesis, Rozos' (1991) results are interestingly similar in both qualitative and quantitative terms to the range of results presented in this thesis. The author agrees with Rozos (1991) that illite and chlorite are the likely dominant clay minerals. It is implied that this is due to the absence of advanced weathering of either the parent rock or the present formation since the afore mentioned minerals are products of the early stages of weathering . This is consistent with the high rhythms of denudation reported by various authors for most of the Neogene and Quaternary formations in Hellas.

In general, any comparison between the mineralogical contents of "marls" from elsewhere and those studied by the author can only be subjected to the wide range of the quoted values and always taking into account the differences arising from different localised geological evolution

4.4.7 Aggregation Ratio

It has long been recognised that there is a discrepancy between the clay minerals' content detected by X - Ray diffraction semi-quantitative analysis and the clay size fraction (2<μm) calculated from the sedimentation test (Dumbleton & West, 1966; Davis, 1967 and others). The difference between the two quantities was ascribed to the aggregation of individual clay minerals into particles of larger size and was expressed by Davis (1967) as the *aggregation ratio* :

$$A_r = \frac{\text{clay minerals content \%}}{\text{clay size fraction \%}}$$

Table 4.4.1 presents the aggregation ratio values for a number of samples considered in this thesis. The presence of clay mineral aggregations in other Hellenic fine grained formations has been reported by other researchers (Cavounidis, 1980; Cavounidis & Sotiropoulos, 1980; Andronopoulos, 1986; Tsiambaos, 1987; Rozos, 1991).

Most of the above mentioned authors attempted to explain the presence of such mineral aggregations by suggesting a cementing agent responsible for "glueing" the clay minerals together. Such agents could be minerals that can form colloidal solutions such as calcium carbonate, pyrite and magnesium oxides.

However, the phenomenon of *ageing* provides a better description of the

mechanisms that contribute to aggregation. There is a natural tendency of the clay minerals to flocculate. Flocculation should be distinguished from aggregation as the latter may additionally incorporate cementation as a mechanism. The presence of cementing agents is not necessary for flocculation to take place. Dispersions of clay minerals in water are classified as *lyophobic colloidal systems*, which in contrast to the *lyophilic colloidal systems* are not in thermodynamic equilibrium state; they tend to coarsen by recrystallisation of the particles to minimise he Gibb's interfacial energy (van Olphen, 1987). The presence or the addition of an *inert* electrolyte (one that does not react chemically with the clay particles) promotes flocculation and further aggregation of the clay mineral particles.

It should also be remembered that naturally occurring clay minerals may reach individual maximum sizes of up to 10 μm (e.g. hydrated muscovite). In this respect, the traditionally held view in the engineering world that clay particles have a maximum size up to 2 μm can prove to be misleading. Equally there is no reason to believe that only clay minerals may be found in the clay size fraction of a soil. As shown in studies with calcretes, the presence of micritic calcite was detected in abundance in the clay size fraction. Similarly amorphous quartz can be found in the clay size fraction of fine grained mudrocks. In such cases it may be expected that the percentage by weight of the clay minerals detected will be less than the percentage by weight of the clay size fraction, thus leading to A_r values below unity. However A_r values below unity have little meaning because they tell us nothing about the degree of aggregation or disaggregation of the clay minerals present.

In table 4.4.1 a number of samples exhibit A_r values below unity. It can be seen that generally the more calcite in a sample the more the chances of any specific sample having $A_r < 1$. Figure 4.4.1 shows that this becomes more apparent for calcium carbonate values in excess of 40% whereas for calcium carbonate values below 40 % there is no trend. Additional data points from Rozos (1991) corroborate the above observation. It can also be seen that there is a boundary line (Fig. 4.4.1) indicating there is a limiting condition (i.e. a lower calcium carbonate value) for any of the marly soils tested to have a specific A_r value. This observation might suggest that for any further decrease of A_r to the left of that line there has to be an increase in calcium carbonate content for a specific soil.

In this respect, it is possible that the presence of micritic calcite in a depositional environment may initially promote the process of flocculation. However, any further infusion of calcium carbonate in the pore water solution over a critical value

seems to have no effect on the clay minerals other than an increased precipitation of micritic calcite from the pore water solution which is consumed in the formation of cementation bonds. Such an increase in calcite content will nevertheless have an effect on the clay size fraction by increasing its percentage by weight for a given soil type. Rozos (1991) too noted that samples with high calcite and/or quartz content were likely to exhibit A_r values below unity.

The apparent paradox of having $A_r < 1$, (which according to Davis (1967) should imply that disaggregation is taking place), with increasing calcium carbonate content, which has been accepted to be a flocculation agent, shows that Davis' definition and quantification of aggregation are inadequate for soils other than those where only clay minerals can be found inside the clay size fraction.

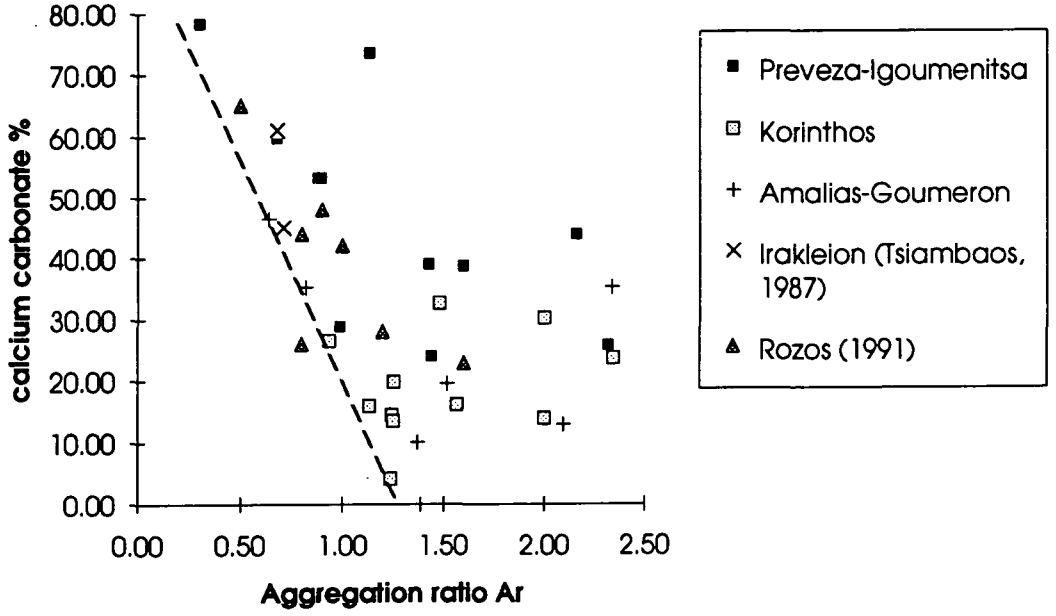

Fig. 4.4.1 The effect of calcium carbonate content on the aggregation ratio of some Hellenic formations.

table 4.4.1 Aggregation Ratio of Hellenic "Marls".

sample -	clay % fraction	clay % minerals	aggregat. ratio	calcium carb. %
XLM.MP	50.00	46.94	0.94	26.53
LL1	53.00	65.98	1.24	14.43
LTS	54.00	67.01	1.24	4.12
KD	41.00	51.49	1.26	19.80
KDAB	55.30	69.23	1.25	13.46
KVT2	46.00	52.13	1.13	15.96
KVTALP	29.00	58.00	2.00	13.86
KVT1HPB	31.00	45.92	1.48	32.65
KKS1	29.00	45.45	1.57	16.16
AGN1	25.00	50.00	2.00	30.21
AGN2	22.00	51.55	2.34	23.71
SLM1T	34.00	10.31	0.30	78.35
SLM4T	35.00	30.85	0.88	53.19
SLM2A	20.00	46.39	2.32	25.77
SLM6A	23.00	36.73	1.60	38.78
SLM21	50.00	49.48	0.99	28.87
SLM20	36.00	51.92	1.44	24.04
ARV3	17.00	36.73	2.16	43.88
ER1	31.00	44.21	1.43	38.95
PFS1A	18.00	20.41	1.13	73.47
RTK	35.00	23.71	0.68	59.79
TKR	38.00	34.04	0.90	53.19
NSA1	58.00	47.47	0.82	35.35
MVG	32.00	67.00	2.09	13.00
KTR2	49.00	31.31	0.64	46.46
PLS	34.00	51.55	1.52	19.59
RDA	22.50	52.53	2.33	35.35
OEN2	43.00	59.00	1.37	10.10
SKF1	51.00	70.75	1.39	0.00
TS71	38.00	27.00	0.71	45.00
TS26	28.00	19.00	0.68	61.00

Data from Rozos (1991)

D6 +	16.00	19.00	1.20	28.00
D16 +	21.00	17.00	0.80	44.00
D17 *	29.00	26.50	0.90	48.00
D18 *	20.00	20.00	1.00	42.00
D25 +	25.00	12.20	0.50	65.00
D28 +	33.00	23.00	0.80	26.00
D29 *	29.00	46.00	1.60	23.00

*denotes semi-quantitative XRD results.
+denotes XRF infered results

4.4.8 Minerals and Grain Size

The sizes of individual minerals as examined under the petrographic microscope can vary quite significantly depending on many and rather complicated processes that a sample has been subjected to during its geological history.

For the sedimentary rocks and soils such processes may include breaking up along cleavage lines or rounding during the weathering of the parent rock, further grinding and differential deposition during transport, varying geochemical conditions during deposition and burial etc. It is then reasonable to assume that samples from different sites but from the same stratigraphic unit may exhibit different characters especially in terms of grain size. However changes in grain size frequently imply changes in the mineralogical contents qualitatively and/or quantitatively

Such relationships are attempted in figures 4.4.2 to 4.4.6. Since the grain sizes of the various clay minerals tend to be confined within relatively narrow bands ranging only few microns in between, it was thought more appropriate that larger diameter mineral particles should be considered. Trends between calcite, quartz and coarse fraction sizes have been examined. In these figures the influence of the local geological conditions can be seen.

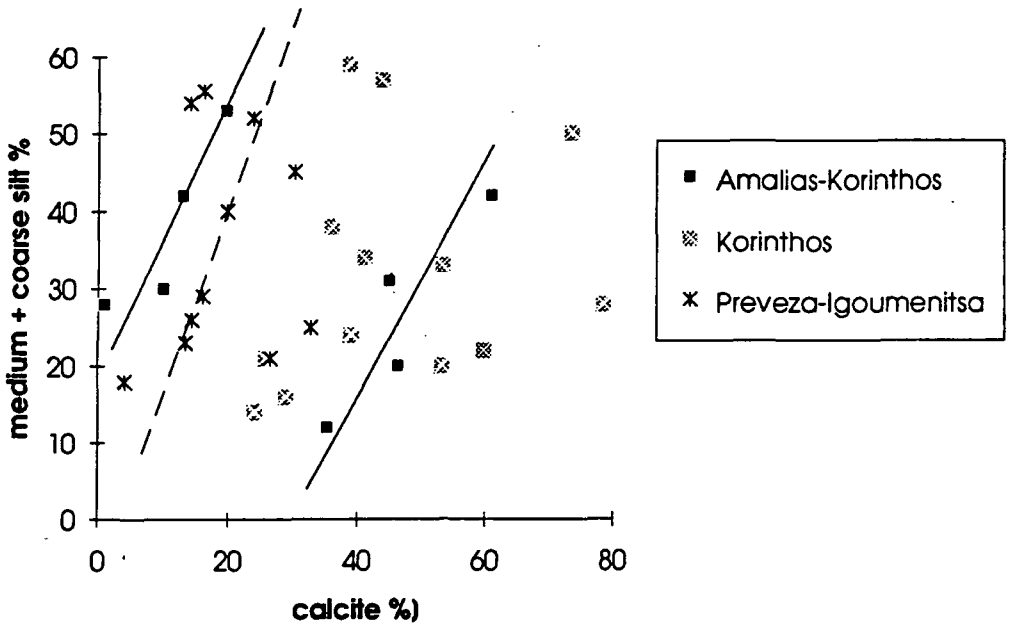

Fig. 4.4.2 Correlation between calcite and the medium plus coarse silt fraction

In fig 4.4.2 no trend can be seen for the Korinthos samples. On the other hand, there are two distinct groupings of samples for the Amalias-Goumeron (continuous line), one at low and one at intermediate calcite contents showing very similar trends of increase in medium plus coarse silt size content. Preveza - Igoumenitsa samples show a clear trend of increasing medium plus coarse silt size content with increasing calcite content.

Figure 4.4.3 shows the correlation between quartz and coarse silt plus sand size contents.Korinthos samples show a weak trend of increased size content with increased quartz content. A similar but clearer trend is shown by the Preveza-Igoumenitsa samples while the Amalias-Goumeron samples showed no trend.

Figures 4.4.4, 4.4.5 and 4.4.6 show correlations between fine silt and quartz, fine silt and calcite and medium silt and calcite contents respectively. There was no correlation of any kind between medium silt and quartz contents. Figure 4.4.4 shows a negative correlation existing for Amalias-Goumeron samples. The samples from the other two areas show a very weak if any trend at all.

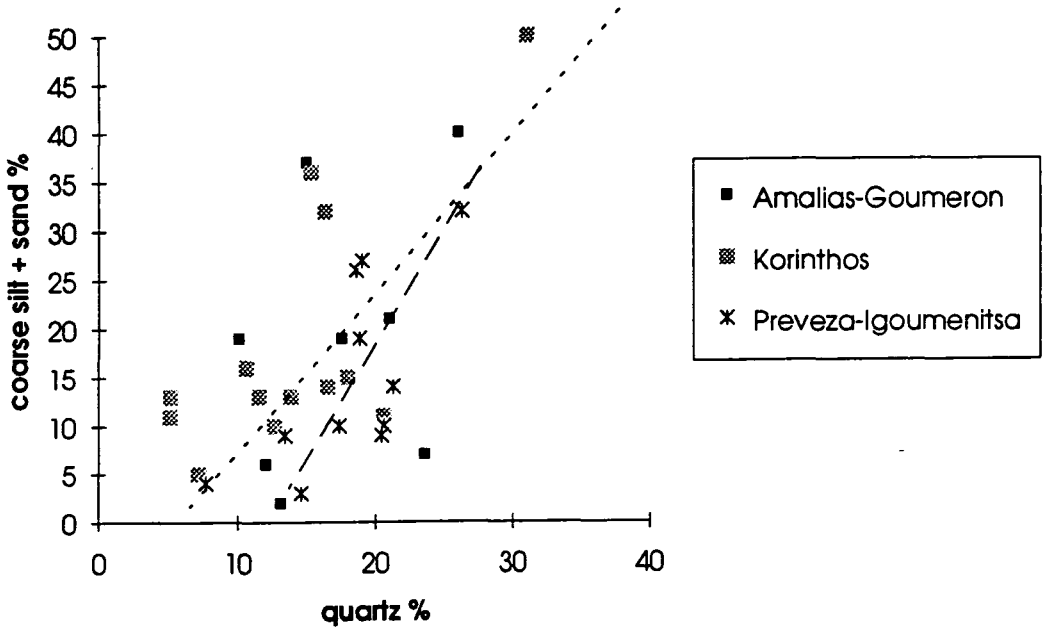

Fig. 4.4.3 Correlation between quartz content and coarse silt plus sand particle size

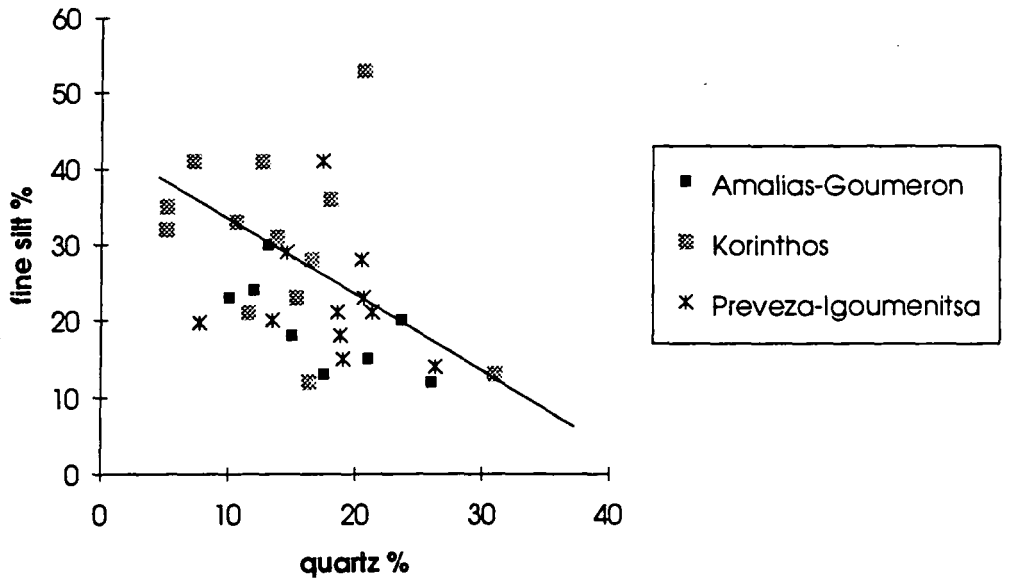

fig. 4.4.4 Correlation between quartz content and fine silt particle size

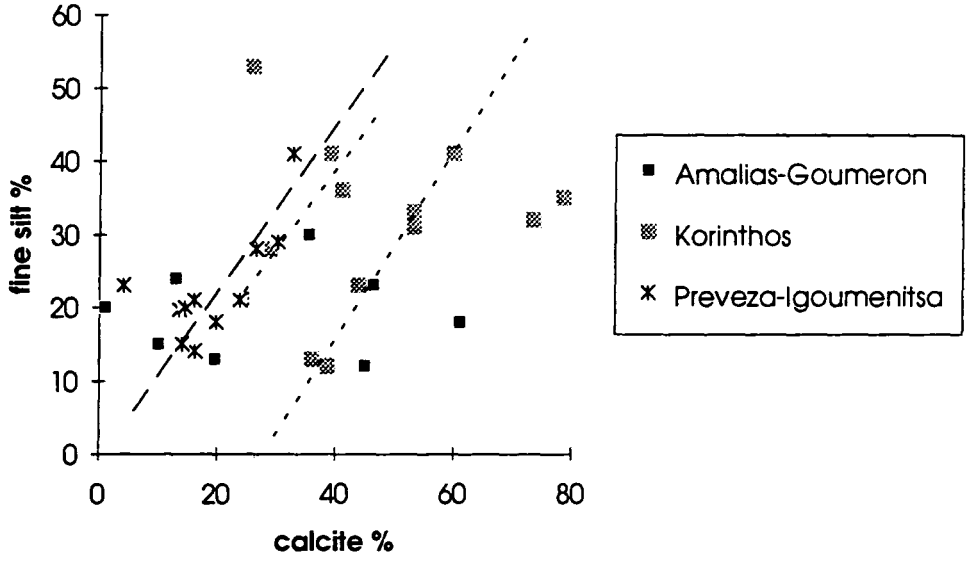

Fig. 4.4.5 Correlation between calcite content and fine silt particle size

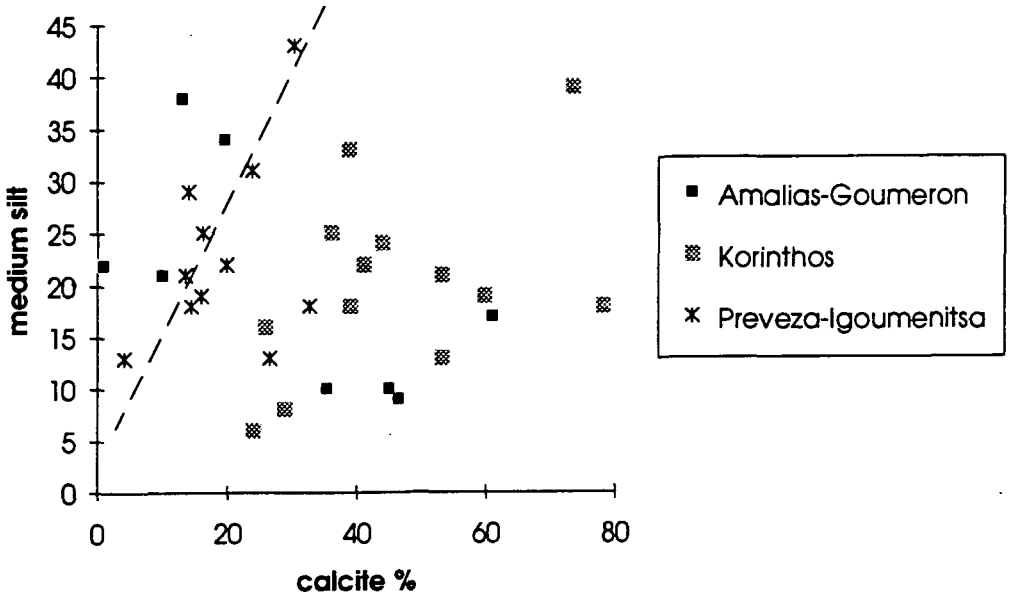

Fig. 4.4.6 Correlation between calcite content and medium silt particle size

In summary, correlations between certain grain sizes and types of minerals exist but their type and magnitude depends on local geological contitions. There is a general trend of positive correlation between calcite and quartz and the coarser members of the silt and sand size fraction. Similar trends were shown to exist for calcite by Tsiambaos (1991) and Hawkins & Mc Donald (1992) who reported a drop in medium and coarse silt size after samples of Irakleion marls and Fuller's Earth were decalcified.

CHAPTER 5
RESIDUAL STRENGTH

5.1 Literature Review

5.1.1 Introduction

The post-peak reduction in the drained shear strength of cohesive soils has been recognised and studied extensively in the laboratory and field by many investigators. The ultimate post-peak drained strength of clay is termed **residual strength.**

The major understanding of residual strength came with Skempton (1964) in the 4th Rankine Lecture. Skempton showed that the strength along any discontinuity in a clay mass is governed by the residual strength of clay. Consequently, most of the work, which has followed since, on the drained residual strength and brittleness of cohesive soils has concentrated on geotechnical problems concerning slope stability, bedding shears, joints or faults, embankments, post failure (back) analysis, as well as on testing techniques, identification of contributing factors and various correlations (Peck, 1967; Skempton & Petley, 1967; Chandler, 1970, 1974, 1977, 1979; Calabresi & Maufredini, 1973; Kenney 1967, 1977; Lupini 1980; Bromhead 1979; and others)

Residual strength is generally determined from one or more of three types of tests: i) reversible shear box (direct shear) test, ii) triaxial compression test & iii) ring shear test. The ring shear apparatus provides lower bound results, whereas the reversible shear box provides upper bound values. The triaxial compression test produces significantly higher values than the other two test procedures. Field values have been obtained by means of back analysis. Later work proves the significance of rate effects and a better insight is given to the practical usage of the various correlations and testing techniques (Lemos, (1986); Hawkins et al., (1988); Tika, (1989); Anayi, (1990); Tsiambaos, (1991); and others).

5.1.2 Major Contributions to the residual strength concept.

5.1.2.1 4th Rankine Lecture (Skempton, 1964)

Following previous work by other researchers Skempton (1964) set the foundations for a comprehensive understanding on the concept of residual strength during his 4th

Rankine Lecture. Skempton (1964) showed that the strength along any discontinuity in a clay mass is governed by the residual strength of the soil. He also reported residual strength measurements from a reversible shear box and reviewed the effect of residual strength on slope stability. Skempton postulated, further, a general correlation between residual strength and clay fraction suggesting a relatively smooth transition from high to low angles of friction levels with increasing clay content. He claimed that the residual strength of a clay is unique for a particular normal effective stress and does not depend on previous consolidation history, sample preparation or initial water content.

5.1.2.2 Lupini's contribution

Lupini (1980) and Lupini et al. (1981) propounded the present understanding of the mechanism of residual strength in terms of shearing mode which was found to be strongly associated with clay mineralogy. Three modes were identified:

i) The turbulent mode occurred in soils dominated by rotund particles or soils with platy particles exhibiting a high coefficient of interparticle friction. Residual strength remains high while no orientation occurs and brittleness is due to dilatant behaviour only. A shear zone is only a zone of different porosity and it is considerably modified by subsequent stress history.

ii) The sliding mode occurs when platy low friction particles are dominant. A low strength shear surface of strongly orientated mineral particles develops and once fully formed behaves independently from subsequent stress changes. The ϕ_r' depends primarily on mineralogy, pore water chemistry and the coefficient of interparticle friction τ/σ_n'

iii) A transitional mode was recognised for samples where no particle size fraction appears dominant, involving the above two modes in different parts of the shear surface. In this mode, ϕ_r' becomes sensitive to small changes in grading of the soil.

It was concluded that correlations between residual strength and index properties and grading cannot be general, while their validity is associated with the degree to which they reflect changes in more fundamental properties such as, particle shape, mineral type, pore water chemistry etc. For prediction purposes such correlations can only be used when the above properties can be regarded as constant throughout a geological body. Finally, the importance of the shape of clay mineral particles on the residual angle of friction is acknowledged. The type of shearing mode and, to a lesser extent, the magnitude of the residual strength, correlates best with the granular void ratio e_g of the soil defined as the volume of platy particles plus voids to the volume of rotund particles. This correlation however, is not effective for the sliding

mode and for soils with high friction platy particles, such as those derived from cemented marls, mudstones and shales, requiring very large particle movements within the soil to produce sufficient clay particles along a concentrated zone for a full residual sliding shear mechanism to develop.

5.1.2.3 Skempton's (1985) contribution

Skempton (1985) presented an extensive review of the most important work following the 4th Rankine Lecture. Skempton concluded that the relationship between σ_n' and τ is non-linear. To overcome problems arising from this non-linearity, he suggested that different residual strength values can be compared to each other only if they correspond to the same normal effective stress levels. The discrepancy of approximately 2° between field parameters and parameters obtained using the ring shear apparatus was once again pointed out, especially for high clay fraction samples. Hence, the amount and suit of clay minerals is of tantamount importance. He claimed that the clay minerals can have little effect on residual strength when clay fraction is less than 20%. Conversely, with clay fraction exceeding 50%, the residual strength depends almost entirely on the character of the clay mineralogical suit. Skempton hinted at aggregation effects for problematic clay fraction to residual strength correlations and concluded that changes of shearing rate within the slow range (0.002-0.1 mm/min) make little difference whereas at rates exceeding 100 mm/min qualitative changes occur through probable disturbances of the original structure of the shear zone.

5.1.3. Slope stability and residual strength

As early as 1846 images of the residual strength concept, or more precisely the post-peak strength reduction, appeared in the literature (La-Gatta, 1970). During the first half of this century, Hvorslev (1936), Tiedman (1937), Haefeli (1938, 1951) and Henkel & Skempton (1954) were among the first few to contribute by demonstrating the existence of post peak reduction in strength and relating such values to slope stability problems. They suggested that the cohesion term c' should be ignored for better results.

In 1961 a report on the Selset slip by Skempton & Brown (1961), explained that if c' was set to zero the calculated factors of safety would fall to about 0.7 or even less. This was in strong contrast to the results from several analyses of very long term slips in overconsol;idated fissured clays where c' was found equal to almost zero. Skempton & Brown (1961) noted that the principal cause of this difference was not

fully understood, but they suggested that this might have been associated with to local overstressing and softening of the clay in the vicinity of the fissures, hinting at progressive failure.
Skempton (1964) showed that the strength along any discontinuity in a clay mass is governed by the residual strength of the soil. Binnie, Clark & Skempton (1967) found that shear zones have a higher average clay fraction than the rest of the clay mass, thus leading to lower strength values.

Following the 4th Rankine Lecture (Skempton, 1964), more studies on progressive failure of slopes were carried out. Slopes in overconsolidated fissured clays and mudrocks alike required special consideration. Large strains occurring locally due to fissuring, result in peak strength being reached and a subsequent decrease towards the critical state value. This phenomenon known as progressive failure may also be caused by considerable non-uniform shear stresses on a slip surface or its reactivation owing to external intervention, such as man-made excavations. Bishop (1967) concluded that slope stability problems usually arise from a non-uniform mobilisation of shear strength, which occurs even in ideally homogeneous soils. Bishop recognised the difficulty in relating in-situ failure surface values to laboratory test results. Again, Bishop (1971) referred to studies indicating significant non-uniformity of shear stress and stress ratio, identifying a possible error directly related to the brittleness of the soil, expressed as brittleness index.

$$I_B = \frac{\tau_{peak} - \tau_{residual}}{\tau_{residual}} \qquad (5.1.1)$$

Bishop added that I_B is strongly influenced by stress level and in anisotropic soils depends on the orientation of the principal stress. He also stated that the post peak displacement are typically associated with migration of water down the slip surface causing a temporary increase in pore pressure. Hence, the peak strength could be mobilised on parts of the slip surface while post-peak and pre-peak strengths would be operating elsewhere. In that manner, a small further displacement should be sufficient to bring the entire surface into a peak and post-peak state. Bjerrum (1967) postulated conditions for progressive failure to be present in overconsolidated plastic clays. These conditions relate to internal lateral force concentrations at the front of an advancing slide, the presence of recoverable strain to produce expansion along the slide and the residual strength to be lower that the peak strength.

The heterogeneity of the materials involved in a landslide is reflected in the landslide's nature as it allows for differing degrees of permeability, frost

susceptibility, slip surfaces concentration and strength loss alike, (Hutchinson et al, 1973). Their analysis on a landslide at Bury Hill, Staffordshire showed that a progressive loosening of the materials involved caused downslope components of movement. Although these components were not predominant they might have contributed to an initial shallow slip surface. Residual values were employed for the back analysis. It was found that laboratory obtained values did not correspond to field estimated values. It was suggested that side friction effects had contributed to the discrepancy.

Newbery & Baker (1981) reported on the Wenallt slope to the north of Cardiff. A 3 dimensional analytical model, JANMAS, was developed based on Janbu's (1973) non-circular failure model. They found that back analysis provided unrealistic values for strength parameters giving a highly misleading impression of the factor of safety for any remedial solution. This was attributed to the combination of side restraint and undulations of the shear surface. They concluded that a failure of the extent observed could have been predicted if the design and back analysis models incorporated laboratory residual strength parameters.

Cavoundidis & Sotiropoulos (1980) found irregularities in stress-strain behaviour of marly formations involved in a number of slides which occurred on excavated slopes in Ipeiros, Hellas. This behaviour was characterised as "quasi-residual" and describes an intermediate stress plateau between peak and residual strength. The authors suggest that if part of a clay slope is characterised by a quasi-residual behaviour a slope failure may cause the reduction of the shear strength along the slip plane only to the quasi-residual level. In this case the slope would be vulnerable to further sliding with a concurrent decrease of the shear strength along the failure plane to the final residual level. Skempton and Coates (1986) postulated that for most failures, like that at Carsington Dam, the critical state of stress conditions cannot be held up as a generalised explanatory mechanism. It was suggested that residual stress conditions provide a better framework for analysis.

Chandler (1984) reported that clays with plasticity index between 20% and 25% show good agreement between laboratory and field residual parameters. For clays with plasticity index greater than 25% it was shown that rapid strain softening and progressive failure are exhibited causing a departure of field values from laboratory obtained values. This discrepancy was also shown by Skempton (1985).

Lemos & Coelho (1991) discuss the strength of pre-existing shear surfaces at or close to residual values, under rapid loading and the implications to slope stability during and after an earthquake. They found static strength at the end of the movements to equal their residual value leading to a factor of safety equal to one. Also Lemos (1991), investigating the displacement rate effects on slopes, showed that for slopes on soils exhibiting a positive rate effect, i.e. increased strength with increased rate of shear, the influence of a change in displacement rate will be small. In sharp contrast, slopes on soils with a negative rate effect could be prone to fast failures of considerable displacements. He claimed that the negative rate effect constitutes an intrinsic soil property.

Finally Davachi et al. (1991) concluded, from their work on the Oldman Dam, Canada, that bedding plane shearing resistance is determined by summing its "primary" and "lesser" components. As primary component the authors suggest the residual angle of friction and as a lesser component the in-situ state, roughness and thickness of the plane, though they could not deliver a quantitative definition of the in-situ state.

5.1.4 Apparatuses for measuring residual shear strength

5.1.4.1 Apparatus Types

Three apparatuses are available for the measurement of shear strength of soils. These are the triaxial compression apparatus, the shear box and the ring shear apparatus.

Skempton's (1964) apparent focus on pre-existing shear surfaces led a number of researchers to use the triaxial apparatus, but, as Bishop, Webb and Lewin (1965) found, the triaxial test suffered from too little displacement. Chandler (1966) devised a correction factor for such measurements in the triaxial cell. Similarly Herrman & Wolfskill (1966) reported that the triaxial test results overestimate residual strength values.

The shear box offered a better alternative. By reversing the direction of shear one can attain large displacements. Most of the early work on residual strength was based on reversible shear box test results (Haefeli (1951); Skempton & Brown, 1961; Borrowicka, 1961, 1965; Horn & Deere, 1962; Skempton 1964; Chandler 1970, Kenney 1967; and many others). Two main restrictions arise from the non-constant shear surface area and the dislodgement of clay minerals during the

reversing of the shearing direction (Bishop et al., 1971). This can lead to an increased value of residual strength compared to field values. Chandler and Hardie (1989) proposed a new shear box technique using a thinner sample. They concluded that with samples having a predetermined shear surface, results came very close to the ones obtained by the thin sample technique and both were in good agreement with residual strength values obtained from back analysis.

To overcome the problems posed by the above mentioned apparatuses, devices based on the torsion principal were used (Hvorslev 1936, 1939; Sembenneli and Ramirez, 1969; and others). The idea was to use a circular specimen which then can be shear tested in a rotational motion. In such a case the attained displacement would be very large. As well as that the sheared surface area would remain constant through the test. In the early seventies, two sophisticated ring shear apparatuses were developed. The first one was by La-Gatta (1970) at Harvard University, USA, and the second one by Bishop et al. (1971) jointly by the Norwegian Geotechnical Institute and Imperial Colllege, University of London, U.K. Their development contributed significantly to the advancement of residual strength measurements. However, their relative complexity necessitated the development of a simpler apparatus. That came with Bromhead's (1979) device, developed at Kingston Polytechnic, UK, later standardised in BS1377:1990 (B.S.I., 1990).

5.1.4.2 Comparative Studies and Testing Methods

The presence of many different apparatuses for laboratory measurement of residual strength parameters led to numerous studies on the accuracy of laboratory estimates when compared with back analysis values of residual strength parameters. The proliferation of such devices also led to comparative studies of different testing procedures and their accuracy in predicting field values.

As already mentioned, the triaxial test procedures were quickly discounted for lacking the ability to generate adequate displacements. Chandler (1966) devised correction charts to overcome this problem and managed to derive identical results for Lias clay samples using reversible shear boxes and triaxial apparatuses (Chandler, 1970). Garga (1970) showed that ring shear test results were independent of loading sequence increments and specimen preparation. James (1970) found that ring shear test results did not correspond to field values of shear along existing planes, reitterating the need to take c' values equal to zero for practical purposes. Calabresi and Manfredini (1973) found that the cohesion intercept c' was equal to zero along joints and bedding planes and that ϕ_r' was reached after a smaller in-situ

displacement compared to that required in laboratory conditions. Chandler (1979) reported that ring shear test results underestimate field residual parameters.

Hutchinson, Bromhead and Lupini (1980) report on test results from Gault clay suggesting very similar ϕ_r' values obtained independently from a Bishop and a Bromhead ring shear apparatus. Bromhead and Curtis (1983) reported that results from a Bromhead ring shear apparatus were more consistent and quicker to obtain than those from reversible shear box. Chandler (1984) reported that clays with PI<20-25% have good agreement between laboratory and field residual parameters. For clays with high PI it was shown that rapid strain softening and progressive failure are exhibited causing a departure of field values from laboratory results. Chandler insisted, again, that ring shear tests underestimate field ϕ_r' values by 2° to 3°, where c' is taken as zero. Skempton (1985) arrived at a similar conclusion. Conversely Newberry & Baker (1981), Bromhead & Dixon (1986), Stark and Eid (1992) showed that the drained residual shear strength obtained from a Bromhead apparatus were in good agreement with field values from a variety of landslides and results from slip surface tests on shear zone materials. Cunningham (1986) concluded that the Bromhead apparatus produced less scatter than the Bishop one and that it provided a less time consuming test. Fell, Sullivan & MacGregor (1988) and Mathews (1988) carried out comparative studies between ring shear and shear box test results. Disparities between the laboratory obtained results were reported. The authors also showed that there was a disagreement between any of the laboratory results and corresponding back analysis values.

Anderson and Hammond (1988) found multi stage testing with the Bromhead apparatus provided good results for clays exhibiting turbulent and transitional behaviour. For clay exhibiting sliding behaviour, lower ϕ_r' values than those obtained from back-analysis were attributed to flattening of the shearing zone caused by subsequent consolidation before every new loading increment. Anayi *et al.* (1988, 1989) and Anayi (1990) proposed modifications to the Bromhead ring shear apparatus to overcome problems associated with losses of material during shearing and lack of reliable and consistent formation of a failure surface. The modification pointed to a thicker sample and vanes on the porous disc. Anayi et al. (1988) proposed a preshearing technique to facilitate the creation of a shear plane, thus reducing, the time required for attaining residual condition. Wykeham-Farrance (1988) made similar propositions.

Stark and Vettel (1992) pointed out that multistage tests tend to overestimate field values due to wall friction, while preshearing prevents an estimate of the drained post peak behaviour of the specimen. They have instead proposed a "flush" test procedure. According to this procedure remoulded soil is added on the surface of the specimen contained and it is allowed to reconsolidate. This would reduce wall friction. Only one test is performed per specimen. The authors claim that contrary to Anayi et al. (1989) the insertion of vanes on the porous discs increases the chances of overestimating residual parameters but no firm evidence was brought forward to support their claim.

5.1.5. Grain Size and Residual Strength

Borowicka (1961, 1965) based on reversible shear box data, suggested that for clays with higher colloidal content, ϕ_r' drops to a final low constant value which was attributed to the scale-like and flake-shape colloid reorienting along the shear plane. Skempton (1964) demonstrated that there is a non-linear relationship between residual strength values and clay fraction. Petley (1966) claimed that soils with clay fractions below 25% exhibit similar residual and peak strength parameters while Binnie, Clark and Skemton (1967) found that shear zones have a higher average clay fraction than the rest of a clay bed and that the higher the clay fraction the lower the residual parameters obtained. Kenney (1967) concluded that residual strength is predominantly dependent on mineral composition and not strictly related to plasticity or the clay size fraction. Townsend & Gilbert (1973, 1974, 1976) found that ϕ_r' depends on clay fraction and mineralogy and that has no relationship with index properties.

Skempton (1985) taking Kenney's (1967) statement into account asserted that any relationship between residual strength and clay fraction covering a wide range of particle size should need the same mineralogy for any comparisons to be valid. Hawkins and Privett (1985, 1986) went further to suggest that as in the case of τ/σ_n' comparisons, so in the case of clay fraction and plasticity correlations with ϕ_r' the effective normal stress level σ_n' has to be quoted for every set of correlations (i.e. different correlations for the various loading or unloading steps during a ring-shear test).

Lemos (1986) attributed the post maximum drop in shear resistance to displacement and displacement rate, as well as to clay fraction, the shape of massive, i.e. silt size and larger, particles and on the relative size of clay and massive particles. Collata et

al. (1989) developed a correlation that links ϕ_r' with the clay fraction and the plasticity for a large number of Italian soils. Tsiambaos (1991) attempted to correlate ϕ_r' and clay fraction & calcium carbonate content for a large number of Irakleion marls, Crete, Hellas. He found some agreement between his findings and the ϕ_r' vs clay fraction correlation by Skempton (1964). He also reported that after decalcification the ϕ_r' values dropped significantly. Similarly Hawkins & McDonald (1992), reporting on Fuller's Earth samples, found that decalcification leads to a drop in silt size particles volume causing a subsequent decrease of residual strength.

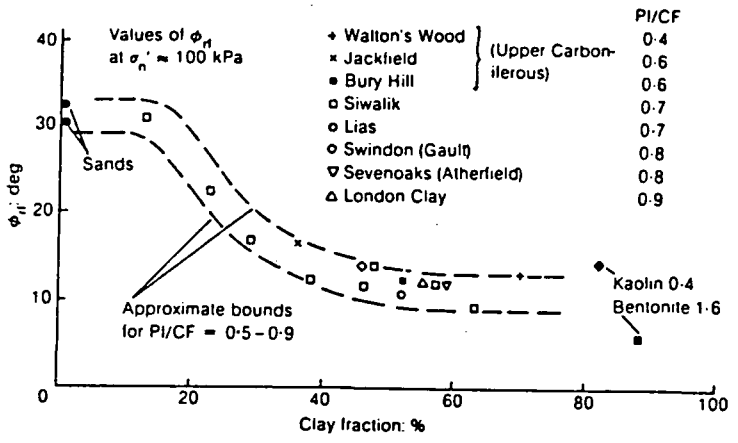

Fig. 5.1.1 Field residual and ring shear tests on sands, kaoline and bentonite (Skempton, 1985)

Tika (1989) suggested five behaviour types for the post peak residual strength against displacement rate variations. These types are closely related to clay fraction and plasticity of the samples tested. She also drew attention to "degradeable soils" containing aggregated clay minerals which tend to break down to their constituent minerals during higher rates of shear. The tendency of some low plasticity silty clays to show a marked drop in shearing resistance beyond a threshold displacement and displacement rate was also shown by Jardine & Christoulas (1991) and Tika & Vassilikos (1991).

5.1.6. Plasticity Indices and Residual Strength

Similarly to the clay fraction, plasticity indices have been a target of many researchers attempting to discover correlations which would enable a quick estimate of residual strength parameters.

Skempton (1964) first indicated that there should be a relationship between plasticity and residual strength for clays. Skempton (1985) specified approximate bounds for plasticity index over the clay fraction (*activity*) pointing out that lower ϕ_r' values are expected for clays and clay shales containing montmorillonite and having *activity*>1.5

Kenney (1967) argued that residual strength is primarily dependent on mineralogy rather than plasticity or clay size fraction. Voight (1973) has pointed out Kenney's (1967) arguement that Atterberg limits should not be discounted as residual parameters indicators since they are equally affected by mineralogy. He showed that there is a relationship of the form:

$$\phi_r'=b/(Ip)^a \qquad (5.1.2)$$

for a number of British and other formations. Kanji (1974) demonstrated that there is such a relationship and estimated parameters *a* and *b* to be equal to 0.466 and 46.6 respectively. Vaughan and Walbanke (1975) reported on the properties of Halloysite and Allophane soils as well as sedimentary and boulder clays. They deduced a relationship similar to Voight's (1973) between ϕ_r' and the inverse of *Ip*, for every group of the tested soils. It is interesting to note the difference between the Halloysite and Allophane soils and the sedimentary and boulder clays which led to two distinct curves with appreciable scatter of points.

Cancelli (1977) presented a correlation between residual strength and liquid limit of an exponential form:

$$\phi_r'=b*w_L^a \qquad (5.1.3)$$

where b = 453.1 and a = -0.85. A similar correlation was presented by Mesri & Cepeda-Diaz (1986) (fig.5.1.2). Saito and Miki (1975) suggested that the "plastic ratio" Ip/w_p should be used for correlations with ϕ_r'. They devised a prediction chart that gave ϕ_r' = 10°-20° for a plastic ratio of 1-2 ($w_L \geq 50\%$) and ϕ_r' = 5°-10° for plastic ratio values greater than 2. Seycek (1978) published data which related $\phi r'$ to the inverse of *Ip* as shown previously by Kanji (1974). Hawkins and Privet (1985), following Skempton's (1985) suggestion that when comparing one clay with another it is best to fix on a "standard" stress, presented correlations between $\phi r'$ and *Ip* for different stress levels, as can be seen on fig.(5.1.3).

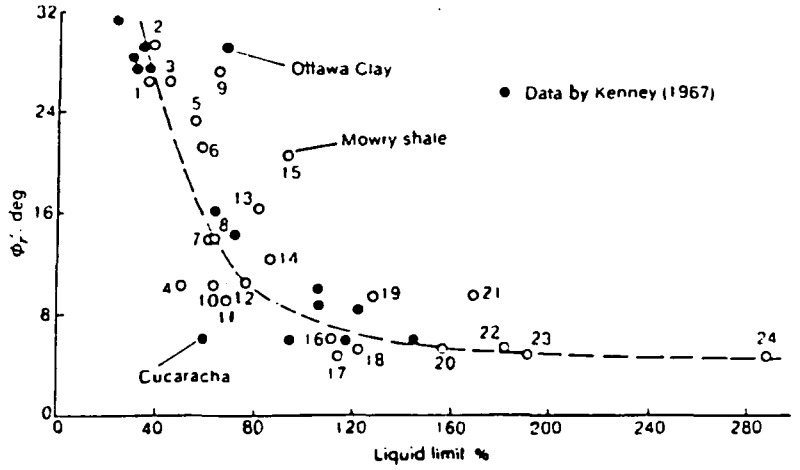

fig 5.1.2 Residual friction angle - liquid limit relationship (Mesri & Cepeda Diaz, 1986)

Similarly Miedema, Byers & McNeary (1981) found relationships between $\phi r'$ and Atterberg limits. Boyce (1984) tested on Zimbabwe soils and, as expected found, higher values of ϕ_r' for low plasticity silty clays than for highly plastic clays. He noted some differences for some silty clays which were explained as aggregation effects.

Collota et al. (1989) proposed a predictive correlation for the residual angle of friction of soils in the form:

$$\phi\ r' = f(CALIP)\ where CALIP = (c.f)^{2} * w_L * Ip * 10^{-5} \qquad (5.1.4)$$

The authors claim that the above expression produces gentler plotted curves and less scatter than previous correlations.

Tsiambaos (1991) reported on correlations found for marls from Irakleion, Crete, pointing at the pivotal role of $CaCO_3$ in determining residual strength parameters. He showed that decalcification increases the plasticity leading to lower strength values. Hawkins and McDonald (1992) working on Fuller's Earth samples found relations between decalcification and increased plasticity to have the same effect on residual strength values as in Tsiambaos' (1991) work. Anayi (1990) however stressing at the non-linear nature of residual strength parameters suggests that any correlation between residual strength and Atterberg limits should only be used as a guide.

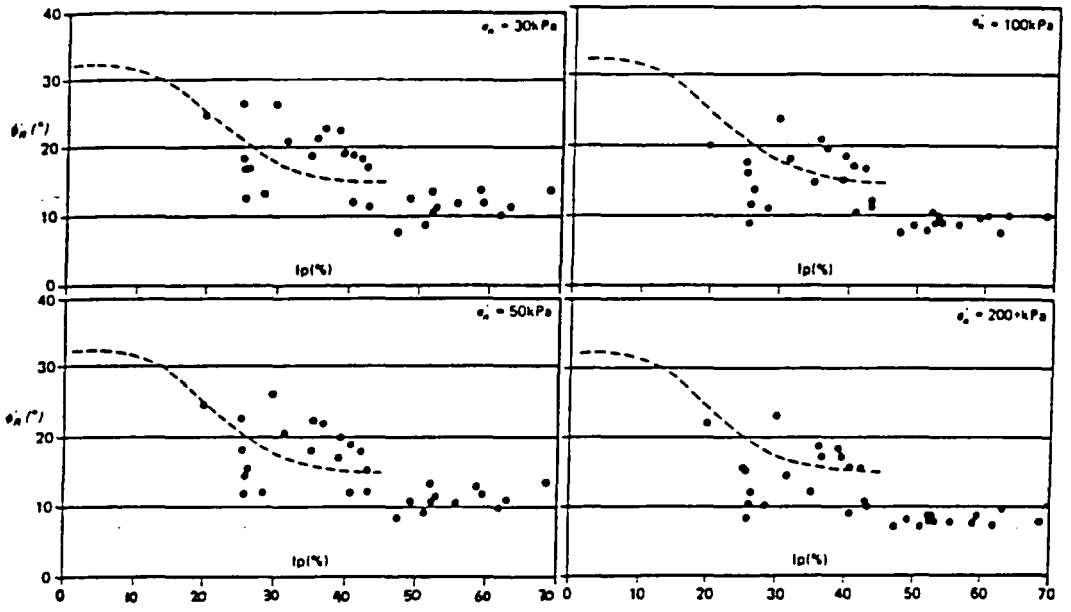

fig. 5.1.3. The relationship between ϕ_r' and *Ip* at different σ_n' . The line is suggested by Ingold (1975) for comparison; (after Hawkins & Privett, 1985)

5.1.7. Mineralogy and Pore Water Chemistry Effects.

The influence of mineralogy and pore water chemistry was recognised early by many researchers. Borowicka (1961, 1965) attributed the "final low constant value" of the angle of friction to the "scale-like" and "flake-shape" colloids reorienting along the shear plane. Additional evidence by Horn & Deere (1968) on interparticle friction, showed that micaceous minerals have a lower friction angle than rougher massive (e.g. quartz, calcite etc) minerals. Skempton (1964) and Petley (1966) also acknowledged the important role of mineralogical differences and the effect on strength parameters.

Kenny (1967) found that mineral shape is an important factor influencing shear strength. Rounded particles of the same size and species exhibited lower values of ϕ_r' than angular particles. Kenney (1967) pointed that the residual strength coefficient τ/σ_n' of massive (i.e. non-clay) minerals is dependent on particle shape and independent of particle size. He also pointed out the effect of hydrous mica and montmorillonite in lowering the residual strength levels. Kenney (1967, 1977)

suggested that the higher the cation concentration and the larger the valence, the greater the increase in residual strength. That was attributed to a net increase of attraction between the clay particles in parallel arrangement.

La-Gatta (1970) claimed that the pore fluid concentration only slightly affects residual strength test results. However, the pore fluid concentration of naturally occurring cations can only produce significant variations in results when significant time is allowed for it to act upon the constituent minerals of a sample.

Ramiah and Purushothamaraj (1971) showed that sample preparation might affect the structure of a clay but that had no visible effect on the resulting residual friction angle at a given normal stress level.

Chattopadhyay (1972) examined the type of cleavage and its mode at large strains for a number of clay minerals. He found that residual strength depends on the mode of cleavage as well as on the bonding energies available along cleavage planes at the shear zone particle contacts. He concluded that illite and other low-crystallinity minerals possess low residual friction angles while more crystalline minerals (e.g. attapulgite) possess higher values. The same author extended the concept of effective stress to include the interparticle stress due to physicochemical environment. He altered the Coulomb-Terzaghi relationship as follows:

$$\tau_r = (\sigma_n' - (R-A)) * \tan\phi_r' \qquad (5.1.5)$$

where (R-A) is the net interparticle stress due to the physicochemical environment. It was found that the application of flocculating and dispersive conditons could increase or decrease ϕ_b' respectively (Ramiah et al., 1970). Therefore the effective stress is not the only stress component affecting the residual strength of clay minerals. The above relationship shows the reason for curved stress envelops developing for clay rich soils at low normal pressures.

Kenney (1977) defined the residual strength of mineral mixtures as

$$R_\phi = \frac{\tan\phi_{r.mix}' - \tan\phi_{r.clay\ mineral}'}{\tan\phi_{r.\ mass\ mineral}' - \tan\phi_{r.clay\ mineral}'} \qquad (5.1.6)$$

indicating that the residual strength is dependent on mineral compositon and relative volumes of clay-mineral matrix and massive mineral.

Townsend and Gilbert (1973, 1974, 1976), Skempton (1985) acknowledge the link between ϕ_r' and clay mineralogy is important. Allam and Sridharan (1983) investigated the mineral to mineral contacts in viscous and non-viscous conditions in clays using the double layer theory developed by Gouy (1910, 1917) and Chapman (1913). They suggest that edge-face linkages or mineral-mineral contacts are inevitable in a soil system possessing considerable shear strength and that the non-viscous behaviour of the system at water contents below liquid limit is explained by means of these linkages. They also indicate that a parallel plate model helps to explain volume change behaviour, but does not adequately account for the shearing resistance of a saturated system of clay particles.

It has been stated (Zen, 1959) that in fine grained sediments the clay mineral-carbonate systems have the best chance of attaining chemical equilibrium. Zen considers that in order to comprehend the mutual relations among the minerals it is not adequate to study the mineral associations from composite samples, nor is it enough to study a few specific minerals in a given sample. Rather, the mineral phases that must be considered depend on the nature of the physico-chemical relations to be examined, and must be decided upon in each case. Carbonates, micritic quartz or iron oxides could form bonds which aggregate clay particles (Davis, 1967; Dumbleton and West 1966). Formation of such bonds, though, is highly dependent upon the depositional history and diagenetic processes.

Brown (1980) showed that carbonates are common clay-associated minerals often forming solid solutions, most frequently those involving the replacement of Mg and/or Mn by Ca and vice versa from clay minerals to carbonate minerals. The presence of appreciable amounts of calcium carbonate in marls and its effect on ϕ_r' was studied by Hawkins, Lawrence and Privett (1986, 1988) Tsiambaos (1991) and Hawkins and McDonald (1992). The above authors have shown that there is a possible correlation between ϕ_r' and calcite. Further more, they have attempted to infer the consequences of weathering caused by calcite depletion. It was reported that there is an appreciable loss of strength with decreasing calcite content for a number of decalcified natural soils and mineral mixtures. Hawkins and McDonald (1992) suggested that calcite loss can be considered as a reduction of silt size particles. Steward and Cripps (1983) likewise found that the ϕ_r' of a shale varied with pore water chemistry and mineralogical changes associated with weathering.

5.1.8. The effects of vertical effective (normal) stress

While many have suspected relationships other than a linear one between vertical effective stress σ_n' and the residual strength parameters and stress ratio (Bishop et al., 1971; Skempton, 1965) it was Garaga (1970) who showed from ring shear tests results a dependency of residual shear strength on vertical effective or normal stress. Townsend and Gilbert (1973, 1974, 1976) reported that ϕ_r' is independent of σ_n' above 150 kPa approximating a straight line through the origin. A similar observation by Kenney (1967) suggested that for clays with high smectite content showed variations of ϕ_r' with σ_n' whereas soils rich in non-clay minerals did not. Kenney (1967) also suggested that perfect clay orientation could be produced at σ_n' beyond 200kPa. Chattopadhyay(1972) found that there is a normal stress dependency between 0-200 Kpa for every clay mineral angle of friction. The angle becomes only independent above 200 KPa.

Chandler (1977) found that back analysis of individual segments of landslides enabled the degree of curvature of the residual strength envelope to be established. Chowdhury and Bertoldi (1977) associated curved strength envelopes with soils of high clay fraction and plasticity. Since then a number of researchers (Lupini et al. 1981; Bromhead & Curtis, 1983; Skempton, 1985; Hawkins & Privett, 1985; Hawkins 1988; Anderson & Sulaiman, 1987; Anayi et al., 1988, Rogers et al., 1989; Anayi, 1990; and others) have been pointing out the dependence of ϕ_r' to σ_n' at low pressure levels. Since many landslides occur at shallow depths, ϕ_r' variations should be taken into account, hence the complete failure envelope must be considered (Skempton, 1985; Hawkins & Privett, 1985). Comparisons of residual strength parameters of various soils will have to be made with reference to their corresponding vertical effective stress level.

Anayi (1990) observed curved envelopes at low normal stresses both loading and unloading sequences. He also suggested that the entire failure envelope should be consulted in every occasion, though he believes that the curvature is more likely to be influenced by experimental error at low normal stress rather than at stresses beyond the critical normal stress value. Anayi (1990) recognised a general trend relating ϕ_r' with $\sigma_n'^{-1/3}$ for purely elastic particle contacts and stress that no empirical relationship can accurately govern the shape and degree of curvature of a residual strength envelope. Lemos (1986) suggested that the expression:

$$\tau / \sigma_{n'} = a + b * \sigma_{n'}^{-1/3} \text{ (Bishop et al., 1971)} \qquad (5.1.7)$$

where a = 0.0924 and b = 0.302 (correlation coefficient : 0.998) best fits the results from tests with a normal effective stress range between 40kPa and 200 kPa.

5.1.9. The role of shear effects on residual strength

As shown in sections 5.1.5 & 5.1.7, residual shear strength is mainly governed by the amount and orientation of clay minerals as well as the type of massive non clay minerals. Once residual conditions are reached one would expect that because of particle orientation the residual shear strength would be independent from rate of displacement. That holds true as long as the rate of shear (or displacement) remains within drained shear conditions. Conversely an increase of rate of shear would lead to increased pore water pressure thus affecting the measurement of strength parameters, (Petley, 1966; Skempton & Hutchinson, 1969; Lupini, 1980; Skempton, 1985).

Sembenneli and Ramirez (1969, 1971) found that changing the rate of displacement during torsion tests influenced the results. Similarly Garga (1970) showed that there is such a relationship. La Gatta (1971) specified that high rates of shear affect ϕ_r' values. Skempton & Hutchinson (1969) deduced from field evidence that for rates of displacement between 5.78×10^{-3}mm/min and 6.34×10^{-7}mm/min, the strength variations lay between -35% and +5%. Skempton (1985) suggested that for a range of rates between 0.002 to 0.01 mm/min the variation of strength values was negligible.

Lemos (1986) carried out extensive research into the effects of shearing rate changes on the residual stress parameters and the various shearing modes as previously identified by Lupini (1980). Lemos discovered that the post maximum shear strength versus displacement rate behaviour can be divided into four types: i) little or no drop in stress ratio τ/σ_n' with displacement rate. The minimum fast shear resistance is normally higher than, or equal to that corresponding to slow shearing. This behaviour is characteristic of soils showing sliding mode in slow shear: ii) a continuous increase in shear resistance with displacement rate. This behaviour has been observed with soils exhibiting sliding to transitional mode of shearing; iii) a drop in fast shearing resistance with displacement. The minimum fast shear resistance is independent of the shear rate and equal to the slow residual strength.

This behaviour is typical of turbulent mode soils; iv) a drastic drop in shearing resistance, with values as low as a third of the slow rate residual strength at very fast rates of shear. This pattern was observed in some low plasticity clays.

Lemos (1986) observed that a shearing zone disturbed by fast shear rates may need a considerable reduction in shear rate before the disturbed clay particles begin to reorientate themselves. Indeed, applying fast shear rates to a previously unsheared remoulded sample leads to higher static shear resistance than a similar sequence applied to a pre sheared sample. He also commented that the drained shear residual strength increases with displacement rate in a manner that suggests a viscous and pore pressure phenomenon. The viscous component predominates over the pore pressure component in highly plastic clays and vice versa in low plasticity clays. Lemos (1986) attributed the post maximum drop in shear resistance to displacement, displacement rate, clay fraction, the shape of massive particles and the relative size of clay and massive particles. It was concluded that soil losses during the test, initial water content and loading rate played no significant role in that drop.

Tika (1989) reported, from extensive experiments, that accelerating to faster shear rates tends to disorder the structure of the shear zone. There is a critical rate of displacement below which very little or no disturbance of the shear zone is observed. The critical rate of displacement increases with both soil plasticity and normal stress. Tika (1989) further developed the classification of soil behaviour introduced by Lemos (1986) suggesting five behaviour types for the post peak residual strength against displacement rate variations: i) constant residual strength irrespective of rate of displacement, corresponding to turbulent mode soils; ii) a moderate increase or decrease in residual strength followed by a dramatic drop to less than half the slow shear value, associated with turbulent to transitional mode soils with Ip=9-21%, typically silts with an average 60% silt size particles; iii) decrease of residual strength with increasing rate of shear followed by an increase and finally a significant drop below the slow shear value at higher displacement rates; typical of transitional mode silty clays with Ip = 24-26%; iv) decrease in residual strength with increasing rate of shear, followed by an increase at higher rates, typical of transitional to sliding mode silty clays with Ip = 26-36%; v) increase of residual strength with increasing rates of shear displacement, typical of sliding mode clays with Ip = 36-51% and clay fraction greater than 48%.

Lemos (1991) investigated the displacement rate effects on slopes and showed that for slopes with soils exhibiting positive rate effects the influence of a change in

displacement rate would be small. In contrast, slopes on soils with negative rate effects could be prone to fast failures of large displacement. He claimed that the negative rate effect constitutes an intrinsic soil property.

5.1.10 Granular Void ratio

Kenney (1977) recognised the importance of the proportions of clay to massive particles present in a mixture. He defined the ratio $R\phi$ for relative residual strength in equation 5.1.6. The definition of equation 5.1.6 led to the definition of volume ratio r_{VC} as:

$$r_{vc} = \frac{\text{volume of clay minerals and water}}{\text{total volume of soil}} \qquad (5.1.8)$$

Lupini et al. (1981) criticised the above expression as ambiguous in that Kenney considered the volume of water to be that associated with the clay minerals. Thus r_{VC} becomes zero in a saturated sand. Alternatively, it would be easier to use the whole volume of water, in which case $r_{VC} = n$ (porosity) for a saturated sand. Lupini et al. (1981) instead proposed that the interference between the rotund particles present in the soil with respect to residual strength calculations is better represented by the void ratio of the granular phase of a soil, the granular void ratio e_g. where:

$$e_g = \frac{\text{volume of platy particles and water}}{\text{volume of rotund particles}} = r_{VC}/(1-r_{VC}) \qquad (5.1.9)$$

The parameter e_g directly reflects changes in packing due to compression. The relative residual strength $R\phi$ of some soil and/or mineral mixtures plotted against e_g. is shown in fig. 5.1.4. The calculation of $R\phi$ from equation 5.1.6 however, presents some problems when testing natural soils. It is difficult to accurately estimate the value of ϕ_r'*clay mineral*. The individual contribution of every clay mineral type may be known but it is particularly difficult to estimate the behaviour of a mixture where the relative grain size distribution is not known. The use of stress ratio τ/σ_n' instead of $R\phi$ is more practical and useful. Figure 5.1.5 shows an example of a stress ratio against granular void ratio graph, where comparisons between natural soils behaviour is attempted. Smaller e_g values indicate a well graded granular phase. Lupini *et al* (1981) noted however that for a large number of soils the determination of e_g would be problematic due to the distorting effects of aggregation of clay minerals or the presence of very fine rock flour within the clay fraction This is particularly important in the way that it reinforces the belief that grain size alone

cannot provide an adequate basis for any predictive model involving residual strength characteristics, such as that presented by Lupini *et al* (1981) attempting to predict the shearing mode of a soil based on its value of granular void ratio *eg* against the residual stress ratio τ_r/σ_n'.

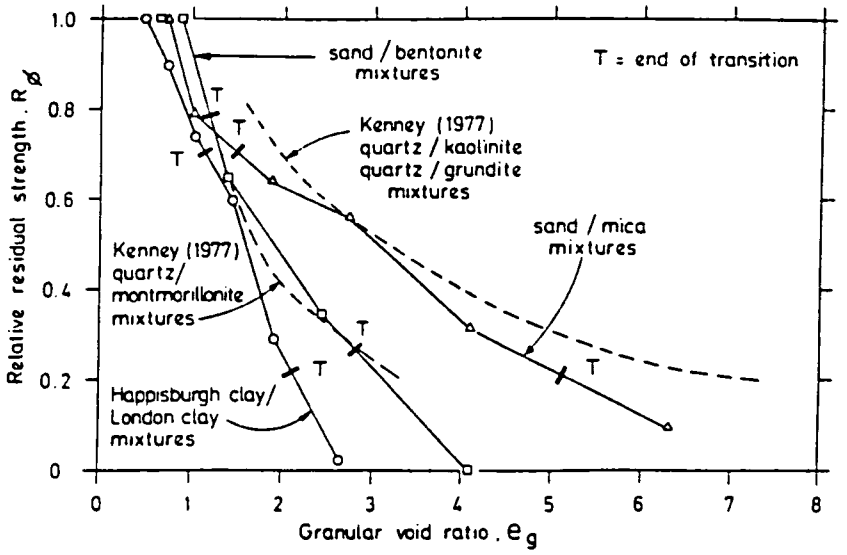

Fig 5.1.4 Relative residual strength, Rϕ, against granular void ratio, e_g, for various soil mixtures (after, Lupini et al, 1981)

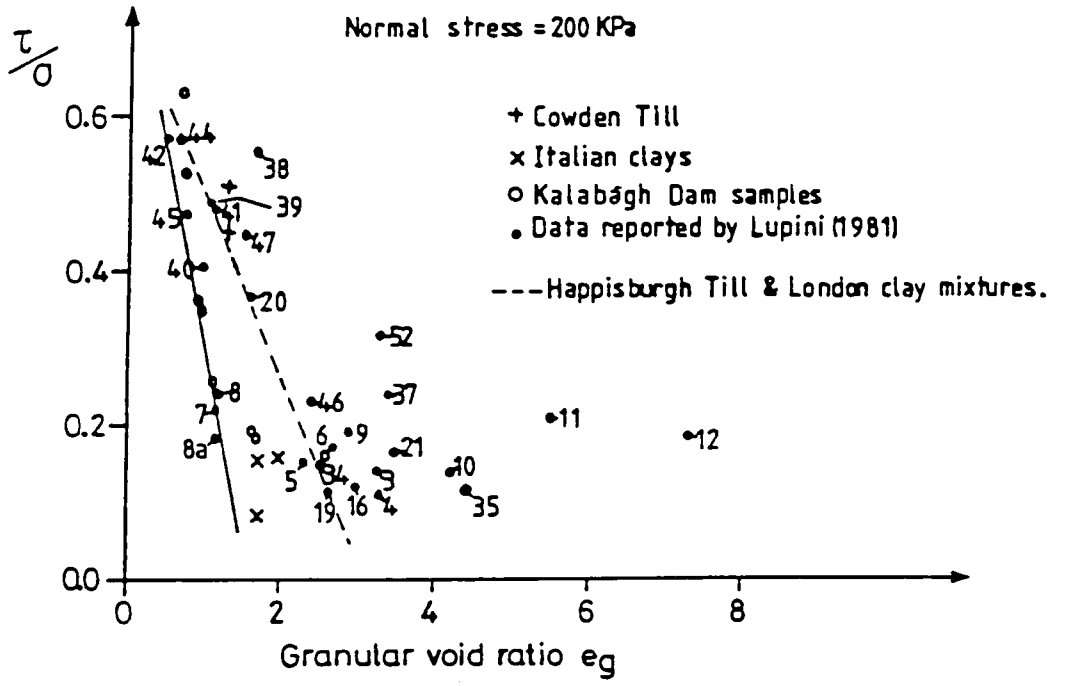

Fig. 5.1.5 Comparison between test results from various natural soils with regard to their granular void ratio, eg. (after Lemos, 1986).

5.2 The residual strength testing programme.

5.2.1. General

The testing programme was completed in two phases. The first phase was conducted in Athens at the Geotechnical Engineering Laboratories, Central Laboratory of Public Works (CPWL), Ministry for the Environment, Physical Planning and Public Works (M.E.P.P.P.W.) under the supervision and assistance of Dr. Tsiambaos and Mr. Ch. Tsaligopoulos. The residual shear strength tests were carried out between April and July 1989 using a Bromhead ring shear apparatus. A total of 10 samples were tested. The second phase took place at the Engineering Geology Laboratories, S.E.C.S, University of Durham under the supervision of Dr. D.G. Toll and the assistance of Mr. B. McEleavy. A total of 20 samples were tested using a prototype Armfield ring shear apparatus. The device was tested, calibrated and further developed from its original state during September 1989 and December 1989. During that period of time trials for comparison against shear box and Bromhed test results were run concurrently with adapting the original device to a testworthy state. Once the credibility of the device was established the testing of 20 samples from Hellenic marls and marly clays took place between February 1990 and June 1992. The long testing time for every sample (at least 15 days) and a number of reruns on samples tested owing to difficulties imposed by the features of the Armfield apparatus and testing failures at the beginning of the programme contributed to the length of the testing programme.

5.2.2. Apparatuses used.

5.2.2.1 Bromhead ring shear apparatus.

The Bromhead ring shear apparatus was used in Athens at the Geotechnical Engineering Laboratories of the Central Public Works laboratory (C.P.W.L.). It was built by Wykeham Farrance following the design invented by Bromhead (1979). The apparatus used for this testing programme is fully described in BS 1377: Part 7: 1990, section 6. The general features of that apparatus are given in figure 5.2.1.

5.2.2.2 Armfield ring shear apparatus.

The Armfield ring shear apparatus is a prototype built by Armfield Technical Education Co. Ltd., Ringwood, Hampshire, England for the Engineering Geology Laboratory at Durham University in the late 1970s. It comprised, in its original

form, two plates separated by a middle set of concentric rings which confined an annular soil specimen. The upper plate was prevented from rotating by a fixed arm on the chassis of the apparatus bolted to the torsion beam through an articulated joint and a proving ring placed diagonally opposite the fixed arm acting on the torsion beam.

The middle concentric confining rings were attached to the upper plate. The lower plate rotated around its centre driven by an electric motor through a 4 speed gearbox. The sample was immersed in a water bath. The normal stress was applied to the upper plate, at its centre, through a system of levers with a loading ratio of 7.5:1.

The shearing heads original configuration of the shearing head posed some problems in accurately measuring the residual shearing resistance of a specimen. At first, the presence of only one proving ring and a fixed position arm to resist any rotation by the upper plate, introduced differential stress distribution around the shear surface as a result of differing stiffnesses between the proving ring and the fixed position arm. Secondly the fixed position of the middle rings relative to the upper plate meant that, once a certain volume of material was extruded during a test, the middle rings would come in contact with the lower plate without any mechanism to rectify the situation, thus introducing, unnecessary non-uniform metal to metal friction. The present configuration has incorporated changes to the shearing head as well as to the frame of the apparatus. The dimensions of the annular specimen have remained the same and these are i) external radius 76mm, ii) internal radius 51mm, iii) height of sample compartment 2mm. Figure 5.2.2 presents a simplifed cross section of the shearing head of the apparatus, and figure 5.2.3 presents a simplified plan view of the shearing head. Photographs 5.2.1 to 5.2.5 show the shearing head components and views of the shearing head and the entire apparatus respectively.

The modified Armfield shearing head (referred to as the shearing head from now on) comprises two main moveable parts. The first comprises the upper plate and middle rings and the second comprises the lower plate. The middle rings are attached to the upper plate by means of six adjustment pins (or bolts). These pins control the distance between the upper plate and the two middle rings, (inner and outer). At relaxation, the middle rings touch the lower plate keeping the upper plate resting on the annular specimen (see fig.5.2.2).

At present the adjustment pins pass through the upper plate and screw into the middle rings. The adjustment pins are screwed till their boltheads touch the upper

plate's surface. Any further tightening results in an upwards movement of the middle rings towards the upper plate, thus creating a gap between the lower plate and the upper section (upper plate plus middle rings) of the shearing head.

Fig. 5.2.1 Bromhead ring shear apparatus (not to scale) from BS 1377:Part 7:1990

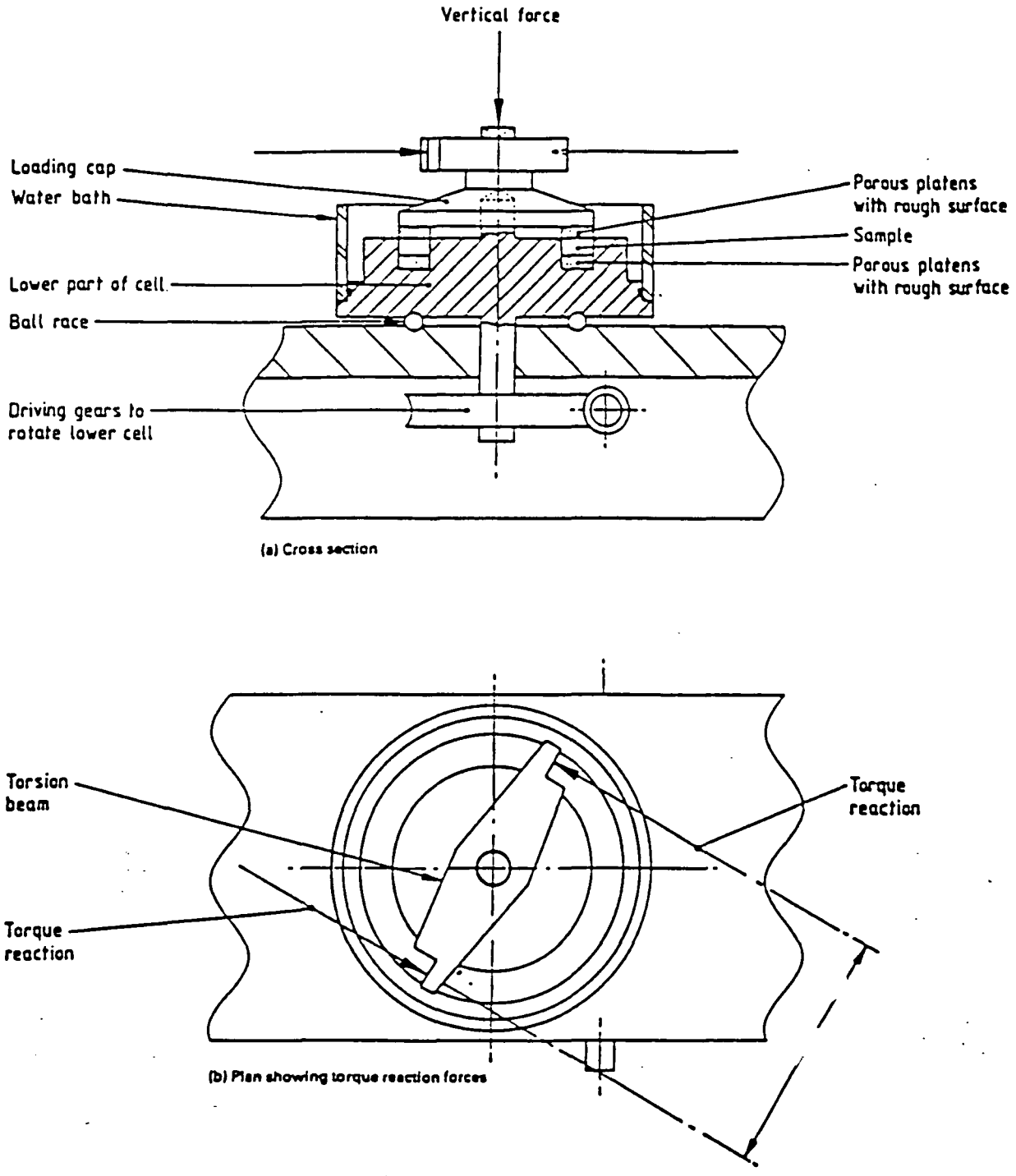

Any loosening of the adjustment pins does not lower the middle rings back towards the lower plate. Lowering of the middle rings can only be achieved by removing the adjustment pins and pushing the middle rings back down towards the lower plate. Whilst this is feasible for the outer middle ring, it is impossible for the inner middle ring without removing the upper plate from the shearing head. Three small pegs fixed on the outer perimeter of the lower plate act as guides as to how much the gap is open at any time. When any of these pegs touches the outer ring of the middle plate it means that at that point the lower plate and middle rings are in contact. In this case metal to metal friction affects the measurements and a further tightening of the nearest adjustment pin is required, to open the gap and prevent further contact.

Both upper and lower plates have radial grooves to allow drainage into the water bath. The porous discs are made of copper and have small vanes incorporated in them to ensure that a shearing plane or a shear zone will not form close to the porous discs, thus enhancing the consistency and definition of the shear plane or zone (Anayi et al, 1989).

The upper plate and middle rings remain held by two proving rings one on either side of the shearing head's diameter and opposing each other (photographs 5.2.3, 5.2.4). The speeds available, referred to as the ratios from now on, and the corresponding angular displacement rates are given in table 5.2.1.

Table 5.2.1

Gear Ratio	Angular Displacement (deg/mm)
1 : 1	2.5174
10 : 1	0.25174
100 : 1	0.025174
1000 : 1	0.0025174

As in the original configuration, the vertical effective stress is applied at the top of the shearing head. The load is provided by a number of weights which are applied on a hanger via a leverage system with a final delivery ratio of 7.5:1 (see photograph 5.2.5). The lower and middle plates are continuously immersed in the water bath which is attached to the lower plate.

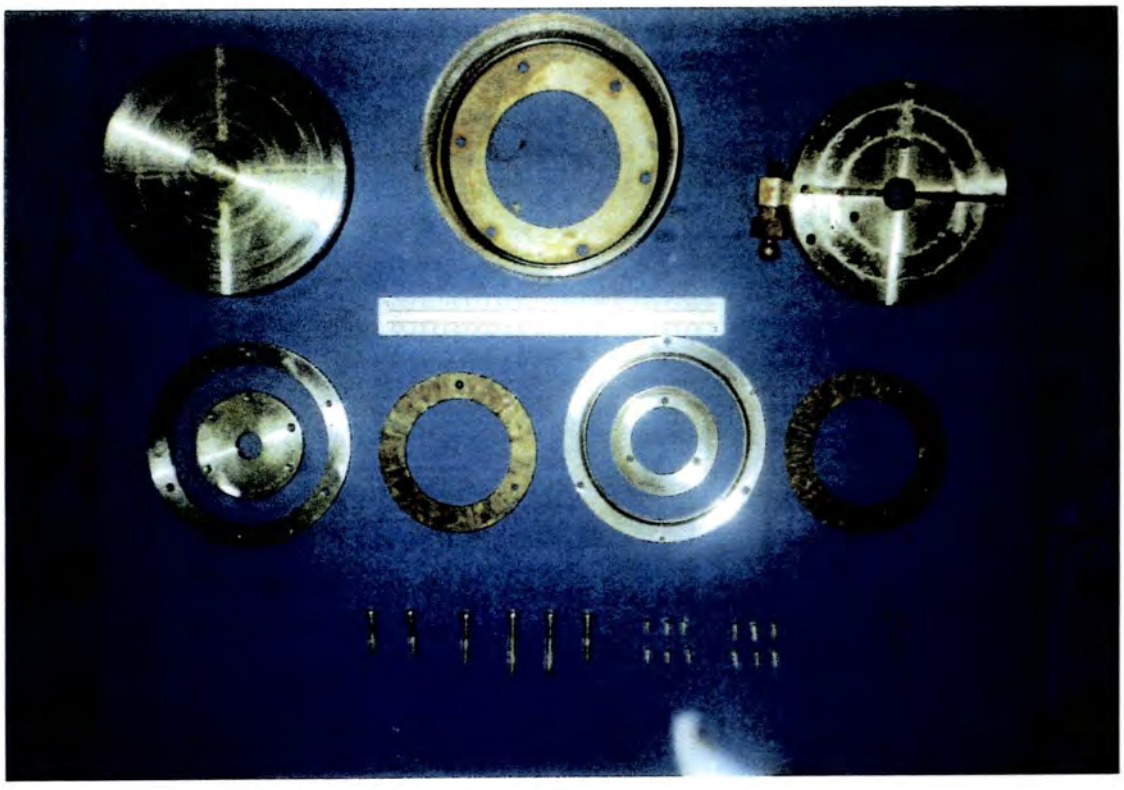

Photograph 5.2.1 Modified Armfield Shearing Head Components from top left to bottom right: lower plate, water bath components, upper plate (loading lid), concentrical rings of the middle section plate, lower porous disc, lower plate wallings, upper porous disc, adjusting pins, connecting screws.

Photograph 5.2.2 View of the perimeter peg indicating that the gap is shut. Note the extruded material at the edge.

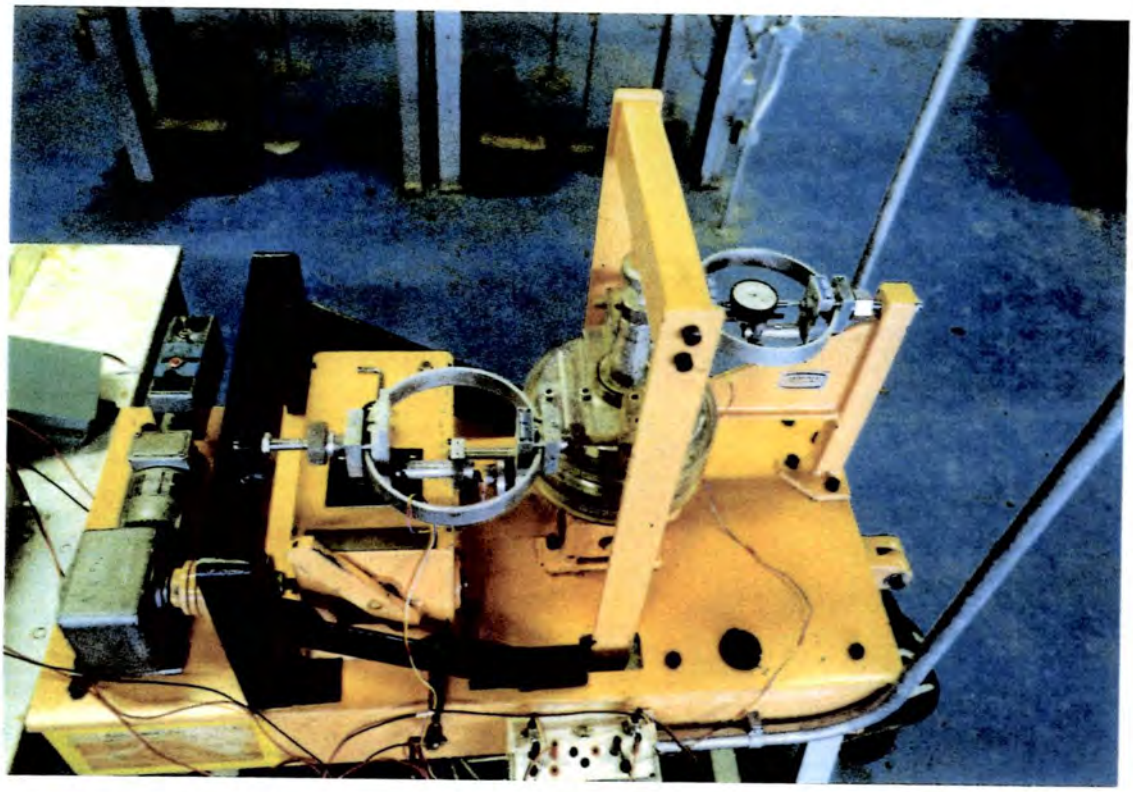

Photograph 5.2.3 Modified Armfield apparatus upper section. From left to right: electric motor, added arm for the second proving ring, gearbox, shearing head and loading lever, original arm for proving ring.

Photograph 5.2.4 View of the modified Armfield apparatus. Note the recording plotter and the power supplies underneath the main unit.

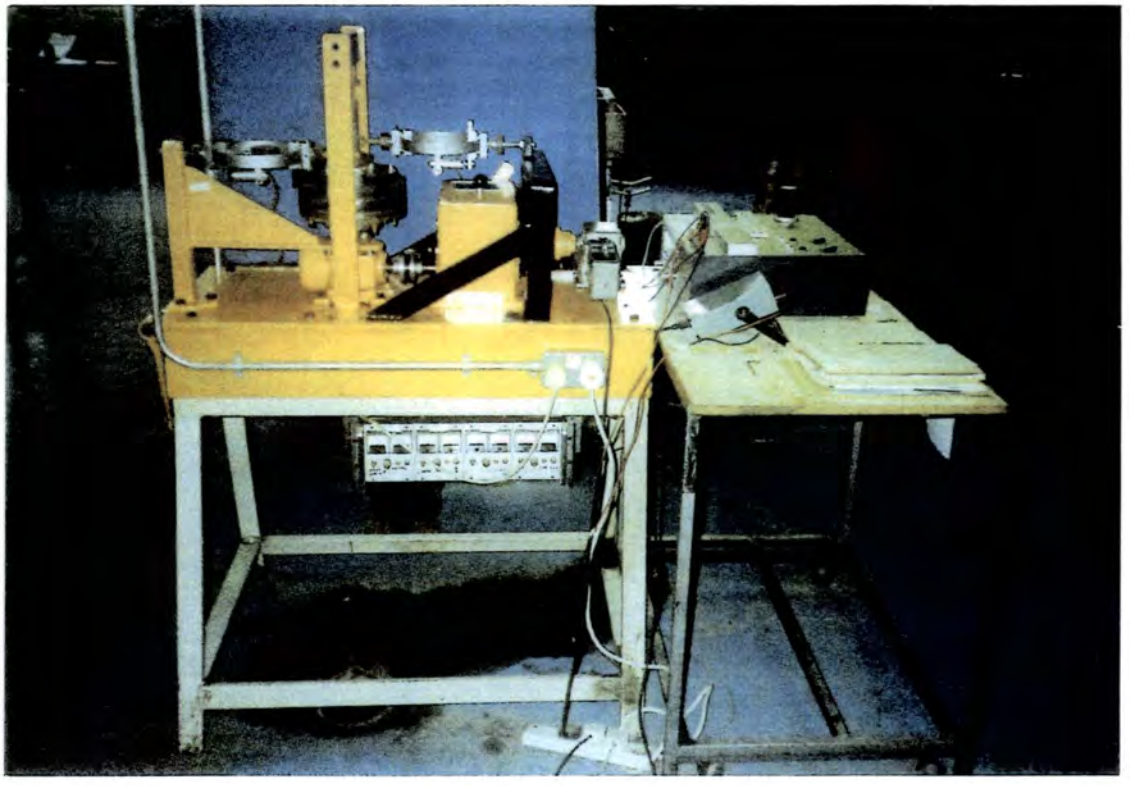

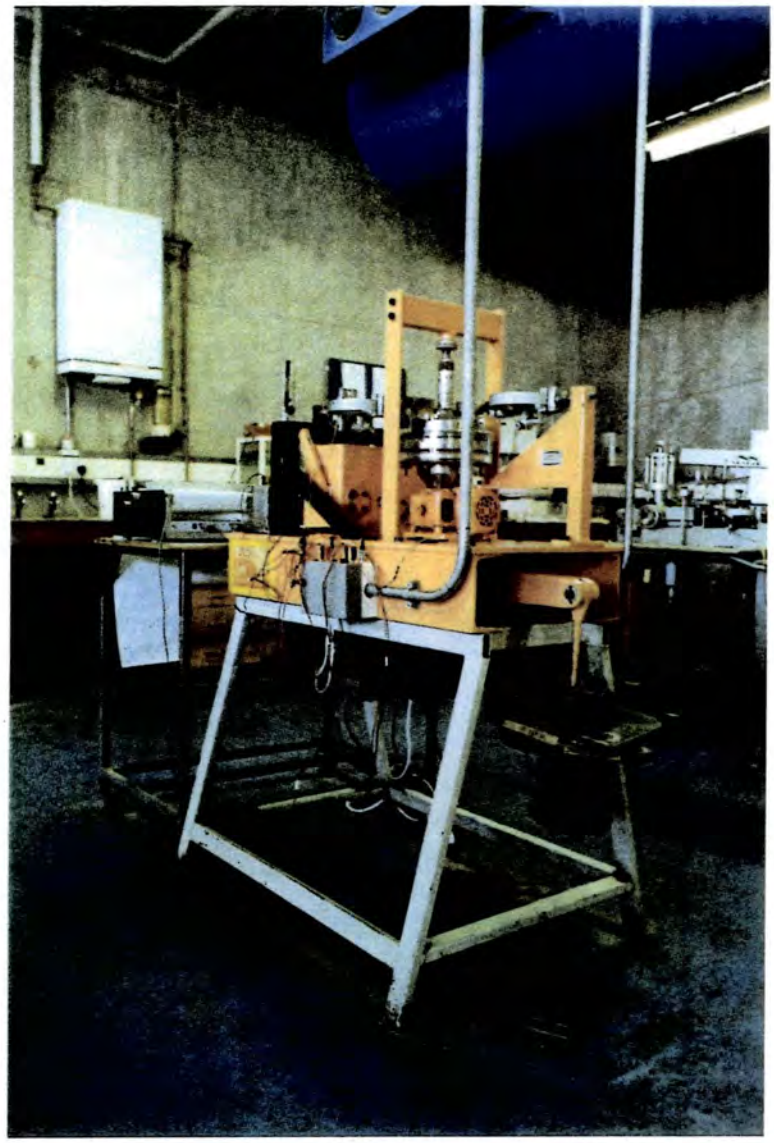

Photograph 5.2.5 Front view of the modified Armfield apparatus. Note the loading arm and the L.V.D. Transducer Channel box to the left. The L.V.D.T. signals are sent directly to an automatic data logger device.

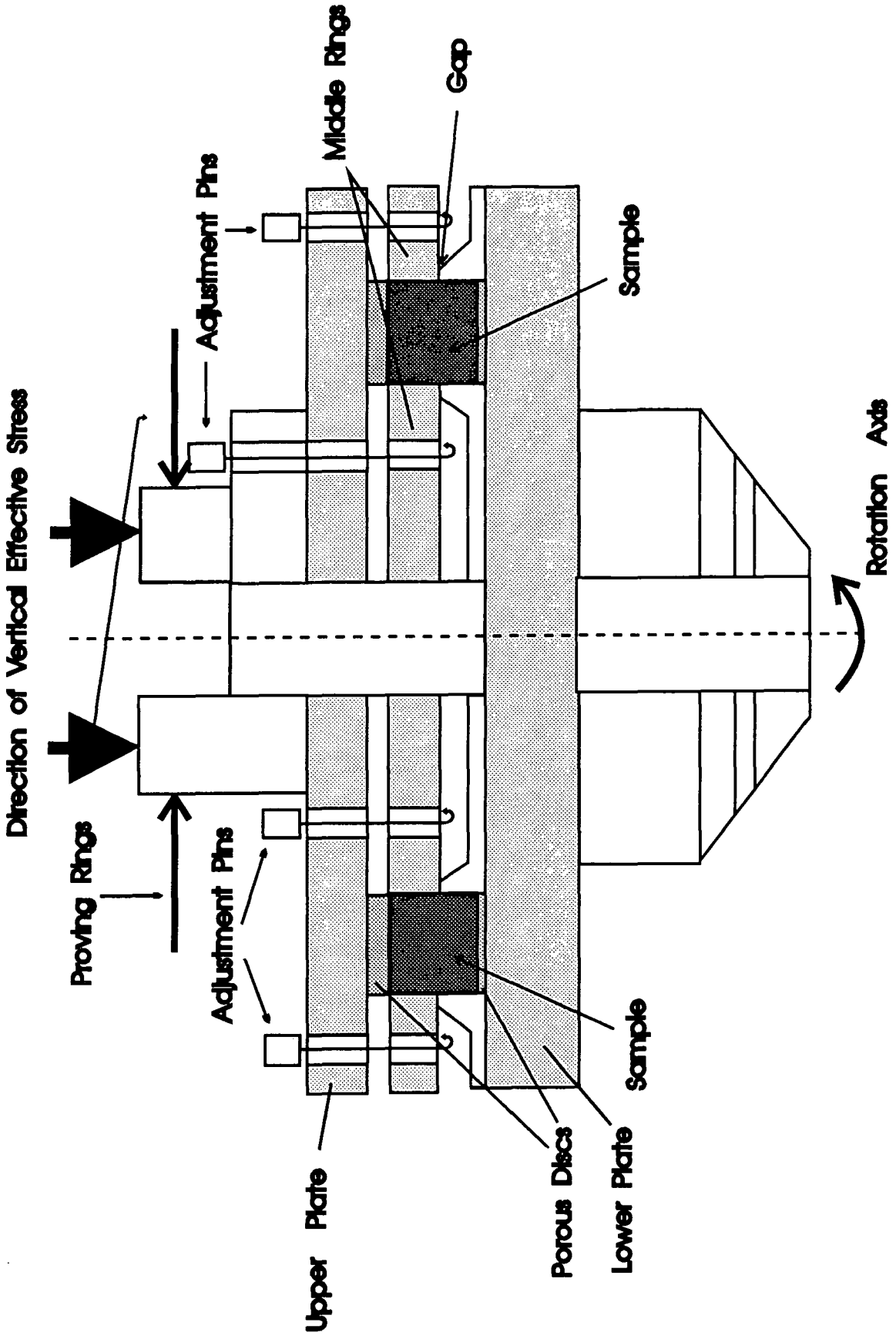

fig.5.2.2. Modified Armfield ring shear apparatus shearing head in cross section (not to scale)

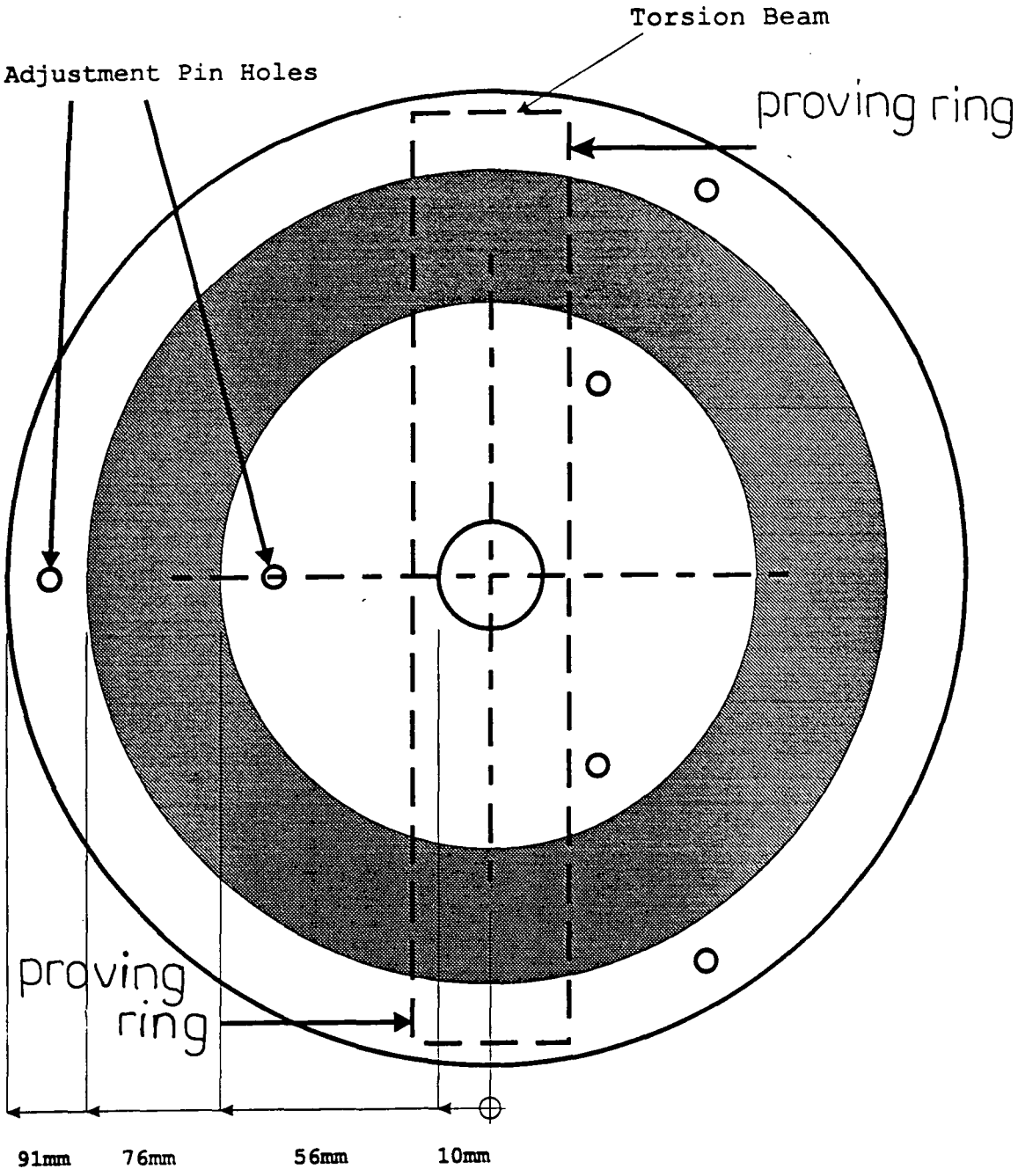

fig 5.2.3. Simplified plan-view of the modified Armfield apparatus shearing head.

5.3. Methods of testing.

5.3.1 Testing with the Bromhead apparatus.

5.3.1.1 Preparation of Specimens.

Specimens were prepared by mechanically crushing samples and dry sieving them through the 420μm size sieve (ASTM D-136). To ensure that enough sample was prepared to form the specimen it was ensured that at least 200 g of sample passed the 420μm sieve. Wherever the material was known, from the grain size distribution curve to be very clayey (clay fraction > 50%) the 75μm sieve was used for dry sieving (sample SLM 20). The part of the sample that passed through the sieve was then wetted to approximately its plastic limit and after a thorough mix was sealed and allowed to cure for 24 hours. After the curing period a small portion of the sample was used for initial moisture content determination. The rest of the sample was then carefully pressed into the annular container by hand. The aim was to prevent any air bubbles from forming within the specimen body. The careful kneading also helps a more even distribution of sample mass through the specimen container. Once the container was full, the surface of the top part of the specimen was further worked with a pallet knife until smooth and level with the surface of the lower plate confining rings. The top plate was finally inserted and carefully placed on top of the specimen and the water bath was filled up.

5.3.1.2. Shearing Procedure

In accordance with Bromhead (1979), Hawkins & Privett (1986), Mesri & Cepeda Diaz (1986), Rogers et al (1989) it was decided to apply a multistage sequence, 50kPa, 100kPa, 200kPa and 400kPa respectively. Shearing started after the specimen was allowed to consolidate under the normal effective stress prescribed for the particular shearing stage. Consolidation was monitored by a vertical transducer, installed on a fixed arm on the apparatus chassis, touching the surface at the top plate of the shearing head. The specimen was allowed to consolidate overnight prior to any shearing stage.

The rate of shearing was chosen to be slow throughout the experiment and fixed at 0.048 degrees/minute. Only for very plastic soils and in order to avoid extrusion of soil from the container, a rate of 0.024 degrees/minute was applied (sample SLM 20). Conversion of angular rotation to linear displacement is performed by

multiplying the angular displacement by a factor of 0.742. A typical run is shown in the form of a shear strength against displacement graph in figure 5.3.1.

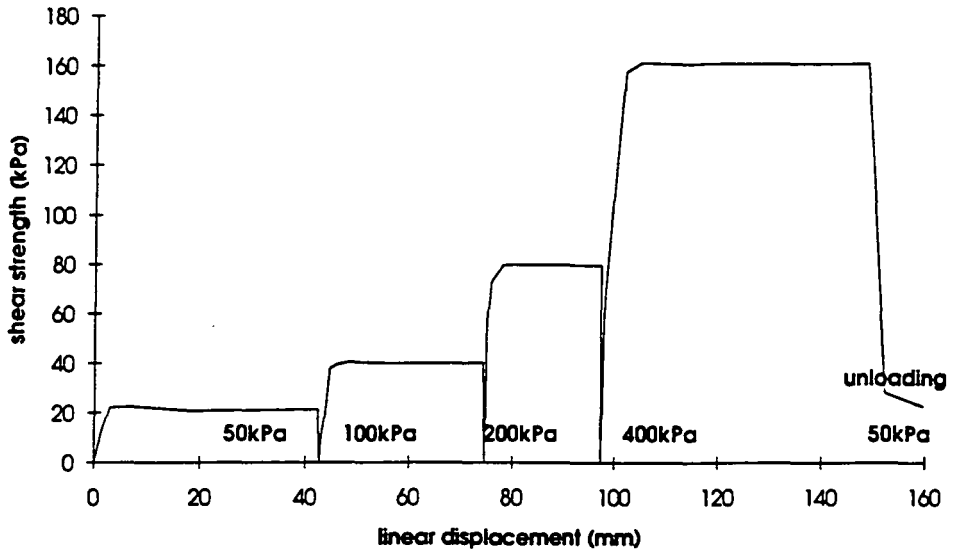

Fig 5.3.1 Shear stress against linear displacement graph for sample SLMB1. There are no strong peak values for any of the shearing stages in this typical run.

At the end of the last loading (400kPa) stage and when residual conditions had been achieved, the specimen was unloaded to the initial test load of 50kPa without halting the experiment. If the shear stress drops to approximately the range of values achieved during the initial 50kPa loading stage, then the experiment was regarded as successful and terminated. Finally the specimen was removed from the shearing head and the final moisture content was determined. The bulk density ranged between 1.92 Mg/m^3 to 1.98 Mg/m^3 and the dry density ranged between 1.35 Mg/m^3 to 1.44 Mg/m^3.

5.3.2 Testing with the Armfield apparatus

5.3.2.1 Preparation of Specimen

Specimens were prepared from mechanically crushed samples dry-sieved and passing the 425μm sieve (BS 1377:1975). The parts of the samples that passed through the 425μm sieve were then wetted to approximately their plastic limit, mixed thoroughly and sealed to cure for 24 hours. After the curing period was completed a small portion of the sample was used for moisture content determination. The rest of the sample was then carefully smeared inside the mould formed by the lower plate (see fig. 5.2.2) and the middle plate, which was mounted

on top of the lower plate, held rigidly in place by two G-clamps. The sample was kneaded to shape by hand. Care was taken at all times that no air bubbles were formed within the specimen. Once the containing mould was filled up, the surface of the specimen was further worked with a pallet knife until smooth and level with the surfaces of the middle plate rings, (see fig. 5.2.2 and photographs 5.3.1, 5.3.2).

The amount of prepared sample required for the formation of the annular specimen needed to be at least 400 grams before wetting. The bulk density of the specimens ranged between 1.94 Mg/m^3 to 1.97 Mg/m^3 while the dry density ranged between 1.39 Mg/m^3 to 1.45 Mg/m^3.

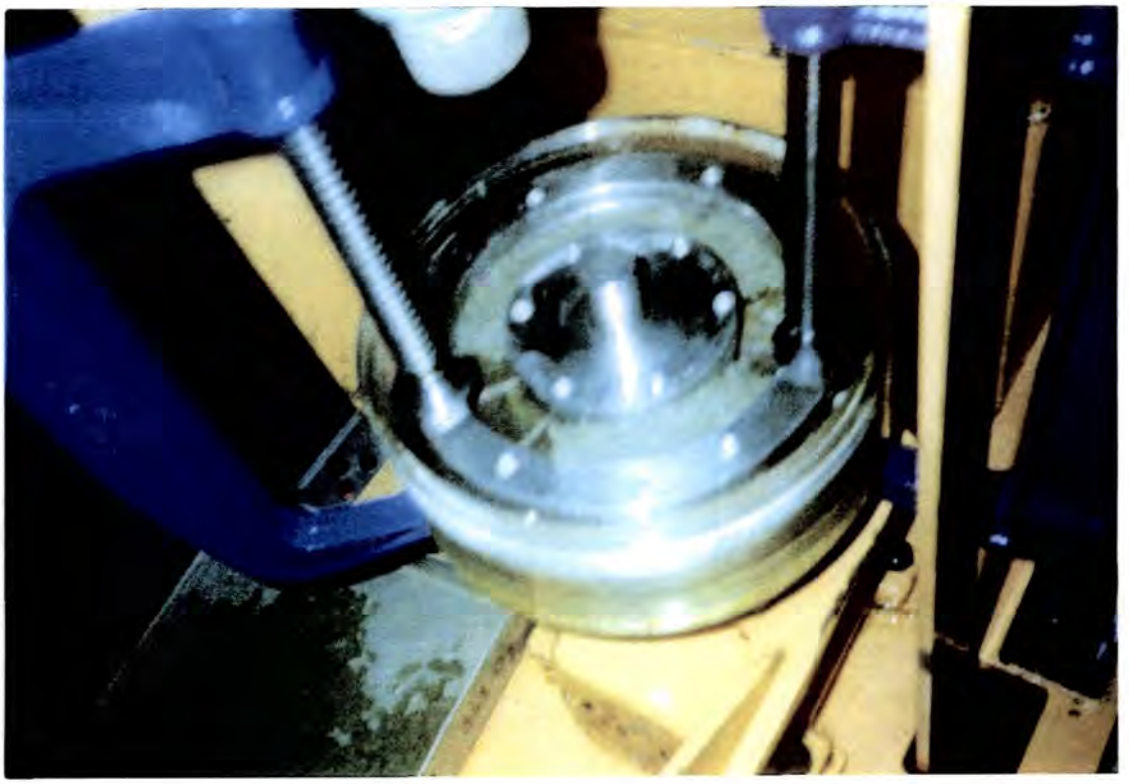

Photograph 5.3.1 The middle plate rings are held firmly on top of the lower plate while the sample is gradually kneaded into the specimen compartment.

5.3.2.2 Shearing Procedure

Due to the inability of the middle rings to move back towards the lower plate once they are lifted away from it, thus exposing the middle part of the specimen (see section 5.2.2) a multistage loading sequence with intermediate consolidation stages could not be applied because it would be impossible to one-dimensionally consolidate the specimen prior to a shearing stage of a higher normal load. Instead,

the specimen was subjected to incremental loading consolidation before any shearing commenced. The final consolidation loading increment was decided to be 1.5 times

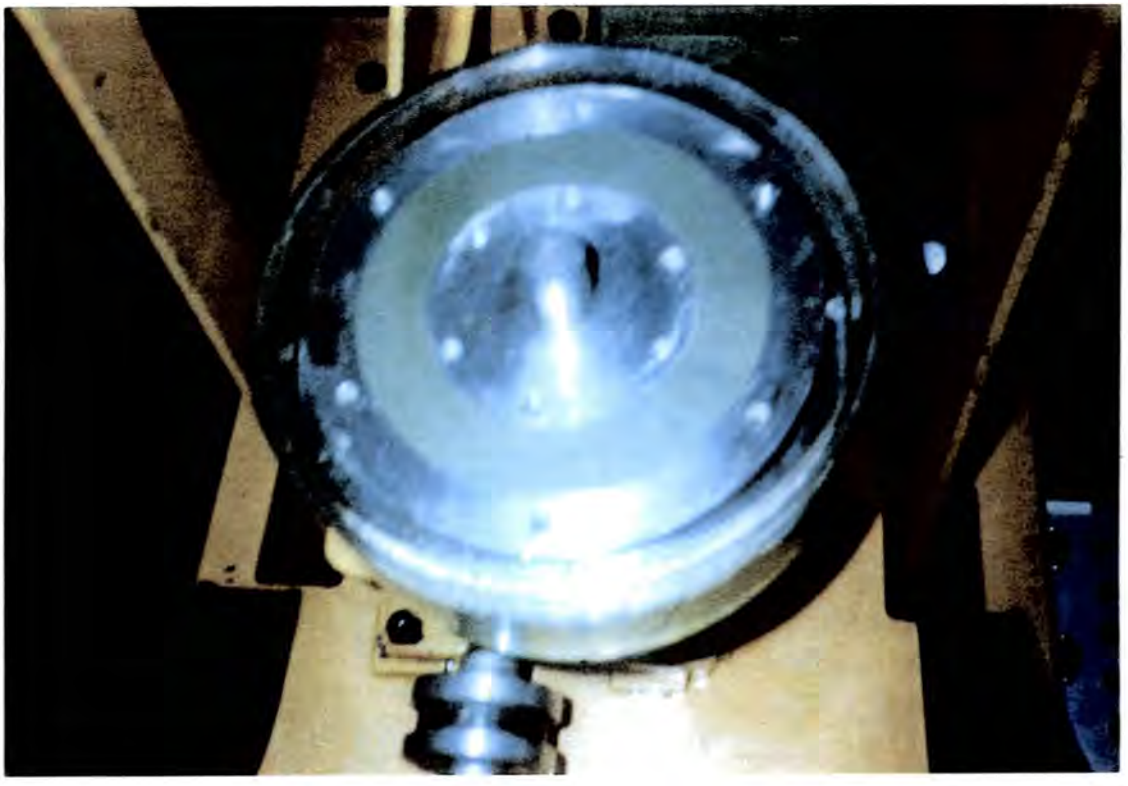

Photograph 5.3.2 The G-clamps are withdrawn and the upper surface of the specimen is levelled with the surface of the middle plate rings before the application of the upper plate.

the heaviest vertical effective load during shearing. This was done in order to further consolidate the specimen thus minimising any further softening of the material along the specimen surface exposed to the water bath (fig. 5.3.2)

For the reasons explained above, a multistage unloading sequence after initial consolidation was the preferred test procedure followed using the modified Armfield ring-shear apparatus. Depending on the local conditions of sampling there were two unloading sequences. The first, for deeper sample depths, was 400 kPa, 200 kPa, 150 and 100 kPa respectively. The second, for shallower sample depths, was 200 kPa, 150 and 100 kPa respectively. The transition from one unloading stage to the next one was rapid involving no halting of the shearing process, thus testing the originally formed shear plane at all stages of the test. The rate of shearing was chosen to be slow and a rate of 0.025174 degrees/minute (see table 5.2.1) was selected as standard. Conversion to linear displacement figures is achieved by

multiplying the angular displacement by a factor of 1.108mm per degree. A typical test (sample OEN2) is shown in fig 5.3.3 in the form of shear stress against linear displacement. After completion of the the specimen was removed from the shearing head and the final moisture content was determined.

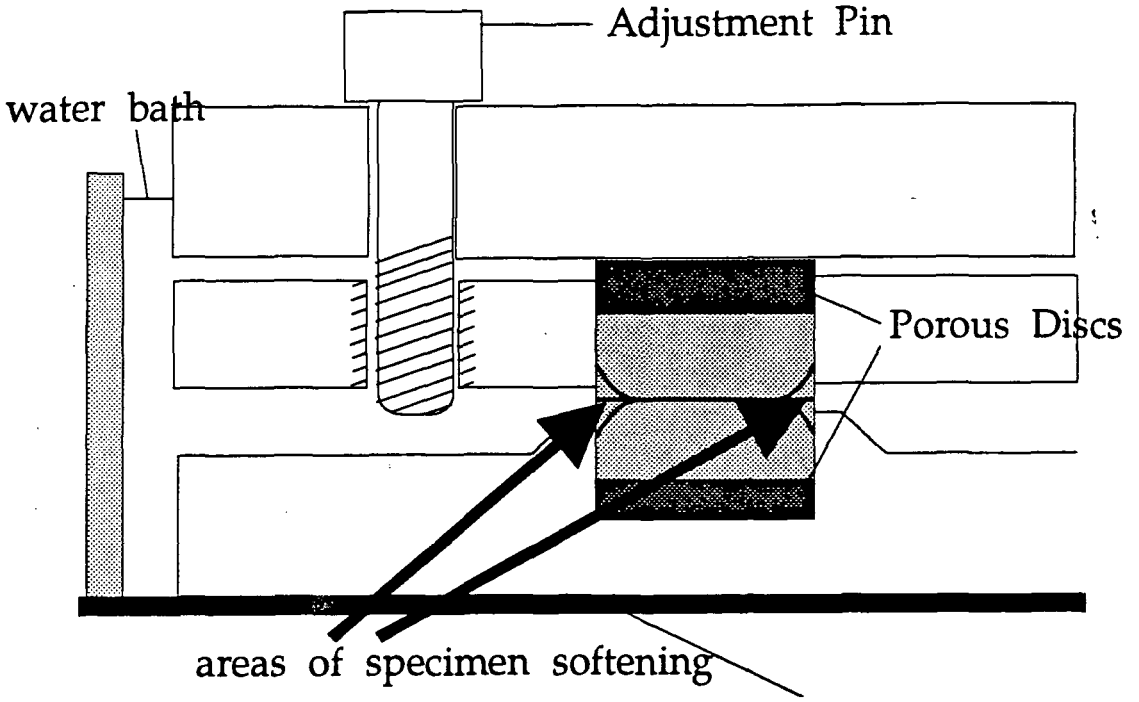

Fig. 5.3.2 Areas of specimen softening and material losses during shearing

5.3.2.3 Comparison against Bromhead ring shear measurements

A series of tests were run to compare the results obtained usng the two pieces of apparatus. Since the testing with the Bromhead apparatus preceded that with the Armfield apparatus, the nearest available gear ratio to the Bromhead apparatus was chosen as standard for the duration of the comparison. Additional runs on lower and higher gear ratios and different sets of loads (either loading or unloading) were also applied in order to examine the effects of such changes on the Armfield test results.

It was found that for the chosen standard gear ratio 100:1 (or 0.025 degrees per minute) and a range of effective normal stress between 400kPa and 50kPa, both the Bromhead apparatus and the modified Armfield apparatus gave results which were in good agreement. At a normal stress of 200kPa the stress ratio of shear stress over normal stress was 0.3995 (21.8°) and 0.406 (22.1°) for Armfield and Bromhead apparatus tests respectively. The full results are shown in Appendix B.

5.3.2.4 Comparisons against reversible shear box measurements

In order to further establish the validity of the results obtained from the modified Armfield apparatus it was felt necessary to also compare its results against reversible shearbox test results. As expected from the studies already published comparing direct shear measurements with ring shear tests, the reversible shear box results were higher than those from the modified Armfield apparatus. The difference was approximately 2 degrees on the residual angle of friction for the same range of effective normal stresses and rates of shearing. The results are given in Appendix B.

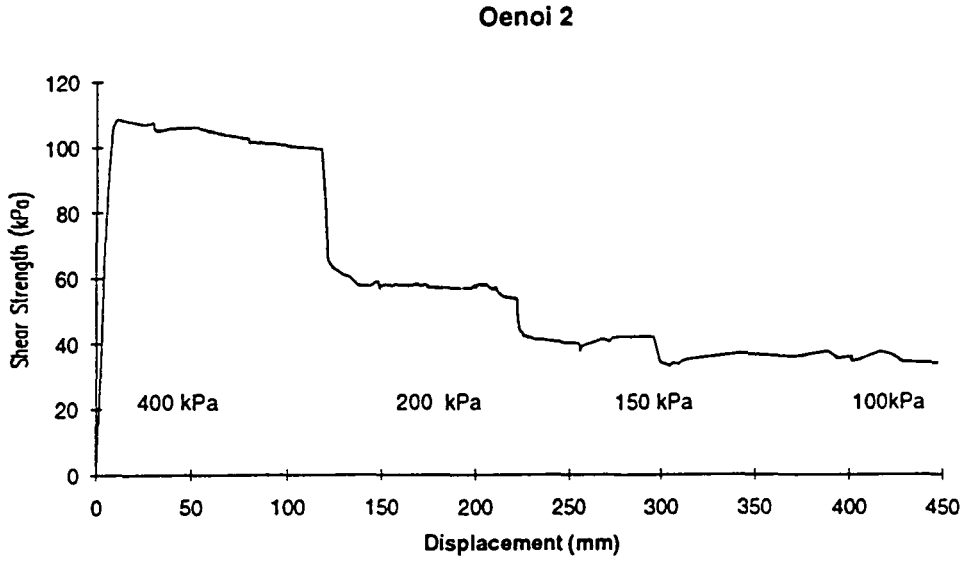

Fig. 5.3.3 Typical shear stress against linear displacement graph. Note the drop in stress between shearing stages.

5.3.3 Experimental Errors

The main difference between the simple Bromhead and the modified Armfield apparatus lies with the presence of a semi-adjustable gap between the moveable parts of the bottom and middle rings in the shearing head of the Armfield apparatus. Hence, the failure plane should form at the mid-height of the sample. However, difficulties may arise from the use of the adjusting pins (see fig.5.2.2) These can be blocked by soil particles jammed inside the grooves of the screwholes. Further, such adjustments require frequent manual observations of the width of the gap during the

experiment. This may prove impractical since tests run non-stop for many days. Any sample loss in excess of that expected may lead to a shutting of the gap and metal to metal friction which affects the true measurements of torque. Any such contact of the moveable parts can be detected on the plotter graph which runs simultaneously with the ring shear apparatus. If this is observed, the data is ignored.

Anayi (1990) criticised such a configuration as it gives rise to fine clay particles being exuded; the continuous extrusion leading to a non-horizontal failure surface. Coarser material then accumulates around the edges of the failure surface. This in turn leads to softening (fig. 5.3.2) and a non-uniform stress distribution across the failure surface and higher strength values. However, the amount of extruded particles varies with the type of sample, the degree of compaction and the relative over consolidation ratio at each shearing stage. It was found that extrusion intensified with higher plasticity and lower O.C.R. This trend can be explained by the tendency of certain plastic soils to expand and relax under low vertical effective stress levels.

Other sources of error ascribed to mechanical friction of the moveable parts of the apparatus can be minimised by good lubrication. A difference in stiffness between the two proving rings could lead to unbalanced application of torque is sometimes a problem and this must be minimised. The apparatus is calibrated assuming that the stresses σ_n' and τ are applied uniformly over the sample's width. The manufacturer suggested that if the stresses reach a maximum at the outer perimeter and are zero at the inner perimeter or vice versa the error involved would vary from -6% to 8% respectively. If the stresses are concentrated at the centre circle of the annulus then the error would be 1.5%.

Movements between the specimen and the confining walls of the shearing head may introduce wall friction. This is not a major problem with the modified Armfield apparatus because failure takes place on a surface exposed to the water bath. On the contrary, in the Bromhead apparatus the failure surface is produced at the top of a thin sample so that, in theory, there should not be any side friction developing around the failure plane (Bromhead, 1979). However, the problem of continuous reduction of specimen thickness in the Bromhead apparatus through consolidation blurr the failure plane definition leading to a failure zone instead. In addition, adhesion between the sample and the bronze porous plates is not reliable and can cause remoulding of the sample surface leading to an increase in water content at the top of the failure plane (Anayi, 1990). The incorporation of vanes on the bronze

porous plates of the Armfield apparatus ensures a better and more consistent definition of the shear plane.

5.3.4 Calibration

All the dial gauges and electrical transducers were subjected to full calibration at the start of the project and frequently checked during the whole programme. The dial gauges were found to comply to the specific tolerances of non-linearity (BS 907:1965). The transducers were of the L.V.D.T type supplied by Penny & Giles Ltd and were calibrated with regard to the corresponding dial gauges.

Every proving ring was originally supplied with a manufacturer's (Wykeham Farance) calibration certificate. The proving rings have a maximum load capacity of 200kN. Recalibrations were carried out and were extended to both loading and unloading.

Photograph 5.3.3 Data acquisition system at the engineering geology laboratory, Durham University.

5.3.5 Data Recording

Measurements were recorded directly from the proving rings dial gauges in the case of the Bromhead apparatus. The exact time and date of the measurement were also recorded alongside the readings taken from the two dial gauges.

In the case of the modified Armfield apparatus, data was recorded automatically via LVDT transducers to a central recording unit (data logger). The data was recorded by the logger at set intervals of time as well as at explicitly instructed intervals of time for all channels connected to active LVDTs. The data is downloaded to a PC at regular intervals and is saved in separate files on the PC's hard disc. The operator can then select the LVDT channels that he/she is interested in and output the data in a format of choice (i.e. ASCII file, spreadsheet file, printer output). The necessary software was developed at S.E.C.S. by Messres. R.P. Welch and T. Nancarrow. The configuration is shown in photograph 5.3.3. Attached to the Armfield's LVDTs was an analogue pen plotter with two channels and variable resolution of plotting scale at different paper speeds.

5.4 Calculating the Shear Strength Parameters

Assuming a uniform distribution of normal stress σ_n' and shear stress τ over the failure surface, the effective normal load can be expressed as:

$$N = \sigma_n' \pi (R_o^2 - R_i^2) \qquad (5.4.1)$$

where *Ro*, *Ri*, are the outer and inner radii. The torque generated with the soil shearing resistance can be expressed as:

$$T = \tau \int_{r=R_i}^{r=R_0} 2\pi r^2 dr = \tau \frac{2}{3}(R_o^3 - R_i^3) = FDa \qquad (5.4.2)$$

where F is the calibration factor of the proving ring, D is the proving ring divisions recorded and *a* is the distance of the proving ring reaction from the axis of the shearing head. The average torque for both ring recording is then expressed as:

$$\overline{T} = \frac{(F_1 D_1 a_1) + (F_2 D_2 a_2)}{2} \qquad (5.4.3)$$

In practical terms, the shear stress for the Bromhead ring shear apparatus is given by the expression

$$\tau_{Bromhead} = \frac{175}{A}\left[\frac{(F_1 D_1) + (F_2 D_{2)}}{2}\right] \qquad (5.4.4)$$

where A is specimen area measured to be 40cm^2. The shear stress for the modified Armfield ring shear apparatus is given below:

$$\tau_{Armfield} = 164\left[\frac{(F_1 D_1) + (F_2 D_2)}{2}\right] \qquad (5.4.5)$$

Once the shear stress levels for every shearing stage are established, the stress ratio τ/σ_n' is calculated for every measurement of shear stress for every shearing stage of a particular test. The lowest consistent set of stress ratio values represents the residual stress ratio for that particular shearing stage. The average stress ratio value of that set is then calculated. Assuming that there is no cohesion intercept (c=0), Coulomb's expression for a particular shearing stage i can be written:

$$\tau_i = \sigma_{n_i}' \tan\left(\phi_{r_i}'\right) \qquad (5.4.6)$$

where τ_i is the shear stress, $\sigma_n'_i$ is the corresponding vertical effective stress and ϕ_{ri}' is the residual angle of friction for the shearing stage i. The residual angle of friction can then be expressed as:

$$\phi_{r_i}' = \arctan\left(\tau_i/\sigma_{n_i}'\right) \qquad (5.4.7)$$

When the residual stress ratio for a number of shearing stages (in practice no more than two) becomes independent of changes in vertical effective stress
i.e.

$$\tau_i/\sigma_{n_i}' \approx \tau_j/\sigma_{n_j}' \qquad (5.4.8)$$

then the specimen has reached its ultimate residual strength. The corresponding angle ϕ'_r is then called ultimate residual angle of friction.

5.5. Test Results

Tables 5.5.1 to 5.5.4 present the test results from Korinthos, Preveza-Igoumenitsa, Amalias-Goumeron and Irakleion samples in the form of stress ratios and their corresponding vertical effective stress. Table 5.5.5 to 5.5.8 present the same tests in the form of residual shear stress and the corresponding vertical effective stress. The type of the apparatus used in every occasion is indicated by a codename, namely "brmd" for Bromhead apparatus and "armfld" for the modified Armfield apparatus. Table 5.5.9 presents the results for all samples in the form of a secant residual angle of friction, as calculated using equation 5.4.7. Figures 5.5.1, 3, 5 and 7 present plots

of stress ratio again normal stress data given in the tables and figures 5.5.2, 4, 6 and 8 present shear stress against normal stress, i.e. the residual shear stress envelopes for the tested samples of each area in the same order as above. All tests are presented individually in Appendix A including shear stress against linear displacement graphs, residual shear stress envelope graphs and stress ratio against vertical effective stress graphs for every tested sample.

Table 5.6.1 presents the results for the granular void ratio e_g of thirteen samples. The results are plotted against τ/σ_n' in figure 5.6.1.

Table 5.5.1
Korinthos

normal stress	residual stress ratio				
	simG4	sim1A	sim7A	sim2T	sim3T
(kPa)	brmd	brmd	brmd	brmd	brmd
50	0.556	0.566	0.516	0.595	0.516
100	0.535	0.545	0.504	0.579	0.512
200	0.523	0.537	0.497	0.578	0.508
400	0.520	0.526	0.484	0.579	0.503
	simB1	simB2	simD2	sim4T	sim20
	brmd	brmd	brmd	brmd	brmd
50	0.433	0.317	0.402	0.523	0.193
100	0.412	0.287	0.369	0.511	0.177
200	0.406	0.276	0.341	0.503	0.182
400	0.408	0.273	0.323	0.499	0.183
	er1	arv3	rtk	psf1a	
	armfld	armfld	armfld	armfld	
100	0.362	0.402	0.451	0.433	
150	0.346	0.338	0.445	0.413	
200	0.325	0.331	0.443	0.406	

Table 5.5.2
Preveza - Igoumenitsa

normal stress	residual stress ratio				
	agn1	agn2	kd	kdAb	kks1
(kPa)	armfld	armfld	armfld	armfld	armfld
100	0.264	0.352	0.447	0.282	0.328
150	0.25	0.350	0.389	0.243	0.326
200	0.226	0.348	0.326	0.245	0.327
400	0.221		0.310		
	kvtA lp	kvt1 hpB	ll1	lts	xml mp
	armfld	armfld	armfld	armfld	armfld
100	0.300	0.332	0.370	0.140	0.427
150	0.268	0.305	0.317	0.124	0.358
200	0.264	0.284	0.277	0.123	0.305
400		0.273	0.262	0.124	0.291

Table 5.5.3
Amalias - Goumeron

normal stress	residual stress ratio					
	ktr2	skf1	mvg	nsa1	pls	oen2
(kPa)	armfld	armfld	armfld	armfld	armfld	armfld
100	0.316	0.261	0.341	0.444	0.471	0.336
150	0.293	0.192	0.285	0.334	0.416	0.269
200	0.288	0.155	0.296	0.302	0.392	0.263
400		0.124		0.292		0.252

Table 5.5.4
Irakleion (Tsiambaos, 1987)

normal stress	res. stress ratio	
	ts71	ts26
(kPa)	brmhd	brmhd
50	0.642	0.618
100	0.573	0.594
200	0.507	0.589
400	0.498	0.587

Table 5.5.5
Korinthos

normal stress	residual shear stress (kPa)				
	simG4	sim1A	sim7A	sim2T	sim3T
(kPa)	brmd	brmd	brmd	brmd	brmd
50	27.8	28.3	25.8	29.8	25.8
100	53.5	54.5	50.4	57.9	51.2
200	104.6	107.4	99.4	115.6	101.6
400	208.0	210.4	193.6	231.6	201.2
	simB1	simB2	simD2	sim4T	sim20
	brmd	brmd	brmd	brmd	brmd
50	21.7	15.9	20.1	26.2	9.7
100	41.2	28.7	36.9	51.1	17.7
200	81.2	55.2	68.2	100.6	36.4
400	163.2	109.2	129.2	199.6	73.2
	er1	arv3	rtk	psf1a	
	armfld	armfld	armfld	armfld	
100	36.2	40.2	45.1	43.3	
150	51.9	50.7	66.8	62.0	
200	65.0	66.2	88.6	81.2	

Table 5.5.6
Preveza - Igoumenitsa

normal stress	residual shear stress (kPa)				
	agn1	agn2	kd	kdAb	kks1
(kPa)	armfld	armfld	armfld	armfld	armfld
100	26.4	35.2	44.7	28.2	32.8
150	37.5	52.5	58.4	36.5	48.9
200	45.2	69.6	65.2	49.0	65.4
400	88.4		124.0		
	kvtA lp	kvt1 hpB	ll1	lts	xml mp
	armfld	armfld	armfld	armfld	armfld
100	30.0	33.2	37.0	14.0	42.7
150	40.2	34.5	47.6	18.6	53.7
200	52.8	38.4	55.4	24.6	61.0
400		76.0	104.8	49.6	116.4

Table 5.5.7
Amalias - Goumeron

normal stress	residual shear stress (kPa)					
	ktr2	skf1	mvg	nsa1	pls	oen2
(kPa)	armfld	armfld	armfld	armfld	armfld	armfld
100	31.6	26.1	34.1	44.4	47.1	33.6
150	44.0	28.8	42.8	50.1	62.4	40.4
200	57.6	31.0	59.2	60.4	78.4	52.6
400		49.6		116.8		100.8

Table 5.5.8
Irakleion (Tsiambaos, 1987)

normal stress	res. shear stress	
	ts71	ts26
(kPa)	brmhd	brmhd
50	32.1	30.9
100	57.3	59.4
200	101.4	117.8
400	199.2	234.8

Table 5.5.9

normal stress	residual effective angle of friction (deg)						
	slmG4	slm1A	slm2T	slm3T	slm4T	slm20	slm21
(kPa)	brmd	brmd	brmd	brmd	brmd	brmd	brmd
50	29.1	29.5	30.8	27.3	27.6	10.9	18.0
100	28.2	28.6	30.1	27.1	27.1	10.0	16.0
150							
200	27.9	28.2	30.0	26.9	26.7	10.3	15.4
400	27.5	27.7	30.1	26.7	26.5	10.4	15.3
	er1	slmB1	slmD2	slm7A	arv3	rtk	psf1a
	armfld	brmd	brmd	brmd	armfld	armfld	armfld
50		23.4	21.9	27.3			
100	19.9	22.4	20.3	26.8	21.9	24.3	23.4
150	19.1				18.7	24.0	22.4
200	18.0	22.1	18.8	26.4	18.3	23.9	22.1
400		22.2	17.9	25.8			
	ktr2	skf1	mvg	nsa1	pls	oen2	
	armfld	armfld	armfld	armfld	armfld	armfld	
50							
100	17.5	14.6	18.8	23.9	25.2	18.6	
150	16.3	10.9	15.9	18.5	22.6	15.1	
200	16.1	8.8	16.5	16.8	21.4	14.7	
400		7.1		16.3		14.1	
	agn1	agn2	kd	kdAb	kks1	kvtA lp	
	armfld	armfld	armfld	armfld	armfld	armfld	
50							
100	14.8	19.4	24.1	15.8	18.1	16.7	
150	14.0	19.3	21.3	13.6	18.1	15.0	
200	12.7	19.2	18.1	13.8	18.1	14.8	
400	12.5		17.2				
	ts71	ts26	kvt1 hpB	ll1	lts	xml mp	
	brmhd	brmhd	armfld	armfld	armfld	armfld	
50	32.7	31.7					
100	29.8	30.7	18.4	20.3	8.0	23.1	
150			13.0	17.6	7.1	19.5	
200	26.9	30.5	10.9	15.5	7.0	17.0	
400	26.5	30.4	10.8	14.7	7.1	16.2	

fig. 5.5.1 Korinthos

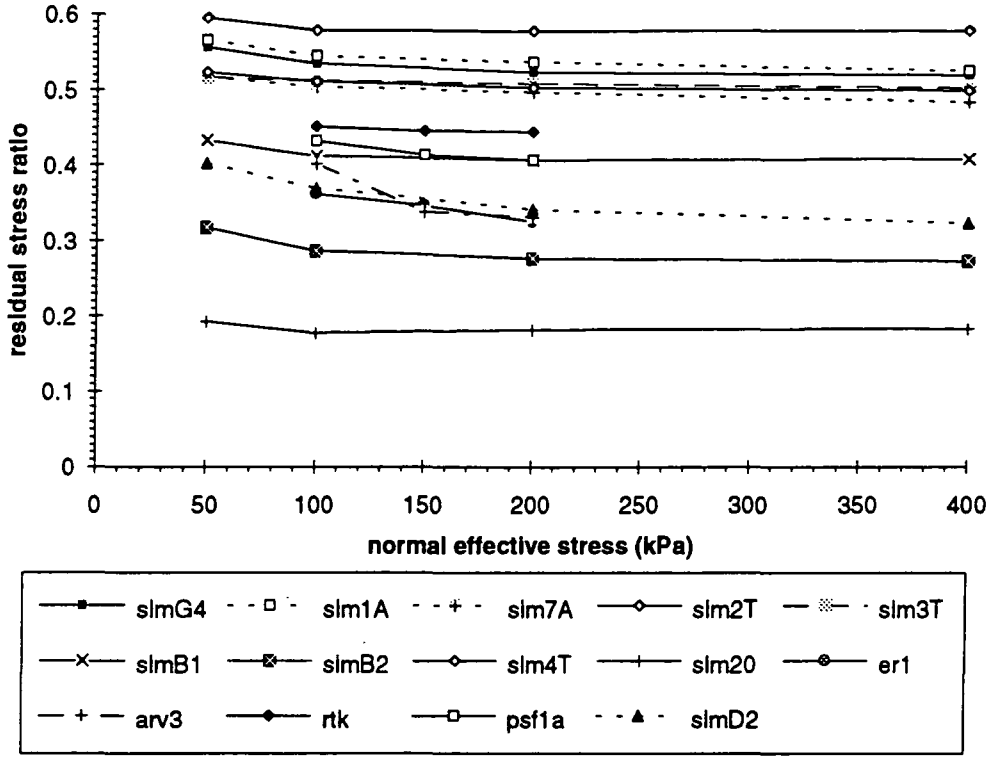

fig. 5.5.2 Korinthos

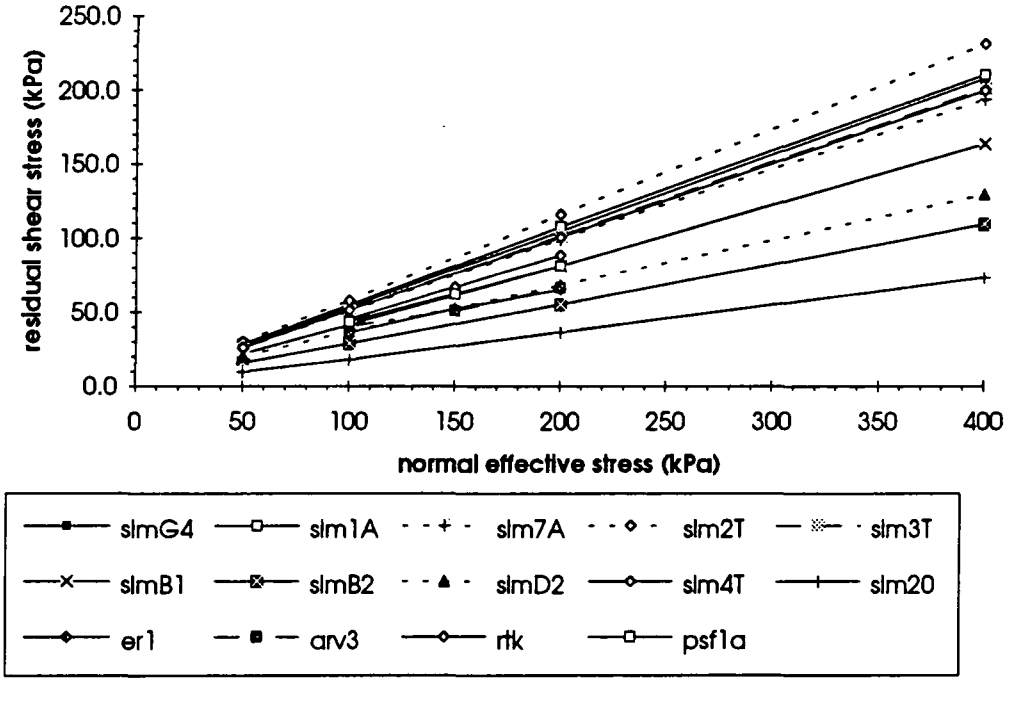

fig. 5.5.3 Preveza - Igoumenitsa

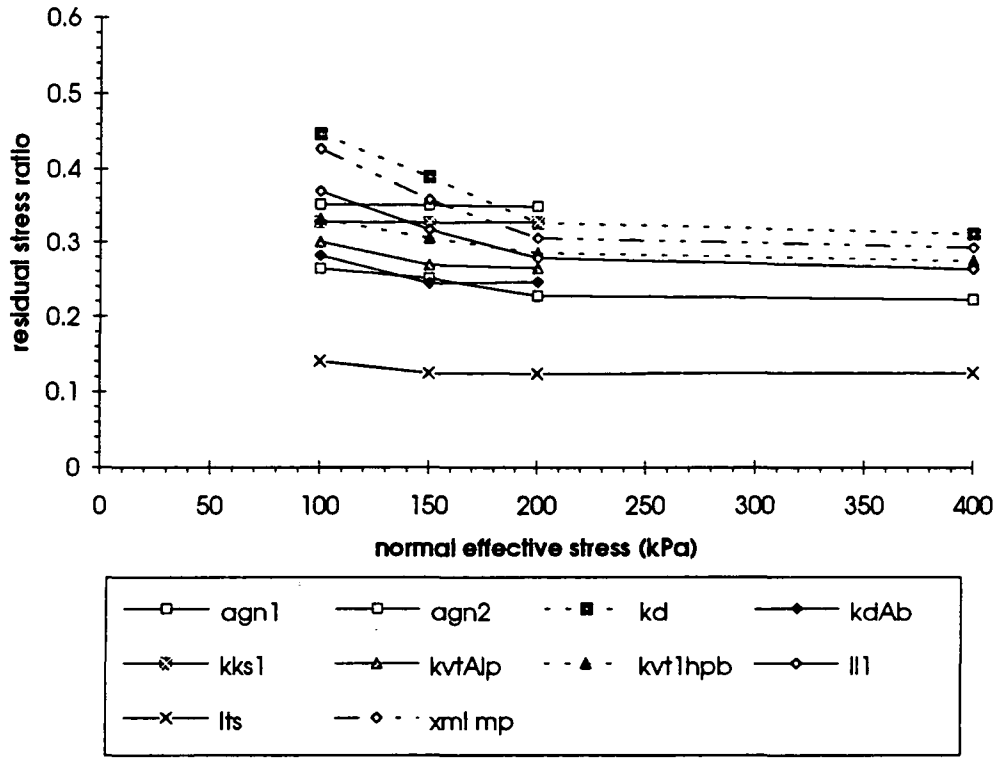

fig. 5.5.4 Preveza - Igoumenitsa

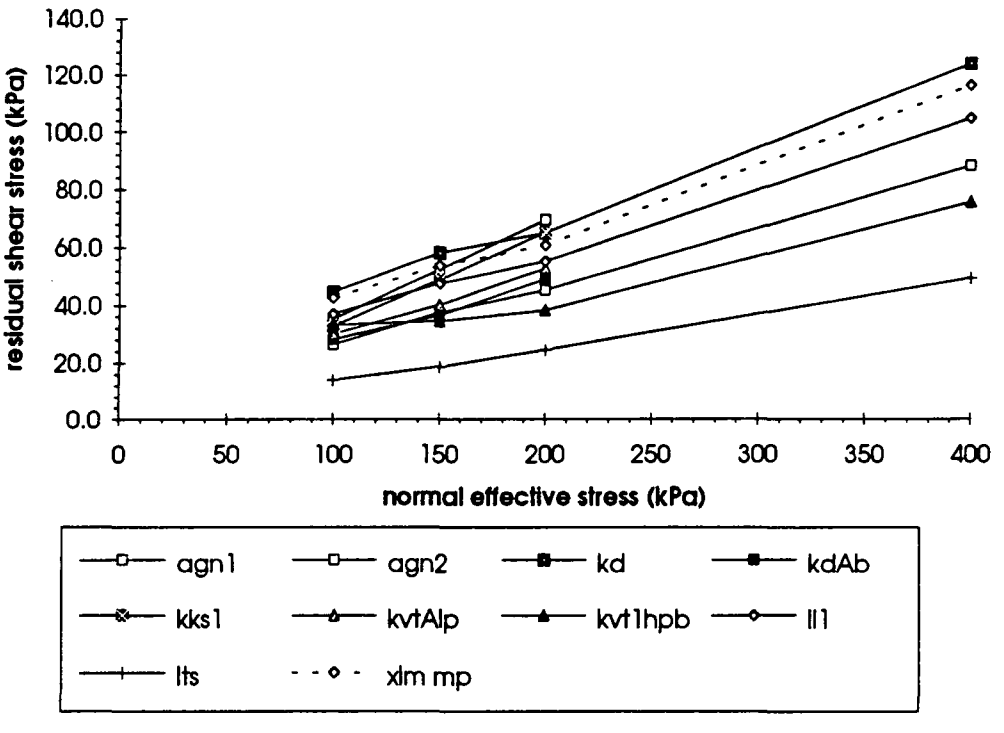

fig. 5.5.5 Amalias - Goumeron

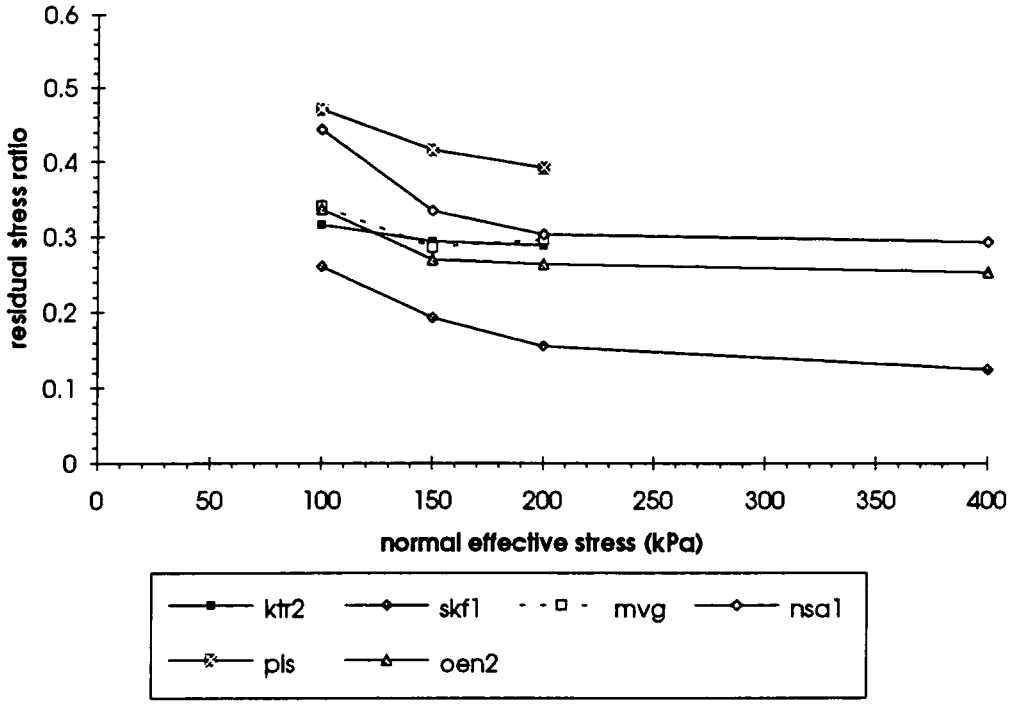

fig. 5.5.6 Amalias - Goumeron

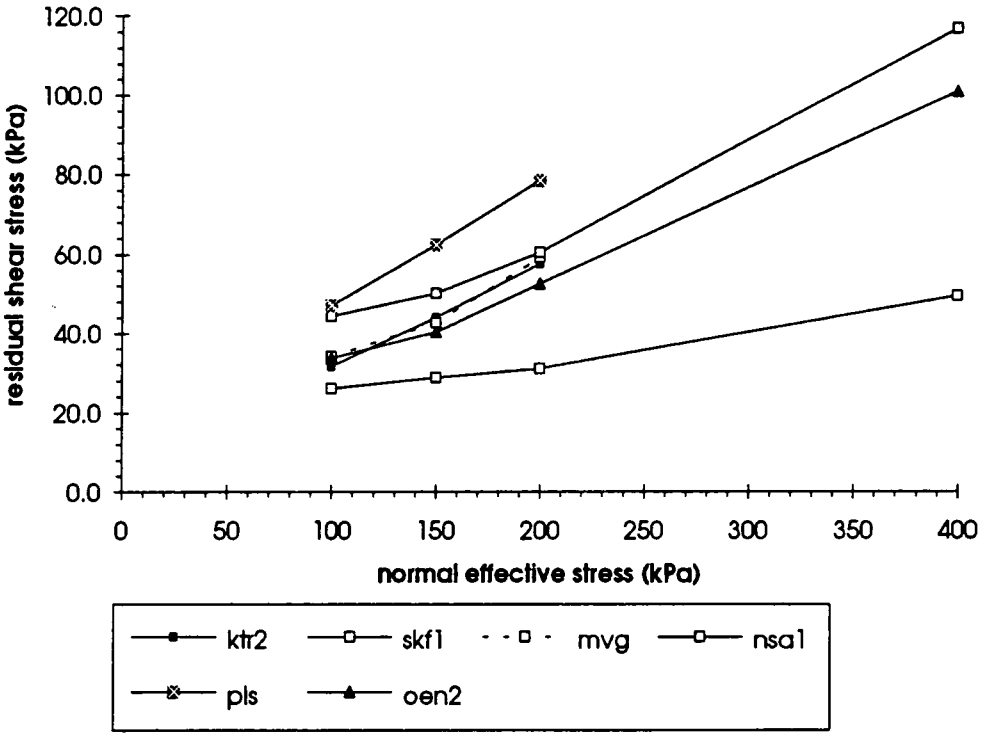

fig. 5.5.7 Irakleion (Tsiambaos, 1987)

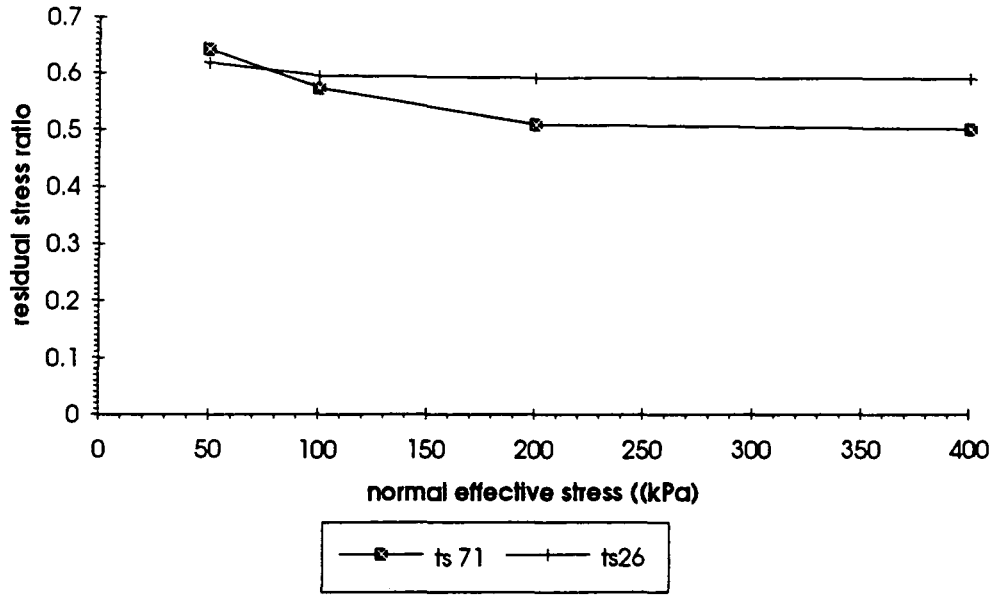

fig.5.5.8 Irakleion (Tsiambaos, 1987)

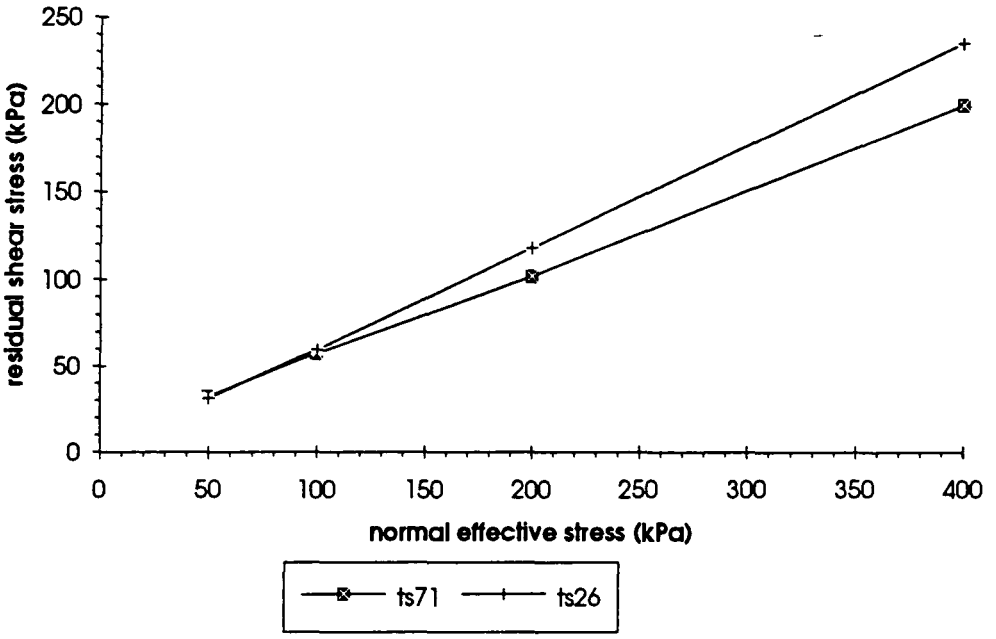

5.6 Analysis of Test results.

5.6.1 Residual stress ratio and shear stress envelopes

Figure 5.5.1 reveals a characteristic flatness of stress ratio to normal effective stress curves for the Korinthos samples relative to curves for samples from the other areas which show a drop in stress ratio for low normal effective stresses between 50 kPa - 200kPa (figs 5.5.3, 5, 7). Test results from both Bromhead and Armfield apparatuses show (with the exception of tests ARV3 and SLM D2) that most of Korinthos samples exhibit only a small drop in residual stress ratio with increasing normal effective stress. For the majority of Korinthos samples the drop in residual stress ratio does not exceed 35% of the value at the begining of the test. This characteristic means a more or less linear increase in shear strength with normal effective stress, with no or very little curving of the shear stress envelope at low normal pressures (fig 5.5.2). Figures 5.5.3, 5.5.5 & 5.5.7 show a more varied behaviour of samples from Preveza-Igoumenitsa, Amalias-Goumeron & Irakleion respectively when compared to Korinthos test results. Residual stress ratio levels may drop by as little as 10% (LTS in fig. 5.5.3) to as much as 150% (NSA1 in fig 5.5.5, TS71 in fig.5.5.7, KVT 1hpb in fig.5.5.3). Curved shear strength envelopes can be found in all three sets of samples.

There are two distinct modes of curvature. The first mode involves an almost linear drop in residual stress ratio values with increasing normal effective stress from 100 kPa to 200 kPa (e.g. KD, AGN1, LL1, XML mp, from fig. 5.5.3; SKF 1, KTR 2, from fig.5.5.5; TS 71, from fig .5.5.8) followed by an almost level section between 200kPa and 400 kPa. This pattern of stress ratio distribution reflects on a pronouncement of the curved section of the envelope of around the 150 kpa normal effective stress . The shape of the curved section of the residual shear strength envelope appears to be convex between 200kPa and 100 kPa effective normal stress.

The second type of curvature of the residual shear strength envelope for the same effective normal stress range (100-200 kPa) is represented by a more exponential like drop of residual stress ratio values with increasing normal effective stress, i.e a sharper drop of ratio values between 100-150 kpa and by comparison a smaller drop between 150-200 kPa normal effective stress. Such a pattern can be seen in cases like KVT 1hpb, LTS, KD ab, KVT Alp, from fig. 5.5.4 and NSA 1, OEN 2 and MVG samples from fig 5.5.6. The shape of the shear strength envelope for the above normal effective stress range becomes more concave.

If no cohesion intercept is assumed (c=0) then further curvature for the shear strength envelope must apply for a number of samples for a normal effective stress range between 0kPa and 50 or 100kPa. It can be seen, however, that the degree of curvature required for a c_r=o envelope varies greatly from sample to sample and more importantly from area to area. Most of the Korinthos envelopes (fig 5.5.2) go through the origin or generally show a small tendency to curve (ARV 3, ER 1, SLM 20). The Preveza-Igoumenitsa test results show (fig 5.5.4) only few envelopes going through the origin (AGN 2, LTS) while the majority show a definite tendency towards a curved shaped envelope for the normal effective stress range between 0kPa and 100 KPa. For some of these envelopes the curvature is shown to be quite pronounced (KVT 1hpb, KD, XML mp, LL1). The Amalias-Goumeron results (fig 5.5.6) follow the Preveza-Igoumenitsa patterns of behaviour with only one envelope going through the axis origin (KTR 2) whilst the rest to a greater (NSA 1, PLS) or a lesser (SKF 1, OEN 2, MVG) extent show a tendency to curve at low normal pressures. The two samples from Irakleion show different envelope characteristics. Sample TS 26 has a linear shear strength envelope that goes through the axis origin (fig 5.5.8) while the envelope of sample TS 71 appears to curve at low normal pressures.

It is interesting to note that results from tests using the Bromhead ring shear apparatus exhibit reduced or no tendency to curved envelopes while test results from samples tested in the Armfield apparatus have shown, by comparison, a greater tendency to curve between 50 kPa and 200 kPa normal effective stress. It can also be observed that, regardless of the apparatus used, soils with low plasticity in general showed low or no tendency to curved envelopes. It can be deduced therefore that for soils with intermediate and high plasticity the type of apparatus used may have played some role in curving the shear strength envelopes. Such a deduction however cannot be substantiated.

It is believed that the different testing procedure used for each apparatus may have played a role which is worth further investigation. In the case of the Bromhead apparatus, the loading sequence was applied such that the soil was consolidated to the normal effective load of the particular shear stage prior to shearing. Hence at any time of the test normal consolidation conditions applied. On the contrary an unloading sequence was chosen for the Armfield apparatus. This means that the soil was consolidated under a load higher than those applied during the the particular shearing stage. Hence over consolidated conditions were introduced. It can be seen that below 150kPa there is a hysteresis in the rate of drop of residual shear strength (fig. 5.5.2, 4, 6

and 8) in both modes of curvature described above, in other words an "apparent" increase in strength compared to what the strength values would be if a linear envelope was assumed for the low normal pressure section of the shear strength envelope.

A plausible mechanism for the curvature of the strength envelopes is thought to be related to the stress relief effects on the samples during unloading. It is believed that increased stress relief could cause a greater degree of swelling to occur within the sample. Such swelling could render the areas beside the shear plane less compact as well as causing dislodgement of swollen clay particles from the shear plane. The disturbance of the shear zone due to unloading would then either increase with further unloading (concave envelopes) or it is probable that it reached a new equilibrium, thus allowing the shear plane to respond to further displacement as it did prior to that disturbance (convex envelopes).

The range of values for the residual stress ratio at normal effective stresses between 200 and 400 kPa is wider for the Korinthos samples than for samples from other areas. This may be partly due to the fact that a larger number of samples from Korinthos have undergone ring shear testing. On the other hand it can be observed from figure 5.5.1 that most of the samples exhibit residual stress ratio values between 0.4 (21.8°) and 0.50 (26.6°) with extremes at 0.581 (30.1°) maximum (SLM 2T) and 0.183 (10.4°) minimum (SLM 20). The Preveza - Igoumenitsa test results (table 5.5.2) shown in figure 5.5.3 suggest a lower residual stress ratio values range, for the same range of normal effective stress, between 0.2 (11.3°) and 0.34 (18.8°) with a low extreme at 0.124 (7°) at LTS. Similarly, for the Amalias - Goumeron set of results the range of most of the results is 0.25 (14°) and 0.3 (16.7°) with an upper extreme at 0.392 (21.4°) at PLS and a low extreme at 0.124 (7°) at SKF1. It can therefore be suggested that the residual strength characteristics of the tested samples are significantly influenced by the geological conditions of the area from these which samples have been obtained

5.6.2. Granular Void ratio

The definition of e_g as the ratio of volume of platy particles and water over volume of rotund particles reflects changes in packing due to compression directly (Lupini et al 1981). The range of normal effective stress taken into consideration in fig. 5.6.1 is between 200kPa and 400 kPa, providing a stress ratio range between 0.124 and 0.433 and a corresponding granular void ratio range between 2.1 and 0.56. The low values of e_g indicate a well graded granular fraction with platy particles much smaller than the rotund ones. Provided that the water used for the experiment and the pore water have

the same chemistry, the values of the Happisburgh-London clay mixtures presented by Lupini et al (1981) should be a useful guide to the type of residual behaviour. These mixtures form a boundary line when plotted as an e_g against τ/σ_n' graph. Most soils lie above this line with those exhibiting turbulent behaviour at $e_g<1$, sliding behaviour at $e_g>2.2$ and a transitional mode in between (Lupini et al, 1981).

It can be seen that only one point in figure 5.6.1 lies above the Happisburgh-London clay mixtures line, corresponding to a clayey and/or least aggregated sample (KD Ab). However the rest of the points lie below the boundary line described. Below this line Lupini et al (1981) suggest that possible sliding shear is expected for a soil sheared against a smooth interface, but they provided no information about the case of samples not sheared against an interface yet having low e_g values .

The results presented in table 5.6.1 are those for which the moisture content at the end of the experiment was determined. Lupini et al (1981) derived an expression similar to the one by Wroth (1979) which can be used for the calculation of the water content at the end of the experiment:

$$w_f = w_L - Ip * \frac{\log(p'_m) - \log(p'_{mL})}{\log(p'_{mP}) - \log(p'_{mL})} \qquad (5.6.1)$$

where P_{mL}' is the mean effective stress at the liquid limit, taken to be 5.5kPa, P_{mp}' is the mean effective stress at plastic limit, taken to be 550 kPa and $P_{m'}$ is the mean effective stress during the test, taken to be the normal effective stress. An attempt was made to use equation 5.6.1 by applying on P_{ml}' and P_{mp}' values calculated from corresponding slurry tests via the expression:

$$e = w * G_s \qquad (5.6.2)$$

and reading off the corresponding value of pressure from an e-logσ_n' graph. The correlations between the experimental moisture content values and the calculated values obtained through applying the set 550 and 5.5kPa for P_{mp}' and P_{ml}suggested by Lupini et al (1981) values and also the estimated ones from the e-log σ_n' plots are given in figures 5.6.2 and 5.6.2 respectively. In neither case do the calculated values agree well with measured values. Therefore, no attempt has been made to calculate values for the tests in which the final moisture content was not determined.

Table 5.6.1

Granular Vold Ratio

sample	granular void ratio	stress ratio
RTK	0.562	0.433
AGN1	1.253	0.221
AGN2	1.319	0.348
LTS	2.087	0.124
XLM.MP	1.124	0.2905
KKS1	1.046	0.3266
KDAB	2.197	0.245
KD	1.249	0.3099
KVTALP	1.454	0.2638
NSA1	1.193	0.2916
SKF1	2.131	0.124
PLS	1.171	0.392
OEN2	1.522	0.252

fig. 5.6.1

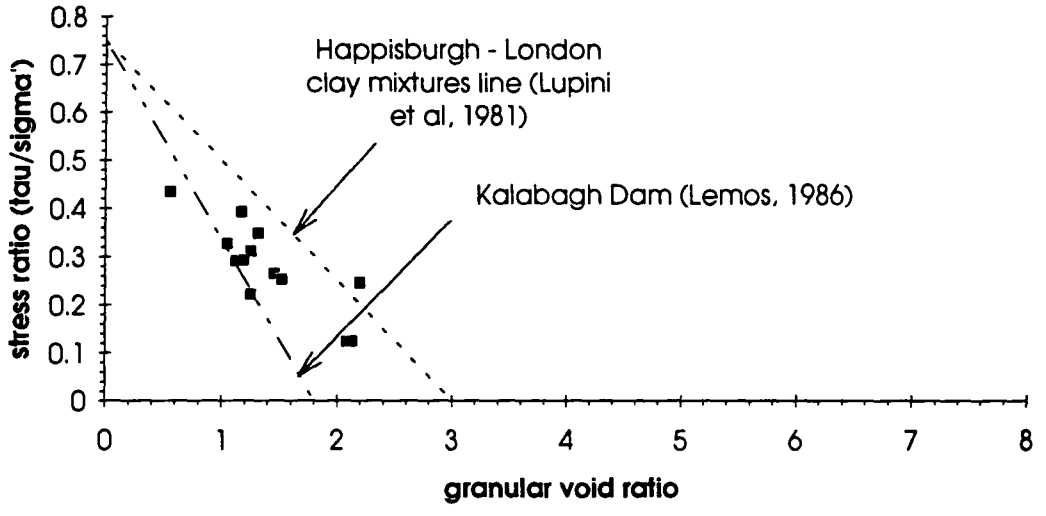

fig. 5.6.2 Ring shear test final moisture content

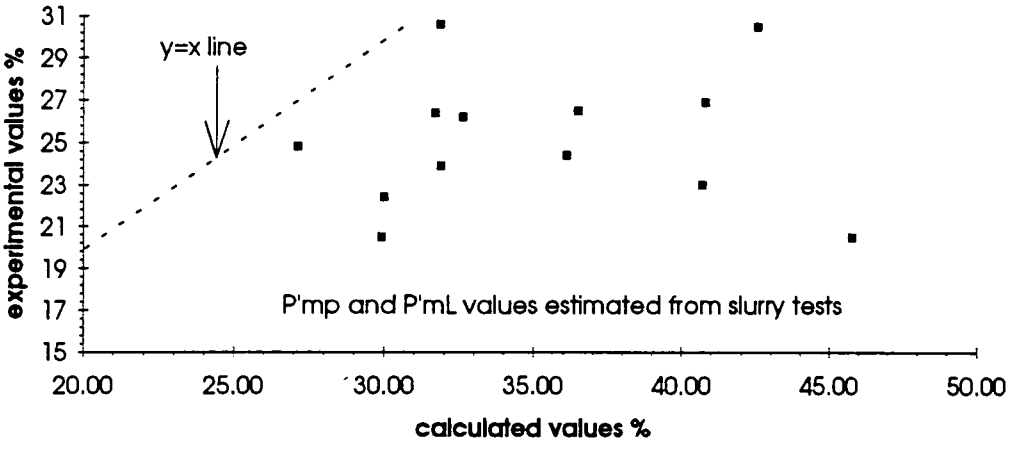

fig. 5.6.3 Ring shear test final moisture content

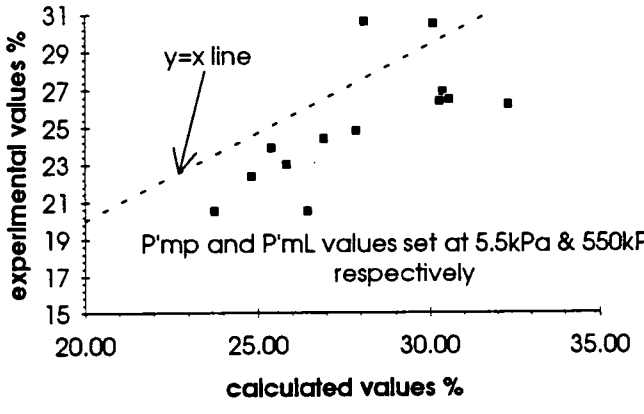

5.7 Discussion

5.7.1 Comparisons with results from other Hellenic formations

Results from other Hellenic formations (Giannaros *et al,* 1992; Kalteziotis, 1992; Tsiambaos, 1991) point at the same range of residual strength parameters obtained during this ring shear testing programme. Specifically Giannaros et al (1992) reported ring shear tests performed on marls from Spathovouni, Korinthos, giving ϕ_r' values from 21 degrees to 27.5 degrees (stress ratios: 0.83 to 0.52) at σ_n'=400kPa. These compare with values of 10 to 27.5 degrees obtained here, although the majority of results fall between 18 and 28 degrees. Giannaros *et al (*1992) have results from samples which lie in the vicinity of the Arvanitis, Rentaiika & Evryteri Roumania sites which yielded results that are in good agreement with the author's results. Unfortunately the nature of the shearing envelopes has not been reported by the authors. It should however be stressed that the term good agreement is used hereby in a lenient manner reflecting the problem arising from the frequent lateral changes of petrological facies within short distances, a local characteristic of Korinthos Neogene and Quaternary materials.

Tsiambaos (1991) reported results for Irakleion marls and argillaceous marls suggesting average ϕ_r' values from 26° to32° for σ_n'=250kPa-600kPa a range well within the data presented here on marls and marly formation from Solomos, Penteskoufi and Rentaiika sites. The same author, in agreement with findings hereby, suggested that curvature is possible by noting different (higher) ϕ_r' values for σ_n'<250kPa.

Kalteziotis (1992) tested a wider range of soils including marly clays and clays as well as marls using a Bromhead apparatus and reported values of ϕ_r' from 10 degrees to 30 degrees at σ_n'=400kPa. Bearing in mind the geographical spread of Kalteziotis' data, the data presented here has produced an equally wide range of ϕ_r' values from 7 degrees to 31 degree at σ_n'= 200kPa - 400kPa.

However, the strong linear nature of the shear stress envelopes found by Kalteziotis for a wide variety of soils does not agree with the findings of this research. It has been shown earlier that the more plastic the soil, the more prone it was to curvature with the less plastic ones having an almost linear envelope. A plausible mechanism (see 5.6.1) that attempted to explain the general trend of suppressing curvature of the shear strength envelope for tests conducted in the Bromhead apparatus (using loading rather

than unloading sequences) could perhaps be of some help to explain the dissagreement between Kalteziotis(1992) and the data presented in this thesis.

5.7.2 Testing Procedures and the curved envelope

5.7.2.1. General

Tests in the Bromhead apparatus were subjected to normally consolidated conditions while tests in the Armfield apparatus were subjected to overconsolidated conditions. It seemed reasonable to use overconsolidation at that time due to device constraints (see sections 5.2.2.2 & 5.4.2.2) and because a model for overconsolidated soil is potentially more valuable to the engineer than one for normally consolidated soil, since overconsolidated conditions are more frequently encountered in nature. As Pender (1978) noted, the potential utility of such a model outweighs the well-known difficulty in interpreting the results of tests on such material because of the inhomogeneity of deformation that develops. As described already in section (5.6.1), the curved part of the shear strength envelope observed between 100kPa and 200kPa normal effective stress is possibly due to increased stress relief caused by unloading during the tests performed in the Armfield apparatus. For the tests performed in the Bromhead apparatus, where loading sequences were preferred, any curvature of the shear strength envelope may be explained by the difference between σ_n' and the swelling pressure developed by the clay minerals during a given loading stage.

5.7.2.2.Physico-Chemical swelling and curved envelope implications

The double layer theory as presented by Sridharan & Javena (1982) explains that compressibility of a clay is controlled primarily by the shearing resistance at the region where two adjacent particles come closest together. This resistance is not equal at all points of contact and volume changes occur by shear displacements and /or sliding between particles. Secondly, compressibility is governed by the long-range electrical repulsive forces, which are mainly of double layer repulsive forces.

Taylor & Cripps (1984) showed that at room temperature (20° C) and pore-water salt concentration at 0.0005 mol/KCl (water content 30%) a micaceous clay exhibits swelling pressure = 232kPa. The presence of more hydrophile minerals such as montmorillonite with average free swell ranging between 100% and 1500% depending on the exchangeable cation (Ca and Na respectively) or even vermiculite or swelling chlorite which do not usually exhibit volume changes to the same extent as smectites but have higher free swell values than average illite with 89% and kaolinite with 28% (Taylor and Smith, 1986) may increase such swell pressure value. Hence, given the

right conditions the swelling pressure of a sample could exceed that applied on the apparatus. The additional disturbance caused by that will affect the linearity of the shear stress envelope.

5.7.2.3 Mechanical swelling and curved envelope implications

On the other hand, mechanical swelling occurs in response to stress unloading in an elastic and time-dependent manner. Mesri et al. (1978) has shown that in samples remoulded to exclude discontinuities and any preferred flow channels, the Terzaghi one-dimensional theory (Terzaghi, 1936) correctly predicts the shape of the percent swell-log time curve up to 60% primary swell. Observed excess negative pressures equilibrated faster than predicted by Terzaghi theory with 50% of the excess negative pressures dissipating 30 times faster. In the case of Bearpaw shale reconstituted samples, the pore pressures eventually became positive, interpreted as being shear induced (Mesri et al. 1978). Part of this swelling, which is in turn part of a natural softening process (Skempton, 1948, 1970), is a chain-reaction nature of particle rearrangement which is a micro-structural readjustment, including particle deformation and reorientation and interparticle slip, a time dependent process.

Mesri et al (1978) showed that the swelling index Cs tends to increase with OCR. The increase in Cs was most pronounced during the decrements that followed sustained secondary swelling and during the first decrements from the maximum pressure at which no secondary compression was allowed. Kirkpatrick et al (1986) showed trends indicating that stress relief effects will not be important if the mean effective stress level from which the clay is unloaded is less than about 100kPa. The above authors found that the more permeable kaolin was more sensitive to the unloading than the illite and produced larger losses of residual negative pore pressure and undrained strength so, as well as the amount of unloading and the OCR, the permeability of the soil has an influence on the behaviour of clay after stress relief. In the case of reconstituted soils the permeability should be a function of mineralogical content, grain size distribution and level of compaction.

5.7.2.4 Concuding remarks

Stress relief induced softening may occur during an incremental unloading ring shear test. The softening which is swelling related can occur on either sides of the shear plane causing micro-structural readjustment, particle deformation and reorientation. The increased water adsorption will cause clay minerals to swell further and thus cause increases in shear stress levels. During an incremental loading ring shear test, swelling will occur when the water bath is first filled unless the first σ_n' increment exceeds the

swelling pressure of the mineral mixture or the natural soil. In both cases the percentage of clay in the samples and the type of clay minerals play a very important role in the extent of swelling. The majority of clay rich engineering soils tested by Privett (1980) were found to have curved residual failure envelopes, the maximum deflection occurring below 200kPa effective normal stress. Kenney(1967) stated that the residual shear strength is dependant mainly on mineralogy and gave examples of curved failure envelopes. He noted that soils with a high proportion of expanding lattice clay minerals show the more pronounced curvature. To that effect, the shape of the shear stress envelope at low normal pressures is suspected to be influenced by swelling induced softening of the material which may disturb the area around the slip surface. More research is needed into these effects.

5.7.3 Granular void ratio

The low values of measured granular void ratio points to a well graded granular fraction with clay particles much smaller in terms of average grain size than the rotund or massive particles. From the grain size distribution curves (see figs. 4.3.1 - 4.3.3) only the former comment can be corroborated. There is a particular difficulty estimating what the average grain size for the clay fraction may be, rendering such comparison difficult. In fig. 5.6.1 it was shown that all but one of the samples exhibited characteristics which do not fit within the Lupini et al. (1981) model for classification of shearing mode depending on stress ratio and granular void ratio values. The reason provided by Lupini et al. (1981) is based on a number of causes which distort the definition of the granular void ratio, such as clay mineral aggregations that break down with displacement and high proportions of very fine rotund particles similar in size to clay particles. Lemos (1986) reported results from Kalabagh Dam which showed that most of the samples lay below the Hapisburgh-London clay mixture line (see fig.5.6.1) . When the granular phase was viewed under optical and electron microscopes it was seen to include a significant proportion of elongated particles of silt size, which seemed to have facilitated the development of sliding shear. Hence smaller values of e_g were needed for transitional shearing to occur.

The samples presented in table 5.6.1 originate from marls, marly clays and cemented mudstones. Therefore the aggregation effect was expected to pose problems in accurately determining e_g. However it is known from the literature that during tests using highly aggregated materials of low plasticity the clay fraction in the residual shear surface was found to be higher than in the adjacent soil (Chandler, 1966, 1969; Clark & Skempton, 1967). The number of exceptions cited in Lupini et al (1981) for

soils not accurately fitting the stress ratio-granular void ratio imposes serious limitations on its usage for any soil that has experienced diagenetic structuring to any degree or any type of fine grained marl.

However if enough care is taken in interpreting relationships that involve the determination of the clay fraction of the above mentioned soil types, an extension to the Lupini et al (1981) model may be considered. Lemos (1986) suggested that if allowance is given to the clay fraction size determination then a new boundary line to the left of that defined by the Happisburgh-London clay mixtures can be considered. He proposed that a steeper and narrower transitional zone should apply, bound by granular void ratios of 0.6 and 1.2. The results presented in fig.5.6.1 lie between Lemos' proposed line and that suggested by Lupini et al (1981). The available data is not adequate to examine how well it fits with the lowest e_g limit suggested by Lemos for a transitional zone. The author found however that at the higher e_g limit the fit is good, if conservative. Samples between e_g=1 and e_g=1.2 show a variable behaviour depending on the level of stress ratio. Highly aggregated AGN1 & KD and NSA1 with a lot of rotund fines (table 5.6.1), all exhibited sliding modes of shear, judging from slip surface observations, hence possessing relatively low stress ratios from 0.22 to 0.3. To accomodate this difference a new e_g=1.1 limit might be considered as more appropriate, though more results need to be made available to corroborate the proposition.

CHAPTER 6
COMPRESSIBILITY OF RECONSTITUTED "MARLS"

6.1 Literature Review

6.1.1 From Sedimentation to Consolidation

Solids suspended in a fluid when left alone will settle under their own gravity until an equilibrium state has arrived. This process is called sedimentation. It is generally accepted that during sedimentation there is no effective stress and the slurry behaves like a fluid. Once a structure is formed and effective stress can be measured, the slurry has become soil, and finite strain-weight consolidation theory has to be used to describe the settlement (Micasa, 1965; Been & Sills, 1981). However, there have been studies that suggest that there may be a transition zone where effective stresses are partially developed (Been & Sills; 1981). Pane & Schiffman (1985) have even introduced an interaction coefficient to account for this transition. A review of the link between sedimentation and consolidation theories is given by Schiffman et al (1988).

In a series of experiments involving slurries with uniform initial void of about 11, Been & Sills (1981), found that the ultimate surface void ratio is 6.5. Now, if the settling process is truely self-weight consolidation, then, as no load is applied to the surface, the void ratio there should remain unchanged. This contradicted the experimental results they reported. To overcome this, Been & Sills (1981) introduced the concept of an "imaginary overburden pressure" and were able to predict quite well the experimental data. However, Tan *et al* (1990) noted that a setback to this approach is that the "imaginary overburden pressure" is not known a priori, since it depends on the ultimate surface void ratio.

More importantly, the settling process may not be a self-weight consolidation but more like sedimentation, since in sedimentation the surface void ratio does change with time. Rates and modes of deposition are likely to vary considerably in nature so there is no reason to anticipate a smooth sedimentation compression curve (Edge & Sills, 1989).

The development of effective stresses is taken to mark the transfer from a suspension with non-Newtonean fluid behaviour to a consolidating soil whose

behaviour may be characterised by the parameters and models of soil mechanics, (Elder & Sills, 1984). Once external load is applied on the slurry and before the slurry develops a structure that can react to external shear stress, compressibility should depend not only on the shearing resistance of the individual particles but it would also be influenced by the geochemical interaction between clay minerals and pore fluid (Bolt,1956; Sridharan & Rao, 1973). Sridharan & Rao (1973) recognised that for natural clays the above mentioned shearing resistance is not equal at all points of contact; volume changes occur by shear displacements and sliding between the particles. In addition, compressibility is governed by the long-range electrical repulsive forces, which are mainly of double layer repulsive forces. Consequently the e-$log\sigma_{v}'$ relationship is significantly influenced by clay type expressed as specific surface area in m^2/g (see table 5.1.1, Sridharan & Jayadeva, 1982).

Table 6.1.1

clay type	**base exchange capacity B: μ eq/g**	**surface area S: m^2/g**
kaolinite	30	15
illite	400	100
montmorillonite	1000	800

6.1.2 Compressibility and Permeability

Hight et al (1987) reported tests on "reconstituted" Magnus clay. They showed that there is a relationship between decreasing void ratio and decreasing vertical permeability with increasing vertical stress. For a stress range applicable to soft clays (20kPa to 300kPa), permeability spanned two orders of magnitude when the soil is consolidated from slurry. The above authors concluded that the net effect of reductions in permeability (k) and compressibility (m_v) with increasing vertical stress levels is that the coefficient of consolidation , $c_v=k/\gamma_w m_v$, where γ_w is the bulk unit weight for water, changes relatively little during virgin consolidation. Lambe and Whitman (1969) have also presented e versus k graphs for a number of reconstituted soils ranging from clays to sandy silts. Tan *et al* (1990) concluded that any permeability versus void ratio relation should depend not only on the concentration of solid particles but also on the initial condition (i.e type of mineral particles, chemistry of the solution medium, clay to non clay mineral ratio) to reflect

the flocculating nature of a clay that affects the soil fabric and consequently the permeability of the clay slurry.

6.1.3 Virgin Compression of Clays

Virgin compression of soils is most commonly expressed by the compression index C_C. This parameter, determined from the slope of a virgin compression curve in void ratio versus logarithm of stress space, quantifies only the compressibility disregarding the volume occupied by the soil at a given stress (Den Haan, 1992). Also, virgin compression curves drawn in this space are generally not straight, but tend to be convex, and therefore C_C comparisons are valid only within a specified stress range which must be quoted.

Sophisticated formulations of the virgin compression of soils, aimed at describing the full relationship between volume and stress over a wide stress range, have appeared regularly in the literature. Of these, various power relationships between a measure of soil volume and vertical effective stress have been most popular. A generalised form of power formulation of virgin soil compression is shown below (from Den Haan, 1992):

$$\frac{v - v_\infty}{v_1 - v_\infty} = \left(\frac{\sigma'_v - \sigma'_{vs}}{\sigma'_{v1} - \sigma'_{vs}} \right)^{-b} \qquad (6.1.1)$$

where v is the specific volume (defined as the ratio between the total soil volume V and the volume of the solids $V_S=1+e$); σ'_v is the effective normal stress; b is dimensionless and has a positive value. The expression 6.1.1 has a vertical asymptote at $\sigma'_v = \sigma'_{vs}$ and a horizontal asymptote at $v=v_\infty$ (fig. 6.1.1). By choosing $\sigma'_{v1} = \sigma'_{vs} + 1$, the equation simplifies to:

$$\frac{v - v_\infty}{v_1 - v_\infty} = \left(\sigma'_v - \sigma'_{vs} \right)^{-b} \qquad (6.1.2)$$

A more simplified form of expression 6.1.2 is deduced if $v_\infty = 1$:

$$\frac{e}{e_1} = \sigma'^{-b}_v \qquad (6.1.3)$$

Expression 6.1.3 has been employed by Garlanger (1972); Mesri, Rokshar & Bohor (1975); Sridharan & Jayadeva (1982); Nagaraj & Srinivasa Murthy (1986) and Jose, Sridharan & Abraham (1990). Similar expressions have been put forward by Juárez-Badillo (1981), Butterfield (1979) and Carrier III & Beckman (1984).

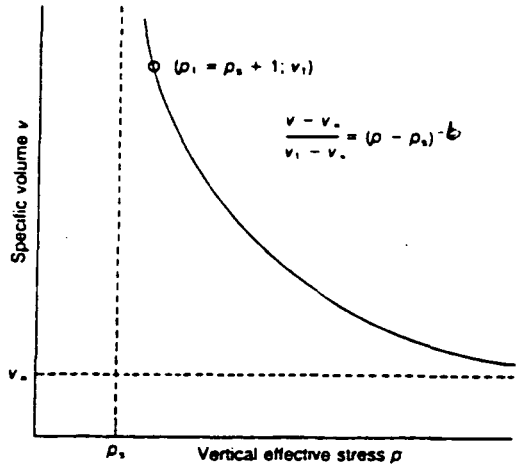

Fig. 6.1.1 Generalised power formulation of virgin compression (expession 6.1.1)

6.1.4 Double Layer Theory and the Compressibility of Clays

The compressibility of pure clays under external load depends not only on the mechanical properties of clay minerals but also on the physicochemical properties of the pore fluid. For example, changes in concentration of ions in the pore fluid, valency of cations or dialectric constant of the pore fluid cause significant changes in compressibility behaviour (Bolt, 1956; Sridharan & Rao, 1973).

Bolt (1956) explained the compressibility of pure clays by considering long-range repulsive forces between the particles. From the diffuse ion distribution around a clay particle in a clay-electrolyte system, the system can be regarded as an osmometer, the semi-permeable membrane of which is formed by the clay particle itself. On applying a load to such a system, a certain amount of pore fluid is pressed out until the difference between the osmotic pressure of the system and of the free liquid pressed out equals the loading pressure. Thus, compressibility will essentially be a function of the double layer repulsive force. Bolt used the Gouy-Chapman theory to predict compressibility behaviour (Chapman, 1913; Gouy, 1910; 1917).

Terzaghi's (1931) view was that physico-chemical activity only occurred after water had entered the system in responce to mechanical causes. Nevertheless it was Terzaghi's principal of effective stress which Lampe (1960) extended to provide the link between *all* the forces which exist in a clay-electrolyte system subject to unloading.

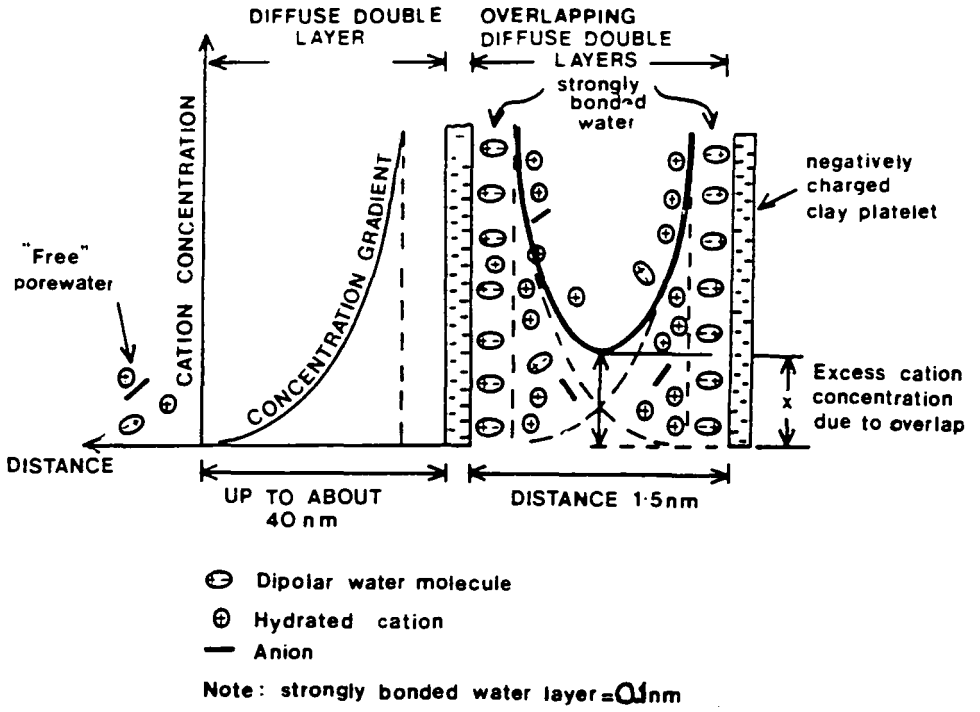

Fig. 6.1.2 Model of double layer system for two clay mineral platelets. Double layer ormed by negatively charged mineral surfaces attracting cations and polar water (from Taylor & Smith, 1986).

Sridharan (1968) examined Lampe's equation and concluded that the average intergranular (effective) stress, $\bar{c}$, may be formulated as follows:

$$\bar{c} = \sigma - \bar{u}_w - \bar{u}_a - R - A \qquad (6.1.4)$$

where $\bar{c}$ is the effective contact stress, σ is the externally applied pressure, $\bar{u}_w$ is the effective porewater pressure, $\bar{u}_a$ is the pore air pressure, R is the total interparticle repulsion over the total interparticle area and A is the total attraction over the total interparticle area. Physico-chemical volume change is governed by repulsive forces, R, since attractive forces, A, are small by comparison within the range of external loadings customarily involved in ground engineering (Taylor & Smith, 1986).

The interaction between clay mineral double layers (fig. 6.1.2) is the primary generator of repulsive forces. In the double layer model there is a balance between coulombic electrical forces and thermal diffusion which largely excludes exchangeable cations from the inner, tightly bonded water layers which total about 1nm in width. The cations which are attracted to negatively charged external surfaces of clay minerals and to internal surfaces of expandable minerals are exchangeable, so clay mineral properties can be changed. More importantly, the cations of the diffuse part of the double layer originate in the free porewater which is

outside the influence of the clay minerals. At spacings below 1.5 nm there is a nett attraction between small particles due mainly to van der Waals' forces. The cations in this case do not form separate double layers but are uniformly distributed between any two clay platelets. When the spacing is greater than 1.5 *nm,* which is beyond the influence of van der Waals' and other surface forces, separate diffuse ion layers form and the minerals will exhibit a nett repulsion

Not all clay minerals are subject to physico-chemical (osmotic) influence, particular those of larger grain size. Mitchell (1960), who performed compression tests on Na-saturated kaolinite, illites and montmorillonites, concluded that double layer theory is not relevant to clay mineral sizes greater than 0.2-1 μm diameter. Kaolinite like granular (non-clay) materials is dominated by the mechanical compressibility concept (Olson & Mesri, 1970; Sridharan & Rao, 1973). According to Olson & Mesri (1970) the behaviour of illite is dependent on the cation present. Sridharan & Rao (1973) showed that although the montmorillonite behaviour complies with the double layer theory, there are quantitative differences between Na-rich and Ca-rich montmorillonites. As with the illites, the monovalent Na allows the development of weaker electrostatic forces thus enhancing the role of the double layer in volume change. Ca-rich illites seem to be influenced by both types of compression mechanisms. Ca-montmorillonite crystalites compact to form irreversible domains which cannot expand to spacings greater than 19-20Å.

6.1.5 Compressibility of Reconstituted Clays and *Intrinsic* Parameters

Leroueil et al (1985) defined four states of structure of clays:
(a) the *intact* state, as it occurs in natural deposits, which is a result of complex geological diagenetic processes;
(b) the *destructured* state, observed when an initially intact clay is submitted to volumetric or shear deformations of such magnitude that the original clay structure is broken (e.g when the preconsolidation pressure has been exceeded);
(c) the *remoulded* state, obtained when sufficient mechanical energy is imparted to a clay mass to reduce its strength to a minimum;
(d) the *resedimented* state, obtained by deposition of clay particles (originally remoulded and mixed to a slurry) by self-weight of the soil column of increasing thickness, which depends on mineralogy and grain size of the soil, the salinity of the dispersion and other environmental factors.
In the 30th Rankine Lecture Burland (1990) suggested that a fifth important state exists, the *reconstituted* state, which is defined as one that has been thoroughly

mixed at a water content equal to or greater than the liquid limit (w_L). He showed that one-dimensional compression curves for some reconstituted clays, covering a wide range of plasticity converge at high normal effective pressures. It was shown that the void ratio at the liquid limit (e_L) was a more fundamental parameter than the liquid limit (w_L).

Burland (1990) introduced the concept of *intrinsic properties* of a given clay as the properties of a clay reconstituted at a water content of between w_L and $1.5*w_L$ (preferably at $1.25*w_L$) without air drying or oven drying, and then consolidated under one-dimensional consolidation. He suggested that the term *intrinsic* had been chosen since it refers to the basic, or inherent, properties of a given soil prepared in a specific manner and which is independent of its natural state. An asterisk is used to denote an intrinsic property (e.g C_c^* is the intrinsic compression index).

The quantities e^*_{100} and e^*_{1000} are the intrinsic void ratios corresponding to σ_n' =100kPa and 1000kPa respectivly. The intrinsic compression index C_c^* is defined as $e^*_{100} - e^*_{1000}$. Hence, e^*_{100} and C_c^* are called the *constants of intrinsic compressibility.* However, there are properties (e.g residual shear strength) which although independent of the natural state of a soil and dependent on constituent grain size and mineralogy, may not qualify as *intrinsic* because Burland's definition restricts the use of the term only to those prepared in the above mentioned specific but quite restricting way.

Burland (1990) suggested that *e-log*σ_v' curves can be normalised by assigning fixed values to e^*_{100} and e^*_{1000}. The normalised parameter I_v is defined such that:

$$I_v = \frac{e - e^*_{100}}{e^*_{100} - e^*_{1000}} = \frac{e - e^*_{100}}{C_c^*} \qquad (6.1.5)$$

Thus the compression curve shown in figure 6.1.3(a) may be transformed to the normalised curve in figure 6.1.3(b), where I_v is the ordinate. From expression 6.1.5 it can be deduced that if $e=e^*_{100}$, $I_v=0$ and when $e=e^*_{1000}$, $I_v=-1$. Burland further suggested that if the void index is less than zero, the sediment is compact and when is greater than zero, the sediment is loose. There is an analogy between the void index and the liquidity index, but it is thought that the void index can be defined in a more direct and accurate manner (from one-dimensional compression) as opposed to the physically complex liquid and plastic limit determination for the liquidity index

Further, Burland (1990) suggested that there is a "reasonably unique" line which can be described with "sufficient accuracy" by the cubic

$$I_v = 2.45 - 1.285x + 0.015x^3 \qquad (6.1.6)$$

where $x = log\sigma_v'$ in kPa. The line is termed the *Intrinsic Compression Line* (ICL) which may either be measured directly for a clay or, if the values for the constants of intrinsic compressibility are known, the ICL may be constructed using the expression 6.1.6.

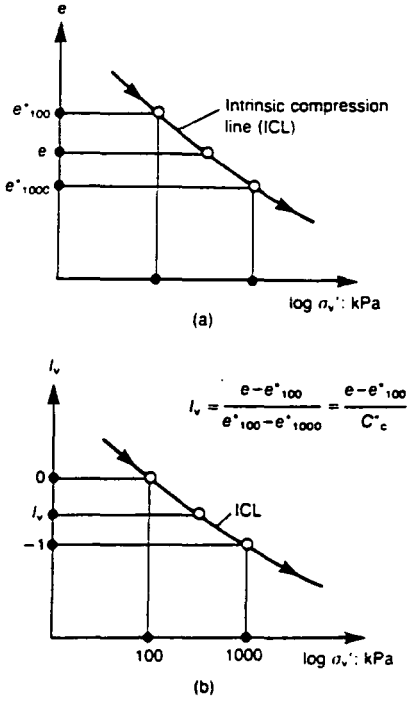

Fig 6.1.3 The use of void index I_v to normalise intrinsic compression curve (Burland, 1990)

Burland (1990) suggested a correlation relating the constants of intrinsic compressibility e^*_{100} and C_c^* and the void ratio at liquid limit e_L expressed by the following equations:

$$e^*_{100} = 0.109 + 0.679e_L - 0.089e_L^2 + 0.016e_L^3 \quad \text{(a)}$$

and (6.1.7)

$$C_C^* = 0.256e_L - 0.04 \qquad \text{(b)}$$

but noted that they are valid only for an e_L range of 0.6 to 4.5, corresponding to liquid limit range of 25 to 160 (assuming an average specific gravity value of 2.4 to 2.8). He compared results from equations 6.1.7a & b with results obtained from

Nagaraj & Srinivasa Murthy (1986) based on physicochemical considerations (double layer theory) and found that there is reasonable agreement apart from significant differences at high and low e_L values. He suggested that small changes in e_L should be taken into account when testing a given clay by correcting e^*_{100} and C_c^* in direct proportion to the changes in e_L. Further, Burland (1990) compared values derived from equations 6.1.7a & b with data from Japanese reconstituted clays at high water contents (Nakase et al, 1988). It was concluded that there was an excellent agreement for C_c^* but all the experimental e^*_{100} values were above the prediction line because of the higher mixing moisture contents used by Nakase et al, (1988). Hence the C_c^* is considered more reliable for comparison purposes. However, Burland (1990) insisted that it is important that the ICL is measured, if possible, directly from oedometer tests.

Leroueil & Vaughan (1990) noted, that in practice, it is difficult to seperate the effect of structure of natural soils from the effect of secondary compression, but evidence of structure may become available by comparing oedometer test results from natural and re-sedimented clays. Such examples have been given by Mesri et al (1975), Locat & Lefebvre (1985), Lapierre (1987) and Leroueil (1988). It is concluded that the *intrinsic compression line* (ICL) can be a valuable reference line for studying the compression characteristics of natural occuring materials, provided they lie above the A-line in the Casagrande plasticity chart.

6.1.6 The Effect of Initial Moisture Content and Load Increment Duration

Skempton (1944) and Leonard & Ramiah (1959) showed that there is an influence of the initial moisture content on the compressibility of a reconsituted clay such that the soil would show quasi-overconsolidation patterns during the first few load increments. They showed that for $p \geq 100$kPa the differences are less. Similarly, Leonard & Ramiah (1959) and Northey (1956) investigated the influence of load increament duration for reconstituted clays. They found that there is very little if no influence at all. Burland (1990) indicated that the void index normalised graphs are insensitive to the above factors.

6.1.7 The Effect of Ageing

There is much evidence that ageing significantly influences the compressibility of reconstituted clays. Leonard & Ramiah (1959) studied the influence of ageing on the one-dimensional compression of a reconstituted clay. They presented results showing creep occuring during ageing and also results with creep being prevented.

In both cases over-consolidation patterns occured during the first few small increments of vertical effective stress. Similar results were obtained by Leonards & Girault (1961).

Burland (1990) considered that the evidence presented by the above authors demonstrate that during ageing a micro-fabric which increases resistance to compression may develop; a resistance that does not depend on volume reduction due to creep. The development of such structures has been observed by Osipov & Sokolov (1978) using scanning electron microscopy. They created pastes of Na-kaolite, illite and montmorillonite which were then placed in layers into "special receptacles". The pastes were allowed to cure for 1min, 1 week, 3 weeks and 1, 2 & 6 months. At the start of the experiment, the samples had good element orientation in the horizontal plane but a sharp decline in orientation was observed after the first week for all three types of minerals used. The authors reported that there was a structural stabilisation beyond the second month. They explained the phenomenon as a result of thixotropic strengthening with time associated with microstructural reorganisation. This reorganisation, according to Osipov & Socolov (1978), is caused by the system tending to come to a thermodynamic equilibrium, due not only to the thinning down of hydrate films at the mineral partical contacts but also to the establishment of an optimum number of such contacts during the formation of the structural network with a certain volumetric periodicity (cellularity). Further, Den Haan (1992) suggested that the void index I_v can be used to depict the relative influence of the postulated non-brittle and brittle components of fabric.

6.2 Testing programme

6.2.1. General

The idea for testing reconstituted "marls" under one-dimensional compression came with the publication of the 30th Rankine Lecture given by Prof. J.B. Burland (1990). The testing programme started in August 1990 and finished in May 1992. All tests were performed in two standard oedometers at the Engineering Geology Laboratory, S.E.C.S., University of Durham. The total number of samples tested was twenty five. Additionally, eleven intact samples were tested to BS1377:1990 specifications. The results of the later can be found in appendix C. Most of the samples tested had also been subjected to residual strength tests.

6.2.2. Equipment

The tests were performed in two Clockhouse Engineering and Instrument Co., type 9200 oedometers complying with BS1377: part 2: 1990 specifications. The confining metal rings used complied with BS1377: part 2: 1990 requirements for minimum internal diameter (50mm). The internal diameter and height of all rings used was accurately measured at the beginning of each test. The load was applied to the cell through a lever arm with a leading ratio of 11:1 applied load over actual dead load. Any vertical movement of the specimen was transfered through the loading cap to a dial gauge and a LVDT potentiometer. The latter was connected to the automatic data logging configuration described in section 5.3.5. Figure 6.2.1 shows the oedometer cell and its recording equipment.

6.2.3. Method of testing

6.2.3.1 Specimen Preparation

Each soil sample was air dried for four days and dry sieved through a 425 μm sieve. Approximately 60 g of the air dried sample were placed and sealed inside a mixing bowl. A small portion (m_i) of the remaining air dried sample was used for moisture content determination.

Once the moisture content of the air dried sample was known to be equal to w_i, the dry mass (m_d) of the specimen in the bowl was calculated as in expression 6.2.1:

$$m_d = m_i(1-w_i) \qquad (6.2.1)$$

The specimen was then wetted to a moisture content equal to 1.5 times its liquid limit, by carefully adding the required quantity of distilled water (m_w) into the mixing bowl:

$$m_w = m_d(1.5*w_L) \qquad (6.2.2)$$

The contents inside the mixing bowl were carefully and thoroughly mixed to form as homogeneous a paste as possible. The bowl was then sealed and its content was allowed to cure for 24 hours. The bowl was then shaken to remove air bubbles formed during the mixing process still trapped inside the paste. The paste was finally transferred with a pallet knife into the confining ring on top of an already saturated porous disc. The transfer was done very slowly and in small portions while the confining ring with the porous disc was shaken on a flat surface using

Fig. 6.2.1 The Oedometer Cell and Recording Configuration used

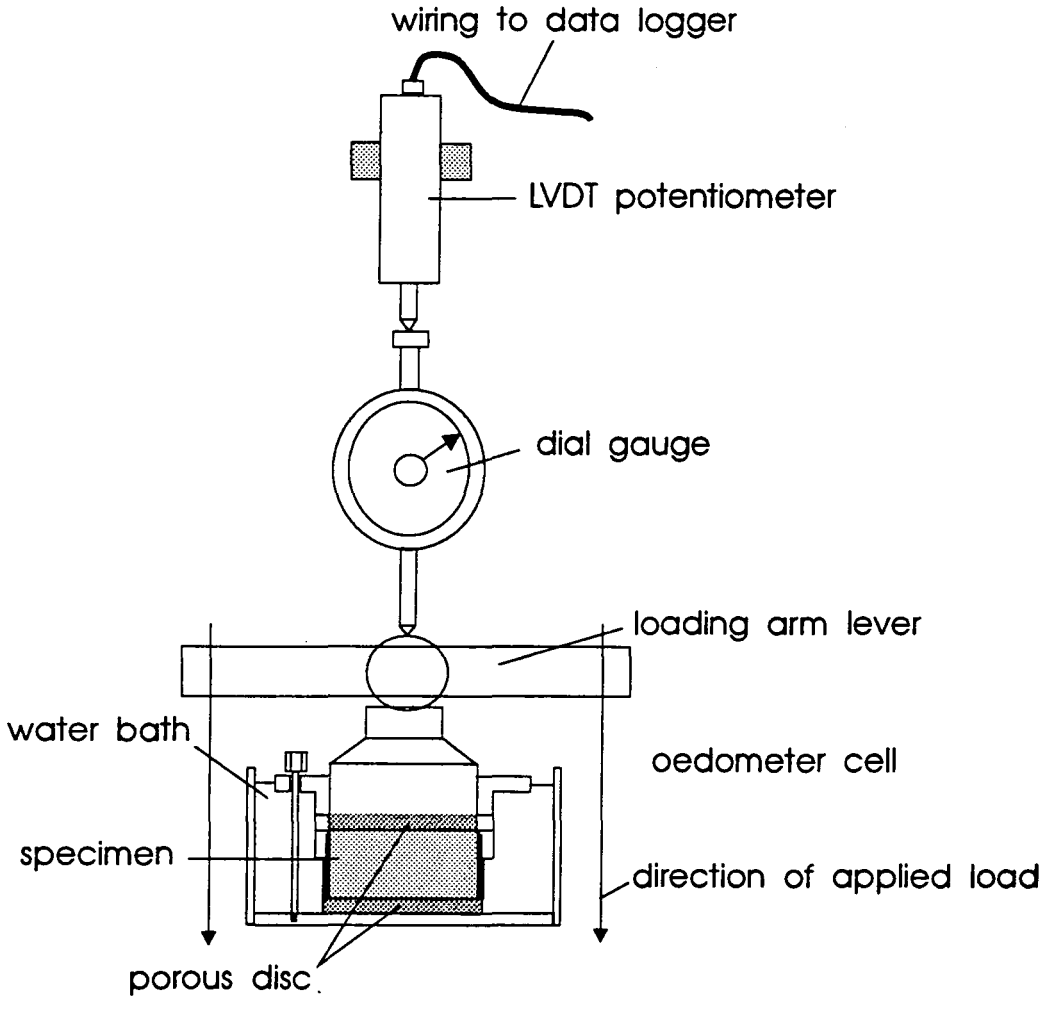

circular movements in a final attempt to minimise any air bubbles. When the confining ring was filled and had a flat specimen surface, the porous disc inside and the loading cap were immediately applied. The water bath was filled with distilled water and the loading arm, still adjusted to zero load, was rested on top of the loading cap.

The readings of the dial gauge and the LVDT were recorded as the initial values prior to loading. Finally from the remaining sample inside the mixing bowl the moisture content at the start of the experiment w_O is determined.

Prior to any new specimen insertion in the oedometer, the exact height of the ring to be used was measured. The whole oedometer was then set up and a metal ring of the same height but smaller diameter was inserted instead of the specimen inside the confining ring. The loading arm was then rested on top of the loading cap and the new position of the balance weights was determined to allow for a completely balanced loading arm at zero load.

6.2.3.2 Testing Procedure

The test procedure has been standardised in BS-1377:1975 for natural soils. The initial pressure would depend on the type of soil and then a sequence of load increments would be applied to the specimen, each being double the previous value. Each load increment would normally be maintained for a period of 24 hours.

In the case of slurry testing, the principal of incremental loading was applied. The initial pressure was set to either 5 kPa or 10kPa depending on the viscosity of the slurry paste. Normally for a fixed water content to liquid limit ratio (w/w_L) the more plastic the soil is the less viscous the water-soil mixture becomes. It was particularly important to ensure that the applied load did not cause sample extrusion especially during the first few load increments. This was achieved by observing the top of the oedometer's loading cap and assessing the rate of consolidation of the primary loading increment as indicators of the slurry's ability to take the next (i.e double the previous) increment or decide to use a smaller incremental step, in order to allow a smoother dissipation of excess pore water pressures.

A typical loading sequence would be 5, 10, 20, 50, 100, 200, 400, 800, 1600 kPa. In certain tests the loading range was extended to 3200kPa and/or included an

additional 1000 kPa step. As already mentioned, occasionally a 35kPa loading step was also included to avoid sample extrusion. Some of the early tests terminated at 400 kPa due to the loading arm coming to a rest on the device's frame. This problem was overcome by inserting extra porous discs underneath the loading cell whenever necessary, thus raising the relative height of the cell and hence lifting the loading arm back to a position close to horizontal. The deformation characteristics of the porous discs were taken into consideration before any calculations took place.

At the end of each 24 hour loading increment, any further consolidation was arrested and the readings of the dial gauge and the potentiometer were taken.

Measurements were taken at set time intervals between the initial value dH_O and the final dH_f, at 10 sec, 15 sec, 30 sec, 1 min, 2 min, 4 min, 8 min, 15 min, 30 min, 1 h, 2 h, 4 h & 8 h. At the end of the loading sequence the specimen was removed from the oedometer and the final moisture content w_f was determined.

6.2.4. Calculation of compression parameters *e*, *Cc*, and *Iv*

The measurements taken during a test were in the form of dial gauge readings in mm and LVDT readings in mV. The readings from the LVDT were selected as the basic for all calculations due to their consistency and accuracy. Dial gauge readings were occassionally used as a cross check on the LVDT readings.

a) The void ratio at the end of the test, assuming full saturation (S_p = 100%), was calculated as follows:

$$e_f = w_f * G_S \qquad (6.2.3)$$

where w_f is the moisture content at the end of the test. The recorded readings (mV) were adjusted to take into account that the starting value was not equal to zero. Hence:

$$r = r_u - r_i \qquad (6.2.4)$$

where r_u is the unadjusted readings, r_i the initial reading prior to the test and r the initialized reading at any stage of the test. If the LVDT calibration constant c is introduced:

$$dH = r * c = (r_u - r_i) * c \qquad (6.2.5)$$

where dH is the compression in mm of any stage of the test. If the void ratio at the start of the test is $e_O = e_f + \Delta e$, where Δe is the total change in viod ratio during the test, then the following expression for any stage of the test becomes:

$$\frac{de}{dH} = \frac{1+e_0}{H_0} = \frac{1+e_f+de}{H_0} \tag{6.2.6}$$

If the above expression is solved with respect to de one arrives to the following expression:

$$de = \frac{dH*(1+e_f)}{H_0 - dH} \tag{6.2.7}$$

where H_O is the initial height of the sample and de is the void ratio change at any stage during the test. Then at the end of the experiment the total reduction of void ratio is as shown in expression 6.2.8.

$$\Delta e = \frac{\Delta H*(1+e_f)}{H_0 - \Delta H} \tag{6.2.8}$$

where $\Delta e = -\int_{e0}^{ef} de = \int_{Ho}^{Hf} dH / V_s = e_0 - e_f$ and $\Delta H = -\int_{H0}^{Hf} dH = H_0 - H_f$, V_S is the volume of solids. From expression 6.2.8 the value of the initial void ratio e_O can be finally calculated. However, if complete saturation is assumed at the start of the test e_O could be calculated from equation 6.2.3 by substituting w_f with w_O the initial moisture content:

$$e_O = G_S * w_O \tag{6.2.9}$$

b) The compression index C_C is the slope of the linear portion of a e-$log\sigma_n'$ plot and is dimensionless. For any two sets of points within that portion of the plot:

$$C_c = \frac{e_1 - e_2}{\log \frac{\sigma'_{v_2}}{\sigma'_{v_1}}} \tag{6.2.10}$$

where σ_v' is the effective vertical pressure.

c) following Burland (1990), any e-$log\sigma_v'$ plot can be normalised by assigning

fixed values to e^*_{100} and e^*_{1000}. The normalising parameter is defined as the void index I_v such that

$$I_v = \frac{e - e^*_{100}}{e^*_{100} - e^*_{1000}} = \frac{e - e^*_{100}}{C_c^*} \qquad (6.2.11)$$

where the quantities e^*_{100} and e^*_{1000} are the intrinsic void ratios corresponding to σ_v' 100kPa and1000 kPa respectively. The intrinsic compression index C_c^* is defined above as $e^*_{100} - e^*_{1000}$.

6.2.5. Presentation of results

Results from the oedometer tests performed on slurries from samples of Korinthos, Preveza-Igoumenitsa and Amalias Preveza are presented in figures 6.2.2 to 6.2.7. Figures 6.2.2 & 6.2.3 present results from Korinthos samples in the e against $\log\sigma_v'$ and I_v against $\log\sigma_v'$ forms respectively. Figures 6.2.4 & 6.2.5 present e against $\log\sigma_v'$ and I_v against $\log\sigma_v'$ graphs based on oedometer test results on Preveza-Igoumenitsa slurry samples. Finally figures 6.2.6 & 6.2.7 present e against $\log\sigma_v'$ and I_v against $\log\sigma_v'$ graphs from oedometer tests on Amalias - Goumeron slurry samples.

Table 6.2.1 presents the *constants of intrinsic compressibility* C_c^* and e^*_{100} together with the Atterberg limits, the void ratio at liquid limit e_L, the ratio of the initial moisture content of the reconstituted material slurry over its liquid limit w_i/w_L, and the corresponding specific gravity for the material.

Appendix C contains e and I_v values for all samples tested in a tabulated form (Korinthos in tables C1 and C4, Igoumenitsa - Preveza in tables C2 and C5, Amalias - Goumeron in tables C3 and C6). Below every I_v against $\log\sigma_v'$ table, the statistical details of regression models (best fit lines) for the I_v values are presented in two forms for every sampling area. In the first, all the I_v values are taken into account and in the second only the I_v values that correspond to $\sigma_v' \geq$ 50kPa are taken into account.

Additionally, appendix C contains the full statistical results of linear regression analysis for the I_v of the samples divided according to their carbonates content in three groups, i.e less than 25%, between 25% and 45% and over 45%. The lower boundary for the carbonates content chosen above was taken from figure 4.4.1 in section 4.4.7. Figure 4.4.1 shows an empirically derived line which marks the

least amount of carbonates required for a given aggregation ratio. It was implied that any excess volume of carbonates above the line for a given aggregatio ratio would only contribute to the mass of the soil. The 25% limit represents the carbonates value for aggregation ratio equal to unity. The 45% limit on carbonates reflects was chosen because it reflects approximately on the argillaceous limestone lower limit (Selley, 1982).

In addition an analysis of the I_v values for the samples divided according to their liquid limit w_L into three groups of less than 40%, between 40% and 50% and over 50% (table C7) is included. For each of these sub-groups there were two statistical tests. As above, in the first test all the I_v values were taken into account and in the second only the I_v values that correspond to $\sigma_{v}' \geq 50$kPa were taken into account The limits on the liquid limit were set at 40% and 50% reflecting major groupings of the tested materials around the said limits.

fig. 6.2.2 Oedometer tests on Korinthos slurries

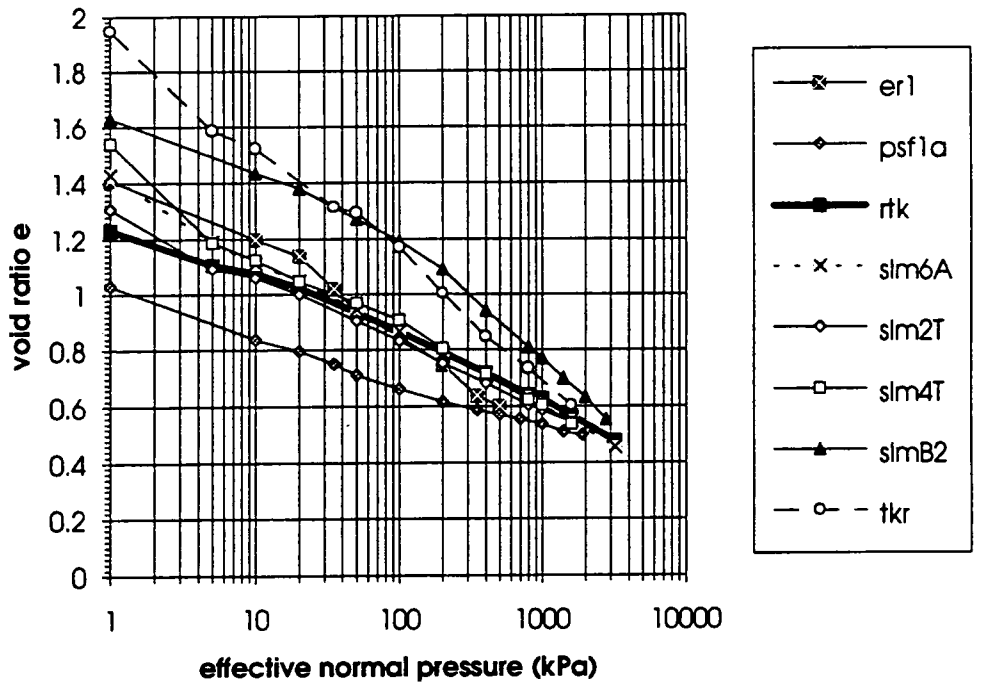

fig.6.2.3 Oedometer tests on Korinthos slurries

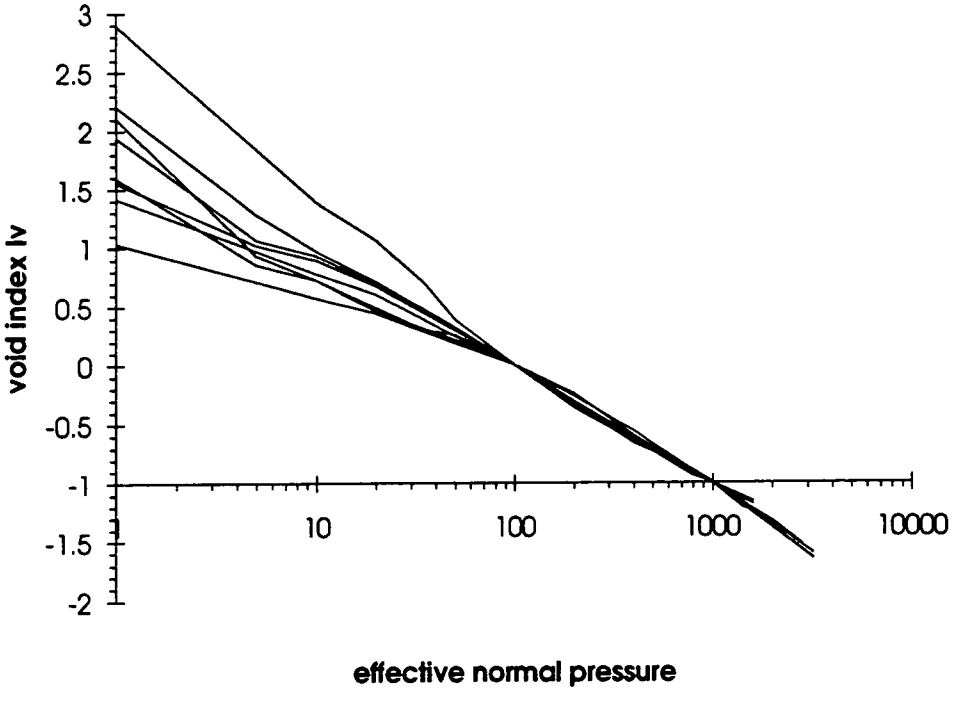

fig. 6.2.4 Oedometer tests on Preveza - Igoumenitsa slurries

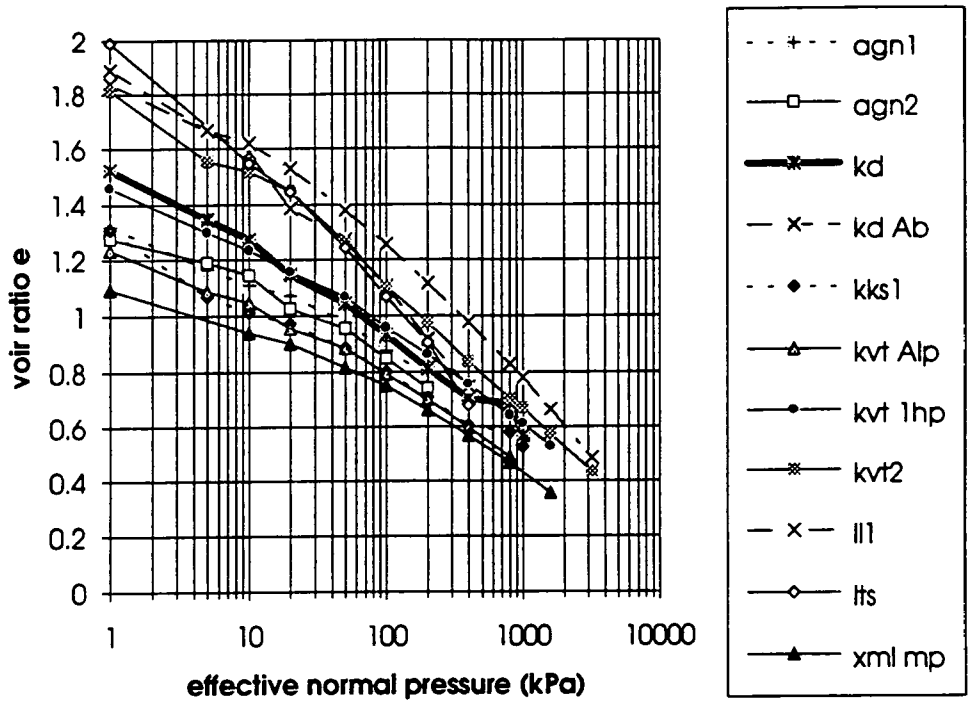

fig.6.2.5 Oedometer tests on Preveza-Igoumenitsa slurries

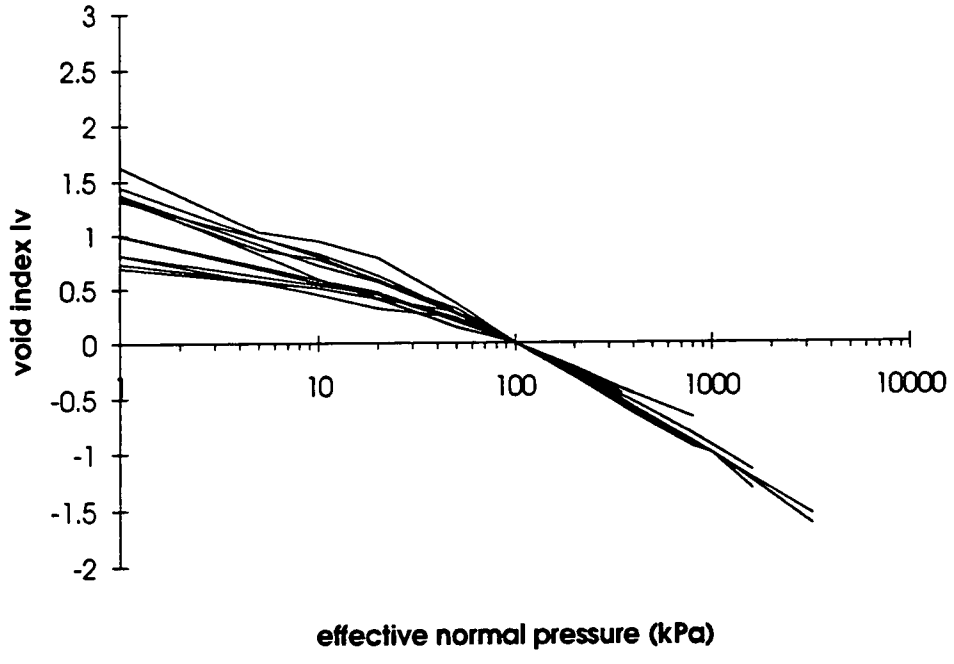

fig. 6.2.6 Oedometer tests on Amalias - Goumeron slurries

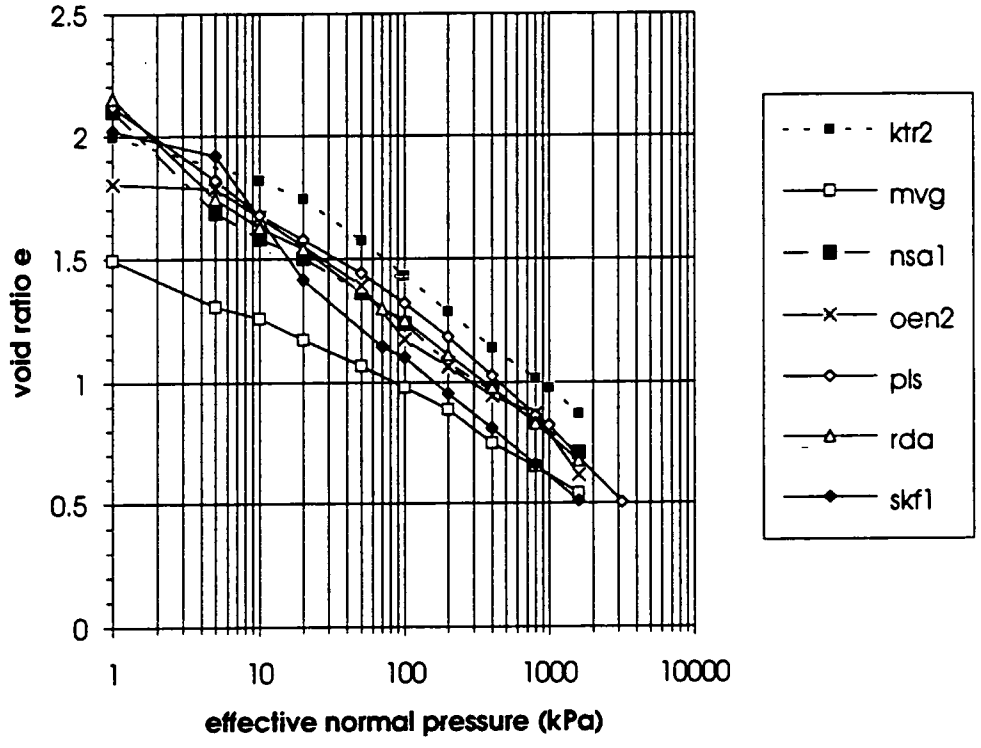

fig.6.2.7 Oedometer tests on Amalias - Goumeron slurries

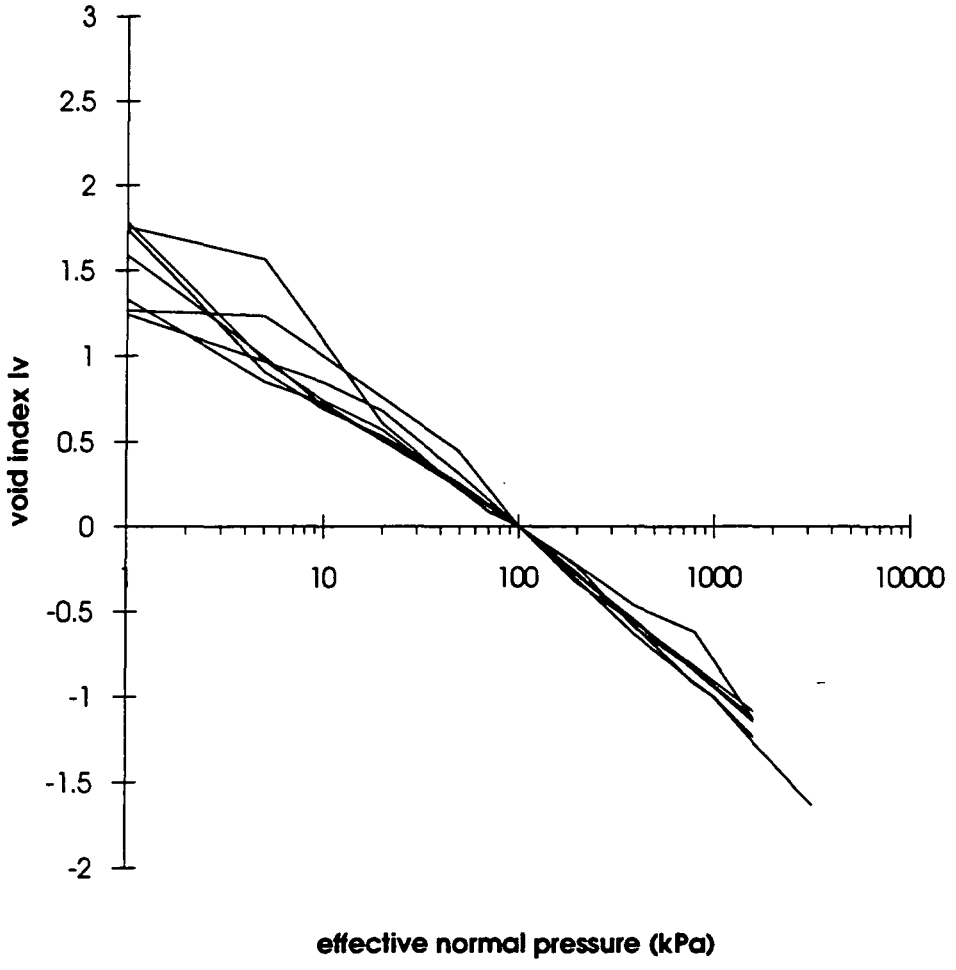

Table 6.2.1

sample	w_L	w_P	w_i/w_L	Gs	e_L	e^*_{100}	C_c^*	
xml MP	48.0	22.00	1.18	2.70	1.318	0.751	0.328	P
ll1	47.30	24.30	1.50	2.70	1.277	1.254	0.474	P
lts	50.90	21.70	1.60	2.65	1.349	1.068	0.645	P
kd	42.70	22.50	1.33	2.68	1.144	1.046	0.363	P
kd A b	56.10	22.80	1.22	2.66	1.492	1.273	0.581	P
kvt2	45.40	19.00	1.37	2.68	1.217	1.105	0.436	P
kvt A LP	44.60	20.00	1.05	2.68	1.195	0.886	0.331	P
kvt1HP b	50.10	22.10	1.21	2.66	1.333	0.958	0.347	P
kks1	42.00	20.00	1.15	2.60	1.092	0.886	0.307	P
agn1	57.30	25.30	1.22	2.67	1.530	0.979	0.351	P
agn2	53.40	23.80	1.31	2.62	1.399	0.958	0.357	P
slm2 T	32.00	22.00	1.50	2.58	0.826	0.832	0.245	K
slm4 T	35.20	18.00	1.50	2.60	0.915	0.906	0.301	K
slm6 A	35.60	19.50	1.60	2.54	0.904	0.864	0.255	K
slm B2	46.50	19.00	1.30	2.70	1.256	1.193	0.423	K
er 1	41.00	21.80	1.15	2.60	1.066	0.937	0.335	K
psf 1 a	32.50	19.10	1.12	2.55	0.829	0.663	0.127	K
rtk	41.00	18.90	1.13	2.60	1.066	0.865	0.236	K
tkr	45.10	21.40	1.56	2.66	1.200	1.169	0.312	K
nsa 1	53.80	23.80	1.52	2.70	1.453	1.242	0.444	A
mvg	45.20	22.30	1.57	2.54	1.148	0.979	0.364	A
ktr2	54.90	22.90	1.10	2.63	1.444	1.432	0.455	A
pls	43.40	21.70	1.70	2.64	1.146	1.322	0.500	A
rda	53.00	24.60	1.53	2.66	1.410	1.253	0.480	A
oen2	46.60	20.00	1.49	2.52	1.174	1.174	0.465	A
skf1	54.70	23.80	1.60	2.65	1.450	1.101	0.489	A

P: PREVEZA-IGOUMENITSA, K: KORINTHOS, A: AMALIAS-GOUMERON

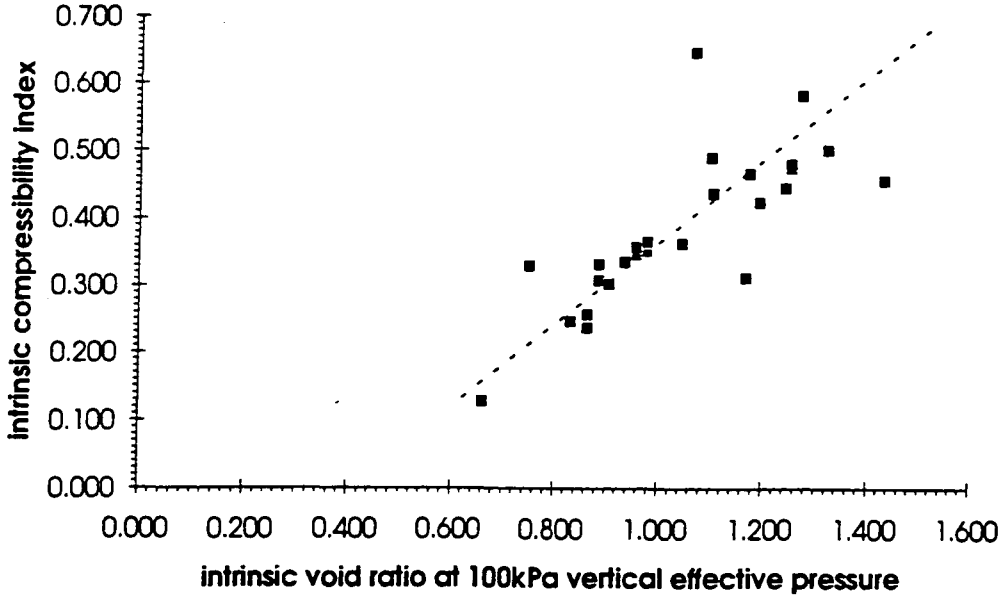

Fig. 6.2.8 Correlation between C_c^* and e^*_{100}.

6.2.6 Analysis of test results

6.2.6.1 The e-logσ_v' curves convergence

Figures 6.2.2 to 6.2.4 show a general trend exhibited by all three groups of samples to converge at high vertical effective stresses. However, the degree of convergence differs for every sample group.

The test results from Korinthos (fig. 6.2.2) show the best convergence of the three groups irrespective of the wide starting values of e_0. For the same range of e_0, Preveza-Igoumenitsa samples show by comparison a weaker tendency for convergence (fig. 6.2.3) while Amalias-Goumeron samples (fig. 6.2.4) exhibit even weaker convergence for the given range of vertical effective stress (5-3,200 kPa).

6.2.6.2 The I_v - logσ_v' curves

The curves presented in figures 6.2.5, 6.2.6 and 6.2.7 have been derived by normalising the ordinate e of the e-logσ_v' graphs according to the expression 6.2.11. The new ordinate is the normalising parameter I_v called the void index.

By normalising the ordinate as above, the compression curves are forced to converge and almost overlap each other for vertical effective stresses in excess of

100kPa. This convergence pattern becomes stronger once the vertical effective stress has reached 50kPa.

There are two distinct points of convergence at 100kPa and 1000kPa owing to the definition of the void index. At these two points the void index becomes 0 and -1 respectively. These two points are shown as junctions through which every curve, for which the I_{v100} and I_{v1000} have been calculated, has to pass. Even when one of the I_{v100} and I_{v1000} has not been calculated for a particular curve (because either e^*_{100} or e_{1000} had not been experimentally determine), it can still be seen that the convergence pattern has essentially been not affected.

Linear regression analysis was performed on the I_v-$log\sigma_v'$ curves from Korinthos, Preveza-Igoumenitsa and Amalias-Goumeron (see appendix C, tables C.4 to C.6). Best fit curves for all three sampling areas obey a cubic polynomial of the form:

$$y = b_3 * x^3 + b_1 * x + b_o \qquad (6.2.12)$$

where y is the void index I_v and x is the $log\sigma_v'$; b_O, b_1 and b_3 are parameters. The term b_2x^2 was very small and was ignored.

As already mentioned in section 6.2.5 there were two statistical tests for every area depending on whether all the loading increments or only those above 50kPa were taken into account.

The polynomials derived from Korinthos samples were:

all increments $y = -0.006 * x^3 - 0.878 * x + 1.787$ (6.2.13)

increments > 50kPa $y = -0.006 * x^3 - 0.886 * x + 1.818$ (6.2.14)

The corresponding coefficients of determination were r^2=0.96 for expression 6.2.13 and r^2=0.996 for expression 6.2.14.

The polynomials derived from Preveza-Igoumenitsa samples were:

all increments $y = -0.0265 * x^3 - 0.484 * x + 1.187$ (6.2.15)

increments > 50kPa $y = -0.0187 * x^3 - 0.626 * x + 1.401$ (6.2.16)

The corresponding coefficients of determination were r^2=0.972 for expression 6.2.15 and r^2=0.991 for expression 6.2.16.

The polynomials derived from Amalias-Goumeron samples were:

all increments $y = -0.0128 * x^3 - 0.719 * x + 1.544$ (6.2.17)

increments > 50kPa $y = -0.0113 * x^3 - 0.755 * x + 1.608$ (6.2.18)

The corresponding coefficients of determination were r^2=0.98 for expression 6.2.17 and r^2=0.985 for expression 6.2.18

It is apparent that the goodness of fit (indicated by r^2) of the expressions improved with the removal of the loading increments up to 50kPa. The same trend was also observed when the samples were grouped according to their liquid limit ,w_L, and their carbonate content.

The regression analysis on the groupings of samples according to carbonate content for loading increments above 50kPa (appendix C, table C.7) showed that the following expressions have very high values of coefficient of determination r^2, averaging 0.99, with standard errors for the y estimate being very similar to those shown for the analysis conducted on samples grouped per sampling area.:

carbonates > 45% $y = 0.0036 * x^3 - 1.097 * x + 2.169$ (6.2.19)

25% > carbonates > 45% $y = -0.015 * x^3 - 0.681 * x + 1.478$ (6.2.20)

carbonates < 25% $y = -0.018 * x^3 - 0.636 * x + 1.422$ (6.2.21)

A closer examination of the above expressions suggests that up to 45% carbonate content, the curves change very little between the up to 25% and between 25%

and 45% sub-groups. The samples with carbonate content over 45% exhibit a somewhat different trend, shown in expression 6.2.19. The full regression analysis results are shown in table C.7 in appendix C.

Similarly, when the samples were grouped according to their plasticity (less than 40%, between 40% and 50% and above 50%) the linear regression analysis showed that the groups are best described (average r^2=0.99) by the following expression:

$$\text{liquid limit} < 40\% \qquad y = -0.0027 * x^3 - 0.982 * x + 1.993 \qquad (6.2.22)$$

$$40\% < \text{liquid limit} < 50\% \qquad y = -0.0148 * x^3 - 0.701 * x + 1.519 \qquad (6.2.23)$$

$$\text{liquid limit} > 50\% \qquad y = -0.0195 * x^3 - 0.589 * x + 1.328 \qquad (6.2.24)$$

The above expressions (6.2.22, 23, 24) refer to data that exclude load increments lower than 50kPa. There is a tendency for increased curvature with increased plasticity shown in the above expressions. The intercept decreases but the parameter attached to x^3 increasingly influences the value of the dependent variable y, especially for values of $x \leq 2$ (i.e $\sigma_v' \leq 100$kPa). The same tendency can also be observed with expressions (6.2.19,20,21) where curvature of the best fit lines for the carbonate content based groups increases with decreasing carbonates content.

6.2.6.3 Constants of intrinsic compressibility

The values for C_c^* and e^*_{100} presented in table 6.2.1 show the wide variety of results obtained during the experimental programme, ranging from 0.127 to 0.645 and 0.663 to 1.432 respectively. However, this wide range of values narrows if the results are grouped into sampling areas.Samples from Preveza-Igoumenitsa show C_c^* values between 0.307 to 0.645 with most of the values falling between 0.328 and 0.436. The e^*_{100} values range from 0.751 to 1.273 with the majority of values falling between 0.886 and 1.068. Samples from Korinthos show values of C_c^* ranging between 0.127 and 0.425 with most of the values falling between 0.236 and 0.335. The e^*_{100} values range from 0.663 to 1.193 with the majority of them falling between 0.832 and 0.937. The Amalias-Goumeron samples show a C_c^* range between 0.364 to 0.500 with the majority

of values lie between 0.444 and 0.480 and an e^*_{100} range from 0.979 to1.432 while the majority of values lie between 1.101 and 1.253 respectively.

Although the above bands of values may still seem to be quite wide, it is clear that individual trends per area can be identified. Korinthos samples show the lowest values of constants of intrinsic compressibility. The highest Korinthos values overlap those from Preveza-Igoumenitsa, with the latter lying within an intermediate band in the present data set. The Amalias-Goumeron samples are the most compressible in the present data set exhibiting the highest values for both C_c^* and e^*_{100}. A weak linear relation between C_c^* and e^*_{100} seems to apply (fig. 6.2.8).

The correlation shown in figure 6.2.8 can be also expressed as:

$$C_c = 0.457 * e^*_{100} - 0.094 \qquad (6.2.25)$$

with coefficient of determination r^2=0.59.

6.3 Discussion

6.3.1 Effects of plasticity on e-logσ_v'-curves

It appears that the curves in the cumulative *e-log*σ_v' graphs 6.2.2, 6.2.3 and 6.2.4 may have been affected by changes in plasticity. This can also be seen in table 6.2.1. So, for instance, samples slmB2 (*Ip*=27.5) and tkr (*Ip*=23.7) in figure 6.2.2, stand out as having higher *e* values from the rest of the Korinthos samples for a σ_v' range of 10 to 1000kPa. Similarly, samples ll1 (*Ip*=23), lts (*Ip*=21.7) and kd Ab (*Ip*=33.3) in figure 6.2.3 appear to have higher *e* values than the rest of the Preveza-Igoumenitsa samples for the same range of σ_v' values. However, caution must be exercised in order to distinguish between the effects of plasticity and the effect of initial moisture content expressed as the mixing ratio w_i/w_L shown in table 6.2.1.

The position of the *e-log*σ_v' curves presented is controlled by their constants of intrinsic compressibility. The effect of plasticity on these constants is shown as relations between the void ratio at liquid limit, e_L, with C_c^* and e^*_{100}, in figures 6.3.1 and 6.3.2. Linear regression lines are shown on the plots. Linear regression analysis showed that the relations shown in figures 6.3.1 and 6.3.2 are weak:

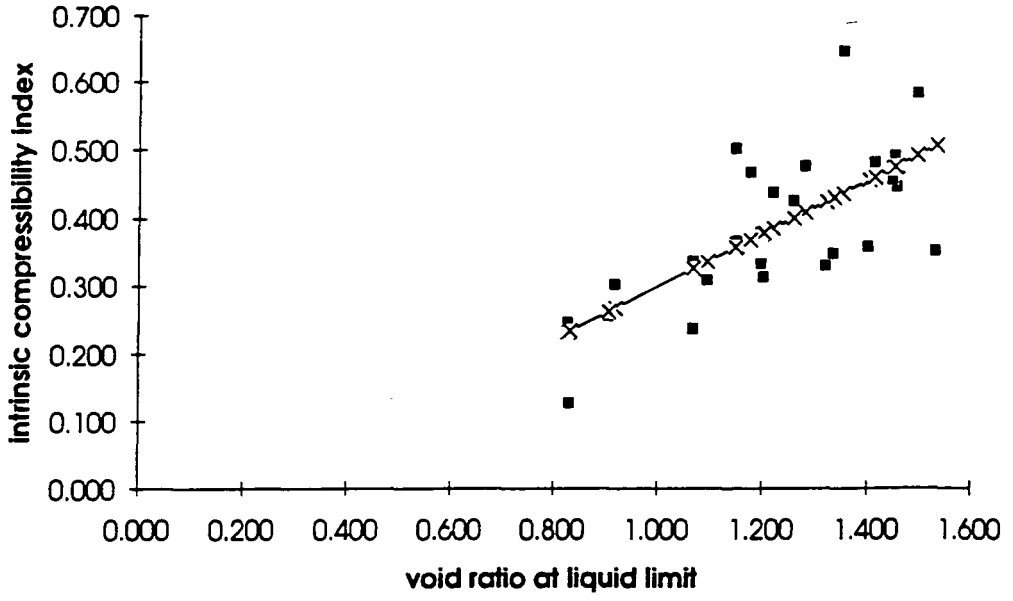

Fig. 6.3.1 Correlation between C_c^* and e_L.

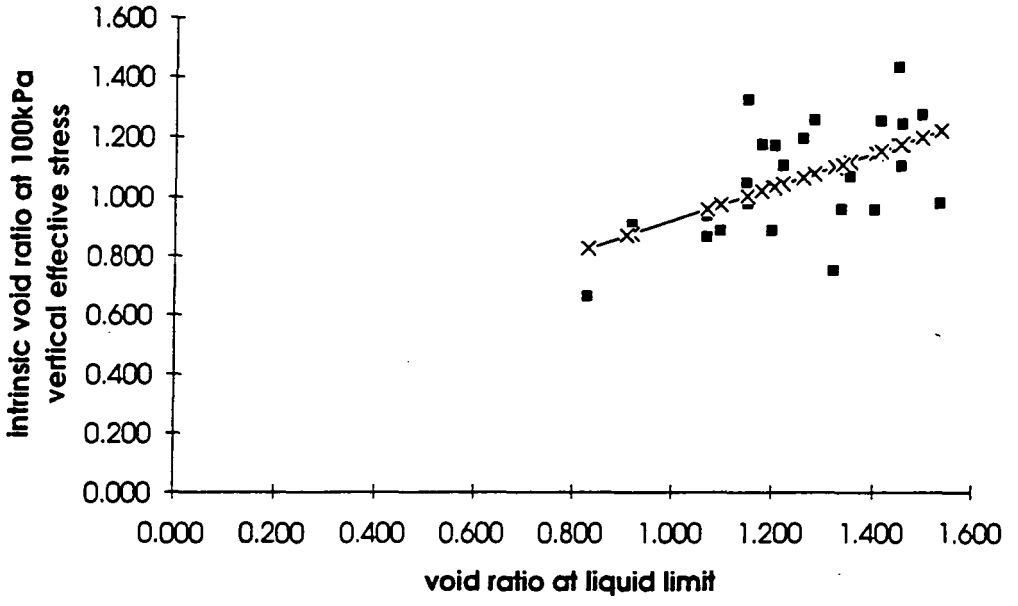

Fig. 6.3.2 Correlation between e^*_{100} and e_L.

$$C_c^* = 0.387 * e_L - 0.088 \qquad (6.3.1)$$

with $r^2=0.59$. Similarly:

$$e^*_{100} = 0.556 * e_L + 0.365 \qquad (6.3.2)$$

with r^2=0.347. The plasticity index *Ip* was not used because it exacerbates errors made during the empirical determination of the Atterberg limits.

6.3.2 The effect of mixing ratio w_i/w_L on the *e-log*σ_v' curves

Leonard & Ramiah (1959) showed that the effect of different mixing ratios is more pronounced with plastic clays, suggesting that at higher w_i/w_L, the values for *e* lie higher than those of lower mixing ratios for the same plastic clay and that convergence may be delayed for as much as one order of magnitude on a *e-log*σ_v' graph when compared to similar tests from less plastic clays.

Such an example can be shown, with some reservation due to some mineralogical differences, for samples xlm MP and ll1. These samples have similar plasticities and the same specific gravity (table 6.2.1) but the mixing ratios are 1.18 and 1.50 respectively. Since $e=wG_S$, the initial void ratios for these two samples could have been identical if the mixing ratios for those two samples were the same. However, the depressed e_0 value for the sample xml MP forces its *e-log*σ_v' curve to show overconsolidated characteristics (fig. 6.2.3) at low σ_v' converging eventually with the one of ll1 at higher stresses.

On the other hand, samples ktr2 and skf1 with similar plasticity and specific gravity (table 6.2.1) show that the difference in mixing ratio has very little affected their relative position in figure 6.2.4 as would be the case if they followed the trend shown above. It appears that although ktr2 and skf1 have comparable C_c^* and e_L values (0.455 & 0.489 and 1.444 & 1.450 respectivly), the former exhibits higher *e* values for the tested range of vertical effective stress.

Significant mineralogical differences are thought to account for this disparity in behaviour. Indeed, ktr2 has a calcite content equal to 45% compared to 0% for skf1 while clay minerals account for 31% and 79% respectively.

6.3.3 Intrinsic compression lines

In the 30th Rankine lecture, Burland (1990) presented results from three reconstituted soils covering a wide range of liquid limits (Argile plastique w_L=128%, London Clay w_L=67.5% and Magnus Clay w_L=35%) and plotted them in the normalised I_v - *log* σ_v' form. He observed that the resulting normalised "intrinsic" compression curves produced a "reasonably unique line"

which he termed the "intrinsic compression line (ICL)" and presented a polynomial expression that best described this line.

Similarly, expressions 6.2.15 to 6.2.26 describe intrinsic compression lines (ICL) based on the data presented in this thesis grouped according to their geographical origin, plasticity and carbonates content, (see section 6.2.6.2).

Figures 6.3.3, 6.3.4 and 6.3.5 show comparisons between the ICLs represented by the expressions 6.2.15 to 6.2.26 and the ICL presented by Burland (1990) for a range of vertical effective stresses between 5kPa and 3,200kPa.

In the first of these figures (6.3.3) the data was divided into three groups according to area of origin (i.e. Korinthos, Preveza-Igoumenitsa, Amalias-Goumeron). The lines representing these groups differ from the Burland's line in terms of the nature of their curvature. All three lines based on results from reconstituted Hellenic "marls" appear convex with degrees of curvature varying from one area group to another. So, the Korinthos ICL is the least curved, Preveza-Igoumenitsa ICL is the most curved and Amalias-Goumeron ICL lies in the middle.

Further, figure 6.3.4 presents the comparison between ICLs of the presented data grouped in terms of their liquid limit and the ICL presented by Burland (1990). These lines show that the differences in curvature between the author's data and that by Burland (1990) shown in figure 6.3.3 persist in the configuration presented in figure 6.3.4. It appears that the more plastic the soil the stronger its tendency to show a convex ICL.

Similarly, when the author's data was grouped in terms of carbonate content and its ICLs were compared to Burland's (1990), the same disparity in behaviour occured as shown in figure 6.3.5, where Burland's line appears concave and the ICLs based on the author's experiments appear convex. It is worth remembering that the expressions 6.2.20 and 6.2.21 which represent the intrinsic compression lines for the 45%<carbonate content<25% and carbonate content<25% are almost identical while expression 6.2.19 which describes the 45%<carbonate content is markedly closer to the one given by Burland in expression 6.1.6. This coincidence is shown in figure 6.3.5 where the lines described by expressions 6.2.20 and 6.2.21 overly each other while the ICL representing the samples with more than 45% carbonates lies closer to the Burland ICL.

It appears, therefore, that the ICLs derived from compression tests on reconstituted Hellenic "marls" differ from each other according to their mineralogy, as this is reflected in terms of liquid limit and carbonate content. The comparison between ICLs derived from data grouped according to their carbonate content and ICLs derived from data grouped according to their liquid limit, point to an inverse relation between the effect of carbonates (mainly calcite) and the effect of liquid limit on the compressibility characteristics of the materials tested.

In summary, the strongest differences in the degree of curvature of the Hellenic "marls" ICLs are practically confined to an area of low vertical effective pressures (up to approximately 50kPa). The differences in terms of the shape of curvature at higher levels of vertical effective stress become less pronounced, however without reaching general agreement. Also, the general trend observed in all nine presented ICLs is that they appear to be convex, unlike the ICL line presented by Burland (1990) which appears to be concave.

It may, therefore, be that the ICL presented by Burland (1990) is not a universally unique line, as suggested, but it is influenced by mineralogical changes and changes in plasticity. However, more research is needed to corroborate the influence of mineralogy and plasticity on the shape of the Intrinsic Compression Line.

Fig. 6.3.3 **Comparison between ICLs grouped per Sampling Area.**

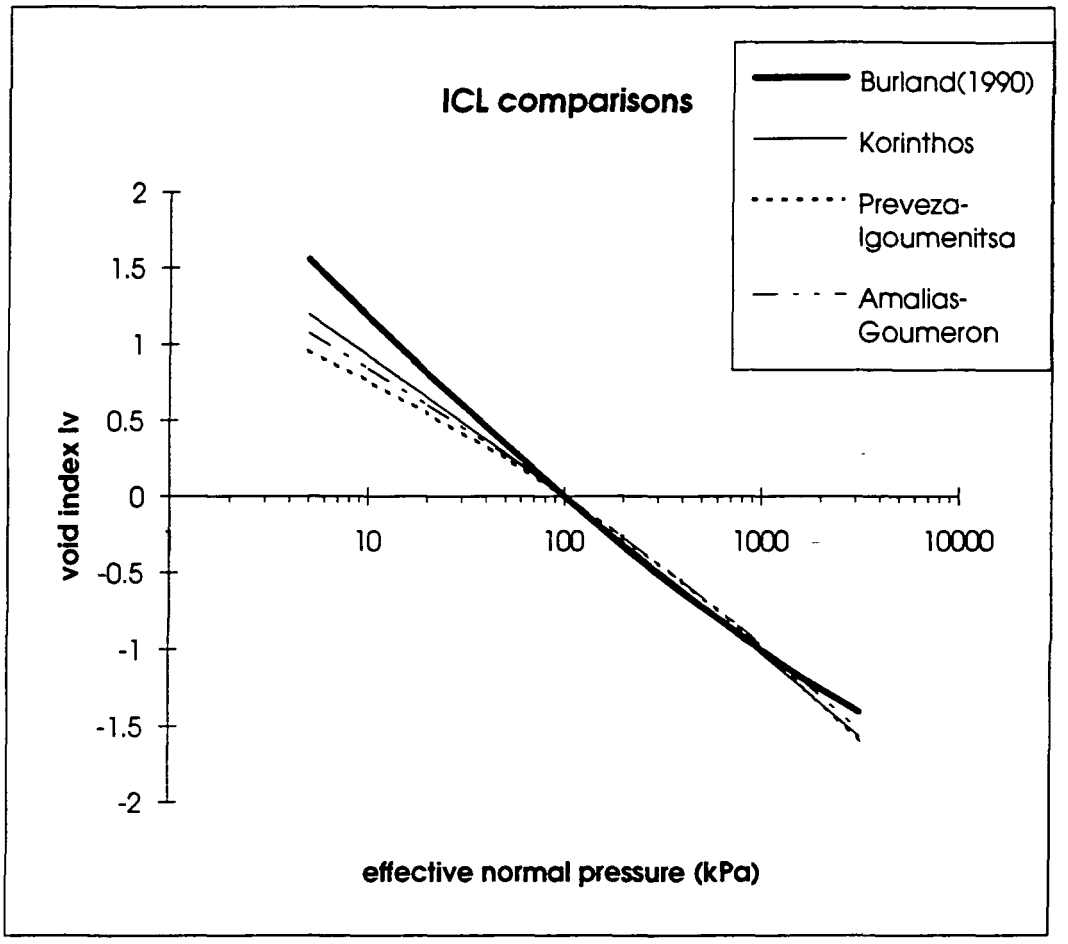

Fig. 6.3.4 Comparison between ICLs grouped according to Liquid Limit.

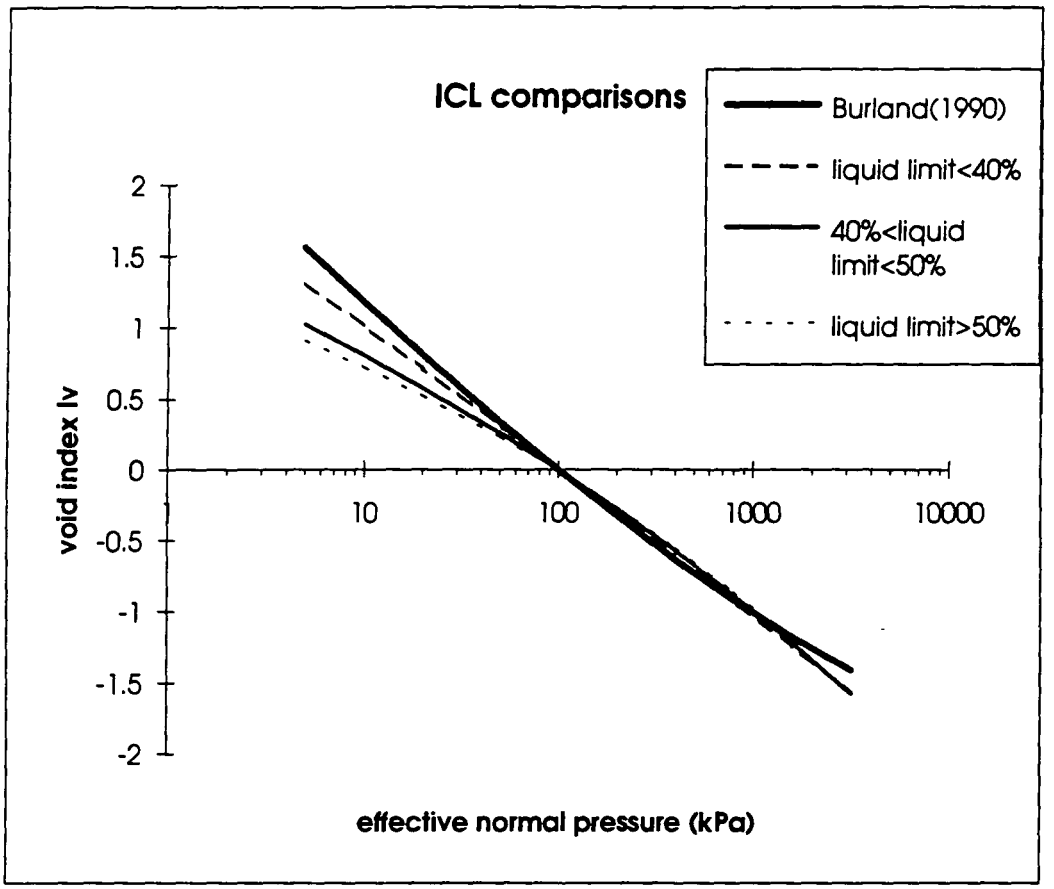

Fig. 6.3.5 Comparison between ICLs grouped according to Carbonate Content.

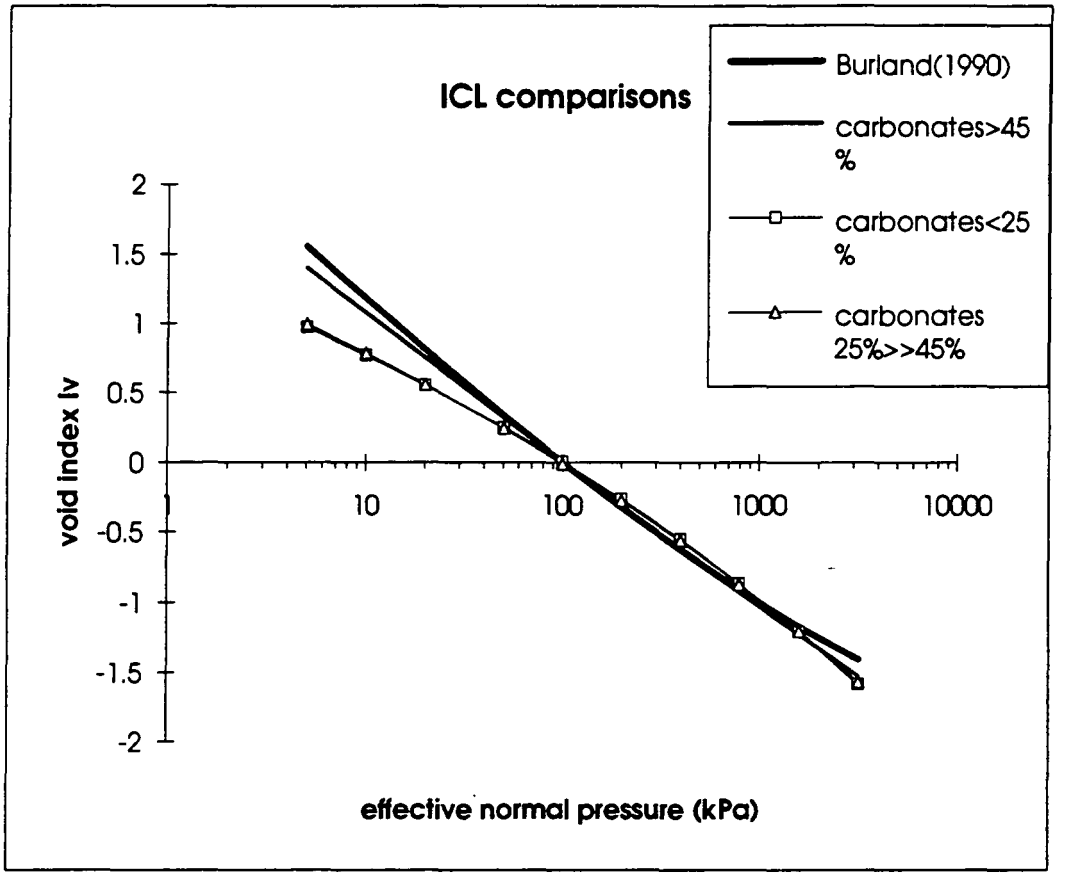

CHAPTER 7
DISCUSSION

7.1 The effects of grain size on the residual strength

7.1.1 General

It has been known for a long time that there is a non-linear relationship between residual strength values and clay fraction (see section 5.1.5, fig. 5.1.1). A similar relationship, inversely proportional to the one identified for the clay fraction, by implication must exist for the coarse size fraction. Additionally, the interaction between clay and coarse size fraction was identified in the form of the granular void ratio (section 5.1.10, fig. 5.1.5), which was in turn used as a modelling parameter for the prediction of the shearing mode of fine grained materials. The granular void ratio is discussed in section 5.7.3.

However there is considerable scatter in any of these correlations. A source of error (and therefore scatter) frequently encountered is the aggregation of clay minerals into particles bigger than 2μm and the presence of very fine rock flour (<2μm) within the clay fraction. Another source of scatter was hinted at by Lupini et al (1981) to be the relative proportions between grain sizes, however without specifying what these relative grain sizes were.

7.1.2 The Effect of Grain Size on the Residual Strength of Hellenic "Marls"

Figure 7.1.1 shows the relationship between the residual angle of friction ϕ_r' and the clay fraction of the Hellenic "marls" tested. Residual angle of friction is taken to be the *arctan* of the stress ratio τ/σ_n' between 200 and 400kPa. Lines depicting the upper and lower bounds of similar graphs presented by Skempton (1964) and Blondeau & Jesseaume (1976) have also been included in figure 7.1.1 to allow comparison.

It can be seen that for a given value or a narrow range of values of clay fraction there is a much wider range of corresponding ϕ_r' values. Because of this wide scatter of values the upper and lower bounds of Skempton (1964) and Blondeau & Jesseaume (1976) are not adequate to describe the tested materials. The reason for this wide scatter of values may be traced to the limiting nature of the two-dimensional

relationship shown in figure 7.1.1, reducing that is the number of input variables required for an accurate solution.

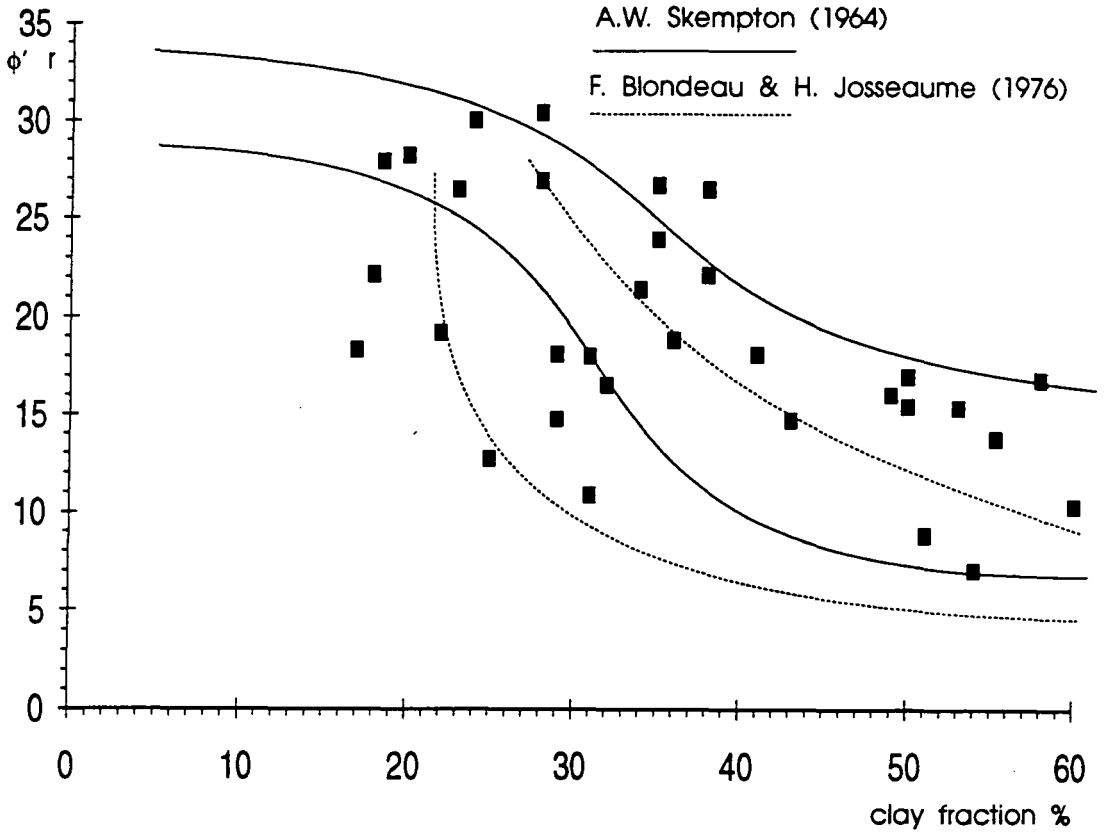

Fig. 7.1.1 The relationship between clay size fraction and the residual angle of friction.

A very similar picture, albeit the inverse, can be drawn if, instead of the clay fraction, the silt size fraction is correlated with the residual angle of friction. The importance of the individual size groups of the silt size fraction with regard to their influence on the residual strength of the tested "marls" is shown in figure 7.1.2. The fine silt size fraction and the medium silt size fraction occupy almost identical areas of the graph especially at an intermediate level between 14° and 22° ϕ_r'. It is tentatively suggested that for the given data population, the fine and medium silt size fractions behave in a very complementary manner over this range of ϕ_r' values. The coarse silt size fraction becomes more prominent for ϕ_r' values in excess of 17°. It should be noted that figure 7.1.2 is not a complete picture of particle size behaviour since the clay fraction is absent and the figure can only serve as an indicator.

The complementary nature of the three silt sub-fractions in influencing the value of

Fig. 7.1.2 The behaviour of silt size sub-fractions with regard to residual strength.

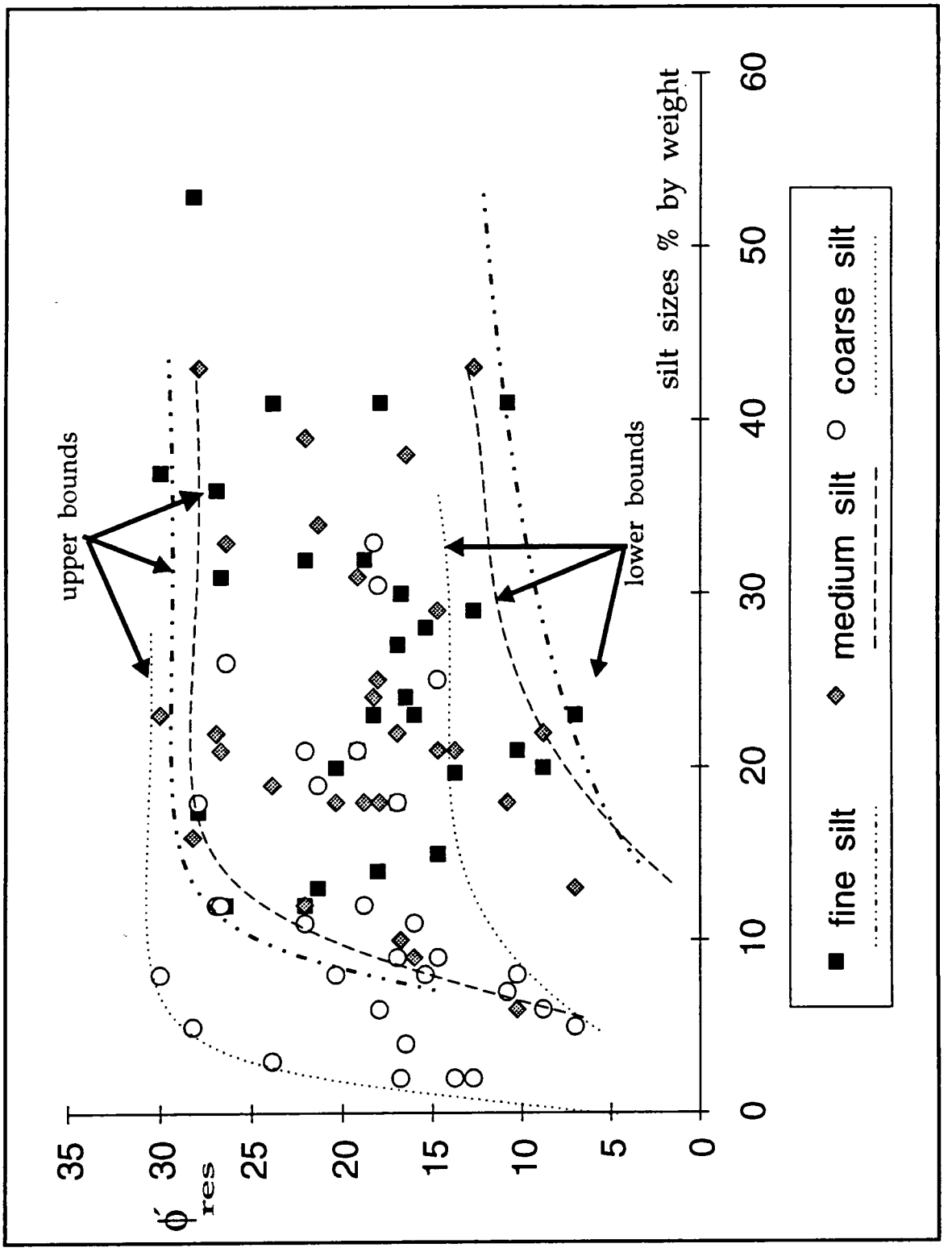

residual angle of friction is better demonstrated in figure 7.1.3. This figure shows that for every clay fraction-ϕ_r' data point, the sum of values for the fine, medium, coarse silt and sand size fractions reduces with decreasing values of residual angle of friction. It can be seen that for some size fractions the reduction is more canonical than for other size fractions. An example of such a trend by a rough grouping of the clay fraction-ϕ_r' data points with regard to changes in fine plus medium silt size values is shown in figure 7.1.3. The graph is divided into three zones A, B and C. Zone A corresponds to fine plus medium silt size values of around and above 50%, zone C represents samples with fine plus medium silt size values around and below 40% and zone B is an intermediate transition zone. However, there are noted exceptions, especially where a particular silt sub-fraction or the sand fraction has a dominant presence (e.g slm2A with 53% fine silt, slmB1 with 17% sand and kks1 with 31% coarse silt). Again, the absence of the rest of the grain size fractions from the consideration shown in figure 7.1.3 may be the reason behind the apparent lack of good fit of the data points with the attempted model of figure 7.1.3. A more complete picture is attempted in figure 7.1.4 where the clay size fraction, the fine

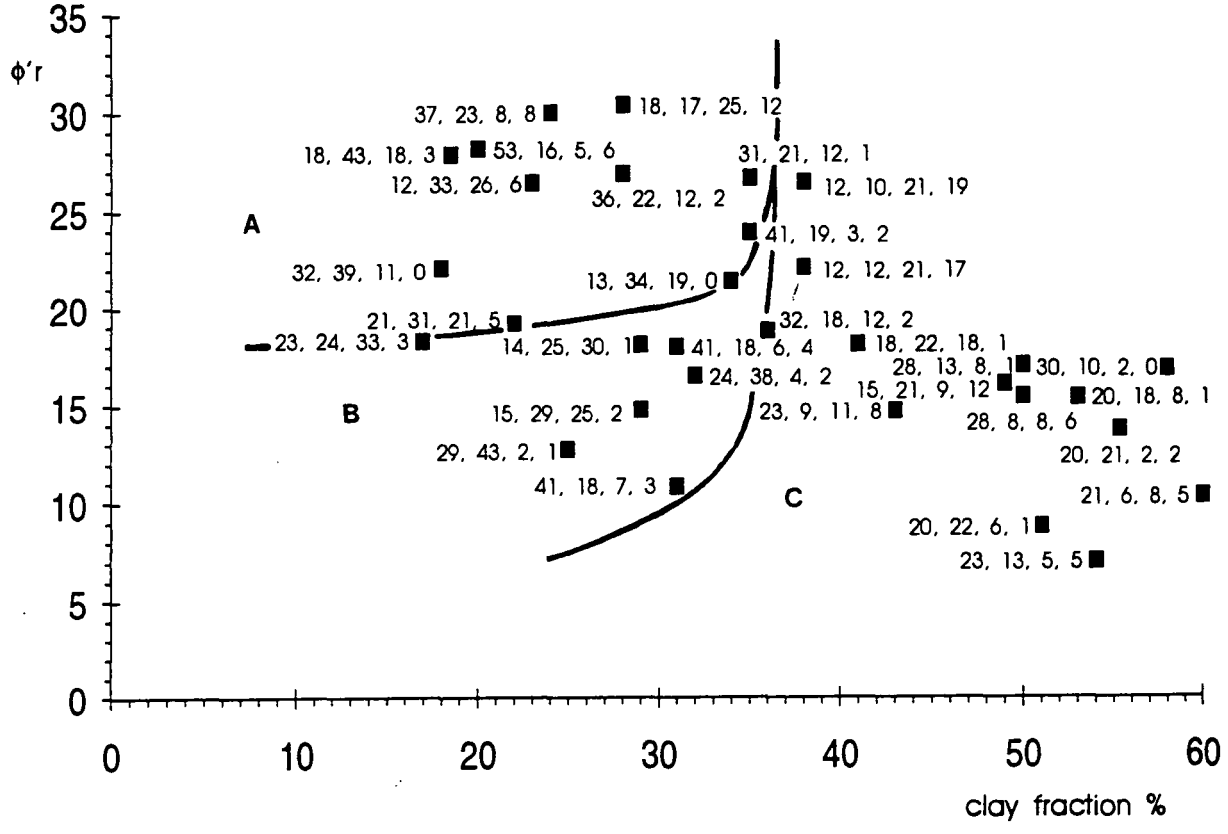

Fig. 7.1.3 Data groups with regard to fine plus medium silt values.

Fig. 7.1.4 A triangular plot presentation of the effects of grain size groups on the residual angle of friction ϕ_r' of Hellenic "marls".

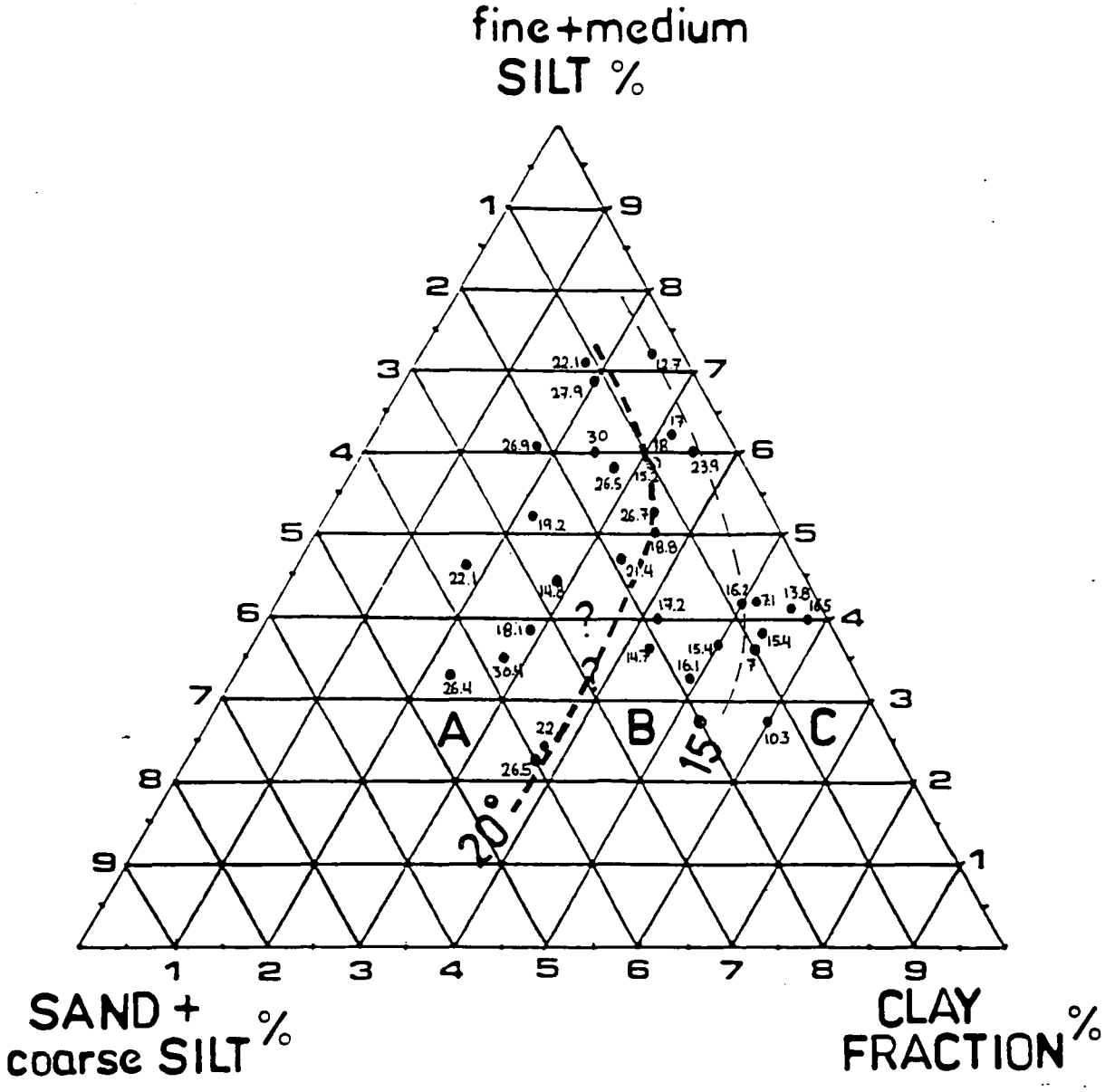

plus medium silt size fraction and the sand plus coarse silt fraction are plotted in a triangular configuration. For every data point, the corresponding value of ϕ_r' is also given. The triangle has been divided into three areas A, B and C depending on the value of the residual angle of friction. Area A contains data points with $\phi_r' \geq 20°$, area B contains data points with values of ϕ_r' between 20° and 15° and area C contains data points with $\phi_r' \leq 15°$.

However, there are a number of data points that are situated inside these areas of the plot and their residual angle values are at odds with the rest of the data points in those areas. Hence, samples kvt1HPb (14.8°), agn2 (19.2°) and kks1 (18.1°) of area A, rtk (23.9°) of area B and nsa1 (16.5°) of area C do not comply with the observed trends as expressed by the area groupings in fig. 7.1.4. Mineralogical idiosyncracies are thought to be responsible for this behaviour mainly affecting parameters such as the aggregation ratio as well as controlling the behaviour of the coarse size fraction (see section 7.2).

Skempton (1985) suggested that any relationship between residual strength and clay fraction covering a wide range of particle size should have essentially the same mineralogy for any comparisons to be valid. Although this might be the purist approach to such analysis, it would become impractical for data sets involving a wide variety of lithological types, where the differences in behaviour will have to be traced by both means of mineralogical and grain size analysis. If the influence of the grain size distribution on the residual strength parameters of a wide ranging data set is to be examined, allowances must be made for the exclusion of mineralogical data.

Lupini et al (1981) and Lemos (1986) suggested that the relative size of clay and "massive" (i.e silt size and over) particles as well as the shape of the "massive" particles control the type of effect that grain size imposes on the residual strength parameters.

However, taking the "massive" fraction as a singular factor affecting relative size ratios as above, leads to oversimplifications especially when examining fine grained geological materials with appreciable amounts of particles in the silt and coarse size fractions (e.g silty clays, clayey silts etc). As figures 7.1.3 and 7.1.4 then suggest, the relative proportions of the individual grain size fractions (clay, silt, sand) and their sub-divisions (fine, medium, coarse) become a dominant factor controlling the residual strength behaviour of a soil.

7.1.3 The effects of grain size as modelled by a computer program

The full data set of grain size distributions and corresponding residual angles of friction was fed into a least squares regression program developed by Dr. S.W. Lavelle at the School of Engineering and Computer Science, Durham University.

7.1.3.1 The program

The program tries to minimise the sum of least squares (equation 7.1.1) between the predicted and the experimental values for a specified set of predictors, where predictor z_i is a function of input variables, e.g x_1-x_2, $1/x_1^3$, $(x_1+x_2)/x_3$ etc.

$$S = \sum_{n=1} (y_i - \hat{y}_{i+1})^2 \qquad (7.1.1)$$

The program allows a set of possible predictors to be specified by the user. Hence, the number of input variables per predictor and the mathematical functions which will describe the relationship between these input variables are interactively determined. Based on that, the program creates every possible combination of input variables to construct a pool of predictors from which the best subset with the minimum least squares for a specific number of parameters is finally selected. The program follows a forward selection procedure by constructing regression models with gradually increasing numbers of parameters (b_0, b_1, b_2,..., b_n). Initially it choses a two parameter model:

$$y=b_0+b_1*z_1 \qquad (7.1.2)$$

where z_1 is chosen to produce the minimum S for any predictor coding. A three parameter model is then produced by keeping the two parameter model and performing the same procedure for the added second predictor. The program carries on in the same manner until the number of parameters specified by the user is reached. Then a reverse procedure attempts to reduce the number of parameters while keeping the same levels of accuracy. The goodness of fit for the model is given by the coefficient of determination r^2 determined as the ratio of the regression sum of squares over the total sum of squares:

$$r^2 = \frac{SSR}{SST} = \frac{SSR}{SSR+SSE} = \frac{\sum_{i=1}^{n} (\hat{y}_i - \bar{y})^2}{\sum_{i=1}^{n} (\hat{y}_i - \bar{y})^2 + \sum_{i=1}^{n} (y_i - \hat{y}_i)^2} \qquad (7.1.3)$$

where $\hat{y}_i$ is the model output, y_i is the experimental output, $\bar{y}$ is the mean of all the experimental outputs, n the number of experiments performed. However the program uses an adjusted coefficient of determination $Adjr^2$ using the Fishers "A"-statistic which takes into account the number of parameters involved in the model.

The program outputs all the models created with all the associated statistical information and leaves the selection of the best model to the user. To assist the user in his\her task a Box-Whisker configuration can be used which plots the error from the models which are constructed using the best predictor codings. Such a plot is shown in figure 7.1.5. It depicts the relative goodness of models produced from the Hellenic "marls" data set. The levels of lack of predictivity are shown as extreme point errors and errors for the 25%, 75% and median population data points.

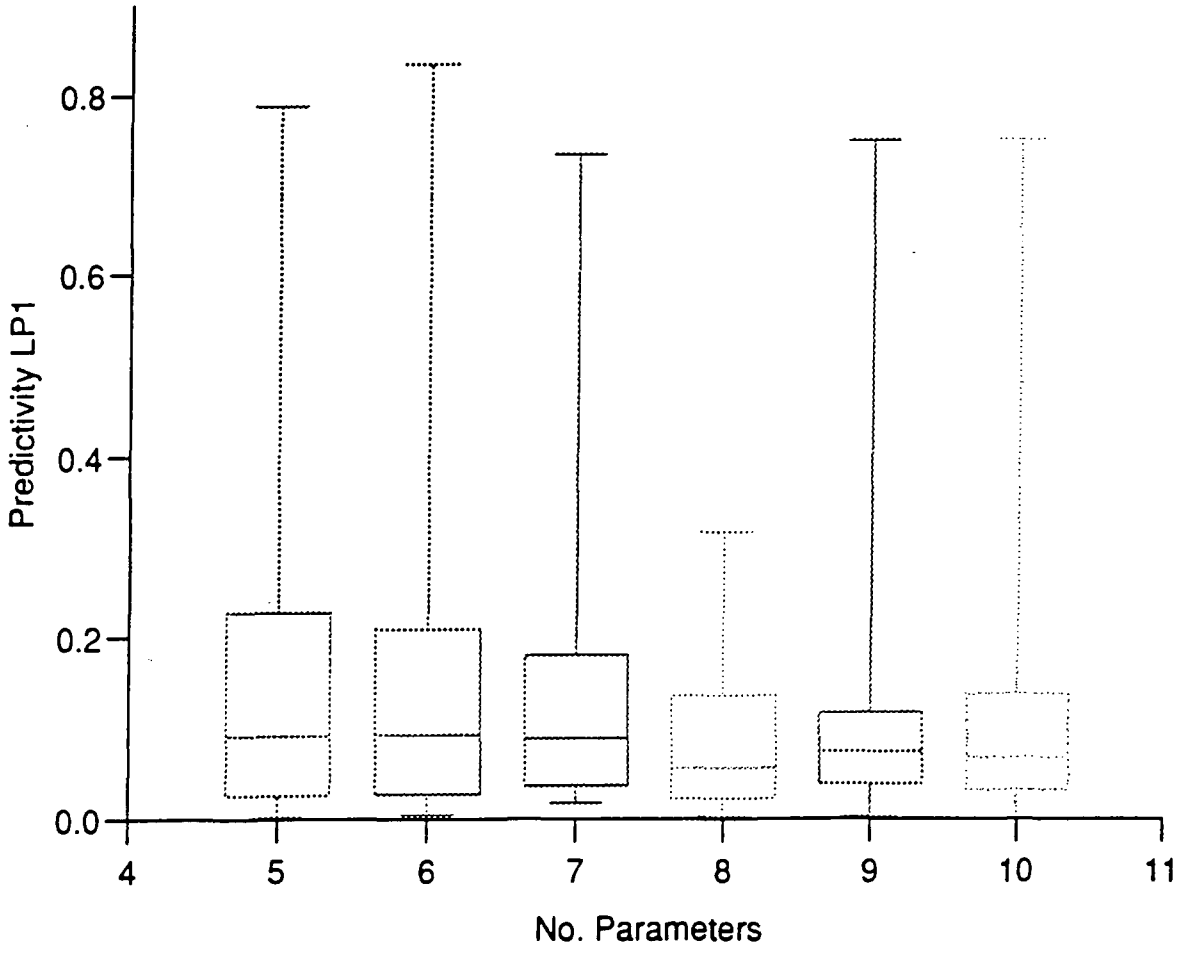

Fig 7.1.5 Box-Whisker plot for the models produced from the Hellenic "marls" data set courtesy of Dr. S.W. Lavelle (S.E.C.S., Durham University).

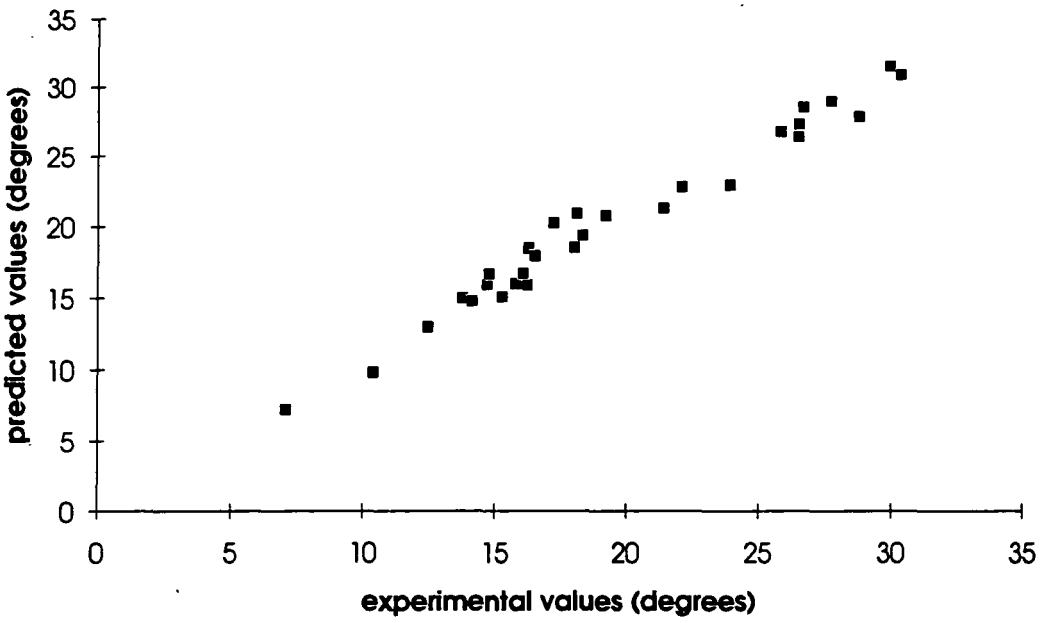

Fig. 7.1.6 Comparison of predicted and experimental values for model 7.1.4.

7.1.3.2 The model

The data set consisted of 32 grain size and residual strength results from Hellenic "marls". The predictors were specified to contain two input variables each using every mathematical function combination. A maximum of ten (10) parameters was allowed. Only predictors with r^2 higher than 0.4 were regarded as significant and were included in the selection pool.

Out of a total 17 models, one with 8 parameters was regarded as the most successful with r^2=0.92 , *Adj* r^2=0.89, residual standard deviation of 2.0 and 22 degrees of freedom:

$$\varphi_{res} = b_0 + b_1 * \frac{e^{clayf}}{e^{sand}} + b_2 * (clayf * sand) + b_3 * \frac{fsilt}{csilt} + b_4 * \frac{csilt^2}{sand^2} + b_5 * \frac{msilt}{csilt^2} + b_6 \frac{clayf^2}{msilt^2} + b_7 * \frac{msilt}{csilt} \qquad (7.1.4)$$

where *clayf* is clay fraction, *fsilt* is fine silt, *msilt* is medium silt, *csilt* is coarse silt, b_0=38.05, b_1=-18.45, b_2=-142.5, b_3=-1.057, b_4=-6.739E-02, b_5=5.69E-02, b_6=-

1.91E-03 and b_7=1.196. Every variable shown in equation 7.1.4 is in the transformed form of:

$$x_i' = \frac{x_i - \bar{x}_i}{\sum \sqrt{(x_i - \bar{x}_i)^2}} \qquad (7.1.5)$$

Figure 7.1.6 shows a comparison between the predicted and the experimental values. A comparison with other prediction models has been shown in figure 7.1.5.

7.1.3.3. Concluding remarks

The model shown in equation 7.1.4 is a numerical model that best fitted the provided input data on the basis of instructions given to the computer program to search for one to one relationships between the constituent grain size fractions with regard to the residual angle of friction.

It must be made clear that this is a data specific model, likely to change depending on type and quantity of input data. Moreover, there was no control over the selection of the predictors. However, it is interesting that the predictors most accurately fitting the data were those that presented forms of different grain size ratios. This is an indication of the importance of relative grain size ratios and is in agreement with past reseach where such relationships were suspected (Bishop et al, 1971; Kenney, 1977; Lupini, 1981; Skempton, 1985).

7.2 The effects of mineralogy on the residual strength

7.2.1 General

There have been numerous studies that linked residual strength characteristics with the mineralogical contents of soils and soil mixtures (see section 5.1.7). Many of the researchers acknowledged the importance of the clay mineralogical suite as a primary cause of strength loss with displacement (Horn & Deere, 1968; Kenney, 1967; 1977; Chattopadhyay, 1972; Skempton, 1964; 1985; Lemos, 1986; and others).

The tendency of certain clay minerals to naturally form aggregations which collapse with further displacement may cause irregularities in the stress-strain behaviour, such as intermediate stress plateaus between peak and residual strength (Cavounidis & Sotiropoulos, 1980).

The study of the contribution of non clay minerals as controls on the residual strength behaviour was often limited because of direct association of such minerals with certain grain sizes. However Kenney (1967) suggested that it is the shape rather than the size of such particles that may or may not cause an increase in residual strength. The effect of the presence of soluble non clay minerals (such as calcite) was studied more recently (Hawkins et al, 1986; 1988; Tsiambaos, 1991; Hawkins & Mc Donald, 1992) showing a positive correlationship between ϕ_r' and calcite content.

7.2.2 Clay minerals associations

Figure 7.1.1 showed that the relationship between clay particle size and residual angle of friction, is non linear and suffers from a lot of scatter. One of the reasons for the scatter is the error introduced by aggregation of clay minerals into silt size particles when determining the clay fraction and the presence of very fine non clay minerals in the clay size fraction (e.g amorphous silica, micritic calcite, etc). However this source of error can be avoided if instead of the clay size fraction, the total proportion of clay minerals (as determined from XRD analysis) is introduced. Figure 7.2.1 presents the relationship between clay minerals content and residual angle of friction.For comparison purposes the upper and lower bounds from the clay size fraction against ϕ_r' relationship shown in 7.1.1 have been included. The data points have moved to the right of the clay size fraction vs ϕ_r' boundaries, however, keeping the same distribution pattern. It can be seen that although the influence of aggregation has been removed, the degree of scatter has not essentially changed. Hence, samples slm2A, kks1, er1, xml MP, nsa1 & kvt1HPb with clay minerals content between 46% and 48% exhibit residual angle of friction values ranging from 28.8° to 15.2°.

Any analysis aiming to model residual strength based on total clay minerals content considerations can only be very general and lacking accuracy. This is because individual clay minerals react differently to shearing depending on their species and geochemistry (Moore, 1991), state of crystallinity and size, though there is thought to be a strong relationship between the latter two. Figure 7.2.2 presents the percentages by weight of the clay minerals or clay mineral groups detected in samples of Hellenic "marls" with respect to the corresponding residual angle of friction.

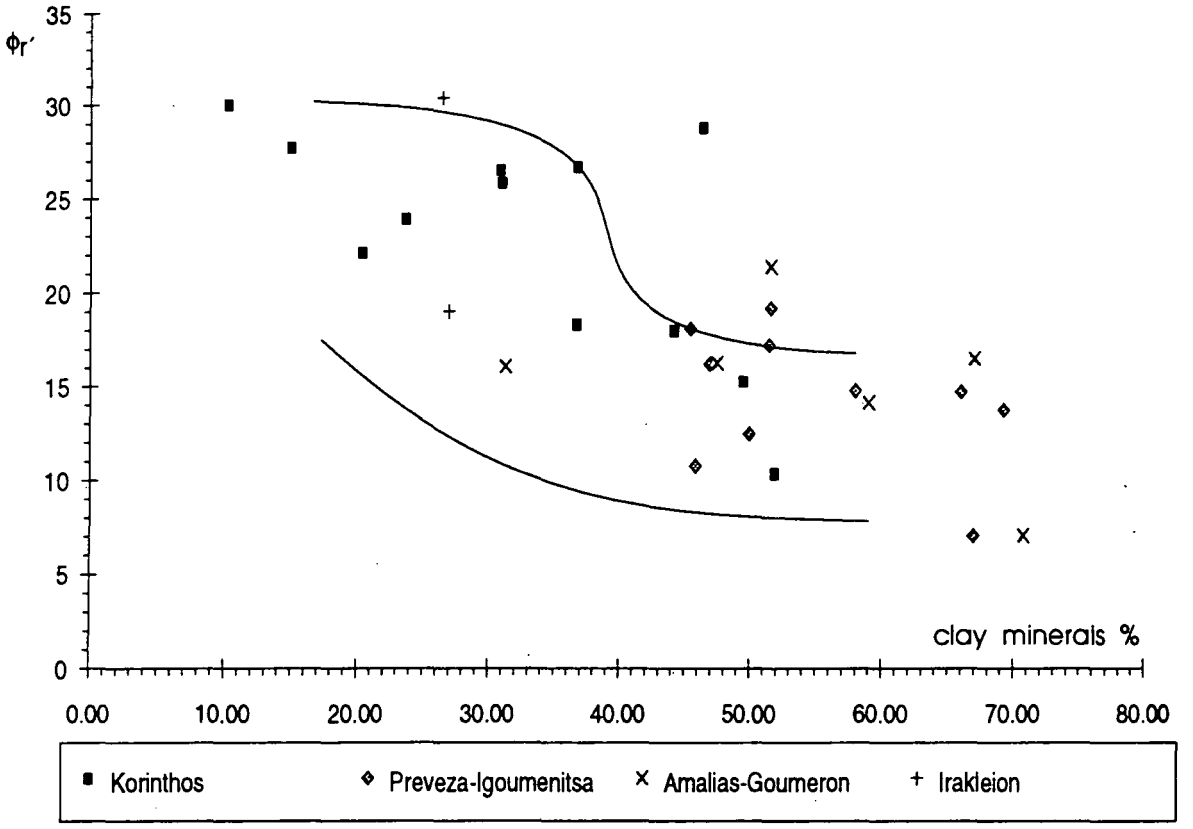

Fig. 7.2.1 The relationship between clay minerals content and the residual angle of friction. The lines represent the clay size fraction vs ϕ_r' relationship shown in 7.1.1.

The mica group minerals (predominantly illite and possibly muscovite) are the dominant species showing a general trend of decreasing content with increasing ϕ_r' values. Chlorites, although not as dominant as the micas, show the same trend as the minerals of the mica group being, though, less sensitive at higher than ϕ_r'=17°. It is, though, interesting that the chlorites generally follow similar peaks and troughs to those of the micas. Smectites and kaolinite show no particular trend, while smectites tend to strongly influence samples on an individual basis acting mostly as replacement to chlorites. Kaolinite is generally in small quantities which do not influence the shearing behaviour of the samples tested.

Linear regression analysis confirmed the relationships between the various clay minerals and ϕ_r' shown in figure 7.2.2. The model for mica group minerals shown below (equation 7.2.1) returns ϕ_r' values with a standard error estimate of 3.7° with a coefficient of determination r^2=0.686; the model for the chlorites (equation 7.2.2) returns ϕ_r' values with a standard error estimate of 4.8° with a coefficient of

determination r^2=0.489; the model for the smectites (equation 7.2.3) returns ϕ_r' values with a standard error estimate of 6.4° with a coefficient of determination r^2=0.095; the model for the sum of chlorites plus smectites (equation 7.2.4) returns ϕ_r' values with a standard error estimate of 4.9° with a coefficient of determination r^2=0.457 implying that the sum is heavily influenced by the chlorites and the tendency of the smectites to frequently act complementary to the chlorites wherever chlorite content is very low.

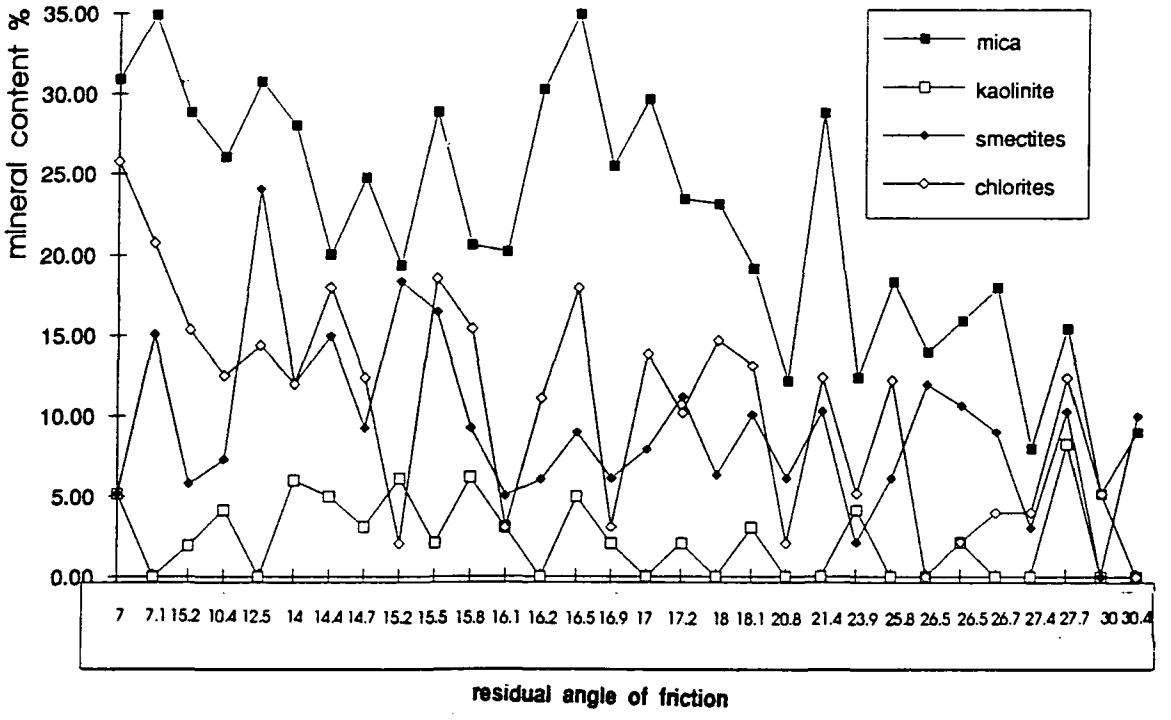

fig 7.2.2 The interaction of detected clay minerals with regard to the residual angle of friction of the corresponding samples of Hellenic "marls".

$$\phi_r' = -0.6687*(\text{mica}) + 33.6627 \qquad (7.2.1)$$

$$\phi_r' = -0.3245*(\text{chlorite})^2 - 0.0157*(\text{chlorite}) + 24.8744 \qquad (7.2.2)$$

$$\phi_r' = -0.5883*(\text{smectite})^2 + 0.0086*(\text{smectite}) + 23.585 \qquad (7.2.3)$$

$$\phi_r' = -0.48*(\text{chlorite} + \text{smectite}) + 28.5738 \qquad (7.2.4)$$

As already discussed in Chapter 4, the determination of the exact mineralogical species reached the level of identifying the quantities of the general representative types without further investigations into the possible type of exchangeable cation

and average mineral size. Such investigations might have helped to achieve a better understanding of the residual strength behaviour of the samples tested.

It is important, however, to note that the dominant species of the clay mineralogical suites examined, i.e chlorites and micas, are according to Mitchell (1976), large and intermediate sized platy minerals with specific areas 50-100m^2g^{-1} and 100-200m^2g^{-1} respectively. However, chlorites can also be very small (<1μm in diameter) with specific areas as high as 300m^2g^{-1} depending on their origin and state of weathering and crystallinity. This variability, which has implications on the value of the friction coefficient τ/σ_n' (Mitchell, 1976), was difficult to determine as it was not always easy to recognise low crystallinity patterns from the small peaks of various mixed minerals on the x-ray diffractogram.

7.2.3 Non clay mineral associations

As for the clay minerals, non clay minerals (also known to engineering researchers as massive or rotund) exhibit a non linear relationship with residual angle of friction as shown in fig. 7.2.3.

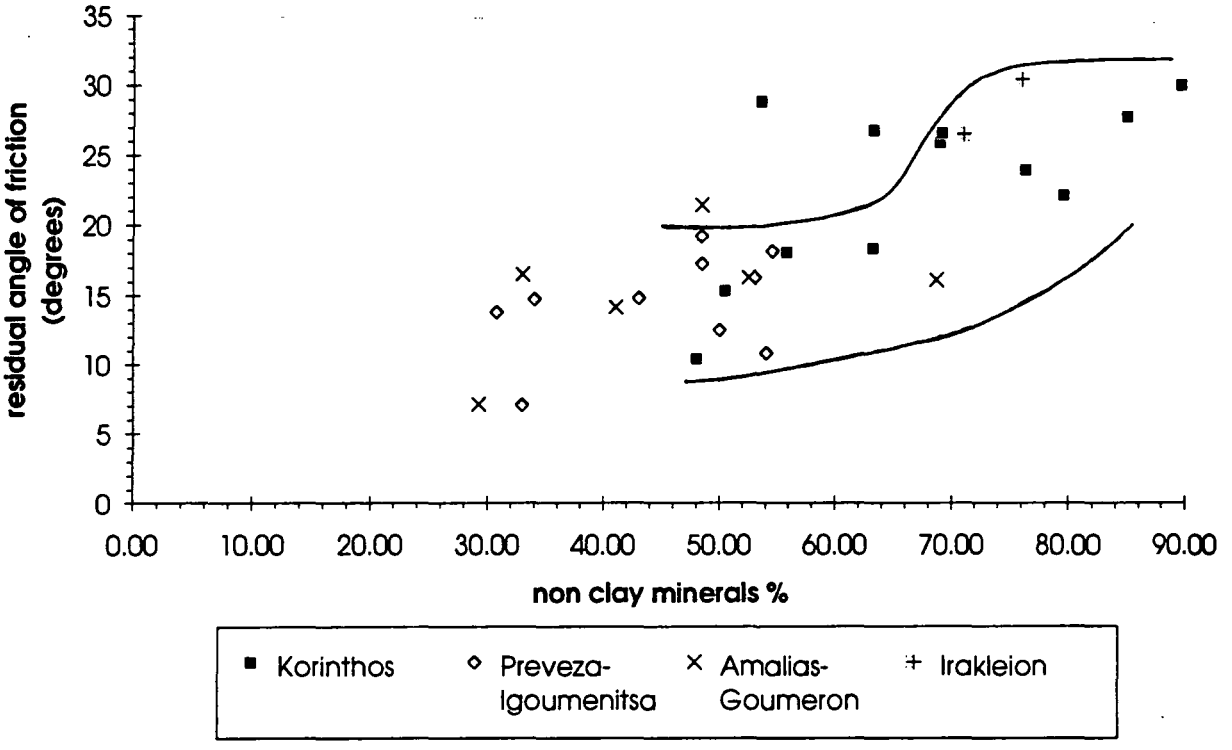

Fig. 7.2.3 Non clay mineral content against residual angle of friction

The distribution of points in figure 7.2.3 is as expected the mirror image of the one

for the clay minerals shown in figure 7.2.1. The continuous lines indicate the upper and lower boundaries for the silt and sand size particles content distribution with regard toϕ_r'. Similarly to figure 7.2.1 the mineral based data points fall to the left of the particle size diagram boundaries. That means that there are more large particles than there are large sized minerals (traditionally accepted to be mainly the non clay ones) pointing to the presence of aggregation.

The contribution of the individual mineral types (e.g. quartz) and mineral groups (e.g. feldspars) with regard to the residual angle of friction of the corresponding samples is shown in figure 7.2.4. It is clear from figure 7.2.4 that the only mineralogical type showing any signs of trend with ϕ_r' is the calcite. Calcite was also identified as an important trend setting mineral with respect to the residual strength of marls and marly clays by Hawkins et al (1988), Tsiambaos (1991) and Hawkins & McDonald (1992). The second important mineral in terms of quantity, quartz, shows a roughly uniform distribution though the entire range of samples. However, quartz complements calcite wherever calcite appears in low quantities. Feldspars and dolomite are not thought to contribute towards any correlation with ϕ_r' either because they are uniformly distributed (feldspars) or because they appear inconsistently and in very small quantities throughout the data set (dolomite).

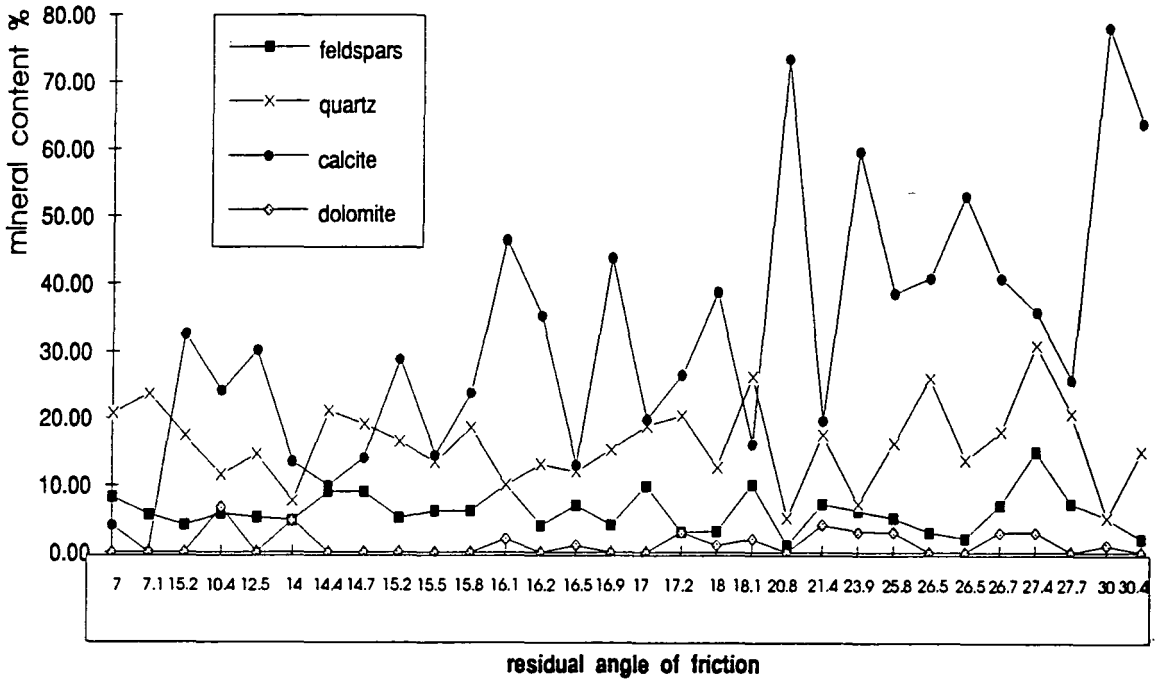

Fig. 7.2.4 The contribution of non-clay minerals to the residual angle of friction

Linear regression analysis confirmed the importance of calcite in influencing the residual angle of friction values and showed enhanced results when the quartz content was considered together with the calcite content:

$$\phi_r' = -0.002*(\text{calcite})^2 + 0.398*(\text{calcite}) + 8.997 \qquad (7.2.5)$$

$$\phi_r' = 0.305*(\text{calcite}) + 0.445*(\text{quartz}) + 1.765 \qquad (7.2.6)$$

Expression 7.2.5 shows a linear regression model for calcite with coefficient of determination r^2=0.497 and standard error for the ϕ_r' estimate of 4.9. If, on the other hand, the influence of calcite and quartz on ϕ_r' is considered, expression 7.2.6 returns ϕ_r' values with a standard error estimate of 4.3° and coefficient of determination r^2=0.605.

7.2.4 Mineralogical suites and ϕ_r'

The individual influence of the clay minerals and the non clay minerals on the residual angle of friction and consequently on the residual strength of the tested Hellenic "marls" has been discussed and a number of correlations have been shown in the previous two sections.

The above relationships, trends and correlations although valid as indicators, have little to do with the "real" soil. The interaction of all those different types and groups of minerals put together would invariably create a composite picture possibly quite different from the picture implied by the correlations based on the individual mineral types and groups. However, it is not always easy or convenient to show on a two axis diagram the relationship or the influence of many variables on an independent parameter without making some simplifying assumptions on the way.

The presence of a standard mineralogical suite (illite (micas), chlorites, smectites (montmorillonites), kaolinite, calcite, quartz, feldspars, dolomite) that covers all the present data set allows some simplifications. Hence, the chlorites can be grouped together with the smectites and the calcite can be grouped with quartz as well as the rest of the non clay minerals since the latter do not noticably influence changes in ϕ_r' levels. Micas, as the most dominant mineral group, are examined individually. The resulting configuration, shown in figure 7.2.5, utilises a triangular plot with its three corners being occupied by the mica group, the chlorites plus smectites and the non-clay minerals (excluding dolomite) respectively.

Fig. 7.2.5 Mineralogical groupings with respect to residual angle of friction.

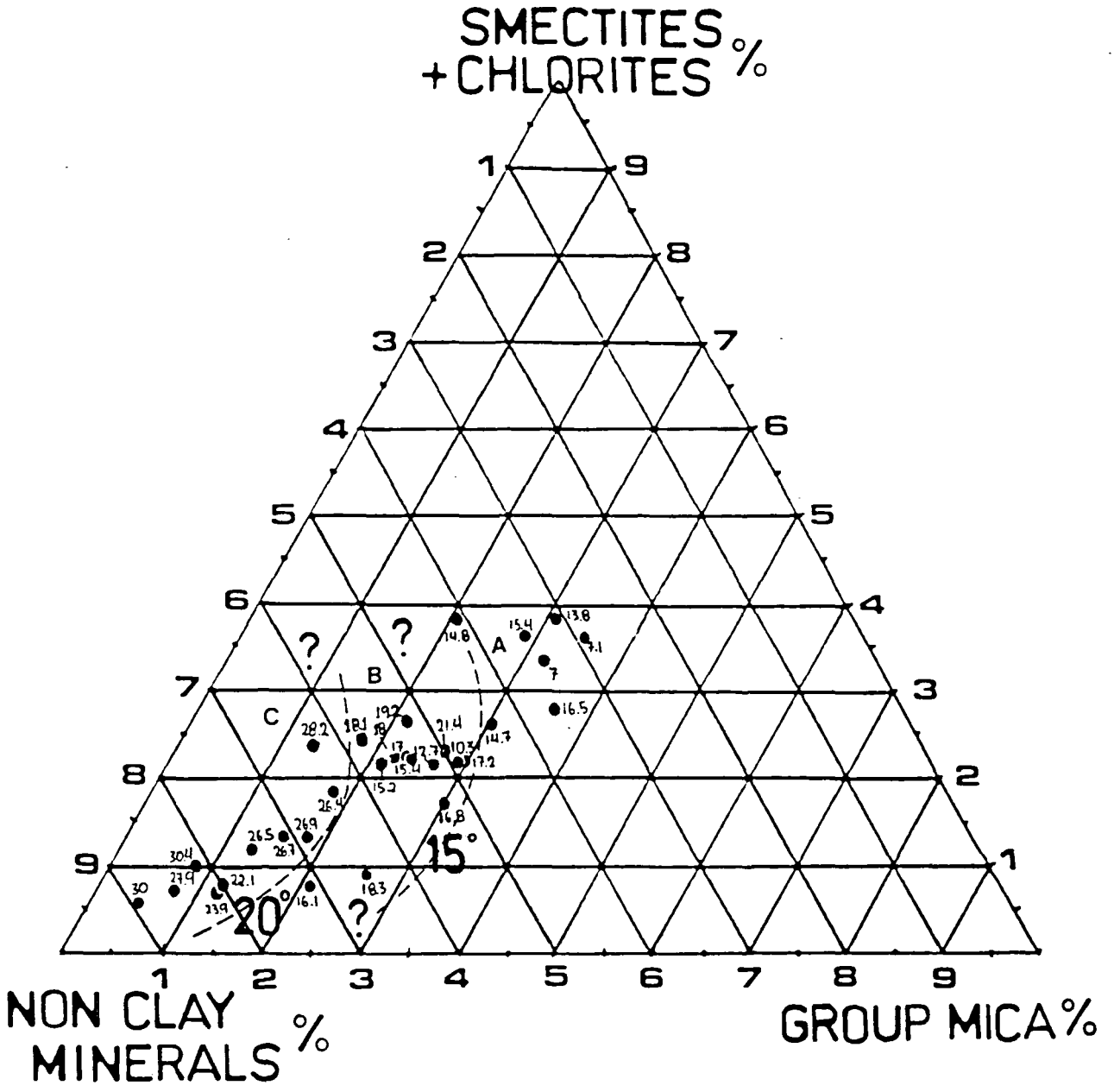

Figure 7.2.5 can be divided into three areas depending on the values of residual angle of friction, namely A ($\phi_r' \leq 15°$), B ($15° \leq \phi_r' \leq 20°$) and C ($\phi_r' \geq 20°$). However, there are data points (samples mvg (16.5°) and ll1 (15.4°) in area A and slm20(10.3°), agn1(12.7°) and pls(21.4°) in area B) that do not fit this layout. A plausible cause for the discrepancy shown by samples mvg, ll1 and pls may lie with the degree of crystallinity, which relates to the shape and grain size of minerals.

Minerals such as the chlorites (mvg: 18%, ll1:18.5%), may contribute to higher levels of residual shear strength when in a crystalline form since they become much less plastic. However, sample lts with 25.7% chlorites exhibits sliding shearing characteristics (as defined by Lupini et al, 1981) with $\phi_r'=7°$. Calcite and quartz may also vary in terms of shape and size distribution from one locality to another depending on their source, transport and depositional enviroment. The sample pls, for instance, with 17.5% quartz and 23.6% carbonates has 34% medium silt size and 19% coarse silt size particles, though part of the silt size particles may be due to aggregation affects (A_r=1.5). Relationships between these two minerals and certain particle sizes have been discussed in Chapter 4, section 4.4.8. Clearly, allowances must be made in fig. 7.2.5 for the absence of grain size considerations.

Samples slm20 and agn1, on the other hand, exhibit lower values of residual strength parameters than their mineralogical suites would suggest. It may also be worth noting that agn1 appears aggregated (A_r=2) while there is a net contribution of non clay minerals in slm20 (A_r=0.87). Despite this difference, the two samples have very similar mineralogical suites which implies that they have quite active clay mineral species present. However, it is quite difficult to confirm this without knowing the precise nature of the clay minerals present (i.e type of exchangeable cation, specific area, etc).

In conclusion, the differences in mineralogical suites will not adequately indicate the behavioural changes of calcareous fine grained soils in relation to their residual strength, unless full identification of the mineralogical species, their particle size and degree of crystallinity is known.

7.3 The effect of aggregation on the residual stress-linear displacement relationship

Cavounidis & Sotiropoulos (1980) studied calcareous fine grained sediments from Ipeiros, W. Hellas, and reported that the drop from peak to residual in consolidated drained triaxial test and direct shear test stress-strain diagrams was interrupted by an intermediate stress plateau. Residual conditions were reached only after considerable displacement. They termed this behaviour as "quasi-residual".

Such stress plateaus were also observed by the author in a number of ring shear test shear stress vs linear displacement graphs, namely agn1, agn2, kd, kks1, ktr2, kvt1HPb, kvtAlp, ll1, lts, mvg and psf1a (see Appendix 1). It was also observed that the more brittle the failure was, the more pronounced such a plateau became. More importantly, all the samples that exhibited such behaviour were, with the exception of ktr2, aggregated with A_r varying from 1.13 (pfs1a) minimum to 2.34 (agn2) maximum. Generally, the greater the aggregation was, the more brittle the peak failure appeared to be.

It is believed that this behaviour is caused by the further break down of aggregated clay mineral assemblances, releasing thus more clay particles along the shear plane and hence further lowering the shearing resistance of the soil. In a similar manner, Tika (1989) drew attention to "degradable soils" containing aggregated clay minerals which tend to break down to their constituent minerals during higher rates of shear. In view of Tika's findings, it appears that aggregations of clay minerals collapse down to their constituents with increased work caused either because of increased rates of shearing or because of prolonged shearing at low rates of shearing. This is compatible with other previous work done on the effects of aggregation (Dumbleton & West, 1966; Davis, 1967; Huang, 1989).

7.4 The effect of plasticity on the residual strength

Plasticity was targeted very early as a source for residual shear strength predictions (see section 5.1.6). A number of different expressions were proposed for that reason mostly based on laboratory work. These expressions varied from power to linear relationships involving either the plasticity index and/or the liquid limit and the plastic ratio (Ip/w_p).

Figures 7.4.1, 7.4.2 and 7.4.3 present relationships between the residual angle of friction and the liquid limit, plastic limit and plastic index respectively. There was no identifiable trend between ϕ_r' and the plastic ratio (Ip/w_p).

Linear regression analysis performed on the figures' 7.4.1, 7.4.2 and 7.4.3 data sets revealed that only liquid limit provided the best correlation out of the three with coefficient of determination r^2=0.662. The correlations with the plastic limit and the plastic index gave much lower value for the coefficients of determination r^2

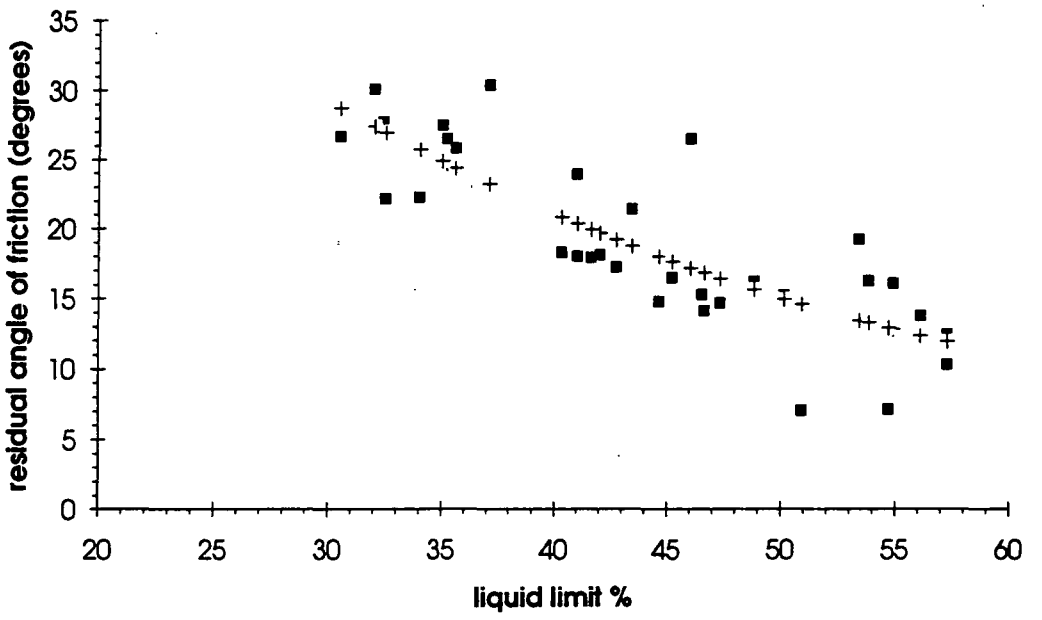

Fig 7.4.1 Correlation between the residual angle of friction and liquid limit.

being equal to 0.463 and 0.459 respectively. However, the standard error for the ϕ_r' estimate was quite high, being 3.78, 4.64 and 4.78 for the correlations between the residual angle of friction and the liquid limit, plastic limit and plastic index respectively. The equations 7.4.1, 7.4.2 and 7.4.3 representing the best fit lines (denoted by crosses in the relevant figures 7.4.1, 7.4.2 and 7.4.3) for the ϕ_r' vs w_L, ϕ_r' vs w_p and ϕ_r' vs Ip correlations.

$$\phi_r' = 0.0107*(w_L)^2 - 1.5647*(w_L) + 66.549 \qquad (7.4.1)$$

$$\phi_r' = 0.325*(w_P)^2 - 15.461*(w_P) + 198.6275 \qquad (7.4.2)$$

$$\phi_r' = 0.0078*(I_P)^2 - 1.0032*(I_P) + 37.7997 \qquad (7.4.3)$$

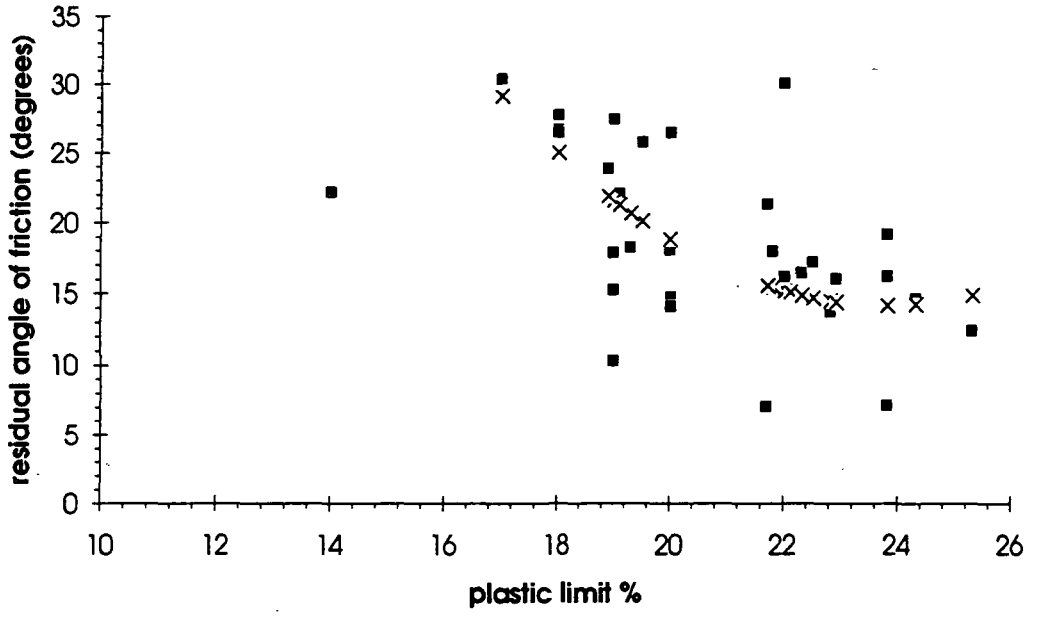

Fig 7.4.2 Correlation between the residual angle of friction and plastic limit.

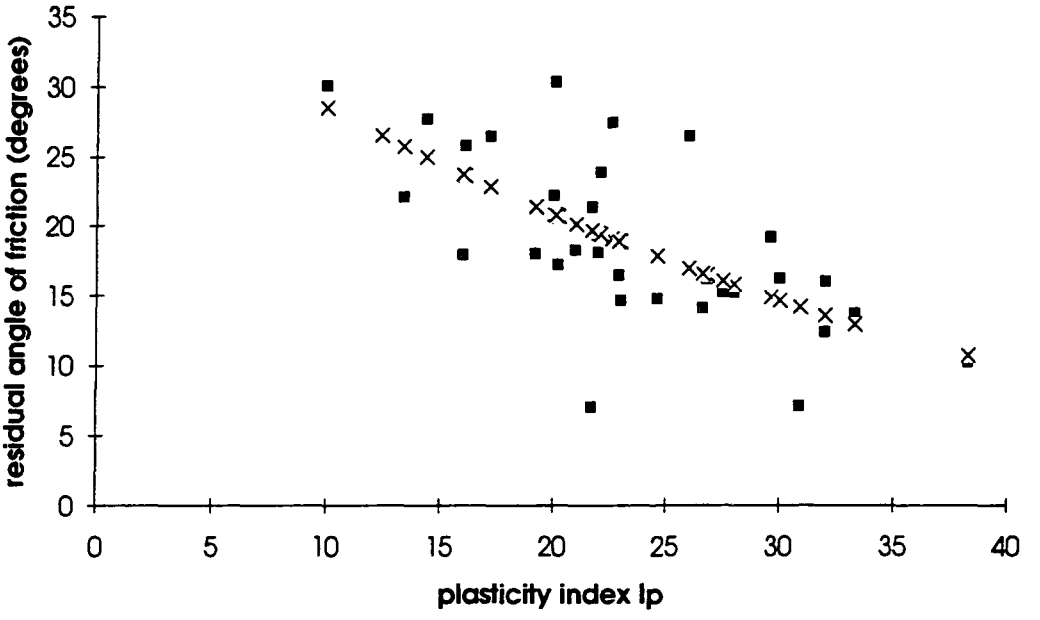

Fig. 7.4.3 Correlation between the residual angle of friction and plasticity index.

All three correlations suffer from a lot of scatter not unusual for correlations that

involve empirical parameters such as the Atterberg limits. Such scatter has been experienced by other researchers (Vaughan & Walbanke, 1975; Cancelli, 1977; Mersi & Cepeda-Diaz, 1986; Tsiambaos, 1991; and others).

The plastic limit may be seen as the moisture content of a fine grained material at failure at 100kPa average undrained cohesion (Skempton & Northey, 1972). However, there is no evidence to suggest that there is any correlation between undrained strength parameters and residual strength parameters. Therefore it makes little sense to try to associate plastic limit and residual strength. Additionally, the physicochemical and mechanical complexities involved in the determination of the Atterberg limits lead to errors which are exacerbated in the plastic index. In conclusion, Atterberg limits may be quick and inexpensive to determine but they do not provide reliable correlations with the residual angle of friction.

7.5 Mineralogical associations with the intrinsic compression index

7.5.1 General

Section 6.1 has demonstrated the complex nature of volume change of a reconstituted fine grained material under one-dimensional consolidation. Mineralogy controls specific gravity; combined grain size and mineralogical considerations control plasticity; grain size distribution controls porosity and mineralogical content controls much of the physicochemical reactions with pore water. These are some of the main factors affecting oedometer test results on reconstituted samples, while thixotropic hardening, further flocculation and the effect of temperature leading to fabric effects must not be discounted.

The effect of plasticity in the form of the void ratio at the liquid limit e_L on the constants of intrinsic compressibility C_c^* and e^*_{100} have been examined and discussed in section 6.3.1. It was found that there was considerable scatter. However, plasticity, in the form of liquid limit, seemed to affect the Intrinsic Compression Lines and a dependence on mineralogy, in the form of calcite content, was also considered (see section 6.3.3). Additionally, variable behaviour recorded as a function of the mixing ratio w_i / w_L was found to depend on differences in mineralogy (see section 6.3.2).

In this section the association between the mineralogical suites identified and the intrinsic compression index C_C^* is further examined.

7.5.2 Mineralogical suites and intrinsic compression

Figures 7.5.1 and 7.5.2 present the clay minerals and non-clay minerals associations with increasing C_C^* values respectively. With respect to totals, the correlation between clays and C_C^* is broadly positive while for the non clay minerals such a correlation is negative. These trends are, however, directly related to the individual behaviour of the dominant mineralogical types or groups, namely micas for the clay minerals and calcite for the non-clay minerals.

The remaining mineral types or groups may or may not follow the general trends above. Regression analysis was performed to confirm the trends implied in figures 7.5.1 and 7.5.2. Mineralogical species and groups were tested individually and/or combined with other species and/or groups. However, the models shown below could not improve further than a maximum coefficient of determination r^2=0.564 and s_{ey}=0.0765 (calcite plus quartz model).

$$C_C^* = 0.0051*(\text{total clay minerals}) + 0.157 \quad (7.5.1)$$

$$C_C^* = -0.0063*(\text{total non clay minerals}) + 0.683 \quad (7.5.2)$$

$$C_C^* = 0.0105*(\text{mica group}) + 0.1546 \quad (7.5.3)$$

$$C_C^* = -0.0042*(\text{calcite}) + 0.505 \quad (7.5.4)$$

$$C_C^* = 0.0114*(\text{chlorites}) + 0.2577 \quad (7.5.5)$$

$$C_C^* = -0.0061*(\text{calcite + quartz}) + 0.638 \quad (7.5.6)$$

$$C_C^* = 0.0082*(\text{smectites + chlorites}) + 0.2177 \quad (7.5.7)$$

$r^2_{7.5.1} = 0.523$, $s_{ey7.5.1} = 0.08$; $r^2_{7.5.2} = 0.516$, $s_{ey7.5.2} = 0.081$;

$r^2_{7.5.3} = 0.536$, $s_{ey7.5.3} = 0.079$; $r^2_{7.5.4} = 0.495$, $s_{ey7.5.4} = 0.082$;

$r^2_{7.5.5} = 0.364$, $s_{ey7.5.5} = 0.092$; $r^2_{7.5.6} = 0.564$, $s_{ey7.5.6} = 0.076$;

$r^2_{7.5.7} = 0.432$, $s_{ey7.5.7} = 0.087$.

None of the above attempted correlations provided a good fit. It is also shown that the standard error estimate for the C^*_C averages 0.082, which means that for sixty nine per cent of the values lie within ± two standard errors.

Fig. 7.5.1 The distribution of clay minerals of the tested samples with respect to their intrinsic compression index C_c^*.

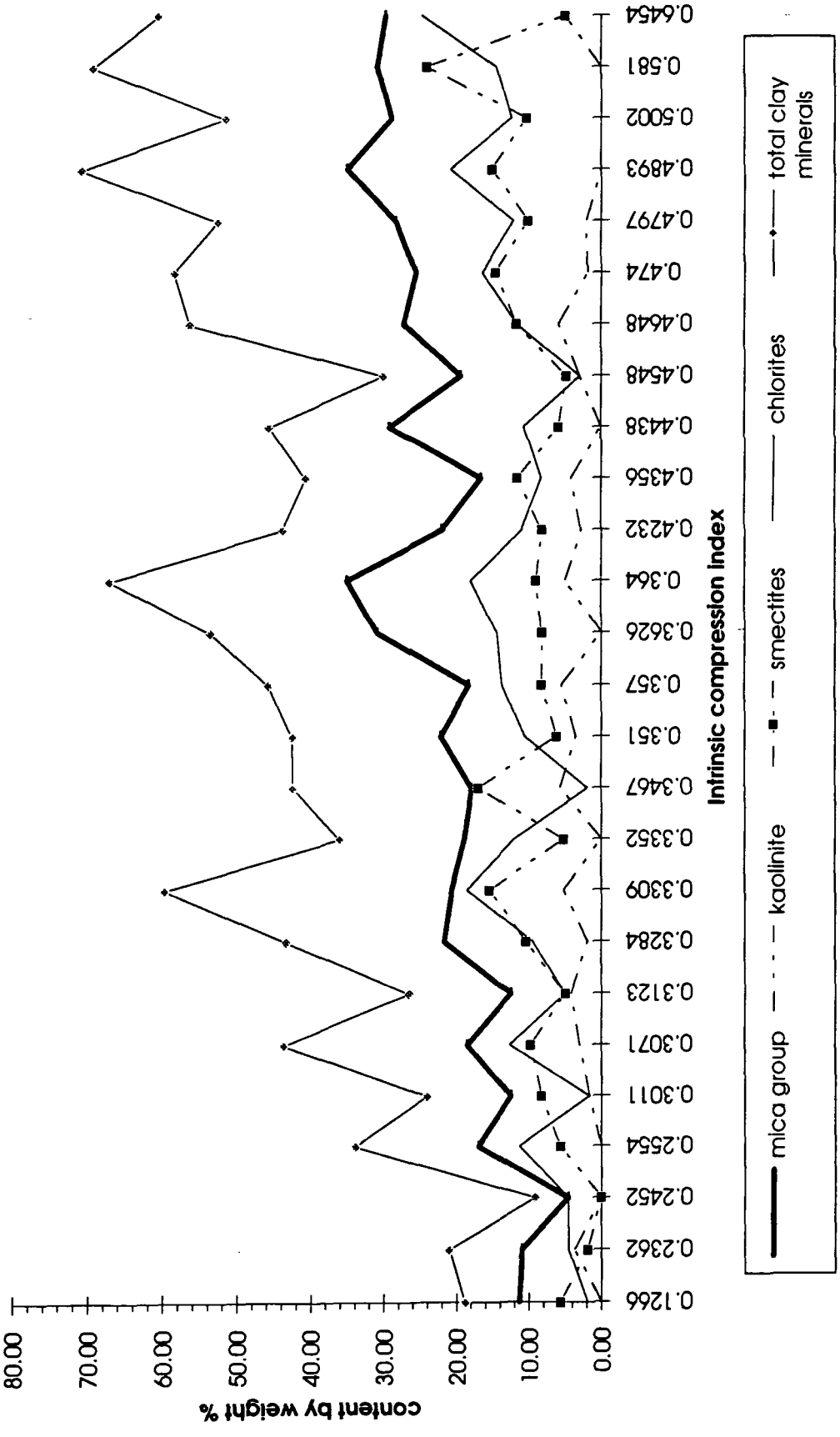

Fig. 7.5.2 The distribution of non-clay minerals of the tested samples with respect to their intrinsic compression index C_c^*.

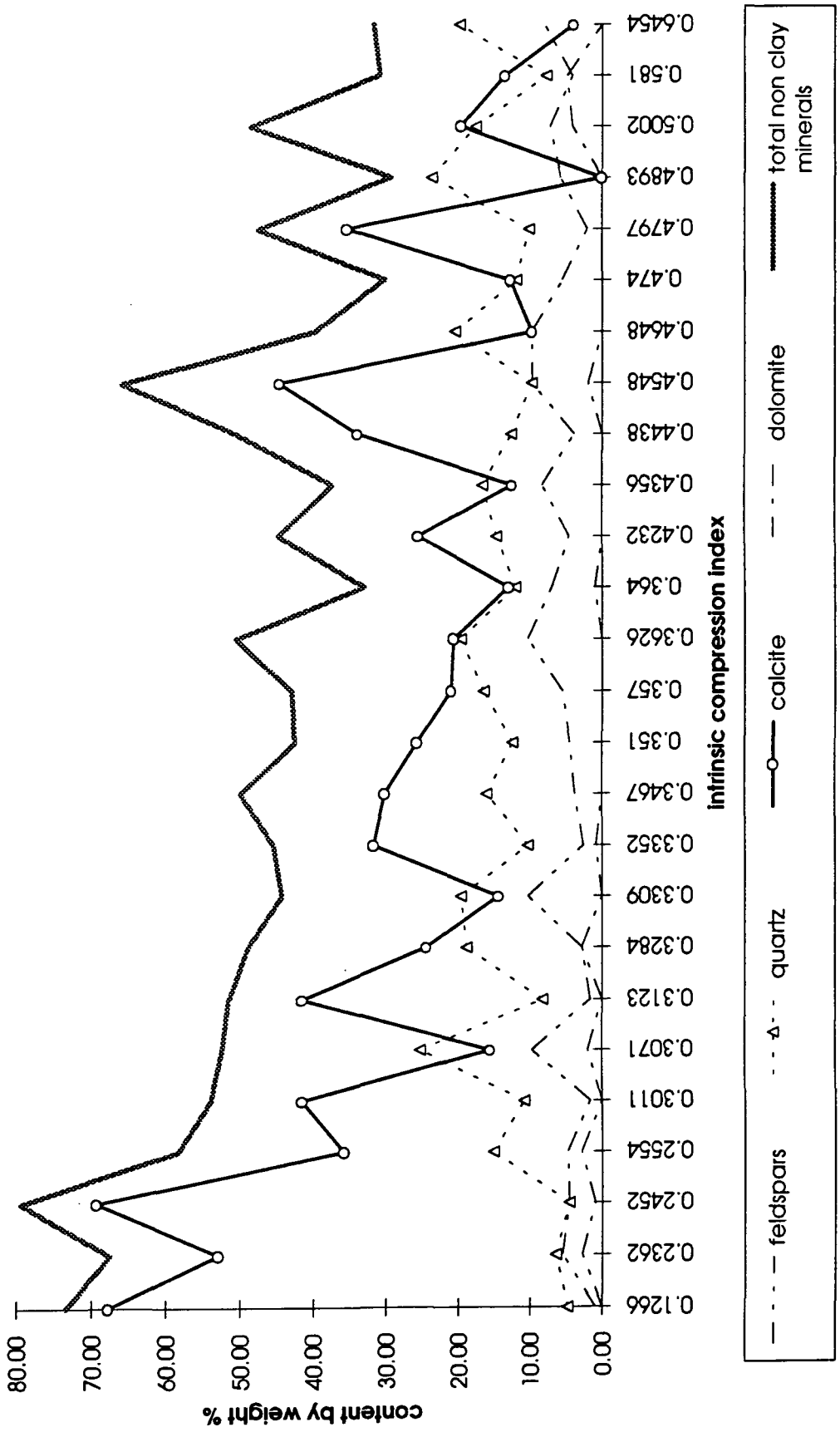

Smectites and quartz contents yielded insignificant trends while kaolinite and dolomite were inconsistent and in too small quantities to have any effect on the general trends. The smectites content, however, when combined with the chlorite content provides an enhanced correlation, when compared to the correlations of smectite content and chlorite content individually. Similarly, when the combined contents of calcite and quartz were tested, they produced a better correlation than the two mineral types produced individually. It should be remembered that similar observations were made and their physical implications with regard to residual shear strength were discussed in sections 7.2.2 and 7.2.3 respectively.

In terms of volume change, smectites are the most active group of species among the clay mineral family with a grain size up to 10μm while chlorites with a grain size up to 1μm exhibit more varied behaviour but with lower activity than the smectites (Christoulas, 1987). In that respect, one could postulate that both combined they contribute more towards the physicochemical aspect of the intrinsic compression of a reconstituted marl or calcareous clay. This mostly affects the behaviour of the reconstituted tested materials at very low pressures (i.e. 5kPa to around 50kPa) when the samples behaved more like high viscosity fluids till they attained a semi-solid state.

On the other hand, calcite and quartz were shown (section 4.4.8) to have some relationship with medium to coarse silt and coarse silt to sand particle size respectively. Additionally, figure 7.5.2 showed that the quartz content increases with decreasing calcite content and vice versa. It could then be inferred that for the majority of the samples tested, calcite and quartz contents cumulatively correspond to the total of medium silt to sand particle size content. When the compression characteristics begin to depend more on the created structure of the reconstituted material, changes in porosity, which are related to grain size distribution, become more relevant to the establishment of drainage paths and the dissipation of excess pore pressure. Hence, the cumulative effect of these two mineralogical species on the compressibility especially of samples with low to intermediate clay minerals content (20% - 50%) can be significant. The distribution of the quartz plus calcite content data points in relation to the intrinsic compression index C_C^* of the corresponding samples is shown in figure 7.5.3. The correlation between the non-clay minerals total content and C_C^* is shown in figure 7.5.4.

Mica group minerals were the most numerous among the clay minerals in the tested samples, influencing the compression characters of the samples more than any other

clay mineral type, group or combination of them. The distribution of the mica group data points (fig. 7.5.5) is an almost identical simulation of the distribution of the total clay minerals content (fig. 7.5.6) with regard to the intrinsic compression index C_c^* of the corresponding sample

One apparent explanation for the considerable scatter shown in the figures above is that the complexity of the phenomena associated with the one-dimensional consolidation cannot be fully described by the variations of one single mineral type or group at a time. Rather it is all the mineral types and/or groups involved as a whole that interactively affect the intrinsic compression index.

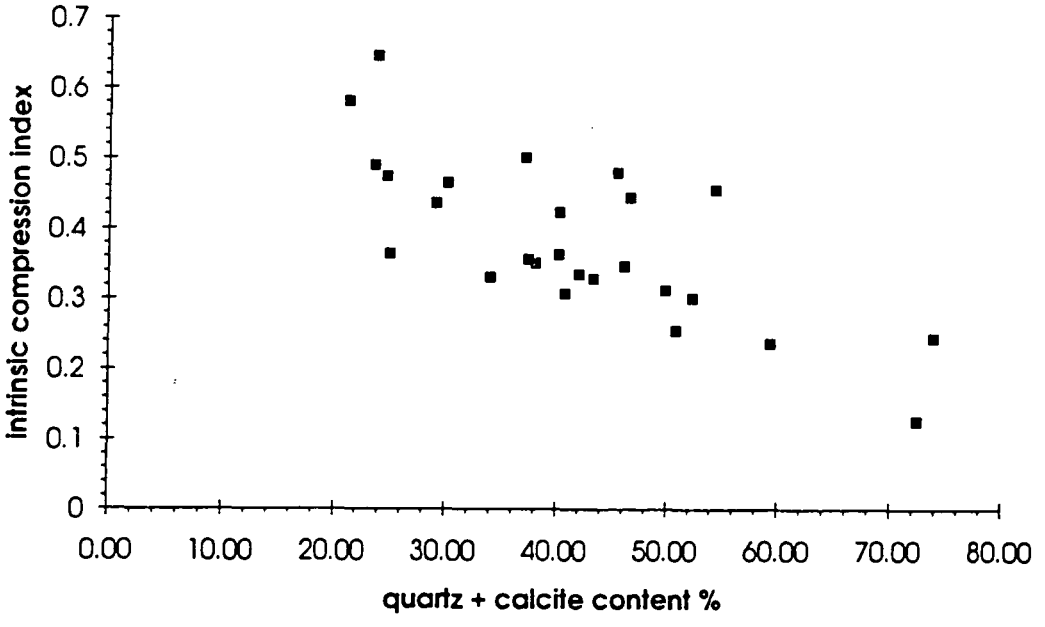

Fig. 7.5.3 The effect of the quartz plus calcite content on the intrinsic compression index C_c^*.

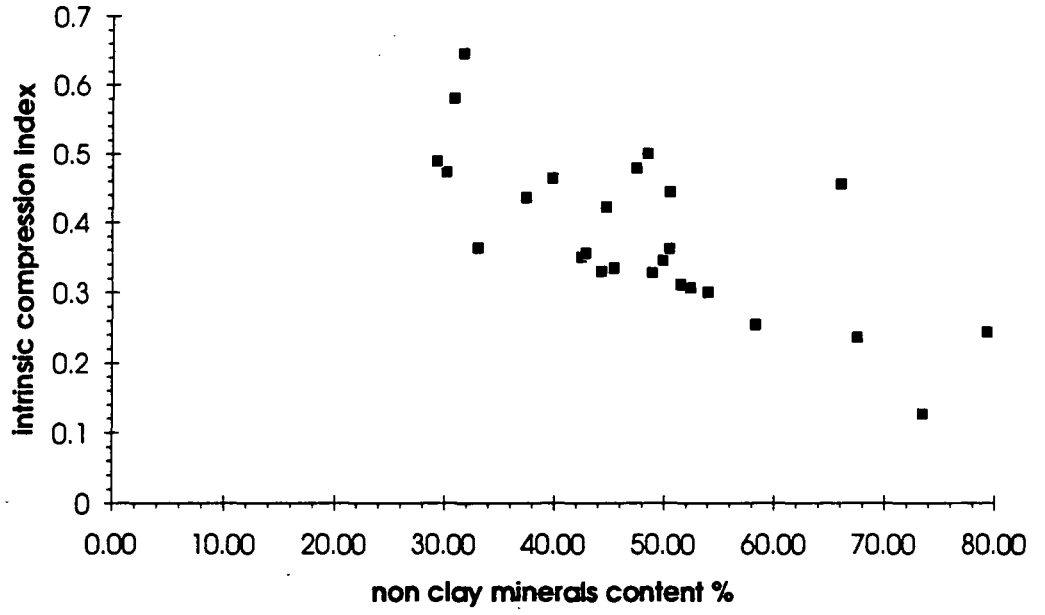

Fig. 7.5.4 Correlation between the non clay minerals content and the the intrinsic compression index $C_c{}^*$.

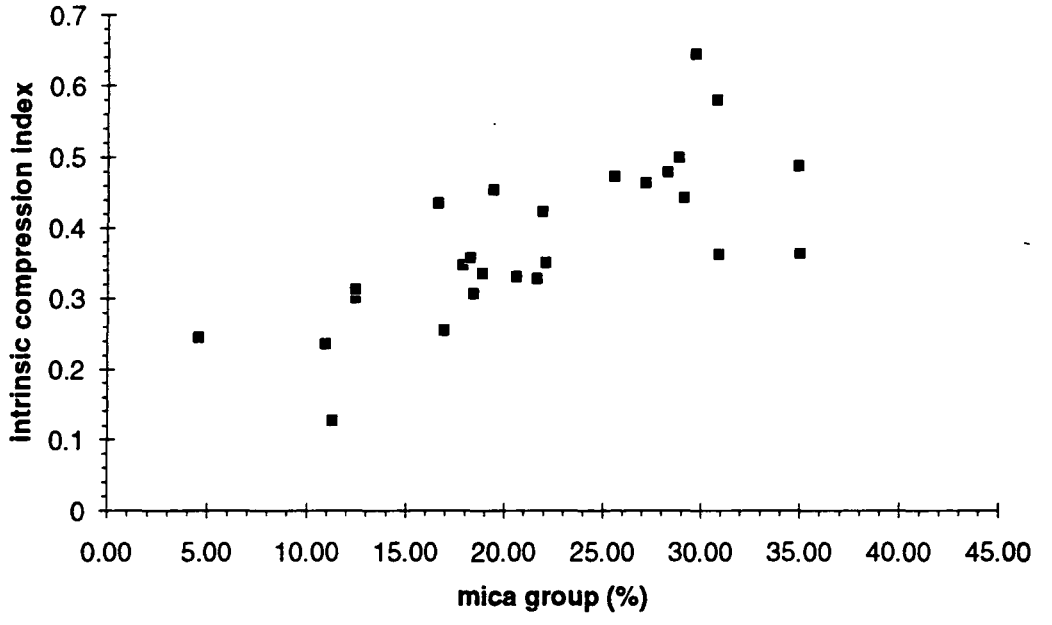

Fig. 7.5.5 The effect of the mica group minerals content on the intrinsic compression index $C_c{}^*$.

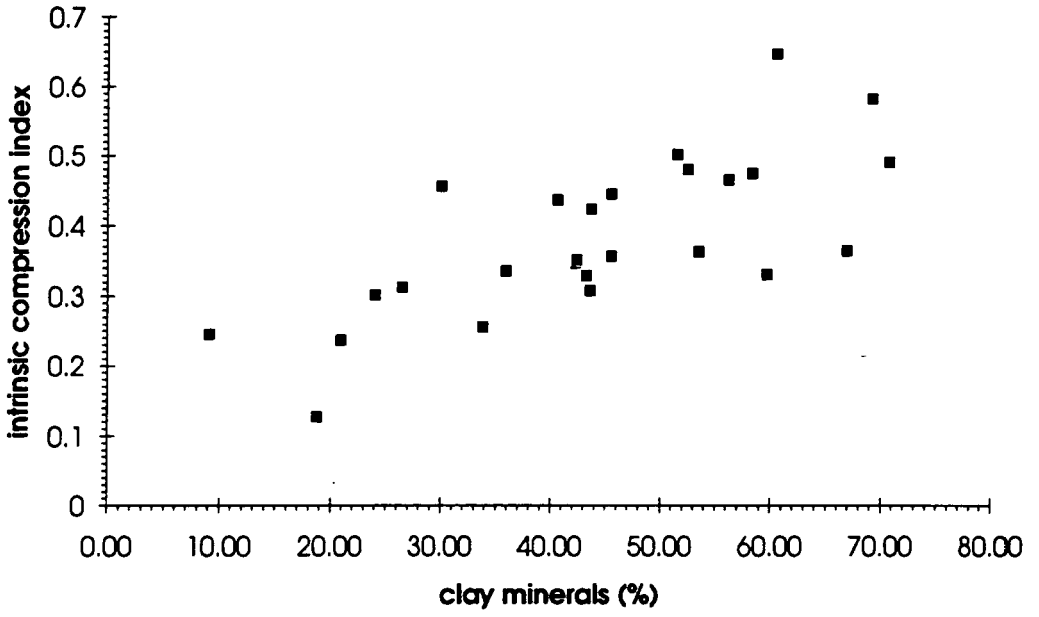

fig. 7.5.6 Correlation between the total clay minerals content and the intrinsic compression index C_c^* .

fig 7.5.7 The mineralogical suites of reconstituted Hellenic "marls" in relation to their corresponding intrinsic compression index C_c* values.

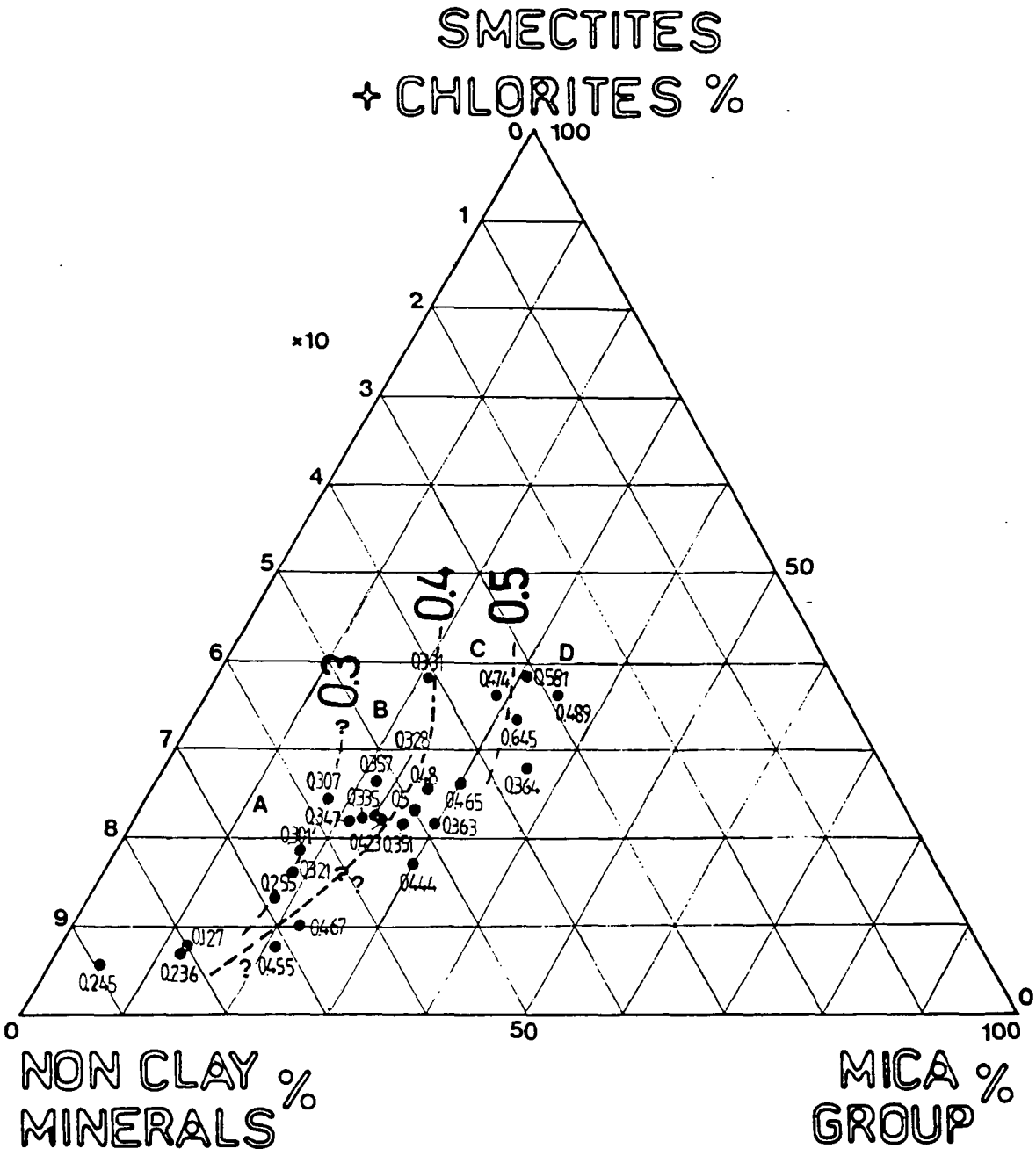

Such an attempt to involve as many mineralogical variables as possible is shown in figure 7.5.7. The full mineralogical suite was broken up into three categories placing more emphasis on the clay minerals present. Hence, the three corners of the triangle are occupied by the mica group minerals content, the cumulative content of the smectites and the chlorites and finally the non-clay minerals content. On every data point the value of its C_C^* was marked.

Two main areas or clusters may be identified, the low to intermediate compression (A and B) and the intermediate to high compression index values (C and D). The areas were delimited by conveniently drawn boundary lines between the data points so that each area described a minimum and a maximum C_C^* value representative of the majority of the data points appearing inside that area. Hence, area A denotes C_C^* values from (theoretically) 0 to 0.300, area B from 0.300 to 0.400, area C from 0.400 to 0.500 and area D from 0.500 and over.

The boundary lines tend to curve in towards the non-clay minerals content along the non-clay minerals - mica group axis. It is interesting to observe that area B appears to thin out and eventually disappears between areas A and C with increasing non-clay minerals content. This might be the result of a continuous reduction of the chlorites and smectite contents while micas remain more or less unchanged, though more data along that boundary line are needed to ascertain this.

However, a closer examination of the areas presented reveals that the scatter of data observed in the figures previously presented was not completely obliterated from figure 7.5.7. Hence, sample skf1 appears in area D instead of C, sample mvg appears in area D instead of B, sample kd appears in area C instead of B and sample agn1 appears in area C instead of area B.

A comparison of the mineralogical contents of samples skf1 and mvg with those of the rest of the area D samples shows that the above samples contain higher proportions of chlorite minerals than smectites. However, sample lts with the highest value of C_C^* (0.645) has also the highest detected value of chlorites content (25.8%). It is known that chlorites have quite variable volume change behaviour, ranging from that of a typical kaolinite to just below that of Ca-montmorillonite (Ca-smectite). Therefore, more needs to be done on the determination of the exact chlorite type. A possible reason behind agn1's misfit arises from its high aggregation ratio (A_r=2) and the consequent reduction of the clay minerals' specific area, though such an occurence did not seem to affect other samples. A slightly higher value of

calcite content for sample agn1 than those from other similar samples might offer an additional explanation for the apparent misfit. However, no specific cause for the misfit of sample kd could be found due to its mineralogical contents.

As shown in figure 7.5.7 there is little to suggest that the mineralogical suites alone can provide accurate clues as to what the behaviour of a reconstituted marl, marly clay and clay may be under one dimensional consolidation. Mineralogy may control part of the initial condition of the slurry prior to one dimensional compression (Tan et al, 1990) and shape up the results at very low pressures, but volume change under one dimensional compression mainly obeys the void ratio-vertical effective stress structural deformation.

On the other hand, a plot such as in figure 7.5.7 helps to group information and to indentify, at least *grosso modo,* behavioural boundaries. Question marks have been inserted in the plot in order to point out areas of the plot that require more data to confirm boundary conditions. Possibly, a configuration that would exclude unnecessary entries such as the feldspars within the non-clay minerals content and would avoid ambiguities such as those introduced by the variable behaviour of the chlorites may be more successful.

7.6 A comparison between reconstituted and intact *e-log*σ_v' curves

The results from eleven one-dimensional consolidation tests on intact samples of some Hellenic "marls" are presented in appendix C. The tests were performed in accordance with the BS1377:1990 standard incremental testing procedure. From the same intact samples, reconstituted specimens were prepared and tested as part of the testing program described in Chapter 6. The results from the oedometer tests on both the intact and their corresponding reconstituted specimens were plotted on *e-log* σ_v' diagrams shown in figures 7.6.2 to 7.6.12.

Vaughan (1988) suggested that the gradient of the compression line for a bonded material would be a function of the initial void ratio rather than the soil grading and plasticity, as in unbonded materials. It is postulated that the stress on a sample is carried partly by the inter-particle contacts and partly by the bonds and that the amount of stress taken up by the bonds is a function of the distance x, the difference between the void ratio of the intact or bonded sample and the void ratio which the

reconstituted of destructured sample would have if loaded from the same initial void ratio and to the same stress level.

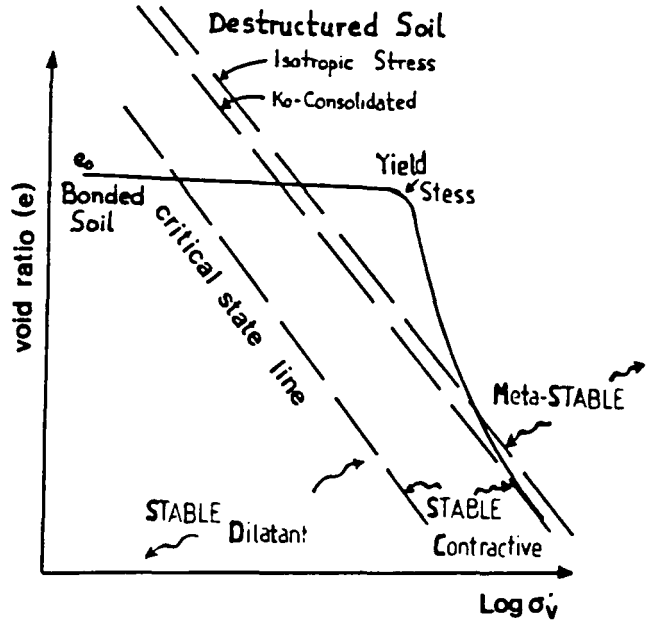

Fig. 7.6.1 One-dimensional compression of soil with bonded structure (from Vaughan, 1988).

The significance of these relative positions between curves from intact and reconstituted samples is shown in diagram 7.6.1. Three porosity states can be recognised for a bonded soil with reference to its position relative to the corresponding virgin consolidation line, each a function of stress level. They are in order of increased instability: i)*stable-dilatant*, ii)*stable-contractive*, and iii)*meta-stable* or *structure permitted.*

The *e-log*σ_v' diagrams may be divided into three broad categories depending on the relative position of the curves. In the first category (fig.7.6.2 to fig.7.6.6) the span of the vertical effective stress of the intact specimen curve is not enough to produce conclusive evidence on the behaviour of the intact material in relation to its reconstituted state. So, for the given range of intact initial void ratio e_O (between 0.3 and 0.4, i.e dense materials), it would be advantageous if the reconstituted *e-log*σ_v' curve had been known in advance of the oedometer test on the intact material so that further increments of σ_v' could have been considered to allow comparisons between the two states.

In the second category (fig. 7.6.7 to fig. 7.6.10) the *e-log*σ_v' curve of the intact sample crosses that of the reconstituted sample or its extention at a particular point. This may be partly because of a more comprehensive range of applied σ_v' and partly because of the higher initial void ratio e_o (around 0.6). According to Vaughan (1988) anything to the right of the reconstituted compression line is in a *metastable* or *structure permitted* contition, in which the natural soil exists at a void ratio which is impossible for the same soil in the reconstituted state at the same vertical effective stress level. The intact sample exists in this state only due to the strength and the stability provided by its bonded structure (Vaughan, 1988).

In the third category (fig.7.6.11 and fig. 7.6.12) the *e-log*σ_v' curve of the intact sample becomes asymptotic to the *e-log*σ_v' curve of the reconstituted sample, keeping to the left of the reconstituted sample's curve. According to Vaughan (1988), the area to the left of the line of the reconstituted sample represents two states of stable conditions, the *stable-dilatant* and the *stable-contractive*, to the left and to the right of the critical state line, refering to a stress domain where the soil could exist in a reconstituted state but it would expand or contract respectively during shear towards the critical state line (fig. 7.6.1).

It can therefore be deduced that testing samples in a reconstituted state helps the extraction of meaningful conclusions about their natural or intact state by providing a useful reference or boundary contition. In any case, experience with the intact materials tested which are characterised by natural low void ratios, shows that such comparisons are possible only if a sufficiently high vertical effective stress is applied, exceeding at all times 1600kPa.

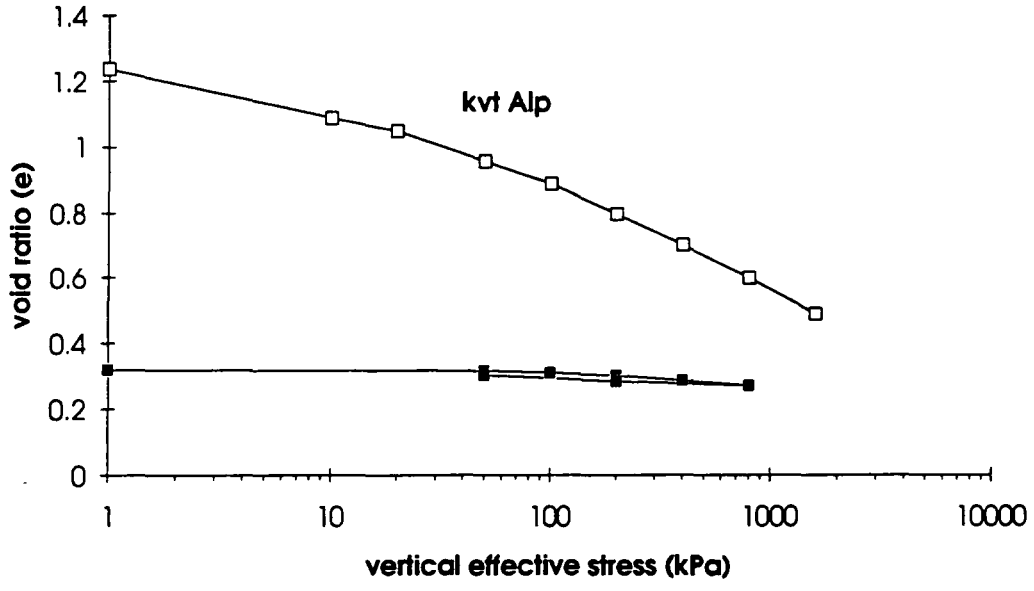

Fig. 7.6.2 Comparison of 1D consolidation of intact and reconstituted sample kvtAlp from Preveza-Igoumenitsa.

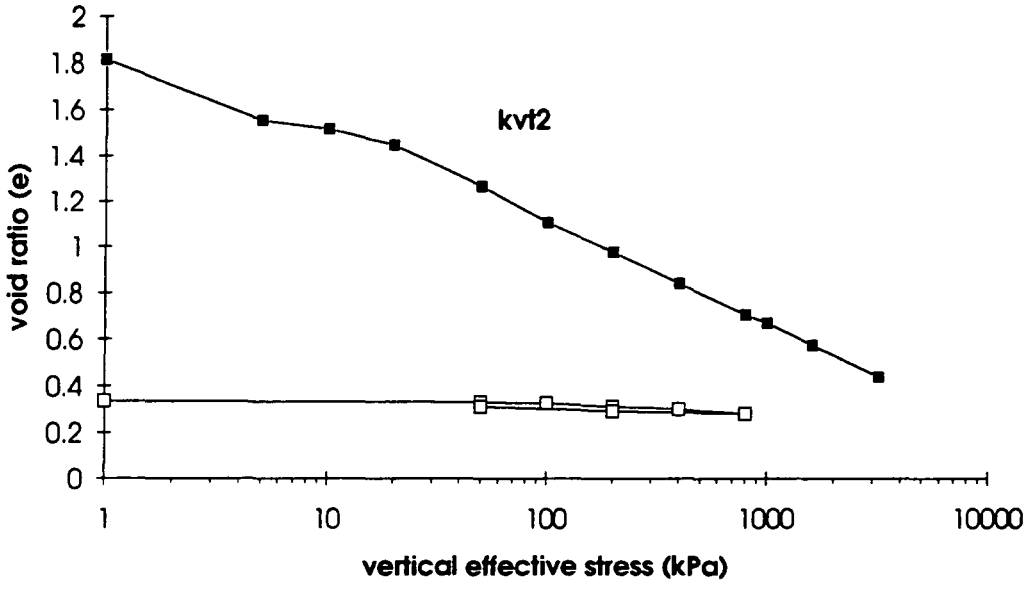

Fig 7.6.3 Comparison between the intact and the reconstituted state of the sample kvt2, Preveza-Igoumenitsa.

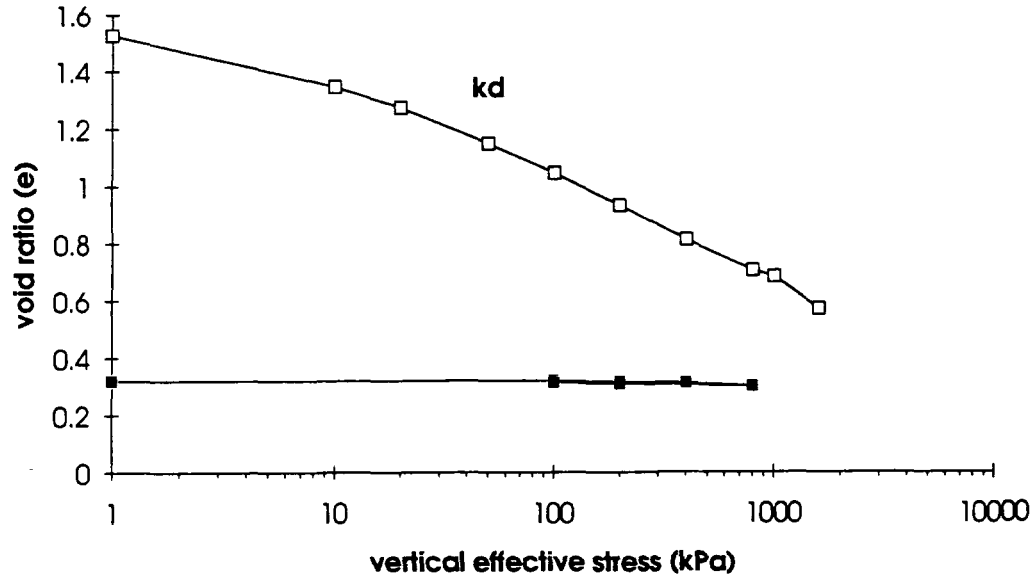

Fig. 7.6.4 Comparison between 1-D compression tests on intact (black boxes) and reconstituted (white boxes) spesimen from the sample kd, Preveza-Igoumenitsa.

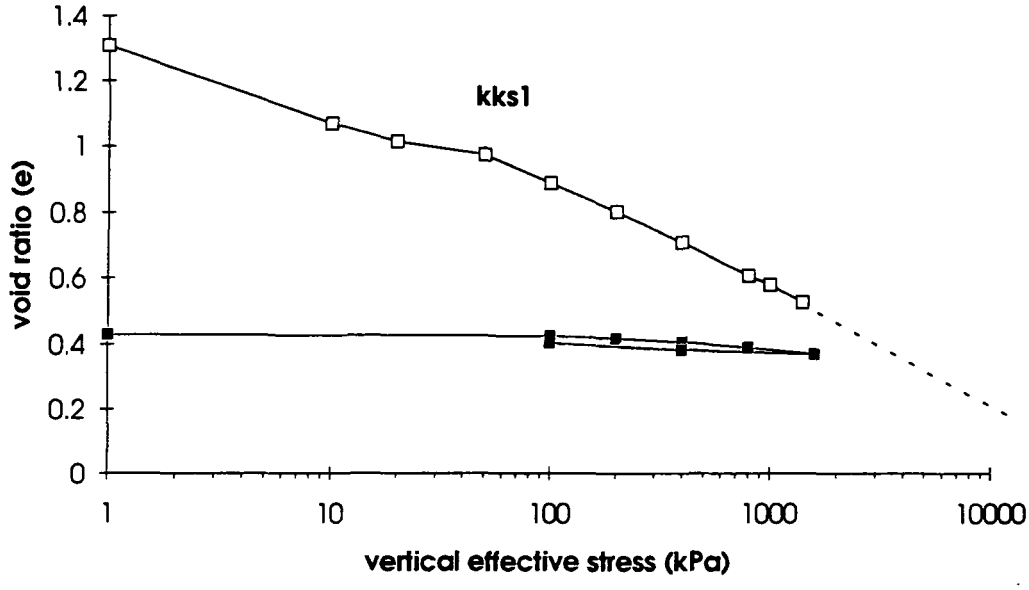

Fig. 7.6.5 Sample kks1 from Preveza-Igoumenitsa. The maximum attained σ_n' of 1600kPa was not enough to produce a meaningful comparison. Notation as above.

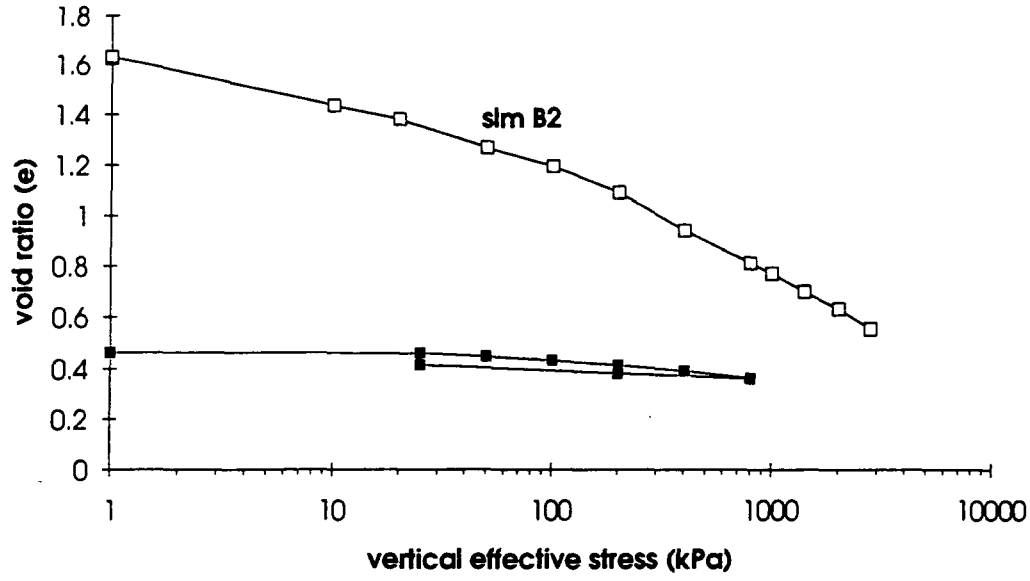

Fig. 7.6.6 Comparison between 1-D compression tests on intact (black boxes) and reconstituted (white boxes) spesimen from the sample slmB2 from Korinthos.

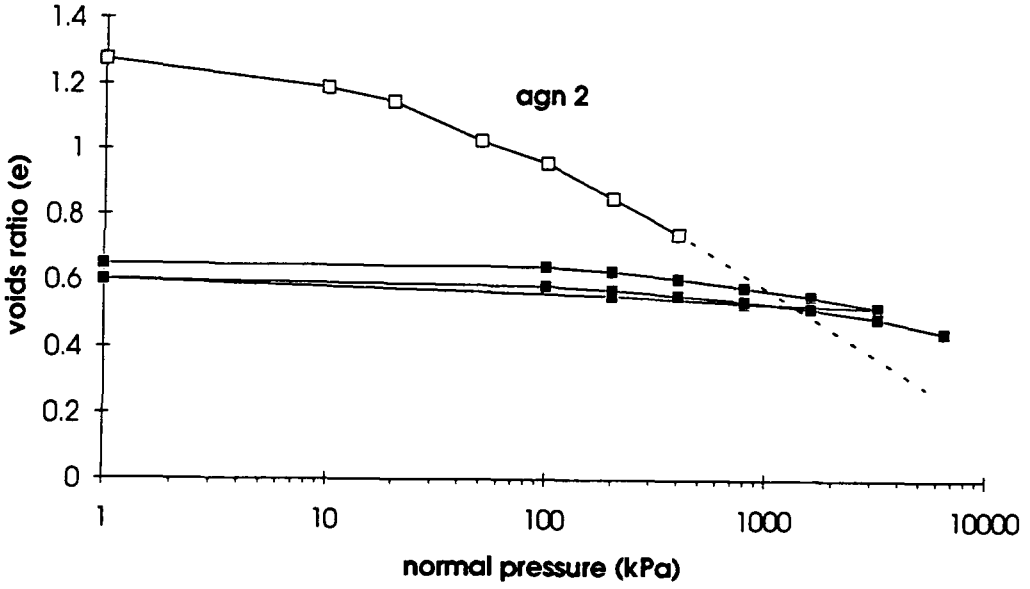

Fig. 7.6.7 Comparison between 1-D compression tests on intact (black boxes) and reconstituted (white boxes) spesimen from the sample agn2, Preveza-Igoumenitsa.

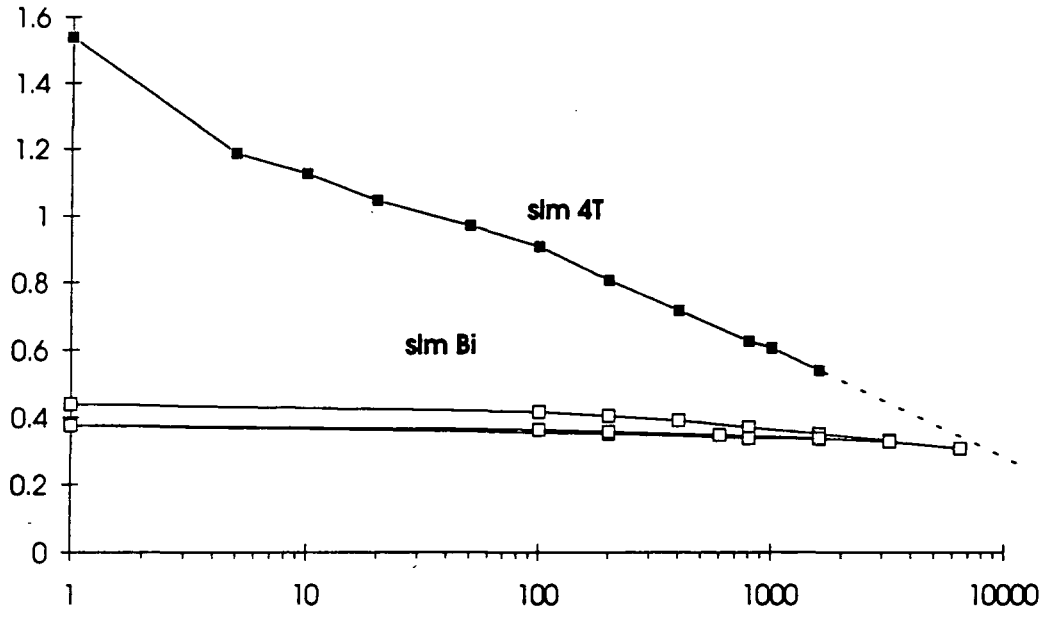

Fig.7.6.8 Samples slm4T and slmBi from Korinthos are from adjacent pits of the same layer. SlmBi crosses into a metastable state at σ_n' approximately equal to 9000kPa.

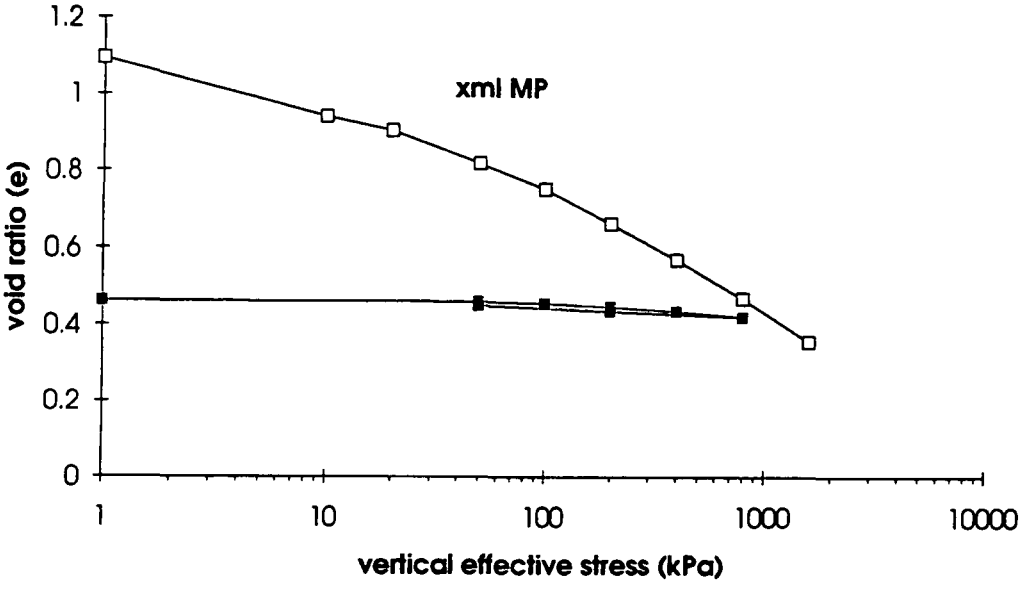

fig.7.6.9 Comparison between intact (black boxes) and reconstituted (white boxes) samples from Xynomelia on the road axis between Preveza and Igoumenitsa.

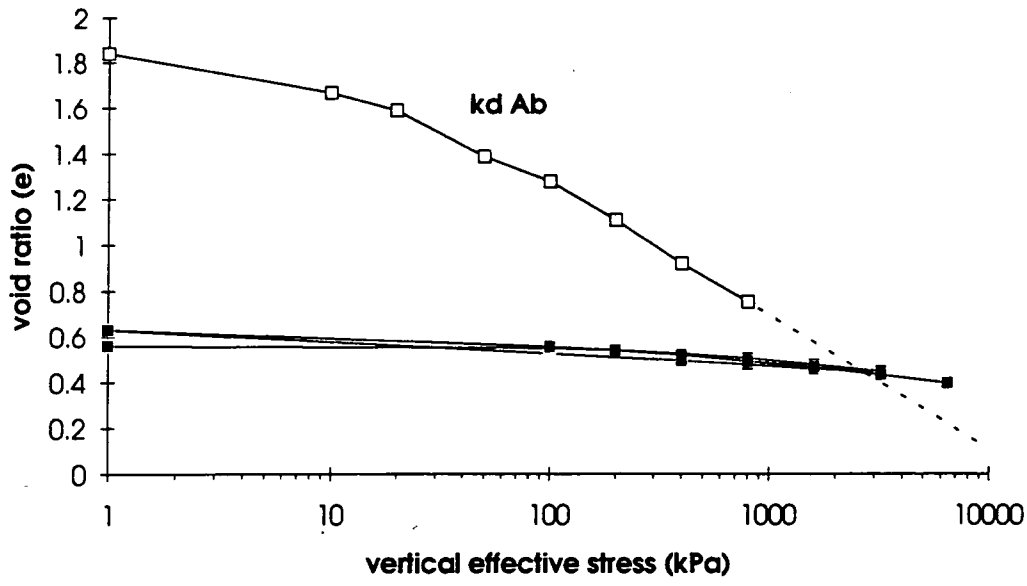

fig. 7.6.10 Sample kdAb (black boxes) from Preveza-Igoumenitsa road axis crosses into its metastable state at approximately 2500kPa.

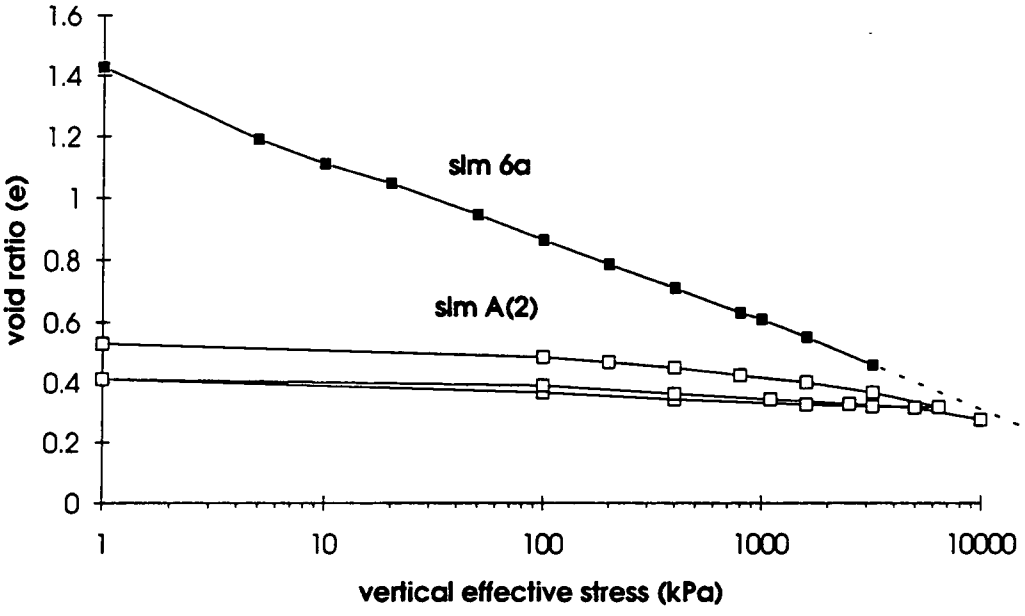

fig. 7.6.11 From the same layer, slm A(2) yields asymptoticly with regard to the virgin line of the sample slm6a from Korinthos.

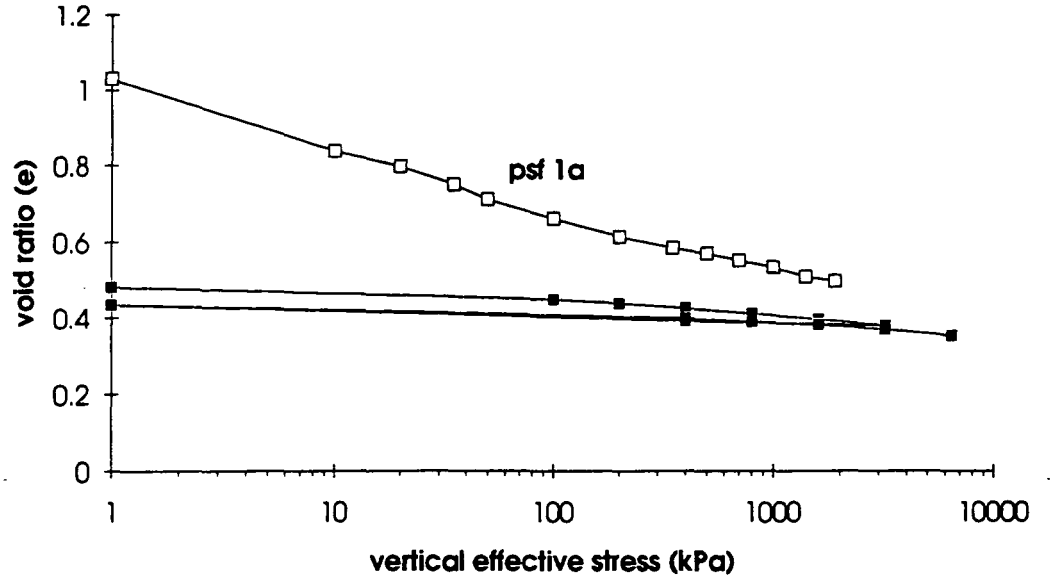

fig. 7.6.12 Asymptotic convergence of the intact (black boxes) and the virgin (white boxes) compression lines for sample psf1a from Korinthos.

CHAPTER 8
SUMMARY AND CONCLUSIONS

8.1 General

Fine grained deposits in post alpine sedimentary successions form a substantial portion of the surface area where human activities take place in Hellas. Only recently has there been a systematic attempt to understand the mechanical behaviour of such materials. In the present thesis, samples from three geologically and geographically different areas of Hellas have been considered and their intrinsic properties of residual shear strength and compression of reconstituted samples, their classification and mineralogy have been analysed. The main findings and the conclusions from this research project are discussed in summary below.

8.2 On the classification and physical characteristics of "marls"

Over consolidated fine grained deposits participating in post alpine sedimentary successions in Hellas have often been characterised as "marls" by practising engineers. However the context within which the term *marl* is used to describe a sedimentary material is ambiguous in engineering terms, while no firm agreement of opinion exists between theoretical geologists as to what criteria (e.g. genetic, mineralogical, tectonic, etc) should be more important when classifying a deposit as *marl*.

The ambiguity in engineering terms rests with the difficulties of engineers to agree on a shear stress based classification between over consolidated soils and weak rocks. The presence of cementation bonds, whether diagenetic or evolved at a later stage (e.g. after uplift has taken place) increases this ambiguity by distorting the traditional soil mechanics relationship between void ratio and stress history, hence opening a new debate on what over consolidation means in cemented materials.

It appears, nonetheless, that there is a minimum consensus in mineralogical terms, where *marl* may be an argillaceous sedimentary material with 30% to 60% by weight calcium carbonate content. In this respect, the formations considered in this thesis have varied considerably, ranging between 0% to 78% by weight calcium

carbonate content, corresponding to a range between *clay* and *calcareous marls* according to Barth et al (1939). The percentage of other non clay minerals (quartz, feldspars, dolomite) remained roughly constant throughout the entire data set. The dominant clay mineral group was the micas (e.g. illites, hydrated muscovites etc). Chlorites of various degrees of crystallinity were detected in almost all the samples considered as the second dominant group. Smectites were present in most samples while kaolinite was detected in some samples. Variations in the contribution of individual clay mineral groups to the total clay minerals' percentage became significant only where the total of clay minerals exceeded 40% by weight.

When all the above mineralogical groups were taken into account, then *marls* were seen as part of the wider mudrocks petrological classification system, such as the one suggested by Selley (1988) and Lindholm (1987). In such a system, the samples considered in this thesis ranged from *sandy mudstone* to *marly limestone.*

The grain size analysis results and the Atterberg limits also varied, offering a range of descriptions from *clayey silts* of low plasticity to *silty clays* of high plasticity and a range of mainly low to intermediate and to a lesser extent high activity characteristics in Skempton's (1953) chart. It was also found that samples pre-treated by oven drying exhibited lower Atterberg limits than samples that were allowed to air dry. The liquid limit of samples with a higher clay size fraction was more affected by oven drying than that of samples with lower clay size fraction values. In shear strength terms, the available bibliography suggested a considerable disparity in values for intact samples, which would not allow the above materials to be examined from a purely soil mechanics or rock mechanics point of view, as already indicated above.

However, there is less ambiguity in character or scatter of test parameters for those materials if they were examined in groups corresponding to their respective area of geological origin. Hence, the samples from the Korinthos area were the richer in calcium carbonate and the poorer in clay minerals. That may have reflected on their plasticity (CL to CI), their grain size (predominantly *clayey silts*) and their field description (*hard light grey, yellowish to light brown marls*). The samples from Igoumenitsa - Preveza showed higher quartz and feldspar contents than the samples from the other two areas and had the same percentage of clay minerals as the Amalias - Goumeron samples. However, on average, the Amalias - Goumeron samples were more plastic (CI to CH), softer in terms of field description (*firm & firm to hard brownish green* to *light blue grey marly clays* and *mudstones*) and

somewhat finer than those from Igoumenitsa - Preveza. The latter exhibited a wider range of values both in terms of plasticity and grain size and had field descriptions of *hard greenish* to *blue grey mudstones.*

The variation of results between samples in those three areas was seen as a direct consequence of the different evolutionary processes that acted upon the sediments from the time of their deposition till the present day. The evolutionary processes include variables such as the material sources in the vicinity of the basin, energy of the deposition environment, the depth of deposition, maximum depth of burial, geochemistry of pore fluids, post deposition tectonic movements (i.e. stress regime), present levels of overburden relief etc.

So, the brackish to lacustrine mainly lagoonal *marly* deposits of Korinthos had predominant sources of material in the limestone rich alpine neighbourhood. Their estimated maximum overburden relief of about 3.5 km since Pliocene times provides an explanation for the degree of lithification that has lead to *hard* soil or *weak* rock type field descriptions, though the development of carbonaceous cementation bonds (diagenetic in this case) distorted the theoretically expected degree of compaction. The less carbonaceous samples from Amalias - Goumeron, though having similar mineralogy with those from Igoumenitsa - Preveza, have been subjected to lower overburden (120 to 600 m) and appeared softer than the latter which have experienced at maximum 2km of overburden. Similarly, the complex deposition environment changes that acted on the Amalias - Goumeron basin lead to soils with a greater variety of grain sizes within the same horizons due to lateral transitions, whereas the presence of only two main depositional environments (Miocene shallow sea and marine Pliocene) in the Preveza - Igoumenitsa area corresponded to two main grain size groups of deposits.

Therefore, it was the local geology that exerted immediate control on the physical and mineralogical characteristics of those Hellenic fine grained sediments collectively referred to as "marls" by practising engineers. It becomes clear that, until there is an engineering classification based on shear strength and void ratio considerations which will adequately delimit existing geological definitions for *marls*, the only tool that can be used with some confidence for the classification of such deposits is their mineralogical suite. Additionally, given the field descriptions of the Hellenic "marls" studied, it would be preferable if *marls* were seen as a special case within the over consolidated mudrock type of soils. Formations extremely rich in calcium carbonate, such as those of the Korinth Canal, should be examined as

exceptional cases, owing to their unique character which lies outside the commonly found *marls'* range of characteristics.

8.3 On the aggregation ratio of "marls"

The use of the aggregation ratio A_r (Davis, 1967) as an indirect indicator of the existence of clay mineral aggregations in Hellenic "marls" has lead to the paradoxical finding of A_r values below unity (implying disaggregation according to Davis), in samples rich in calcium carbonate, a well known cementing agent. The presence of non clay minerals (such as calcite, quartz etc) under 2 μm in grain size would increase the apparent clay fraction leading to A_r values below unity. However such values do not rule out the presence of clay mineral aggregates.

Therefore additionally, a boundary line was found when calcium carbonate content was projected against A_r. This indicated that minimum A_r values were lower in the more calcium carbonate rich samples. For carbonate contents less than 20%, A_r was always greater than 1.0. For carbonate contents above 20% and below 40%, A_r had values below as well as above 1.0. For samples with higher than 40% carbonate contents, A_r was always less than 1.0, suggesting a greater amount of micritic calcite (<2 μm) was present in the clay size fraction.

Such results in themselves do not preclude the presence of aggregated clay minerals within the soil sample, nor do they mean that disagregation is taking place. They do however point to the presence of other non clay minerals in the clay size fraction. The current definition of aggregation ratio is successful for soils where the clay size fraction consists only of clay minerals.

8.4 On the residual strength of "marls"

The residual strength of the Hellenic "marl" samples tested was ascertained using a standard Bromhead and a modified Armfield prototype ring shear apparatus once trial tests comparing the two apparatuses and a shear box had been carried out. The shear box results were approximately 2° higher than the results from the two ring shear devices over the same normal stress range, as expected from past research literature.

Different testing procedures were adopted for the two ring shear apparatuses owing to their different design philosophies. This was done in order to minimise losses of sample material through the gaps between the shearing plates and hence ensure the smooth running of tests and achieve the best possible compatibility of results. Thus a loading sequence of 50kPa increments in normal stress σ_n', starting at 50kPa and finishing at 400kPa, with consolidation taking place inbetween increments, was adopted for the standard Bromhead. For the modified Armfield, which has similar design features with the Bishop (Imperial College & N.G.I) device, uninterrupted unloading sequences of 200, 150 & 100 kPa or 400, 200, 150 & 100 kPa σ_n' decrements were adopted depending on the estimated present overburden pressure experienced by a given sample. Prior to shearing, the sample was consolidated to a load equal to 1.5 times the heaviest load used during the test.

The two ring shear devices showed almost identical stress ratio (τ/σ_n') at residual values for the same sample, hence very similar values of residual angle of friction. However, the shape of the shear strength envelopes differed at low σ_n' with the Bromhead device generally indicating less curved envelopes than the modified Armfield apparatus. The testing procedure followed for the tests carried out in the standard Bromhead meant that normally consolidated conditions applied during shearing. So, it is reasonable to expect that no stress relief had taken place. That, in conjunction with on average lower percentage of clay minerals in the samples tested in the standard Bromhead, led to very little or no curvature of the failure envelope at low pressure. If, however, the swelling pressure of the clay minerals exceeded the normal pressure imposed during a shearing stage in the Bromhead apparatus, then it is reasonable to expect that curving of the shear stress envelope could develop.

On the other hand the majority of the tests carried out in the Armfield ring shear apparatus gave curved envelopes for the same range of σ_n'. The curved nature of that part of the failure envelopes sugests that there is hysterisis in the shear stress for decreasing normal stress. It is suggested that the curvature is related to mechanical swelling in the vicinity of the shear plane in response to the incremental unloading in the Armfield device during testing, resulting in progressively higher over consolidation ratios experienced by the sample. That could result in some disorientation and dislodgement of particles along the shear surface. The increased disorder along the shear zone would contribute to increased shearing resistance along the shear plane. Such curvature was observed especially in clay rich samples and

could be further exacerbated by physicochemical swelling of the sample's expanding lattice clay minerals.

For a range of σ_n' between 200 and 400kPa, Korinthos samples exhibited, on average, higher values of final τ/σ_n' between 0.400 and 0.520 (ϕ_r' between 21.8° and 27.5°) than samples from the other two areas. The tests showed that the drop in τ/σ_n' did not on average exceed 35% between the first (σ_n'=50-100kPa) and last (σ_n'=200-400kPa) shearing stages, thus ensuring almost linear shear strength envelopes.

For the same range of σ_n', Preveza-Igoumenitsa samples exhibited, on average, a lower range of final τ/σ_n' than Korinthos with values between 0.200 and 0.340 (ϕ_r' equivalent 11.3° and 18.8°). The drop in τ/σ_n' between first (σ_n' = 100kPa) and last (σ_n' = 200-400kPa) shearing stages varied from 10% to 150%. Curved residual shear stress envelopes were observed.

Amalias-Goumeron samples showed, for the same range of σ_n', an average range of final τ/σ_n' between 0.25 and 0.300 (ϕ_r' equivalent 14° and 16.7°). The drop in stress ratio σ_n' varied as above from 10% to 150% between the first (σ_n' =100kPa) and the last (σ_n' = 200-400kPa) shearing stage of a test. Curved residual shear stress envelopes were observed.

An intermediate stress plateau between peak and residual strength was observed in some tests. It is believed that this is related to the presence of aggregations of clay minerals which break down with further displacement causing a further loss of strength.

The results obtained from both apparatuses were generally compatible with the findings of the mineralogical and grain size analysis. The low plasticity samples (high in non clay minerals) from Korinthos showed similar behaviour at residual stress conditions to the Irakleion marls (Tsiambaos, 1987), thus exhibiting the highest values of stress ratio τ/σ_n'. On the other hand, the higher plasticity samples (richer in clay minerals) from Preveza - Igoumenitsa and Amalias - Goumeron exhibited lower values of stress ratio τ/σ_n' than those of Korinthos and Irakleion.

Atterberg limits, though quick and inexpensive to produce following the B.S 1377:1975 specifications, could not provide reliable correlations with ϕ_r' mainly due to their empirical nature and the errors that are involved in their determination.

It was shown that although the trend already identified in the literature between ϕ_r' and calcium carbonate exists, it was statistically insufficient to make good predictions (r^2 = 0.497, ϕ_r' error estimate = 4.9°). When the combined influence of calcite (calcium carbonate) and quartz on ϕ_r' was examined, it was found that the trend was enhanced (r^2 = 0.605, ϕ_r' error estimate = 4.3°). Hence, the importance hitherto placed solely on calcite may be misleading. The minerals of the mica group were the most influential (r^2 = 0.686, ϕ_r' error estimate = 3.7°). The chlorites showed comparable statistical importance with the calcite, whereas the smectite content showed no correlation with the residual strength parameters.

On the whole, plotting only one mineralogical component against a complicated parameter such as the residual angle of friction expectedly leads to statistical scatter. The presence of scatter in a graph indicates the lack of consideration of other factors which also exert influence on the measured parameter. Therefore, the simultaneous use of all mineralogical components should reduce the scatter found in the above correlations. When the tested "marls" were plotted in a triangular classification chart, where the mica group, the smectite plus chlorite groups and the non clay minerals group occupied the ends of the triangle. Three concave zones, pointing away from the non clay minerals pole, could be identified where ϕ_r' values developed from above 20°, to between 15° and 20° and below 15° towards the two other clay minerals poles.

However, a number of samples did not fit the above described zones. A closer inspection of these samples revealed that the differences in mineralogical suites could not adequately reflect the behavioural changes of "marls" in relation to their residual strength. That could only happen when the particle size distribution for the mineralogical species, the specific type of the clay minerals involved (i.e. type of exchangeable cation, specific area etc) and the degree of crystallinity of the mineralogical species became known. The latter could become important when chlorites were detected in relatively high quantities (i.e. over 12%) given the wide range of specific areas that they may exhibit.

The low values of granular void ratio e_g measured point to a well graded granular fraction with clay particles much smaller in terms of average grain size than the rotund (or massive) particles. The samples tested fell inside the exceptions cited by Lupini et al (1981) as not fitting their model of shearing mode behaviour because of aggregation effects. However, an extension to the left of the Lupini et al (1981)

model was considered alongside a similar proposition by Lemos (1986) which allows for aggregated, diagenetically bonded fine grained soils to be modelled.

The grain size distribution results generally suffered from problems similar to the mineralogical suites when they were used as prediction indicators for the residual strength of the tested Hellenic "marls". The non linear relationship between the clay fraction and the residual strength parameters was confirmed. Looking, however, at the scatter in that relationship, it was recognised that for the same clay fraction content a wide range of residual angles of friction were determined. The entire grain size distribution curve had to be taken into account, since it was realised that there was a gradual coarsening of the rest of the grain size distribution curve with increasing ϕ_r' for a given clay size fraction content. A triangular plot was employed in order to investigate the effect of the entire grain size distribution curve on the residual angle of friction. The clay fraction, the fine plus medium silt and the coarse silt plus fine sand contents were used to determine the three poles of the triangle. Three broad zones were identified where the samples exhibited ϕ_r' values that progressed from below 15°, 15° to 20° and above 20° respectively as data points got closer to the coarser poles.

However here too, a number of data points did not fit that general outlook. Apart from the distorting effects of particle aggregation on the grain size distribution curve, mineralogical idiosycracies (such as the presence of calcite and quartz in the clay fraction or the presence of highly active clay minerals) are thought to have played a part in the misfit of these data points.

On the other hand, it is suggested that the relative size of clay and "massive" particles (i.e. silt size and over) as well as the shape of the latter control the type of effect that the grain size imposes on the residual strength parameters (Lupini *et al*, 1981; Lemos, 1986). However, the results of this investigation suggest that a collective "massive" particles approach is oversimplified, especially with soils where the so called "massive" particles are present in large quantities. It is rather the relative proportions of the grain size fractions and fraction sub-divisions (i.e. fine, medium, coarse silt) and their internal ratios which provide a better indicator of the residual strength behaviour of a soil. It was shown that such ratios have better predictive power when incorporated in a numerical model. The model was picked from a pool of computer generated models for its optimum use of parameters and goodness of predictions. The common characteristic of all those models was that they all used ratios of grain size fractions and fraction sub-divisions.

In summary, the residual strength characteristics of the tested Hellenic "marls" reflect the geological identity of the areas from which they have been sampled. Although a number of correlations may be helpful to draw a picture about the residual strength of such materials, it is only the combination of grain size distribution ratios and detailed mineralogical considerations, assuming that there is no change in the pore fluid geochemistry, that can fully describe the reaction of a soil to shearing at large displacements. Simple models which attempt to predict the behaviour of a formation subjected to residual shearing conditions are useful as long as the user of such models is aware of the simplifications made which affect the accuracy of the solutions expected.

8.5 On the intrinsic compressibility of Hellenic "marls"

Compressibility test results from broken down soil-water mixtures (slurries) prepared at moisture contents approximately between one to one and a half times the liquid limit (reconstituted state according to Burland, 1990), showed that there was a general trend of $e\text{-}log\sigma_v'$ lines to converge at high vertical effective stress levels. The compression lines thus produced were free of any stress history (fabric) effects and would only depend on the particle and mineral types present, provided that no changes in pore water chemistry occurred during the tests. The linear portion of such lines was seen as the extension of their virgin consolidation lines, the constants of which were named constants of intrinsic compressibility. Burland (1990) suggested that a normalisation with respect to the void ratios at 100kPa and 1000kPa on the y axis of the $e\text{-}log\sigma_v'$ plot produced an unique concave curve, insensitive to composition, plasticity and loading rate, which was termed *intrinsic compression line* or ICL.

Samples from Korinthos showed values of the constants of intrinsic compressibility C_c^* ranging on average between 0.236 and 0.335 and e^*_{100} ranging on average between 0.832 and 0.937. Samples from Preveza-Igoumenitsa showed on average C_c^* values from 0.328 to 0.436 and e^*_{100} ranging on average between 0.886 and 1.068. Samples from Amalias-Goumeron showed C_c^* ranging on average between 0.444 and 0.480 and values of e^*_{100} on average between 1.101 and1.253.

The values of C_c^* and e^*_{100} shown above were in some agreement with the range of plasticities identified for the corresponding areas (see also section 8.2). Hence, the

low plasticity Korinthos "marls" were shown to be the least compressible and had the smallest intrinsic void ratio of the rest of the samples. The intermediate plasticities of the Preveza - Igoumenitsa samples generally corresponded well with the test results, which fell between the low Korinthos and the intermediate to high plasticity Amalias - Goumeron ones. However, the correlation between plasticity and the constants of intrinsic compressibility C_c^* and e^*_{100} suffered from considerable scatter. This may be due to the fact that plasticity (as a function of mineralogical composition) exerts control on the initial experimental condition and thus influence the results at very low pressures. The influence of the mixing ratio w_i / w_L on the shape of the e-$log\sigma_v'$ compression curves was also thought to have added to the scatter observed.

The variation of C_c^* with the contents by weight of individual mineralogical species and groups of species was considerable too. The best correlation was produced by the sum of calcite plus quartz content (r^2=0.564, s_{ey}=0.076) while the correlation with the total sum of clay minerals was closely second best. Micas were the most dominant clay mineral group. Smectites and quartz yielded insignificant trends. When the chlorites plus smectites sum was considered, it produced a better correlation with C_c^* than the individual species did.

In terms of volume change, smectites, being the most active group, and the chlorites, being the second most active group, when both combined would contribute more towards the physicochemical aspect of intrinsic compression of a reconstituted "marl" mainly at very low pressures (5 to 50kPa) until the sample attained a semi-solid state. On the other hand, when the compression characteristics began to depend more on the created structure of the reconstituted "marl", changes in porosity, which are related to grain size distribution, influenced the further establishment of drainage paths. It was shown that there was a relationship between the calcite and quartz present with the medium silt to fine sand grain sizes. Hence, their cumulative effect in forming the reconstituted fabric especially of samples with low to intermediate clay minerals content (20% to 50%) and therefore influencing the intrinsic compressibility characteristics can be important. Kaolinite and dolomite presence was inconsistent and in too small quantities to have any effect.

The complexity of the phenomena associated with the one-dimensional consolidation of reconstituted "marls" cannot be fully described by the variation of one single mineral type or group at the time. Rather it is all the mineral types and groups involved as a whole that interactively affected the constants of intrinsic

compressibility and the intrinsic compression index. However, mineralogy controls only the initial conditions and the compression at very low pressures. Volume change of reconstituted Hellenic "marls" under one dimensional compression at intermediate and higher vertical stresses mainly obeyed the classic soil mechanics void ratio-vertical stress predicted deformation.

An attempt to involve as many mineralogical variables as possible led to the use of a triangular classification chart, where the three poles were occupied by the sum of non clay minerals, the micas group and the sum of smectites and chlorites contents respectively. The values of C_c^* were noted beside each point. Four zones were identified progressing from low C_c^* values close to the non clay minerals poles to higher C_c^* values closer towards the other two clay mineral poles (less than 0.3, from 0.3 to 0.4, from 0.4 to 0.5, higher than 0.5). However inconsistencies did occur in the model. The misfit of a number of points was thought to have been caused by variable behaviour of some mineral types such as various chlorites and the different development of drainage paths due to variability in grain size distribution.

The intrinsic compression curves were grouped in terms of liquid limit (w_L<40%, 40%<w_L<50%, 50%<w_L) and calcite content (c.c.<25%, 25%<c.c.<45%, 45%<c.c.) of the respected samples. It was found that every group could be described individually by its own ICL. The accuracy of polynomial descriptions of ICLs as derived by linear regression analyses increased when the σ_v' increments up to 50 kPa were ignored. The shape of these ICLs was generally convex in contrast to the single line proposed by Burland (1990). The degree of curvature increased with increasing liquid limit and decreased with increasing calcite (calcium carbonate) content.

Given the differences established in terms of mineralogy and plasticity between the three sampling areas, it was expected that such variations in curvature would be seen if the data was grouped in terms of area of origin. That has been confirmed when the shape of the ICLs which corresponded to samples from Korinthos (least curved), Amalias-Goumeron (mostly curved) and Preveza-Igoumenitsa (intermediately curved) were examined. The differences in the degree of curvature were most notable in the area of low σ_v' values (up to 50kPa) and very high ones (over 1000kPa) due to the normalisation with respect to the void ratios at 100kPa and 1000kPa on the *y* axis of the *e-log*σ_v' plot.

In light of the behaviour of the reconstituted samples of Hellenic "marls" under one

dimensional consolidation it is concluded that the ICL presented by Burland (1990) is not, after all, a universally unique line but it is influenced by mineralogy and plasticity, and hence is prone to local geological effects. It would generally be more useful, if ICLs reflected a narrower data set more representative of a specific group of formations either in terms of area or in terms of petrological type. In either cases it becomes clear that the *intrinsic compression line*, as defined by Burland (1990), cannot serve as a unique reference line for studying the compression of naturally occurring materials.

On the other hand, the intrinsic compression curves can provide valuable reference for the extraction of conclusions on the state of an intact sample's structure under one-dimensional consolidation (metastable or structure permitted, stable-dilatant, stable-contractive). A small number of intact samples of Hellenic "marls" was tested under one dimensional consolidation and their results were projected against results from reconstituted samples of the same "marls". It was found that with intact materials characterised by natural low void ratio, such as those tested, comparisons between the reconstituted and the intact states will only be possible if the applied vertical effective stress exceed 1600kPa.

8.6 Proposals for further research

The acquisition of objective knowledge is a continuous struggle of analytical criticism and constant re-evaluation of the "truths" that a piece of research has come up with. After all there are no such "truths" or theories that have been proved. Theories are simply reconfirmed until someone presents data that do not obey those "truths". However, the level of such re-evaluation and questioning quite frequently has its starting point at the basics of testing methodologies and practices which often reveal philosophical bias of researchers. The revelation and recognition of such bias, however, promotes objective knowledge.

Often enough, owing to different reasons, shortcuts or simplifications in research have to be made. Frequently, such shortcuts in academic scrutiny come wherever testing procedures have been standardised and documented by internationally accepted bodies (e.g. B.S.I., A.S.T.M. etc). In such cases, following the standard methods for the routine identification of some parameters becomes the norm, especially if it has been thought that these parameters do not form the "cutting edge" of a particular project.

The determination of the Atterberg limits and the grain size analysis curve for naturally bonded soils or heavily aggregated soils is an area where such shortcuts were taken. Nonetheless, the prescribed methods for the determination of the above parameters are quite vague in terms of pre treatment. The main question lies with the aggregated clay minerals which occur naturally in Hellenic "marls" and the optimum way of removing them prior to any of the above mentioned tests. Dumbleton & West (1966) studied the effect of time dependent disaggregation achieved by mechanical means on plasticity and Huang (1989) looked at methods of disaggregation and their effect on the intensity of X-ray diffraction peaks. However, the question of which might be the optimum combination of pre treatment method and procedure, which will remove the majority if not all of the aggregations prior to the determination of physical characteristics of bonded materials, remains largely unresolved. Any attempt to answer such questions will first have to carefully examine the usefulness of the complete removal of mineral aggregations from a soil even when it is known that some of them survive real life situations and most of the tests in geotechnical engineering, thus behaving like stable particles.

The use of scanning electron microscopy has not in the past seen a lot of use in geotechnical engineering. The images obtained have been used mostly to show the state of a sample's fabric, the orientation of particles along a shear surface and the identification of degrees of crystallinity and shape of particles. However the picture that a reader gets is fragmented, limited by surface area that can be covered and not showing medium scale features which could have been revealed if a petrographic microscope thin section was used. Such thin sections (as shown by Lemos, 1986) would be very useful for examining cross sections of annular specimens sheared to residual conditions. Although a thin section cannot unveil the nature of the very small clay minerals it could however provide a better picture of the deformation that had taken place during shearing through the entire specimen.

Through the course of the data analysis of this thesis it became apparent that the mineral identification of the samples tested created questions about the behaviour of the mineralogical suite as a whole. The behaviour of the mineralogical suite, with regard to the intrinsic properties tested here, was thought to have been influenced by the grain size distribution of the individual minerals and their properties with reference to water adsorption and shearing. The techniques used in this research could not differentiate between various types of chlorites, or various types montmorillonites or mixed layer expansive clays present (nor the degree of their

crystallinity). The shape of the peaks of those minerals (and of the hydrated micas in that respect), which can provide valuable clues about their crystallinity, could be affected by the presence of substantial amounts of calcite which acts as a peak's depressant. This has serious implications for *marls*. The suggestion of leaching the calcite prior to the XRD determination of the composition of the clay minerals suite is fundamentally flawed. The use of acids to leach the calcite out of the sample can alter some of the sensitive minerals, such as some chlorites and montmorillonites. Wherever the presence of calcite is too strong, so that the combined non clay minerals content exceeds 70% in total, the precise knowledge of the clay mineralogy is not important.

Generally though, one has to become more specific about the type of chlorites or montmorillonites present in a suite and find out more about the shape of the mineral crystals if safer inferences about mechanical properties can be deduced from the mineralogical analysis. Hence a more sophisticated sampling method is required. It may be advantageous if the pipette method for the determination of grain size is used. Samples collected in testing tubes, which represent grain size fractions, could be allowed to air-dry and then carefully extracted from the tubes and tested using X-ray diffractometry. In that way, at least one would be able to relate the presence of some minerals to a particular grain size fraction. It is also hoped that the resolution for the clay fraction would substantially increase, thus allowing more detailed examination of the ensuing diffraction peaks.

Questions over the influence of the testing procedures and the type of equipment on the determination of residual strength characteristics arise from this research. Although compatible final residual angle of friction results were obtained, it became clear that the failure envelopes produced by the Bromhead and the modified Armfield apparatusses differed at low normal stress levels. It is difficult to suggest what was predominantly responsible for this disparity because different testing procedures were employed for each of the two machines. There have already been studies on various testing procedures on a particular type of ring shear apparatus or studies on various types of ring shear apparatusses using the same procedure (see the literature review on Chapter 5). However the author feels that none of these studies looked adequately into the ways that the constituents of a soil specimen react to a change in procedure (e.g. loading or unloading stages of normal stress during a test) or a change in equipment (e.g. different thickness of specimen, position of shear plane relative to the porous discs). Therefore it would be useful to attempt to differentiate between these two influencing factors (different machine, different

procedure) and identify the ways that these may individually influence the shape of the failure envelope of "marls" at low normal stresses.

This thesis argues that creating residual angle of friction predictive models based on physical and mineralogical characteristics, is a complicated process which requires data of high detail and clarity in order to deliver good quality results. However further development of our understanding on how mineralogy or grain size disrtibution of "marls" affect the residual angle of friction remains important. The triangular representations proposed in this thesis can help in this direction but they are by no means complete. More results from ring shear tests are needed to expand or even revise the presented zones. Caution is urged, so that the ring shear results incorporated into the triangular representations have been tested for their compatibility.

When Burland (1990) presented his ideas on the *intrinsic compression line* he largely based his work on Skempton's (1970) data set which excluded clays with calcium carbonate contents in excess of 20%. This thesis showed that variations in plasticity and calcium carbonate content affected the shape of such lines. It was concluded that groupings of ICLs reflected more accurately the variations of the composition of the tested materials. The formations examined in this thesis belong to a relatively narrow range of materials despite the efforts of the author to include a wide variety of naturally occuring "marls". Therefore soft pure clays, expansive soils and over consolidated clays can be tested in order to examine the behaviour of their groups in terms of *intrinsic compression* and thus provide a complete picture of the available ICLs.

It was shown that a lot of the differences in ICL shape occured at low pressures where physicochemical reactions to loading play an important role. It was further postulated from the literature that at intermediate and high pressures the $e\text{-}log\sigma_v'$ classic soil mechanics approach is more realistic in describing the compression of a reconstituted "marl" sample. However, the transition phase between the physicochemical mechanism and the soil mechanics approach remains an area where a lot of questions can be raised. First of all, where in terms of vertical pressures does this transition take place? Is the magnitude of this transition range of pressures related to the mineralogical composition of the material, the grain size distribution or both? What is the likely mixing ratio during this transition and how much is this ratio dictated by the sample's composition? Answers to these questions may shed

light into the area between deposition and compression under self-weight and compression due to overburden pressure of natural materials.

The study of Hellenic "marls" is far from complete. This research has looked into some aspects of their nature and studied the intrinsic properties of residual strength and the compressibility of reconstituted samples. One of the most prominent features that came out from this thesis is that there is a strong relationship between performance of these materials and their geological origin. The three areas that have been studied are by no means the only areas were such materials occur. Wherever post-alpine formations are found in Hellas, "marls" are going to be present. Therefore, extensive 1:25,000 engineering geological mapping that will cover these formations, encompassing at least the physical characteristics, unconfined compressive strength values and field descriptions of the state of the formations (e.g. fresh, weathered, residual), is needed to lay the foundation for more detailed work. Most of the problematic slopes can then be identified using remote sensing techniques (e.g aerial photography) and be noted on the maps. The examination of existing discontinuities and the determination of minimum and maximum piezometric levels in the slopes are two other valuable parameters which can be included in such maps. Slope stability problems associated with "marls" need to be additionally investigated on the basis of material reaction to seasonal variations of moisture content. Such variations lead to the opening up of desiccation cracks and the consequent filling up with water during wet periods. Such cracks can reach appreciable depths. The study of partial saturation effects on the shear strength of intact "marls" could yield important clues about the seasonal variations of strength. To that end, the understanding of the suction mechanisms of "marls" which lead to seasonal shrinking and swelling, should help to answer questions on the progressive weakening of slope materials, a possible contributor to progressive failure of slopes.

Further, the engineering geological investigation of the Hellenic "marls" should aim at the gathering of shear strength information from triaxial tests numerous enough so that it can be statistically manipulated. A second, more specialised, approach should look into the fabric of such materials and examine the constitutional relationship between the various mineral grains and their response to triaxial loading and one dimensional consolidation. So, answering questions pertaining to the placement of *marls* on the spectrum between over consolidated soils and *weak* rock would aid a more precise classification of *marls* within the mudrocks family. To that end, the creation of a sound framework, within which these materials can be examined, may

be helped by the findings of this thesis which, if enriched with results from more areas, could provide the lower bounds of the behaviour of Hellenic "marls".

REFERENCES AND BIBLIOGRAPHY

Abu-Sharar T.M., Bingham F.T. & Rhoades J.D. (1987) *Stability Of Soil Aggregates As Affected By Electrolyte Concentrations And Composition.* Soil Sci. Soc. Am., Vol: 51 pp 309 - 314.

Abu-Sharar T.M., Bingham F.T. & Rhoades J.D. (1987) *Reduction In Hydraulic Conductivity In Relation To Clay Dispersion And Disaggregation.* Soil Sci. Soc Am., Vol: 51 pp 342 - 436.

Allam M.M. & Sridharan A. (1985) *The Shearing Resistance Of Saturated Clays.* Geotechnique Vol: 35 pp 119 - 122.

American Society for Testing and Materials (1984) *Standard Methods for Classification of Soils for Engineering Purposes*, ASTM Designation D2487-1983.

Anagnostopoulos A.G., Kalteziotis N., Tsiambaos G.K., & Kavadas M. (1991) *Geotechnical Properties Of The Corinth Canal Marls.* Geotechnical & Geological Engineering, Vol: 9 (1) pp 1 - 26, Chapman & Hall Ltd.

Anayi J.T. (1990) *Residual Strength Of Clay At Low Normal Stresses.* Ph.D. Thesis, Loughborough University of Technology, England, UK.

Anayi J.T., Boyce J.R. & Rogers C.D.F. (1989) *Modified Bromhead Ring Shear Apparatus.* Journal of Geotechnical Testing, ASTM Vol: 12 (2), pp 171 - 173.

Anderson W.F. (1988) *Effective Stresses on the Shafts of Bored and Cast-in-situ Piles in Clay,* Proceedings of the International Seminar on Deep foundations on Bored and Augered Piles / GHENT. Ghent State University, USA, pp 387 - 394.

Anderson W.F. & Hammond F. (1988) *Effects of Testing Procedure In Ring Shear Tests.* Journal of Geotechnical Testing, GTJODJ, Vol: 11 (3), Sept. 1988, pp 204 - 207 ASTM.

Anderson W.F. & Sulaiman J.I. (1987) *Mobilisation of Shaft Adhesion on Bored and Cast-in-situ Piles*, Proceedings of the International Conference on Foundations and Tunnels, Edinburgh University, U.K., Vol: 1, pp 160 - 166.

Anderson W.F., Young K.Y. & Sulaiman J.I. (1985) *Shaft Adhesion on Bored and Cast-in-situ Piles*, Proceedings of the 11th International Conference of Soil Mechanics and Foundation Engineering, San Francisco, California, USA, pp 1333 - 1336.

Andronopoulos B. (1985) *The Geology And Structure Of The Pireas Marls.* Hellenic Society Soil Mechanics & Foundation Engineering, Technical Chamber Of Greece, Athens, pp 5 - 20.

Aoyagi K., Chilingarian G.V. & Yen T.F. (1987) *Clay Mineral Diagenesis In Argillaceous Sediments And Rocks.* Energy Sources, Vol: 9, pp 99 - 109. Taylor & Francis, U.K.

Arkin Y. & Michaeli L. (1989) *Strength And Consistency Of Artificial Clay-Carbonate Mixtures: Simulation Of Natural Sediments.* Engineering Geology, Elsevier, Vol: 26 (3), pp 201 - 215, March 1989, Netherlands.

Attewell P.B. & Farmer I.W. (1976) *Principles of Engineering Geology*, Chapman and Hall, ISBN 0 412 114003.

Aubouin J. (1965) *Geosynclines, Developments in Geotechnics*, Vol: 1, Elsevier, Amsterdam, 335 p.

Bailey S.W. (1980) *Structures Of Layer Silicates.* In: "Crystal Structures Of Clay Minerals And Their X-Ray Identification", G.W. Brindley & G. Brown (Eds.). Mineralogical Society Monograph No. 5, Mineralogical Society, London, 1980, pp 1 - 115.

Barth, T.F.W., Correns C.W. & Eskola P. (1939) *die Eutstehung der Gesteine*, Springer-Verlag, Berlin.

Been K. & Sills G.C. (1981) *Self-Weight Consolidation Of Soft Soils: An Experimental And Theoretical Study.* Geotechnique Vol: 31 (4), pp 519 - 535.

Binnie G.M., Clark J.F. & Skempton A.W. (1967) *The Effect Of Discontinuities In Clay Bedrock On The Design Of Dams In The Mangla Projects.* Proc. 9th Conference Progress Large Damns, Vol: 1, pp 165 - 183.

Bishop A.W. (1967) *Progressive Failure with Special Reference to the Mechanism Causing it*, Panel discussion, Proceedings of the Geotechnical Conference in Olso, Vol: 2, pp 142 - 150.

Bishop A.W., Green G.E., Garga V.K., Andresen A. & Brown J.D. (1971) *A New Ring Shear Apparatus And Its Application To The Measurement Of Residual Strength.* Geotechnique Vol: 21 (4), pp 273 - 328.

Bishop A.W., Webb D.L., & Lewin P.I. (1985) *Undisturbed Samples Of London Clay From Ashford Common Shaft; Strength Effective Stress Relationship.* Geotechnique Vol: 15 (1), pp 1 - 31.

Bizon J.J, Dourthe P., La Treille M., Perrier P., Rochet J., Savoyat E. & Katsikatsos G. (1967) *Kanalakion Sheet*, Geological map of Greece, 1:50,000, Institute of Geology and Subsurface Research, Athens.

Bjerrum L. (1967) *Progressive Failure in Slopes of Overconsolidated Plastic Clay and Clay Shales*, Journal of Soil Mechanics and Foundation Engineering Division, ASCE, Vol: 95 (SM5), pp 3 - 49.

Bjerrum L. (1973) *Problems of Soil Mechanics and Construction on Soft Clays*, Eighth International Conference on Soil mechanics and Foundation Engineering, Moscow, Vol: 3, pp 111 - 159.

Blatt H., Middleton G.V. & Murray R.C. (1980) *Origin Of Sedimentary Rocks.* Prentice-Hall Inc., New Jersey. ISBN 0-13-642710-3

Blondeau F. (1973) *The Residual Strength of Some French Clays; Measurement and Application to a Natural Slope Landslide.* Geologia Applicate e Idrogeologia, Vol: 8, pp 125 - 141.

Bolt G.H. (1956) *Physicochemical Analysis Of The Compressibility Of Pure Clays.* Geotechnique Vol: 6 (2), pp 86 - 93.

Bornovas J., Lalechos L. & Filippakis N. (1972) *Korinthos Sheet*, Geological map of Greece 1:50,000, Institute of Geology and Subsurface Research, Athens.

Borowicka H. (1961) *The Mechanical Properties of Soils*, Proceedings of the 5th International Conference of Soil Mechanics and Foundation Engineering, Vol: 1, pp 39 - 41.

Borowicka H. (1965) *The Influence of Colloidal Content on Shear Strength of Clay*, Sixth International Conference of Soil Mechanics and Foundation Engineering, vol: 1, pp 175 - 178.

Boyce J.R. (1984) *The Residual Strength of Some Soils in Zimbabwe*, Proceedings of the 8th Regional Conference for Soil Mechanics and Foundation Engineering for Africa, Harare, Vol: 4, pp 73 - 80.

Brackley I.J.A. (1975) *A Model Of Unsaturated Clay Structure And Its Application To Swell Behaviour.* 6th Regional Conference For Africa On SMFE, Durban, S. Afrca. Sept. 1975, pp 71 - 79.

Bressani L.A. (1990) *Experimental Properties Of Bonded Soils.* Ph.D. Thesis, Imperial College of Science, Technology & Medicine, University Of London, U.K.

Brindley G.W. & Brown G., (Eds.) (1980) *Crystal Structures Of Clay Minerals And Their X-Ray Identificiation.* Mineralogical Society Monograph No. 5, Mineralogical Society, London.

British Standards Institution, BS 1377 (1975) *Methods of Testing soils for Civil Engineering Purposes*, London.

British Standards Institution, BS 1377 (1990) *Methods of Testing Soils for Civil Engineering Purposes*, London.

Bromhead E.N. (1978) *Large Landslides in London Clay at Herne Bay, Kent*, Quarternary Journal of Engineering Geology, London, Vol: 11, pp 291 - 304.

Bromhead E.N. (1979) *A Simple Ring Shearing Apparatus. Ground Engineering, Vol: 12 (5), pp 40 - 44.*

Bromhead E.N. (1984) *Slopes And Embankments (Chapter Three)* In: "Ground Movements & Their Effects On Structures". P.B. Attewell & R.K. Taylor (Eds.), pp 46 - 75. Surrey University Press, Glasgow. ISBN: 0-903384-36-1

Bromhead E.N. (1986) *The Stability of Slopes*, Surrey University Press, Chapman & Hall.

Bromhead E.N. & Curtis R.D.. (1983) *A Comparison of Alternative Methods of Measuring the Residual Strength of London Clay*, Ground Engineering, Vol: 16, pp 39 - 41.

Bromhead E.N. & Dixon N. (1986) *The Field Residual Strength Of London Clay And Its Correlation With Laboratory Measurements, Especially Ring Shear Tests.* Geotechnique Vol: 36 (3), pp 449 - 452.

Brooks M. & Ferentinos G. (1984) *Tectonics and Sedimentation in the Gulf of Corinth and the Zakynthos and Kefallinia Channels, W. Greece*, Tectonophysics, Vol: 101, pp 25 - 54.

Brown G. (1980) *Associated Minerals* In: "Crystal Structures Of Clay Minerals And Their X-Ray Identification". G.W. Brindley & G. Brown (Eds.), pp 361 - 407. Mineralogical Society Monograph No. 5, Mineralogical Society, London, U.K.

Bucher F. & Kynlule A.L. (1980) *Residual Shear Strength of Tropical soils*, Seventh Regional Conference for Africa on Soil Mechanics and Foundation Engineering, Vol: 1, pp 83 - 94.

Burland J.B. (1990) *On the Compressibility and Shear Strength of Natural Clays*, Thirtieth Rankine Lecture, Geotechnique, Vol: 40 (3), pp 329 - 378.

Butterfield R. (1979) *A Natural Compression Law For Soils, (An Advance On e-logp'). Geotechnique Vol: 29 (4), pp 469 - 480.*

Calabresi G. & Manfredini G. (1973) *Shear Strength Characteristics of the Jointed Clay of S. Barbara*, Geotechnique, Vol: 23 (2), pp 233 - 244.

Camapum D.E., Carvalho J., Crispel J.J. & Legrand C. (1986) *Influence De L'Etat De Contrainte Du Saturation Sur Le Compotement Mecanique D'Une Marne Compactee.* Annales De L'Institute Technique Du Batimient Et Des Travaux Publique. No. 444, Mai 1986, Serie: Sols Et Fondations 196, Inst. Techn. Batiment Et Des Travaux Publique.

Cancelli A. (1977) *Residual Shear Strength and Stability Analysis of Landslides in Fissured Overconsolidated Clays*, Bulletin of the International Association of Engineering Geologists, Vol: 16, pp 193 - 197.

Carrier W.D. III (1985) *Consolidation Parameters Derived From Index Tests.* Geotechnique Vol: 35 (2), pp 211 - 213.

Carrier W.D. & Beckman J.F. (1984) *Correlations Between Index Tests And The Properties Of Remoulded Clays.* Geotechnique Vol: 34 (2), pp 211 - 228.

Carroll D. (1970) *Clay Minerals; a Guide to their X-ray Identification*, Special Paper 126, Geological Society of America, Boulder, Colorado, USA.

Casagrande A. (1948) *Classification and Identification of Soils*, Transactions of the American Society of Civil Engineers, Vol: 113, pp 901 - 992.

Cavounidis S. & Sotiropoulos E. (1980) *Hypotheses For Progressive Failure In A Marl.* Journal Of Geotechnical Engineering Division ASCE, Vol: 106, No. GT6, pp 659 - 671.

Cavounidis S., Tika T. & Dounias G.T. (1988) *Greek Marls Under the Microscope*, Proceedings of the First Hellenic Conference of Geotechnical Engineering,

Technical Chamber of Greece, Hellenic Society of Soil Mechanics and Foundation Engineering, Vol: 1, pp 59 - 63 (in Greek).

Chandler R.J. (1966) *The Measurement of Residual Strength in Triaxial Compression*, Geotechnique, Vol: 16 (3), pp 181 - 186.

Chandler R.J. (1969) *The Effect Of Weathering On The Shear Strength Properties Of Keuper Marl.* Geotechnique Vol: 19 (3), pp 321 - 334.

Chandler R.J. (1970) *The Degredation Of Lias Clay Slopes In An area Of The East Midlands.* Quarterly Journal Of Engineering Geology, Vol: 2, pp 161 - 181.

Chandler R.J. (1972) *Lias Clay: Weathering Processes And Their Effect On Shear Strength.* Geotechnique Vol: 22 (3), pp 403 - 431.

Chandler R.J. (1974) *Lias Clay: The Long-Term Stability Of Cutting Slopes.* Geotechnique Vol: 24 (1), pp 21 - 38.

Chandler R.J. (1977) *Back Analysis Techniques for Slope Stabilisation Works, a Case Record*, Geotechnique, Vol: 20 (3), pp 181 - 186.

Chandler R.J. (1979) *Stability of a Structure Constructed in a Landslide; Selection of Soil Strength Parameters*, British Geotechnical Society, Vol: 3, pp 175 - 182.

Chandler R.J. (1984) *Recent European Experience of Landslides in Overconsolidated Clays and Soft Rocks*, Proceedings of the 4th International Symposium on landslides, Toronto, pp 61 - 81.

Chandler R.J. & Apted J.P. (1988) *The Effect Of Weathering On The Strength Of London Clay.* Quarterly Journal Of Engineering Geology, London, Vol: 21, pp 59 - 68.

Chandler R.J. & Hardie T.N. (1989) *Thin-Sample Technique Of Residual Strength Measurement.* Geotechnique Vol: 39 (3), pp 527 - 531.

Chapman D.L. (1913) *A Contribution to the Theory of Electrocapillarity*, Philosophical Magazine, Vol: 25 (6), pp 475 - 481.

Chattopadhyay P.K. (1972) *Residual Shear Strength of Some Pure Clay Minerals*, Ph.D Thesis, University of Alberta, Edmonton, Canada.

Chowdury R.N & Bertolodi C. (1977) *Residual Shear Strength on Soils from Two Natural Slopes*, Australian Geomechanics Journal, pp 1 - 9.

Christaras B. (1991) *A Comparison Of The Casagrande And Fall Cone Penetrometer Methods For Lquid Limit Determination In Marls From Crete, Greece.* Engineering Geology, An Internation Journal, Elsevier. Vol: 31 (2), pp 131 - 142.

Christoulas S., Kalteziotis N., Tsiambaos G. & Sabatakakis N. (1987) *Engineering Geology Of Soft Clays, Examples From Greece.* In: "Embankments On Soft Clays, Special Publication". Bulletin Of The Public Works Research Center, Ministry Of Environment, Physical Planning and Public Works, Athens.

Cita M.B. (1972) *Studi Sul Pliocene e Sugli Studi di Passagio del Miocene al Pliocene I. il Significato Della Transgressione Pliocenica Alla Luce Delle Nuoue Scoperte uel Mediterraneo*, Riv. Hal. Paleont., vol: 78 (3), pp 527 - 594.

Clews J.E. (1989) *Structural Controls on Basin Evolution: Neogene to Quarternary of the Ionian Zone, Western Greece*, Journal of the Geological Society, London, vol: 146, pp 447 - 457.

Collier R.E.L.L. (1990) *Eustatic And Tectonic Controls Upon Quaternary Coastal Sedimentation In The Corinth Basin.* Journal Of Geological Society, London. Vol: 147, pp 301 - 314.

Collota T., Cantoni R., Pavesi V., Ruberi E & Moretti P.C. (1981) *A Correlation Between Residual Friction Angle Graduation and the Index Properties Of Cohesive Soils.* Geotechnique Vol: 39 (2), pp 343 - 346.

Comninakis P.E. & Papazachos B.C. (1970) *A Catalogue of Earthquakes in the Mediterranean and the Surrounding Area for the Period 1901-1977*,

Publications of the Geophysical Laboratory, Aristoteleion University, Thessaloniki, Greece, Vol: 5, pp 1 - 96 (in Greek).

Crawford C.B. (1988) *On The Importance Of Rate Of Strain In The Consolidation Test.* Geotechnical Testing Journal, GTJODJ, Vol: 11 (1), March 1988, pp 60 - 62, ASTM.

Cripps J.C. & Taylor R.K. (1986) *Engineering Characteristics Of British Over-Consolidated Clays And Mudrocks, I Tertiary Deposits.* Engineering Geology, Vol: 22, pp 349 - 376. Elsevier Science Publishers B.V., Amsterdam.

Cripps J.C. & Taylor R.K. (1987) *Engineering Characteristics Of British Over-Consolidated Clays And Mudrocks, II Mesozoic Deposits.* Engineering Geology, Vol: 23, pp 213 - 253. Elsevier Science Publishers B.V., Amsterdam.

Ctori P. (1989) *The Effects Of Temperature On The Physical Properties Of Cohesive Soil.* Ground Engineering, Vol: 22 (5), British Geotechnical Society, pp 26 - 27.

Cullen R.M. & Donald I.B. (1971) *Residual Strength Determination in Direct Shear*, First Australian-New Zealand Conference on Soil Mechanics and Geomechanics, vol: 1, pp 1 - 10.

Cripps J.C., Coulthard J.M., Culshaw M.G., Forster A., Hencher S.R., Moon C.F. (eds) (1993) *The Engineering Geology of Weak Rock*, Proceedings of the 26th Annual Conference of the Engineering Group, Geological Society of London, University of Leeds, September 1990, Engineering Geology Special Pubication No.8, A.A. Balkema, Rotterdam, ISBN 90 6191 167 2.

Cunningham P.P. (1986) *A Comparison on the Norwegian Geotechnical Institute/Imperial College and the Bromhead Ring Shear Machines with Tests Performed on Grey Cowden Till*, MSc Thesis, City University, London.

Datta M., Gulhuti S.K. & Rao G.V. (1982) *Engineering Behaviour of Carbonate Soils of Ludia and Some Observations on Classification of Such Soils*, in

"Geotechnical Properties, Behaviour and Performance of Calcareous Soils", ASTM Special Technical Publication 777, pp 113 - 140.

Davachi M.M., Sinclair B.J., Hartmaier H.H., Baggott B.L. & Peters J.E. (1991) *Determination of the Oldman River Dam Foundation Shear Strength*, Canadian Geotechnical Journal, Vol: 28, pp 698 - 707.

Davi E. (1971) *Petrology*, Agricultural University, Athens, p 386, (in Greek).

Davis A.G. (1967) *The Minerology And Phase Equilibrium Of The Keuper Marl.* Quarterly Journal Of Engineering Geology, Vol: 1, pp 25 - 38.

Davis A.G. (1968) *The Structure Of Keuper Marl.* Quarterly Journal Of Engineering Geology, Vol: 1, pp 145 - 153.

Davis G.A. & Worrall W.E. (1971) *The Absorption Of Water By Clays.* Trans. British Ceramic Society, Vol: 70 (2), pp 71 - 75.

De Beer E. (1967) *Shear Strength Characteristics of the Boom Clay*, Proceedings of the Geotechnical Conference, Oslo, Vol: 1, pp 83 - 88.

Den Haan E.J. (1992) *The Formulation Of Virgin Compression Of Soils.* Geotechnique Vol: 42 (3), pp 465 - 483.

Dimitrov S. (1955) *Stand Und Aufgaben Der Untersuchungen Der Magmatischen Und Metamorphen Komplexe Bulgarieus.* Isz. Ak. Naut. SSSR, Ser, Geol. 1, Moskva.

Dimitrov S. (1959) *Kurze Ubersicht Der Metamorphen Komplexe In Bulgarien.* Freiberger Forchungsh, C57 pp 62 - 72.

Doutsos T. (1980) *Postalpine Geodynamic Thessaliens (Griechenland)*, Z. dt. geol. Ges., vol: 131, pp 685 - 698.

Doutsos T. & Ferentinos G. (1984) *Post Alpine Crustal Deformation of North Aegean Region (Greece)*, Geol. Balcanica, Vol: 14 (6), pp 36 - 46.

Doutsos T., Kontopoulos N. & Frydas d. (1987) *Neotectonic Evolution of Northwestern continental Greece*, Geologische Rundschan, vol: 76, pp 433 - 450.

Doutsos T., Kontopoulos N. & Poulimenos G. (1988) *The Corinth-Patras Rift As The Initial Stages Of Continental Fragmentation Behind An Active Island Arc, (Greece).* Basin Research, Vol: 1, pp 177 - 190.

Dumbleton M.J. & West G. (1966) *Studies of the Keuper Marl: Mineralogy*, Road Research Laboratory Report No. 40, Road Research laboratory, 25 p.

Dumbleton M.J. (1967) *Origin And Mineralogy Of African Clays And Keuper Marl.* Quarterly Journal Of Engineering Geology, Vol: 1, pp 39 - 45.

Edge M.J. & Sills G.C. (1989) *The Development Of Layered Sediment Beds In The Laboratory As An Illustration Of Possible Field Processes.* Quarterly Journal Of Engineering Geology, Geological Society Of London, Vol: 22 (4), pp 271 - 279.

Elder D. McG. & Sills G.C. (1984) *Time and Stress Dependent Compression in soft Sediments*, ASCE Symposium on Prediction and Validation of Consolidation, San Francisco.

Fell R., Sullivan T.D. & MacGregor J.P. (1988) *Influence of Bedding Plane Shear in Slope Stability in Sedimentary Rocks*, Fifth International Symposium of Landslides, Switzerland, pp 129 - 134.

Fleming R.W., Spencer G.S. & Banks D.C. (1970) *Empirical Study of Behaviour of Clay Shale Slopes*, N.C.G, Technical Report No. 15 (2 volumes), U.S. Army Engineering Nuclear Cratering Group, Livermore, California.

Fleury J.J, de Wever P. & Izart A. (1981) *Goumeron sheet*, Geological Map of Greece 1:50,000, Institute of Geology and Mineral Exploration, Athens.

Folk R.L. (1980) *Petrology of Sedimentary Rock*, Hemphill, Austin, Texas, USA.

Fookes P.G., Dearman W.R. & Franklin J.A. (1971) *Some Engineering Aspects Of Rock Weathering With Field Examples From Dartmoor And Elsewhere.* Quarterly Journal Of Engineering Geology, Vol: 4, pp 139 - 185.

Fytrolakis N. (1973) *Contribution To The Knowledge Of The Change Of Properties Of Clays And Marls With Regard To Mineralogical Contitions.* Bulletin Of Geological Society Of Greece, Vol: 10 (2), pp 1 - 12, Athens, (In Greek).

Galanopoulos A. (1968) *On the Quantitative Determination of Earthquake Risk,* Aunali di Geolisica, Vol: 21, pp 193 - 206.

Garga V.K. (1970) *Residual Shear Strength under Large Strains and the Effect of Sample Size on the Consolidation of Fissured Clay,* Ph.D Thesis, Imperial College, University of London, UK.

Garlanger J.E. (1972) *The Consolidation Of Soils Exhibiting Creep Under Constant Effective Stress.* Geotechnique Vol: 22 (1), pp 71 - 78.

Gasios E., Constantinides C.H., Boukovalas G & Pachakis M. (1988) *Long-Term Stability Of Embankments On Unstable Slopes.* Proceedings of First Hellenic Conference Of Geology Engineering, Athens Feb. 1988, Technical Chamber Of Greece, Hellenic Society of Soil Mechanics And Foundation Engineering. Vol: 1, pp 259 - 264. (In Greek).

Giannaros C.H., Pachakis M & Christodoulias I. (1992) *Long-Term Stability Problems Of Marly Cutting Slopes On The Korinth Tripolis Motorway.* Proceedings of The 2nd Greek National Conference On Geotechnical Engineering, Thessaloniki, October 1992, Technical Chamber Of Greece & Hellenic Society Of Soil Mechanics And Foundation Engineering (in Greek).

Gibbs H.J. & Holtz W.G. (1956) *Engineering Properties Of Exapnsive Clays.* Trans Am. Society Of Civil Engineering, Vol: 121 (1), Papaer 2814.

Gillott J.E. (1968) *Clay In Engineering Geology.* Elsevier Publishing Co., Amsterdam.

Goodman E.R. (1980) *Rock mechanics,* John Wiley & sons, New York, 478 p.

Gouy G. (1910) *Sur la constitution de la Charge Electrique à la Surface d'un Electrolyte*, Annales Physique (Paris), Série 4 (9), pp 457 - 468.

Gouy G. (1917) *sur la Fonction Electrocapillaire*, Annales Physique (Paris), Série 9 (7), pp 129 - 184.

Grainger P. (1984) *The Classification Of Mudrocks For Engineering Purposes.* Quarterly Journal Of Engineering Geology, Vol: 17, pp 381 - 387.

Grefesheim F.D. (1988) *Laboratory Testing of Slope Stability Design Parameters in Overconsolidated Clay*, Fifth International Symposium of Landslides, Switzerland, pp 169 - 174.

Griffiths F.J. & Joshi R.C. (1989) *Change In Pore Size Distribution Due To Consolidation Of Clays.* Geotechnique, Vol: 39 (1), pp 159 - 167.

Grim R.E. (1968) *Clay Minerology.* Second Edition, McGraw-Hill, New York.

Hageman J. (1979) *Benthic foraminiferal Assemblages from Plio-Pleistocene Open Bay to Lagoonal Sediments of the Western Peloponnesus (Greece)*, Utrecht Micropaleontology Bulletin, No. 20.

Hardy R. & Tucker M. (1988) *X-Ray Powder Diffraction Of Sediments.* In "Techniques In Sedimentology", M. Tucker (ed.), Blackwell Scientific Publications, Oxford, pp 191 - 216. ISBN: 0-632-01372-9.

Hatzidimitriou P.M., Papadimitriou E.E., Mountrakis D.M. & Papazachos B.C. (1985) *The Seismic Parameter b of the Frequency Magnitude Relation and its Association with the Geological Zones in the Area of Greece*, Tectonophysics, vol: 120, pp 141 - 151.

Hawkins A.B. (1988) *Stability of Inland Soil Slopes; Some Geotechnical Considerations*, Fifth International Symposium on Landslides, Switzerland, pp 181 - 186.

Hawkins A.B. & Privett K.D. (1985) *Measurements And Use Of The Residual Shear Strength Of Cohesive Soils.* Ground Engineering Vol: 18 (8), pp 22 - 29.

Hawkins A.B. & Privett K.D. (1986) *Residual Strength; Does BS 5930 Help or Hinder?*, Geological Society, Engineering Geology Special Publication No. 2: "Site Investigation Practice, Assessing BS 5930", pp 279 - 283.

Hawkins A.B., Lawrence M.S. & Privett K.D. (1986) *Clay Minerology And Plasticity Of The Fuller's Earth Formation Bath, UK.* Clay Minerals, 21, pp 293 - 310.

Hawkins A.B., Lawrence M.S. & Privett K.D. (1988) *Implications Of Weathering On The Engineering Properties Of Fuller's Earth Formation.* Geotechnique Vol: 38 (4), pp 517 - 532.

Hawkins A.B. & McDonald C. (1992) *Decalcification And Residual Shear Strength Reduction In Fuller's Earth Clay.* Geotechnique Vol: 42 (3), pp 453 - 464.

Head K.H. (1980) *Manual Of Soil Laboratory Testing.* Volume 1: "Soil Classification And Compaction Tests". Pentech Press Ltd., Plymouth, UK. ISBN: 0-7273-1302-9.

Heezen B.C., Ewing M. & Johnson G.L. (1966) *The gulf of Corinth Floor*, Deep Sea Research, Vol: 13, pp 381 - 411.

Henkel D.J. & Skempton A.W. (1954) *A Landslide of Jackfield, Shropshire in Heavily Overconsolidated Clay*, Geotechnique, Vol: 5 (2), pp 131 - 137.

Herrman H.G. & Wolfskill L.A. (1966) *Residual Shear Strength of Weak Shales*, Technical Report No.3-669, "Engineering Properties of Nuclear Craters, Report 5", M.I.T., Cambridge, Massachusetts, USA.

Hight D.W., Jardine R.J. & Gens A. (1987) *The Behaviour of Soft Clays*, in "Embankments on Soft Clays", Special Publication, Bulletin of the Public Works Research Centre, Ministry for the Environement, Physical Planning and Public works, Athens.

Horn H.M. & Deere D.V. (1962) *Frictional Characteristics of Minerals*,Geotechnique, Vol: 12 (4), pp 319 - 335.

Holtz W.G. & Gibbs H.J. (1956) *Engineering Properties Of Expansive Clays.* Trans. ASCE Vol: 121, pp 641 - 677.

Huang Scott L. (1989) *The Influence Of Disaggregation Methods On X-Ray Diffraction Of Clay Minerals.* Journal Of Sedimentary Petrology, Vol: 59 (6). Society Of Econimic Paleontologists & Mineralogists, pp 997 - 1001.

Huergo P.J., Christoulas S.G. & Tsiambaos G.K. (1987) *Some Geotechnical Aspects Of Iraklion Marls.* Bulletin Of The Association Of Engineering Geologists, Vol: 24 (1), pp 93 - 103.

Hutchinson J.N., Bromhead E.N. & Lupini J.F. (1980) *Additional Observations of the Folkestone Warren Landslides*, Quarternary Journal of Engineering Geology, London, Vol: 13, pp 125 - 137.

Hutchinson J.N., Somerville S.H. & Petley D.J. (1973) *A Landslide In Periglacially Disturbed Etruria Marl At Bury Hill, Staffordshire.* Quarterly Journal Of Engineering Geology, Vol: 6, pp 377 - 404.

Hvorslev M.J. (1936) *A Ring Shearing Apparatus for the Determination of the Shearing Resistance and Plastic flow of Soils*, Proceedings of the 1st International Conference of Soil Mechanics and Foundation Engineering, Boston, USA, Vol: 2, pp 125 - 129.

Ingold T.S. (1975) *Variation of Effective Residual Angle of Shearing with Plasticity Index*, Midlands Soil Mechanics and Foundation Engineering Symposium on Glacial Materials, pp 221 - 224.

Jackson J.A., King G. & Vita-Finzi C. (1982) *The Neotectonics of the Aegean: an Alternative view*, Earth and Planetary Science Letters, Vol: 61, pp 303 - 318.

Jacobshagen V., Dürr S., Kockel F., Kopp K.O. & Kowalczky G. (1978) *Structure and Geodynamic Evolution of the Aegean region*, in "Alps, Apennines, Hellinides", Closs, Roeder & Schmidt (eds), pp 537 - 564.

James P.M. (1970) *Time Effects and Progressive Failure in Clay Slopes, Ph.D Thesis, Imperial College, University of London, UK.*

Jardine R.J. & Christoulas S. (1991) *Recent Developments in Defining and measuring Static Piling Parameters*, Proceedings of the International Conference on Deep Foundations, Paris, Presse de l'Ecole Nationale des Ponts et Chaussées, pp 713 - 745.

Jose B.T., Sridharan A. & Abraham B.M. (1989) *Log-Log Method For Determination Of Preconsolidation Pressure.* Geotechnical Testing Journal, ASTM, Vol: 12 (3), pp 230 - 237.

Juarez-Badillo E (1981) *General Compressibility Equation For Soils.* Proceedings Of 10th International Conference Of Soil Mechanics, Stockholm. Vol: 1, pp 171 - 178.

Jung J. (1969) *Précis de Petrographie*, Masson, Paris.

Kaltetziotis N. (1992) *The Residual Shear Strength Of Some Clayey Soils.* Geotechnical & Geotechnical Engineering, An International Journal. Chapman & Hall, London. (Paper Submitted For Publication).

Kalteziotis N., Dimitrakopoulos P. & Pachakis M. (1989) *Long-Term Stability Problems Of Cutting Slopes Along The Igoumenitsa-Preveza National Road.* Bulletin Of The CPWL, Vol: 103 -104, pp 107 - 121, MEPPPW, Athens. (In Greek, with English Transaltion).

Kamberis E. (1987) *Geological And Petroleogeological Study Of N.W. Peloponnesos.* Ph.D. Thesis, National Technical University (Metsovion Polytechnion), Dept. Of Mettalurgy And Mining Engineering, Athens, Greece. (In Greek).

Kanji M.A. (1974) *The Relationship Between Drained Friction Angles and Atterberg Limits of Natural Soils*, Geotechnique, vol: 24 (4), pp 671 - 674.

Kanji M.A. & Wolle C.M. (1977) *Residual Strength — New Testing And Microstructure.* Proceedings Of The 9th International Conference Of Soil Mechanics, Tokyo. Vol: 1, pp 153 - 254.

Kenney T.C. (1967) *The Influence Of Mineral Composition On The Residual Strength Of Natural Soils.* Proceedings Of Geotechnical Conference, Oslo. Vol: 1, pp 123 - 129.

Kenney T.C. (1977) *Residual Strength Of Mineral Mixtures.* Proceedings Of The 9th Internaltional Conference Of Soil Mechanics, Tokyo. Vol: 1, pp 155 - 160.

Keraudren B. & Sorel D. (1987) *The Terraces of Corinth (Greece), a Detailed Record of Eustatic Sea Level Variations During the last 500,000 Years,* Marine Geology, Vol: 77, pp 99 - 107.

King G.C.P, Tselentis A., Gomberg J., Molnar P, Roecker S.W., Sinvhal h., Soufleris C. & Stock J.M. (1983) *Microearthquake Seismicity and Active Tectonics of Northwestern Greece,* Earth and Planetary Science Letters, Vol: 66, pp 279 - 288.

Kirkpatrick W.M., Khan A.J. & Mirza A.A. (1986) *The Effects Of Stress Relief On Some Overconsolidated Clays.* Geotechnique, Vol: 36 (4), pp 511 - 525.

Kissel C. & Laj C. (1988) *The Tertiary Geodynamical Evolution of the Aegean Arc: a Paleomagnetic Reconstruction,* Tectonophysics, Vol: 146, pp 183 - 201.

Kober L. (1931) *Das Alpine Europa.* Borntrager (Ed.). Berlin.

Kostopoulos S. (1988) *Geotechnical Consideration Of The Hellenic Marls.* Proceedings Of The First Hellenic Conference Of Geotechnical Engineering, Feb. 1988, Athens. Technical Chamber Of Greece, Hellenic Society Of Soil Mechanics & Foundation Engineering, Vol: 1, pp 63 - 68. (In Greek).

Koukis G. (1977) *Research On The Geological Structure And Physical-Mechanical Properties Of The Neogene Sediments In The Area Of Pyrgos-Ilias.* Bulletin Of Central Laboratory Of Public Works, Quarterly Scientific Review, April - June 1977, Vol: 2, pp 69 - 79. (In Greek With English Summary).

Koukis G. (1985) *Engineering Geological Conditions in the Area of the Zakynthos Open-Air Theatre Foundations*, Bulletin of the Central Public Works Laboratory, Quarterly Scientific Review, Athens, Vol: 3-4, pp 3 - 14.

Koukis G. & Ziourkas K. (1989) *Landslide Movements In The Greek Territory: A Statistical Approach,* Mineral Wealth Vol: 58, Jan - Feb 1989, pp 39 - 58. Scientific Society Of The Mineral Wealth Technologists. (In Greek With English Summary).

Kronenberg P., Meyer W. & Pilger A. (1970) *Geologie Der Rila-Rhodope Masse Zwischen Strimon Und Nestos.* Beith. Geolo. Jb., Vol: 88, pp 133 - 180.

Krumbein W.C. (1933) *The Dispersion Of Fine-Grained Sediments For Mechanical Analysis.* Journal Of Sedimentary Petrology, Vol: 3, pp 121 - 135.

Krynine D.P. & Judd W.R. (1957) *Principles of Engineering Geology and Geotechnics*, McGraw-Hill, New York.

La Gatta D.P., (1970) *Residual Strength of Clays and Clay Shales by Rotation Shear Test*, Harvard Soil Mechanics Series, No. 86, Cambridge, Massachusetts, Harvard University, USA.

La Gatta D.P. (1971) *The Effect of Rate of Displacement on Measuring the Resifual Strength of Clays*, Report of the U.S. Army Engineers Waterways Experiment Station, Vicksburg, Mississipi, Contract No. DAC W39-69-C-0028, Harvard University, Cambridge, Massachusetts, USA.

Lampe T.W. (1960) *A Mechanistic Picture of Shear Strength in Clay*, Proceedings of the Conference of Shear Strength of Soils, Colorado, USA, pp 503 - 532.

Lapierre C. (1987) *Evolution De La Texture Et De La Permeabilite De L'Argile De Louisville Durant La Consolidation.* M.Sc. Thesis, Universite Laval, Quebec.

Leeder M.R. & Gawthorpe R.L. (1987) *Sedimentary Models for Extensional Tilt Block/Half Graben Basins*, in "Continental Extensional Tectonics", Coward M.P., Dewey J.F. & Hancock P.L. (eds.), Geological Society, London, Special Publication No, 28, pp 139 - 152.

Lehane B.M. & Jardine R.J. (1992) *Residual Strength Characteristics of Bothkennar Clay*, Geotechnique, Vol: 42 (2), pp 363 - 368.

Lemos L.J.L. (1986) *The Effect Of Rate On Residual Strength Of Soil.* Ph.D. Thesis, Imperial College of Science, Technology & Medicine, London University, UK.

Lemos L.J.L. (1991) *Shear Strength of Shear Surfaces Under Fast Loading*, Tenth European Conference on Soil Mechanics and Foundation Engineering, Italy.

Lemos L.J.L. & Coelho P.A.L.F. (1991) *Displacements of Slopes Under Earthquake Loading*, Second International Conference of Geotechnical Engineering and Soil Dynamics, St. Louis, Missouri, USA.

Lemos L.J.L, Skempton A.W & Vaughan P.B. (1985) *Earthquake Loading on Shear Surfaces in Slopes*, Proceedings of the 14th International Conference on soil Mechanics and Foundation Engineering, San Francisco, USZ, Session 7B, pp 1 - 7.

Leonard G.A. & Girault P. (1961) *A Study Of The One-Dimensional Consolidation Test.* Proceedings Of The 5th International Conference On Soil Mechanics, Paris. Vol: 1, pp 213 - 219.

Leonard G.A. & Ramiah B.K. (1959) *Time Effects In The Consolidation Of Clay.* ASTM Special Technical Publication No. 254, pp 116 - 130, Philedelphia ASTM.

Leroueil S. (1988) *Recent Developments In Consolidation Of Natural Clays.* 10th Canadian Geotechnical Colloquium, Canadian Geotechnical Journal, Vol: 25 (1), pp 85 - 107.

Leroueil S., Kabbaj M., Tavenas F. & Bouchard R. (1985) *Stress-Strain-Strain rate relation For The Compressibility Of Sensitive Natural Clays.* Geotechnique Vol: 35 (2), pp 159 - 180.

Leroueil S., Tavenas f., Brucy F., La Rochelle P. & Roy M. (1979) *Behaviour of De-Structured Natural Clays*, Journal of the Geotechnical Engineering Division, ASCE, Vol: 106 (GT6), pp 759 - 778.

Leroueil S. & Vaughan P.R. (1990) *The General And Congruent Effects Of Structure In Natural Soils And Weak Rocks.* Geotechnique Vol: 40 (3), pp 467 - 488.

Lindholm R.C. (1987) *A Practical Approach To Sedimentology.* Alen & Unwin, London. ISBN: 0-04-551132-2.

Littleton I. & Farmilo M. (1977) *Some Observations on Liquid Limit Values with Reference to Penetration and Casagrande Tests*, Ground Engineering, Vol: 10, pp 39 - 40.

Locat J. & Lefebvre G. (1985) *The Compressibility And Sensitivity Of An Artificially Sedimented Clay Soil: The Grande-Baleine Marine Clay, Quebec.* Marine Geotechnology Vol: 6 (1), pp 1 - 27.

Lupini J.F., Skinner A.E. & Vaughan P.R. (1981) *The Drained Residual Strength Of Cohesive Soils.* Geotechnique Vol: 31 (2) pp 181 - 213.

Makris J. (1973) *Some Geophysical Aspects of the Evolution of the Hellenides*, Bulletin of the Geological Society of Greece, Athens, Vol: 10, pp 206 - 213 (in Greek).

Maksimovic M. (1989) *On The Residual Shearing Strength Of Clays.* Geotechnique Vol: 39 (2), pp 347 - 351.

Mathews M.C. (1987) *The Engineering Application of Direct and Simple Shear Testing*, A report of the discussion organised by the British Geotechnical Society at the Royal Institution of Chartered Surveyors.

McKenzie D.P. (1972) *Active Tectonics of the Alpine-Himalayan belt: the Aegian Sea and Surrounding Region*, Geophysical Journal of the Royal Astrophysical Society, Vol: 55, pp 217 - 254.

McKown A.F. & Ladd C.C. (1982) *Effects Of Cementation On The Compressibility Of Pierre Shale.* In: "Geotechnical Properties, Behaviour & Performance Of Caleareous Soils", ASTM STD 777, K.R. Demars & R.C. Chaney (Eds). American Society For Testing And Materials, pp 320-339.

Mégard F. & Philip H. (1976) *Plio-Quarternary Tectono-Magmatic Zonation and Plate Tectonics in the Central Andes*, Earth and Planetary Science Letters, Vol: 33, pp 231 - 238.

Mesri G & Cepeda-Diaz A.F. (1986) *Residual Shear Strength Of Clays And Shales.* Geotechnique Vol: 36 (2), pp 269 - 274.

Mesri G. & Olson R.E. (1970) *Shear Strength of the Montmorillonite*, Geotechnique, Vol: 20 (3), pp 261 - 276.

Mesri G., Rokhsar A. & Bohar B.F. (1985) *Composition And Compressibility Of Typical Samples Of Mexico City Clays.* Geotechnique Vol: 28 (3), pp 281 - 307.

Mesri G., Ullrich C.R. & Choi Y.K. (1978) *The Rate Of Swelling Of Overconsolidated Clays Subjected To Unloading.* Geotechnique Vol: 28 (3), pp 281 - 307.

Meulenkamp J.E. (1986) *Aspects of the Late Cenozoic Evolution of the Aegean Region*, in "Geological Evolution of the Mediterranean Basin", Stanley D.J. & Wezel F.C. (eds), new York, Springer-Verlag, Chapter 15, pp 307 - 321.

Micasa M. (1965) *The Consolidation Of Soft Clay: A New Consolidation Theory And Its Application.* Civil Engineering In Japan, pp 21 - 26.

Miedema D., Byers J. & McNeary R. (1981) *Residual Shear Strength Determination of Overconsolidated Nespelem Clay*, in "Laboratory Shear Strength of Soils", ASTM, STP7H0, Yong R.N. & Townsend F.C. (eds), ASTM, pp 594 - 609.

Ministry for the Environment, Physical Planning and Public Works (1986) *Specifications for Laboratory Tests in Soil mechanics*, Division of

Geotechnical Engineering (EK1), General Secretariat of Public workds, MEPPPW Designation E106-86.

Mitchell J.E. (1960) *The Application of Colloidal Theory to the Compressibility of Clays*, Interparticle Forces in Clay-Water-Electrolyte Systems, CSIRO, Melbourne.

Mitchell J.E. (1976) *Fundamentals of Soil Behaviour*, John Wiley & Sons, New York, USA.

Monopolis D. & Bruneton A. (1982) *Ionian Sea (Western Greece): its Structural Outline Deduced from Drilling and Geophysical Data*, Tectonophysics, vol: 83, pp 227 - 242.

Moon C.F. & White K.B. (1985) *A Comparison Of Liquid limit Test Results.* Geotechnique Vol: 35 (1), pp 59 - 60.

Moore R. (1991) *The Chemical and Mineralogical Controls upon the Residual Strengths of Pure and Natural Clays*, Geotechnique, vol: 41 (1), pp 35 - 47.

Morgenstern N.R. & Eigenbrod K.D. (1974) *Classification Of Argillaceous Soils And Rocks.* Proceedings Of Journal Of Geotechnical Division ASCE 100: 1137 - 1156.

Morgenstern N.R. & Tchalenco J.S. (1967a) *Microstructural Observations on Shear Zones from Slips in Natural Clays*, Proceedings of the Geotechnical Conference, Oslo, pp 147 - 152.

Morgenstern N.R. & Tchalenco J.S. (1967b) *The Optical Determination of Preferred Orientation in Clays and its Application to the Study of Microstructure in Overconsolidated Kaolins*, Proceedings of the Royal Society, London, A300, pp 235 - 250.

Moundrakis D.M. (1985) *Geology of Greece*, University Studio Press, Thessaloniki, Greece, 207 p. (in Greek).

Muhunthan B. (1991) *Liquid Limit And Surface Area Of Clays.* Geotechnique Vol: 41 (1), pp 135 - 138.

Müller G. (1967) *Methods in Sedimentary Petrology*, John Wiley & Sons, New York.

Nagaraj T.S. & Srinivasa Murthy B.R. (1986) *A Critical Reapraisal Of Compression Index Equations.* Geotechnique Vol: 36 (1), pp 27 - 32.

Nagaraj T.S., Murthy B.R., Vatsala A. & Joshi R.C. (1990) *Analysis Of Compressibility Of Soils.* Journal Of Geotechnical Engineering, Geotechnnical Engineering Division, ASCE Vol: 116 (1). Plus: Discussion by S. Leroueil & K. McManis In Vol: 117 (1), pp 163 - 168.

Nakamura K. & Uyeda (1980) *Stress Gradient in Arc-Back Acr Regions and Plate Subduction*, Journal of Geophysical Research, Vol: 85, pp 6419 - 6428.

Nakase A, Kamei T & Kusakabe O. (1988) *Constitutive Parameters Estimated By Plasticity Index.* Journal Of Geotechnical Engineering, Division ASCE Vol: 114 (7), pp 844 - 858.

Newbery J. & Baker D.A.B (1981) *The Stability of Cuts on the M4 North of Cardiff*, Quarterly Journal of Engineering Geology, London, Vol:14, pp 195 - 205.

Northey R.D. (1956) *Rapid Consolidation Tests For Routine Investigations.* Proceedings Of The 2nd Australian-New Zealand Conference On Soil Mechanics, pp 20 - 26.

Olmstead L.B. (1931) *Dispersion Of Soils By A Supersonic Method.* Journal Of Agricultural Research, Vol: 42, pp 842 - 852.

Osipov V.I. & Sokolov V.N. (1978) *A study of the Nature of the Strength and Deformation Properties of Clay Soils with the Help of the Scanning Electron microscope*, Bulletin of the International Association of Engineering Geology, Vol: 17, pp 91 - 94.

Oslon R.E. (1974) *Shearing Resistance of Kaolinite, Illite and Montmorillonite*, Journal of the Soil Mechanics and Foundation Engineering Division, ASCE, Vol: 100 (GT11), pp 1215 - 1229.

Pachakis M.D., Constantinidis C.V. & Bouckovalas G. (1988) *Long-Term Stability Of Cutting Slopes In A Marly Formation On The Basis Of Field Evidence.* Proceedings Of The 5th International Symposium On Landslides, C. Bonnard, (ed.), A.A. Balkema, Rotterdam, Brookfield.

Panagiotopoulos D.G., Scordilis E.M., Hatzidimitriou P.M., Rocca A.C. & Papazachos B.C. (1985) *Further Evidence on the Deep Tectonics of the Aegean and Eastern Mediterranean Area*, Nineteenth Conference of the European Seismology Commission, Moscow, October 1984, Vol: 1, pp 1 - 14.

Pane V. & Schiffman R.L. (1985) *A Note On Sedimentation And Consolidation.* Geotechnique Vol: 35 (1), pp 69 - 77.

Papazachos B.C. (1973) *Distribution of Seismic Foci in the Mediterranean and Surrounding Area and its Tectonic Implication*, Geophysics Journal, Royal Astronomic Society, London, vol: 33, pp 419 - 428.

Papazachos B.C. (1988) *Active Tectonics In The Aegean And Surrounding Area.* In: "Seizmic Hazard In Mediterranean Regions." Proceedings Of Summer School (1986) by European Mediterranean Seismological Centre And Institute De Physique Du Globe De Strasbourg, J. Bonnin, M. Cara, A. Cisternas & R. Fantechi (Eds.), Kluwer Academic Publishers (For The Commission Of The European Communities), Netherlands. ISBN: 90-277-2779-1.

Papazachos B.C. & Kiratzi A.A. (1984) *Seismic Faults in the Aegean Area*, Tectonophysics, Vol: 106, pp 71 - 85.

Papazachos B.C. & Kiratzi A.A. (1986a) *Seismotectonic Properties of the Aegean Area that Restrict Valid Geodynamic Models*, Second Wegener Conference, Dionysos, Greece, pp 1 - 16.

Papazachos B.C. & Kiratzi A.A. (1986b) *Probabilities of Occurrence of Large Earthquakes in the Aegean and the Surrounding Area During the Period 1986-2006*, Publications of the Geophysics Laboratory, Aristoteleion University, Thessaloniki, Greece, vol: 4, pp 1 - 22. (in Greek)

Paul M.A., Peacock J.P. & Wood B.F. (1992) *The Engineering Geology of the Carse Clay of the National Soft Clay Research site*, Bothkennar, Geotechnique, Vol: 42 (2), pp 183 - 198.

Peck R.B. (1967) *Stability of Natural slopes*, Journal of Soil Mechanics and Foundations Division, ASCE, Vol: 93 (SM4), pp 403 - 417.

Pender M.I. (1978) *A Model For The Behaviour Of Overconsolidated Soil.* Geotechnique Vol: 28 (1), pp 1 - 25.

Perrin R.M.S. (1971) *The Clay Mineralogy of British Sediments*, Mineralogical Society, London.

Petley D.J. (1966) *The Shear Strength of Soils at Large Strains*, Ph.D Thesis, University College London, UK.

Petley D.J. (1980) *Comparison of Residual Strength from laboratory Tests and back Analysis*, Proceedings of the International Symposium on Landslides, New Delhi, Vol: 3, pp 99 - 104.

Philip H. (1988) *Recent And Present Tectonics In The Mediterranean Region.* In: "Seizmic Hazard In Mediterranean Regions." Proceedings Of Summer School (1986) by European Mediterranean Seismological Centre And Institute De Physique Du Globe De Strasbourg, J. Bonnin, M. Cara, A. Cisternas & R. Fantechi (Eds.), Kluwer Academic Publishers (For The Commission Of The European ommunities), Netherlands. ISBN: 90-277-2779-1.

Potter P.E., Maynard J.B. & Pryor W.A. (1980) *Sedimentology of Shale*, Springer, Berlin.

Privett K.D. (1980) *The Engineering Geology Of Slopes In The South Cotswolds.* Ph.D. Thesis, University Of Bristol, U.K.

Ramiah B.K., Dayala N.K. & Purushothamaray P. (1970) *Influence of Chemicals on the Residual Strength of Silty Clays*, Soil and Foundations, vol: 10, pp 25 - 36.

Rao S.M., Sridharan A. & Chandrakaran S. (1989) *Influence Of Drying On the Liquid Limit Of A Marine Clay,* Geotechnique Vol: 39 (4), pp 715 - 719; plus Discussion by T.S. Ramanatha Ayyar, N. Balasubramanian, V. Raman & S. Esa kku, Geotechnique 40(4), pp 673 - 676.

Rogers C.D.F., Boyce J.R. & Anayi J.T. (1989) *The Residual Shear Strength Of Sedimentary Clays,* 1st South American Symposium On Landslides, pp 201 - 213, Paipa, Colombia. August 1989.

Rowlands G.O., Arabi M. & Delpak R. (1987) *Lime And The Plasticity Of Clays.* R. Highways And Transportation, Institution Of Highways, May 1987, Vol: 3415, pp 21 - 27.

Rozos D.E. (1991) *Engineering Geological Conditions in Achaia Province, Geomechenaical Caharacteristics of the Plio-Pleistocene Sediments (Ph.D Thesis),* Engineering Geology Investigations No 15, Institute of Geology and Mineral Exploration, Athens. (in Greek with extensive English summary).

Saito T. & Miki G. (1975) *Swelling and Residual Strength Characteristics of Soils Based on Newly Proposed Plastic Ratio Chart,* Japanese Society of Soil Mechanics and Foundation Engineering, vol: 15 (1), pp 61 - 68.

Schiffman R.L., Vicks S.G. & Gibson R.E. (1988) *Behaviour And Properties Of Hydraulic Fills.* Geotechnical Special Publication No. 21, D.J.A. Van Zyl & S.G. Vicks (Eds.), ASCE, pp 166 - 202.

Scordilis E.M., Karakaisis g.F., Karakostas B.C., Panagiotopoulos D.G. & Papazachos B.C. (1985) *Evidence for Transform Faulting in the Ionian Sea: the Cephalonia Island Earthquake Sequence of 1983,* Pure and Applied Geophysics, Vol: 123. pp 387 - 397.

Seed B.H., Woodward R.J. & Lundgren R. (1964) *Fundamental Aspects Of Atterberg Limits.* Journal Of The Soil Mechanics Foundations Division, Proc. ASCE, Nov. 1964 (SM6). Vol: 90, pp 75 - 105.

Selley R.C. (1982) *An Introduction To Sedimentology.* 2nd Edition, Academic Press Inc., London. ISBN: 0-12-636362-5.

Selley R.C. (1988) *Applied Sedimentology.* Academic Press Ltd., London. ISBN: 0-12-636366-8

Sembenneli P. & Ramirez L. (1969) *Measurement of Residual Strength of Clays with a Rotation Shear Machine*, Speciality Session No. 16, Proceedings of the 7th International Conference on Soil Mechanics and Foundation Engineering, Mexico, Vol: 3, pp 528 - 529.

Seychek J. (1970) *Residual Strength of Soils*, Bulletin of the Internation Association of Engineering Geologists, vol: 17, pp 73 - 75.

Sherwood P.T. (1967) *Classification Tests On African Red Clays And Keuper Marl.* Quarterly Journal Of Engineering Geology, Vol: 1, pp 47 - 55.

Sherwood P.T. & Ryley M.D. (1968) *An Examination of Cone Penetrometer Methods for Determing the Liquid Limit of Soils*, Road Research Laboratory Report No. 233, Road Research Laboratory, Crowthorne, U.K.

Skempton A.W. (1944) *Notes On The Compressibility Of Clays.* Quarterly Journal Of Geological Society, London. Vol: 100, pp 119 - 135.

Skempton A.W. (1953) *The collodal Activity of Clay*, Proceedings of the 3rd International Conference on Soil Mechanics and Foundation Engineering, Zurich, Vol: 1, pp 57 - 61.

Skempton A.W. (1964) *Long-Term Stability of Clay Slopes*, Fourth Rankine Lecture, Geotechnique, Vol: 14 (2), pp 77 - 101.

Skempton A.W. (1985) *Residual Strength Of Clays In Landslides, Folded Strata And The Laboratory.* Geotechnique Vol: 35 (1), pp 3 - 18.

Skempton A.W. & Brown J.D. (1961) *A Roadside in Boulder Clay at Sellset, Yorksire*, Geotechnique, vol: 11 (4), pp 280 - 293.

Skempton A.W. & Coates D.J. (1984) *Failures in Earthworks, the Carsington Dam Failure*, Institution of Civil Engineers, London.

Skempton A.W. & Northey R.D. (1972) *The Sensitivity of Clays*, Geotechnique, Vol: 27, pp 195 - 300.

Smart P. (1970) *Residual Shear Strength*, Journal of Soil Mechanics and Foundation Engineering Division, Proceedings of the ASCE, Vol: 96 (SM6), pp 2181 - 2183.

Smith J.T. (1978) *Consolidation and Other Geotechnical Properties of Shales with Respect to Age and Composition*, PhD. Thesis, University of Durham, U.K.

Soliman H.A. & Zygoyannis N. (1980) *Geological and Paleaontological Studies in the Mesohellenic Basin, Northern Greece*, Geological and Geophysical Research, IGME, Athens, Vol: 22, pp 1 - 66.

Sridharan A. (1968) *Some Studies on the Strength of Partly Saturated Clays*, Ph.D Thesism Purdue University, Lafayette, Indiana, USA.

Sridharan A. & Jayadeva M.S. (1982) *Double Layer Theory And Compressibility Of Clays.* Geotechnique Vol: 32 (2), pp 133 - 144.

Sridharan A. & Rao G.V. (1973) *Mechanisms Controlling Volume Change Of Saturated Clays And The Role Of The Effective Stress Concept.* Geotechnique Vol: 23 (3), pp 359 - 382.

Sridharan A. & Rao A.S. (1982) *Mechanisms Controlling The Secondary Compression Of Clays.* Geotechnique Vol: 32 (3), pp 249 - 260.

Sridharan A., Rao S.M. & Murthy M.S. (1986) *Liquid Limit Of Montmorillonite Soils,* Geotechnical Testing Journal, GTJODJ, American Society For Testing And Materials, Vol: 9 (3), pp 156 - 159.

Stark T.D. & Eid H.T. (1992) *Comparison of field and laboratory residual strengths,* Proceedings, ASCE Specialty Conference on Stability and Performance of Slopes and Embankments, Vol: 2, University of California, Berkeley, CA, ASCE, New York.

Stark T.D. & Vettel J.J. (1992) *Bromhead Ring Shear Test Procedure.* Geotechnical Testing Journal, GTJODJ, Vol: 15 (1), pp 24 - 32.

Steward H.E. & Cripps J.C (1983) *Some Engineering Implications of Chemical Weathering of Pyritic Shale*, Quarternary Journal of Engineering Geology, London, Vol: 16, pp 281 - 289.

Stewart I.S. & Hancock P.L. (1988) *Normal Fault Zone Evolution And Fault Scarp Degredation In The Aegean Region.* Basin Research, Vol: 1, pp 139 - 153.

Stewart I.S. & Hancock P.L. (1991) *Scales Of Structural Heterogeneity Within Neotectonic Normal Fault Zones In The Aegean Region.* Journal Of Structural Geology, Vol: 13.

Takahashi H. (1959a) *Effects Of Dry Grinding On Kaoline Minerals, I: Kaolinite.* Bulletin Of The Chemical Society Of Japan, Vol: 32, pp 235 - 263.

Takahashi H. (1959b) *Wet Grinding On Kaoline Mineral.* Bulletin Of The Chemical Society Of Japan, Vol: 32, pp 381 - 387.

Tan T.S., Yong K., Leong E.C., & Lee S.L. (1990) *Sedimentation Of Clayey Slurry.* Journal Of Geotechnical Engineering, Vol: 116 (6), pp 885 - 898. ISSN: 0733-9410.

Taylor R.K. (1971) *Deformation and Physico-Chemical Properties of Certain sediments with Particular Reference to Colliery spoil*, Ph.D Thesis, University of Durham, UK.

Taylor R.K. (1988) *Coal Measures Mudrocks: Compositions, Classification And Weathering Processes,* Quarterly Journal Of Engineering Geology, London, Vol: 21, pp 85 - 99.

Taylor R.K. & Smith T.J. (1986) *The Engineering Geology Of Clay Minerals: Swelling, Shrinking And Mudrock Breakdown,* Clay Minerals, The Mineralogical Society, Vol: 21, pp 235 - 260.

Taylor R.K. & Spears D.A. (1981) *Laboratory Investigations of Mudrocks*, Quarternary Journal of Engineering Geology, Geology Society London, vol: 14, pp 291 - 309.

Technical Chamber Of Greece (1985) *Proceedings Of Meeting: Geotechnical Problems Of The Pireas Marl.* Hellenic Society Of Soil Mechanics And Foundation Engineering, Technical Chamber Of Greece, Athens. (In Greek).

Terzaghi K. (1931) *The Influence of Elasticity and Permeability on the Swelling of Two-Phase Systems*, in "Colloid Chemisty, 3", Chemical Catalog Company, New York, pp 65 - 88.

Terzaghi K. & Peck R.B. (1967) *Soil Mechanics in Engineering Practice, (2nd edition)*, John Wiley and Sons, New York.

Thorington S. (1980) *A Laboratory Investigation Of Calcretes From Botswana.* Overseas Unit, Working Paper No. 93, TTRL, Crowthorne, U.K. Sept. 1980.

Tiedman B. (1937) Über die Schubfestogkeit bindiger Böden, Bautechnik, Vol: 15, pp 400 - 403.

Tika T.M. (1989) *The Effect of Rate of Shear on the Residual Strength of Soil*, Ph.D Thesis, Imperial College, University of London, U.K.

Tika T.M. & Vassilikos T. (1991) *Clay on Steel Ring Shear Tests and their Implications for Displacement Piles*, Geotechnical Testing Journal, A.S.T.M., Vol: 14 (4), pp 457 - 463.

Townsend D.L. (1965) *Discussion*, Canadian Geotechnical Journal, Vol: 2, pp 190 - 193.

Townsend F.C. (1985) *Geotechnical Characteristics of Residual Soils*, Journal of Geotechnical Engineering, ASCE, Col: 111, pp 77 - 93.

Townsend F.C. & Gilbert P.A. (1973) *Residual Strength of Clay Shales*, Geotechnique, vol: 23 (2), pp 267 - 271.

Townsend F.C. & Gilbert P.A. (1974) *Engineering Properties of Clay Shales*, Report 2, in "Residual Strength of Clays and clay Shales", STP-559, Philadelphia, ASTM, pp 43 - 65.

Tselentis G.A. & Makropoulos K (1986) *Rates of Crustal Deformation in the Gulf of Corinth (Central Greece) as Determined from Seismicity*, Tectonophysics, Vol: 24, pp 55 - 61.

Tsiambaos G. (1987) *The Engineering Geological Characteristics Of The Herakleion Marls, Crete.* Ph.D. Thesis, Dept. Of Geology, University Of Patras, Patra, Greece. (In Greek).

Tsiambaos G. (1991) *Correlation Of Minerlogy And Index Properties With Residual Strength Of Iraklion Marls,* Engineering Geology, Elsevier, Vol: 30 (3/4), pp 357 - 369.

Underhill J.R. (1989) *Late Cenozoic Deformation Of The Hellenide Foreland, Western Greece.* Bulletin Of The Geological Society Of America, Vol: 101, pp 613 - 634.

Underwood L.B. (1967) *Classification and Identification of Shales*, Journal of the Soil Mechanics and Foundation Division, ASCE, Vol: 93 (SM6), pp 97 - 116.

Van Olphen H. (1987) *Dispersion And Flocculation.* In:"Chemistry Of Clays And Clay Minerals", Mineralogical Society Monograph No. 6, A.C.D. Newman (Ed.), Mineralogical Society, Longman Scientific & Technial, pp 203 - 224. ISBN: 0-582-30114-9.

Vaughan P.R. (1988) *Characterising The Mechanical Properties Of In Situ Residual Soil,* 2nd International Conference On Geomechanics In Tropical Soils, December 1988, Singapore.

Vaughan P.R., Lemos L.J.L. & Tika T.M. (1985) *Strenght Loss on Shear Surfaces due to Rapid Loading*, Eleventh International Conference on Soil Mechanics and Foundation Engineering, San Francisco, California, Vol: 4, pp 1955 - 1958.

Vaughan P.R., Maccarini M. & Mokhtar S.M. (1988) *Indexing The Engineering Properties Of Residual Soil,* Quarterly Journal Of Engineering Geology, London, Vol: 21, pp 69 - 84.

Vaughan P.R. & Walbancke H.J. (1975) *The Stability of Cut and Fill Slopes in Boulder Clay*, Proceedings of the Symposium on Engineering Behaviour of Glacial Materials, Midland Society of Soil Mechanics, Birmingham, U.K., pp 209 - 219.

Velde B. & Meunier A. (1987) *Petrologic Phase Equilibria In Natural Clay Systems.* In: "Chemistry Of Clays And Clay Minerals", Mineralogical Society Monograph No. 6, A.C.D. Newman (Ed.), Mineralogical Society, Longman Scientific & Technical, pp 423 - 458. ISBN: 0-582-30114-9.

Vita-Finzi C. & King G.C.P. (1985) *The Seismicity, Geomorphology And Structural Evolution Of The Corinth Area Of Greece,* Phil. Trans. Royal Society London, Vol: A 314, pp 379 - 407.

Voight B. (1973) *Correlation Between Atterberg Plasticity Limits And Residual Shear Strength Of Natural Soils,* Geotechnique Vol: 23 (2), pp 265 - 267.

Voumoos M.M. (1965) *Determination of Organic matter for Classification of Soil Samples*, Proceedings of the 6th International Conference on Soil Mechanics and Foundation Engineering, Vol: 1, pp 77 - 79.

Wild S., Arabi M. & Leng Ward G. (1989) *Fabric Development In Lime Treated Clay Soils.* Ground Engineering, Vol: 22 (3), April 1989, British Geotechnical Society, pp 35 - 37.

Williams A.A.B. & Donaldson G.W. (1980) *Building on Expansive Soils in Southern Africa 1973-1980*, Proceedings of the 4th International Conference on Expansive Soils, ASCE, Denver, pp 834 - 844.

Wood D.M. (1982) *Cone Penetrometer and Liquid Limit*, Geotechnique, Vol: 32 (2), pp 152 - 157.

Wood D.M. & Wroth C.P. *The Use of the Cone Penetrometer to Determine the Liquid Limit of Soils*, Ground Engineering, vol: 11, pp 37 - 42.

Wroth C.P. (1979) *Correlations Of Some Engineering Properties Of Soils,* Proceedings Of The 2nd International Conference On The Behaviour Of Offshore Structures, Vol: 1, pp 121 - 132.

APPENDIX A

RING SHEAR TEST RESULTS

APPENDIX A

TABLE OF CONTENTS

sample	page
agn 1	1
agn 2	2
kd	3
kks 1	4
kd Ab	5
arv 3	6
ktr 2	7
er 1	8
kvt 1 hpb	9
kvt Alp	10
ll1	11
lts	12
mvg	13
nsa 1	14
oen 2	15
pls	16
psf 1a	17
rtk	18
skf 1	19
xml mp	20
slm 0320	21
slm B1	22
slm B2	23
slm G4	24
slm 1A	25
slm 7A	26
slm 2T	27
slm 3T	28
slm 4T	29
slm D2	30
slm 20	31

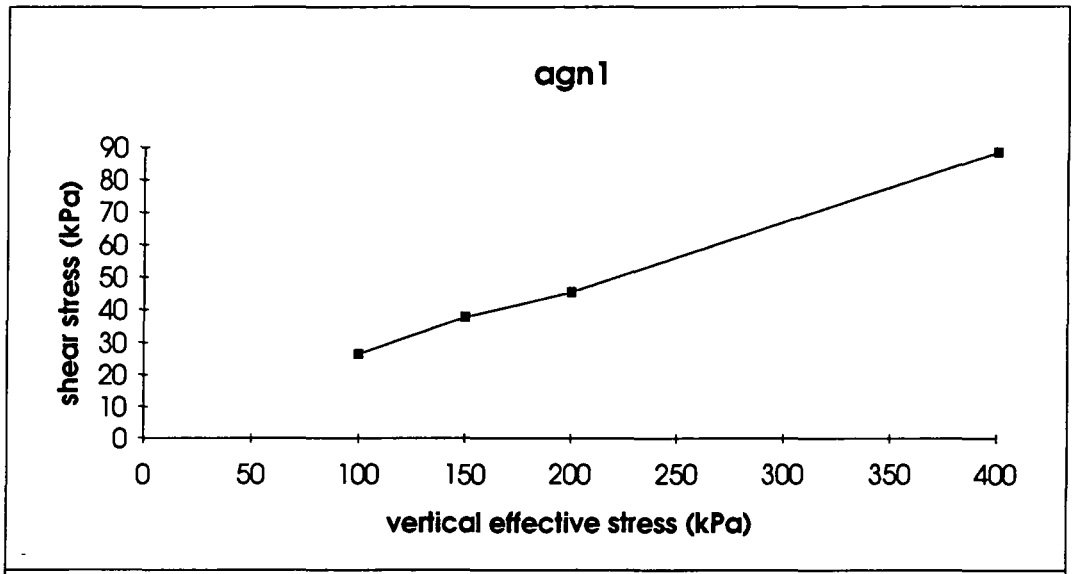
agn1
shear stress (kPa)
0
10
20
30
40
50
60
70
80
90
0
50
100
150
200
250
300
350
400
vertical effective stress (kPa)

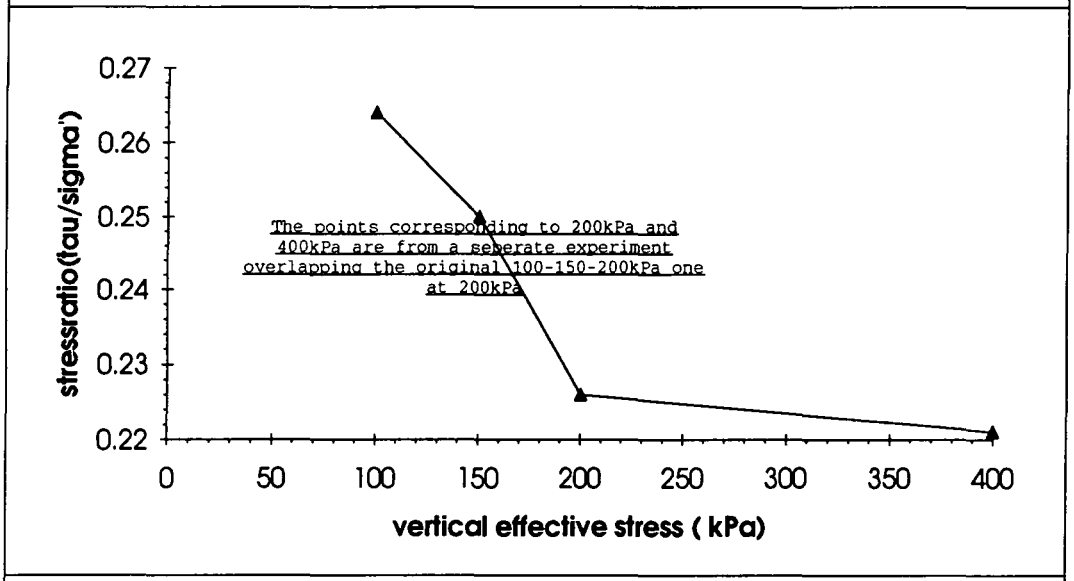
stressratio(tau/sigma')
0.22
0.23
0.24
0.25
0.26
0.27
The points corresponding to 200kPa and 400kPa are from a seperate experiment overlapping the original 100-150-200kPa one at 200kPa
0
50
100
150
200
250
300
350
400
vertical effective stress (kPa)

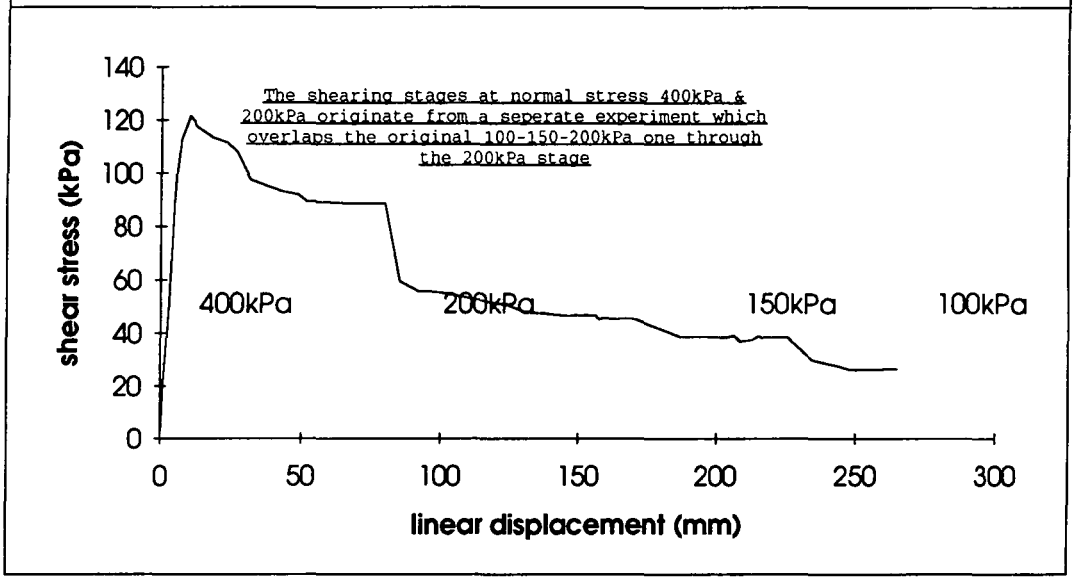
shear stress (kPa)
0
20
40
60
80
100
120
140
The shearing stages at normal stress 400kPa & 200kPa originate from a seperate experiment which overlaps the original 100-150-200kPa one through the 200kPa stage
400kPa
200kPa
150kPa
100kPa
0
50
100
150
200
250
300
linear displacement (mm)

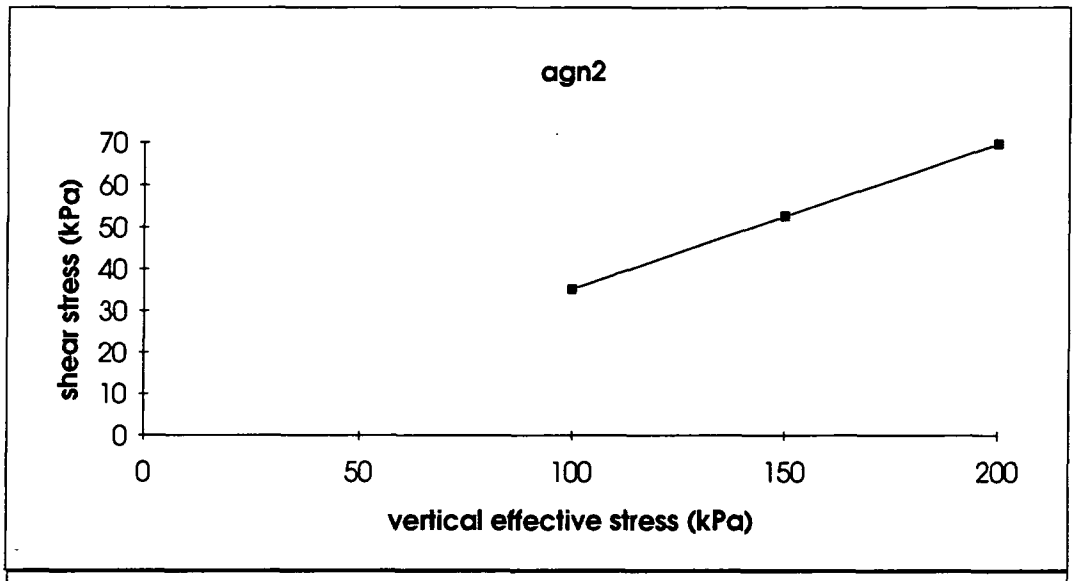
agn2
shear stress (kPa)
70
60
50
40
30
20
10
0
0
50
100
150
200
vertical effective stress (kPa)

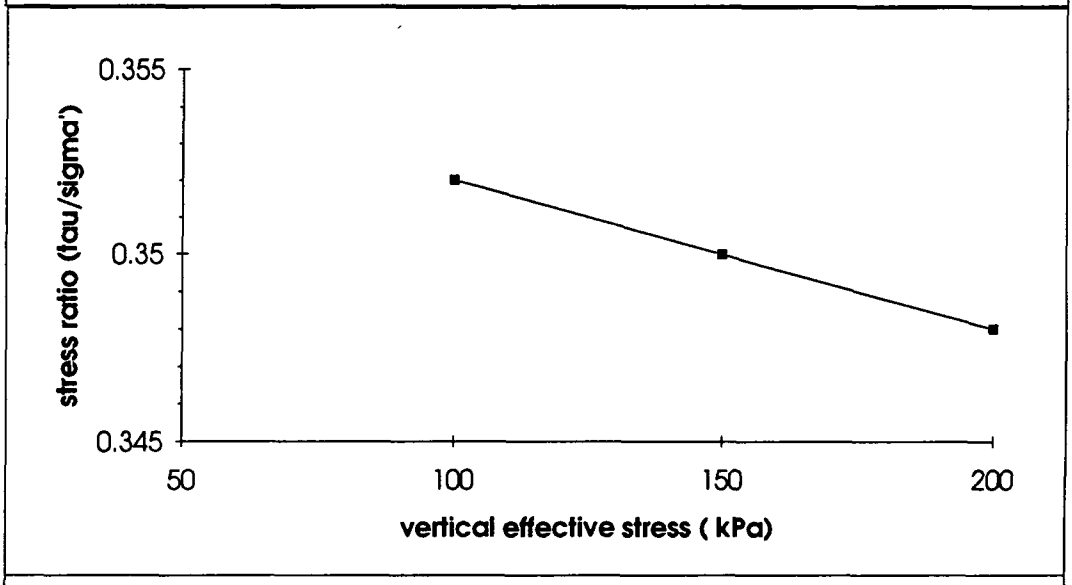
stress ratio (tau/sigma')
0.355
0.35
0.345
50
100
150
200
vertical effective stress (kPa)

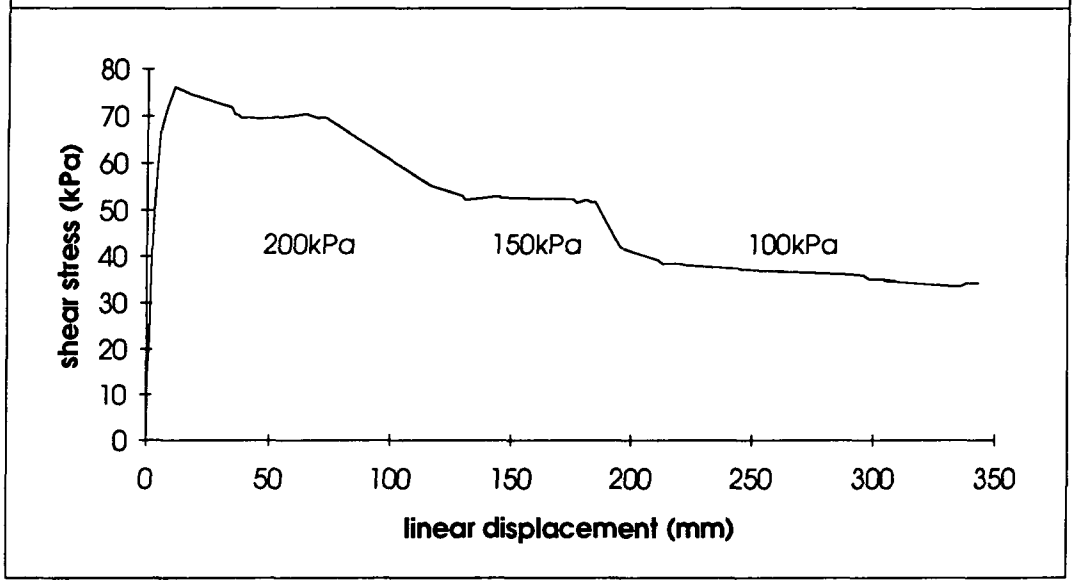
shear stress (kPa)
80
70
60
50
40
30
20
10
0
200kPa
150kPa
100kPa
0
50
100
150
200
250
300
350
linear displacement (mm)

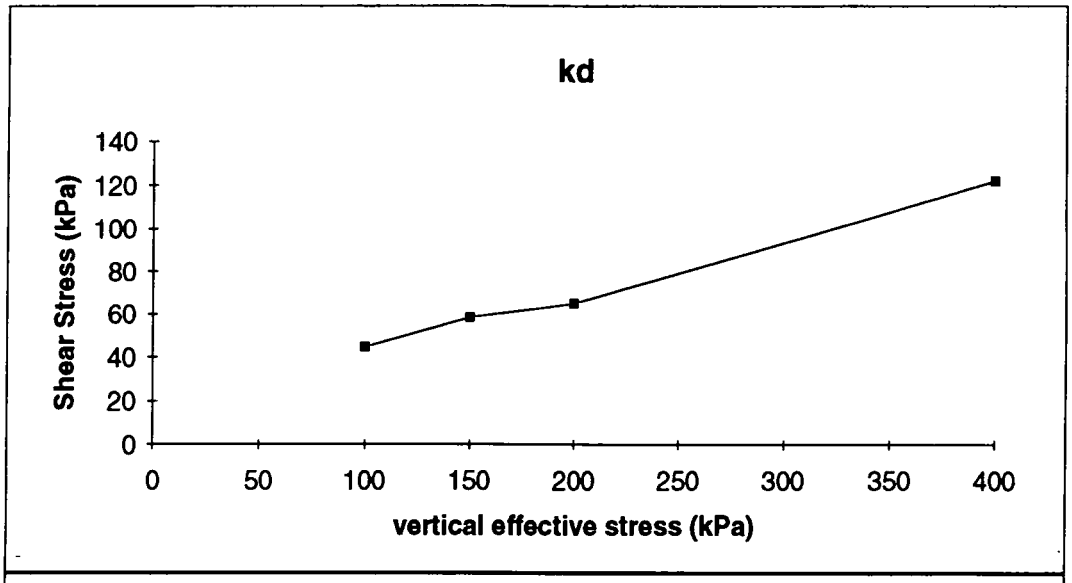
kd
Shear Stress (kPa)
140
120
100
80
60
40
20
0
0
50
100
150
200
250
300
350
400
vertical effective stress (kPa)

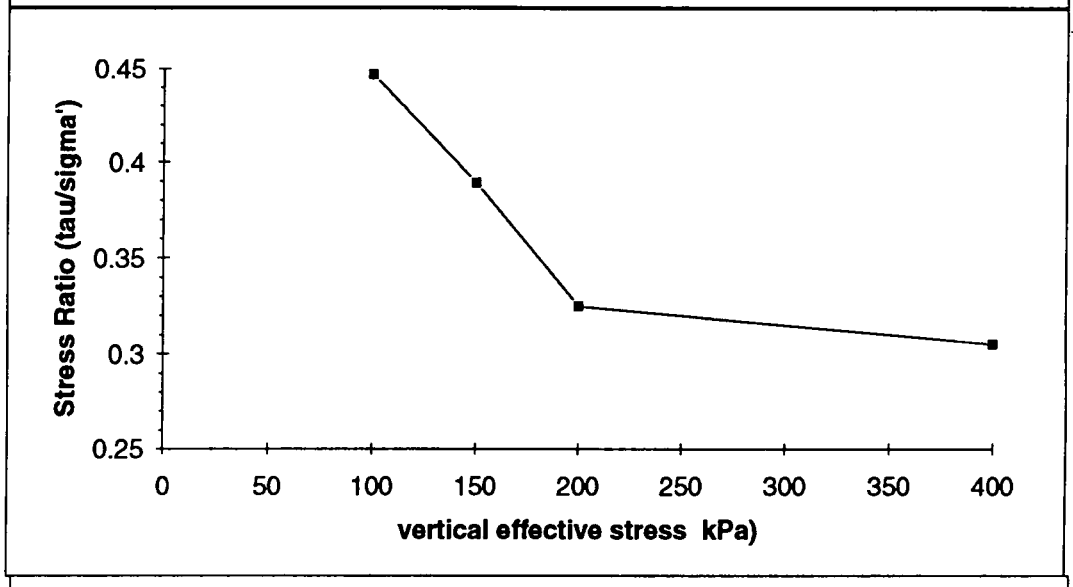
Stress Ratio (tau/sigma')
0.45
0.4
0.35
0.3
0.25
0
50
100
150
200
250
300
350
400
vertical effective stress kPa)

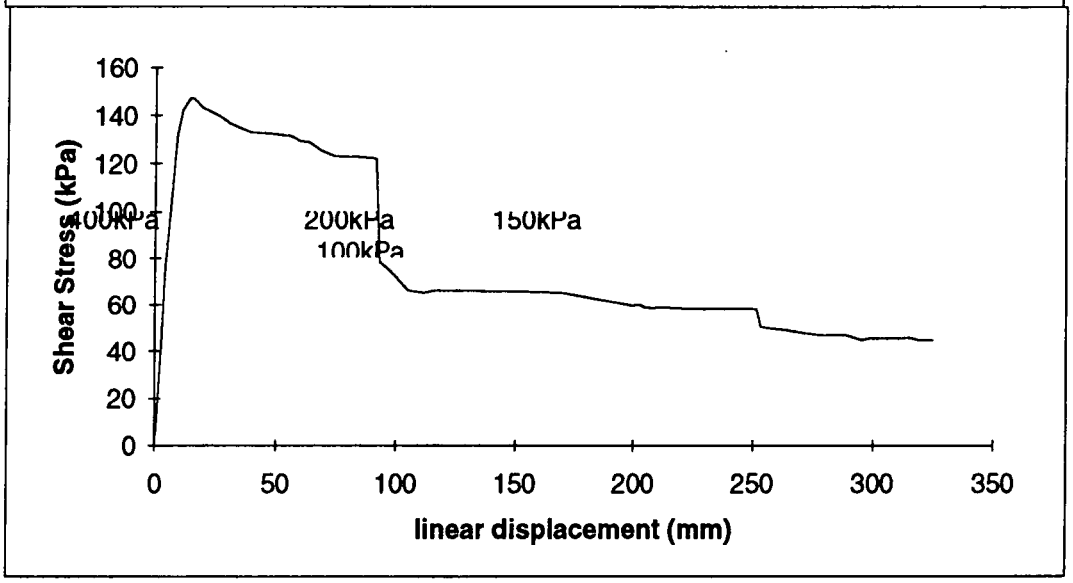
Shear Stress (kPa)
160
140
120
100
80
60
40
20
0
100kPa
200kPa
100kPa
150kPa
0
50
100
150
200
250
300
350
linear displacement (mm)

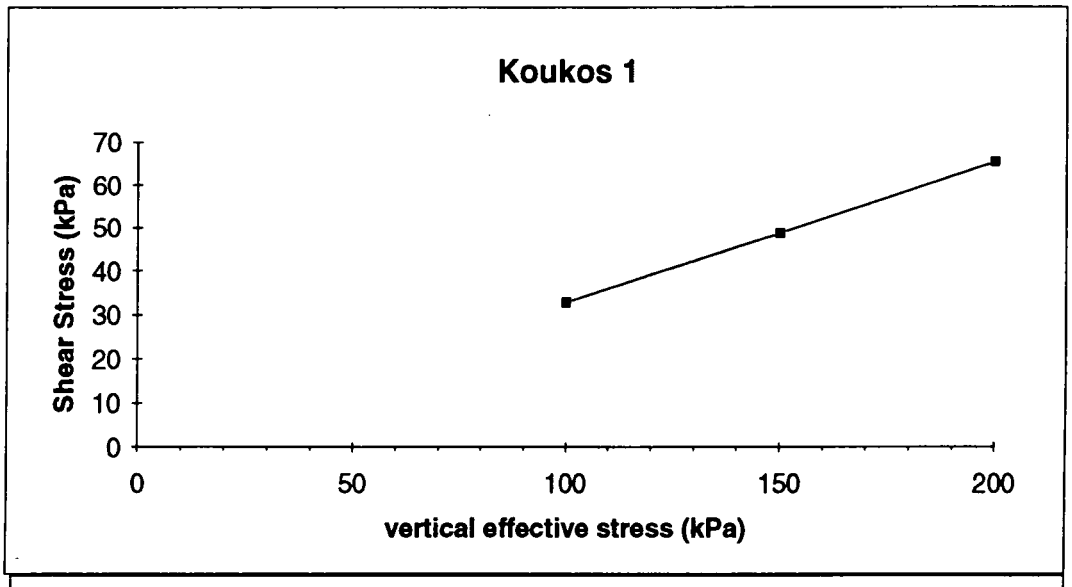
Koukos 1
Shear Stress (kPa)
70
60
50
40
30
20
10
0
0
50
100
150
200
vertical effective stress (kPa)

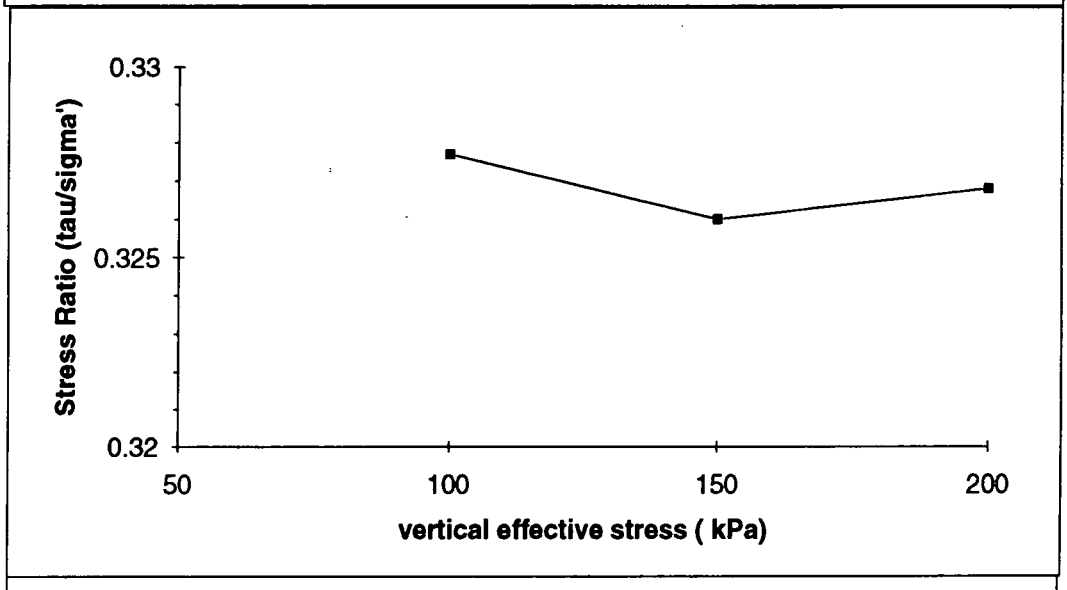
Stress Ratio (tau/sigma')
0.33
0.325
0.32
50
100
150
200
vertical effective stress (kPa)

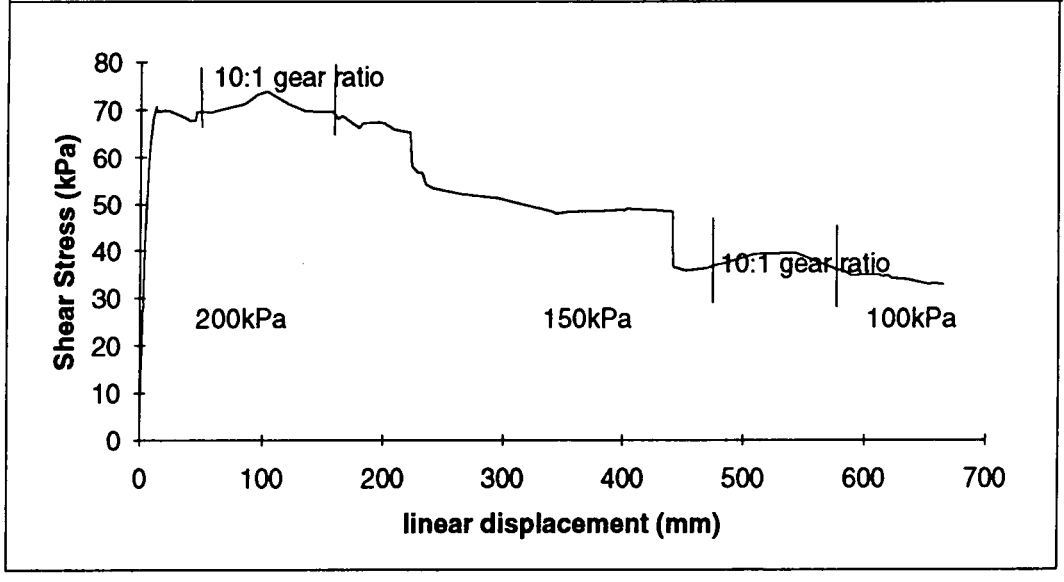
Shear Stress (kPa)
80
70
60
50
40
30
20
10
0
10:1 gear ratio
10:1 gear ratio
200kPa
150kPa
100kPa
0
100
200
300
400
500
600
700
linear displacement (mm)

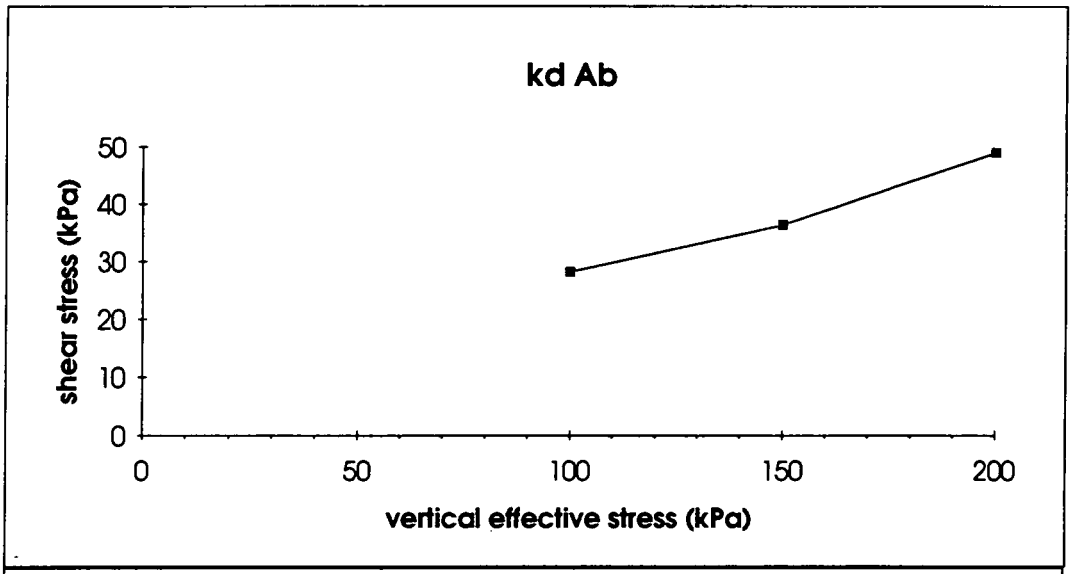
kd Ab
shear stress (kPa)
0
10
20
30
40
50
0
50
100
150
200
vertical effective stress (kPa)

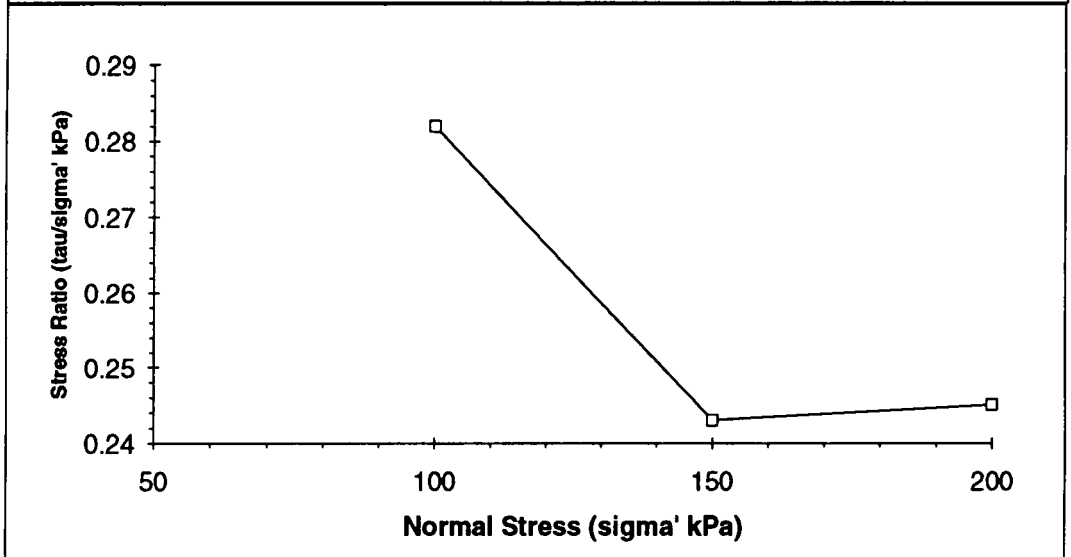
Stress Ratio (tau/sigma' kPa)
0.24
0.25
0.26
0.27
0.28
0.29
50
100
150
200
Normal Stress (sigma' kPa)

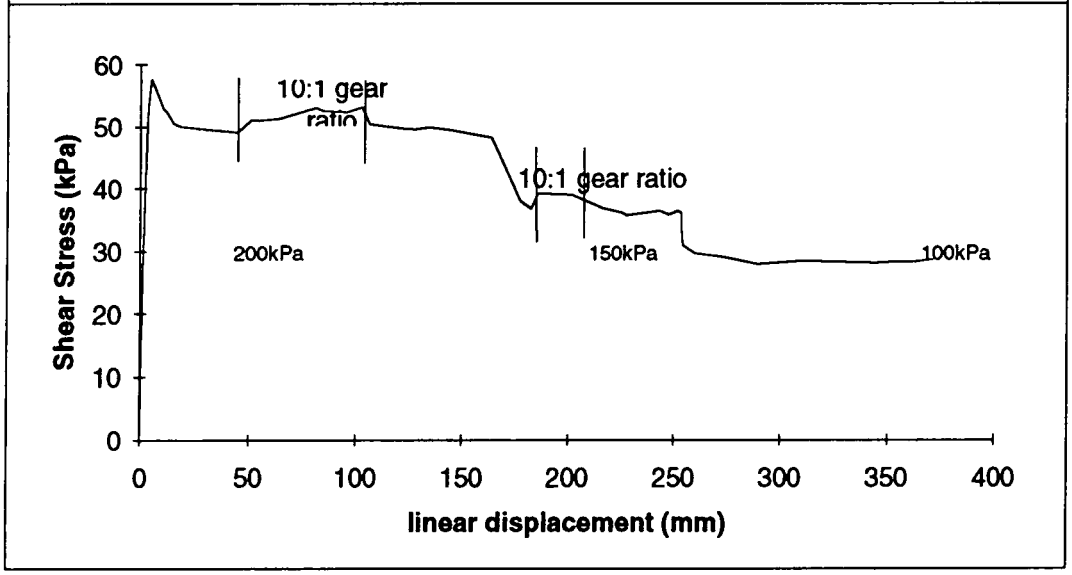
Shear Stress (kPa)
0
10
20
30
40
50
60
10:1 gear ratio
10:1 gear ratio
200kPa
150kPa
100kPa
0
50
100
150
200
250
300
350
400
linear displacement (mm)

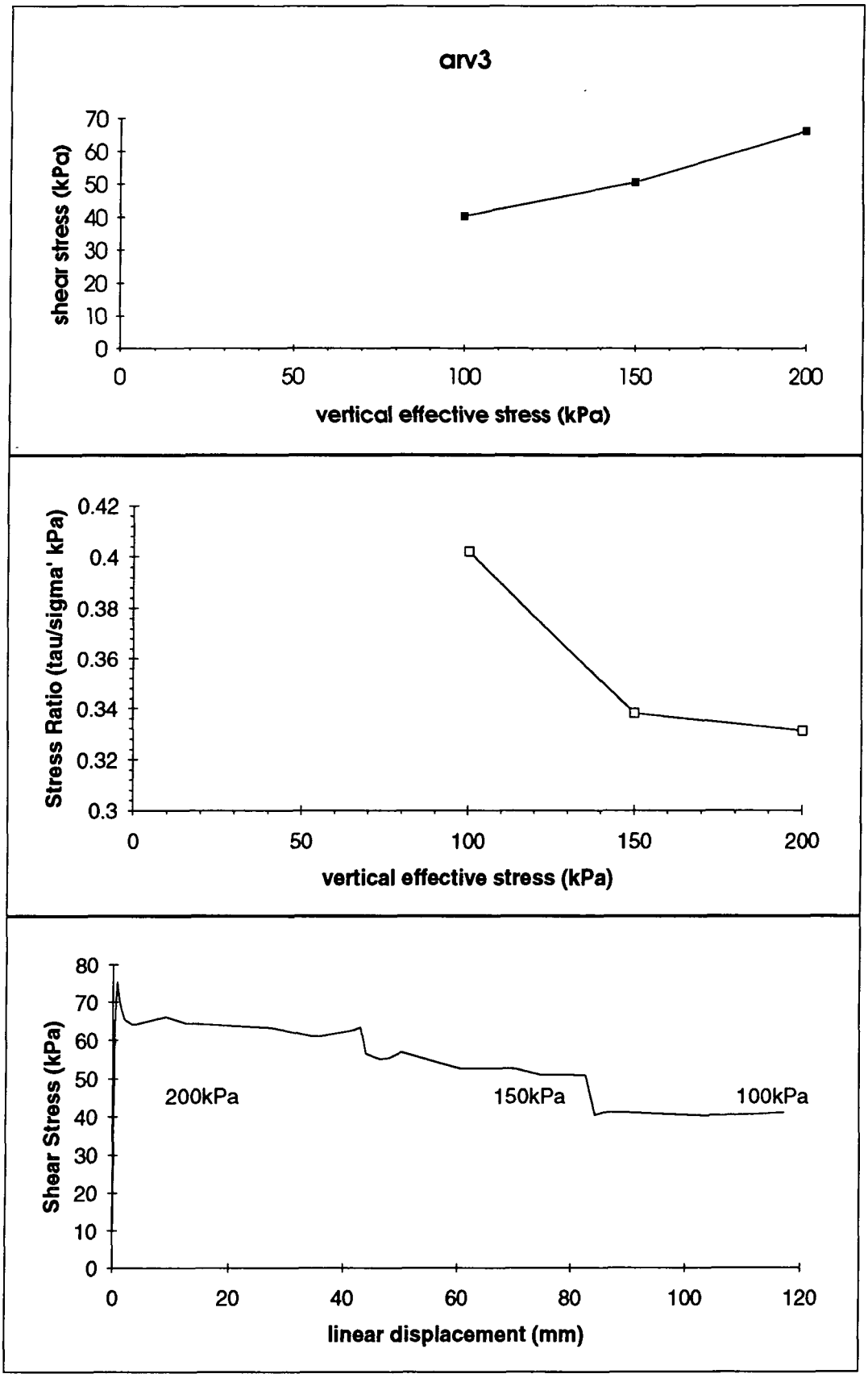
arv3
shear stress (kPa)
70
60
50
40
30
20
10
0
0
50
100
150
200
vertical effective stress (kPa)
Stress Ratio (tau/sigma' kPa)
0.42
0.4
0.38
0.36
0.34
0.32
0.3
0
50
100
150
200
vertical effective stress (kPa)
Shear Stress (kPa)
80
70
60
50
40
30
20
10
0
200kPa
150kPa
100kPa
0
20
40
60
80
100
120
linear displacement (mm)

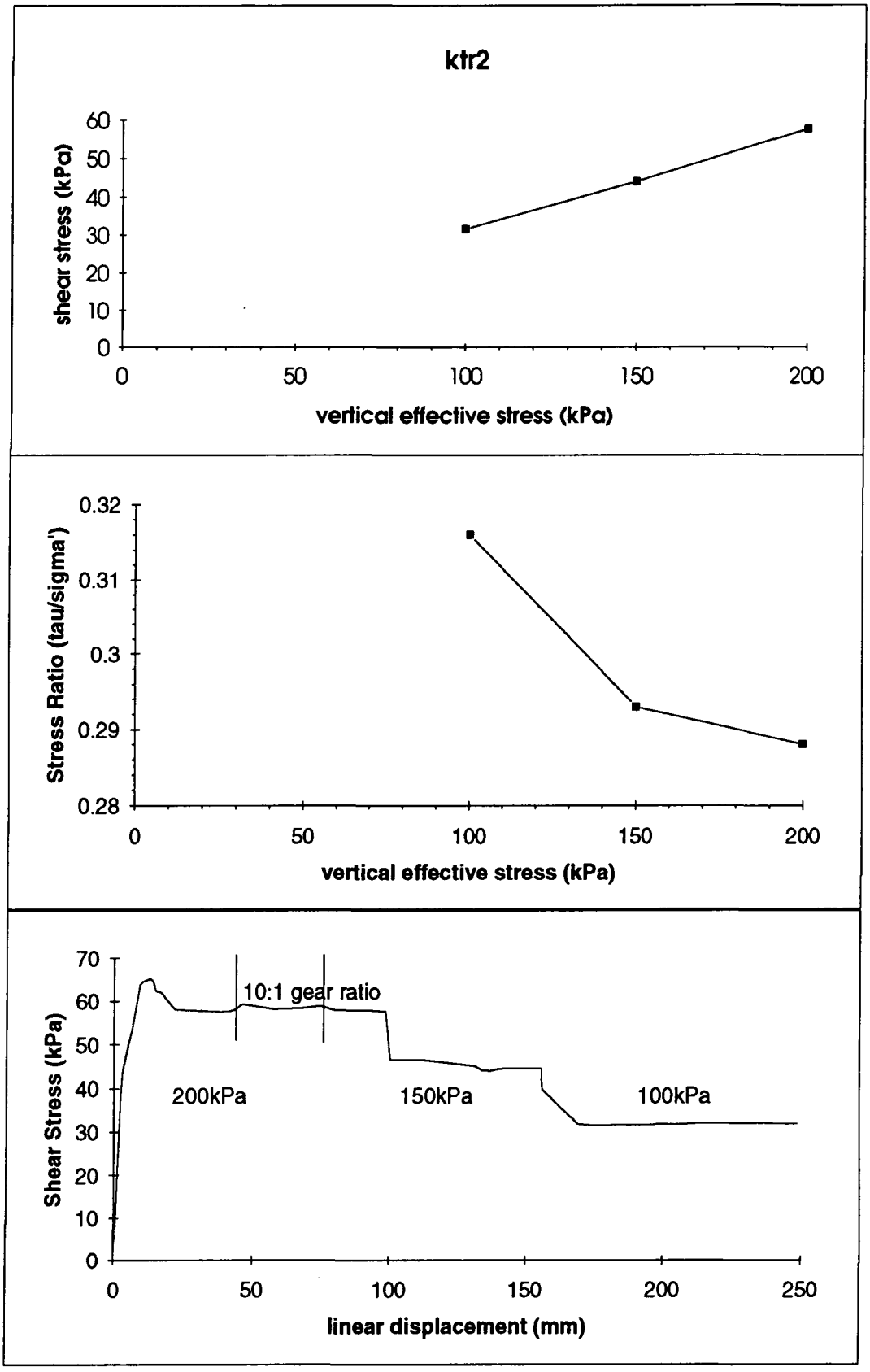
ktr2
shear stress (kPa)
60
50
40
30
20
10
0
0
50
100
150
200
vertical effective stress (kPa)
Stress Ratio (tau/sigma')
0.32
0.31
0.3
0.29
0.28
0
50
100
150
200
vertical effective stress (kPa)
Shear Stress (kPa)
70
60
50
40
30
20
10
0
10:1 gear ratio
200kPa
150kPa
100kPa
0
50
100
150
200
250
linear displacement (mm)

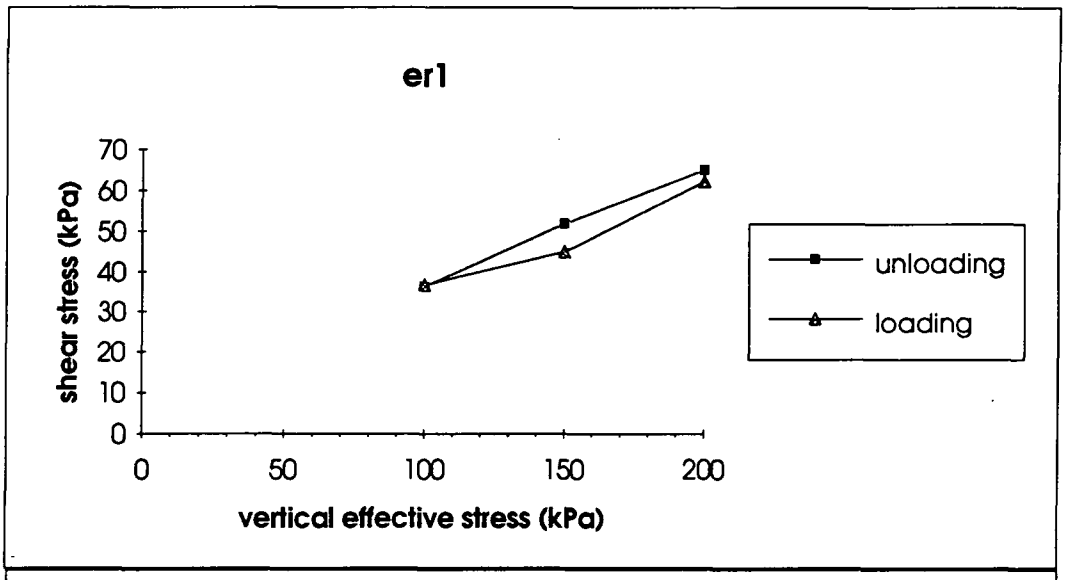
er1
shear stress (kPa)
70
60
50
40
30
20
10
0
0
50
100
150
200
vertical effective stress (kPa)
unloading
loading

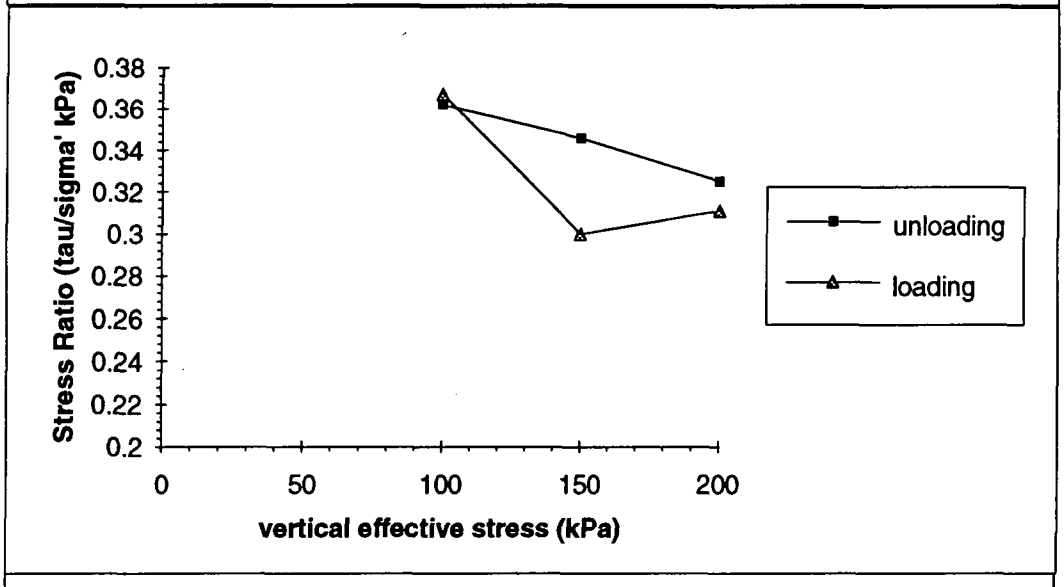
Stress Ratio (tau/sigma' kPa)
0.38
0.36
0.34
0.32
0.3
0.28
0.26
0.24
0.22
0.2
0
50
100
150
200
vertical effective stress (kPa)
unloading
loading

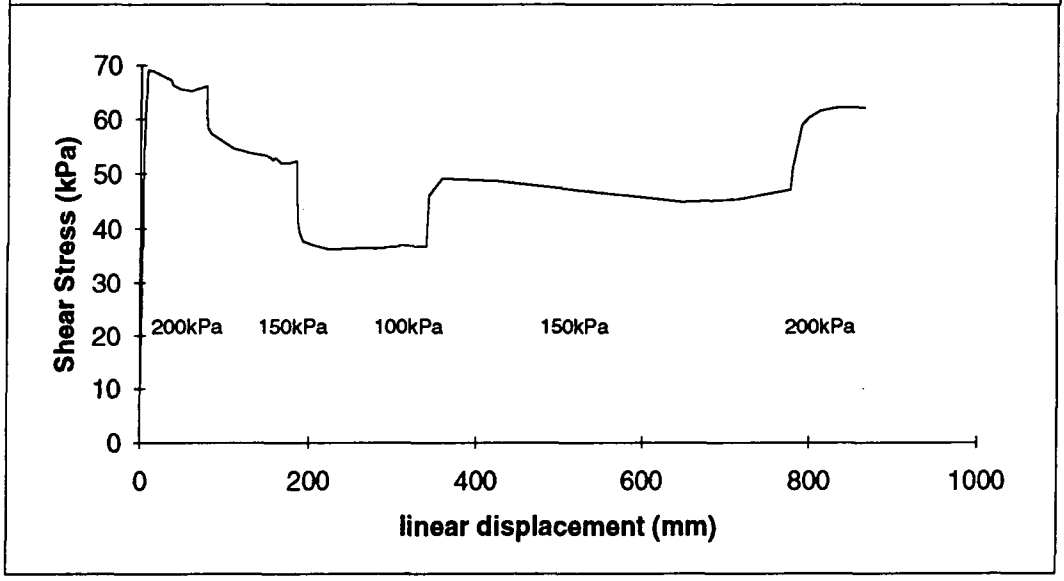
Shear Stress (kPa)
70
60
50
40
30
20
10
0
200kPa
150kPa
100kPa
150kPa
200kPa
0
200
400
600
800
1000
linear displacement (mm)

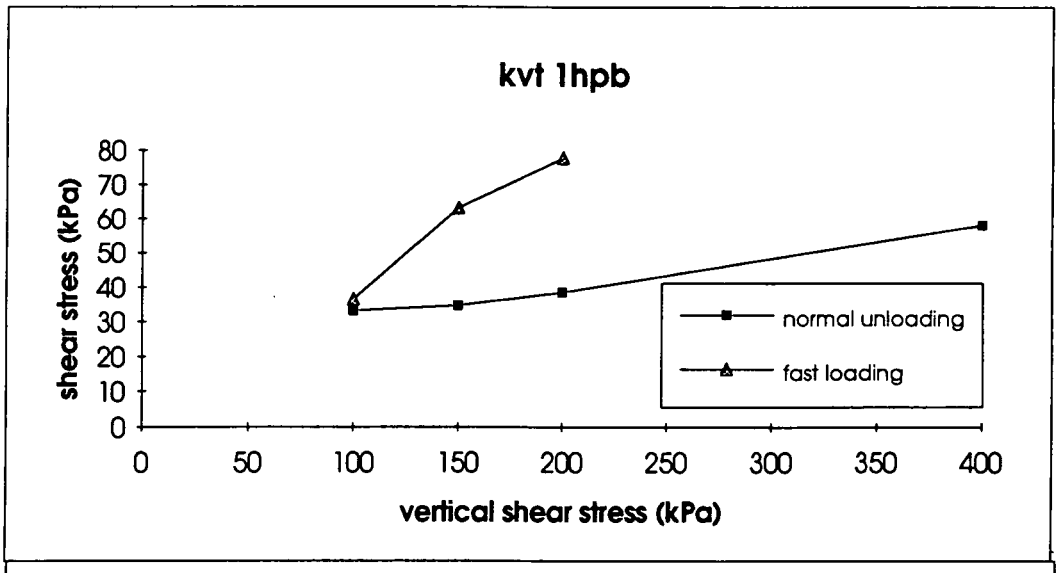
kvt 1hpb
shear stress (kPa)
80
70
60
50
40
30
20
10
0
0
50
100
150
200
250
300
350
400
vertical shear stress (kPa)
normal unloading
fast loading

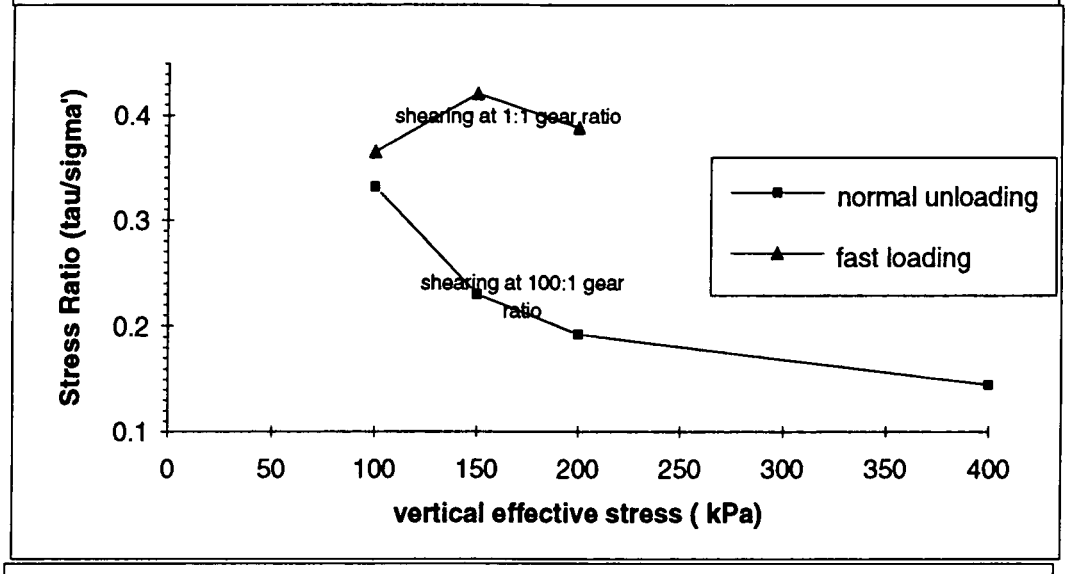
Stress Ratio (tau/sigma')
0.4
0.3
0.2
0.1
0
50
100
150
200
250
300
350
400
vertical effective stress (kPa)
shearing at 1:1 gear ratio
shearing at 100:1 gear ratio
normal unloading
fast loading

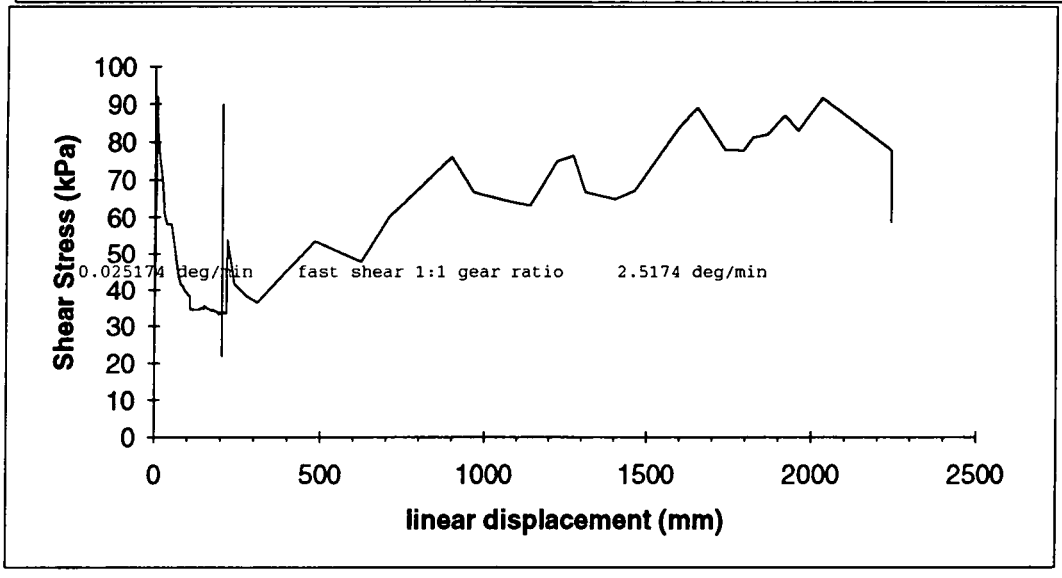
Shear Stress (kPa)
100
90
80
70
60
50
40
30
20
10
0
0
500
1000
1500
2000
2500
linear displacement (mm)
0.025174 deg/min
fast shear 1:1 gear ratio
2.5174 deg/min

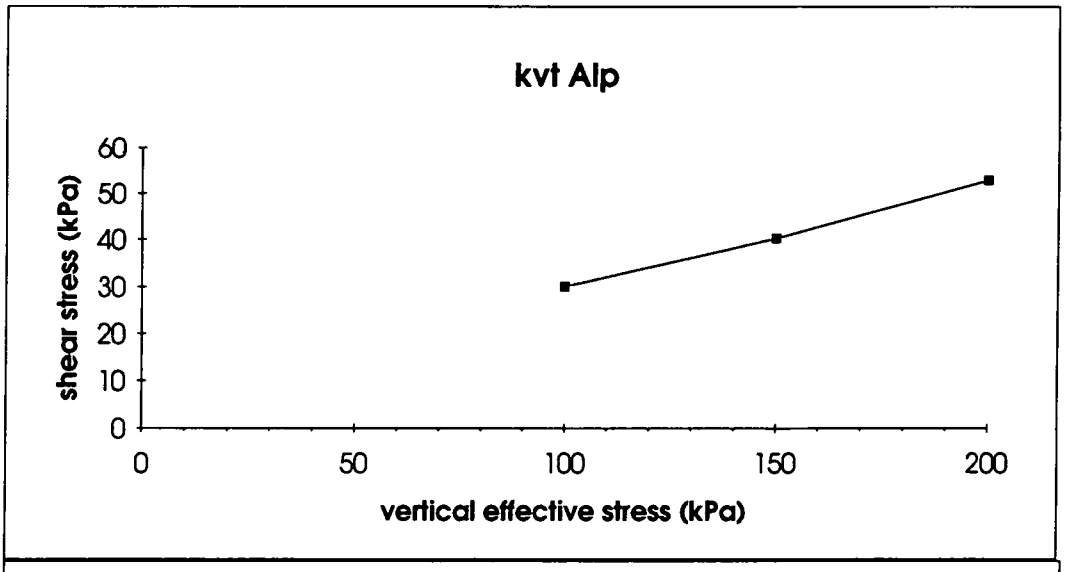
kvt Alp
shear stress (kPa)
60
50
40
30
20
10
0
0
50
100
150
200
vertical effective stress (kPa)

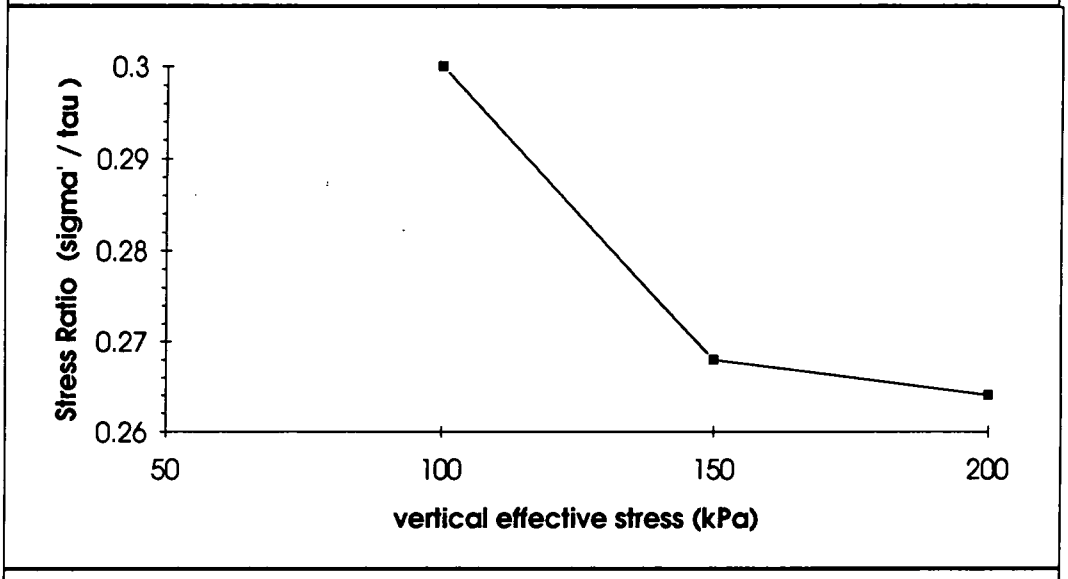
Stress Ratio (sigma' / tau)
0.3
0.29
0.28
0.27
0.26
50
100
150
200
vertical effective stress (kPa)

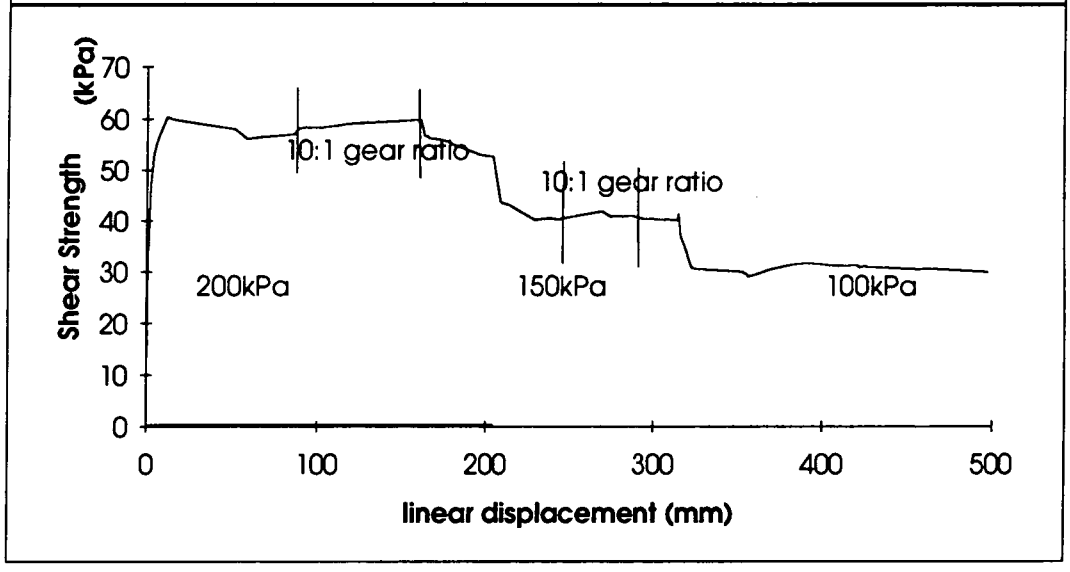
Shear Strength (kPa)
70
60
50
40
30
20
10
0
10:1 gear ratio
10:1 gear ratio
200kPa
150kPa
100kPa
0
100
200
300
400
500
linear displacement (mm)

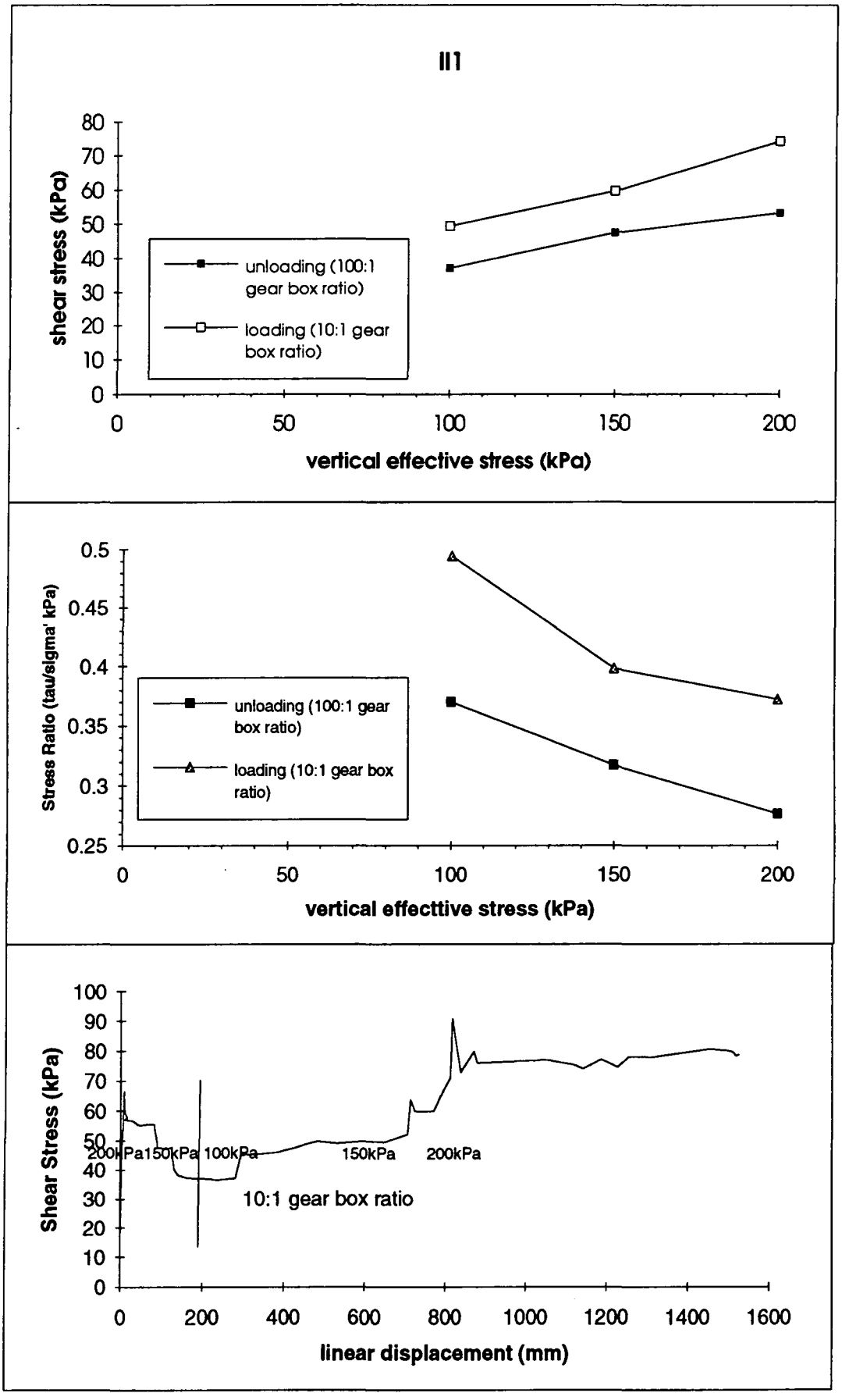
III
shear stress (kPa)
80
70
60
50
40
30
20
10
0
unloading (100:1 gear box ratio)
loading (10:1 gear box ratio)
0
50
100
150
200
vertical effective stress (kPa)
Stress Ratio (tau/sigma' kPa)
0.5
0.45
0.4
0.35
0.3
0.25
unloading (100:1 gear box ratio)
loading (10:1 gear box ratio)
0
50
100
150
200
vertical effecttive stress (kPa)
Shear Stress (kPa)
100
90
80
70
60
50
40
30
20
10
0
200kPa
150kPa
100kPa
150kPa
200kPa
10:1 gear box ratio
0
200
400
600
800
1000
1200
1400
1600
linear displacement (mm)

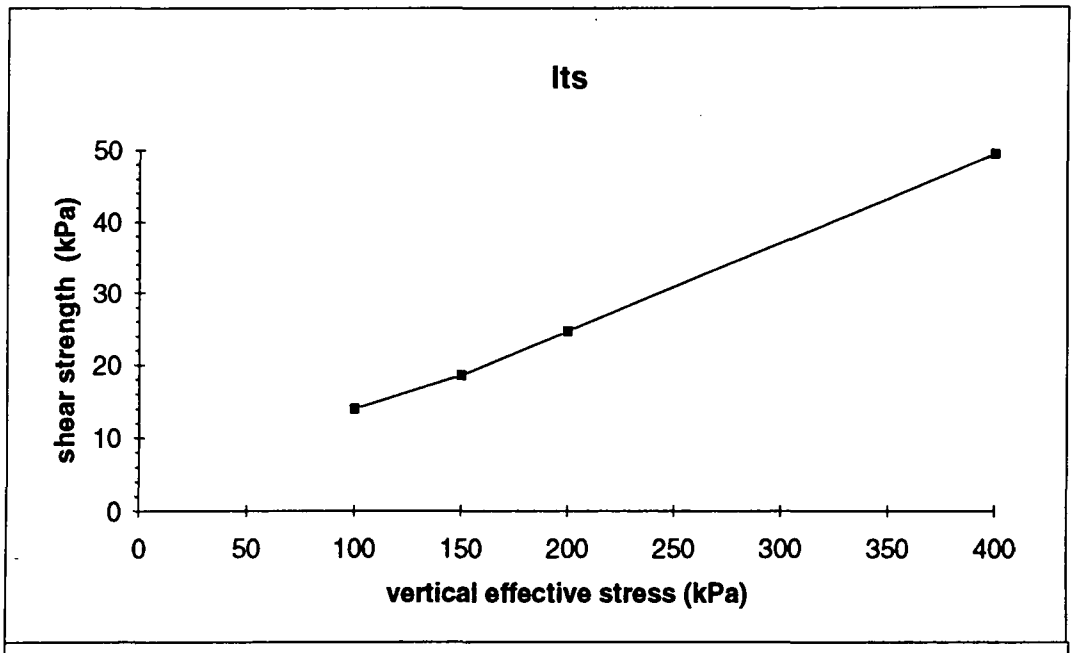
lts
shear strength (kPa)
50
40
30
20
10
0
0
50
100
150
200
250
300
350
400
vertical effective stress (kPa)

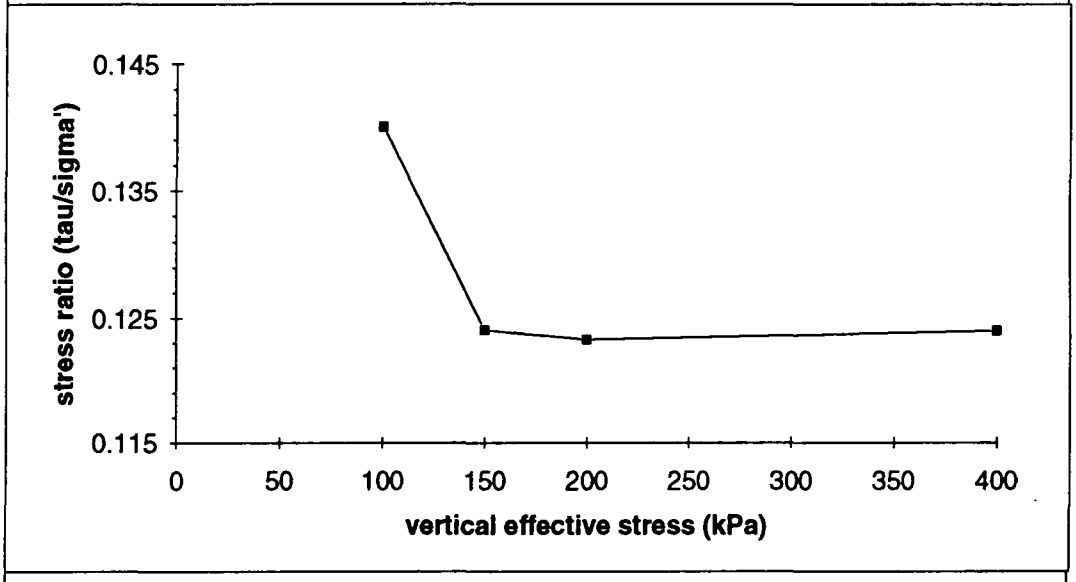
stress ratio (tau/sigma')
0.145
0.135
0.125
0.115
0
50
100
150
200
250
300
350
400
vertical effective stress (kPa)

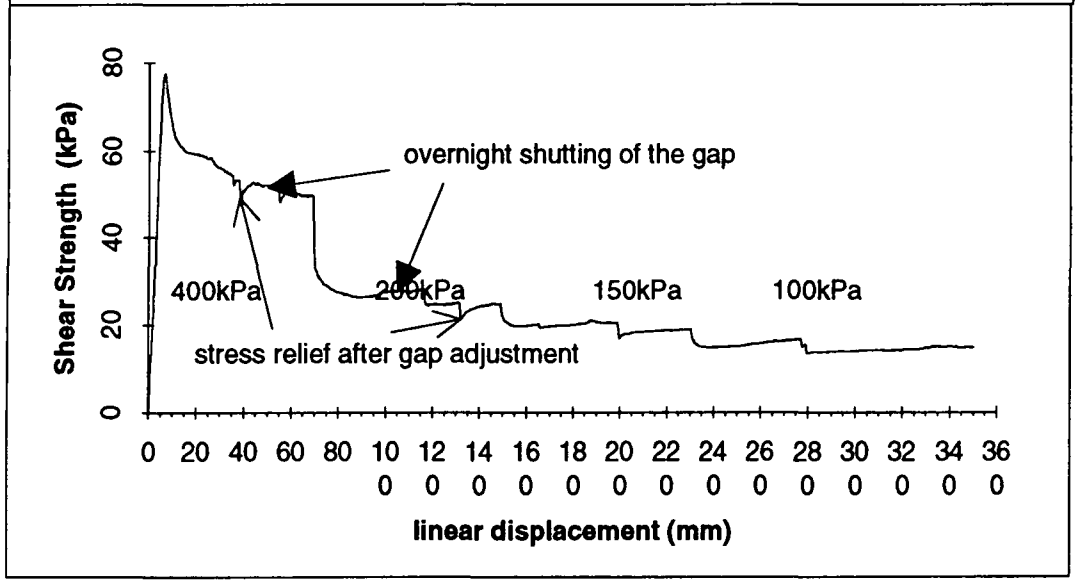
Shear Strength (kPa)
80
60
40
20
0
overnight shutting of the gap
400kPa
200kPa
150kPa
100kPa
stress relief after gap adjustment
0 20 40 60 80 10 12 14 16 18 20 22 24 26 28 30 32 34 36
0 0 0 0 0 0 0 0 0 0 0 0 0 0
linear displacement (mm)

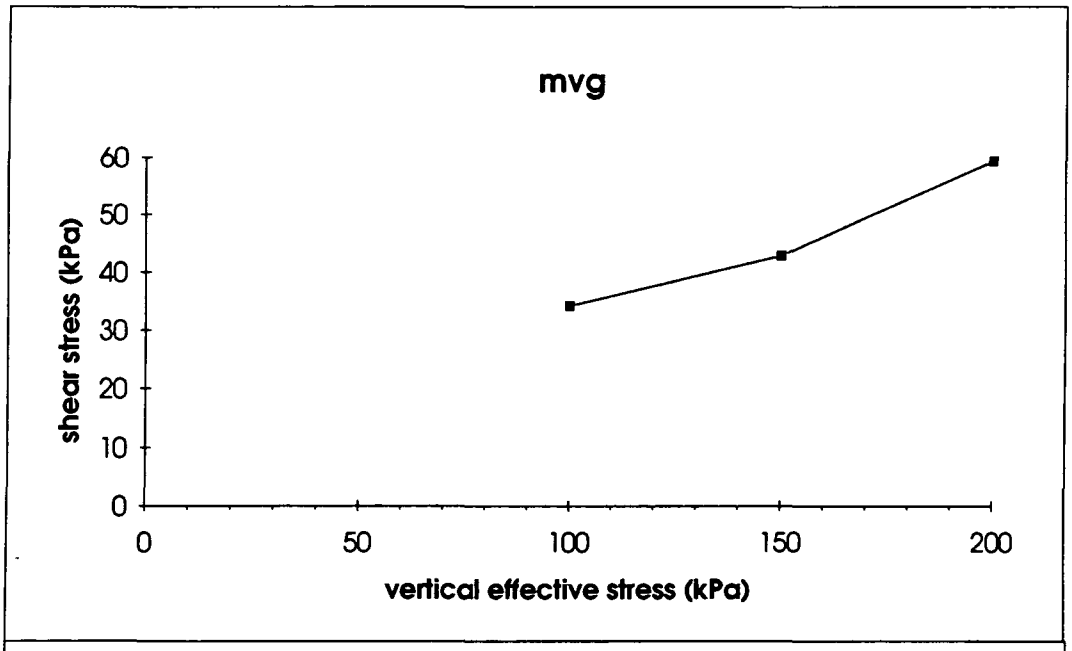
mvg
shear stress (kPa)
60
50
40
30
20
10
0
0
50
100
150
200
vertical effective stress (kPa)

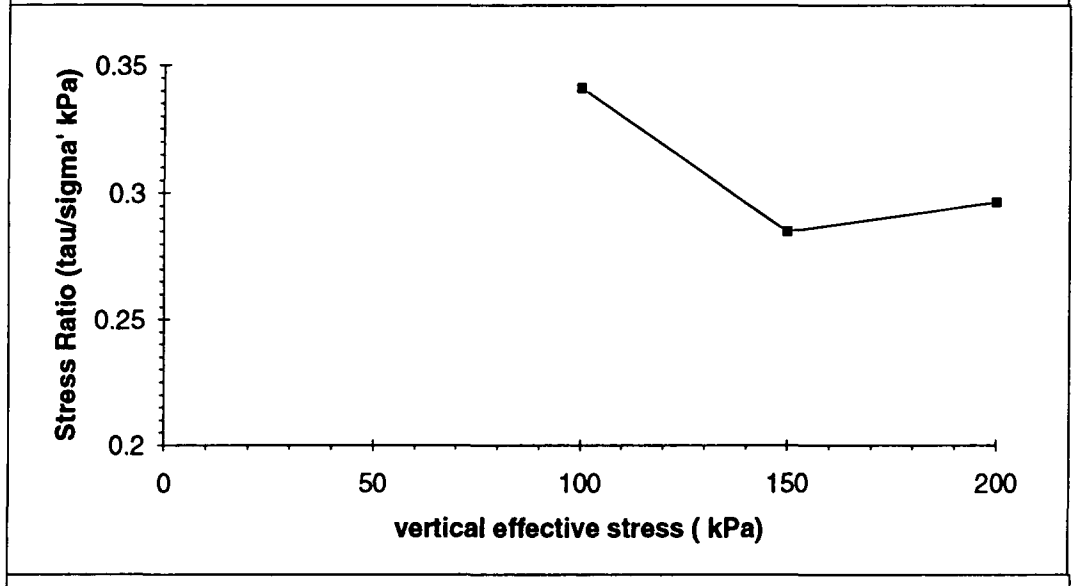
Stress Ratio (tau/sigma' kPa)
0.35
0.3
0.25
0.2
0
50
100
150
200
vertical effective stress (kPa)

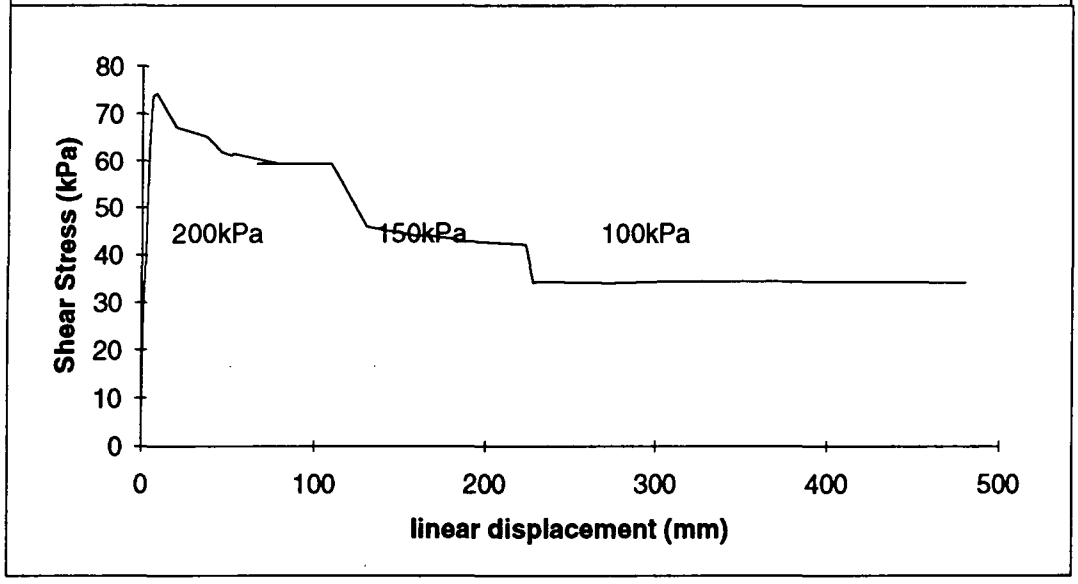
Shear Stress (kPa)
80
70
60
50
40
30
20
10
0
200kPa
150kPa
100kPa
0
100
200
300
400
500
linear displacement (mm)

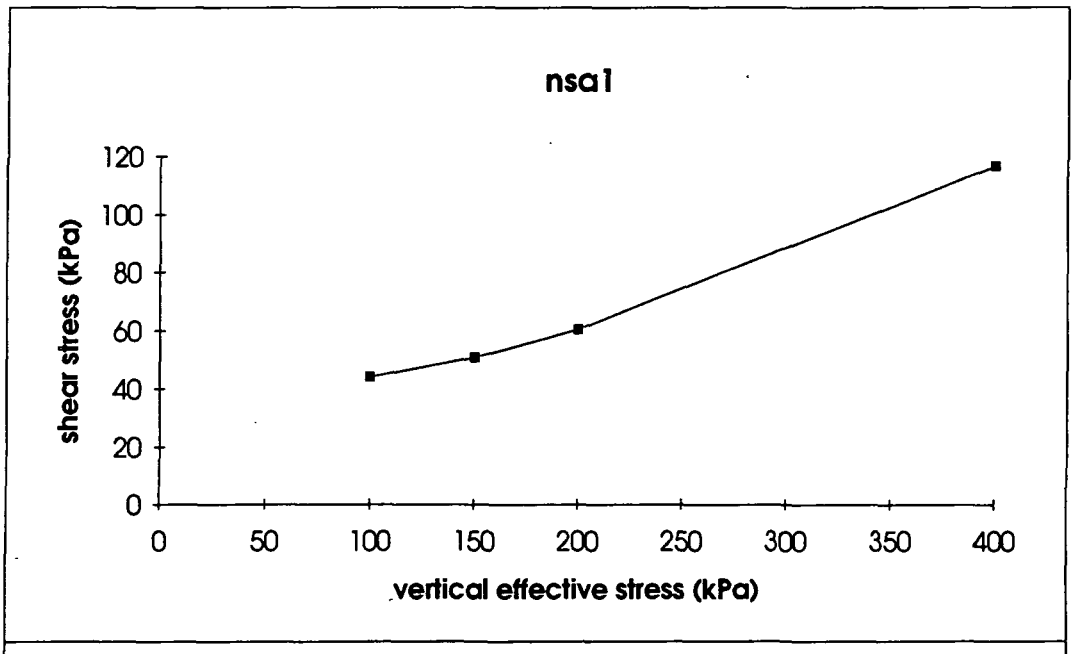
nsa1
shear stress (kPa)
120
100
80
60
40
20
0
0
50
100
150
200
250
300
350
400
vertical effective stress (kPa)

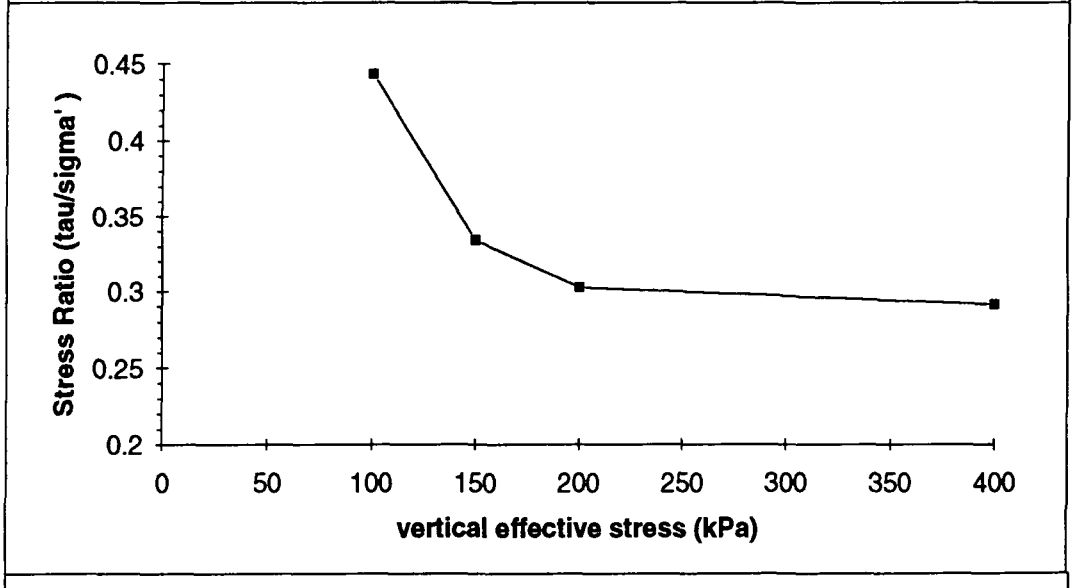
Stress Ratio (tau/sigma')
0.45
0.4
0.35
0.3
0.25
0.2
0
50
100
150
200
250
300
350
400
vertical effective stress (kPa)

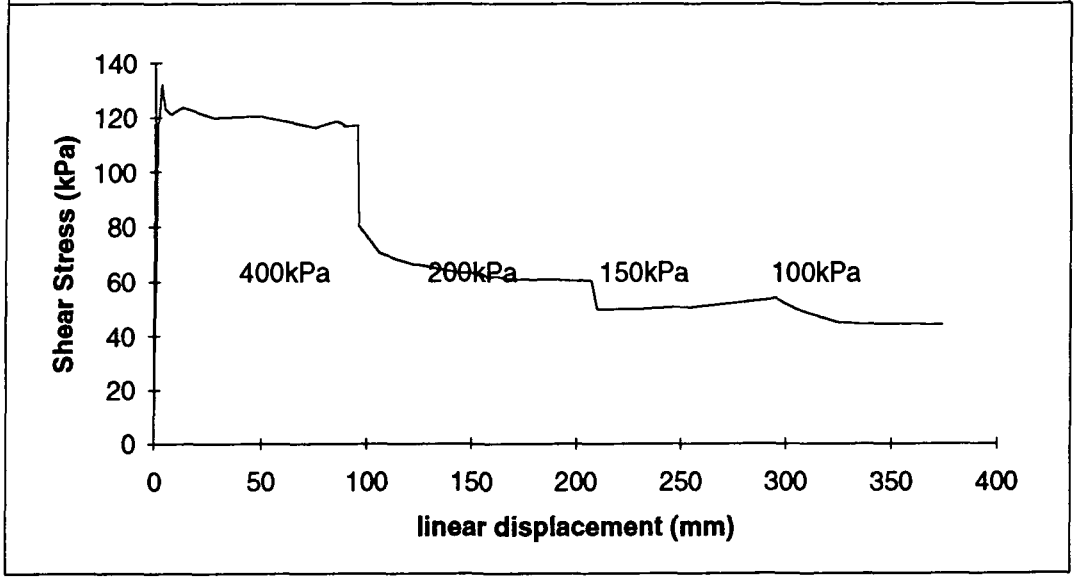
Shear Stress (kPa)
140
120
100
80
60
40
20
0
400kPa
200kPa
150kPa
100kPa
0
50
100
150
200
250
300
350
400
linear displacement (mm)

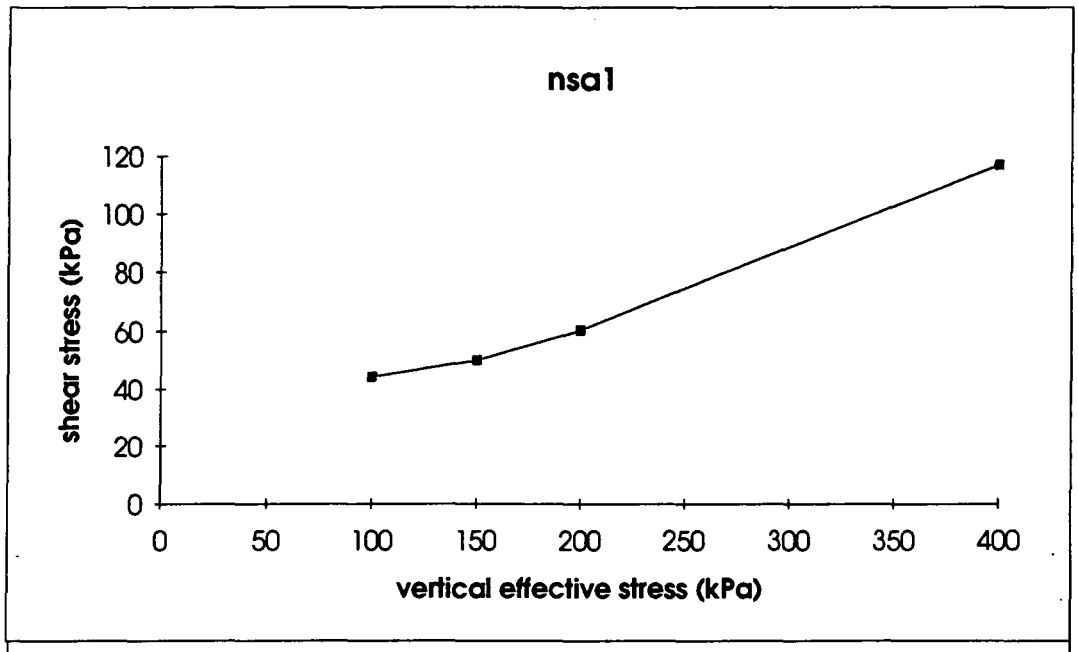
nsa1
shear stress (kPa)
120
100
80
60
40
20
0
0
50
100
150
200
250
300
350
400
vertical effective stress (kPa)

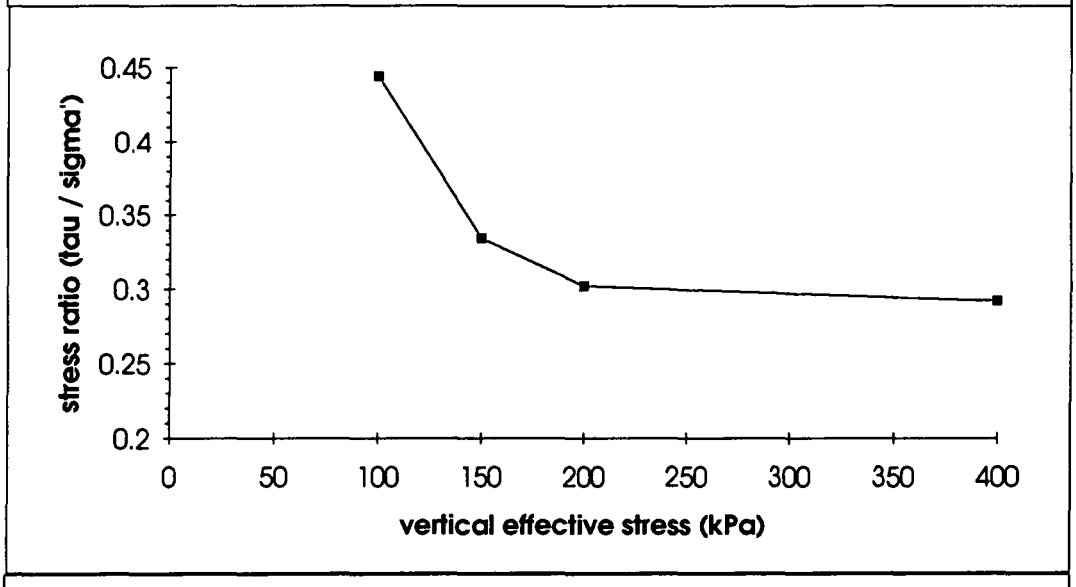
stress ratio (tau / sigma')
0.45
0.4
0.35
0.3
0.25
0.2
0
50
100
150
200
250
300
350
400
vertical effective stress (kPa)

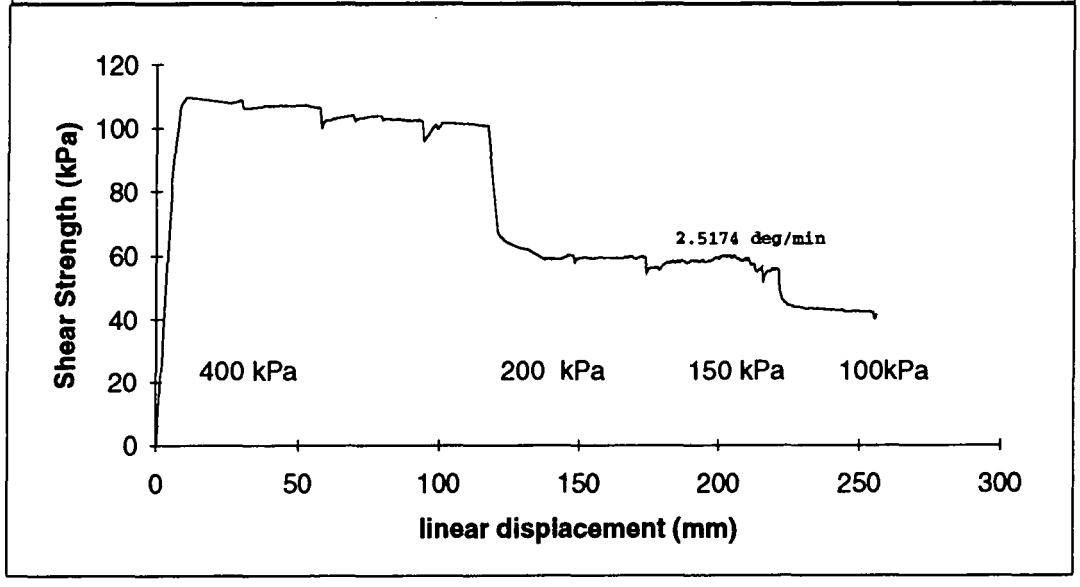
Shear Strength (kPa)
120
100
80
60
40
20
0
2.5174 deg/min
400 kPa
200 kPa
150 kPa
100kPa
0
50
100
150
200
250
300
linear displacement (mm)

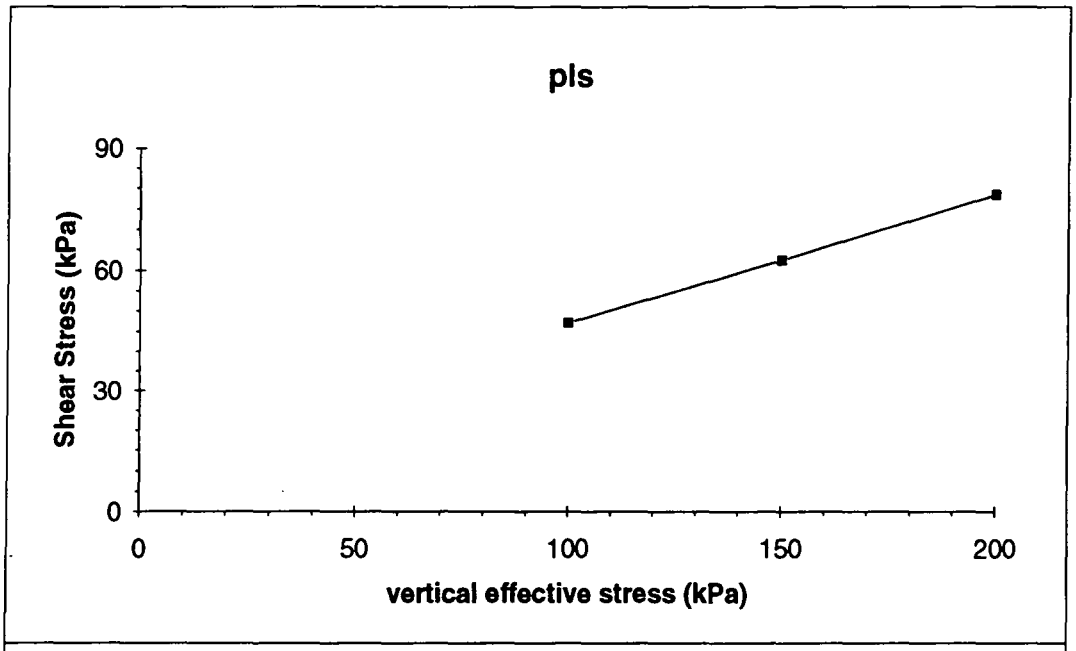
pls
Shear Stress (kPa)
90
60
30
0
0
50
100
150
200
vertical effective stress (kPa)

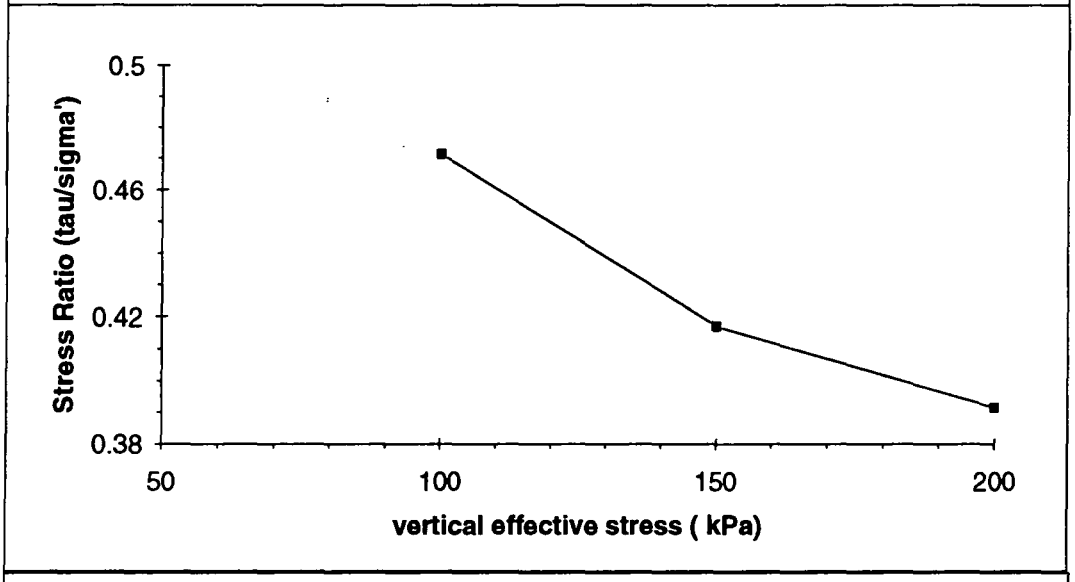
Stress Ratio (tau/sigma')
0.5
0.46
0.42
0.38
50
100
150
200
vertical effective stress (kPa)

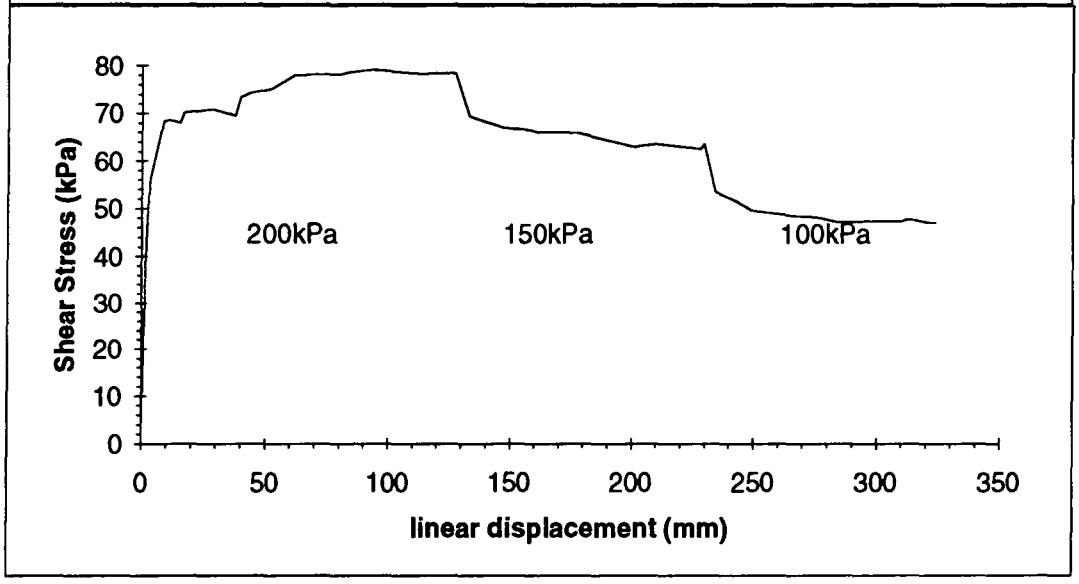
Shear Stress (kPa)
80
70
60
50
40
30
20
10
0
200kPa
150kPa
100kPa
0
50
100
150
200
250
300
350
linear displacement (mm)

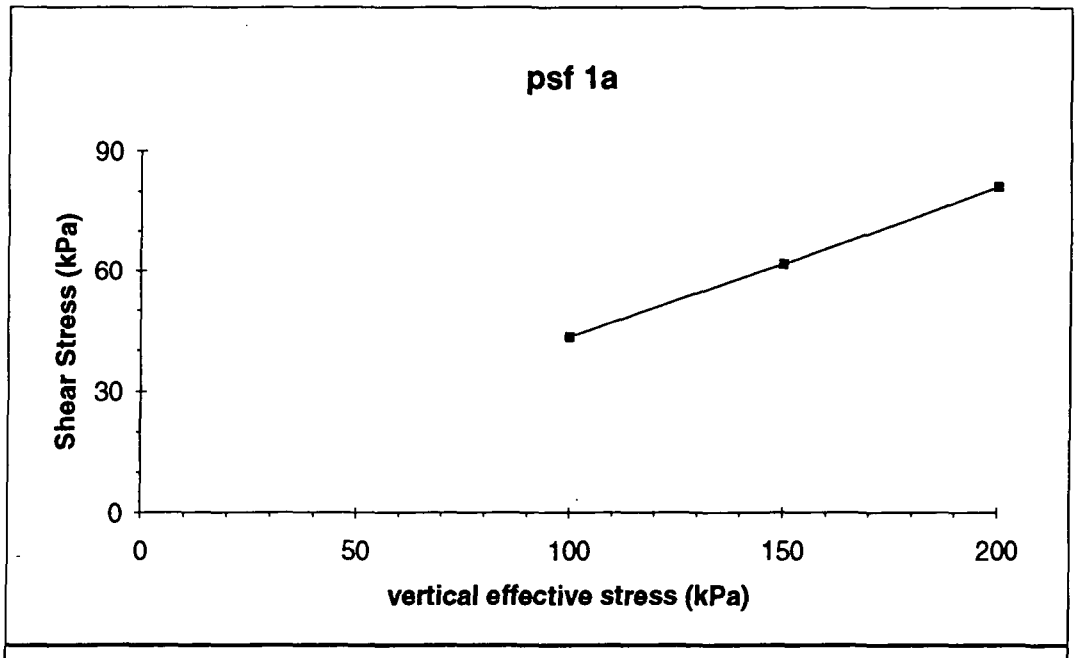
psf 1a
Shear Stress (kPa)
90
60
30
0
0
50
100
150
200
vertical effective stress (kPa)

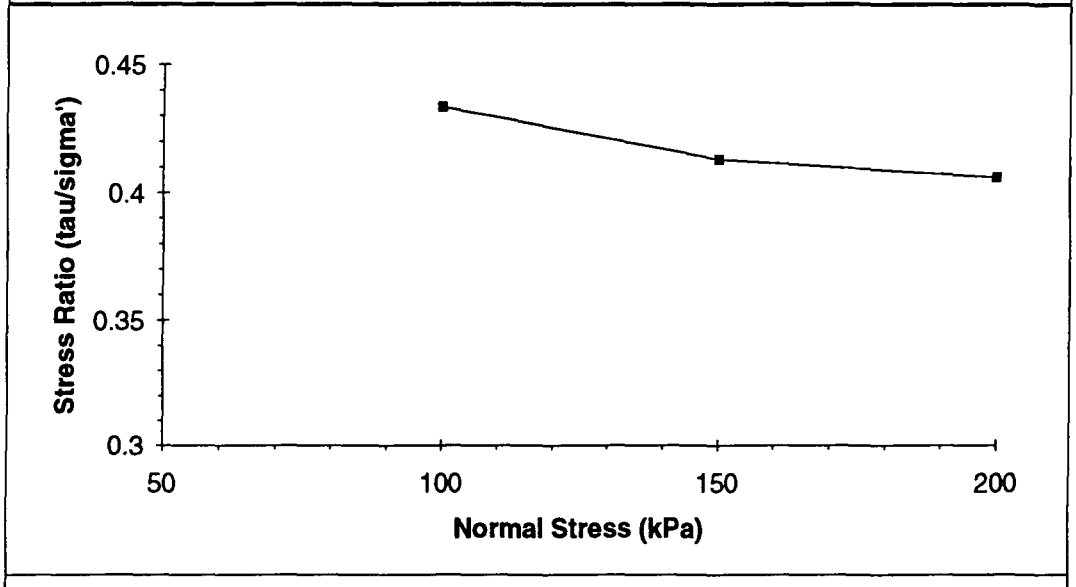
Stress Ratio (tau/sigma')
0.45
0.4
0.35
0.3
50
100
150
200
Normal Stress (kPa)

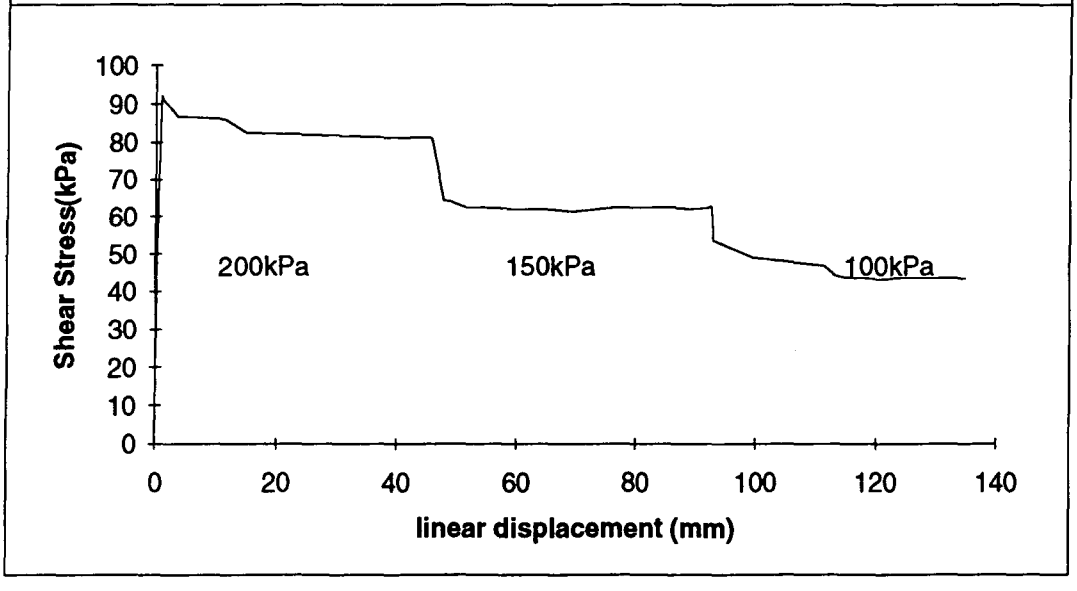
Shear Stress(kPa)
100
90
80
70
60
50
40
30
20
10
0
200kPa
150kPa
100kPa
0
20
40
60
80
100
120
140
linear displacement (mm)

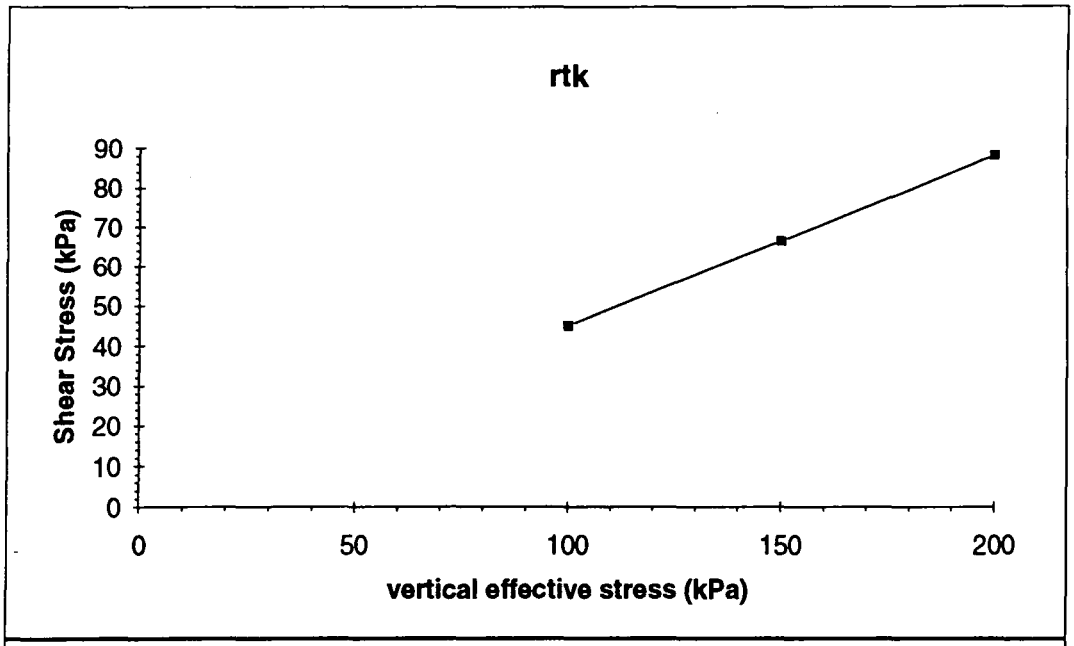
rtk
Shear Stress (kPa)
90
80
70
60
50
40
30
20
10
0
0
50
100
150
200
vertical effective stress (kPa)

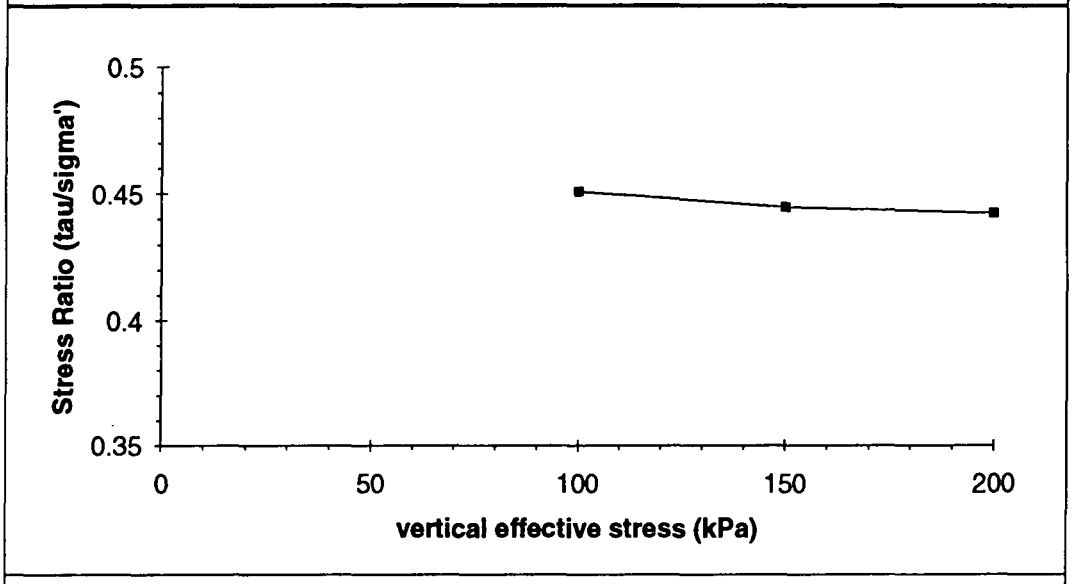
Stress Ratio (tau/sigma')
0.5
0.45
0.4
0.35
0
50
100
150
200
vertical effective stress (kPa)

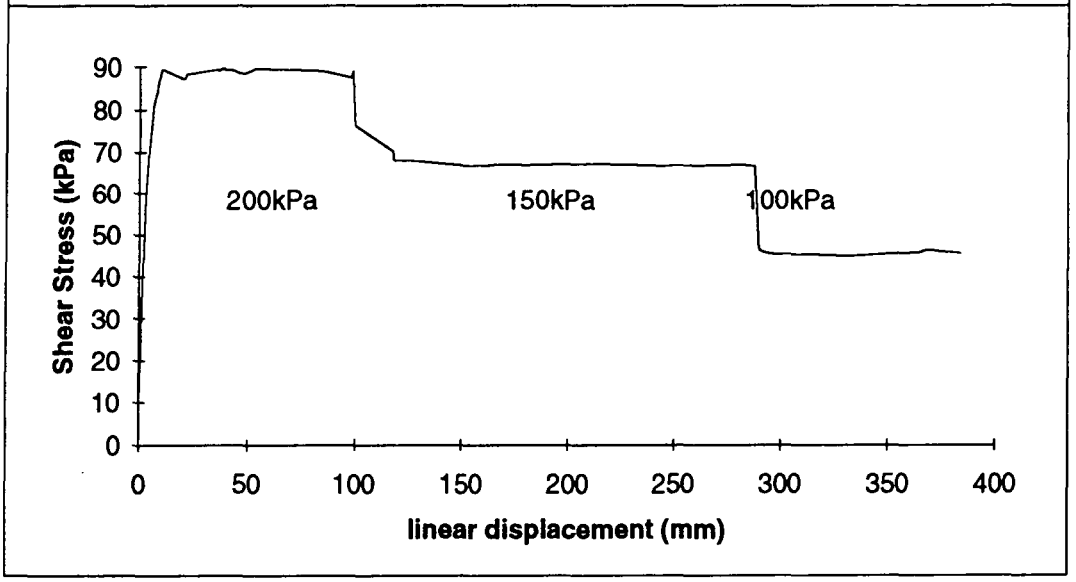
Shear Stress (kPa)
90
80
70
60
50
40
30
20
10
0
200kPa
150kPa
100kPa
0
50
100
150
200
250
300
350
400
linear displacement (mm)

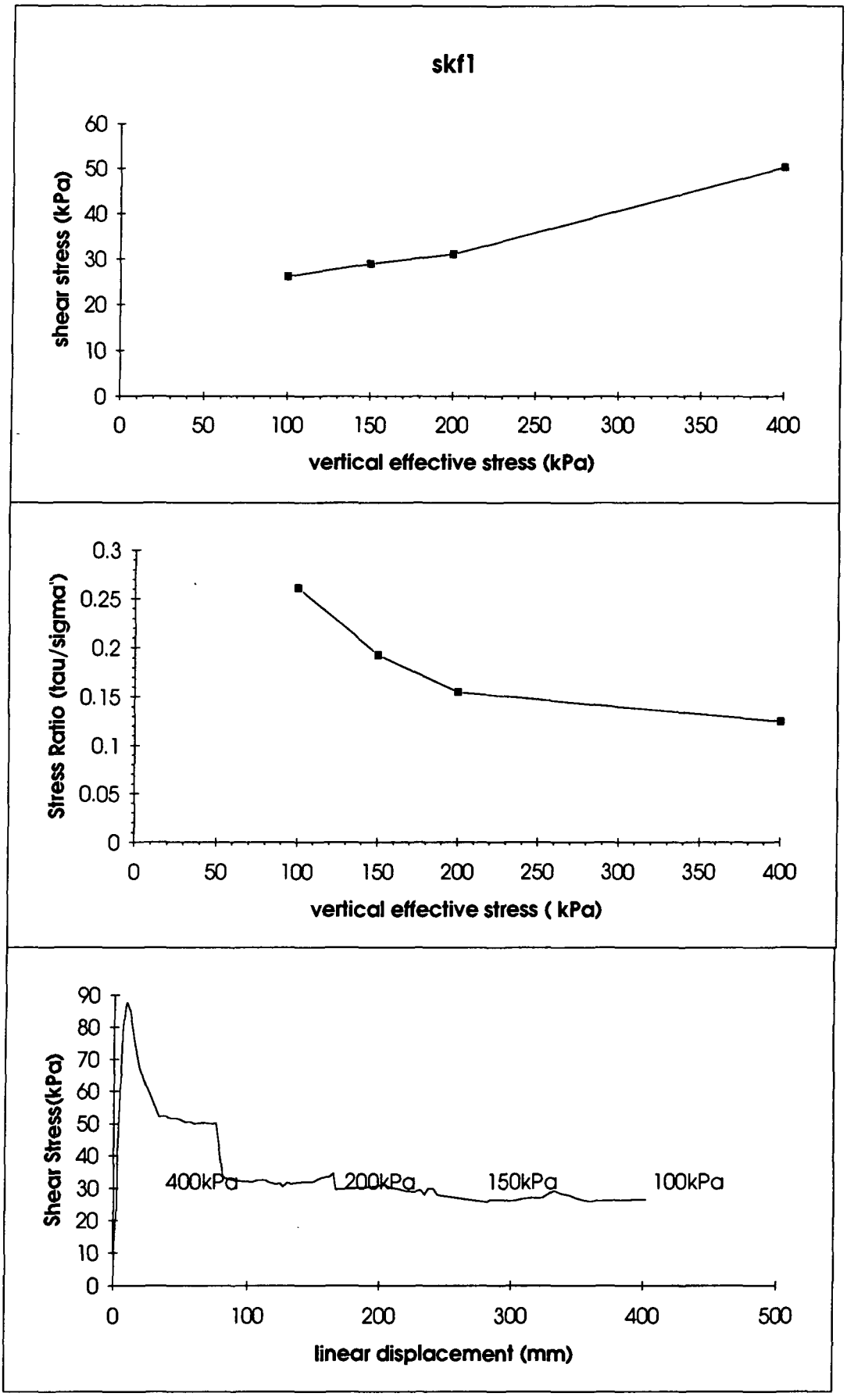
skf1
shear stress (kPa)
0
10
20
30
40
50
60
0
50
100
150
200
250
300
350
400
vertical effective stress (kPa)
Stress Ratio (tau/sigma')
0
0.05
0.1
0.15
0.2
0.25
0.3
0
50
100
150
200
250
300
350
400
vertical effective stress (kPa)
Shear Stress(kPa)
0
10
20
30
40
50
60
70
80
90
400kPa
200kPa
150kPa
100kPa
0
100
200
300
400
500
linear displacement (mm)

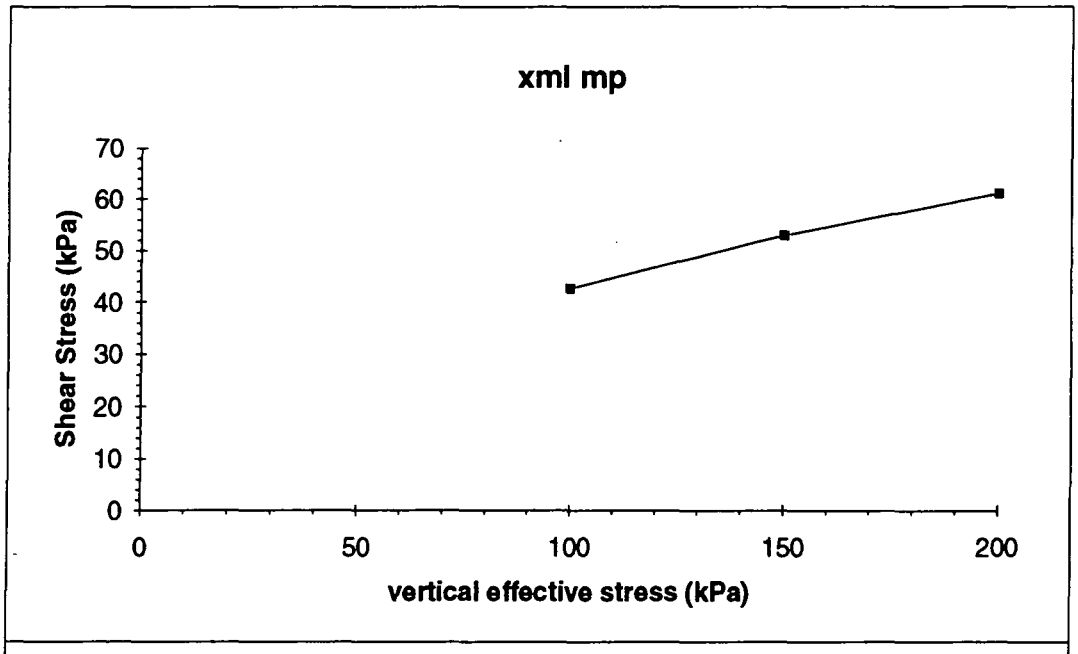
xml mp
Shear Stress (kPa)
70
60
50
40
30
20
10
0
0
50
100
150
200
vertical effective stress (kPa)

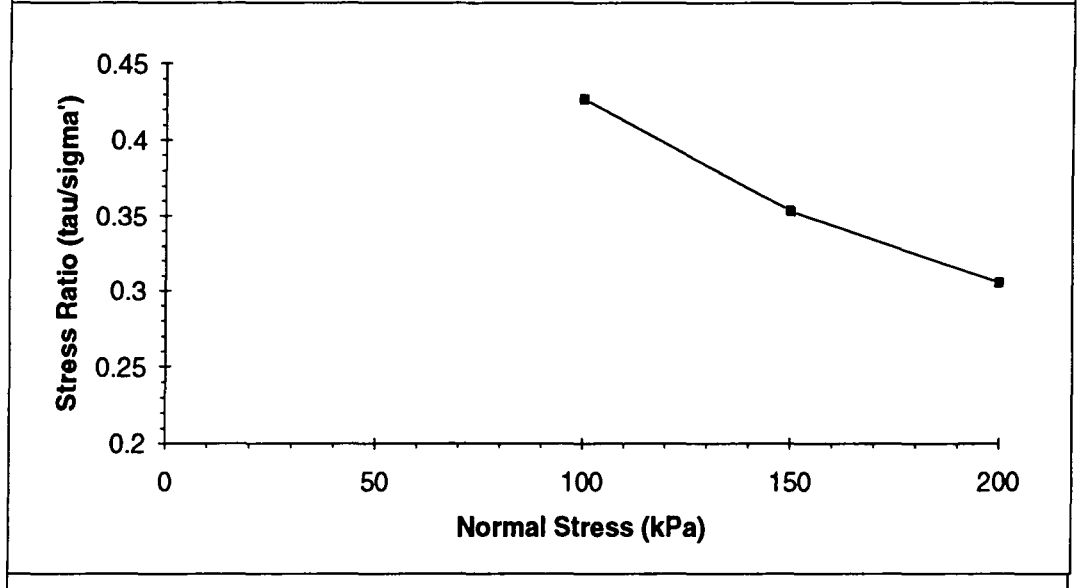
Stress Ratio (tau/sigma')
0.45
0.4
0.35
0.3
0.25
0.2
0
50
100
150
200
Normal Stress (kPa)

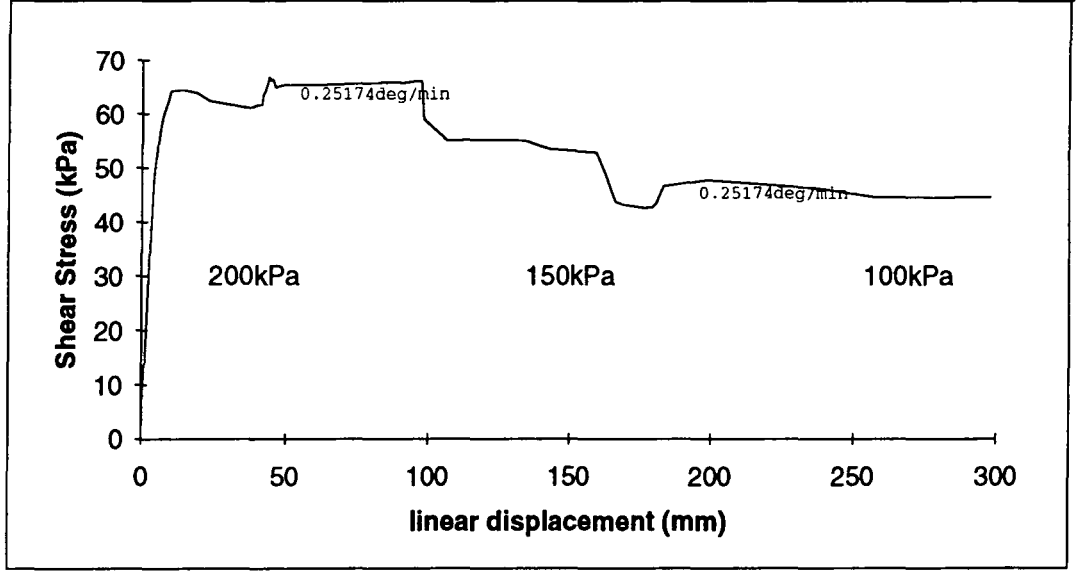
Shear Stress (kPa)
70
60
50
40
30
20
10
0
0.25174deg/min
0.25174deg/min
200kPa
150kPa
100kPa
0
50
100
150
200
250
300
linear displacement (mm)

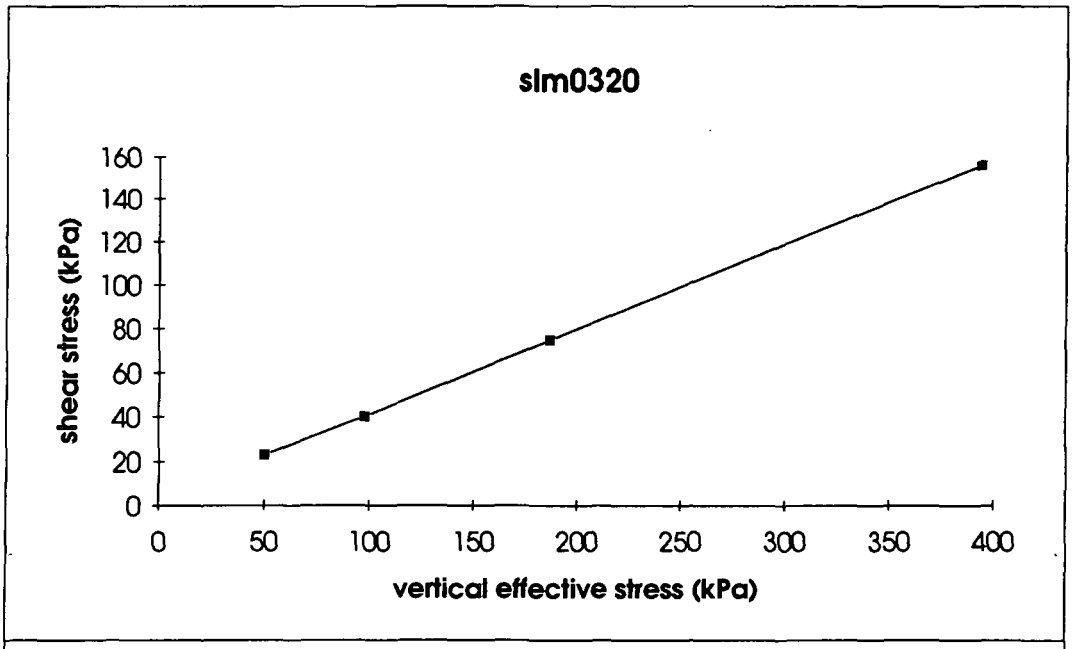
slm0320
shear stress (kPa)
160
140
120
100
80
60
40
20
0
0
50
100
150
200
250
300
350
400
vertical effective stress (kPa)

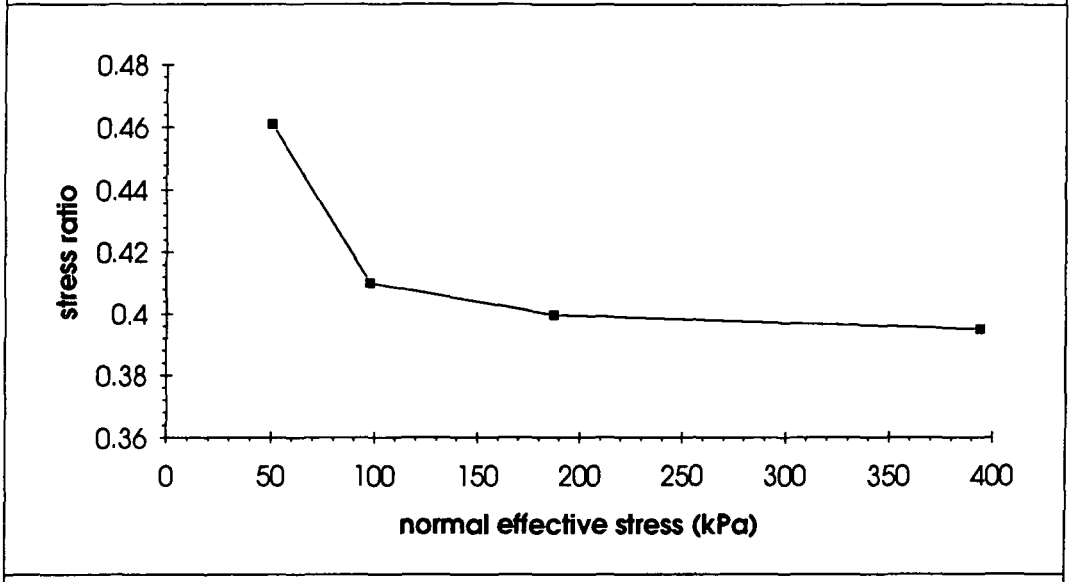
stress ratio
0.48
0.46
0.44
0.42
0.4
0.38
0.36
0
50
100
150
200
250
300
350
400
normal effective stress (kPa)

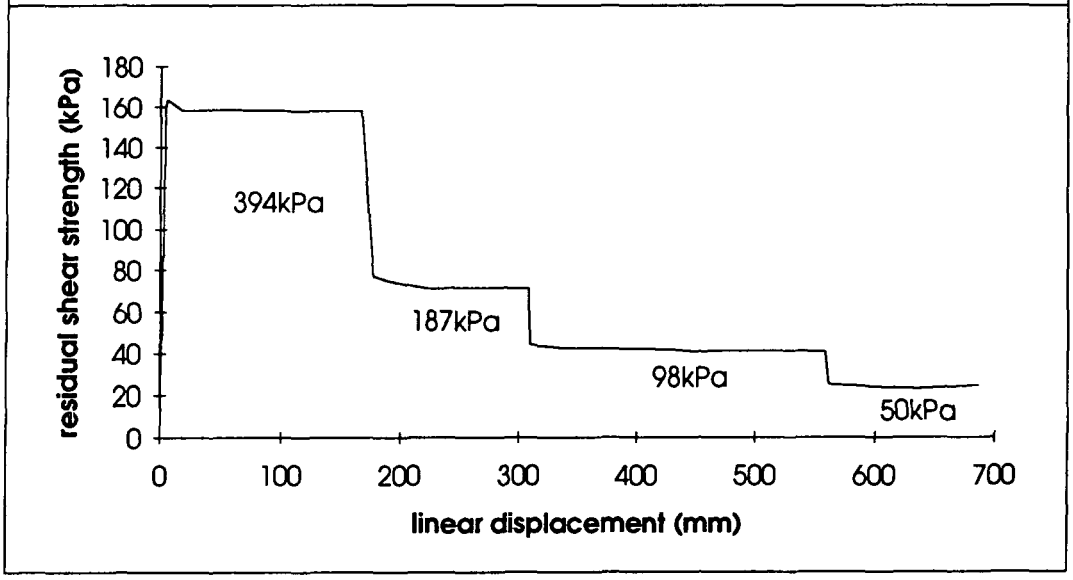
residual shear strength (kPa)
180
160
140
120
100
80
60
40
20
0
394kPa
187kPa
98kPa
50kPa
0
100
200
300
400
500
600
700
linear displacement (mm)

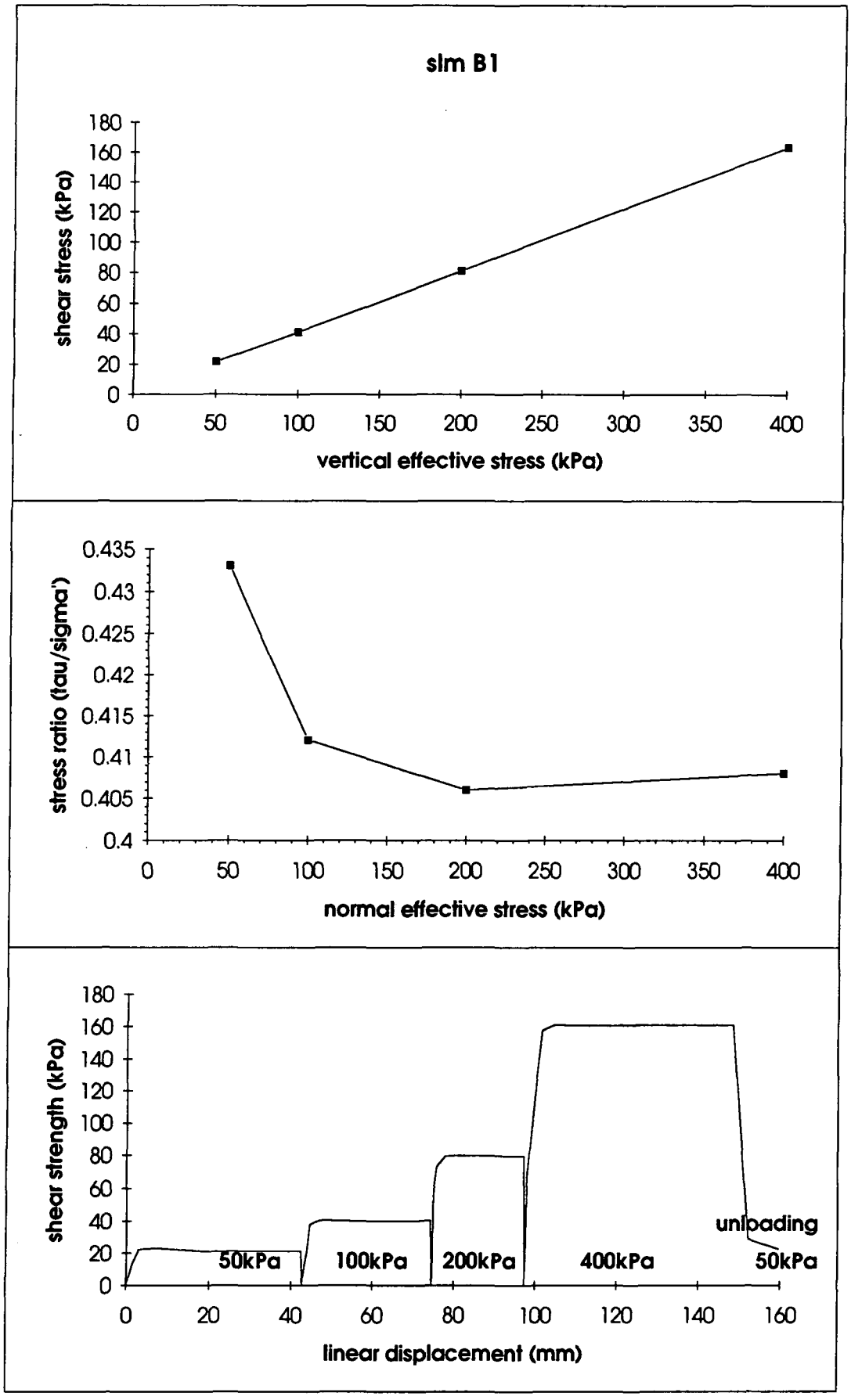
slm B1
shear stress (kPa)
180
160
140
120
100
80
60
40
20
0
0
50
100
150
200
250
300
350
400
vertical effective stress (kPa)
stress ratio (tau/sigma')
0.435
0.43
0.425
0.42
0.415
0.41
0.405
0.4
0
50
100
150
200
250
300
350
400
normal effective stress (kPa)
shear strength (kPa)
180
160
140
120
100
80
60
40
20
0
50kPa
100kPa
200kPa
400kPa
unloading
50kPa
0
20
40
60
80
100
120
140
160
linear displacement (mm)

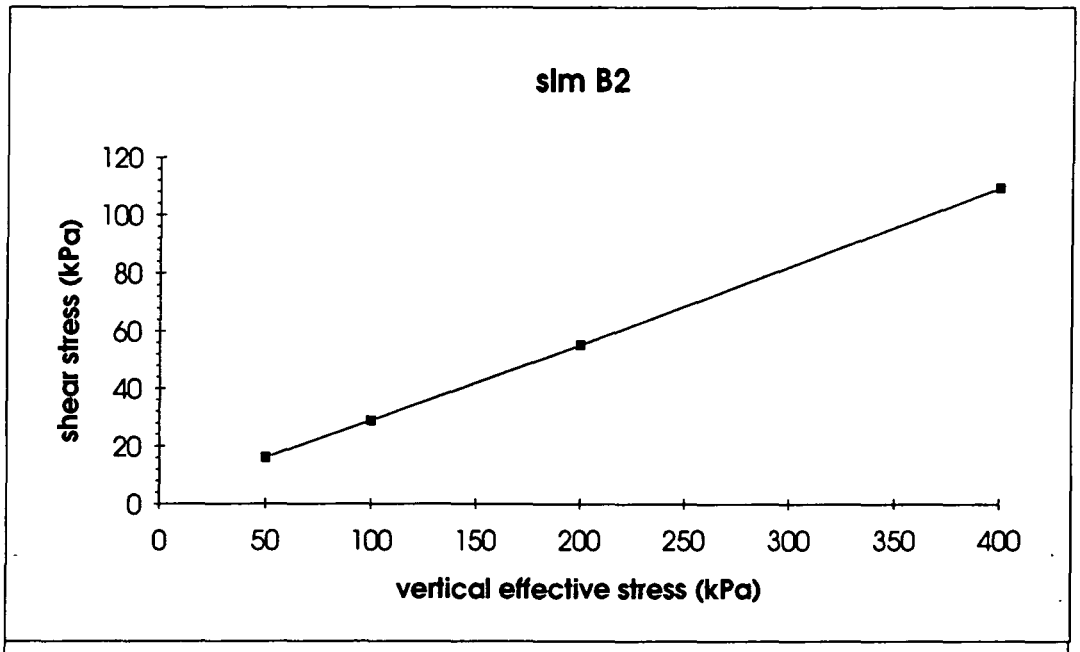
slm B2
shear stress (kPa)
120
100
80
60
40
20
0
0
50
100
150
200
250
300
350
400
vertical effective stress (kPa)

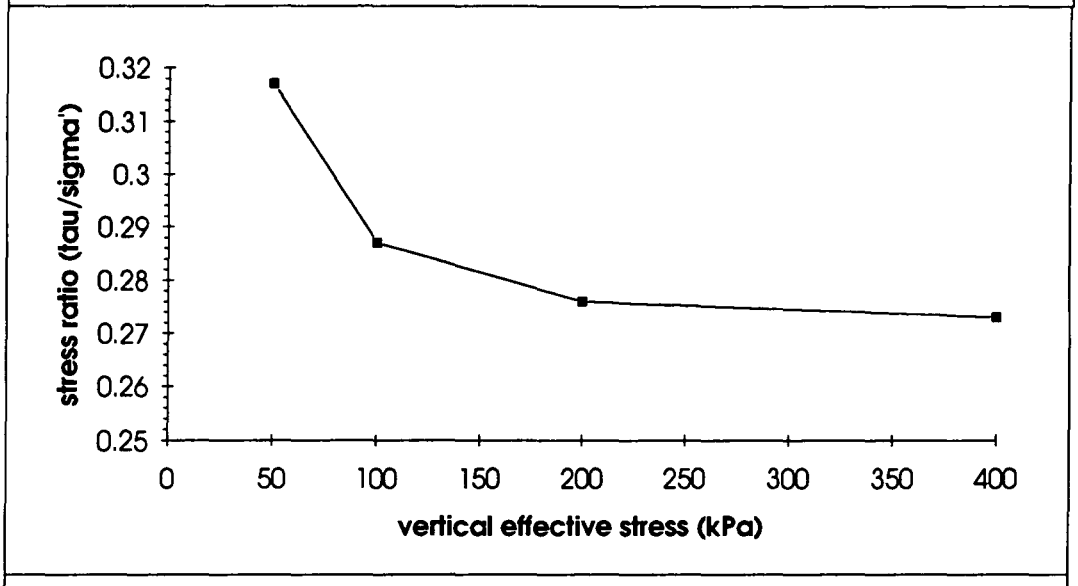
stress ratio (tau/sigma')
0.32
0.31
0.3
0.29
0.28
0.27
0.26
0.25
0
50
100
150
200
250
300
350
400
vertical effective stress (kPa)

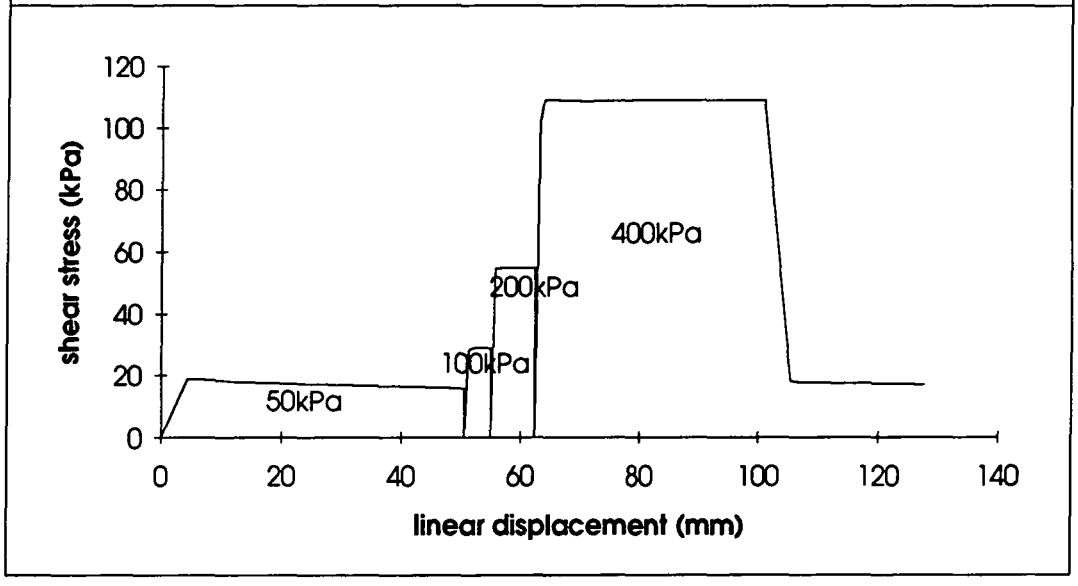
shear stress (kPa)
120
100
80
60
40
20
0
50kPa
100kPa
200kPa
400kPa
0
20
40
60
80
100
120
140
linear displacement (mm)

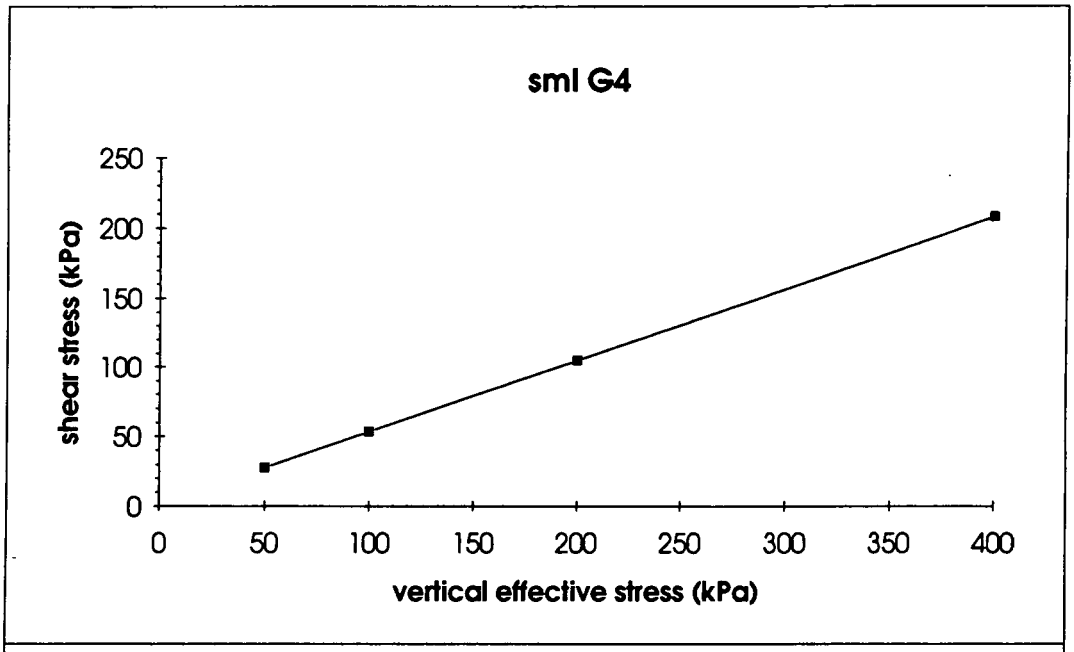
sml G4
shear stress (kPa)
250
200
150
100
50
0
0
50
100
150
200
250
300
350
400
vertical effective stress (kPa)

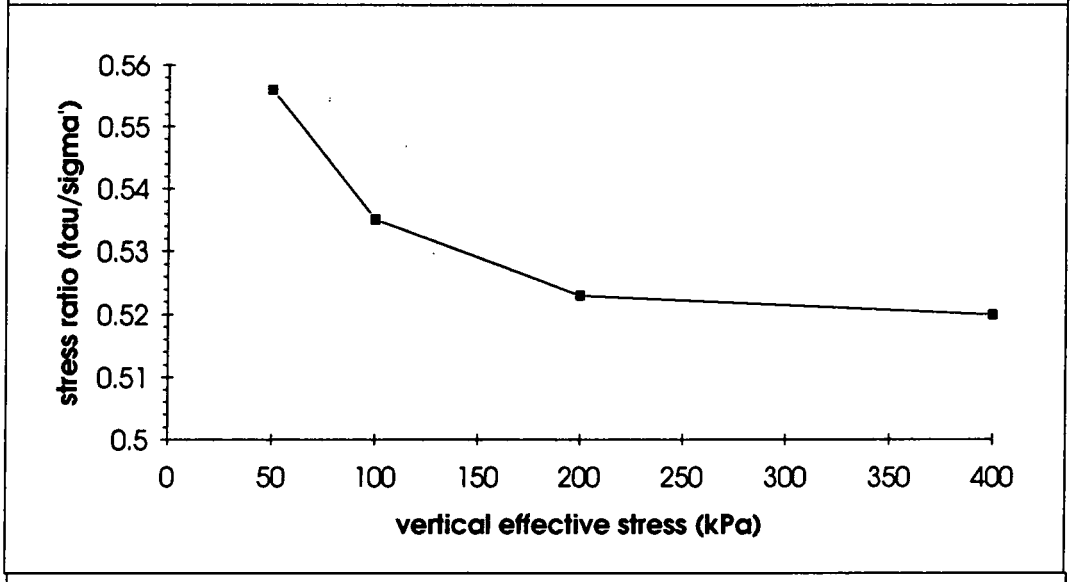
stress ratio (tau/sigma')
0.56
0.55
0.54
0.53
0.52
0.51
0.5
0
50
100
150
200
250
300
350
400
vertical effective stress (kPa)

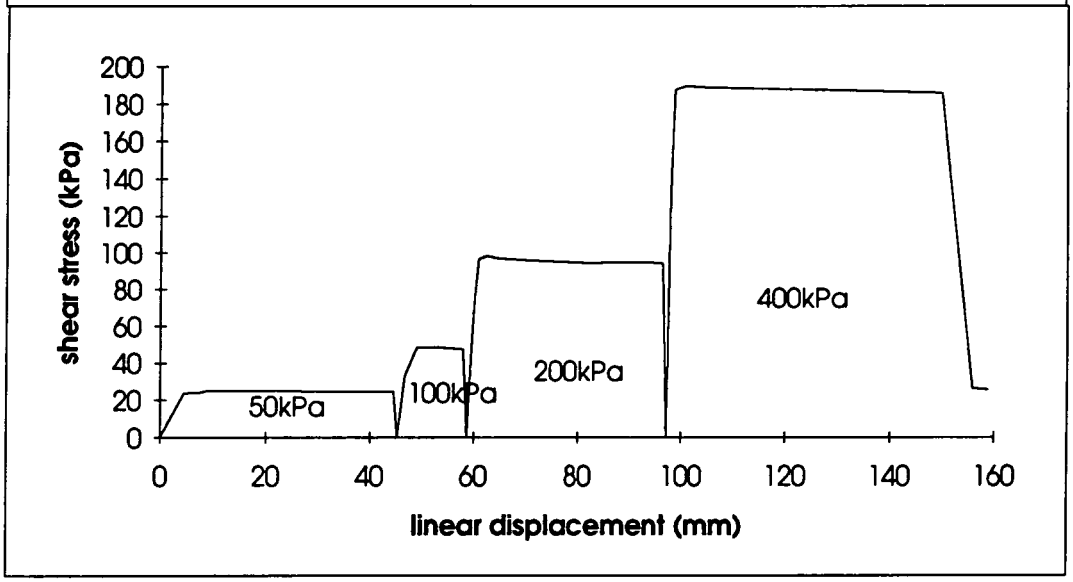
shear stress (kPa)
200
180
160
140
120
100
80
60
40
20
0
0
20
40
60
80
100
120
140
160
50kPa
100kPa
200kPa
400kPa
linear displacement (mm)

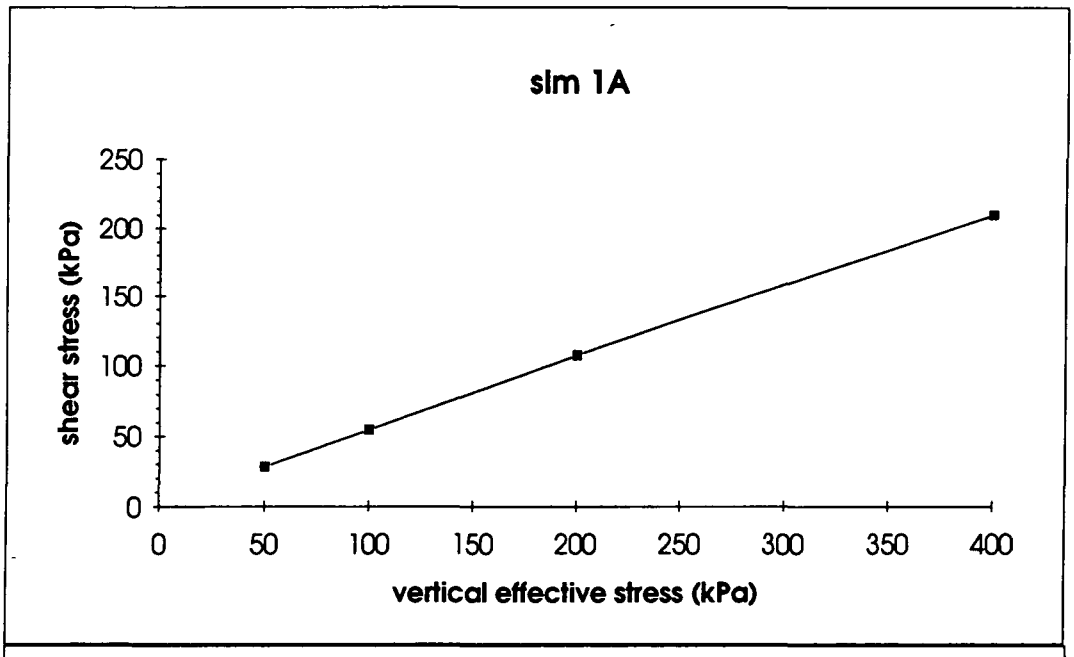
sim 1A
shear stress (kPa)
250
200
150
100
50
0
0
50
100
150
200
250
300
350
400
vertical effective stress (kPa)

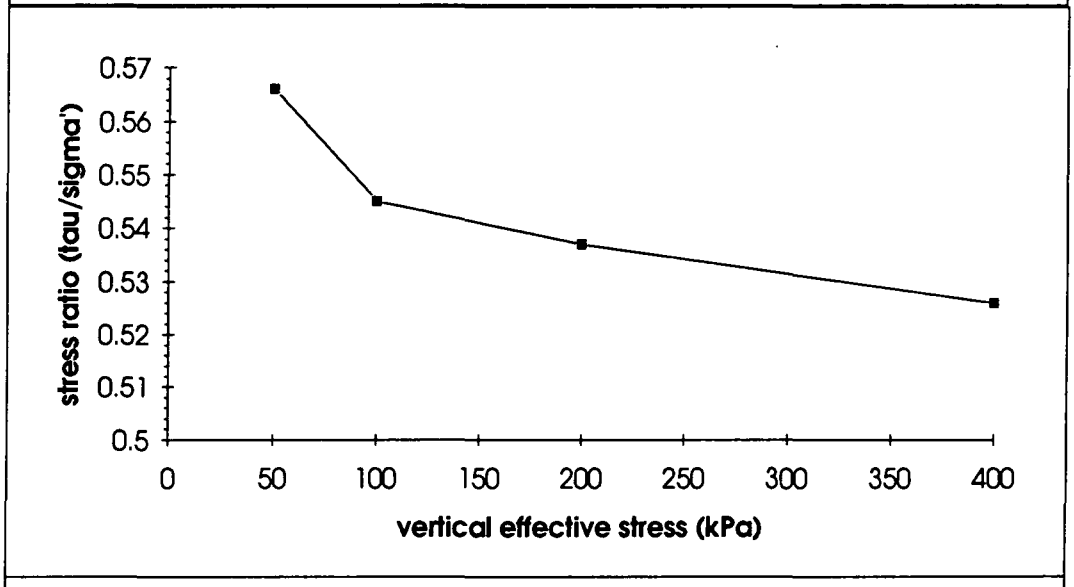
stress ratio (tau/sigma')
0.57
0.56
0.55
0.54
0.53
0.52
0.51
0.5
0
50
100
150
200
250
300
350
400
vertical effective stress (kPa)

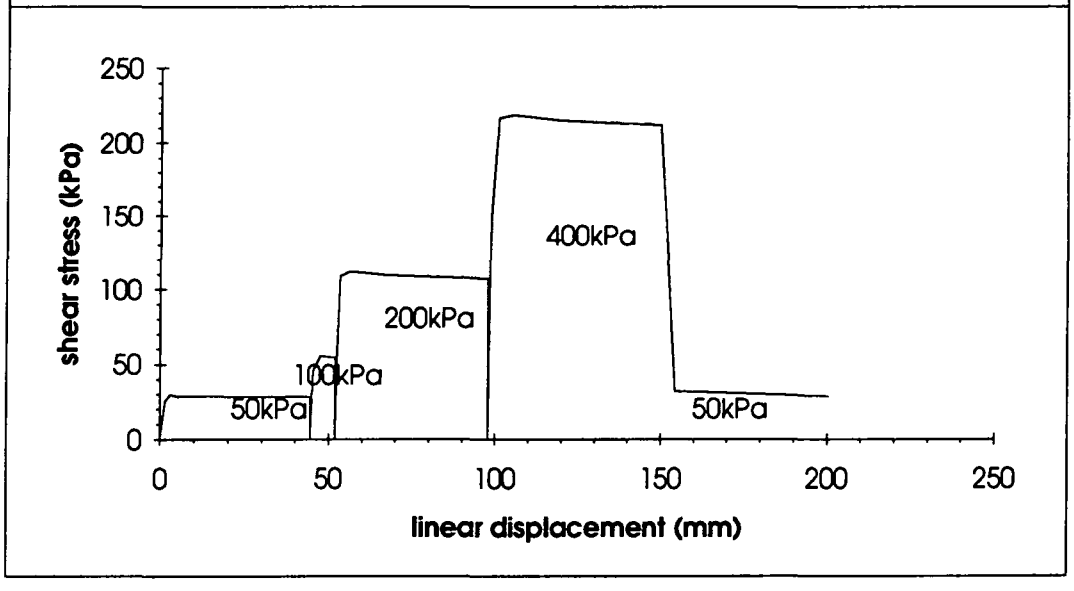
shear stress (kPa)
250
200
150
100
50
0
50kPa
100kPa
200kPa
400kPa
50kPa
0
50
100
150
200
250
linear displacement (mm)

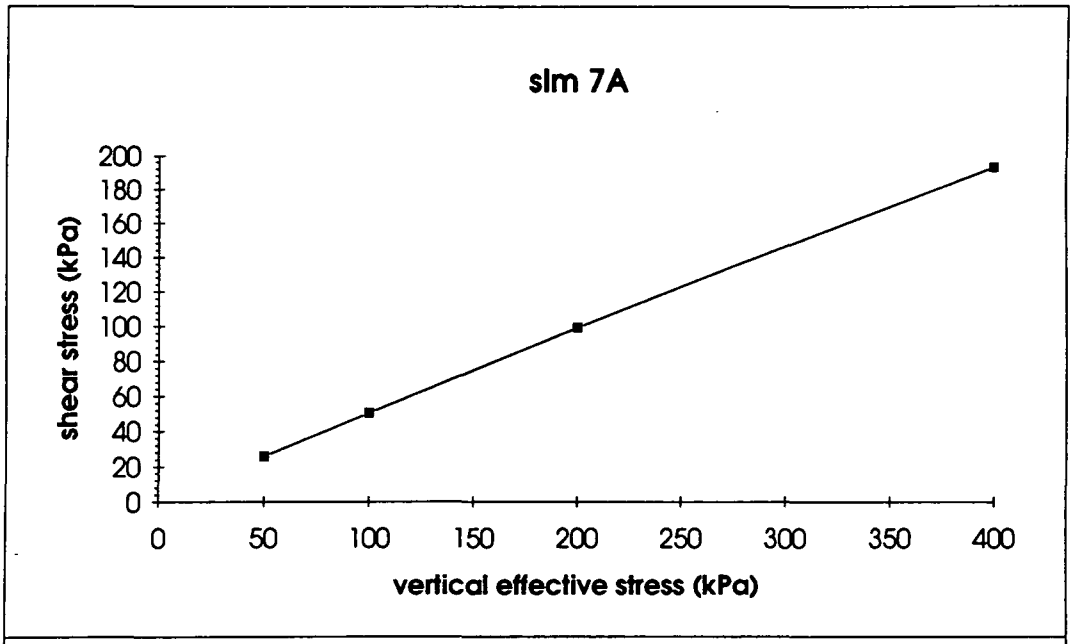
slm 7A
shear stress (kPa)
200
180
160
140
120
100
80
60
40
20
0
0
50
100
150
200
250
300
350
400
vertical effective stress (kPa)

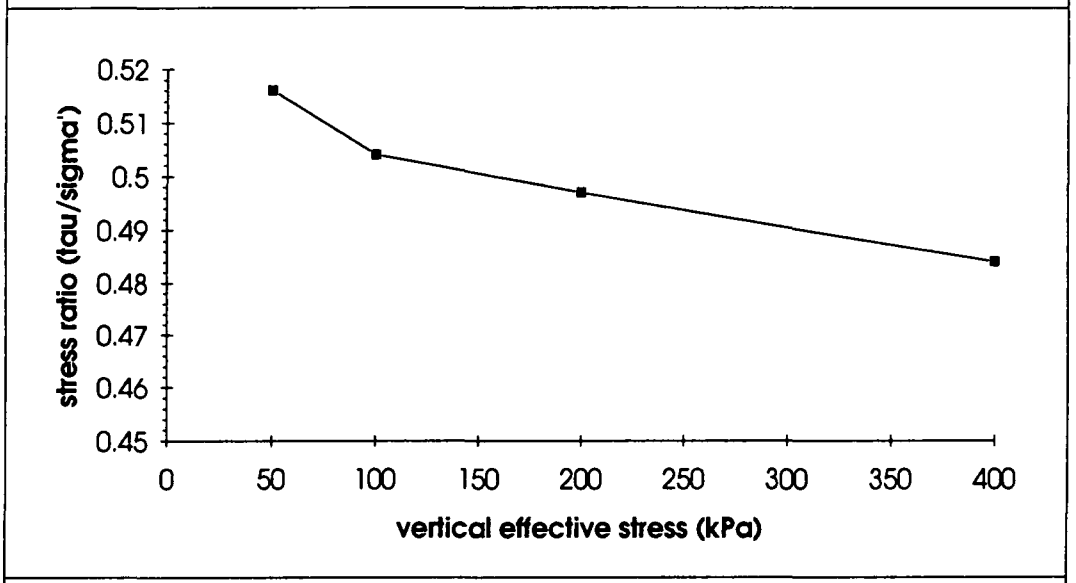
stress ratio (tau/sigma')
0.52
0.51
0.5
0.49
0.48
0.47
0.46
0.45
0
50
100
150
200
250
300
350
400
vertical effective stress (kPa)

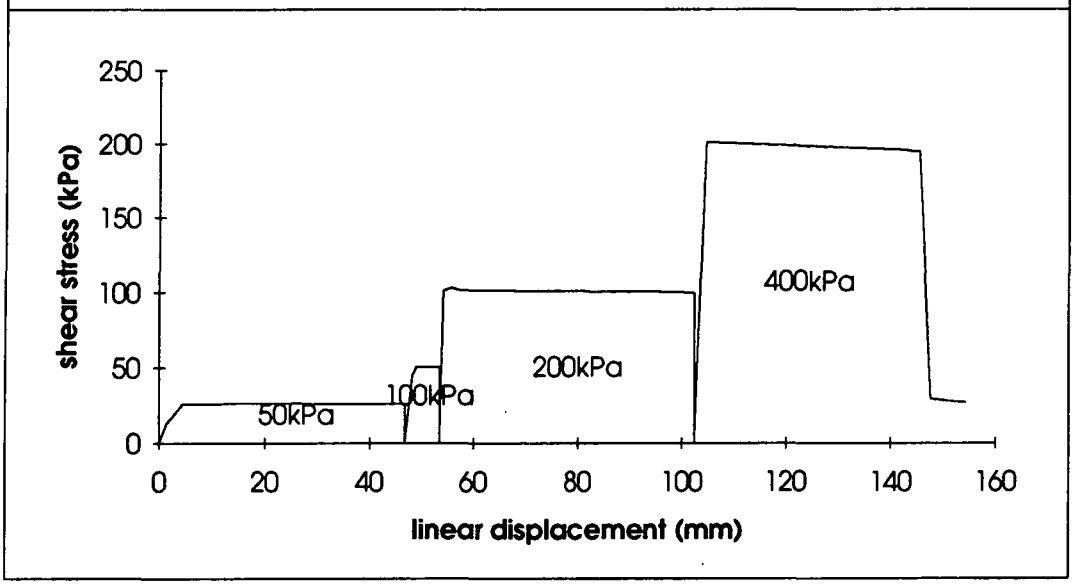
shear stress (kPa)
250
200
150
100
50
0
50kPa
100kPa
200kPa
400kPa
0
20
40
60
80
100
120
140
160
linear displacement (mm)

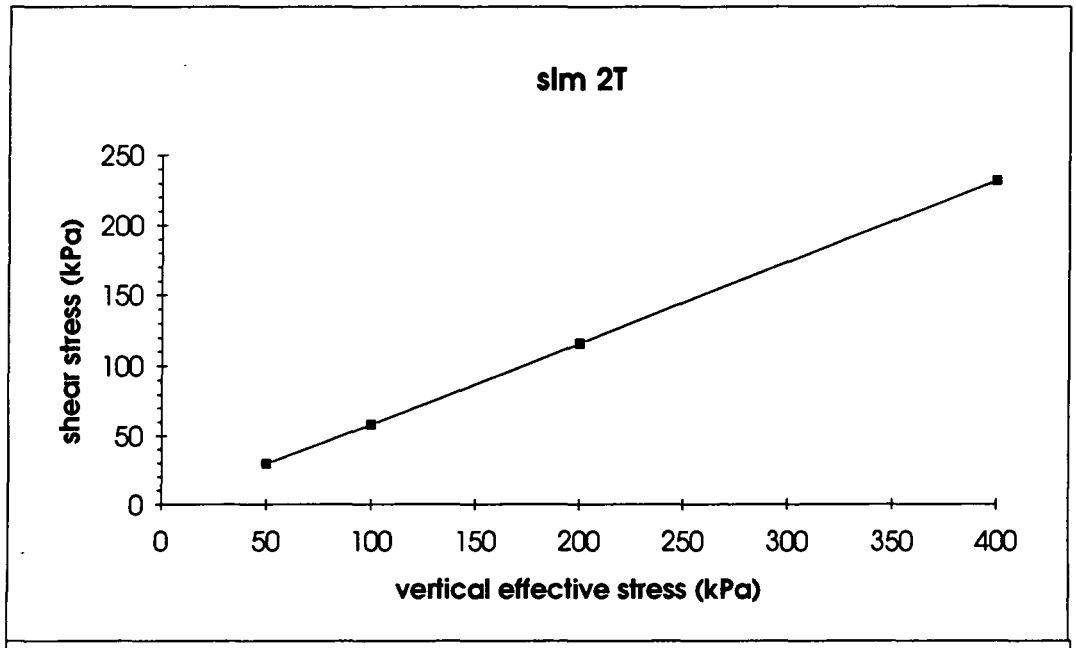
slm 2T
shear stress (kPa)
250
200
150
100
50
0
0
50
100
150
200
250
300
350
400
vertical effective stress (kPa)

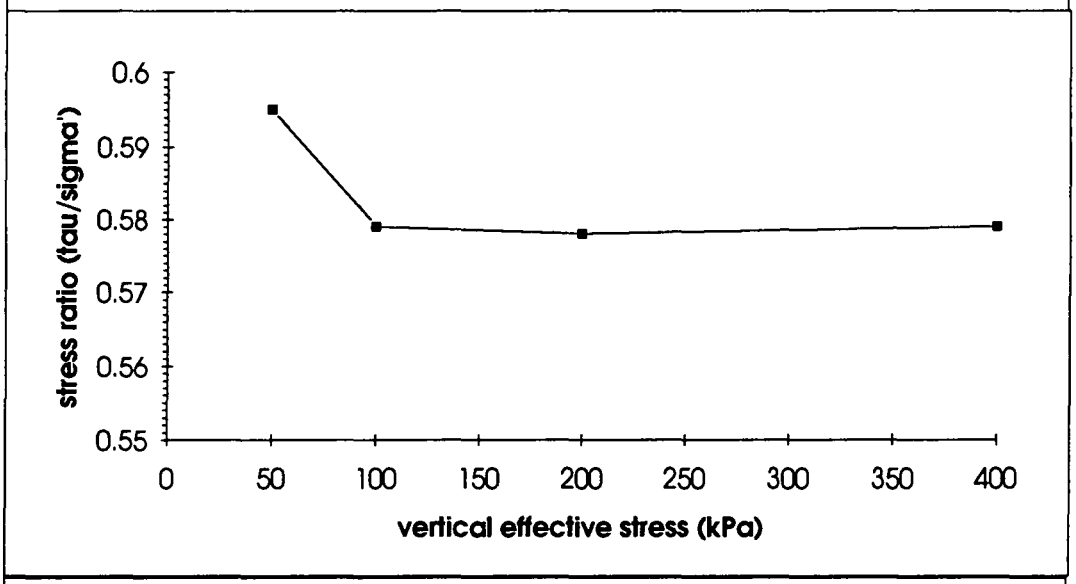
stress ratio (tau/sigma')
0.6
0.59
0.58
0.57
0.56
0.55
0
50
100
150
200
250
300
350
400
vertical effective stress (kPa)

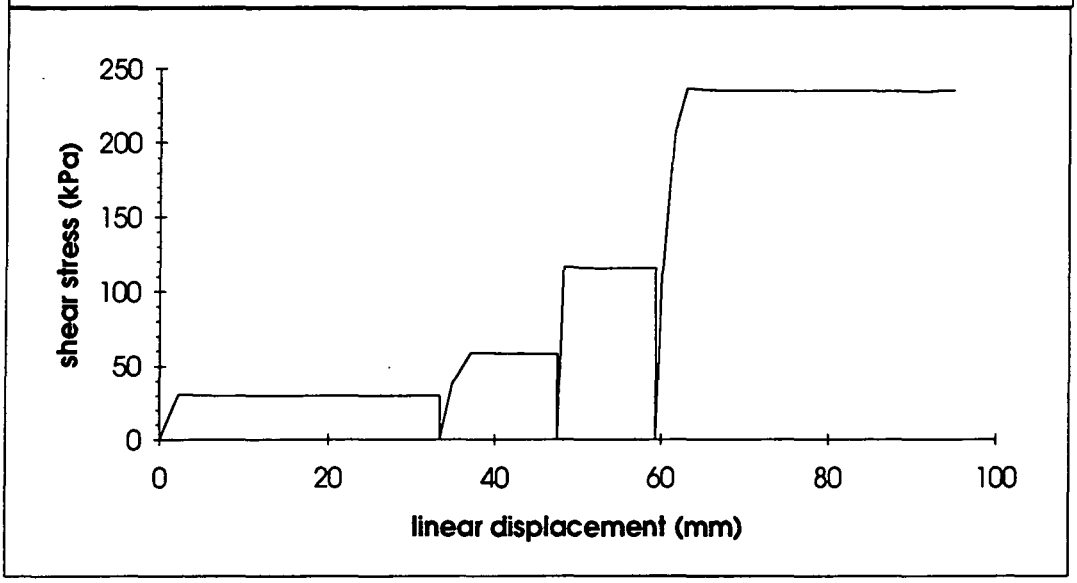
shear stress (kPa)
250
200
150
100
50
0
0
20
40
60
80
100
linear displacement (mm)

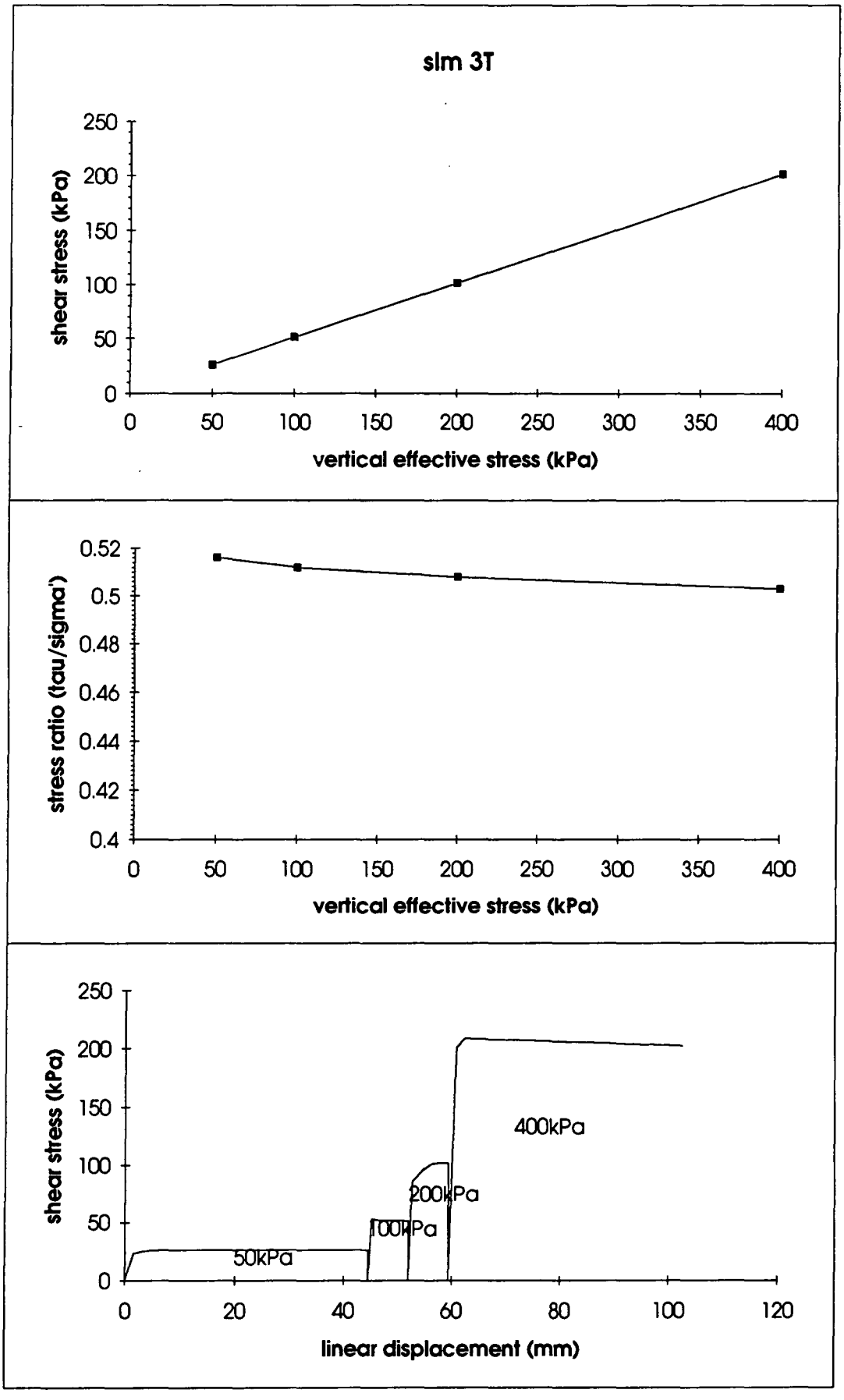
slm 3T
shear stress (kPa)
250
200
150
100
50
0
0
50
100
150
200
250
300
350
400
vertical effective stress (kPa)
stress ratio (tau/sigma')
0.52
0.5
0.48
0.46
0.44
0.42
0.4
0
50
100
150
200
250
300
350
400
vertical effective stress (kPa)
shear stress (kPa)
250
200
150
100
50
0
50kPa
100kPa
200kPa
400kPa
0
20
40
60
80
100
120
linear displacement (mm)

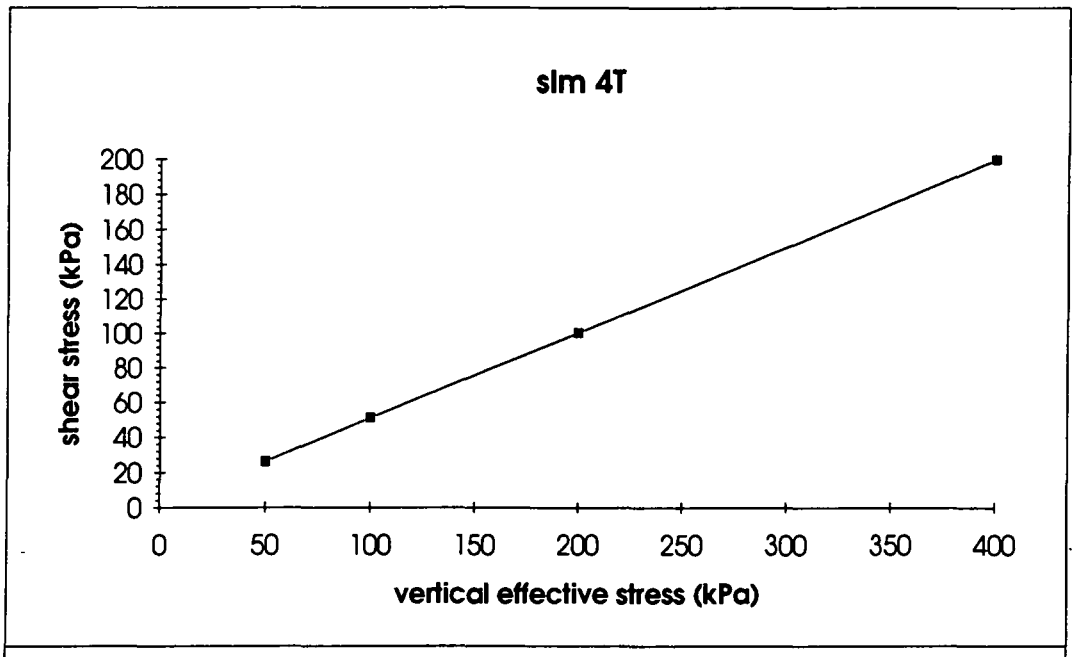
slm 4T
shear stress (kPa)
200
180
160
140
120
100
80
60
40
20
0
0
50
100
150
200
250
300
350
400
vertical effective stress (kPa)

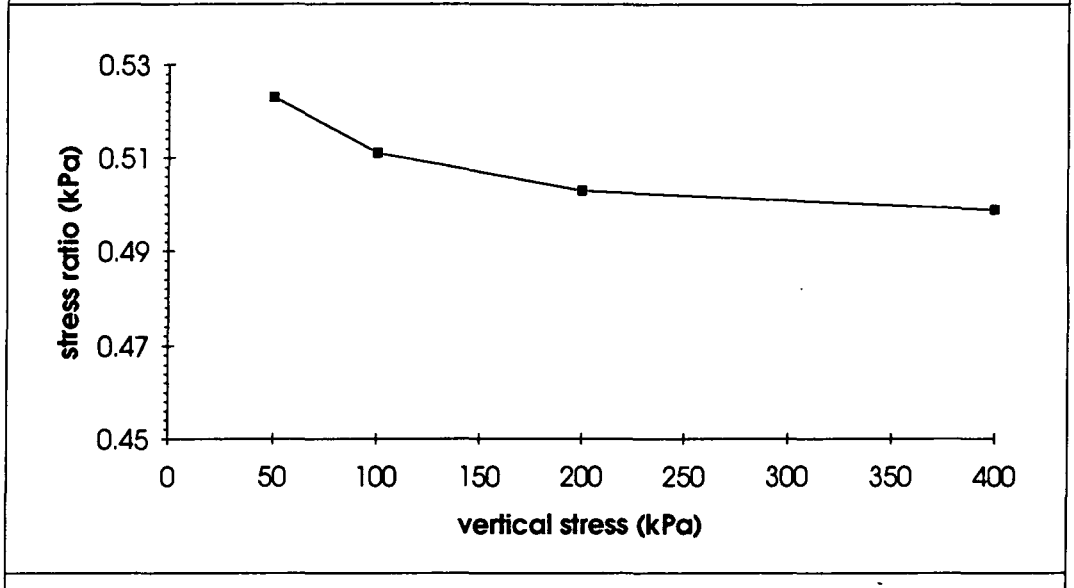
stress ratio (kPa)
0.53
0.51
0.49
0.47
0.45
0
50
100
150
200
250
300
350
400
vertical stress (kPa)

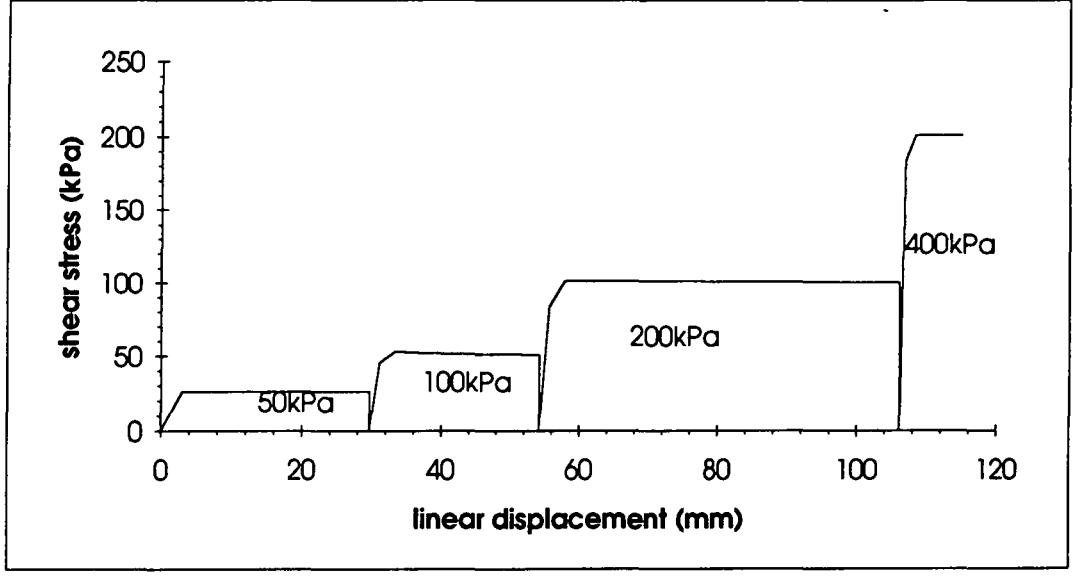
shear stress (kPa)
250
200
150
100
50
0
0
20
40
60
80
100
120
linear displacement (mm)
50kPa
100kPa
200kPa
400kPa

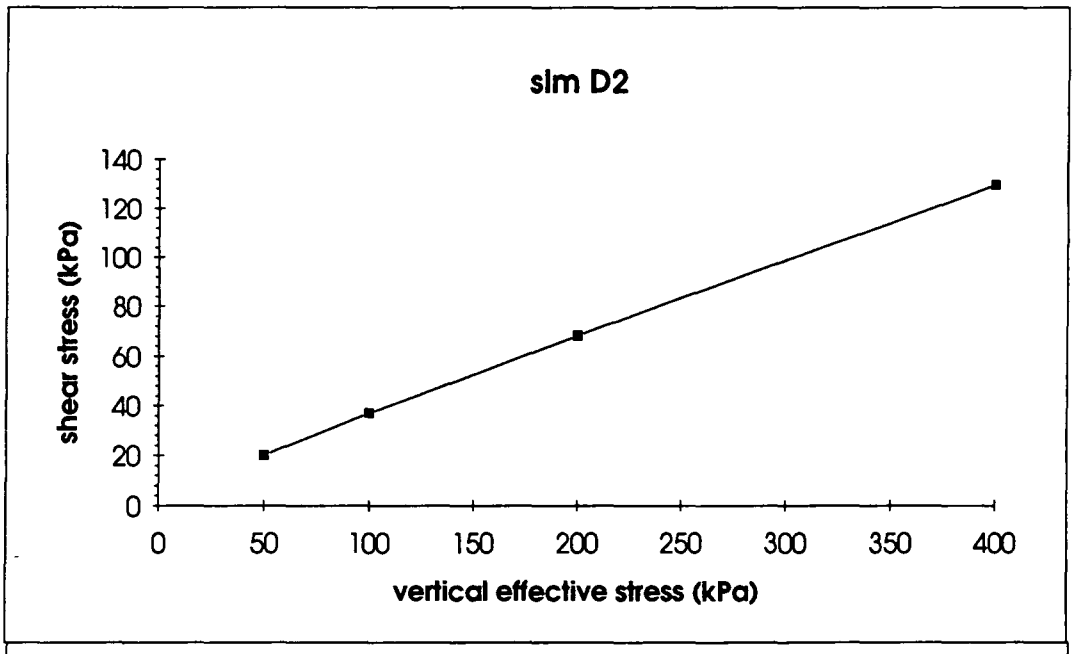
sim D2
shear stress (kPa)
140
120
100
80
60
40
20
0
0
50
100
150
200
250
300
350
400
vertical effective stress (kPa)

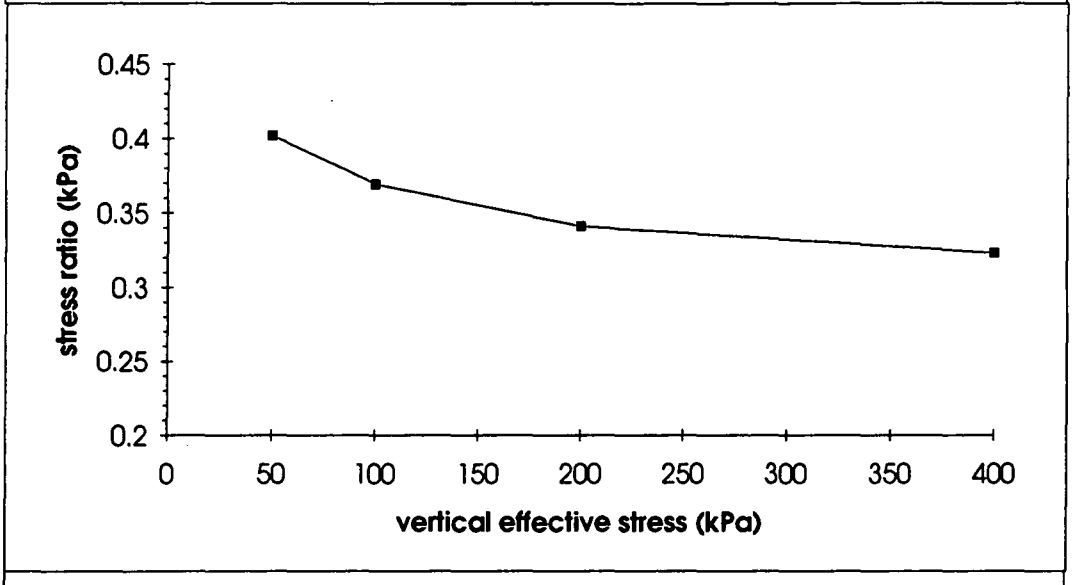
stress ratio (kPa)
0.45
0.4
0.35
0.3
0.25
0.2
0
50
100
150
200
250
300
350
400
vertical effective stress (kPa)

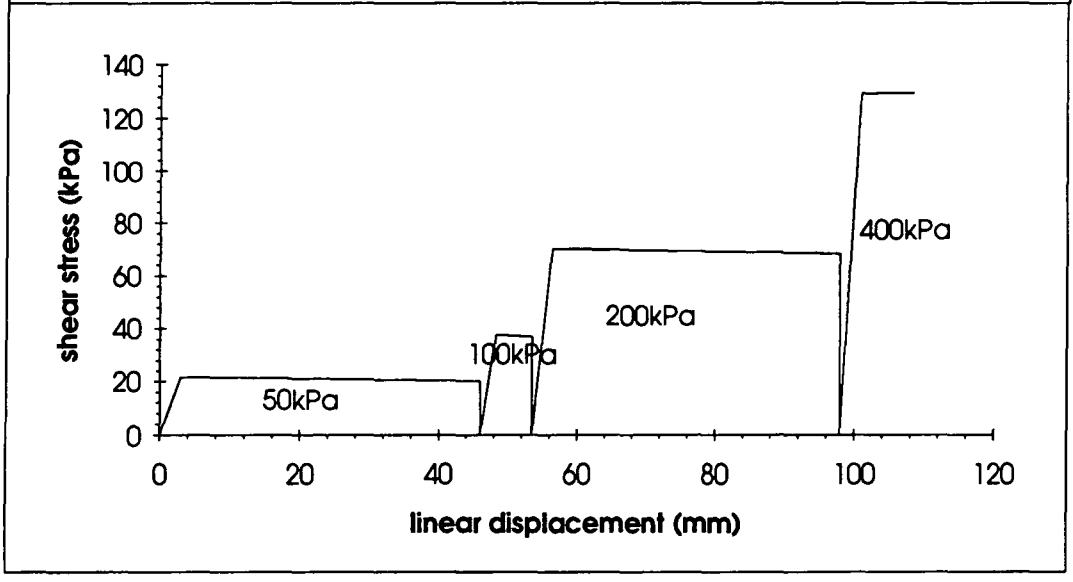
shear stress (kPa)
140
120
100
80
60
40
20
0
0
20
40
60
80
100
120
linear displacement (mm)
50kPa
100kPa
200kPa
400kPa

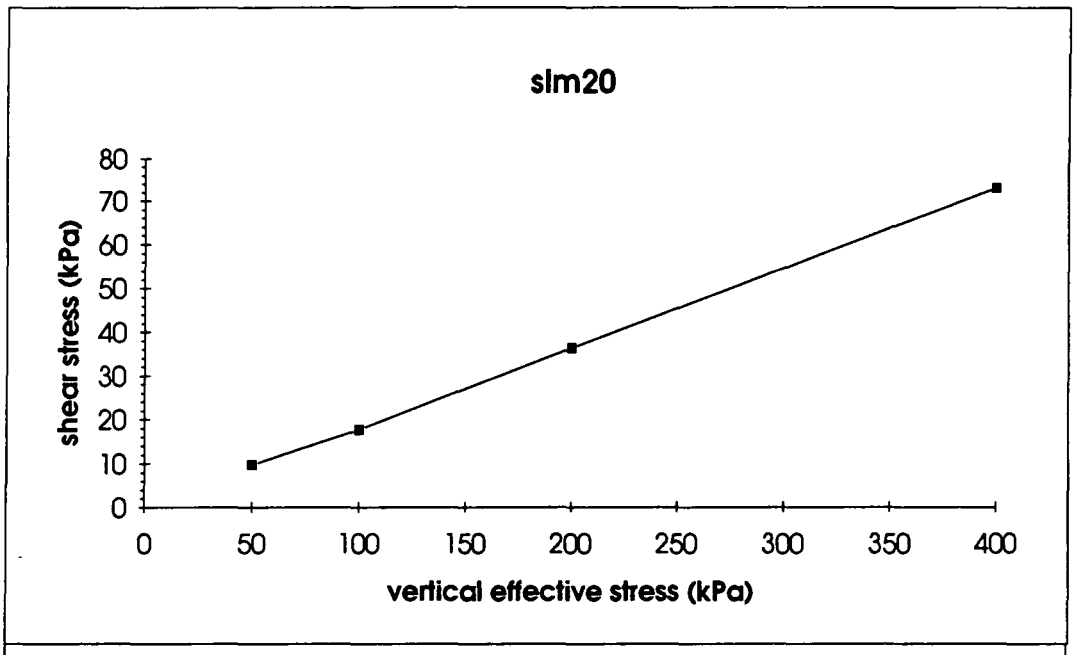
slm20
shear stress (kPa)
80
70
60
50
40
30
20
10
0
0
50
100
150
200
250
300
350
400
vertical effective stress (kPa)

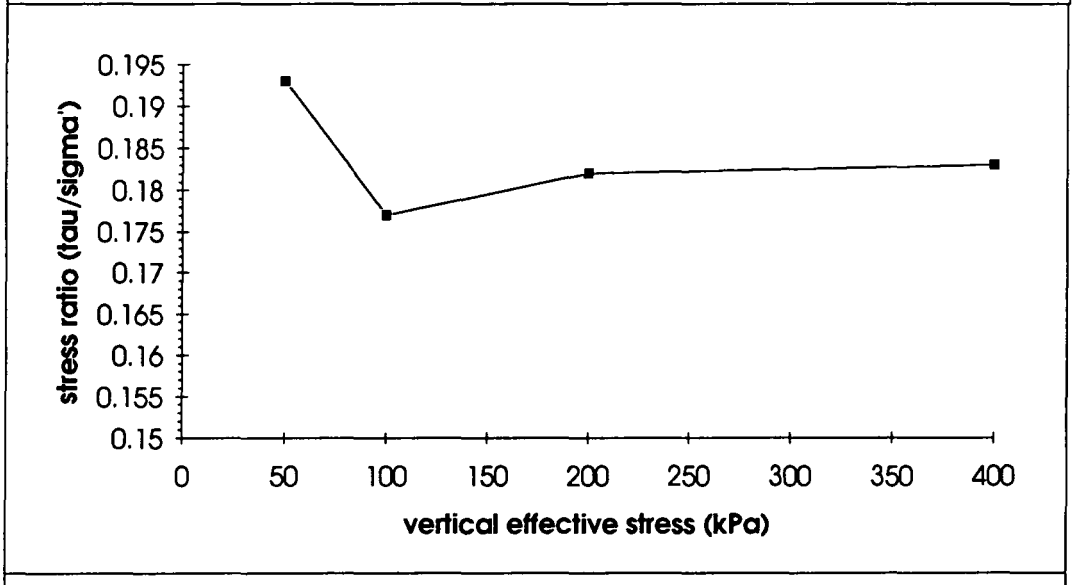
stress ratio (tau/sigma')
0.195
0.19
0.185
0.18
0.175
0.17
0.165
0.16
0.155
0.15
0
50
100
150
200
250
300
350
400
vertical effective stress (kPa)

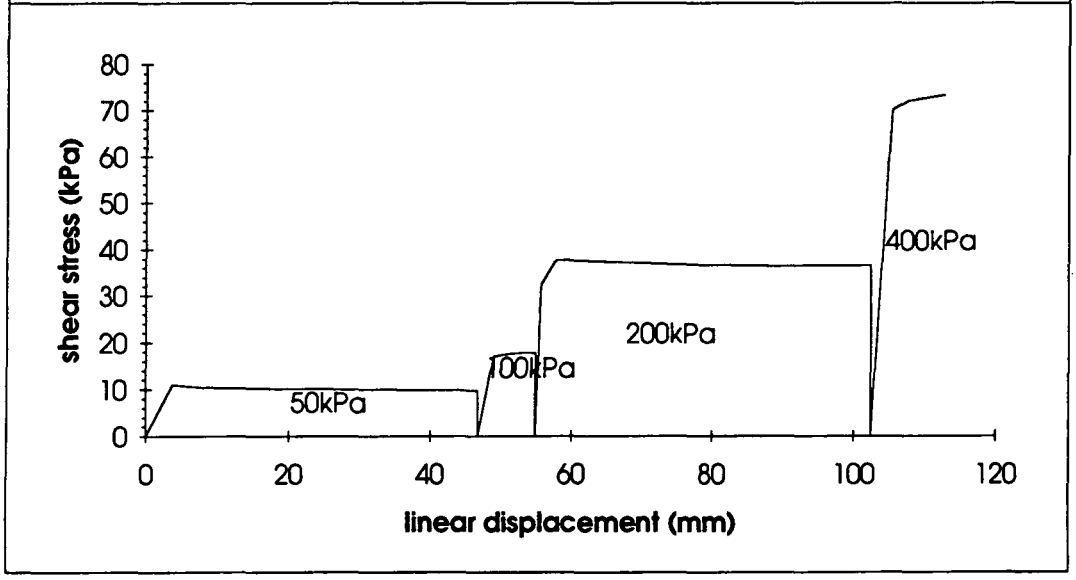
shear stress (kPa)
80
70
60
50
40
30
20
10
0
50kPa
100kPa
200kPa
400kPa
0
20
40
60
80
100
120
linear displacement (mm)

Ring shear test final moisture content calculation
with pressure values estimated from slurry tests

sample	wL	wP		Gs	eL	eP	PwL	PwP	log PwL	log PwP	m.c. final
xml LP	48.8	22		2.7	1.3176	0.594	5	480	0.69897	2.681241	27.14
ll1	47.3	24.3		2.7	1.2771	0.6561	95	1670	1.977724	3.222716	41.33
lts	50.9	21.7		2.65	1.34885	0.57505	33	525	1.518514	2.720159	31.89
kd	42.7	22.5		2.68	1.14436	0.603	72	1660	1.857332	3.220108	36.12
kd 1 b	56.1	22.8		2.66	1.49226	0.60648	30	3200	1.477121	3.50515	42.57
kvt A LP	44.6	20		2.68	1.19528	0.536	22	1580	1.342423	3.198657	31.90
kvt 1 HP b	50.1	22.1		2.66	1.33266	0.58786	5	1150	0.69897	3.060698	31.11
kks1	42	20		2.6	1.092	0.52	18	1500	1.255273	3.176091	30.02
agn1	57.3	25.3		2.67	1.52991	0.67551	5	600	0.69897	2.778151	32.64
agn2	53.4	23.8		2.62	1.39908	0.62356	5	770	0.69897	2.886491	31.72
slm4 T	35.2	18		2.6	0.9152	0.468	100	2340	2	3.369216	31.42
slm6 A	35.6	19.5		2.54	0.90424	0.4953	75	2400	1.875061	3.380211	31.04
slm B2	46.5	19		2.67	1.24155	0.5073	63	3310	1.799341	3.519828	38.48
er 1	41	21.8		2.6	1.066	0.5668	50	1585	1.69897	3.200029	33.30
psf 1 a	32.5	19.1		2.55	0.82875	0.48705	15	2240	1.176091	3.350248	25.57
rtk	41	18.9		2.6	1.066	0.4914	15	2630	1.176091	3.419956	29.92
nsa 1	53.8	23.8		2.7	1.4526	0.6426	30	2400	1.477121	3.380211	40.81
mvg	45.2	22.3		2.54	1.14808	0.56642	5	1000	0.69897	3	29.26
ktr2	54.9	22.9		2.63	1.44387	0.60227	100	5011	2	3.699924	49.23
pls	43.4	21.7		2.64	1.14576	0.57288	260	2820	2.414973	3.450249	45.79
oen2	46.6	20		2.52	1.17432	0.504	100	2300	2	3.361728	40.72
skf1	54.7	23.8		2.65	1.44955	0.6307	20	1000	1.30103	3	36.51

Ring shear test final moisture content calculation
with pressure values set according to Lupini et al, 1981

sample	wL	wP		Gs	eL	eP	PwL	PwP	log PwL	log PwP	m.c. final
xml LP	48.8	22		2.7	1.3176	0.594	5.5	550	0.740363	2.740363	27.89
ll1	47.3	24.3		2.7	1.2771	0.6561	5.5	550	0.740363	2.740363	29.35
lts	50.9	21.7		2.65	1.34885	0.57505	5.5	550	0.740363	2.740363	28.11
kd	42.7	22.5		2.68	1.14436	0.603	5.5	550	0.740363	2.740363	26.94
kd 1 b	56.1	22.8		2.66	1.49226	0.60648	5.5	550	0.740363	2.740363	30.12
kvt A LP	44.6	20		2.68	1.19528	0.536	5.5	550	0.740363	2.740363	25.40
kvt 1 HP b	50.1	22.1		2.66	1.33266	0.58786	5.5	550	0.740363	2.740363	28.25
kks1	42	20		2.6	1.092	0.52	5.5	550	0.740363	2.740363	24.83
agn1	57.3	25.3		2.67	1.52991	0.67551	5.5	550	0.740363	2.740363	32.33
agn2	53.4	23.8		2.62	1.39908	0.62356	5.5	550	0.740363	2.740363	30.30
slm4 T	35.2	18		2.6	0.9152	0.468	5.5	550	0.740363	2.740363	21.78
slm6 A	35.6	19.5		2.54	0.90424	0.4953	5.5	550	0.740363	2.740363	23.04
slm B2	46.5	19		2.67	1.24155	0.5073	5.5	550	0.740363	2.740363	25.04
er 1	41	21.8		2.6	1.066	0.5668	5.5	550	0.740363	2.740363	26.02
psf 1 a	32.5	19.1		2.55	0.82875	0.48705	5.5	550	0.740363	2.740363	22.04
rtk	41	18.9		2.6	1.066	0.4914	5.5	550	0.740363	2.740363	23.75
nsa 1	53.8	23.8		2.7	1.4526	0.6426	5.5	550	0.740363	2.740363	30.39
mvg	45.2	22.3		2.54	1.14808	0.56642	5.5	550	0.740363	2.740363	27.33
ktr2	54.9	22.9		2.63	1.44387	0.60227	5.5	550	0.740363	2.740363	29.93
pls	43.4	21.7		2.64	1.14576	0.57288	5.5	550	0.740363	2.740363	26.47
oen2	46.6	20		2.52	1.17432	0.504	5.5	550	0.740363	2.740363	25.84
skf1	54.7	23.8		2.65	1.44955	0.6307	5.5	550	0.740363	2.740363	30.59

APPENDIX B

COMPARISON BETWEEN ARMFIELD AND BROMHEAD RING SHEAR APPARATUSES AND A SHEAR BOX RESULT.

APPENDIX B
TABLE OF CONTENTS

SLM0320 Armfield 1st Run	1
SLM0320 Armfield 2nd Run	2
SLM0320 Armfield 3rd Run	3
SLM0320 Bromhead	4
Table of Test Runs Results	5
SLM0320 Shear Box Test Run	6
-//-	7

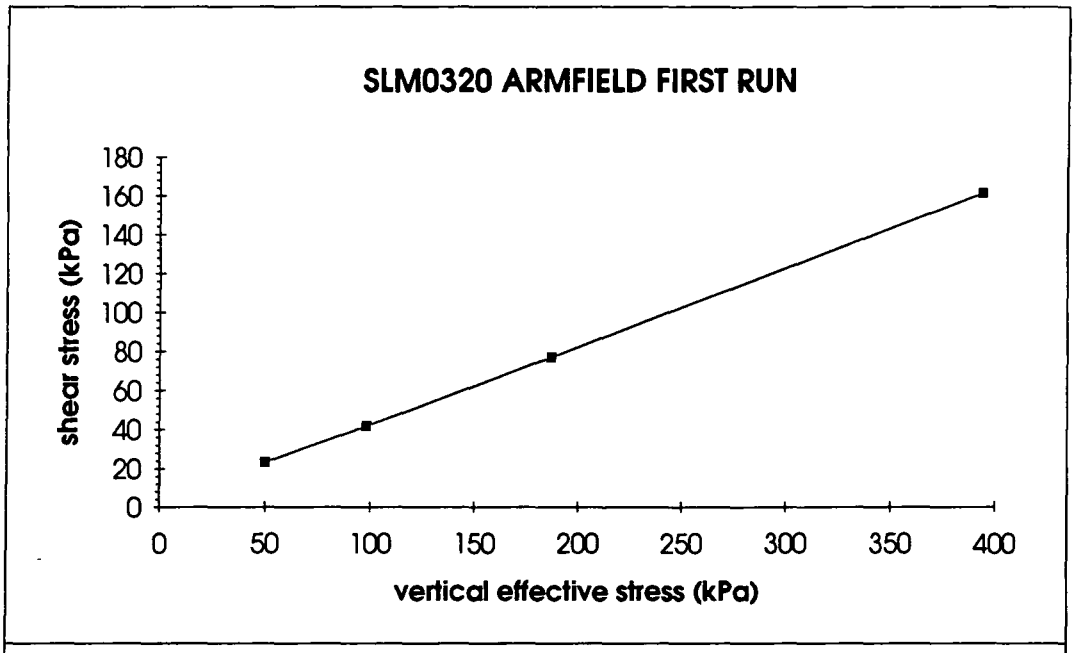
SLM0320 ARMFIELD FIRST RUN
shear stress (kPa)
180
160
140
120
100
80
60
40
20
0
0
50
100
150
200
250
300
350
400
vertical effective stress (kPa)

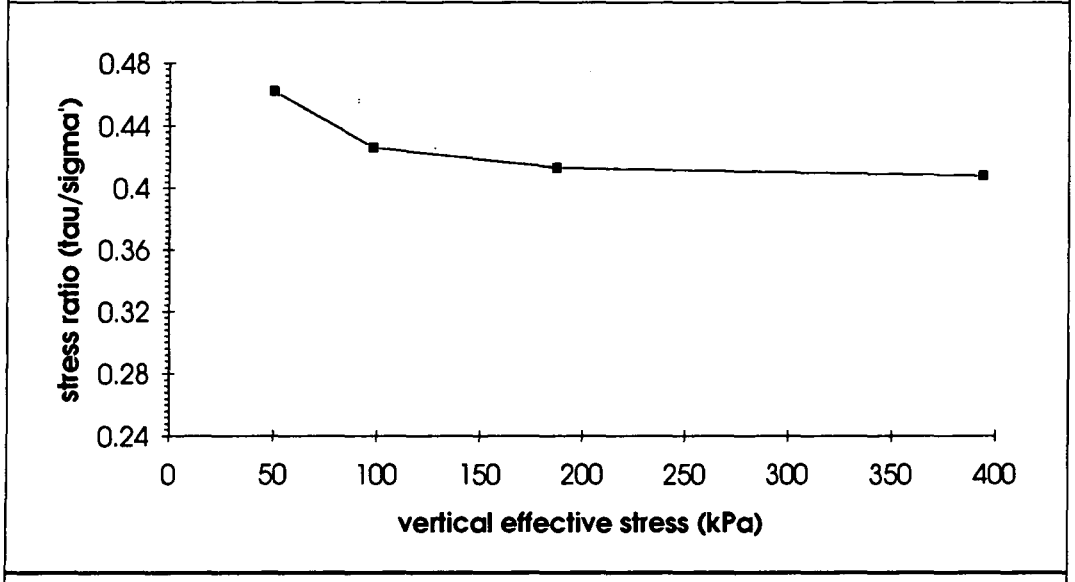
stress ratio (tau/sigma')
0.48
0.44
0.4
0.36
0.32
0.28
0.24
0
50
100
150
200
250
300
350
400
vertical effective stress (kPa)

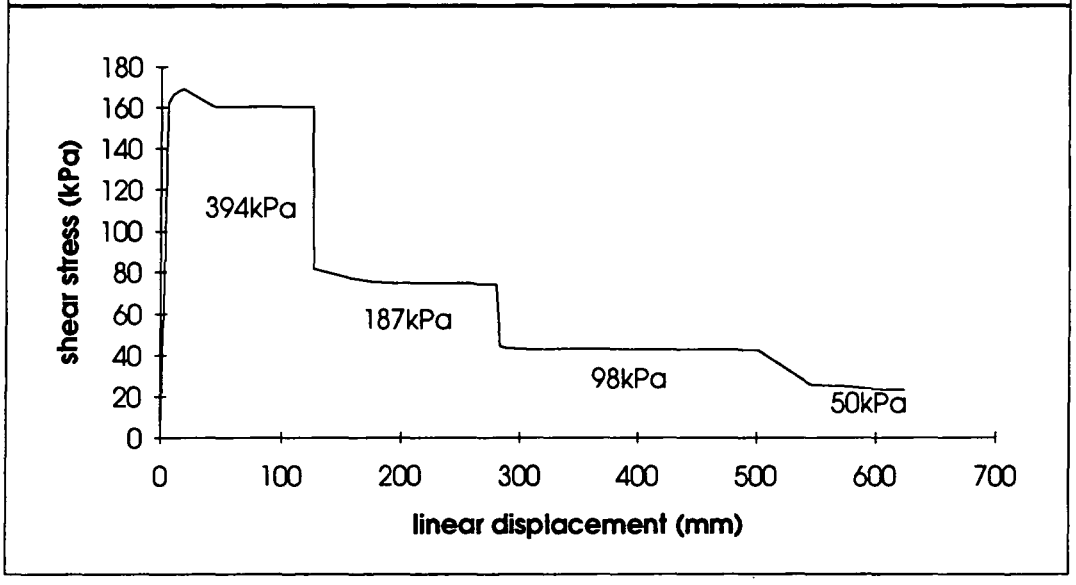
shear stress (kPa)
180
160
140
120
100
80
60
40
20
0
394kPa
187kPa
98kPa
50kPa
0
100
200
300
400
500
600
700
linear displacement (mm)

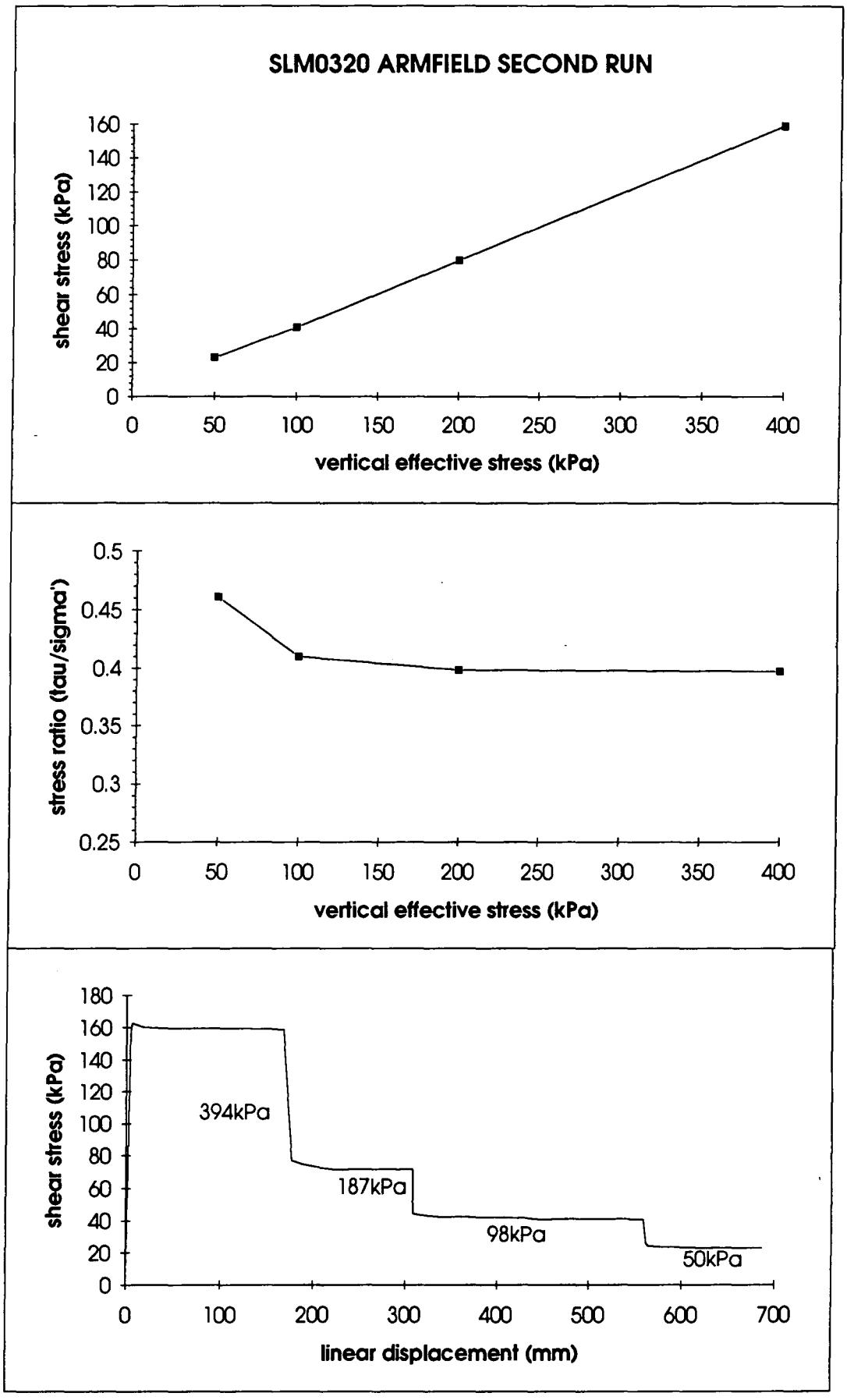
SLM0320 ARMFIELD SECOND RUN
shear stress (kPa)
0
20
40
60
80
100
120
140
160
0
50
100
150
200
250
300
350
400
vertical effective stress (kPa)
stress ratio (tau/sigma')
0.25
0.3
0.35
0.4
0.45
0.5
0
50
100
150
200
250
300
350
400
vertical effective stress (kPa)
shear stress (kPa)
0
20
40
60
80
100
120
140
160
180
394kPa
187kPa
98kPa
50kPa
0
100
200
300
400
500
600
700
linear displacement (mm)

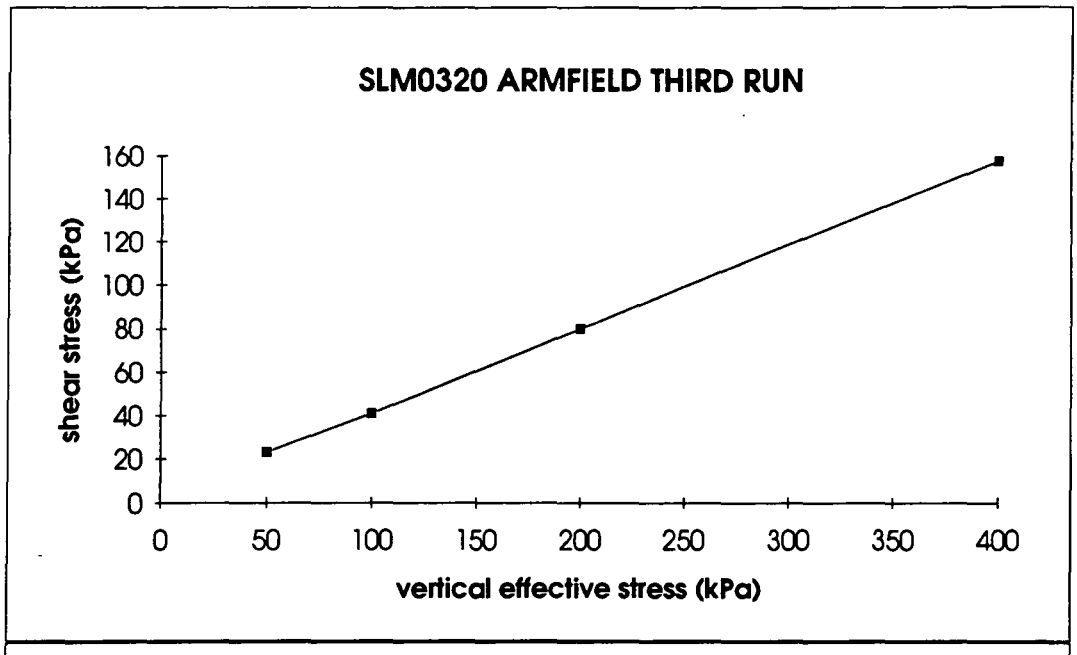
SLM0320 ARMFIELD THIRD RUN
shear stress (kPa)
0
20
40
60
80
100
120
140
160
0
50
100
150
200
250
300
350
400
vertical effective stress (kPa)

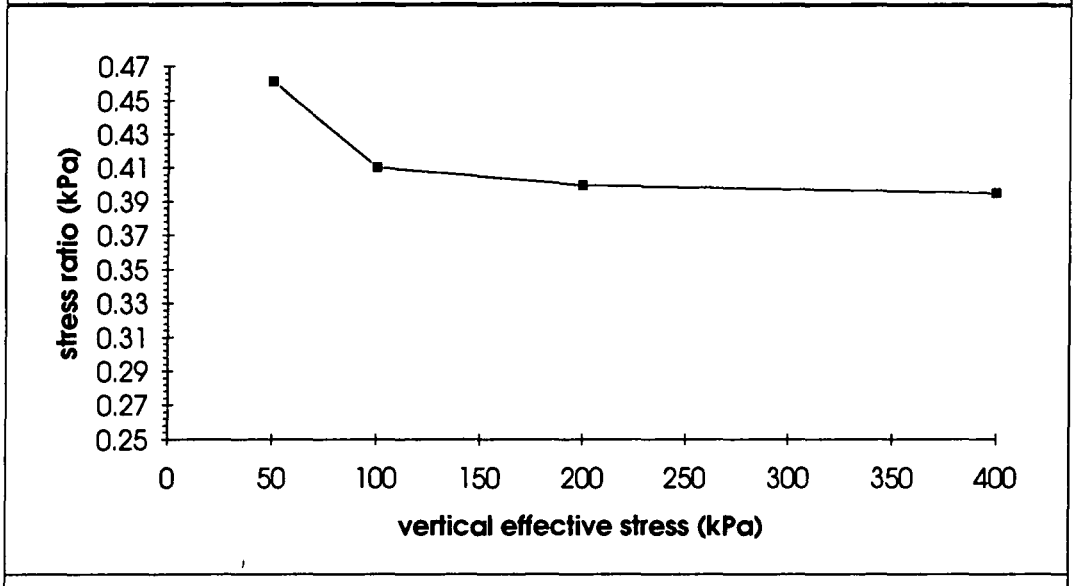
stress ratio (kPa)
0.25
0.27
0.29
0.31
0.33
0.35
0.37
0.39
0.41
0.43
0.45
0.47
0
50
100
150
200
250
300
350
400
vertical effective stress (kPa)

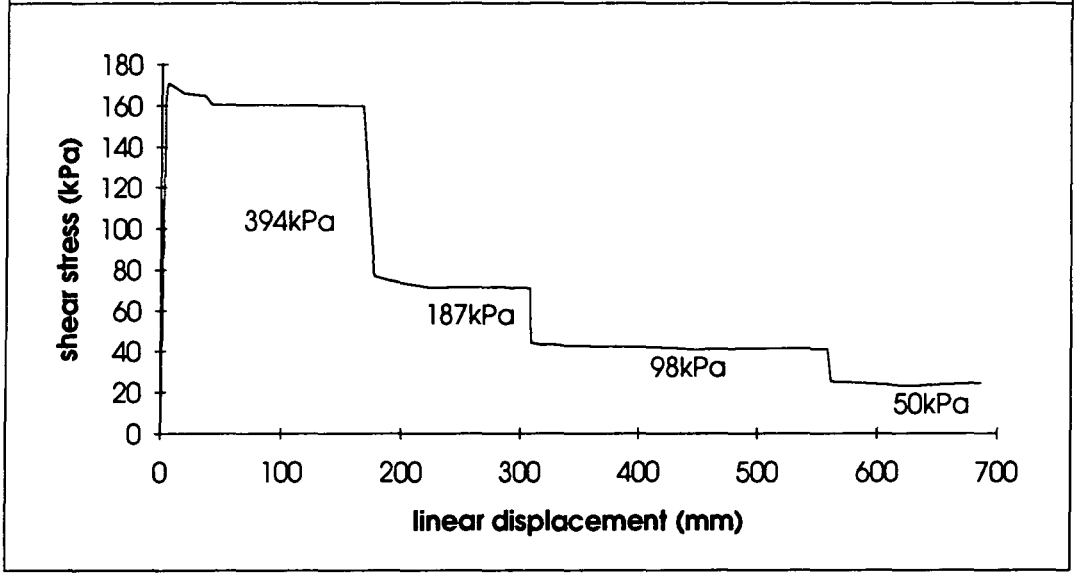
shear stress (kPa)
0
20
40
60
80
100
120
140
160
180
394kPa
187kPa
98kPa
50kPa
0
100
200
300
400
500
600
700
linear displacement (mm)

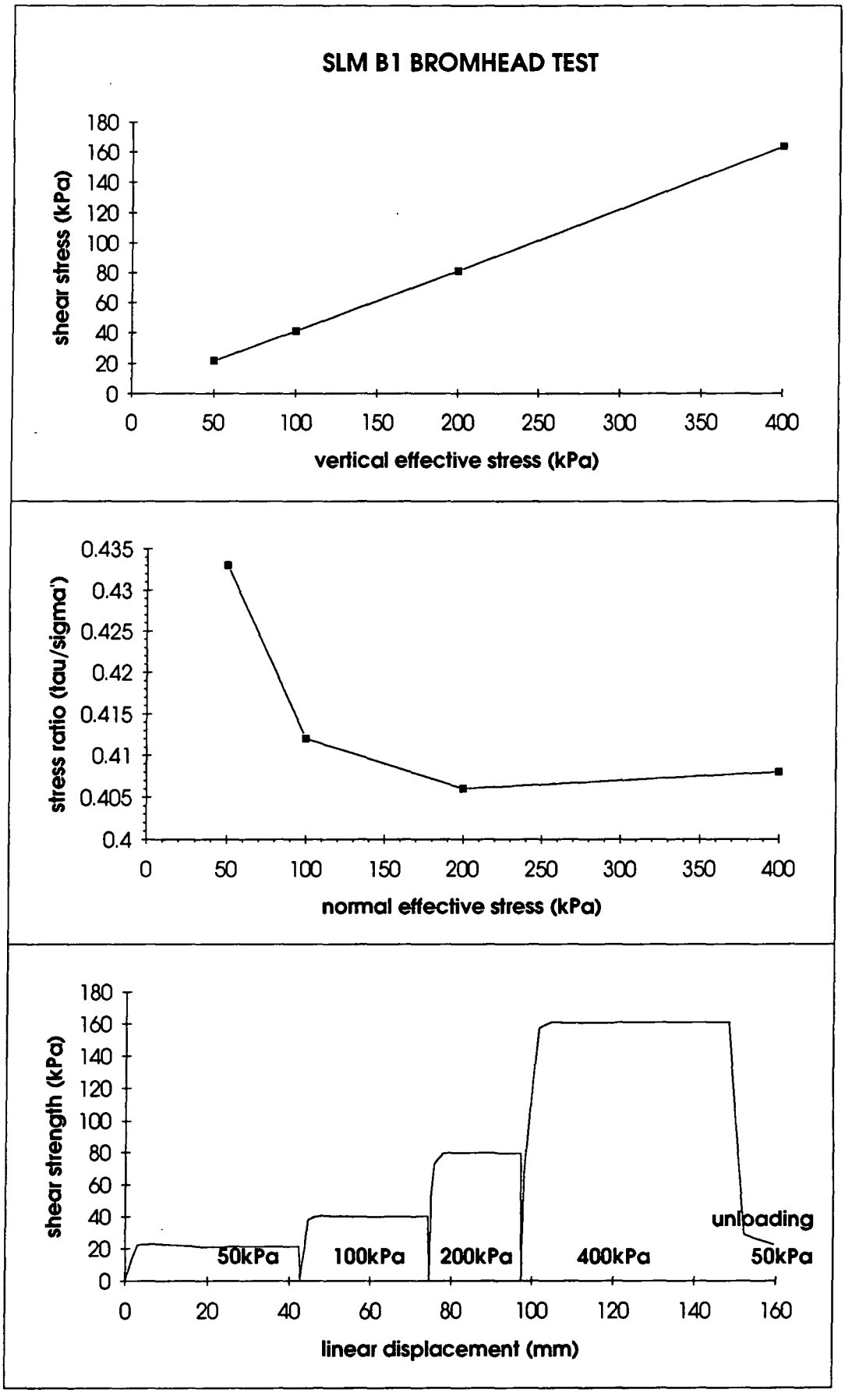
SLM B1 BROMHEAD TEST
shear stress (kPa)
180
160
140
120
100
80
60
40
20
0
0
50
100
150
200
250
300
350
400
vertical effective stress (kPa)
stress ratio (tau/sigma')
0.435
0.43
0.425
0.42
0.415
0.41
0.405
0.4
0
50
100
150
200
250
300
350
400
normal effective stress (kPa)
shear strength (kPa)
180
160
140
120
100
80
60
40
20
0
50kPa
100kPa
200kPa
400kPa
unloading
50kPa
0
20
40
60
80
100
120
140
160
linear displacement (mm)

TABLE OF TEST RUNS RESULTS

(Stress values in kPa)

ARMFIELD 1

stress ratio	vertical eff.stress	shear stress
0.408	394	160.75
0.413	187	77.23
0.426	98	41.75
0.462	50	23.10

ARMFIELD 2

stress ratio	vertical eff.stress	shear stress
0.397	400	158.80
0.398	200	79.60
0.410	100	41.00
0.461	50	23.05

ARMFIELD 3

stress ratio	vertical eff.stress	shear stress
0.395	400	158.00
0.400	200	79.90
0.410	100	41.00
0.461	50	23.05

BROMHEAD

stress ratio	vertical eff.stress	shear stress
0.408	400	163.20
0.406	200	81.20
0.412	100	41.20
0.433	50	21.65

SHEAR BOX

stress ratio	vertical eff.stress	shear stress
0.427	600	256.00
0.433	300	130.00
0.453	150	68.00

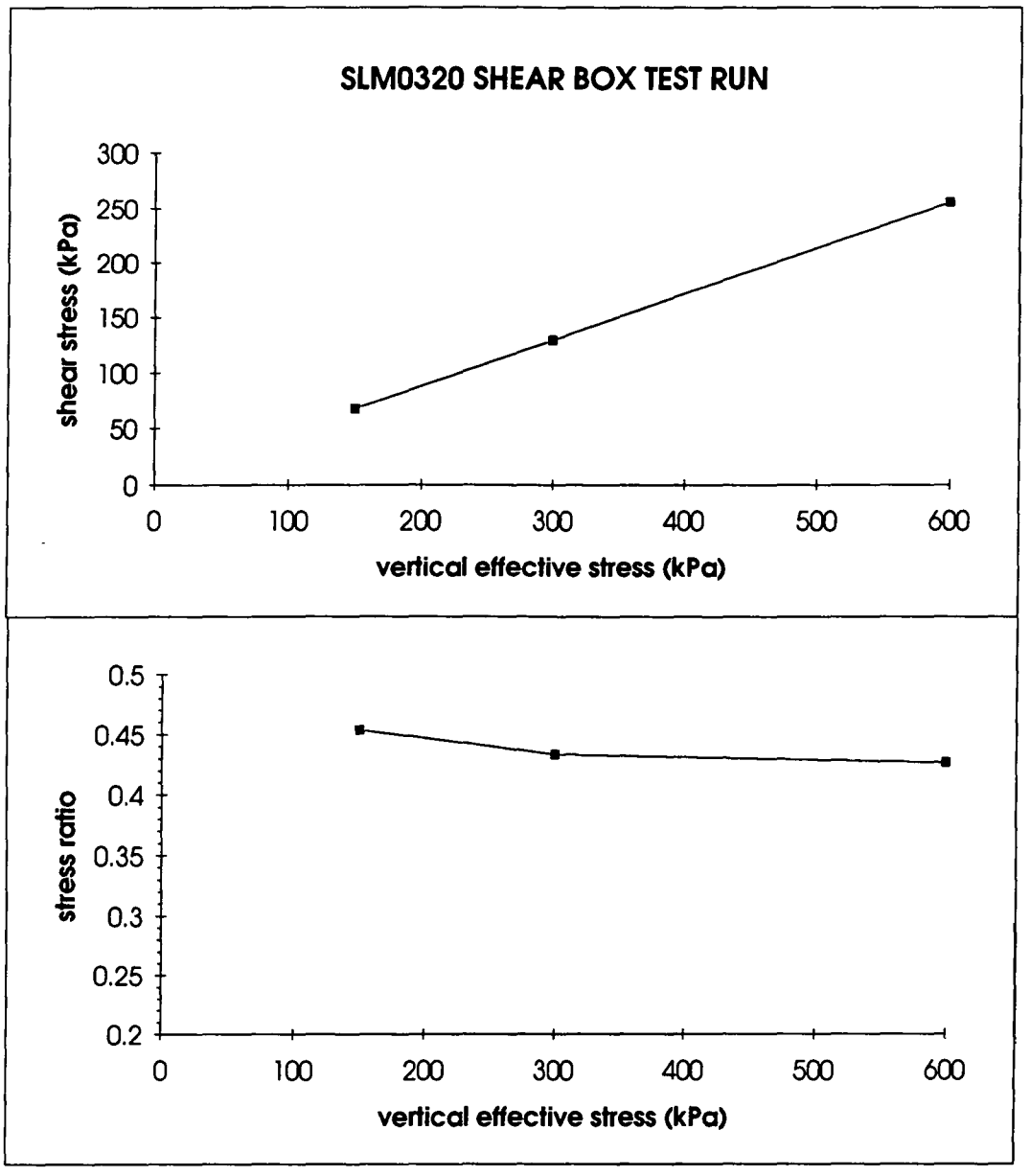

The above shown multireversal shear box test was conducted in accordance to Head (1982) 12.3.9 slow drained test on clays and silts and 12.3.10 residual shear strength test description and recommentations. The rate of shearing was kept at 1.463mm/hour. The specimen was an over consolidated very stiff clayey silt of low plasticity measuring 60x60x40mm prior to the test, density=2.15gr/cub.cm, initial moisture content=11.7%.

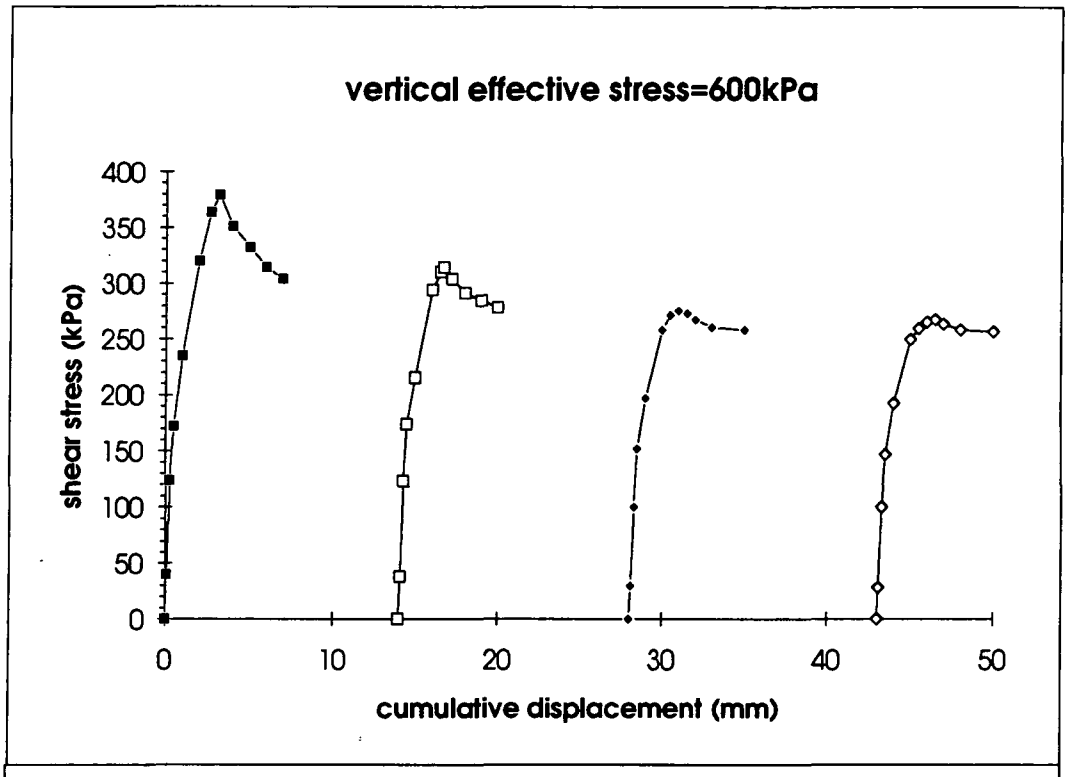
vertical effective stress=600kPa
shear stress (kPa)
400
350
300
250
200
150
100
50
0
0
10
20
30
40
50
cumulative displacement (mm)

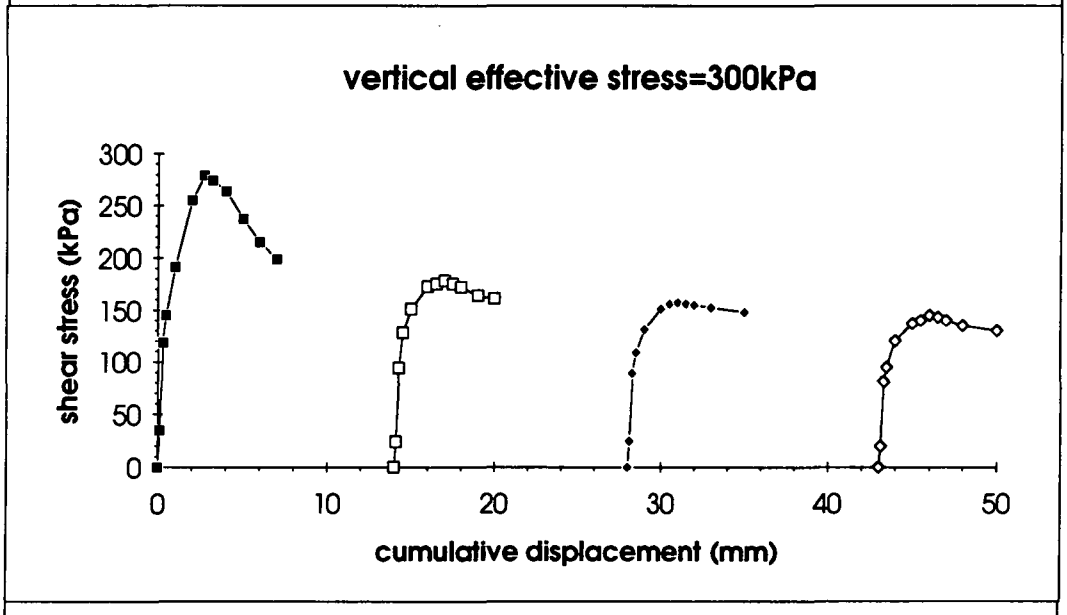
vertical effective stress=300kPa
shear stress (kPa)
300
250
200
150
100
50
0
0
10
20
30
40
50
cumulative displacement (mm)

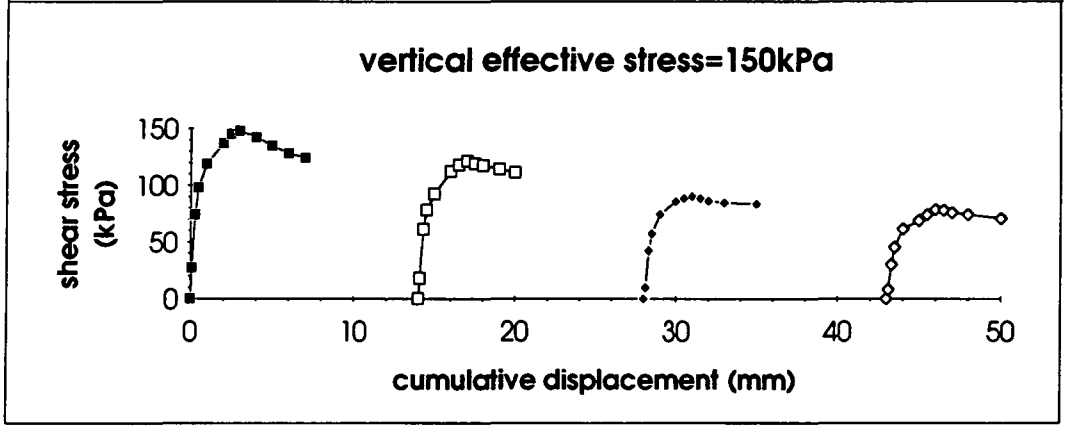
vertical effective stress=150kPa
shear stress (kPa)
150
100
50
0
0
10
20
30
40
50
cumulative displacement (mm)

APPENDIX C

RESULTS FROM ONE DIMENTIONAL CONSOLIDATION OF RECONSTITUTED AND INTACT HELLENIC "MARLS"

APPENDIX C
TABLE OF CONTENTS

Table C.1 Korinthos e-logσ'_v Slurry Test Results.....	C.1
Table C.2 Preveza-Igoumenitsa e-logσ'_v Slurry Test Results.....	C.2
Table C.3 Amalias-Goumeron e-logσ'_v Slurry Test Results.....	C.3
Table C.4 Korinthos I_v-logσ'_v Slurry Test Results.....	C.4
Table C.5 Preveza-Igoumenitsa I_v-logσ'_v Slurry Test Results.....	C.5
Table C.6 Amalias-Goumeron I_v-logσ'_v Slurry Test Results.....	C.6
Table C.7 Carbonates and Plasticity groupings Statistics of Slurry Test	C.7
Table C.8 Korinthos e-logσ'_v Intact Test Results.....	C.8
Table C.9 Preveza-Igoumenitsa e-logσ'_v Intact Test Results.....	C.9
Table C.10 Compression Indices.....	C.10

N.B In the following pages σ'_v will be presented as *p*.

TABLE C.1
KORINTHOS
SLURRY TESTS

ER 1 slurry		PSF 1a slurry		RTK slurry		SLM 6A slurry	
p(kPa)	e	p(kPa)	e	p(kPa)	e	p(kPa)	e
1	1.411	1	1.0293	1	1.232	1	1.4275
10	1.1977	10	0.8378	5	1.1052	5	1.1905
20	1.1382	20	0.797	10	1.0754	10	1.1106
50	1.0175	35	0.7509	20	1.0232	20	1.0465
100	0.9365	50	0.7115	50	0.9339	50	0.9448
200	0.8471	100	0.6625	100	0.8648	100	0.864
400	0.7484	200	0.6163	200	0.7916	200	0.7847
800	0.6369	350	0.5881	400	0.7184	400	0.709
1000	0.6013	500	0.5722	800	0.643	800	0.63
		700	0.5546	1000	0.6286	1000	0.6086
		1000	0.5359	1600	0.5675	1600	0.5495
		1400	0.5101	3200	0.477	3200	0.4555
		1900	0.498				

SLM 2T slurry		SLM 4T slurry		SLM B2 slurry		TKR slurry	
p(kPa)	e	p(kPa)	e	p(kPa)	e	p(kPa)	e
1	1.3077	1	1.5399	1	1.63116	1	1.9472
5	1.0921	5	1.1864	10	1.4352	5	1.5875
10	1.0593	10	1.1237	20	1.38	10	1.5236
20	1.0007	20	1.0448	50	1.26935	35	1.3137
50	0.9041	50	0.9686	100	1.19333	50	1.2926
100	0.8315	100	0.9063	200	1.08998	100	1.16943
200	0.753	200	0.8053	400	0.94007	200	1.0027
400	0.6838	400	0.7161	800	0.80997	400	0.846
800	0.6058	800	0.6247	1000	0.77014	800	0.7341
1000	0.5863	1000	0.6052	1400	0.70004	1600	0.6038
1600	0.5414	1600	0.5374	2000	0.63217		
				2800	0.5524		

TABLE C.2
PREVEZA-IGOUMENITSA
SLURRY TESTS

AGN 1 slurry		AGN 2 slurry		KD slurry		KD Ab slurry	
p(kPa)	e	p(kPa)	e	p(kPa)	e	p(kPa)	e
1	1.3188	1	1.27459	1	1.5249	1	1.8392
20	1.1651	10	1.18904	10	1.34486	10	1.6644
35	1.11067	20	1.14561	20	1.27236	20	1.5881
50	1.07388	50	1.02665	50	1.14816	50	1.3838
100	0.97846	100	0.95794	100	1.04586	100	1.2729
200	0.87704	200	0.84992	200	0.93386	200	1.1055
350	0.788	400	0.743	400	0.81326	400	0.9164
				800	0.70426	800	0.748
				1000	0.68326		
				1600	0.56916		

KKS 1 slurry		KVT Alp slurry		KVT 1hp B slurry		KVT 2 slurry	
p(kPa)	e	p(kPa)	e	p(kPa)	e	p(kPa)	e
1	1.30755	1	1.2339	1	1.4597	1	1.8133
10	1.06849	10	1.087	5	1.2998	5	1.5548
20	1.01275	20	1.0483	10	1.2348	10	1.5167
50	0.97296	50	0.957	20	1.1567	20	1.4475
100	0.88639	100	0.8864	50	1.0678	50	1.2644
200	0.80076	200	0.7946	100	0.9584	100	1.1047
400	0.70657	400	0.7001	200	0.8631	200	0.9778
800	0.6061	800	0.5985	400	0.7556	400	0.838
1000	0.57926	1600	0.488	800	0.6416	800	0.7039
1400	0.5265			1000	0.6117	1000	0.6691
				1600	0.5283	1600	0.573
						3200	0.4352

LL 1 slurry		LTS slurry		XLM mp slurry	
p(kPa)	e	p(kPa)	e	p(kPa)	e
1	1.8893	1	1.99001	1	1.093
5	1.6656	10	1.54744	10	0.941
10	1.6193	20	1.44568	20	0.9035
20	1.5283	50	1.24391	50	0.817
50	1.3789	100	1.06834	100	0.751
100	1.2536	200	0.9056	200	0.662
200	1.1154	400	0.67979	400	0.569
400	0.9776			800	0.468
800	0.83			1600	0.3556
1000	0.7796				
1600	0.663				
3200	0.4842				

TABLE C.3
AMALIAS - GOUMERON
SLURRY TESTS

KTR 2 slurry		MVG slurry		NSA 1 slurry		OEN 2 slurry	
p(kPa)	e	p(kPa)	e	p(kPa)	e	p(kPa)	e
1	1.997	1	1.4961	1	2.1017	1	1.801
10	1.8167	5	1.3098	5	1.6878	5	1.7835
20	1.741	10	1.2607	10	1.5816	10	1.667
50	1.5726	20	1.1753	20	1.5037	50	1.3929
100	1.4315	50	1.0687	50	1.3664	100	1.1744
200	1.2881	100	0.979	100	1.2418	200	1.0615
400	1.1411	200	0.8876	200	1.0788	400	0.9423
800	1.0147	400	0.7466	400	0.9617	800	0.8679
1000	0.9767	800	0.6513	800	0.8367	1600	0.6148
1600	0.8683	1600	0.5407	1600	0.7075		

PLS slurry		RDA slurry		SKF 1 slurry	
p(kPa)	e	p(kPa)	e	p(kPa)	e
1	2.1182	1	2.1515	1	2.0194
5	1.8185	5	1.7425	5	1.9171
10	1.6753	10	1.6256	20	1.4175
20	1.577	20	1.5391	70	1.1468
50	1.442	70	1.2999	100	1.1014
100	1.3223	100	1.2533	200	0.9514
200	1.1855	200	1.1118	400	0.8085
400	1.027	400	0.9757	800	0.6595
800	0.8606	800	0.8295	1600	0.5088
1000	0.8221	1600	0.6757		
1600	0.6885				
3200	0.5053				

TABLE C.4
KORINTHOS
SLURRY TESTS

ER 1 slurry		PSF 1a slurry		RTK slurry		SLM 6A slurry	
p(kPa)	Iv	p(kPa)	Iv	p(kPa)	Iv	p(kPa)	Iv
1	1.415573	1	2.897314	1	1.554615	1	2.206343
10	0.779236	10	1.384676	5	1.017782	5	1.278387
20	0.60173	20	1.062401	10	0.891617	10	0.965544
50	0.241647	35	0.698262	20	0.670618	20	0.714565
100	0	50	0.387046	50	0.292549	50	0.316366
200	-0.26671	100	0	100	0	100	0
400	-0.56116	200	-0.36493	200	-0.30991	200	-0.31049
800	-0.89379	350	-0.58768	400	-0.61981	400	-0.60689
1000	-1	500	-0.71327	800	-0.93903	800	-0.91621
		700	-0.85229	1000	-1	1000	-1
		1000	-1	1600	-1.25868	1600	-1.2314
		1400	-1.20379	3200	-1.64183	3200	-1.59945
		1900	-1.29937				

SLM 2T slurry		SLM 4T slurry		SLM B2 slurry		TKR slurry	
p(kPa)	Iv	p(kPa)	Iv	p(kPa)	Iv	p(kPa)	Iv
1	1.942088	1	2.104284	1	1.034594	1	1.589134
5	1.062806	5	0.930256	10	0.57154	5	0.854198
10	0.929038	10	0.722019	20	0.441102	10	0.723638
20	0.690049	20	0.45998	50	0.179636	35	0.294771
50	0.296085	50	0.206908	100	0	50	0.25166
100	0	100	0	200	-0.24422	100	0
200	-0.32015	200	-0.33544	400	-0.59845	200	-0.34066
400	-0.60237	400	-0.63168	800	-0.90588	400	-0.66083
800	-0.92047	800	-0.93524	1000	-1	800	-0.88946
1000	-1	1000	-1	1400	-1.16565	1000	-1
1600	-1.18312	1600	-1.22517	2000	-1.32602	1600	-1.15569
				2800	-1.51452		

x^3	x	b	x^3	x	b
all increments			**increments>50kPa**		
-0.00623	-0.87789	1.787518	-0.00649	-0.88638	1.818454
0.004083	0.050643	0.059161	0.002157	0.04344	0.071672
0.960318	0.196529	#N/A	0.99639	0.033371	#N/A
1064.819	88	#N/A	7866.218	57	#N/A
82.25411	3.398868	#N/A	17.52031	0.063478	#N/A

linear regression models of the form y=b+b1*x+b2*x^3 where y=Iv, x=log(vertical effective stress in kPa), also see key below:

b2	b1	b
se b2	se b1	se b
r^2	se y	#
F	df	#
ss reg.	ss resid.	#

where se is the standard error, r^2 is the coefficient of determination, F is the F statistic , df is the degrees of freedom, ss reg is the regression sum of squares and ss resid is the residual sum of squares.

TABLE C.5
PREVEZA-IGOUMENITSA
SLURRY TESTS

AGN 1 slurry		AGN 2 slurry		KD slurry		KD Ab slurry	
p(kPa)	Iv	p(kPa)	Iv	p(kPa)	Iv	p(kPa)	Iv
1	0.813315	1	0.691466	1	1.321125	1	0.732695
20	0.446016	10	0.504651	10	0.8246	10	0.506534
35	0.315944	20	0.409814	20	0.624655	20	0.407815
50	0.228027	50	0.150041	50	0.282129	50	0.143486
100	0	100	0	100	0	100	0
200	-0.24236	200	-0.23588	200	-0.30888	200	-0.21659
350	-0.45515	400	-0.46936	400	-0.64148	400	-0.46125
				800	-0.94208	800	-0.67913
				1000	-1		
				1600	-1.31467		

KKS 1 slurry		KVT Alp slurry		KVT 1hp B slurry		KVT 2 slurry	
p(kPa)	Iv	p(kPa)	Iv	p(kPa)	Iv	p(kPa)	Iv
1	1.371276	1	1.003176	1	1.445919	1	1.626722
10	0.592909	10	0.579099	5	0.984713	5	1.033287
20	0.411422	20	0.467379	10	0.797231	10	0.945822
50	0.281868	50	0.203811	20	0.571964	20	0.786961
100	0	100	0	50	0.315547	50	0.366621
200	-0.27881	200	-0.26501	100	0	100	0
400	-0.58548	400	-0.53782	200	-0.27488	200	-0.29132
800	-0.91261	800	-0.83112	400	-0.58494	400	-0.61226
1000	-1	1600	-1.15012	800	-0.91376	800	-0.92011
1400	-1.17178			1000	-1	1000	-1
				1600	-1.24055	1600	-1.22062
						3200	-1.53696

LL 1 slurry		LTS slurry		XLM mp slurry	
p(kPa)	Iv	p(kPa)	Iv	p(kPa)	Iv
1	1.341139	1	1.379044	1	0.997085
5	0.869198	10	0.716851	10	0.553936
10	0.771519	20	0.564593	20	0.444606
20	0.579536	50	0.262696	50	0.19242
50	0.264346	100	0	100	0
100	0	200	-0.2435	200	-0.25948
200	-0.29156	400	-0.58137	400	-0.53061
400	-0.58228			800	-0.82507
800	-0.89367			1600	-1.15277
1000	-1				
1600	-1.24599				
3200	-1.62321				

regression models key as shown in table C.4

x^3	x	b	x^3	x	b
all increments			**increments>50kPa**		
-0.02647	-0.48362	1.186918	-0.0187	-0.62562	1.400826
0.002581	0.029792	0.034516	0.003253	0.062798	0.101166
0.971739	0.128402	#N/A	0.990612	0.051389	#N/A
1702.004	99	#N/A	3323.718	63	#N/A
56.12186	1.632212	#N/A	17.55466	0.166371	#N/A

TABLE C.6
AMALIAS - GOUMERON
SLURRY TESTS

KTR 2 slurry		MVG slurry		NSA 1 slurry		OEN 2 slurry	
p(kPa)	Iv	p(kPa)	Iv	p(kPa)	Iv	p(kPa)	Iv
1	1.243404	1	1.329306	1	1.748475	1	1.267395
10	0.846966	5	0.850386	5	0.906873	5	1.231998
20	0.680519	10	0.724165	10	0.690931	10	0.996359
50	0.310246	20	0.504627	20	0.532534	50	0.44195
100	0	50	0.230591	50	0.253355	100	0
200	-0.3153	100	0	100	0	200	-0.22836
400	-0.63852	200	-0.23496	200	-0.33144	400	-0.46946
800	-0.91645	400	-0.59743	400	-0.56954	800	-0.61994
1000	-1	800	-0.84242	800	-0.82371	1600	-1.13188
1600	-1.23835	1600	-1.12674	1600	-1.08642		

PLS slurry		RDA slurry		SKF 1 slurry	
p(kPa)	Iv	p(kPa)	Iv	p(kPa)	Iv
1	1.591164	1	1.784621	1	1.760644
5	0.992003	5	0.971985	5	1.564442
10	0.705718	10	0.739718	20	0.606252
20	0.509196	20	0.567852	70	0.087073
50	0.239304	70	0.092589	100	0
100	0	100	0	200	-0.28769
200	-0.27349	200	-0.28114	400	-0.56176
400	-0.59036	400	-0.55156	800	-0.84753
800	-0.92303	800	-0.84204	1600	-1.13656
1000	-1	1600	-1.14763		
1600	-1.26709				
3200	-1.63335				

regression models key as shown in table C.4

x^3	x	b	x^3	x	b
all increments			**increments>50kPa**		
-0.01283	-0.71947	1.544394	-0.01127	-0.75504	1.608027
0.003033	0.035103	0.039303	0.005379	0.105682	0.172078
0.980586	0.122891	#N/A	0.984696	0.065227	#N/A
1692.023	67	#N/A	1319.006	41	#N/A
51.10645	1.011845	#N/A	11.22345	0.174435	#N/A

Table C.7

all increments			increments>50kPa		
x^3	x	b	x^3	x	b
Carbonates > 45%			**Carbonates > 45%**		
-0.00561	-0.89619	1.821672	0.003587	-1.09732	2.168745
0.005204	0.061765	0.070451	0.00396	0.075346	0.12029
0.957985	0.201705	#N/A	0.992348	0.050131	#N/A
729.6254	64	#N/A	2723.309	42	#N/A
59.36969	2.603843	#N/A	13.68778	0.105549	#N/A
25%> Carbonates > 45%			**25%> Carbonates > 45%**		
-0.01619	-0.65876	1.436533	-0.0153	-0.68106	1.478434
0.003513	0.041887	0.048551	0.002704	0.053327	0.086727
0.965979	0.157857	#N/A	0.995082	0.037946	#N/A
1093.169	77	#N/A	4956.872	49	#N/A
54.48089	1.918746	#N/A	14.27493	0.070556	#N/A
Carbonates < 25%			**Carbonates < 25%**		
-0.02175	-0.57077	1.327698	-0.01796	-0.63654	1.421751
0.002742	0.03225	0.037159	0.003648	0.071772	0.116667
0.967618	0.148099	#N/A	0.986227	0.06346	#N/A
1673.345	112	#N/A	2577.807	72	#N/A
73.40381	2.456525	#N/A	20.76283	0.28996	#N/A
liquid limit <40%			**liquid limit <40%**		
-0.00237	-0.96698	1.942423	-0.00271	-0.98174	1.993395
0.004527	0.055509	0.064386	0.00312	0.059449	0.094628
0.96741	0.185985	#N/A	0.993549	0.049308	#N/A
964.7306	65	#N/A	3388.578	44	#N/A
66.74058	2.248367	#N/A	16.47714	0.106976	#N/A
40%<liquid limit <50%			**40%<liquid limit <50%**		
-0.02066	-0.58593	1.336502	-0.01485	-0.70111	1.519635
0.001907	0.023465	0.027355	0.003053	0.060471	0.098288
0.984512	0.105547	#N/A	0.989921	0.056771	#N/A
3591.4	113	#N/A	3732.383	76	#N/A
80.01767	1.25884	#N/A	24.05849	0.244943	#N/A
liquid limit >50%			**liquid limit >50%**		
-0.02058	-0.58019	1.327912	-0.01948	-0.58922	1.328132
0.003665	0.040605	0.045859	0.003652	0.068859	0.109643
0.955939	0.164946	#N/A	0.989615	0.051474	#N/A
954.6221	88	#N/A	2620.462	55	#N/A
51.9449	2.39422	#N/A	13.88638	0.145728	#N/A

TABLE C.8
KORINTHOS
TESTS ON INTACT SAMPLES

SLM B2 intact		SLM A(2) intact		SLM B intact		PSF 1a intact	
p(kPa)	e	p(kPa)	e	p(kPa)	e	p(kPa)	e
1	0.463	1	0.527	1	0.4384	1	0.4806
25	0.461	100	0.483	100	0.4154	100	0.4488
50	0.448	200	0.466	200	0.4043	200	0.4401
100	0.433	400	0.447	400	0.3905	400	0.4273
200	0.415	800	0.423	800	0.3704	800	0.4133
400	0.393	1600	0.398	1600	0.3517	1600	0.3982
800	0.363	3200	0.365	3200	0.333	3200	0.3805
200	0.382	6400	0.316	1600	0.3353	1600	0.3844
25	0.414	3200	0.320	800	0.3387	800	0.3886
		1600	0.326	200	0.3505	400	0.3935
		400	0.342	1	0.3757	1	0.4343
		100	0.366	100	0.3619	400	0.4005
		1	0.409	200	0.3582	800	0.3912
		100	0.388	600	0.3481	1600	0.383
		400	0.362	1600	0.3374	3200	0.3708
		1100	0.342	3200	0.3279	6400	0.3544
		2500	0.327	6400	0.3074		
		5000	0.314				
		10000	0.274				

TABLE C.9
PREVEZA-IGOUMENITSA
TESTS ON INTACT SAMPLES

KVT Alp intact		KVT 2 intact		XML mp intact		KKS 1 intact	
p(kPa)	e	p(kPa)	e	p(kPa)	e	p(kPa)	e
1	0.318	1	0.334	1	0.463	1	0.428
50	0.314	50	0.33	50	0.46	100	0.425
100	0.308	100	0.323	100	0.454	200	0.417
200	0.3015	200	0.31	200	0.446	400	0.405
400	0.286	400	0.297	400	0.435	800	0.389
800	0.2702	800	0.279	800	0.42	1600	0.3693
200	0.284	200	0.291	200	0.435	400	0.3823
50	0.301	50	0.31	50	0.45	100	0.403

KD 1b intact		AGN 2 intact		KD intact	
p(kPa)	e	p(kPa)	e	p(kPa)	e
1	0.558	1	0.649	1	0.319
100	0.548	100	0.642	100	0.3182
200	0.538	200	0.628	200	0.3144
400	0.522	400	0.606	400	0.3093
800	0.503	800	0.581	800	0.299
1600	0.475	1600	0.555	200	0.308
3200	0.445	3200	0.521	100	0.313
1600	0.455	1600	0.526		
800	0.473	800	0.535		
400	0.492	200	0.553		
1	0.628	1	0.600		
100	0.553	100	0.584		
200	0.538	200	0.571		
400	0.516	400	0.556		
800	0.490	800	0.540		
1600	0.465	1600	0.519		
3200	0.430	3200	0.490		
6400	0.395	6400	0.446		

TABLE C.10
COMPRESSION INDICES

	Cc 0.8-1.6MPa	Cc 3.2-6.4MPa	in situ m.c %	first yield(kPa) Casagrande
AGN2	0.101	0.248	13.2	520
KD	0.045	N/A	12.5	710
KDAb	0.068	0.168	16.1	550
KKS1	0.081	N/A	15.6	650
KVT2	0.073	N/A	13.6	390
KVTALP	0.068	N/A	12.7	320
XLM MP	0.058	N/A	18.2	450
SLMB2	0.098	N/A	13.5	825
SLMB(i)	0.062	0.062	10.3	650
SLMA(2)	0.083	0.163	17.5	550
PSF1a	0.045	0.087	2.00	850

APPENDIX D

GEOLOGICAL MAPS

Peneios Reservoir

dam

scale
1:50.000
based on AMALIAS SHEET (KAMBERIS, 1987)
based on GOUMERON SHEET (IGME, 1981)

0 500 1000 2000 m

NESIA

SOUNION

KENTRON

TL183

LAÏAS

KAMBOS

AVGI

DAFNI

KERAMIDIA

EFYRA

TZAMI

MVG

MEROVIGLI

SIMOPOULON

To CHAVARION

DAFNIOTISSA

KRYONERION

OENI

OENIDI

KALO PAIDI

RIVER LADON

RODIA

ALTOPHOLIA

PERISTERION

To GERAKION

SKOUFA

KOUTSOHERA

KTR20

KTR10

ASTERAIIKA

PLS PALAIOSTANI

PERDIKOVRYSI

To OLYMPIA

PALAIOLANTHI

MOYZAKION

21°25'

21°30'

21°35'

- Road
- Secondary Road
- Elevation Point
- River
- Tributary river, stream
- Sampling point
- Geological Boundary
- Probable Geological Boundary
- Fault
- Probable Fault
- Steep slope, scarp
- Landslip

al — Alluvial recent deposits.

Pleistocene, Kryoneri formation, coarse facies conglomerates, sands. psephitic conglomerates.

Plio-pleistocene, Keramidia formation, blue, grey-blue clays with lenses of coarse grain sandstones

1 — Vounagron formation, intercalations of sandstones and argillaceous successions. Clays and silts are more dominant in the upper stratigraphical units. Conglomerates were not found. Sandstones of various grain sizes dominate the lower units. The fine grained facies are fossiliferous.

2 — **Upper Pliocene** Peristerion formation, mainly whitish conglomerates (1) with intercalations of sandstones and silty clays (2), blue with lenses of lignite

Oenoi - Prophetis Helias formation, clays grey-green, marls, marly clays and conglomerates at the base.

22°50'

22°55'

37°55'

KORINTHOS GULF

CITY OF KORINTHOS

scale 1:50,000

PERYIALION

ASSOS

LECHAION

PATRA-KORINTHOS-ATHENS NATIONAL ROAD

JSAKIRI

ARCHAIA KORINTHOS

AKROKORINTHOS

SOLOMOS JUNCTION

SOLOMOS

RACHIANI STREAM

RENTAIIKA

PENTESKOUFI

MBE:KIANIKA

AYIA SOTIRA

POTAMIA STREAM

PLATANI STREAM

VELINIATIKA

ROUMANIA

SPATHOVOUNION

Prophetes Helias

ARVANITIS

0 500 2000 m

LEGEND

- ROAD
- AGRICULTURAL TRACK
- SAMPLING POSITION
- STREAM
- GEOLOGICAL BOUNDARY
- POSSIBLE GEOLOGICAL BOUNTARY
- FAULT
- POSSIBLE FAULT
- ELEVATION POINT
- TALUS, ALLUVIAL FAN
- LANDSLIP

N.B. This map is based on the Korinthos Sheet of the Geological Map of Greece (I.G.M.E, 1969) by DR. J. Bornovas, N. Lalechos and N. FILIPAKIS. Stratigraphy by Dr. G. Christodoulou and St. Tsaila-Monopolis.

Qal1 / Qcn — Holocene, Recent deposits (Qal1) loose, mixed facies; Recent talus cones (Qcn),

Qel — Mainly elluvial deposits, loam & loamy sand from weathering of the Pliocene or Tyrrhenian sandy marls Red coloured.

Qdl2 — Pleistocene, Red clayey sand overlying the tyrrhenian beds Thickness 5-10m,

Qdl1 — Tyrrhenian marine-near shore deposits: conglomerates, marls, sands present in terraces from 20m to 300m elevation. 5-10m thick.

Pl.m / Plc — Pliocene, marls, yellowish to white, sometimes light grey or blueish with intercalations of sandstones, psephitic conglomerates and marly limestones. Lacustrine facies dominate the upper parts. Lignite beds in marls of the upper parts by Solomos and Penteskoufi.

Basic conglomerates (c), coarse, cohesive, polygenetic sometimes with plenty of marly cement.

Jm.k / sh — Midde Jurassic, Thin plated to thin bedded limestones (k) with shales (sh) made up of sandstones, clays and brown to green marls.

scale
1:5,000
detail from
KORINTHOS
SHEET No
6366/2

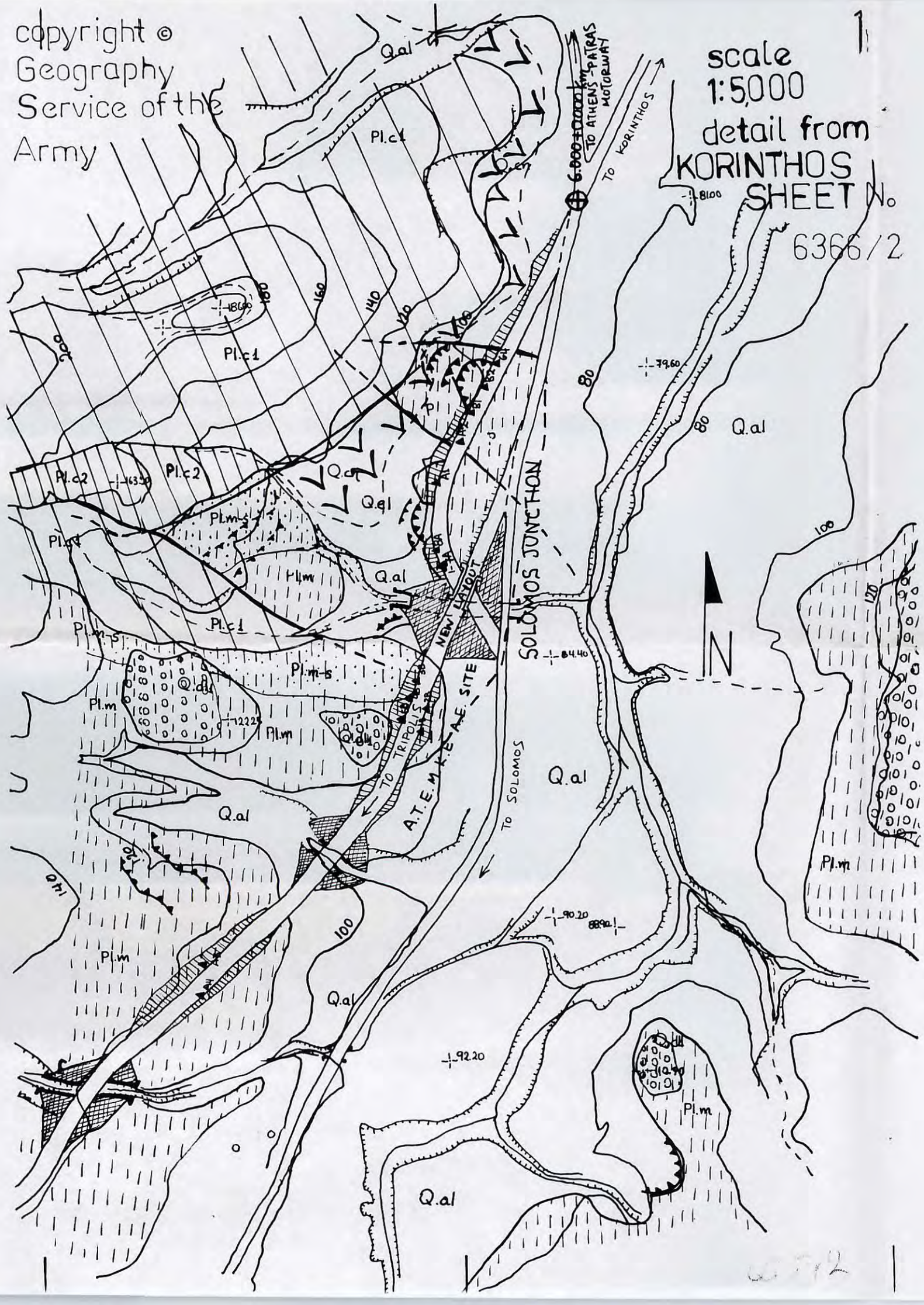

embankment materials

Q.al — Alluvial deposits. Loose mostly coarse grained sands and sandy silty clays.

Q.cn — Recent talus cones

Q.dl — Terragenous materials probably related to Tyrrhenian marine near coast. Coarse grained overlying marly formations deposited in paleorelief. Mainly loosened conglomerates. with marly matrix

Pleistocene

Pl.c1 — Conglomerates, no bedding identified, loosened, attaining thickness in excess of 50m. Terrestrial origin with red sandy clayey matrix.

Pl.c2 — Cohesive beds of conglomerates with thin bands of sandy silt; maximum thickness 15m.

Pliocene

Pl.m-s — Grey sandstone with intercalations of green grey and grey brown clayey marl. The thickness of the sandstone beds does not exceed 0.3m.

Pl.m — Marls, clays, sandy and silty marls intercalated. The upper members are coarser than the lower overconsolidated hard materials.


TO Igoumenitsa
20°30'
39°10'
Pl.m
LOUTSA
Ji.k
Pl.c
AGIOS NIKOLAOS
GOURNAKI
VRACHOS
TSOUMBA
LAKKA
LIGIA
KREVATINA
KASTRO DESPOS
RIZA
MEGA DENDRON
KYMONELIA
KASTROSYKIA
ARCHANGELOS
KANALI
KOYKOS
IONIAN SEA
20°35'
39°05'
20°40'
TO Preveza
scale 1:50,000
based on KANALAKION SHEET (I.G.M.E)
N
0
500
2000m
The Kanalakion Sheet of the geological map of Hellas was mapped by J.J. BIZON, M. LATREILLE, P. DOURTHE, J. ROCHET, E. SAVOYAT, P. FERRIER, of the French Institute of Petroleum and G. KATSIKATSOS of I.G.M.E. First Published in 1967.
road
secondary road
elevation point
stream
landslip
sampling site
fault
probable fault
geological boundary
probable geological boundary
al
Quaternary Alluvial deposits near coast and fluvial, loose, forming terraces to the south of Riza as a result of coastal erosion. Mixed facies. Recent talus cones (scl).
scl
Pl.m
Pliocene Archaggelos formation. Mixed facies series consisting of conglomerates (Pl.c), argillaceous silts and sands, marly clays and marls (Pl.m). The entire succession has an estimated thickness of 700m on average
Fine grained facies intercalate with sandstones medium to coarse grain size to form steep slopes.
Pl.c
Ms-m G
Vindobanian - Upper Miocene
Series of blue marls, rich in microfauna with banks of gypsum (G). Thin bands of sandstones of varying grain size. The upper members of the series become coarser.